UNIVERSITÉ DE GRENOBLE

THÈSE

Pour obtenir le grade de

DOCTEUR DE L'UNIVERSITÉ DE GRENOBLE

Spécialité : **Matériaux, Mécanique, Génie civil, Electrochimie**

Arrêté ministériel : 7 août 2006

Présentée par

Varvara GRIBOVA

Thèse dirigée par **Catherine PICART** et
codirigée par **Rachel AUZELY-VELTY**

préparée au sein du **Laboratoire des Matériaux et du Génie Physique** et **du Centre de Recherches sur les Macromolécules Végétales** dans **l'École Doctorale I-MEP^2 : Ingénierie - Matériaux, Mécanique, Environnement, Energétique, Procédés, Production**

Films biomimétiques multicouches pour les applications dans l'ingénierie tissulaire musculo-squelettique

Thèse soutenue publiquement le **25 novembre 2013**,
devant le jury composé de :

Mme Catherine COIRAULT Chargée de Recherche, INSERM, Paris	Rapporteur
Mr Christophe TRIBET Directeur de Recherche, CNRS, Paris	Rapporteur
Mme Cécile GAUTHIER-ROUVIERE Directeur de Recherche, INSERM, Montpellier	Examinateur
Mr Didier BOTURYN Directeur de Recherche, CNRS, Grenoble	Président du jury
Mr Benoît FRISCH Directeur de Recherche, CNRS, Strasbourg	Examinateur
Mme Rachel AUZELY-VELTY Professeur des Universités, Université Joseph Fourier, Grenoble	Co-directeur de thèse
Mme Catherine PICART Professeur des Universités, Institut Polytechnique de Grenoble, Grenoble	Directeur de thèse

Biomimetic multilayer films for musculoskeletal tissue engineering applications

Table of contents

Acknowledgements

I am deeply indebted to a number of people for making this thesis a reality.

I first thank my advisors, Pr Catherine Picart and Pr Rachel Auzély-Velty, for their individual and collaborative efforts to guide and shape my research, professional and personal development during these three years in Grenoble. No doubts that meeting you in June 2010 was one of the most important events in my life, and I do not have enough words to describe everything you learned me.

I would like to thank Dr Catherine Coirault and Dr Christophe Tribet for the honor they made me by accepting to evaluate my work, and Dr Cécile Gauthier-Rouvière, Dr Benoît Frisch and Dr Didier Boturyn for accepting to participate in the thesis committee.

In also thank Cécile for her precious advices, and I am deeply grateful to Dr Corinne Albigès-Rizo and Dr Manuel Théry for their collaboration and expertise.

I would like to thank all my colleagues from LMGP and CERMAV laboratories.

I thank Virginie Charrière, Josiane Viboud and Anne Fracchia for their administrative assistance. Also, this work would not be possible without our excellent microscopy engineer Isabelle Paintrand. I also thank Isabelle Jeacomine for her help with NMR.

I specially thank my best girls Laure Fourel and Jing Jing, who supported me from the very first days of my thesis and who always helped me with everything, and Flora Gilde and Claire Holtzinger, who were close during all the three years and who shared with me all the good and bad moments. I thank Raphaël Guillot, Fabien Dalloneau, Jimmy Mergy for being such great engineers (we can rely on you, guys!), and Claire Monge and Thomas Boudou for scientific discussions and interesting collaborations. I thank all the great people whom I had pleasure to know and without whom I can barely imagine my lab life at one moment or another, among them Xiqiu Liu, Anne Valat, Min Hai, Naresh Saha, Laurent Nault, and Thomas Ballet. I also had the pleasure of advising an excellent intern Hugo Cheyron, and I thank him for making me proud.

I am extremely grateful to Pr Mitsuru Akashi at Osaka University for the opportunity of collaboration with his laboratory – it was an extraordinary experience! I also thank all the people who helped me during my stay in Japan: Natsuko Hashimoto for her administrative assistance, Akihiro Nishiguchi for teaching me the new methods, Paninee Chetprayoon and Chun-Yen Liu for their friendship. I would like to specially thank Dr Michiya Matsusaki for sharing with me his passion for the science and for his contagious ideas that have led me till obtaining a post-doctoral fellowship for my future research work in Japan.

And I would like of course to thank my family, and especially my mother, who has always been my Friend Number One, for always supporting me, believing in me, for her continuous love. Without whom I could not have made it here. And Dominique, for showing me with his example – how strong a person can be and how precious every day of the life is.

I thank my wise friend Zahia Hamidouche, who guided me in the beginning of my scientific life, and my beloved best friends from more or less far away: Elena, Nelly, Katia.

Finally, I recognize that this research would not have been possible without the financial assistance of the Region Rhônes-Alpes, which provided me with a PhD fellowship, and the European Commission via an ERC Starting grant 2010 (GA 259370, BIOMIM). I also thank Society for Cell Biology – France (SBCF) for providing me with a travel fellowship for visiting the excellent Gordon Research Conference in the USA.

Abbreviations

Polymers
ALG: Alginate
CHI: Chitosan
GAG: Glycosaminoglycan
HA: Hyaluronic Acid
HEP: Heparin
PA: Poly(acrylamide)
PDMS: Poly(dimethylsiloxane)
PEG: Poly(ethylene glycol)
PEI: Poly(ethylenimine)
PGA: Poly(L-glutamic acid)
PLGA: Poly(lactic-glycolic) acid
PLLA: Poly-(L-lactic) acid
PLL: Poly(L-lysine)
PSS: Poly(styrene sulfonate)

Reactifs and solvents
BrdU: 5-Bromo-2'-deoxyuridine
DMSO: Dimethylsulfoxide
EDC: 1-Ethyl-3-(3-dimethylamino-propyl) carbodiimide
EDTA: Ethylene diamine tetraacetic acid
EdU: 5-Ethynyl-2'-deoxyuridine
EGTA: Ethylene Glycol Tetraacetic Acid
FBS: Fetal Bovine Serum
FITC: Fluorescein Isothiocyanate
HEP: Heparin
HEPES: 4-(2-Hydroxyethyl)-1-piperazine ethane sulfonique acid
PBS: Phosphate buffered saline
SDS: Sodium Dodecyl Sulfate
S-NHS: N-hydroxysulfo succinimide
TBS: TRIS-Buffered Saline
TRIS: 2-Amino-2-hydroxymethyl-propane-1,3-diol

Techniques and equipment
FTIR: Fourier Transform Infrared spectroscopy
LbL: Layer-by-Layer
NMR: Nuclear Magnetic Resonance
QCM-D: Quartz Cristal Microbalance with Dissipation
SEM: Scanning Electron Microscopy

Proteins and enzymes
ALP: Alkaline Phosphatase
BMP: Bone Morphogenic Protein
BSA: Bovin Serum Albumin
COL: Collagen
EGF: Epidermal Growth Factor
FAK: Focal Adhesion Kinase
FGF: Fibroblast Growth Factor
FN: Fibronectin
G: Gelatin
GAG: Glycosaminoglycan
GFP: Green Fluorescent Protein
HSPG: heparan sulfate proteoglycans
LAM: Laminin
PDGF: Platelet-Derived Growth Factor
rhBMP-2: Human Recombinant Bone Morphogenic Protein 2
RGD: Arginine - Glycine – Asparagine
SDC-1: Syndecan-1
VEGF: Vascular endothelial growth factor

Cell culture
DM: Differentiation Medium
DMEM: Dulbecco's Modified Eagle's Medium
ES: Embryonic Stem (cells)
FBS: Fetal Bovine Serum
GF: Growth Factor
GM: Growth Medium
HSC: Hematopoietic Stem Cells
HUVEC: Human Umbilical Vein Endothelial Cells
iPS: Induced Pluripotent Stem (cells)
MSC: Mesenchymal Stem Cells
SFM: Serum-Free Medium
siRNA: Small Interferent RNA

Other
ANOVA: Analysis Of Variance
BM: Basement Membrane
ECM: Extracellular Matrix
MW: Molecular Weight
PEM: Polyelectrolyte Multilayer (films)
RT: Room Temperature

General Introduction

The loss or failure of an organ or tissue is one of the most important problems in human health care. Because of the shortage of organs and tissues available for donation, physicians and scientists are searching for alternatives.

Tissue engineering applies the principles of biology and engineering to the development of functional substitutes for damaged tissue. Current tissue engineering approach consists in combining cells, engineering and biomaterials to improve the biological functions of damaged tissues or to replace them. Production of "artificial tissues" is still challenging and requires collaboration of scientists from different domains like cell biology, chemistry, materials and polymer science.

Different types of tissues may be engineered by this approach, and among them skeletal muscle, which is one of the major tissues of the human body. Skeletal muscle tissue engineering holds promise for the replacement of muscle due to an injury following a surgery or due to a trauma, and for the treatment of muscle diseases, such as muscle dystrophies or paralysis. Engineered muscle tissues models are also required for pharmaceutical assays and fundamental studies of muscle regeneration.

Satellite cells, muscle stem cells, are now considered as a powerful source for the regeneration of skeletal muscle, but also of several other tissues. A major limitation to the study and clinical applications of satellite cells consists in a rapid lost of their stem properties *in vitro*. The development of skeletal muscle is known to strongly depend on the interaction of muscle cells with their surrounding extracellular matrix (ECM), which provides them a variety of physical and biochemical signals. These are now recognized as being key parameters in numerous cellular processes, from adhesion to regulation of the cell fate. Moreover, mature skeletal muscle has a complex three-dimensional (3D) organization of aligned muscle fibers surrounded by ECM.

Thus, engineering of a functional muscular tissue requires complex environments mimicking *in vivo* niche, to control cell adhesion, proliferation, differentiation and properly organize the cells. To this end, materials with tunable mechanical and chemical/biochemical properties for myoblast expansion and differentiation *in vitro,* as well as for the studies of myogenesis on controlled 2D microenvironments or in 3D scaffolds, are crucially needed.

In this context, layer-by-layer (LbL) films offer numerous possibilities for the development of substrates with well-controlled mechanical and biochemical properties. The technique was introduced in the early 1990s and has attracted an increasing number of researchers in recent

years due to its high versatility and wide range of advantages they present for biomedical applications. Polyelectrolyte multilayer (PEM) films are currently emerging as a new kind of biomaterials coating that can be used to guide cell fate. They can be used either as 2D materials for investigation of cellular behavior on defined substrates, or for coating of 3D constructions such as implants or tissue engineering scaffolds.

In this thesis work, we used layer-by-layer (LbL) assemblies for two goals. The first consisted in the development of multifunctional biomimetic thin films for the control of skeletal muscle cell fate on 2D substrates. We used LbL films made of polypeptides, which can be stiffened by chemical cross-linking and can be specifically functionalized by grafting of biomimetic peptides onto their surface. In addition, we combined the peptide-grafted films with substrate microtopography. Such approach is promising for the development or multifunctional materials that combine the different stimuli present in *in vivo* ECM. This part of the project was conducted in collaboration between two Grenoble laboratories, LMGP and CERMAV, one specialized in biomaterials and other in polymer chemistry.

In the second part, we used LbL assemblies for the construction of 3D skeletal muscle microtissues by "cell-accumulation technique". This part was conducted in collaboration with the laboratory of Pr Mitsuru Akashi from Osaka University, Japan. The method consists in coating myoblasts with fibronectin-gelatin nanofilms mimicking the ECM, before seeding them onto a substrate where the cells self-organize. Such approach makes it possible to rapidly build 3D tissues and is promising for the *in vitro* construction of tissue models.

During this project I had opportunity to work with people from different disciplines, trying to adapt their know-how to biological science. Being a cell biologist, according to my Master diploma, I could acquire new knowledge and competences in biomaterials, nanomaterials, chemical synthesis and discover methods for the analysis of synthesized products and different tools for the characterization of materials. This experience was very enriching both in human and in professional senses.

My strong wish is to continue collaboration with people from different scientific fields in order to create "smart" materials for the control of cellular processes and develop new approaches for the construction of artificial tissues.

CHAPTER I – Introduction

This chapter serves to introduce important concepts of the biomaterials field and present the possibilities offered by different types of biomaterials for musculo-skeletal tissue engineering. It is divided in three parts.

First, the importance of cell-surrounding environment will be demonstrated. An overview of the different types of stimuli presented by the surrounding matrix will be given.

Second, an overview of currently existing biomaterials and their properties will be done and the concept of tissue engineering will be presented. The emphasis of this discussion will be on the currently existing methods for modification of biomaterials properties for better control of cellular behavior and tissue regeneration. LbL films as a type of highly versatile biomaterial offering numerous advantages for biomedical applications will be presented.

Finally, the focus will be done on skeletal muscle tissue engineering, current approaches and challenges in this field. The applications of LbL films for the control skeletal muscle stem cell fate will be discussed.

The objectives of this thesis will be presented at the end of the chapter.

I.A. THE CELL ENVIRONMENT

I.A.1. General presentation of the extracellular matrix

Our body is made of several types of tissues (skin, muscle, bone, cartilage…) whose properties and functions strongly depend on their composition. Tissues are composed of cells embedded within an extracellular matrix (ECM) made of proteins, polysaccharides and other bioactive molecules such as growth factors (Hynes 2009; Frantz et al. 2010). Tissues differ in cell types that compose them, but also in ECM composition and quantity (Halfter et al. 2013). For instance, tissues like cartilage are predominantly made of the ECM, while in brain it is only a minor constituent.

ECM properties are extremely dynamic and are spatially- and temporally-controlled during development. From the earliest stages of embryogenesis and throughout the life, the ECM plays a role in development and morphogenesis, induces stem cells to differentiate into mature tissue cells, provides structural support to the cells and determines tissue architecture and function (Adams and Watt 1993; Gullberg and Ekblom 1995; Reilly and Engler 2010; Rozario and DeSimone 2010).

The ECM molecules are synthesized intracellularly, secreted by exocytosis and remodeled by the cells. Abnormal ECM deposition is a characteristic feature of many diseases, and a number of pathologies involve changes in matrix properties (Jarvelainen et al. 2009; Frantz et al. 2010). Deposition of amyloid fibers takes place in Alzheimer's, Parkinson's, Huntinghon's diseases, atherosclerosis and rheumatoid arthritis, diabetes mellitus type 2 (Meredith 2005; Rambaran and Serpell 2008). In the liver, pancreas, kidney and lung fibrosis significantly affects organ functions (Zeisberg and Kalluri 2013). Fibrosis is characterized by changes in the composition and amount of many ECM proteins. Duchenne muscular dystrophy is also characterized by an increase in connective tissue (Klingler et al. 2012). Recently, evidence of important ECM remodelling in adipose tissue and, in particular, during the development of obesity was discovered (Divoux and Clement 2011).

I.A.2. Composition of the extracellular matrix

The ECM is composed of several types of macromolecules (Fig. I-1): glycosaminoglycans (GAGs), which are polysaccharide chains usually covalently linked to a protein core, and proteins, including collagen, elastin, fibronectin, and laminin. Bioactive molecules, such as growth factors (GF), are often bound to ECM components and presented to the cells in a matrix-bound manner (Fig. I-1)

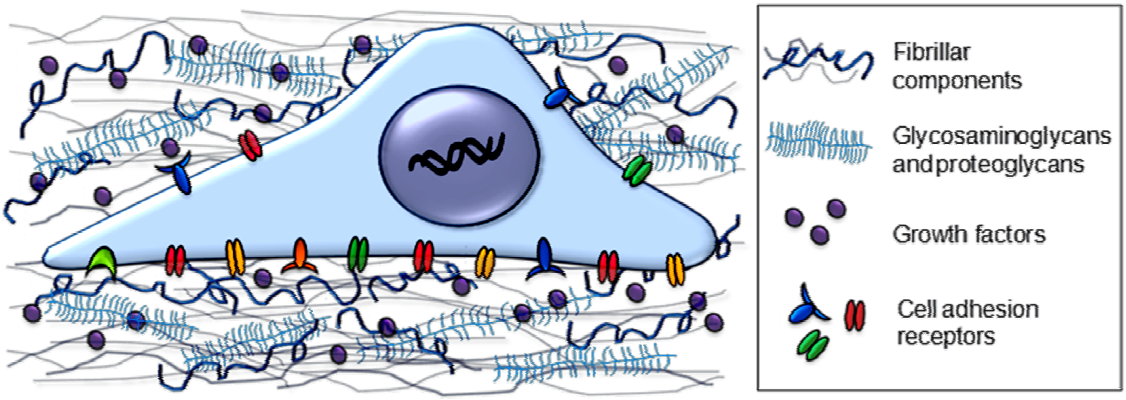

Figure I-1. Composition of the extracellular matrix. *The glycosaminoglycans and proteoglycans form a highly hydrated substance in which the fibrous proteins are embedded. Growth factors bind to ECM components and are presented to the cells in a matrix-bound manner. The cell senses its environment through cell surface receptors, especially cell adhesion and cell/cell receptors.*

Extracellular matrix includes the interstitial matrix and the basement membrane. Interstitial matrix is ia highly hydrated network present in the intercellular spaces. The negatively-charged proteoglycan molecules form a highly hydrated substance in which the fibrous proteins are embedded. This gel allows rapid diffusion of nutrients and bioactive molecules, while fibrous proteins strengthen and organize the matrix. Basement membranes (BM) are the thin sheets of ECM that surround muscle cells, Schwann cells, fat cells and underlies epithelial and endothelial cells (Yurchenco 2011; Halfter et al. 2013). BM proteins emerged about 500 million years ago during the evolution of metazoan species, and they are the evolutionary oldest ECM proteins (Hynes 2012). BM contain collagen, proteoglycans and laminin, which is the major glycoprotein of the BM (Durbeej 2010). A core network of cross-linked collagen is associated with laminin, laminin-binding glycoprotein nidogen and a very large and complex heparan sulfate proteoglycan perlecan (Yurchenco 2011; Hohenester and Yurchenco 2013). Mutations in genes encoding components of the skin basement membrane are associated with inherited skin disorders such as epidermolysis bullosa, which is characterized by skin fragility, mechanically induced blisters and erosions of the skin and mucous membranes (Bruckner-Tuderman and Has 2013).

Laminin, a major glycoprotein of the BM, consists of the three subunits: α, β and γ, and contains many distinct domains with different structure and functions (Engel and Furthmayr 1987; Beck et al. 1990) (Fig. I-2). At present, 5 α, 3 β and 3 γ chains are known for mouse and human, that form 16 laminin isoforms (Miner and Yurchenco 2004). Laminins can self-assemble into a sheet through interactions between the ends of the laminin arms. Cellular receptors specifically recognizing laminins are mainly integrins, *α*-dystroglycan, syndecans, and other cell surface molecules (Miner and Yurchenco 2004).

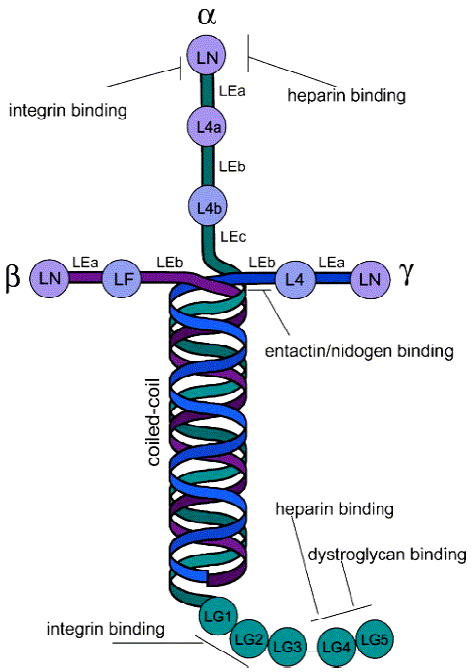

***Figure I-2. Scheme of laminin heterotrimeric structure**. Laminin α chain is depicted in green, β in violet and γ in blue. Laminin α chain consists of: the N terminal globular domain (LN); tandem rod domains of epidermal growth factor (LEa, LEb, LEc), separating the LN, L4a and L4b globular domains; the laminin coiled-coil (LCC) domain that tangles with the LCC domains of the β and γ chains; and the C-terminal laminin globular (LG) domains. Sites of binding to different cell surface receptors are indicated.Adapted from (Nguyen and Senior 2006).*

Collagen, elastin and fibronectin are major components of the ECM fibrillar network.

Collagens are a family of fibrous proteins found in all multicellular animals. They are major components of skin and bone and constitute about 25% of the total protein mass of the body. Collagen molecule has triple-stranded helical structure made of three collagen polypeptide chains. Collagen triple helices can be further cross-linked and form sheet-like structures (Fig. I-3A). Collagens play structural roles and contribute to mechanical properties, organization, and shape of tissues (Ricard-Blum 2011).

Fibronectin, a large glycoprotein found in all vertebrates, is a dimer composed of two very large subunits joined by disulfide bonds at one end. One of the FN isoforms, plasma fibronectin, is soluble and circulates in the blood and other body fluids. In other forms, fibronectin dimers are cross-linked to one another by additional disulfide bonds and assemble on the cell surface and are deposited as highly insoluble fibers (Fig. I-3B) (Ruoslahti 1988a).

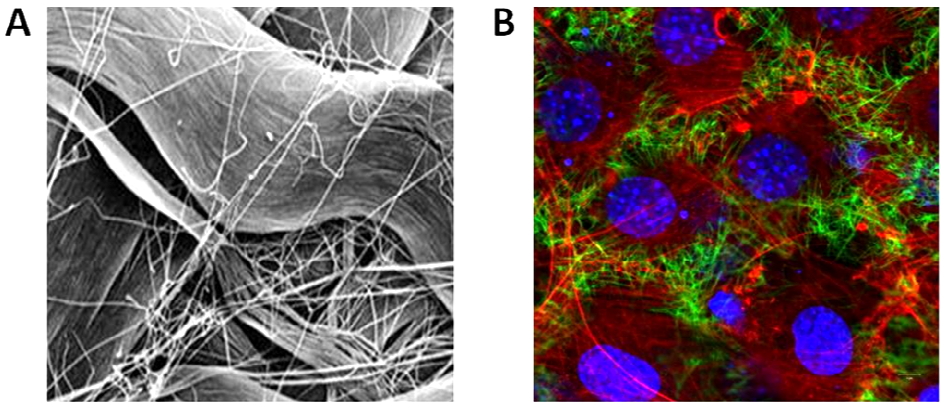

Figure I-3. Extracellular matrix fibrillar components. *(A) Fibrillar and sheet-like collagen network (image by Thomas Caceci, http://vetmd.vt.edu). (B) Fibronectin matrix (labeled in green) secreted by C2C12 myoblasts in culture.*

Elastin is one of the major components of elastic fibers. Soluble tropoelastin is crosslinked into amorphous elastin by lysyl oxidase, making from it a highly stretchable molecule, which is a major provider of tissue elasticity. Elastin is the dominant ECM protein in arteries, comprising 50% of the dry weight of the largest artery - the aorta (Debelle and Tamburro 1999).

Glycosaminoglycans (GAG) are a heterogeneous group of negatively charged polysaccharides that are covalently linked to protein to form proteoglycan molecules (except for hyaluronan which is not linked to a protein core). They occupy a large volume and form hydrated gels in the extracellular space. Some proteoglycans, such as syndecans or glypicans, are also found anchored to the cell surface (Fig. I-4) (Ruoslahti 1988b).

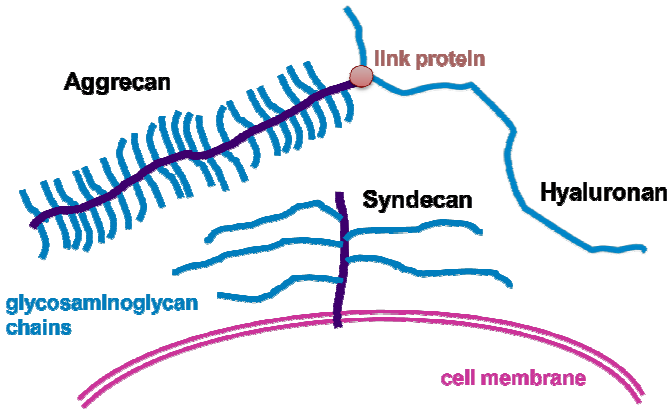

Figure I-4. Scheme showing some proteoglycans and other GAGs of the extracellular space. *An example of membrane-bound proteoglycan is syndecan which has several heparan sulfate chains attached to a core protein. Aggrecan is a common proteoglycan of the interstitial space that form hydrated gels in complexes with the free polysaccharide hyaluronan.*

I.A.3. Cell adhesion receptors

Deciding which protein to express, when to divide, when to specialize, and when to commit or get into apoptosis are processes that permanently occur within the cells. These decisions are taken in response to the environmental stimuli such as extracellular signaling molecules (growth factors, cytokines…) and ECM. All the signals provided by the environment are transmitted from the outside by cell surface receptors and activate signaling pathways that regulate gene expression, protein synthesis and thus contribute to the control of cell fate (Fig. I-5).

The discovery of the integrins in the 1980s (Ruoslahti 1988a) allowed understanding of the physical linkages between intracellular and extracellular compartments that serve to mediate adhesion and bidirectional flow of the signals. Adhesion is of fundamental importance to a cell, as it provides anchorage, cues for migration, and signals for growth and differentiation. There are two principal types of cell adhesion: cell-matrix adhesion and cell-cell adhesion. Integrins appear to be the primary mediators of cell-matrix adhesion, and they also serve as one of the many families of molecules active in cell-cell adhesion (Ruoslahti 1988a; Hynes 1992; Hynes 2002). Later it became clear that a group of cell-surface associated proteoglycans named syndecans might act as co-receptors for the ECM and for certain growth factor receptors (Ruoslahti 1988b). Later, dystroglycan have emerged as another type of receptors that link the cytoskeleton to the ECM (Gullberg and Ekblom 1995; Matsumura et al. 1997).

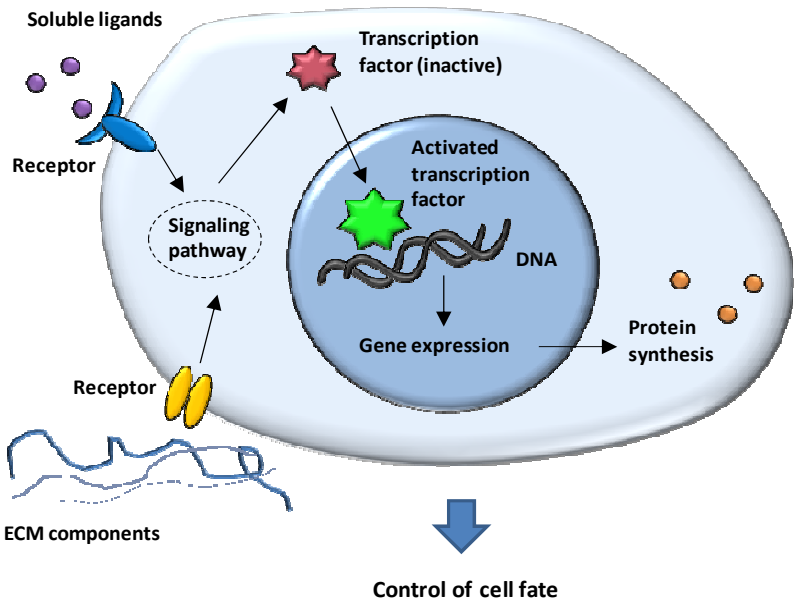

Figure I-5. Schematic presentation of signal transduction by cell surface receptors. *Cell interaction with environmental cues (soluble ligands, extracellular matrix components) activate signaling pathways that regulate gene expression and protein synthesis.*

The first **integrin** to be discovered bound to fibronectin (Ruoslahti and Pierschbacher 1987; Ruoslahti 1988a) but it was soon found that several ECM components bind to similar types of receptors (Hynes 1992; Ruoslahti 1996b). Integrins are transmembrane heterodimeric molecules composed of α and β chains. So far, 24 distinct heterodimeric isoforms have been identified, composed of various combinations of the 18 α and 8 β chains (Hynes 1992). Generally the subunits possess a small intracellular domain, a single transmembrane spanning region, and a large extracellular domain, and link the intracellular compartment with the ECM (Fig. I-6). The name integrin was given to denote the importance of these receptors for the integrity of both the cytoskeleton and the ECM (Ruoslahti and Pierschbacher 1987; Ruoslahti 1988a).

From the large integrin repertoire that exists for each specific cell type, cells are known to sense the underlying substrates mainly via $\alpha_v\beta_3$ and $\alpha_5\beta_1$, through focal complexes and focal adhesions. The $\alpha_v\beta_3$ and $\alpha_5\beta_1$ integrins serve as receptors for a variety of extracellular matrix proteins with the exposed arginine-glycine-aspartic acid (RGD) sequence. The tripeptide sequence RGD is present in many ECM proteins, including fibronectin, vitronectin, fibrinogen, von Willebrand factor, thrombospondin, laminin, osteopontin, bone sialo protein, and some collagen isoforms (Ruoslahti 1996b), and binds to a wide range of integrin receptors.

Focal adhesions are protein assemblies on the cytoplasmic side of the cell membrane where integrin receptors mechanically link the extracellular matrix to the actin cytoskeleton. Focal adhesions originate from the maturation of small focal complexes; they associate with actin stress fibres and are a place for cell traction (Fig. I-6). The transformation of focal adhesions into even bigger fibrillar adhesions is driven by integrin and cytoskeletal-generated tension (Zamir and Geiger 2001b; Zamir and Geiger 2001a; Hynes 2002; Bershadsky et al. 2006).

Syndecans are transmembrane heparan sulfate proteoglycans that bind a variety of ECM components, including fibronectin, laminin, tenascin, thrombospondin, vitronectin, and the fibrillar collagens. Their polysaccharide chains allow interaction with a variety of growth factors, so that syndecans act as “regulators” of growth factor receptor activation.

The syndecan family includes 4 members named Syndecan-1 to -4, which are expressed in cell type-specific manner (Bernfield et al. 1999). Syndecan-1 (SDC-1), or cell surface antigen CD138, is the most studied of all the syndecans in cancer research. Altered expression of SDC-1 has been detected in several different tumor types and (Beauvais and Rapraeger 2004). SDC-1 is also known to mediate fibroblast growth factor-2 binding and activity (Filla et al. 1998).

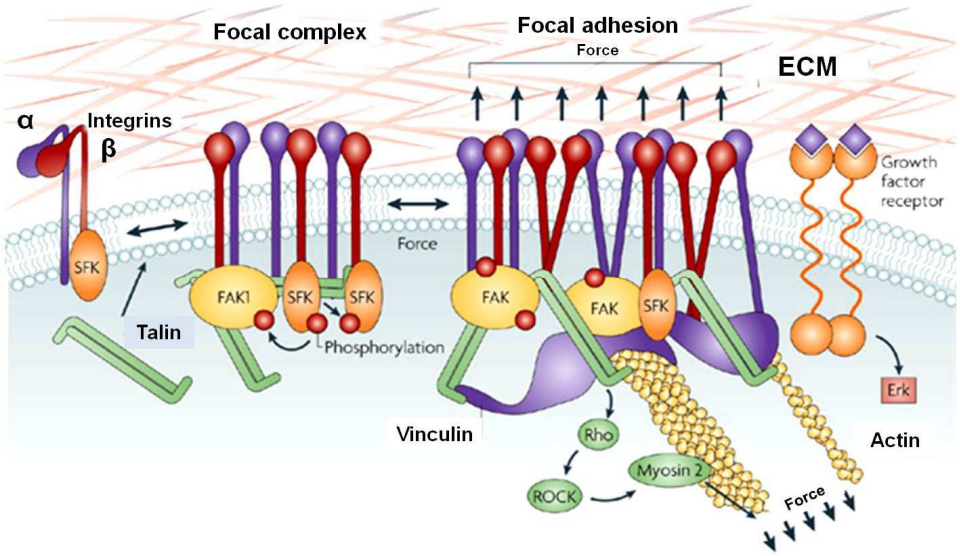

Figure I-6. Integrin-mediated bidirectional signaling between the intracellular and extracellular compartments and focal adhesion formation. *The majority of integrins exist at the plasma membrane in a resting, inactive state in which they can be activated by inside–out or outside–in cues. With regard to outside–in activation, when cells encounter a mechanically rigid matrix or are exposed to an exogenous force integrins become activated, which favours integrin oligomerization or clustering, vinculin–talin association, and Src and focal adhesion kinase (FAK) stimulation of RhoGTPase-dependent actomyosin contractility and actin remodelling. Focal adhesions mature with the recruitment of a repertoire of adhesion plaque proteins, including α-actinin to facilitate actin association, and adaptor proteins such as paxillin, which foster interactions between multiple signalling complexes to promote growth, migration and differentiation. From (Butcher et al. 2009).*

For a long time, syndecans were considered as co-receptors (Fig. I-7). Recently, their independent role in mediating cell adhesion and signaling has emerged (Couchman 2003). Also, synergistic control of cell adhesion by integrins and syndecans has been described (Morgan et al. 2007), although the mechanisms and precise roles of this interplay remain unclear. SDC-1 was shown to support integrin α2β1-mediated adhesion to collagen in Chinese hamster ovary cells, suggesting a previously unknown link between integrin-α2β1 and SDC-1 (Vuoriluoto et al. 2008). Hozumi et al. showed that syndecan-1/4 and integrin-α2β1 binding peptides derived from laminin-α1 synergistically accelerated cell adhesion (Hozumi et al. 2010).

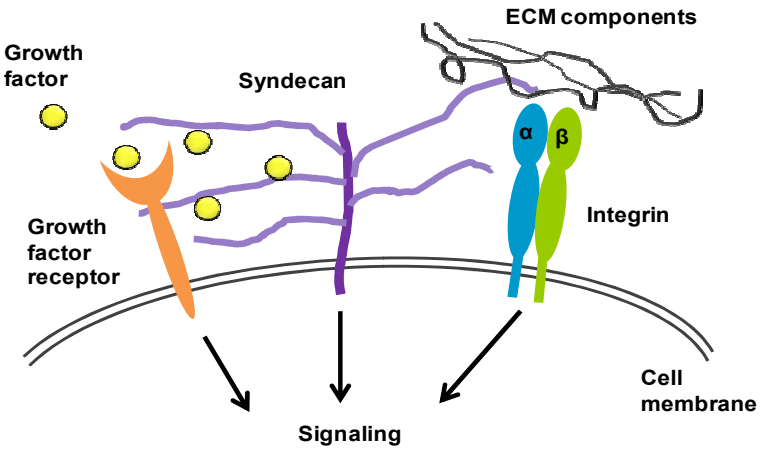

Figure I-7. Some of syndecan functions. *Syndecans modulate growth factor signaling through binding growth factors by their polysaccharide chain, bind extracellular matrix components and participate in synergistic control of cell adhesion with integrins.*

Dystroglycan (DG) is a component of dystrophin-glycoprotein complex which, in muscle cells, forms an important receptor system for ECM (Gullberg and Ekblom 1995). DG was shown to be crucial for maintaining the integrity of sarcolemma and protecting muscle from damage. (Matsumura et al. 1997; Cohn et al. 2002; Han et al. 2009). (Fig. I-8). DG is also expressed in peripheral nerves (Masaki et al. 2003), where it plays diverse roles in Schwann cells such as myelination and maintenance of myelin and nodal structures (Masaki and Matsumura 2010).

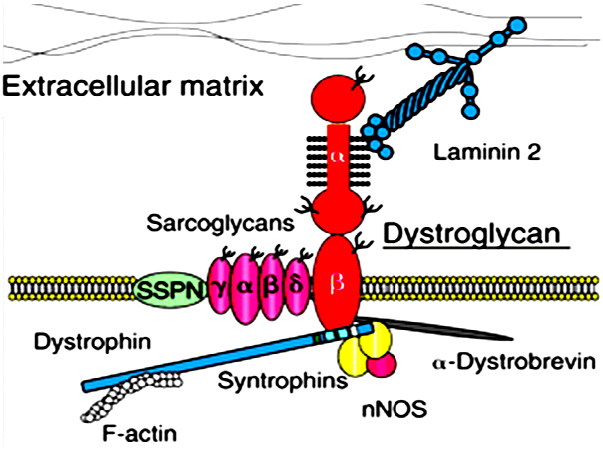

Figure I-8. Schematic representation of dystroglycan within the dystrophin-glycoprotein complex binding ECM. *Dystroglycan is composed of α and β subunits. It binds with high affinity to the LG domains of laminin α chain from the extracellular side, and dystrophin intracellularly. Adapted from (Barresi and Campbell 2006).*

Cadherins are cell surface receptors that ensure association between cells through the calcium-dependent assembly of cell-cell junctions (Fig. I-9). Cell-cell adhesion is important for the maintenance of normal tissue architecture and function. (Hirohashi and Kanai 2003). Originally considered as cell adhesion molecules, cadherins were shown to be involved in cell signaling and communication, morphogenesis, angiogenesis and possibly neurotransmission (Angst et al. 2001).

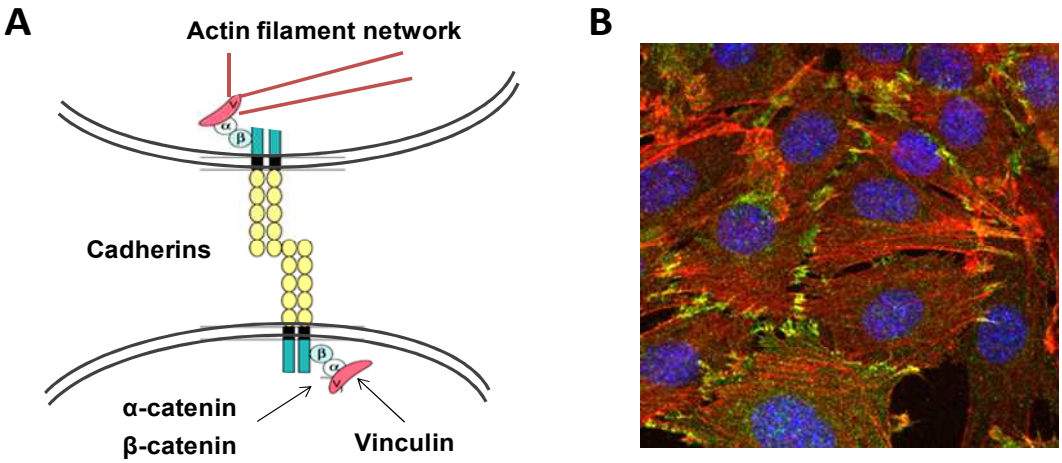

Figure I-9. Cadherin-mediated cell-cell adhesion *(A) Cadherin homodimers interact with homodimers of the neighbouring cell. Intracellularly they bind to their cytoplasmic partners a-catenin, b-catenin, vinculin, and to the actin filament network. Adapted from (Angst et al. 2001). (B) Cell-cell junctions in C2C12 myoblast monolayer culture. N-cadherin is labeled in green, actin in red and nuclei in blue.*

I.A.4. Signals provided by the extracellular matrix

It is increasingly accepted that cell fate depend on the reciprocal and dynamic interactions of cells with their microenvironment that includes stimuli defined by neighboring cells, soluble bioactive molecules and ECM (Hynes 2009). Importantly, the ECM provides to the cells a variety of physical and biochemical signals that are now recognized as being key parameters in regulating numerous cellular processes (adhesion, differentiation etc.). In Figure I-10, different types of stimuli provided by the ECM are described.

Biochemical stimuli are provided to the cells by the surrounding biological molecules that compose the matrix (fibrillar proteins, glycoproteins, proteoglycans/glycosaminoglycans) and by soluble molecules that are often presented in a matrix-bound form (GF, cytokines, chemokines…) (Fig. I-10). For this type of interactions, composition and conformation of the ECM molecules is of the utmost importance (Garcia et al. 1999). Growth factors can bind to the ECM via the glycosaminoglycan side chains or the protein cores of matrix molecules. ECM binding of growth factors can have a number of biological consequences. By limiting diffusion, the ECM provides a local store of growth factor that persists after growth factor production has ceased; for example, matrix bound FGF is degraded more slowly than free FGF, prolonging its activity (Klagsbrun 1990).

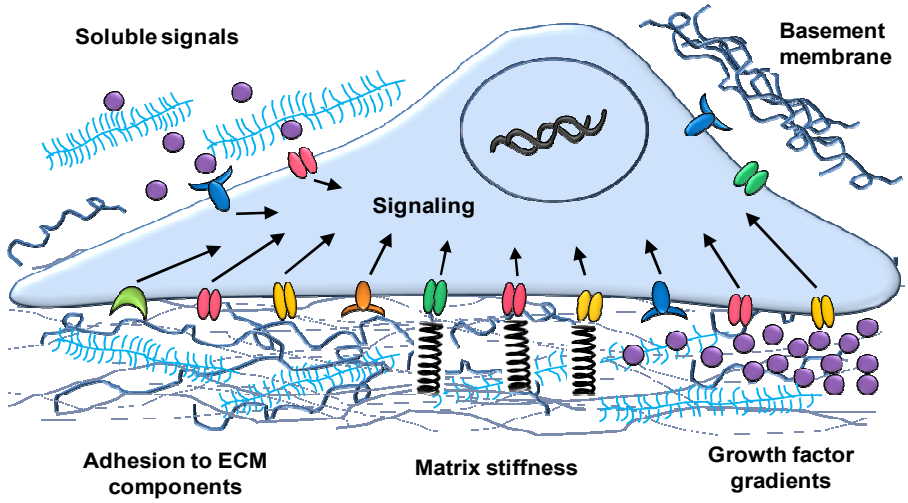

Figure I-10. Different types of stimuli provided by the extracellular matrix (ECM). *Biochemical stimuli are provided to the cells by the surrounding biological molecules: polysaccharides and proteins. ECM composition and cross-linking of the ECM proteins determines the stiffness of the matrix, thus providing mechanical stimuli. Bioactive molecules such as growth factors can form gradients and promote cell directional migration.*

Young's modulus (E), or elastic modulus, is defined as a ratio between a shear stress over a relative deformation for a homogeneous and isotropic sample. It serves a measure of the stiffness of an elastic material and is used to characterize materials, but also the live tissues. Stiffness of

the tissues can vary from around 1 kPa (liver) to several tens of GPa for bone (Nemir and West 2010) (Fig. I-11). The difference between the values is due to the properties of tissue-specific ECM. The stiffest tissues, ligaments and bone, contain a big quantity of collagen fibers that can be cross-linked together and significantly stiffen the matrix. As for bone, the high stiffness of its matrix is explained by the presence of inorganic hydroxyapatite.

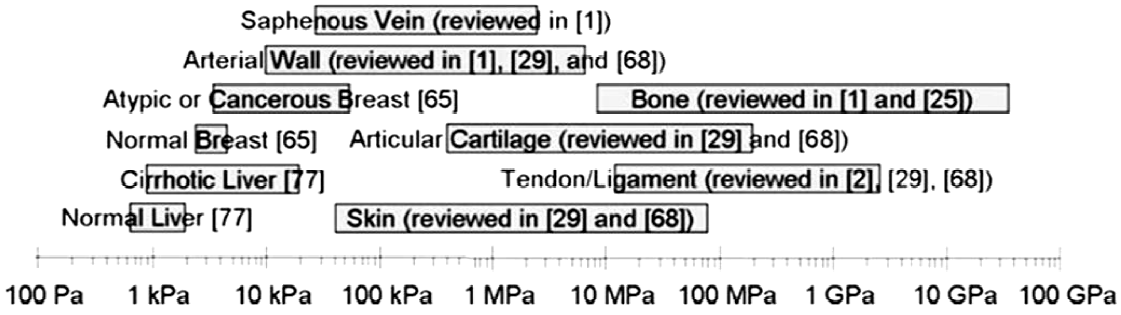

Figure I-11. Range of stiffness found in selected human tissues. *Stiffness of the tissues can vary from around 1 kPa (liver) to several tens of GPa for bone. Adapted from (Nemir and West 2010).*

Cells are mechano-sensors known to transduce a mechanical signal into a biochemical signal, or *vice versa*, via integrins, that exhibit conformational changes in response to mechanical stimuli (Hynes 2002). Many cell types are sensitive to the mechanical properties of the underlying substrate and respond by increasing their adhesion, spreading and proliferation (Mammoto and Ingber 2009; Schaller 2010).

Another important characteristic of the ECM is its **topography**. Matrix is a more or less porous structure that determines the diffusion of nutritive elements and cell migration. The matrix is constantly remodeled by the cells. Matrix proteases are secreted to degrade the matrix proteins when the matrix is too dense, and new matrix proteins are secreted when the matrix is too sparse. Matrix remodeling process is involved in inflammation, tissue repair, and metastatic cancer invasion (Wolf and Friedl 2011). Topographical features are important for the function of many tissues. For instance, muscle fibers must be aligned to allow proper contraction. Stem cell niche is a microenvironment where stem cells are found, and which regulates their fate (Schofield 1978; Scadden 2006).

The native ECM is also a highly anisotropic environment. **Gradients** in biochemical (growth factors, cytokines, etc.) and physical signals (matrix porosity, stiffness, etc.) are often implicated in cellular processes such as adhesion, proliferation, migration, and differentiation (Kucia et al. 2005; Lortat-Jacob 2009).

I.A.5. Transition

Until recently, cell biologists commonly used glass substrates or tissue culture polystyrene substrates to investigate cellular behavior *in vitro*. However, such substrate is very different from the natural cell environment and may significantly affect cell behavior *in vitro* compared to *in vivo* conditions (Fig. I-12).

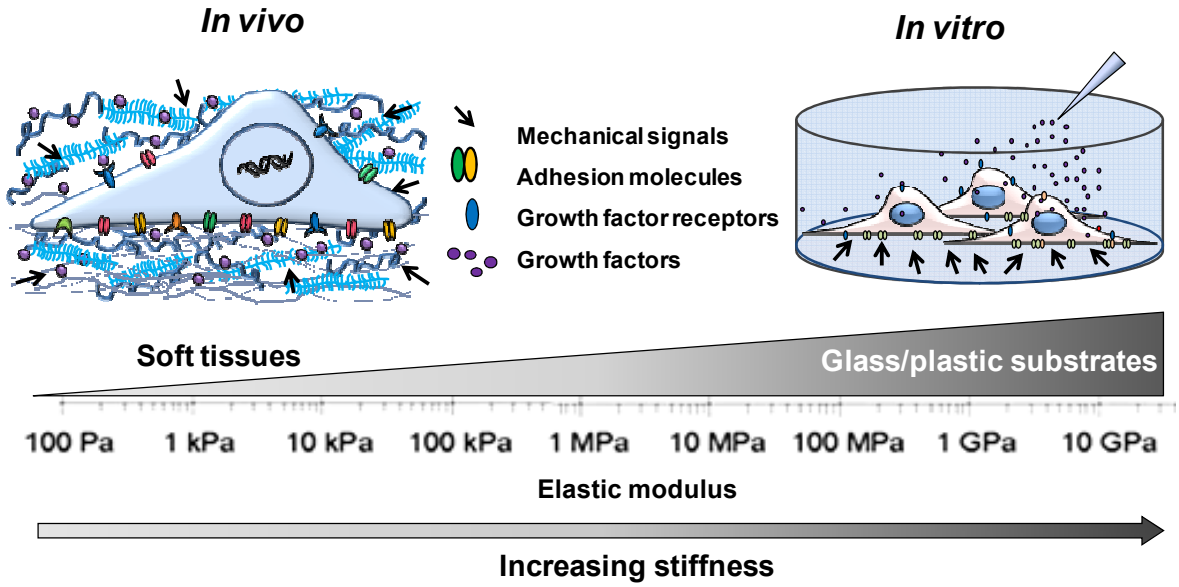

Figure I-12. Differences in cell microenvironment in vivo and in vitro. *In vivo, cells are surrounded by the extracellular matrix that provides a variety of physical and biochemical signals. In vitro, cells are usually cultured on substrates which are much stiffer than the majority of tissues. Bioactive molecules such as growth factors are delivered in solution, while in vivo, they are usually presented in a matrix-bound form.*

Nowadays, classical approaches of cell biology and biochemistry are being completed by interdisciplinary approaches aiming to reproduce natural cell environment, in order to study the cells in more physiological conditions. The development of micro- and nanotechnologies makes it possible to create substrates and matrices that precisely mimic the natural cell environment. Engineered artificial matrices find numerous applications in the field of implantable materials, but also in tissue engineering and drug delivery.

In the next part, we will present biomaterials and how their properties can be modulated to render them more physiologically relevant, but also to intentionally control cellular processes, for applications in tissue engineering field. We will particularly focus on layer-by-layer (LbL) films and on the possibilities that such films offer for the development of substrates with well-controlled mechanical and biochemical properties.

I.B. BIOMATERIALS AND TISSUE ENGINEERING

I.B.1. Definitions and historical overview

Below are two definitions of biomaterials from 1986 and 1992 Biomaterials Consensus Conferences:

"A nonviable material used in a medical device, intended to interact with biological systems."(1st Biomaterials Consensus Conference, 1986, Chester, UK)

"A material intended to interface with biological systems to evaluate, treat, augment, or replace any tissue, organ, or function of the body." (2nd Biomaterials Consensus Conference, 1992, Chester, UK)

As we can notice, the definitions remain partially similar, but the second describes a much larger field of application. Indeed, biomaterials first appeared mostly to replace a part of the human body (prosthesis). The main requirements for this type of materials were its ***mechanical properties*** and ability to partially replace the function of the missing body part.

The first surgical acts making use of biomaterials took place in the end of 19th century. In 1891, Pr Glück produced an ivory ball and socket joint that he fixed to bone with nickel-plated screws. Metal-on-metal total hip replacements were first implanted in the 1930s. In 1938, Smith-Petersen introduced a vitallium mould arthroplasty using a cup made from cobalt-chrome alloy (Smith-Petersen 1948). Integration of the material into human body now required it to be ***biocompatible***, i.e. nontoxic and not promoting the immune response.

Today, this type of biomaterials is largely used for many medical applications (Fig. I-13). For example, hollow polymeric tubes replace the blood vessels; metals are used to fix fractures and cements to fill the bone defects. Artificial skin saves the lives of burned people. Many of us have contact lens or dental implants. However, for certain applications, integration of biomaterials with surrounding native tissue may be limited or tissue repair is not satisfying yet (Castner and Ratner 2002).

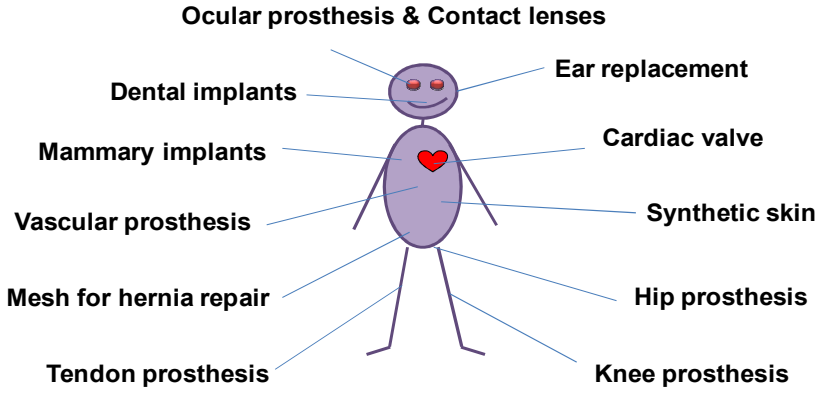

Figure I-13. Overview of the different applications of biomaterials. *Implants and prosthesis can be made of metals, ceramics, and polymers (synthetic or natural).*

But as the progress goes on, biomaterials evolve too. Development of materials science, in particular polymer science, opened new possibilities for biomaterials design. Numerous aspects of biomaterials properties are known to affect cell behavior, so all of these parameters must be carefully adjusted, as they have an influence on subsequent cellular and tissue events. Among them, materials surface chemistry and morphology, bulk and mechanical properties, degradability and biochemical functionality. Changing the surface roughness and porosity of the bone implant improves osteointegration (Hertz and Bruce 2007; Le Guehennec et al. 2007). Contact lenses with good wettability are generally better tolerated by the eye (Gorbet and Postnikoff 2013; Tighe 2013). Molecules promoting cell adhesion have already been included in the design of biomaterials, as many cells need to adhere for their survival (Newham and Humphries 1996). More recently, other parameters like mechanical properties of biomaterials (Pelham and Wang 1997; Engler et al. 2006) and delivery of growth factors (Fan et al. 2007) have also been taken into account.

Such modification of biomaterial's surface properties allows not only to improve the biocompatibility and integration, but also to induce a specific response of the host tissue. These materials are ***biomimetic*** and/or ***bioactive***. By combining different technologies, it is now possible to create materials with precise control over their multiple properties, making them ***multifunctional***.

The scheme of biomaterials evolution, from just biocompatible to those presenting additional functionalities, is shown in Figure I-14.

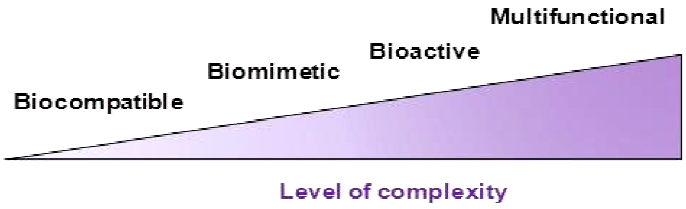

Figure I-14. Evolution in the development of biomaterials. *Integration of the material into human body requires it to be biocompatible. Modification of biomaterial's surface properties allows to improve its biocompatibility and integration, but also to induce a specific response of the host tissue -- these are biomimetic materials. "Smart" bioactive and multifunctional materials participating in tissue regeneration by stimulating specific cell response or responding to changes of physiological conditions are currently being designed.*

Such materials find numerous applications in the field of implantable (Hubbell 1999) and injectable (Li et al. 2012a) materials, for targeted and controlled drug delivery (Matsusaki and Akashi 2009), but also for tissue engineering, and as model materials for fundamental studies of cell-material interaction (Lutolf and Hubbell 2005; Stevens and George 2005). In this work, we focus on the design of biomaterials for tissue engineering applications.

Tissue engineering applies the principles of biology and engineering to the development of functional substitutes for damaged tissue, and was pioneered about 20 years ago by Langer and colleagues from MIT (Langer and Vacanti 1993). Current tissue engineering approach consists in combining cells, engineering and biomaterials to improve the biological functions of damaged tissues (bone, cartilage, blood vessels, skin…) or replace them.

The cells can be taken from the patient or from a compatible person, and biomaterials will support cell attachment and provide them with the appropriate cues to organize the cells into a tissue- or organ-like structure. Here, biomaterials must be "smart" enough to stimulate the regeneration of tissues by controlling and guiding the cells (Lutolf and Hubbell 2005; Stevens and George 2005). Such tissues and organs, grown from a patient's own cells, should avoid the problems of immune rejection. In addition to having a therapeutic application, tissue engineering can have diagnostic applications: the tissue is made *in vitro* and used for testing drug metabolism and toxicity. Besides *in vitro* tissue engineering, the tissue formation and repair may take place *in vivo* due to achievements in the field of injectable hydrogels, which allow *in vivo* delivery in a minimally invasive way (Li et al. 2012a).

I.B.2. Current challenges in tissue engineering

The progress in the field of artificial scaffolds for tissue engineering has been impressive. For instance, cartilage (DeNovo® NT Natural Tissue Grafts) and skin (Apligraf™) are already on the market, and engineered bladders are in clinical trials (Atala et al. 2006).

These tissues all consist of a small number of cell types, and/or are either flat planes or hollow constructs, that are relatively simple to produce. However, organs such as the lungs, heart, liver, and kidneys are bigger, they contain dozens of cell types, and they have a complex architecture with a network of blood vessels.

Production of such constructs is still challenging and requires collaboration of scientists from different domains like cell biology, chemistry, materials and polymer science. The main challenges are represented in Figure I-15 and include stem cell amplification, biomaterial's design and tissue maturation/organization.

I.B.2.a) Cell amplification

Stem cells can be defined as unspecialized cells that can renew their own population while also supplying cells that differentiate into the specialized tissue-specific cell types (Janzen and Scadden 2006). (Fig I-16). This presents important issues for tissue engineering, as stem cells can be amplified *in vitro* and differentiated into a specific cell type.

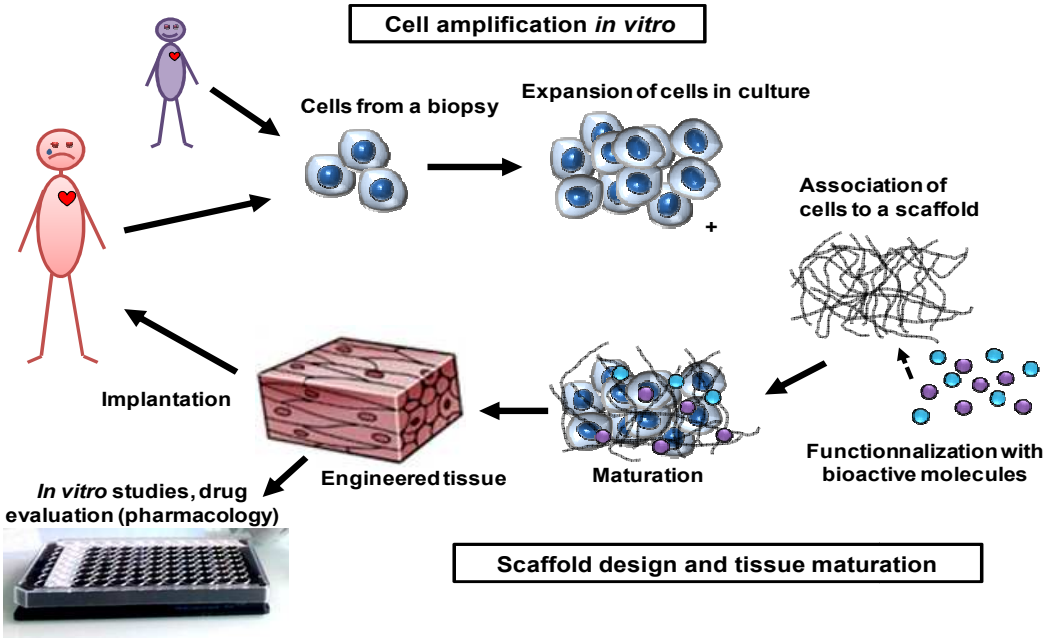

Figure I-15. Current challenges in tissue engineering. *A goal of biomaterials scientists is to design the scaffolds in which cells can adhere, proliferate, differentiate and synthesize their own matrix to regenerate tissues. Adult tissues contain very few stem cells, so they have to be amplified in vitro in order to get enough cells to fill the scaffold. As most of the tissues are 3D structures, spatio-temporal properties of the materials are very important to properly organize the tissue.*

In vivo, stem cells are localized in "niches" — specific tissue compartments that regulate their involvement in tissue regeneration and repair (Schofield 1978). Without this niche, stem cells generally have limited function and, when cultured *in vitro*, they may rapidly lose their stem properties. For this reason scientists are studying the various components of the niche, in order to identify the important factors regulating stem cells *in vivo* (Lutolf et al. 2009b). Reproducing such factors *in vitro* by the mean of biomimetic materials will allow the precise control of stem cell fate.

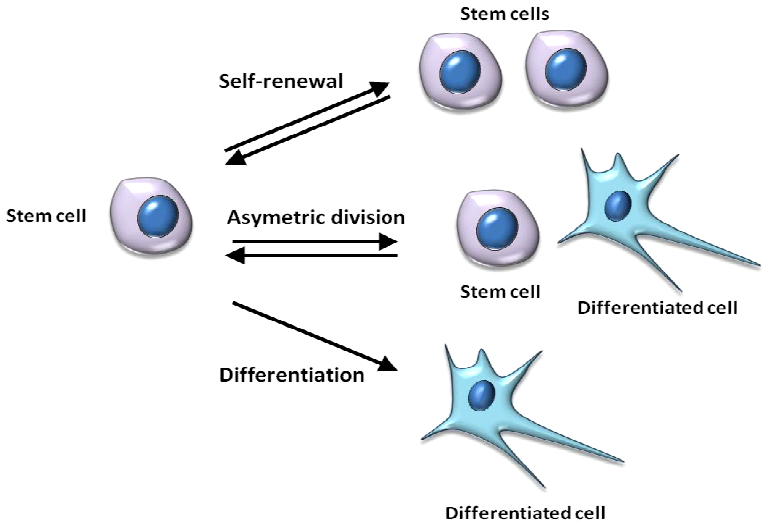

Figure I-16. Possible fates of stem cells. *Stem cells are unspecialized cells that can renew their own population and/or supply cells that differentiate into the specialized tissue-specific cell types.*

I.B.2.b) Scaffold design and tissue maturation

Probably the most important step is to design biocompatible scaffolds in which cells can adhere, proliferate, differentiate and synthesize their own matrix to regenerate tissue (Lutolf and Hubbell 2005; Stevens and George 2005). Stiff polymeric materials can be employed as scaffolds when mechanical strength is needed, and soft hydrogels can be used for soft tissues (Drury and Mooney 2003).

As described in the part ***I.A. The cell environment,*** cells respond to a variety of stimuli, including biochemical, topographical and mechanical signals originating from their *in vivo* micro-environment. All of these parameters must be carefully adjusted by appropriate biomaterial's design, to provide it with new functionalities and induce a specific cell response.

As most of the tissues are 3D structures, spatio-temporal properties of the materials are very important to properly organize the tissue. Last but not least, developing tissues may require supply of different bioactive molecules or presentation of different adhesive ligands at different times of tissue maturation. This will require controlled molecule delivery by the biomaterial.

Different approaches for the biomaterials design are described below.

I.B.3. Design of synthetic and natural polymeric materials for tissue engineering (Review article 1)

In a first part of my PhD thesis, we made a literature review of synthetic and natural polymeric materials with well-characterized and tunable mechanical and biochemical properties. We also highlighted how biochemical signals can be presented to the cells by combining them with these biomaterials (Gribova et al. 2011).

Here, we will give a short overview of the different types of polymeric materials, including synthetic and natural ones. For more details, the reader is referred to the review article that can be found in Annexe I. We will also present important aspects that have to be taken into account when designing biomimetic materials.

Polymeric 2D substrates and 3D scaffolds made of either synthetic or natural polymers are the most widely used in the development of biomimetic and bioactive materials due to their high versatility: they can be tuned in terms of composition, rate of degradation, mechanical and chemical properties, and thus offer a wide range of possibilities to control cellular processes and tissue regeneration. If surface properties of the materials are taken into consideration, they are viewed as 2D materials and cells will interact with them from their basal side. In the case of hydrogels, that are usually uses as 3D materials, their bulk (volumic) properties are important, as

the cells embedded in the hydrogel are fully surrounded by it. Accumulating evidence has shown that there is a significant difference in cell behavior in 2D and 3D microenvironments (Lee et al. 2008). However, it is important to underline that both 2D and 3D studies of cell/material interactions are required, as these studies provide complementary information. For instance, 2D materials may serve for cell amplification or for coating of other materials, while 3D materials are required for fabrication of thick tissue constructs.

Both synthetic and natural polymers present some advantages and drawbacks in terms of their applications as biomimetic substrates. The main properties of natural and synthetic materials, from 2D to 3D materials are summarized in Table I-1.

Synthetic polymers can be tuned in terms of composition, rate of degradation, mechanical and chemical properties. Among the mostly employed synthetic polymers, polyacrylamide (PA) gels, polydimethylsiloxane (PDMS) and polyelectrolyte multilayer films made of synthetic polyelectrolytes, which are used as 2D culture substrates; crosslinked networks of poly(ethylene glycol) (PEG) are often used as a 3D hydrogels with cells embedded inside. The coupling strategy is often required for synthetic materials, which do not have any natural interaction with biomolecules (Table I-1).

PROPERTIES	NATURAL	SYNTHETIC
2D → 3D	PEM-films Fibrin Collagen Hyaluronan Alginate IPN Composites	PA gels PDMS PEG
Physical/mechanical properties	- Viscoelasticity - Physical architecture - Porosity (nm to µm scale) - Degradability (proteases)	- Pure elasticity - No physical architecture - Small porosity - Non biodegradabile (unless grafted with MMP peptides)
Biochemical properties	- Non specific interactions (electrostatic, H-bonds) - Specific (natural ligands)	- Inertness - Need grafting with ligands
Main disadvantage	- Difficulty to decouple mechanics and chemistry	- High swellability (for PEG) - Stability over time
Main advantage	-Biomimetism (natural presence in tissues)	-Versatility of the control

Table I-1. Summary of the main properties of natural and synthetic materials, from 2D to 3D materials, which are used in mechano-sensitivity studies. *This includes their physical/mechanical and biochemical properties. Their main disadvantages and advantages are also given. (Gribova et al. 2011).*

Natural polymers can be derived from animals (collagen, fibrin, chitosan) or from plants/algae (cellulose, alginate, agarose). They can be used as 2D or 3D hydrogels or as thin multilayer films. Multilayer films made by self-assembly of polypeptides and polysaccharides are emerging as a new class of materials with well-defined properties.

Natural polymers have the advantage of being components of native ECM matrices, i.e. they provide compositional uniqueness such as stimulating a specific cellular response and serve both as mechanical as well as biochemical signals (Table I-1). Natural materials are also particularly interesting due to their unique structural properties. Their nano- and microstructure are similar to that of native tissues in terms of functional groups and structural organization. Interestingly, natural materials exhibit low and high affinity interactions with ECM proteins and growth factors, and can be favorably exploited to present these stimuli. Conversely, natural materials have also some drawbacks. They are more fragile, polydisperse, and not always pure. In addition, their natural bioactivity makes it difficult to fully decouple the effect of mechanics from chemistry.

The modifications of synthetic and natural polymeric materials are summarized in Figure I-17 and include modifications of mechanical and biochemical properties, as well as control of material's topography and degradability.

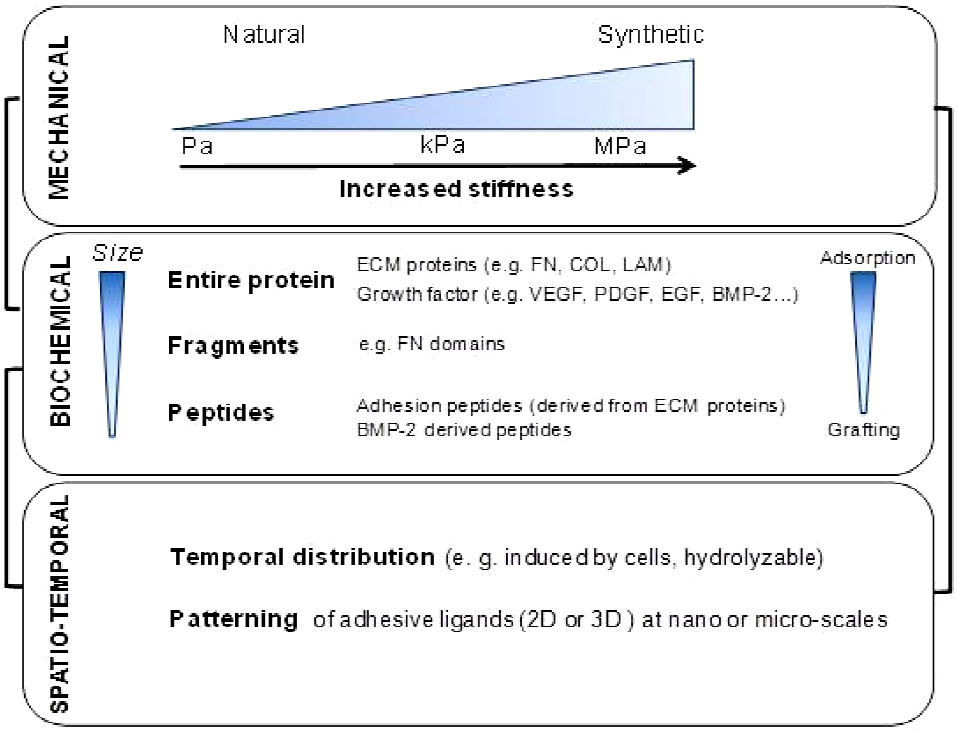

Figure I-17. Scheme presenting the three major ways of control of the cell microenvironment using engineered materials *: mechanical properties with typical variation in elastic moduli from few Pa to tens of MPa; biochemical properties obtained by adsorbing or grafting entire proteins, protein fragments as well as peptides; spatio-temporal properties, e.g. hydrolytically degradable materials or controlled presentation of ligands by nano and micropatterning. Adapted from (Gribova et al. 2011).*

I.B.3.a) Control of mechanical properties

Cells are mechanosensors known to transduce a mechanical signal into a biochemical signal, or *vice versa,* via specific proteins that are known to play a key role in this process. Among those are integrins, transmembrane receptors that exhibit conformational changes in response to mechanical stimuli (Ingber 1991). Many cell types are sensitive to the mechanical properties of the underlying substrate and respond by increasing their adherence, spreading and proliferation. How the cells exert forces on to a substrate and how these forces are transmitted at the molecular level inside the cells are key questions, which have been and are still being investigated. This has also led to the development of new materials that would, ideally, make possible independent variation in mechanical and biochemical properties.

In a pioneer study by Discher's group, decoupling (or independent adjusting) of the mechanical and chemical properties has been achieved, using model synthetic gels such as polyacrylamide gels grafted with COL at increasing densities.(Engler et al. 2004a). The same group showed that altering polyacrylamide gel stiffness made possible MSC differentiation into neurons on soft PA gels, bone cells on stiff gels that mimicked collagenous bone (Engler et al. 2006) and myoblasts for gels of intermediate stiffness (Fig. I-18).

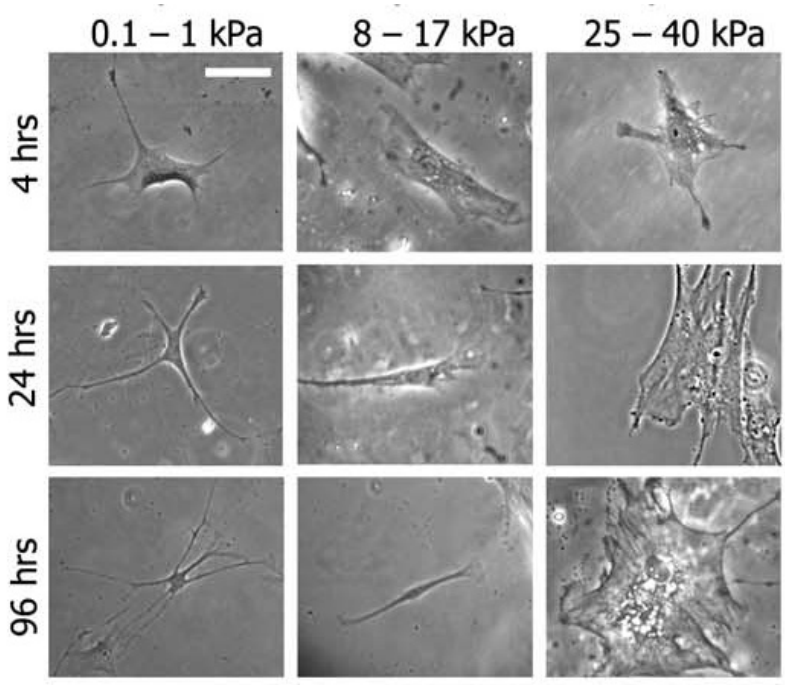

Figure I-18. Effect of substrate stiffness on cell differentiation. *Human MSCs (hMSCs) exhibit neurogenic, myogenic and osteogenic phenotypes when cultured on collagen-coated polyacrylamide (PAAm) hydrogels with stiffness similar to brain (0.1–1 kPa), muscle (8–17 kPa) and nascent bone (>34 kPa), respectively. From (Engler et al. 2006).*

Other types of synthetic and natural polymeric materials with controlled mechanical properties have been developed, such as PEG hydrogels (Lutolf et al. 2003b; Gilbert et al. 2010; Moon et al. 2010), PDMS (Trappmann et al. 2012), alginate gels of varying stiffness (Genes et al. 2004; Boontheekul et al. 2007), hyaluronan (Young and Engler 2011), and polyelectrolyte multilayer films made of biopolymers (Ren et al. 2008). Recently, Post and coworkers (Boonen et al. 2009) showed, using PA gels of varying rigidity and protein coating that proliferation was influenced only by rigidity, whereas differentiation was influenced both by rigidity and by protein coating.

For more detailed presentation of materials used for mechanosensitivity studies, the reader is referred to the review article in Annexe I (Gribova et al. 2011). An overview of the main strategies used to modulate mechanical properties of synthetic and natural materials is given in Figure I-19. Although a full decoupling of mechanical and chemical properties is the ideal goal, this is in fact very difficult to achieve, because many of the cross-linking strategies are based on a chemical modification of the material. In addition, in case of synthetic materials that usually provide poor adhesive properties, biochemical ligands have to be added by grafting it or by adsorbing it. This also involves modification of materials surface.

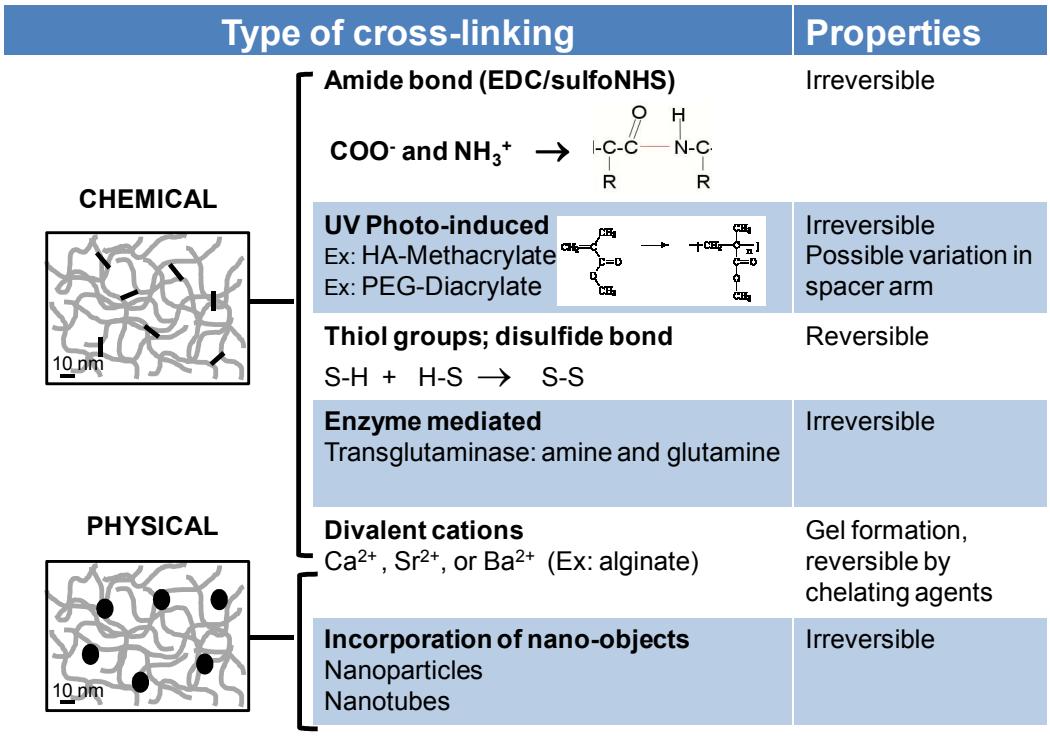

Figure I-19. Overview of the main strategies used to modulate mechanical properties of synthetic and natural materials. *The methods are essentially based on chemical cross-linking, as physical cross-linking is so far barely employed for biomaterials. We have classified cross-linking by divalent cations at the border between chemical and physical cross-linking, as addition of cations changes the film chemistry but, at the same time, induces a physical gelation (no need for covalent crosslinks). From (Gribova et al. 2011).*

I.B.3.b) Biochemical functionalization

Synthetic polymers such as PA, PDMS and PEG hydrogels are poorly adhesive due to their inertness and lack of specific adhesive motifs. In the case of natural materials, although cells may possess specific receptors recognizing the material, their naturally high hydration and softness often render them poorly adhesive, too. Such low cell attachment has been observed for hydrated polysaccharides such as HA and ALG. Researchers have thus designed strategies for giving additional biochemical functionality to different types of synthetic and natural materials.

Biochemical functionalization has up to now mostly focused on improving cell adhesion by presenting cell **adhesive ligands**: adsorbing cell adhesion proteins (collagen, fibronectin, etc.) or grafting adhesion peptides. Recent developments have begun, however, to present not only adhesive signals, but also signals triggered by **growth factors** (FGF, BMP, VEGF, NGF), which modulate cell proliferation and differentiation. Notably, presentation of a biochemical signal from a biomaterial in a "matrix-bound" manner is important for mimicking physiological conditions, as many bioactive molecules are bound to the ECM matrix *in vivo*.

Two main strategies of functionalization are usually employed: **covalent coupling** or **physical adsorption** of the bioactive molecules (entire proteins, fragments or peptides) (Fig. I-20). The coupling strategy is often required for synthetic materials, which do not have any natural interaction with biomolecules. Conversely, natural materials, that exhibit low and high affinity interactions with ECM proteins and growth factors can be favorably exploited to present these stimuli. Summary of the main functionalization strategies for 2D and 3D materials are shown in Figure I-20. Examples of molecules usually immobilized are also indicated.

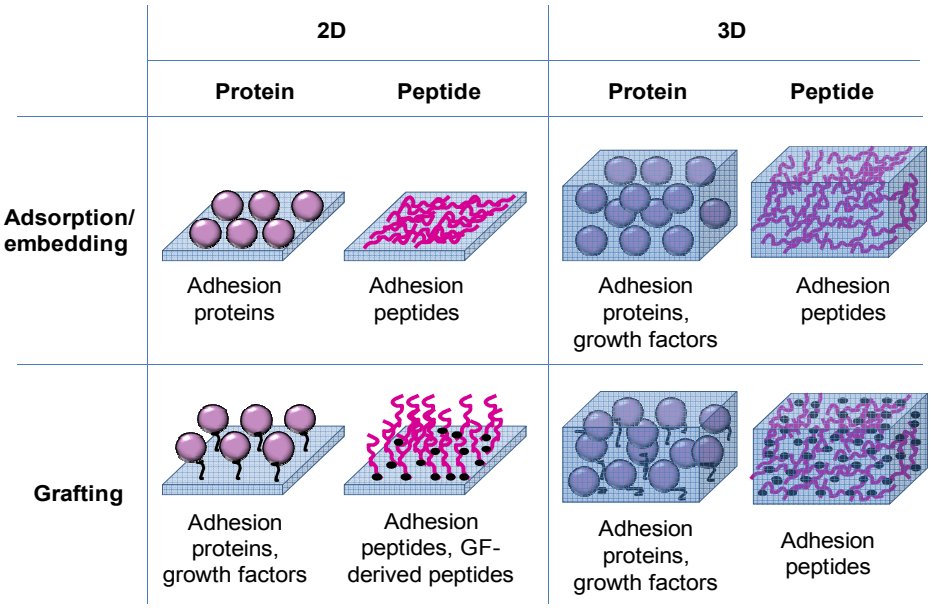

Figure I-20. Main strategies for immobilization of bioactive molecules on 2D substrates or in 3D hydrogels. *The molecules can be either grafted or attached by adsorbtion due to specific or non-specific interactions. Covalent links are represented as black dots or black dashes.*

The advantage of grafting is that it provides good control of surface composition, a stable link and limits release of the functional group into the culture medium. Covalent grafting of short bioactive peptides or protein fragments is more frequently performed than that of full length ECM proteins, which is more difficult to handle. A key issue is to preserve the bioactivity of the grafted molecules, especially entire proteins, because their activity depends on their 3D conformation. Grafting of proteins/peptides can be performed in solution on hydrogel components, prior to formation of the 2D or 3D biomaterial, or directly at the surface of a biomaterial.

Proteins can be coupled to polymers via their amino-groups using sulfo-SANPAH **(**sulfosuccinimidyl 6-(4'-azido-2'-nitrophenylamino)hexanoate**)** cross-linker (Kandow et al. 2007) or carbodiimide coupling chemistry (Grabarek and Gergely 1990). Thiol groups of proteins or peptides are another target for coupling reactions. They can be grafted to polymers via maleimide linker molecules or reacted with acrylates under defined experimental conditions (Hern and Hubbell 1998; Mann et al. 2001; Peyton et al. 2006).

For more detailed presentation of the grafting strategies, as well as for more details on adsorption and grafting of **full-length molecules** including ECM proteins and GF, the reader is referred to the review article in Annex I (Gribova et al. 2011). Here, we will focus on the recent developments that use **bioactive peptides** and are aimed to achieve a better selectivity, i.e. target a particular cell surface receptor and thus create substrates/scaffolds with well-defined properties.

In entire proteins (ECM proteins or GF), many different active sequences can be recognized by cell surface receptors. Using a bioactive fragment makes it possible to enhance the specificity of the interaction and to target one particular partner to better control cellular processes. Such short sequences are, however, often less bioactive than entire molecules, because of the loss of active site spatial architecture, which is defined by protein's specific conformation (Ruoslahti 1996a).

The most common grafted peptides are derived from ECM proteins, mainly fibronectin (Petrie et al. 2008), collagen (Lutolf et al. 2003c; Trappmann et al. 2012), laminin (Hozumi et al. 2009; Urushibata et al. 2010), and vitronectin (Doran et al. 2010) (Table I-2). More recently, peptides that exhibit protease sensitive sequences have been grafted to the biomaterials, to add biodegradability in response to cellular activity (Raeber et al. 2007).

The **tripeptide sequence RGD** is very popular, as it is present in many ECM proteins, including fibronectin, vitronectin, fibrinogen, von Willebrand factor, thrombospondin, laminin, osteopontin, bone sialoprotein, and some collagen isoforms (Ruoslahti 1996a). It binds to a wide range of integrin receptors in a non-selective manner, i.e. is not specific to a given integrin

receptor. The literature about the various forms of RGD-containing peptides is rich and the reader is referred to more specialized reviews (Ruoslahti 1996b; Hersel et al. 2003).

The recent developments are aimed to achieve a better selectivity, i.e. target a particular cell surface receptor, integrin or non-integrin. To this end, several strategies have been investigated: i) synthesis of cyclic RGD peptides (Hsiong et al. 2009), or RGD peptide multimerization to enhance avidity with particular cell adhesion receptors (Suzuki et al. 2003b), ii) using a more selective peptide sequence that is not based on RGD but contains other key sequences or iii) associating two different bioactive peptides derived from the same ECM protein (Benoit and Anseth 2005) or from different ones (Rezania and Healy 1999) (Table I-2). Thus, collagen-mimetic peptides (Picart et al. 2005; Reyes et al. 2007; Weber et al. 2007), laminin-derived peptides (Hozumi et al. 2009; Werner et al. 2009; Urushibata et al. 2010) and fibronectin-derived peptides or fragments (Benoit and Anseth 2005; Petrie et al. 2008) are increasingly used for their higher selectivity.

ECM protein	PEPTIDE SEQUENCE	TARGETED RECEPTOR	CELL TYPE	REFERENCE
COLLAGEN (Type I)	GFOGER	Integrin $\alpha2\beta1$	Primary bone marrow stromal cells	Reyes et al., *Biomaterials* 2007 [94]
	CGPKGDRGDAGPKGA	Integrins $\alpha1\beta1$, $\alpha2\beta1$	Primary human osteoblasts	Picart et al. *Adv. Funct. Mater*. 2005 [76]
	DGEA	Integrin $\alpha2\beta1$	MIN6 b-cells	Weber Biomaterials 2007 [95]
FIBRONECTIN (FN)	rhFN fragment FNIII7-10 (with RGD and PHSRN)	Interin $\alpha5\beta1$	Osteoblasts	Petrie et al., *Biomaterials* 2008 [83]
			hESC, hMSC	Doran et al., *Biomaterials* 2010 [75]
	RGD-PHSRN	Inegrin $\alpha5\beta1$	Osteoblasts	Benoit and Anseth, *Biomaterials* 2005 [90]
LAMININ (LAM)	RKRLQVQLSIRT ($\alpha1$ chain LAM-1, LG4 module)	Syndecans	Human dermal fibroblasts, neural PC12	Hozumi et al, *Biomaterials* 2009 [83]
	ATLQLQEGRLHFXFDLGKGR, X: Nle ($\alpha1$ chain, LG4 module)	Integrin $\alpha2\beta1$		
	PPFLMLLKGSTRFC (LG3 of the lam-5 $\alpha3$ chain)	Integrins $\alpha6\beta4$, $\alpha3\beta1$	Oral keratinocyte cell line, TERT-2 OKF-6	Werner et al., *Biomaterials* 2009 [96]
	IKLLI (LAM $\alpha1$ chain)	Integrin $\alpha3\beta1$	MIN6 b-cells	Weber, *Biomaterials* 2007 [95]
	IKVAV (LAM $\alpha1$ chain)	110 kDa laminin receptor protein		
	YIGSR (LAM $\beta1$ chain)	67 kDa laminin receptor protein		
VITRONECTIN	rhVN, N-terminal Somatomedin B and RGD domain	Plasminogen activator inhibitor-1 (PAI-1), integrin receptors	hESC	Doran et al., *Biomaterials* 2010 [75]
Multiple ECM proteins	RGDSPC	Integrins	MC3T3-E1 preostoblasts	Zouani et al., *Biomaterials* 2010 [100]
			Human foreskin fibroblasts	Lutolf et al., *Nature Biotech*. 2003 [84]
	G4RGDSP	Integrins	Primary human bone marrow stromal cells, MC3T3-E1 preosteoblasts, mouse bone marrow stromal D1 cell line	Hsiong et al. *Tissue Eng*. 2009 [92]
	Cyclic RGD: G4CRGDSPC	Integrin receptors, higher specifity for $\alpha V\beta3$		
	MMP-sensitive peptide: Ac-GCRD-GPQGIWGQ-DRCG-NH2	Matrix metalloproteinases (MMP)	Human foreskin fibroblasts	Lutolf et al. *Nature Biotech* 2003 [84]

Table I-2. Peptide sequences used for targeting adhesion receptors of four main ECM proteins. *The targeted receptor (or receptor family) as well as cell type used in the study are indicated. From (Gribova et al. 2011).*

We are now progressively entering a new era, where peptides with higher specificity, high biological activity as well as targeting other receptors than integrins are being designed (Table I-2). Indeed, it is now acknowledged that besides integrin receptors, other families of receptors including syndecans (Bellin et al. 2009) and growth factor receptors play key roles in early cellular events. Recent developments also include grafting the peptide sequence of growth factors, mostly bone morphogenetic protein 2 (BMP-2) derived peptides (Saito et al. 2003; Saito et al. 2005; He et al. 2008b; Zouani et al. 2010; Moore et al. 2011; Zouani et al. 2013), but also BMP-9 (Marquis et al. 2008; Bergeron et al. 2009).

I.B.3.c) Micro- and nanotopography

Material's topographical cues are recognized to be a powerful tool for regulating cell functions. Scaffold architecture and substrate topography affect cell adhesion, migration, growth and differentiation (Curtis and Wilkinson 1997; Rapier et al. 2010; Nikkhah et al. 2012).

Surfaces of biomaterials are rarely flat at a molecular level: such surfaces only occur after cleavage of single crystal materials in particular planes. Thus, most of the materials possess "natural" or "accidental" topography. Otherwise, nano- and micropatterned surfaces and scaffold can be intentionally fabricated, in order to investigate the effects of spatial parameters on the cellular processes and/or to control these processes. Many micro- and nanofabrication processes have been employed to control substrate characteristics in both 2D and 3D environments. Among them, optical and electron beam lithography, soft lithography, and printing technologies (Falconnet et al. 2006; Khademhosseini et al. 2006). Patterning on biomaterial surfaces and scaffold topography are important for fundamental studies of cell–cell and cell–substrate interactions, and in biomedical applications such as tissue engineering, cell-based biosensors and diagnostic devices. For instance, in the field of tissue engineering, one of the main issues is to engineer scaffold with controlled architecture, to obtain a properly organized tissue *in vitro*.

The basic principle of materials patterning is to create controlled spatial arrangement of surface chemical and physical properties. Gradients are also being developed and used to understand how cells respond to these cues (Burdick et al. 2004; Kutejova et al. 2009).

"Physical" topography includes surface roughness (Lampin et al. 1997; Fan et al. 2002; Chung et al. 2003; Yamakawa et al. 2003; Ranella et al. 2010), stiffness patterns (Chien et al. 2009), grooved substrates (Teixeira et al. 2003; Monge et al. 2012), and micropillars (Ghibaudo et al., Biophys J, 2009). Several examples of physical topography are shown in Figure I-21.

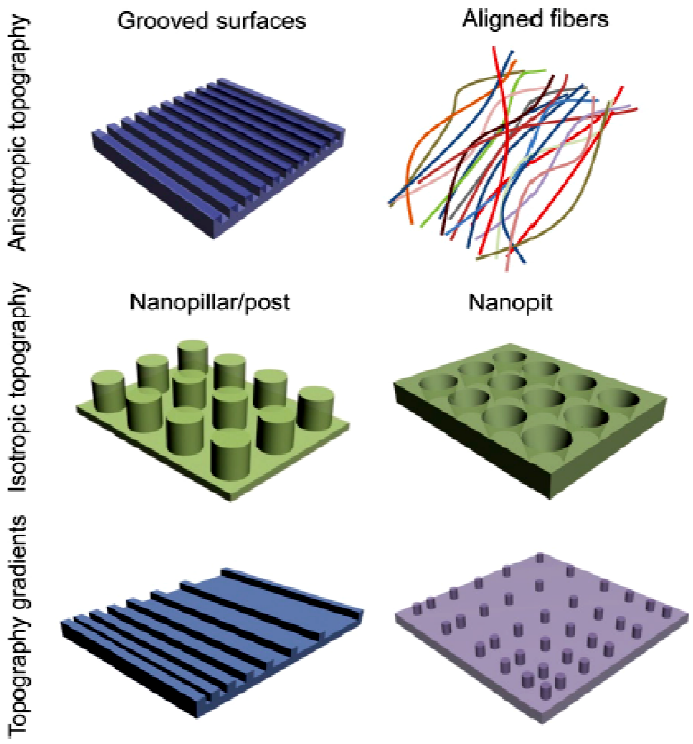

Figure I-21. Nanotopographically defined in vitro cell culture tools. *Schematics of three representative nanotopography geometries commonly used as cell culture substrates. Anisotropic topographies are directionally dependent, in this case, providing cues along a single axis. Isotropic topographies are uniform in all directions, providing cues along multiple axes. Topography gradients provide cues through gradual changes in physical features (e.g., groove spacing) along a particular direction (Kim JBC 2012)*

Chemical/biochemical topography includes micro- or nano- patterned domains of adhesive molecules (Gallant et al. 2002; Wu et al. 2010). Chemical patterning achieved using spatial cell-adhesive molecular organization regulates different cell functions depending on its scale. Micropatterned surfaces can be used to orient the cells or to control their geometry. The geometry of the cell adhesive microenvironment was shown to direct cell surface polarization, internal organization and division (Thery and Bornens 2006; Thery et al. 2006; Pitaval et al. 2010). Moreover, cell adhesive surface geometry may also regulate cell differentiation (Guvendiren and Burdick 2010). Nanopatterned topographical features such as matrix ligand density (Ranucci and Moghe 2001; Berg et al. 2004) are important for cell adhesion, proliferation, and differentiation.

The porosity of the material must be considered when designing 3D scaffolds, as it is an important parameter for cell migration within the scaffolds. Also, porosity can greatly influence cell adhesion and interaction with the matrix components. Depending on the porosity of the scaffold, the cells can sometimes behave as on 2D surfaces, i.e. interact with their environment only from the basal side even in 3D materials (Figure I-22).

Another important parameter of 3D materials is degradability. It was shown that the degradation rate of hydrogel can influence differentiation of mesenchymal stem cells (Khetan et al. 2013). In this study, MSCs within HA hydrogels of equivalent elastic moduli with different cell-mediated degradation exhibited variable degrees of cell spreading and favoured either osteogenesis or adipogenesis.

In case of dense polymeric hydrogels, specific peptide crosslinkers may be introduced into the polymer network. Such peptides are cleavable by secreted metalloproteases and allow cell progression through the gels (Lutolf et al. 2003a). Invasion and growth of different cell types in engineered synthetic ECM may be controlled selectively by the choice of protease specific peptide crosslinker (Bracher et al. 2013).

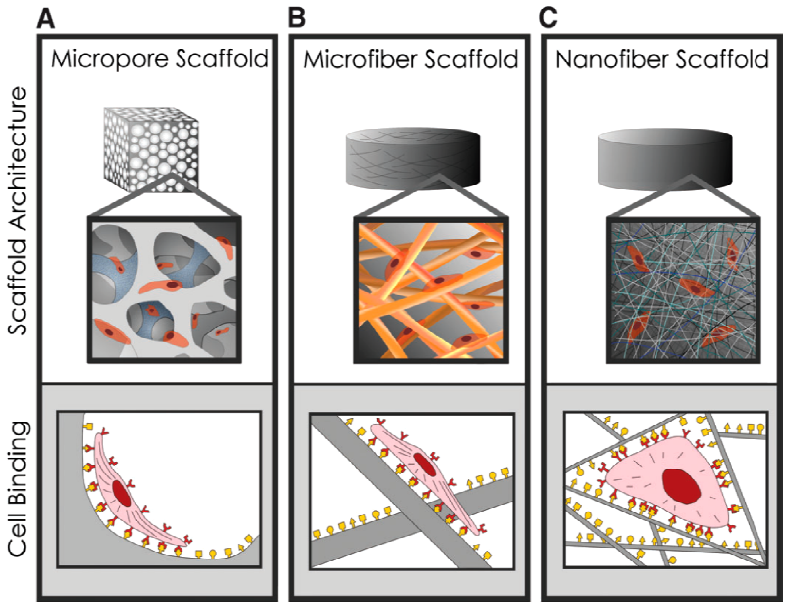

Figure I-22. Scaffold architecture affects cell binding and spreading. *(A and B) Cells binding to scaffolds with microscale architectures flatten and spread as if cultured on flat surfaces. (C) Scaffolds with nanoscale architectures have larger surface areas to adsorb proteins, presenting many more binding sites to cell membrane receptors. Adapted from (Stevens and George 2005).*

I.B.3.d) Multifunctional materials and high-throughput screening

Control over biochemical and mechanical properties of materials in a spatially-controlled manner has to be achieved to investigate the respective role of each parameter, as well as to produce innovative multifunctional biomaterials (Huebsch and Mooney 2009). New methodological developments emerging from soft lithography and microfluidics can be combined to further develop these 2D and 3D biomaterials (Lutolf et al. 2009). Importantly, these technologies can be applied to a wide range of polymeric biomaterials currently in use.

This will make it possible to incorporate spatial control which is crucial for developing complex microenvironments (Marklein and Burdick 2010).

Current technologies also allow creation of *in vitro* platforms for high-throughput screening (Ranga and Lutolf 2012). Example of the creation of such platform is shown in Figure I-23. Recently, PEG microgels with modular dimension, stiffness and surface-tethered biomolecule composition were created by combining hydrogel engineering with droplet microfluidic technology (Allazetta et al. 2013). Such approach allows to combine multiple gel components and additives, providing opportunity to generate a huge diversity of microgels for cell manipulation and screening applications.

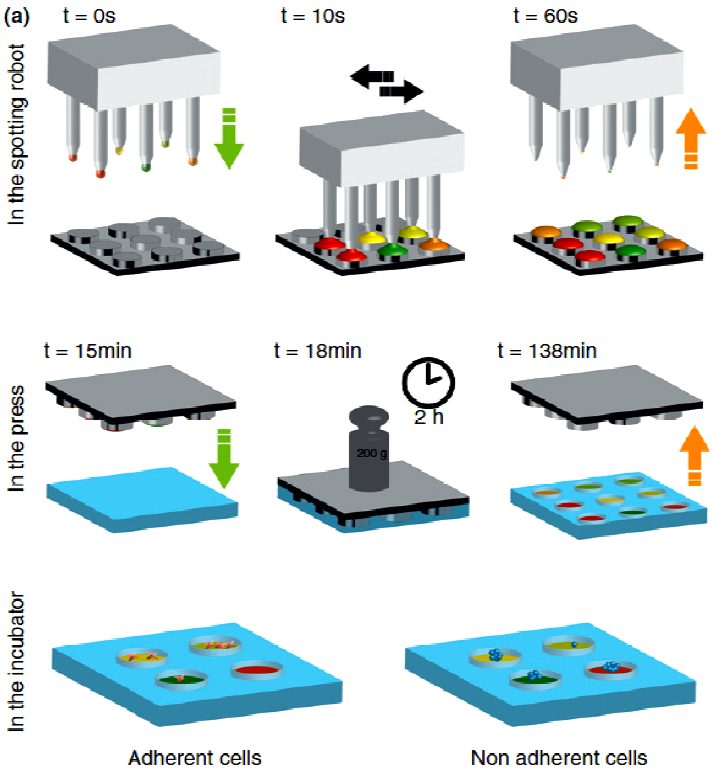

Figure I-23. Example of a state-of-the-art combinatorial biomaterial microarray to probe biochemical and biophysical niche effectors. *A DNA spotter with solid pins can be used to spot different protein solutions on micropillars of a microfabricated silicon stamp. The printed stamps can be pressed against a thin (partially crosslinked) hydrogel layer. Finally, the stamp can be demolded to obtain an artificial niche microarray suitable for both adherent or nonadherent stem cells. Adapted from (Ranga and Lutolf 2012).*

I.B.4. Polyelectrolyte multilayer (PEM) films as thin polymeric substrates (Review article 2)

Layer-by-layer (LbL) films offer numerous possibilities for the development of substrates with well-controlled mechanical and biochemical properties, and have become a highly studied class of biomaterials over the past decade. The technique was introduced in the early 1990s by Decher, Möhwald, and Lvov (Decher et al. 1992; Lvov et al. 1994; Decher 1997) and has attracted an increasing number of researchers in recent years due to its high versatility and wide range of advantages they present for biomedical applications. Polyelectrolyte multilayer (PEM) films are currently emerging as a new kind of biomaterials coating that can be used to guide cell fate (Boudou et al. 2010; Leguen et al. 2007; Detzel et al. 2011). They can be used either as 2D materials for investigation of cellular behavior on defined substrates, or for coating of 3D constructs such as implants or tissue engineering scaffolds.

The reader is referred to our recent review article (Gribova et al. 2012) (please find in Annexe II) for detailed presentation of different possibilities of controlling cell behavior by means of PEM film composition, presentation of bioactive molecules and modulation of mechanical properties. Here, we will present a principle of LbL deposition method and give a short description of the main techniques used for the control of PEM film properties.

The LbL deposition method consists in the alternate adsorption of polyelectrolytes that self-organize on the material's surface, leading to the formation of polyelectrolyte multilayer (PEM) films (Fig. I-24) (Decher et al. 1992; Lvov et al. 1994; Decher 1997).

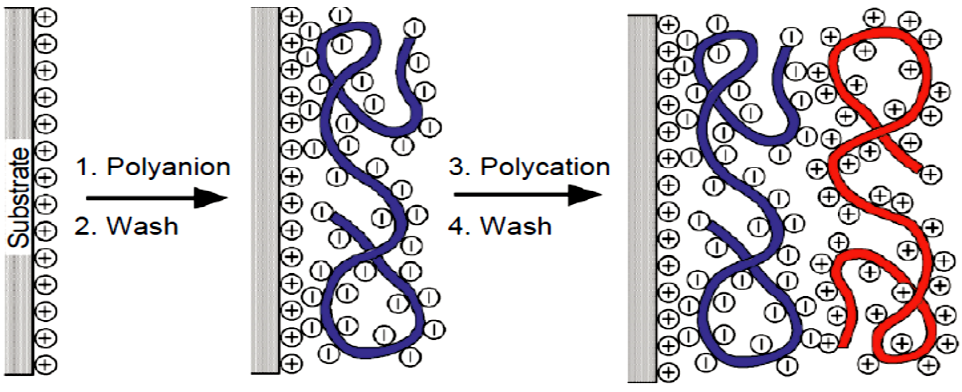

Figure I-24. Schematic of layer-by-layer deposition method. *Simplified molecular picture of the first two adsorption steps, depicting film deposition starting with a positively charged substrate. Adapted from (Decher 1997).*

The method was originally developed by dipping the substrate (e.g. glass slides or silicon wafer) in the different polyelectrolyte solutions. The analogous method consists in depositing the solutions on the substrate by spin-coating (Fig. I-25a and b). Polyelectrolytes can also be deposited onto small particles, which can be further dissolved to give hollow microcapsules, that can be used for drug delivery and many other applications (Antipov and Sukhorukov 2004; Becker et al. 2010), or onto viable cells (Wilson et al. 2011). Such coating helped to maintain cell viability and function upon *in vivo* transplantation. Nowadays, other methods of LbL assembly are being developed, such as film deposition by spraying (Fig. I-25c), which is much faster and easier to adapt at an industrial level (Izquierdo et al. 2005; Schaaf et al. 2012).

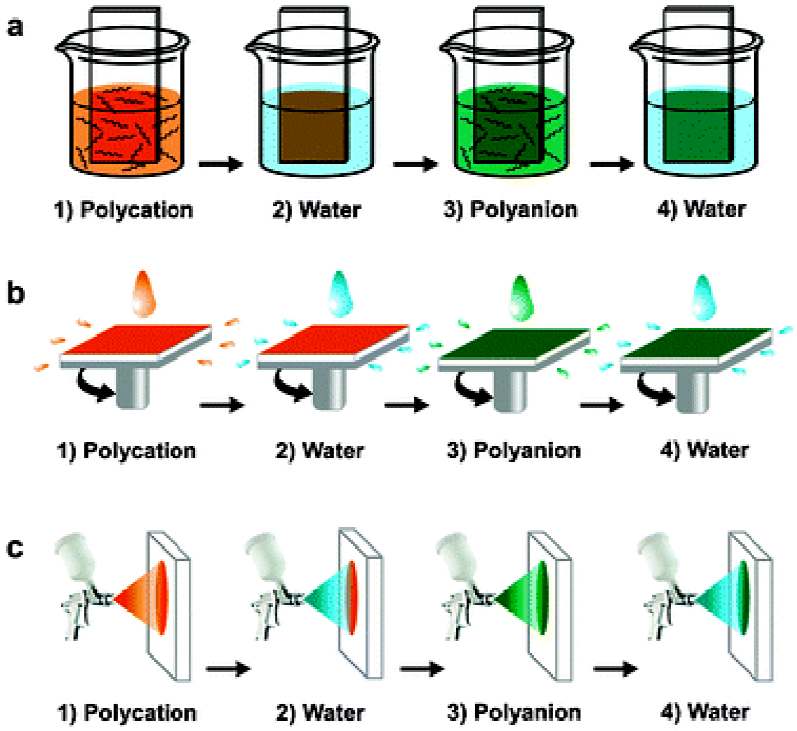

Figure I-25. Construction of layer-by-layer assemblies using different deposition techniques. *(a) by the dipping method. (b) by spin coating a solution onto the substrate . (c) by spraying. From (Li et al. 2012b).*

The procedure of LbL deposition is relatively simple and versatile, as it is possible to modulate film growth and internal structure by choosing the nature of polyelectrolytes and assembly parameters such as pH and ionic strength (Shiratori and Rubner 2000). PEM film fabrication can be performed under mild conditions in an aqueous environment, which is a great advantage when using biopolymers and bioactive molecules, which are often very sensitive molecules and can easily lose their properties if using harsh chemistry. Also, films can be either stratified or can exhibit some interdiffusion, which makes it possible to use them either as barriers (Garza et al. 2005) or as compartments for the loading of bioactive molecules (Crouzier

et al. 2009). Importantly, as will be shown below, PEM films appear highly suitable for immobilization of biomolecules with preserved bioactivity.

Besides polyelectrolytes, other types of components can be assembled using LbL method, among them proteins (Johansson et al. 2005; Zhang et al. 2005), nanoparticles, nanowires and carbon nanotubes (Jan and Kotov 2007; Srivastava and Kotov 2008; Zhang et al. 2012), and even living cells (Matsusaki et al. 2007; Chetprayoon et al. 2013).

Advantageously, multiple parameters of the films can be controlled. The films can be functionalized by bioactive molecules such as adhesive peptides (Berg et al. 2004; Picart et al. 2005; Tsai et al. 2009) and charged with growth factors for local delivery (Crouzier et al. 2009; Crouzier et al. 2011b; Macdonald et al. 2011; Shah et al. 2011; Guillot et al. 2013). The different strategies of incorporing bioactive molecules inside or on top of PEM films are summarized in Figure I-26. Biochemical stimuli may also be delivered in response to external stimuli. Cyto-mechanoresponsive surface that becomes cell-adhesive through exhibition of arginine-glycine-aspartic acid (RGD) adhesion peptides under stretching has been described (Davila et al. 2012). The controlled presentation of bioactive molecules to cells by means of the engineered PEM films offers a new tool for biophysicists who are interested in unraveling the subtle interplay between cell adhesion receptors, growth factor receptors and mechano-transduction pathways.

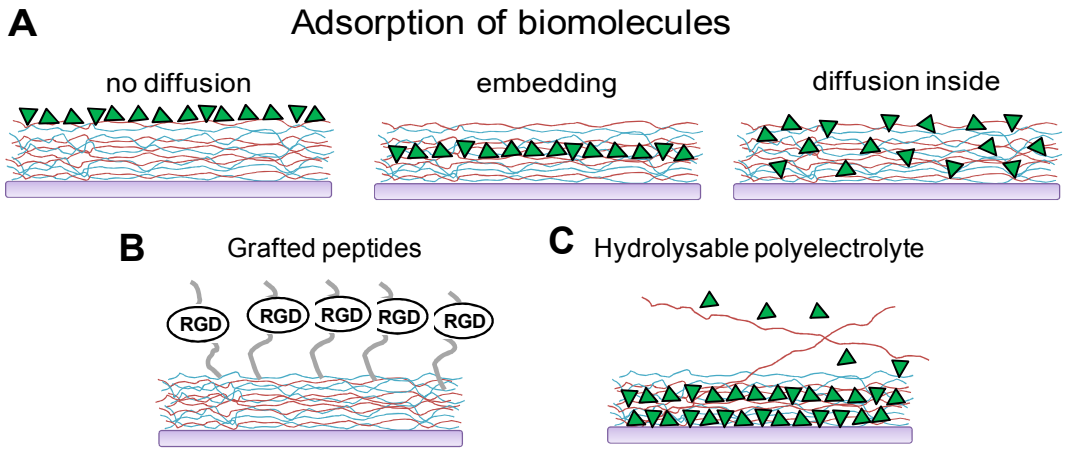

Figure I-26. Scheme representing different possibilities of incorporing bioactive molecules inside or on top of PEM films. *(A) Adsorption of the bioactive molecule can be achieved after film buildup or at a certain step during build up. In case of diffusion, the bioactive molecule can be loaded in the "bulk" of the film; (B) Very small molecules such as bioactive peptides can be grafted to one of the polyelectrolytes; (C) if one of the components is hydrolysable, then the bioactive molecule can be delivered in solution. From (Gribova et al. 2012)*

The mechanical properties of the films can be modulated by several techniques, including chemical cross-linking by carbodiimide (Richert et al. 2004) and photo-crosslinking using photosensitive derivatives of the polyelectrolytes (Olugebefola et al. 2006; Pozos Vazquez et al. 2009). The main techniques are shown in Figure I-27.

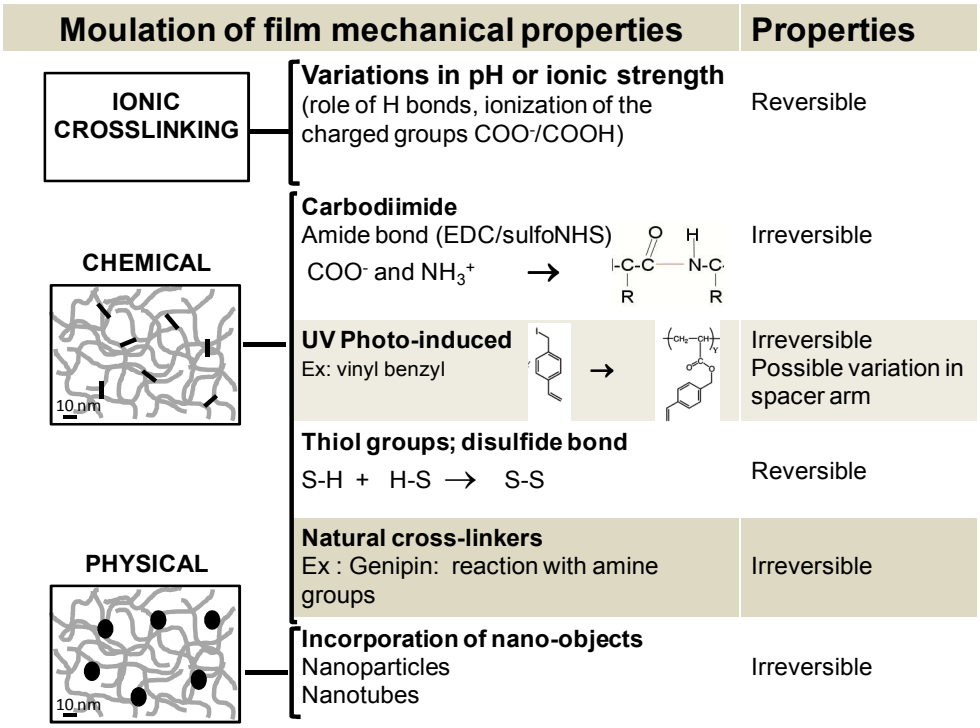

FIGURE I-27. Overview of the main strategies used to modulate mechanical properties of polyelectrolyte multilayer films. *The methods are essentially based on ionic cross-linking, chemical cross-linking and physical cross-linking. From (Gribova et al. 2012)*

The films can also be micropatterned to have (X-Y) architecture by combining with microfabrication techniques such as photolithography, microcontact printing or microfluidics (Berg et al. 2004; Chien et al. 2009; Monge et al. 2012; Almodovar et al. 2013). Furthermore, they can be deposited on various types of supporting materials, including metals, polymers and ceramics, which are already approved as implantable materials (Boudou et al. 2010). Interestingly, PEM films can also be fabricated as free-standing membranes (Ono and Decher 2006; Larkin et al. 2010; Pennakalathil and Hong 2011).

The versatility of PEM films makes of them a valuable tool for the studies of the effects of different stimuli, physical and biochemical, on cellular processes, and for the control of cell fate.

I.B.5. Transition

Skeletal muscle tissue engineering holds promise for the replacement of muscle due to an injury and for the treatment of muscle diseases, such as muscle dystrophies or paralysis, but is also required for pharmaceutical assays. To this end, complex environments with tunable mechanical and chemical/biochemical properties mimicking *in vivo* muscle ECM are needed.

In the next part, we will focus on skeletal muscle tissue engineering using skeletal muscle multipotent stem cells, and give an overview of the current approaches that exist for the *in vitro* 2D and 3D engineering of skeletal muscle.

The emphasis of this discussion will be on the applications of polyelectrolyte multilayer films for the control of the cell fate of skeletal myoblasts.

I.C. SKELETAL MUSCLE TISSUE ENGINEERING

Skeletal muscle is one of the major tissues of the human body. An average adult male is made up of 42% of skeletal muscle and an average adult female is made up of 36% (as a percentage of body mass). Skeletal muscle is anchored by tendons to bone and is used for locomotion.

Skeletal muscle tissue engineering holds promise for the replacement of muscle due to an injury following a surgery or due to a trauma and for the treatment of muscle diseases, such as muscle dystrophies or paralysis.

Engineered muscle tissues models are also required for pharmaceutical assays, in particular for the development and evaluation of drugs against diabetes, because skeletal muscle plays a crucial role in insulin-mediated uptake and disposal of blood glucose (Jensen et al. 2011). *In vitro* engineered models of diseased muscle may find use for the examination of the functional effects of patient-specific mutations.

Besides clinical and pharmacological applications, *in vitro* engineered muscle tissue models are also needed for fundamental studies. Structural, biochemical, cellular, and functional changes in skeletal muscle ECM contribute to the deterioration in muscle mechanical properties with aging (Kragstrup et al. 2011). Muscle atrophy is of particular interest to the spaceflight community, since the weightlessness results is a loss of as much as 30% of mass in some muscles (Narici and de Boer 2011)

Different fields that require engineered skeletal muscle tissues are schematically represented in Figure I-28.

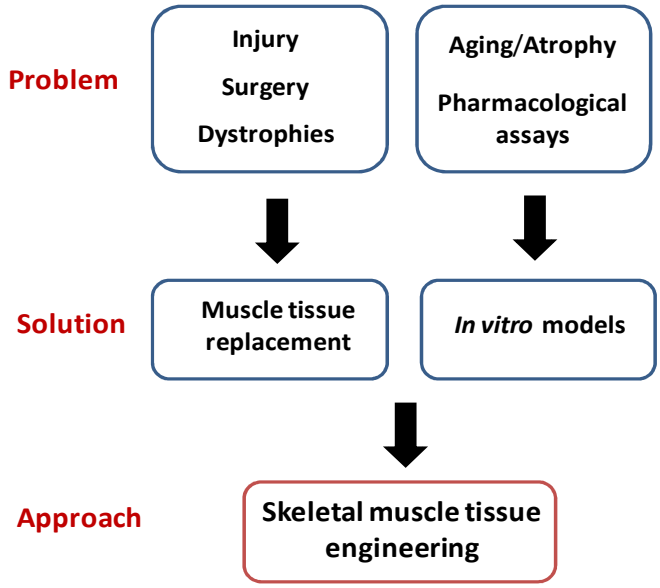

Figure I-28. Schematic representation of different fields that require engineered skeletal muscle tissues. *Skeletal muscle tissue engineering holds promise for the replacement of muscle due to an injury. They are also required as models for pharmaceutical assays and for fundamental studies.*

I.C.1. Skeletal muscle organization and extracellular matrix

The development of skeletal muscle is known to strongly depend on the interaction of muscle cells with their surrounding extracellular matrix. Mature skeletal muscle has a complex three-dimensional (3D) organization of aligned muscle fibers surrounded by ECM (Fig. I-29). The ECM of skeletal muscle consists of two distinct structures: the basement membrane delineating individual myofibres and interstitial connective tissue layers including endomysium, perimysium and epimysium which connect muscle fibers, fascicles, and bundles (Trotter and Purslow 1992; Gillies and Lieber 2011). The interstitial connective tissue consists mostly of collagens type I, III and V, and fibronectin (Light and Champion 1984).

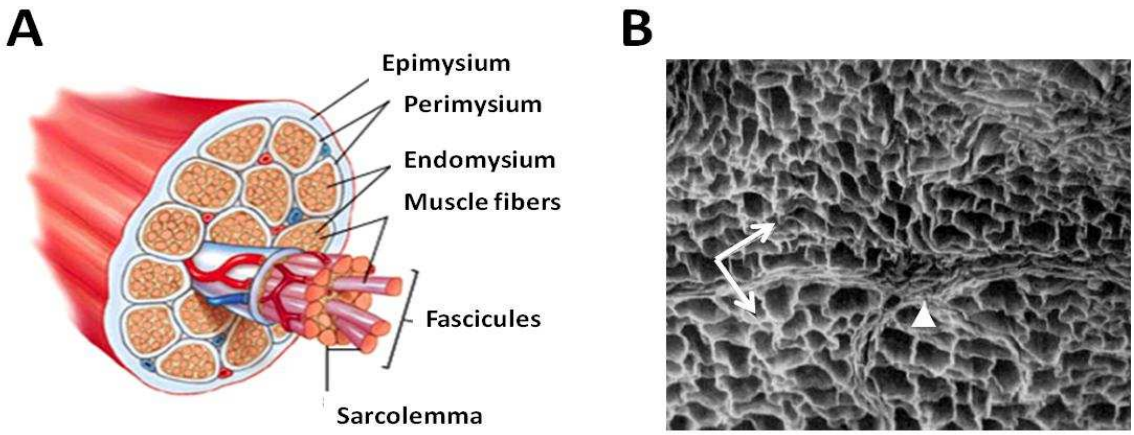

Figure I-29. Muscle organization and extracellular matrix*. (A) Schematic diagram of the gross organization of muscle tissue. Muscle ECM can be categorized as epimysium (surrounding the muscle), perimysium (surrounding muscle fascicles), and endomysium (surrounding muscle fibers). (B) Scanning electron microscopy of the collagenous endomysial network around muscle fibers Low power overview of the endomysium reveals an array of "tubes" into which muscle fibers insert (arrows) as well as a thickened area surrounding the fibers that is presumably perimysium (arrowhead). Adapted from (Trotter and Purslow 1992) and (Gillies and Lieber 2011).*

Skeletal muscle basement membrane (BM) contains collagen type IV, laminin and heparan sulfate proteoglycans and is composed of two layers: an internal, felt-like basal lamina (BL) directly linked to the plasma membrane, and an external, fibrillar reticular lamina (Sanes 2003) (Fig. I-30).

Basal lamina plays an important role in maintaining sarcolemma integrity, which is required for muscle function (Gillies and Lieber 2011; Hinds et al. 2011; Thorsteinsdottir et al. 2011). The laminin-α2 chain, which is a component of laminin-211, -221 and -213, is the predominant laminin alpha chain expressed in adult skeletal muscle (Miner and Yurchenco 2004). The laminin-α2 chain is involved in anchoring myofibers to the basal lamina, promoting muscle cell integrity and survival (Miyagoe et al. 1997).

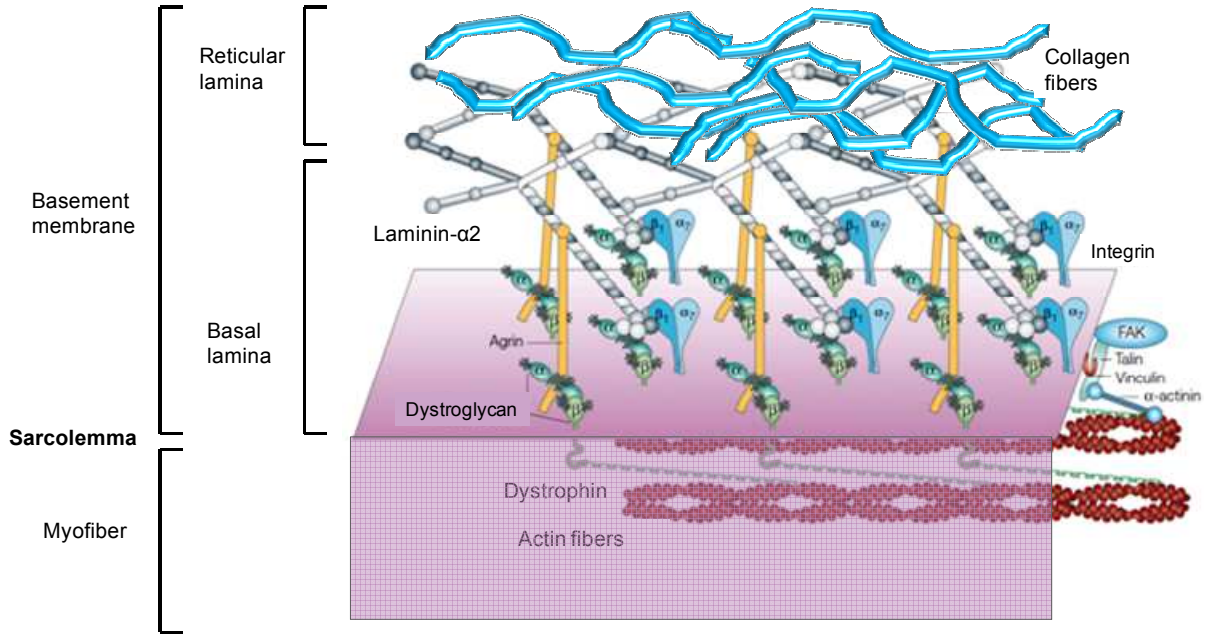

Figure I-30. Schematic presentation od skeletal muscle basement membrane. Skeletal muscle basement membrane (BM) surround myofibers and is composed of two layers: basal lamina and reticular lamina. *Basal lamina is linked to sarcolemma via dystroglycan and integrin interaction with laminin globular domains. Adapted from (Bezakova and Ruegg 2003).*

It was shown that, *in vivo*, local irradiation enhances the laminin content in the host muscle microenvironment and provides a better engraftment of human myoblasts (Silva-Barbosa et al. 2008). In another study, injection of laminin-111 restored the regeneration in *mdx* mice and protected muscle from exercise-induced damage (Rooney et al. 2009a; Rooney et al. 2009b). Laminin-111 (α1, β1, γ1), which is the most widely studied laminin isoform, is expressed during embryonic development, but is absent in postnatal normal or dystrophic skeletal muscle. Goudenege et al. showed that intramuscular injection of laminin-111 increased muscle strength and resistance in *mdx* mice and improved proliferation and drastically increased migration *in vitro* (Goudenege et al. 2010). These data provide combined *in vivo* and *in vitro* evidence that laminins may serve as a novel therapeutic agent for patients with congenital myopathies.

Among various cell surface receptors, integrins are the most characterized and have been shown to be crucial for skeletal muscle development and function (Mayer 2003; Perkins et al. 2010). For instance, β_3 integrin was found to be crucial for myogenic differentiation of C2C12 myoblasts, and to mediate satellite cell differentiation (Liu et al. 2011), while β_1-integrin, which is constitutively expressed in skeletal muscle, has earlier been shown to be dispensable to myogenesis (Hirsch et al. 1998).

Dystroglycan is a component of dystrophin-glycoprotein complex which, in muscle cells, forms an important receptor system for ECM (Gullberg and Ekblom 1995; Durbeej et al. 1998b).

Dystroglycan interaction with laminin-α2 chain was shown to be crucial for maintaining the integrity of sarcolemma and protecting muscle from damage (Matsumura et al. 1997; Durbeej et al. 1998b; Cohn et al. 2002; Han et al. 2009; Munoz et al. 2010). Mutations that lead to loss of dystroglycan result in the loss of other members of the dystrophin-glycoprotein complex along the sarcolemmal membrane, and deficits in most of these proteins cause muscular dystrophies (Durbeej et al. 1998a). Defects in the glycosylation of a-dystroglycan cause muscular dystrophies called dystroglycanopathies (Hewitt 2009; Muntoni et al. 2011).

In parallel, syndecans, transmembrane heparan sulfate proteoglycans, were shown to play an important role in myogenesis. Syndecan-3 and syndecan-4 specifically mark skeletal muscle satellite cells and are implicated in satellite cell maintenance and muscle regeneration (Cornelison et al. 2001). Syndecan-1 expression was found downregulated during myoblast differentiation (Larrain et al. 1997), and its overexpression inhibited the differentiation (Larrain et al. 1998; Velleman et al. 2004) and promoted proliferation (Velleman et al. 2007).

Besides biochemical properties, mechanical properties of the muscle ECM are important. Muscle is a soft tissue with Young's modulus around 10 kPa. In dystrophic muscle, a more fibrotic tissue and an increased rigidity of the diaphragm have been observed as compared to normal diaphragm (Stedman et al. 1991). This leads to an abnormal muscle function.

I.C.2. Skeletal muscle stem cells

Although several cell types may contribute to muscle repair *in vivo* or used for skeletal muscle generation *in vitro*, and among them ES cells, MSC or mesoangioblasts (for review, see Rossi et al. 2010), the canonical myogenic progenitor is the muscle satellite cell, characterized by its specific location on muscle fibers under the basal lamina (Fig. I-31) (Mauro 1961). These cells are multipotent and are now considered as a powerful source for the generation of several tissues. Besides skeletal muscle (Bischoff 1975), they are able to give smooth muscle (Le Ricousse-Roussanne et al. 2007), bone (Katagiri et al. 1994; Schindeler et al. 2009) or fat tissue (Teboul et al. 1995; Wada et al. 2002). This makes of them interesting candidates for engineering of muscle and other tissues.

I.C.2.a) Muscle regeneration

The process of muscle formation requires that satellite cells become activated, proliferate, differentiate, and fuse together to form multinucleated myotubes (Fig. I-32). For skeletal myoblasts, cell cycle arrest is necessary to undergo differentiation.

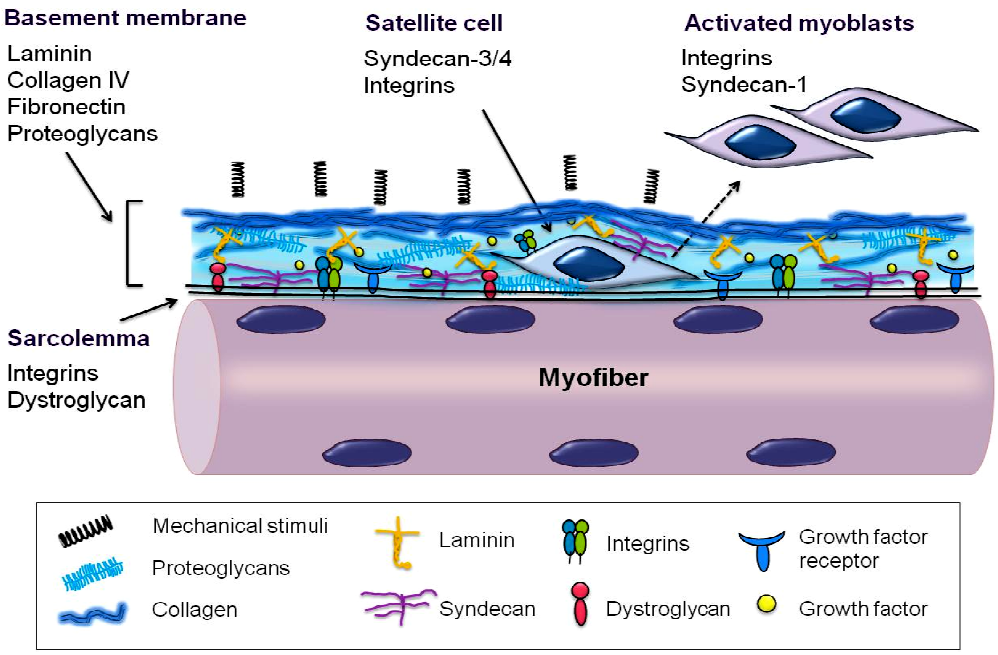

Figure I-31. Skeletal muscle microenvironment surrounding satellite cell. *Different components of the extracellular matrix, as well as cell surface receptors, are indicated. The elements are not drawn to scale.*

During myogenic differentiation, a highly ordered process of temporally separable events that begins with the expression of myogenic transcription factors such as myogenin, and is followed by cell cycle arrest takes place (Andres and Walsh 1996).

A major limitation to the study and clinical application of muscle progenitors is a rapid loss of their muscle stem cell properties once they are removed from their *in vivo* environment (Cosgrove et al. 2009). For this reason, myoblast cell lines are often used for the *in vitro* studies of myogenic differentiation. Several myoblast cell lines are available, such as C2C12 or MM14 mouse myoblasts. These cells are able to reproduce processes that take place during *in vivo* differentiation of skeletal muscle progenitors (Bach et al. 2004). C2C12 myoblasts are a subclone of C2 myoblasts (Yaffe and Saxel 1977) which differentiate in culture after serum removal (Blau et al. 1983).

Using cell lines presents, however, several disadvantages. Some studies show that the expression of surface markers, as well as response to environmental stimuli, is different for primary myoblasts and cell lines (Boontheekul et al. 2007; Grabowska et al. 2010). This indicate that one must be cautious in generalizing results obtained with cell lines to more physiologically relevant processes (e.g., tissue regeneration), as significantly different or even opposing results may be obtained for primary cells.

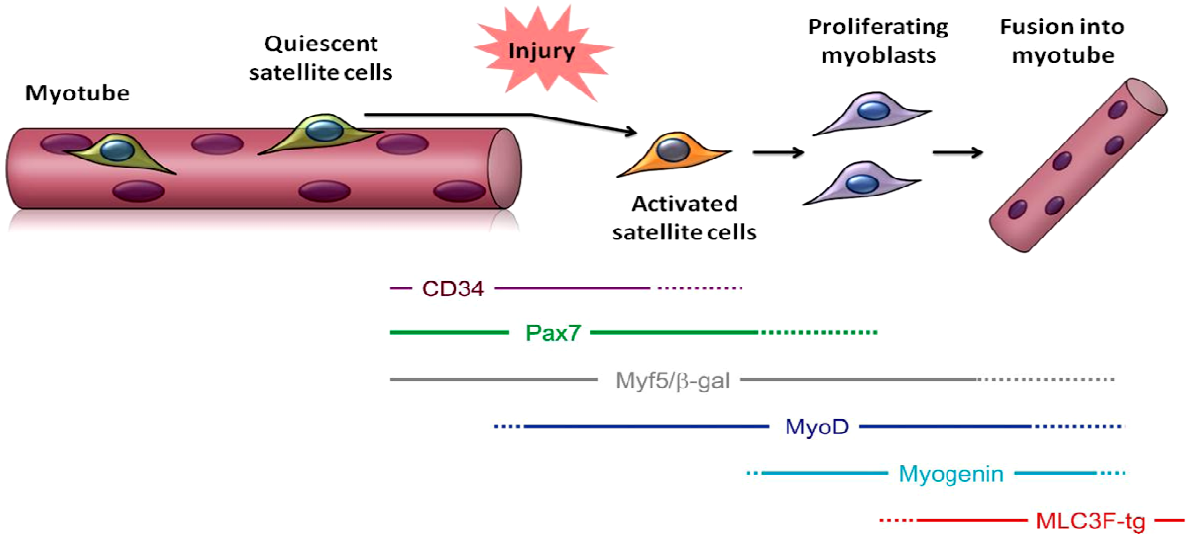

Figure I-32. Muscle regeneration. *The process of muscle formation requires that muscle precursor cells become activated, proliferate, differentiate, and fuse together to form multinucleated myotubes. Different markers (adapted from Zammit et al. 2006) expressed during this process are indicated.*

I.C.2.b) Osteogenic differentiation of muscle progenitors

Besides regeneration of skeletal muscle, muscle stem cells *in vivo* can also contribute to bone repair (Schindeler et al. 2009). *In vitro*, C2C12 myoblasts can undergo osteogenic differentiation when treated with BMP-2 growth factor (Katagiri et al. 1994).

Bone morphogenetic protein-2 (BMP-2) is a member of a large BMP family (Gautschi et al. 2007). BMP-2 through 7 and BMP-9 have the unique ability to induce differentiation of mesenchymal stem cells into osteoblasts (Chen et al. 1991; Yamaguchi et al. 1991; Hughes et al. 1995; Mayer et al. 1996). Recently, it was shown that BMP-4 plays a role in the control of skeletal muscle stem cell fate: it stimulated satellite cell division and inhibited myogenic differentiation, thus permitting population expansion (Ono et al. 2011).

BMP-2 has two epitopes referred to as the ‘‘wrist epitope’’ and the ‘‘knuckle epitope’’, forms dimers and bind to BMP receptors type I and type II on the cell surface to initiate their activities (Fig. I-33A). The cytoplasmic domain of the BMP-bound BMP receptor type II phosphorylates the BMP receptor type I (Wrana et al. 1994) (Fig. I-33B). The phosphorylated BMP receptor type I then phosphorylates Smad1, which is a cytoplasmic signaling molecule specifically mediating the action of BMP-2. Phosphorylated Smad1 moves into the nucleus and promotes osteoblastic differentiation by controlling the expression of several genes (Fig. I-33B). Differentiating osteoblasts have elevated alkaline phosphatase (ALP) activity and form bone tissue by promoting the secretion of bone matrix.

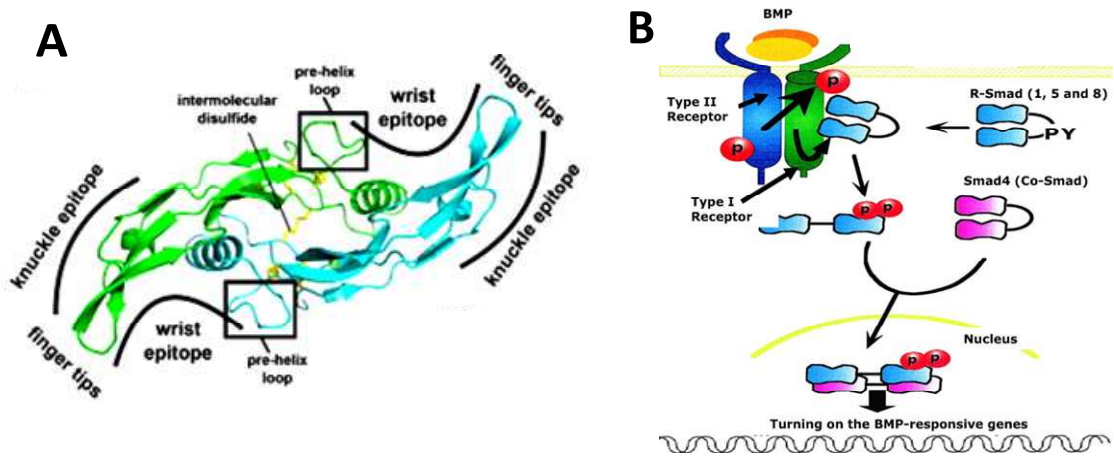

Figure I-33. Representation of BMP-2 with its epitopes and BMP signaling pathway. *(A) The butterfly-shaped architecture of the dimeric ligand resembles two hands assembled palm-to-palm. The convex side of the fingers termed knuckle epitope is the binding interface for type II receptors. Type I receptor binding occurs in the so-called wrist epitope formed by the concave side of the fingers and the palm of the ligand. Adapted from (Mueller and Nickel 2012).(B) BMP dimer binds to BMP receptor type II which recruits type I receptors, so that a hetero-tetramer is formed with two receptors of each type. The proximity of the receptors allows the type II receptor to phosphorylate the type I receptor. Activated type I receptors phosphorylate R-smads or receptor regulated Smads (Smad1/5/8) which form complex with Smad4. Activated Smad complexes regulate gene expression of several target genes.*

I.C.3. Current approaches for skeletal muscle tissue engineering

Therapeutic treatments for skeletal myopathies and loss of functional muscle require either the implantation of differentiated muscle tissue constructs (*in vitro* tissue engineering) or the injection of muscle-precursor cells into sites of disfunction for subsequent formation of new muscle tissue (*in vivo* tissue engineering). Both of these approaches require artificial matrices, either for cell amplification *in vitro* before injection, or for their differentiation and organization into functional muscle tissue. Current approaches in muscle tissue engineering include the development of 2D substrates with controlled stiffness and/or ligand presentation, as well as creation of 3D muscle tissue models. The main approaches are summarized in Figure I-34 and will be further described in more details.

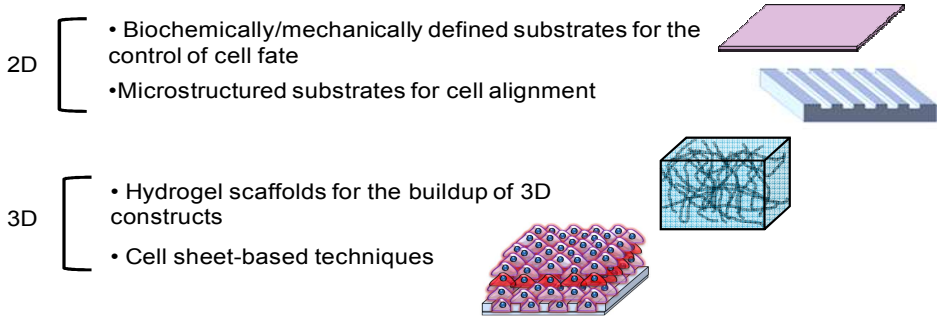

Figure I-34. Current approaches for skeletal muscle tissue engineering. *2D substrates with controlled stiffness, ligand presentation and topography are used for studies of cellular processes and for the control of cell organization. 3D muscle tissue models are being developed using biomimetic scaffolds or hierarchical cell manipulation.*

I.C.3.a) 2D models

Modulation of substrate biochemical properties

Flat substrates are widely used to study the effects of different signals on skeletal muscle cell fate. Many studies of muscle cell differentiation *in vitro* are conducted using full-length ECM proteins such as fibronectin (Grossi et al. 2007; Bajaj et al. 2011), laminin (Grossi et al. 2007; Munoz et al. 2010; Serena et al. 2010), or collagen (Engler et al. 2004b; Boonen et al. 2009).

These full-length molecules contain, however, many active domains able to interact with different cell surface receptors and thus may influence very different cell processes. To precisely control myogenic differentiation, more defined substrates are needed. Currently, coupling of RGD peptide is the most widely used strategy to control myoblast adhesion in a more specific manner. It was shown that RGD peptide was necessary to promote myoblast attachment to alginate hydrogels, and that myoblast differentiated only on alginate gels with specific combination of monomeric ratio and RGD grafting density (Rowley and Mooney 2002). RGD was used to study myoblast adhesion and differentiation in 2D versus 3D alginate gels (Boontheekul et al. 2007) or in PEG hydrogels (Hume Acta Biomat 2012). In another study, RGD-peptides were found to significantly improve myoblast cell adhesion onto grooved polystyrene substrates (Wang et al. 2012).

There are only very few works where specific cell receptors are targeted. Munoz et al. used short laminin globular (LG4-5) modules of the laminin-α2 chain that binds α-dystroglycan. When incorporated into poly(2-hydroxyethyl methacrylate), this fragment promoted myotube attachment and prevented anoikis (Munoz et al. 2010). In another study, syndecan-1 antibody was used to study the effect of syndecan-mediated signaling on C2C12 myoblast adhesion and migration (Chakravarti et al. 2005).

Modulation of substrate mechanical properties

Besides biochemical properties, mechanical properties of the substrate can affect muscle cell adhesion, spreading, proliferation and differentiation. Different types of synthetic and natural materials are being used to study and control the cell fate of muscle cells *in vitro*: model synthetic PA gels coated with collagen (Engler et al. 2004b), PEG hydrogels (Gilbert et al. 2010), alginate gels of varying stiffness (Boontheekul et al. 2007) and polyelectrolyte multilayer films made of biopolymers (Ren et al. 2008). Recently, Post and coworkers (Boonen et al. 2009) showed, using PA gels of varying rigidity and protein coating, that proliferation was influenced only by rigidity, whereas differentiation was influenced both by rigidity and by protein coating.

Topographical cues

One of the main issues of *in vitro* skeletal muscle tissue engineering is to obtain a properly organized tissue. On flat tissue culture polystyrene, myotubes are randomly organized, while natural muscle cells are perfectly aligned. This disorganization severely interferes with differentiation studies. Notably, synchronous contraction is very important, as the primary function of skeletal muscle is the generation of a longitudinal force (Stern-Straeter et al. 2007). Thus, the controlled alignment of myotubes *in vitro* could have significant applications clinically.

It has been shown that myoblast adhesion and the subsequent formation of myotubes *in vitro* are sensitive to microstructured topography. To guide muscle cell alignment *in vitro*, different types of microstructured substrates such as silicon microgrooves or wavy patterns, as well as aligned nanofibers prepared by electrospinning, have been used (Huang et al. 2006; Lam et al. 2006; Charest et al. 2007; Gingras et al. 2009; Aviss et al. 2010; Huang et al. 2010; Bajaj et al. 2011; Monge et al. 2012).

I.C.3.b) 3D models

One of the current challenges in muscle tissue engineering is to construct 3D well-organized muscle tissues. Another important challenge consists in vascularizing such engineered tissues, since blood supply is necessary to bring nutritive elements and oxygen to the cells in thick constructs (Koning et al. 2009). The most commonly used method for 3D muscle tissue construction consists in myoblast association to polymeric scaffolds.

Scaffolds made of synthetic materials

Different scaffolds made of synthetic materials have been developed (Levenberg et al. 2005; Shah et al. 2005; Williamson et al. 2006). Levenberg et al. have used a polymer scaffold composed of 50% poly- (L-lactic acid) (PLLA) and 50% poly(lactic-glycolic) acid (PLGA) to construct a prevascularized skeletal muscle 3D constructs by co-culturing myoblasts, endothelial cells and fibroblasts (Levenberg et al. 2005). This scaffold was also used to evaluate the effect of the stiffness on myoblasts. The results indicated that compliant scaffolds were insufficient to withstand cell forces, while excessively firm scaffolds could not lead to parallel oriented myotube organization (Levy-Mishali et al. 2009). In another study, a UV-photopatterned thiol-ene mold was employed to produce long channels within a PEG–RGD hydrogel, where skeletal myoblasts formed multiple cell layers within the channels (Hume Acta Biomat 2012).

Scaffolds made of natural materials

However, natural matrices such as collagen gels (Bian and Bursac 2009), matrigel (Vandenburgh et al. 2008; Bian et al. 2012) or fibrin gels (Chiron et al. 2012) present advantages compared to synthetic scaffolds, because they possess cell adhesion ligands that can interact with integrins and thus naturally allow cell anchorage. In addition, some of the scaffolds, e.g. fibrin gels, have the capacity to bind specifically many growth factors (Janmey et al. 2009). Interestingly, application of a continuous strain to a fibrin gel induced myotube alignment in the direction of the applied strain (Matsumoto et al. 2007). In another study, human myoblasts were embedded in a fibrin matrix cast between two posts, and myoblasts also aligned along the longitudinal axis of the gel (Chiron et al. 2012). Cell-interactive alginate gels with tunable degradation rate and stiffness were used to study the effects of mechanical stiffness and degradability on proliferation and differentiation of primary myoblast versus C2C12 myoblast cell line (Boontheekul et al. 2007).

Cell sheets

Another widely used method to create 3D muscle constructs is cell sheet-based tissue engineering. A thermoresponsive polymer poly(N-isopropylacrylamide) (PNIPAAm), grafted on a cell culture substrate, allows confluent cells to be detached as a single cell sheet and to create scaffold-free 3D tissues by layering multiple cell sheets (Yamada et al. 1990; Akiyama et al. 2004). Sasagawa et al. developed prevascularized 3D tissues using human umbilical vein endothelial cells (HUVECs) sandwiched between two myoblast sheets (Sasagawa et al. 2010). Recently, myoblast sheets with well-aligned orientation were fabricated to create 3D oriented myoblast and myotube constructs (Takahashi et al. 2013).

I.C.4. PEM films for the control of cell fate of skeletal myoblasts

Due to their versatility, PEM films can be used as model biomaterial surfaces for guiding the cell fate of skeletal muscle progenitors. Stiffness, biochemical properties and topography of PEM films can be controlled independently or simultaneously, thus providing a wide platform for investigation of the effects of different stimuli on skeletal muscle regeneration.

Here, we will present recent achievements in controlling adhesion and differentiation of skeletal myoblasts using PEM films as biomimetic substrate with controlled properties.

I.C.5.a) Differentiation towards myogenic pathway

PEM films made of hyaluronan (HA) and PLL are a model substrate for cell adhesion and differentiation studies due to their mechanical and biochemical properties. HA is a major constituent of the ECM, and PLL appears to be biocompatible (Tryoen-Toth et al. 2002). (PLL/HA) films can be cross-linked in a tunable manner, which leads to increased stiffness, while other parameters such as film roughness, wettability and serum protein adsorption are not significantly modified (Schneider et al. 2005).

(PLL/HA) films of controlled stiffness were used to investigate the effects of the stiffness on C2C12 myoblast adhesion, proliferation and differentiation (Ren et al. 2008). Stiff films (E(0)>320 kPa) promoted the formation of focal adhesions and organization of the cytoskeleton, as well as an enhanced proliferation, whereas softer films (E(0) from 3 to 320 kPa) were not favorable for cell anchoring, spreading, or proliferation. Cell differentiation into myotubes was also greatly dependent on film stiffness. This study revealed that stiffer (PLL/HA) films (E(0) > 320 kPa) were favorable for the differentiation of C2C12 myoblasts, whereas softer films were not favorable for differentiation (Fig. I-35).

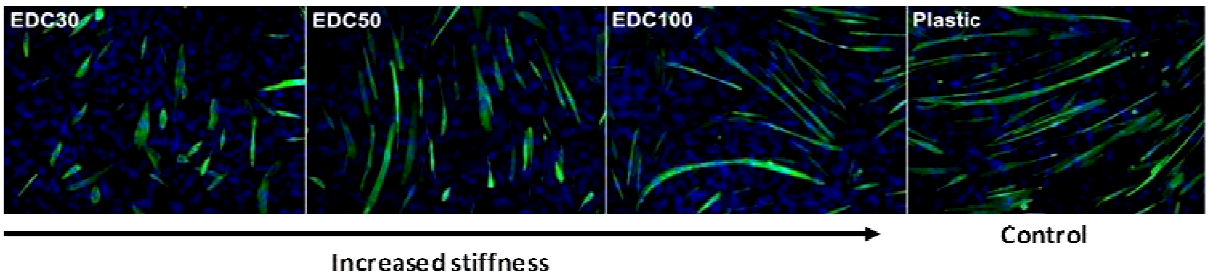

Figure I-35. Effect of (PLL/HA) film stiffness on C2C12 myoblast differentiation. *Stiffer (PLL/HA) films (here, EDC 50 and EDC 100, corresponding to higher cross-linking degrees) were more favorable for the myogenic differentiation of C2C12 myoblasts, as compared to softer films (here, EDC10). Troponin T is labeled in green and nuclei in blue. From (Ren et al. 2008).*

C2C12 myoblast adhesion and proliferation was also studied on three types of multilayer films made from poly(L-lysine)/hyaluronan, chitosan/hyaluronan, and poly(allylamine hydrochloride)/poly(L-glutamic acid). The results showed that, for all films, adhesion and proliferation was controlled by film cross-linking, independently of their internal chemistry. The cell spreading areas correlated with the film stiffness (Boudou et al. 2011). The mechanisms of C2C12 myoblast adhesion on (PLL/HA) films, including integrin clustering, integrin and actin cytoskeleton connection, and focal adhesion formation, were also studied (Ren et al. 2010).

More recently, (PLL/HA) films were also used to orient and confine myoblasts. When combined with molded PDMS, they were used to reproduce *in vitro* the natural organization of myotubes in a regular and parallel network (Monge et al. 2013). Multilayer films made of PLL

and a photoreactive hyaluronan derivative, which can be photo-crosslinked through a photomask to create stiffness patterns, were used to create spatial patterns of rigidity (Monge et al. 2013). These films allowed cell confinement on the stiffer areas in case of circular micropatterns, and myoblast alignment on linear patterns.

Interestingly, an approach for the controlled detachment of C2C12 myoblasts cell sheets from (PLL/HA) films with a topmost layer of fibronectin was proposed (Zahn et al. 2012). Adding a low concentration of nontoxic ferrocyanide to the cell culture medium resulted in erosion of the polyelectrolyte multilayer and rapid detachment of viable cell sheets (Fig. I-36). This technique is promising to cell sheet engineering and could potentially be used for skeletal muscle regenerative medicine (Zahn et al. 2012).

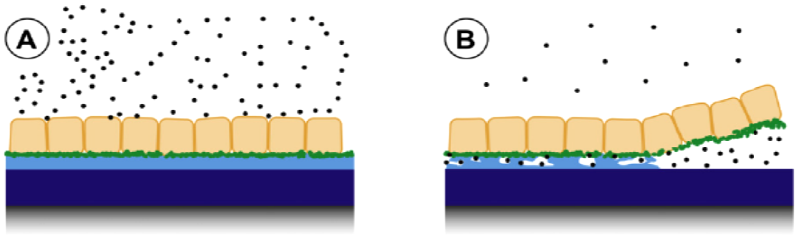

Figure I-36. Schematic representation of ferrocyanide-induced cell sheet detachment. *(A) Polystyrene culture dishes (gray) are coated with an (HA/PLL) film; the first block (dark blue) is crosslinked and the second block is native (light blue). Confluent cell sheets (orange) are grown on a fibronectin adhesion layer (green). (B) Upon addition of ferrocyanide (black) the native (HA/PLL) multilayer dissolves resulting in the detachment of the cell sheet and the fibronectin layer. From* (Zahn et al. 2012).

Besides HA-based PEM films, C2C12 myoblast cell adhesion was also studied on multilayer films made of synthetic polymers. The effect of terminal layer and of different film composition (e.g. varying PSS molecular weight) of poly(sodium-4-sulfonate) (PSS) and poly(allylamine hydrochloride) (PAH) films on C2C12 cell behaviour was investigated (Ricotti et al. 2011). A ”double-sheet” PDMS with stiffness microdomains coated with Dextran Sulphate Salts/Protamine (DXS/PRM) multilayers promoted C2C12 myoblasts alignment and differentiation. In another study, $(PAH/PSS)_5$-coated microgrooves allowed C2C12 skeletal muscle regeneration without switching to their optimal differentiative culture medium (Palamà et al. 2013).

I.C.5.b) Differentiation towards osteogenic pathway

Besides using PEM films for myogenic differentiation of skeletal myoblasts, (PLL/HA) films were used to guide myoblasts towards the osteogenic pathway (Crouzier et al. 2009; Crouzier et al. 2010). As already mentioned, C2C12 myoblasts can undergo osteogenic differentiation when treated with BMP-2 growth factor (Katagiri et al. 1994).

In vivo, soluble bioactive molecules (GF, cytokines, chemokines…) have natural affinity to ECM components and are often presented in a matrix-bound form. This property can be used for incorporation and targeted *in vivo* drug delivery. For instance, BMP-2 and BMP-7 are now approved by the US Food and Drug Administration (FDA) for delivery in absorbable collagen sponges (Bessa et al. 2008). Currently, multiple studies have convincingly demonstrated rhBMP-2 to be a safe, effective treatment option to enhance bone healing in many animal models and in humans (For review, see (Ghodadra and Singh 2008)).

It was shown that crosslinked (PLL/HA) layer-by-layer films can also serve as a reservoir for delivery of BMP-2 (Fig. I-37A). C2C12 culture on (PLL/HA) films charged with rhBMP-2 (recombinant human BMP-2) induced myoblasts differentiation into osteoblasts in a dose-dependent manner. Low doses of surface-adsorbed rhBMP-2 blocked C2C12 differentiation into myotubes, while higher doses allowed the development of an osteogenic phenotype, as measured by ALP production (Fig. I-37B). The rhBMP-2-containing films could sustain three successive culture sequences while remaining bioactive, thus confirming the important and protective effect of rhBMP-2 immobilization.

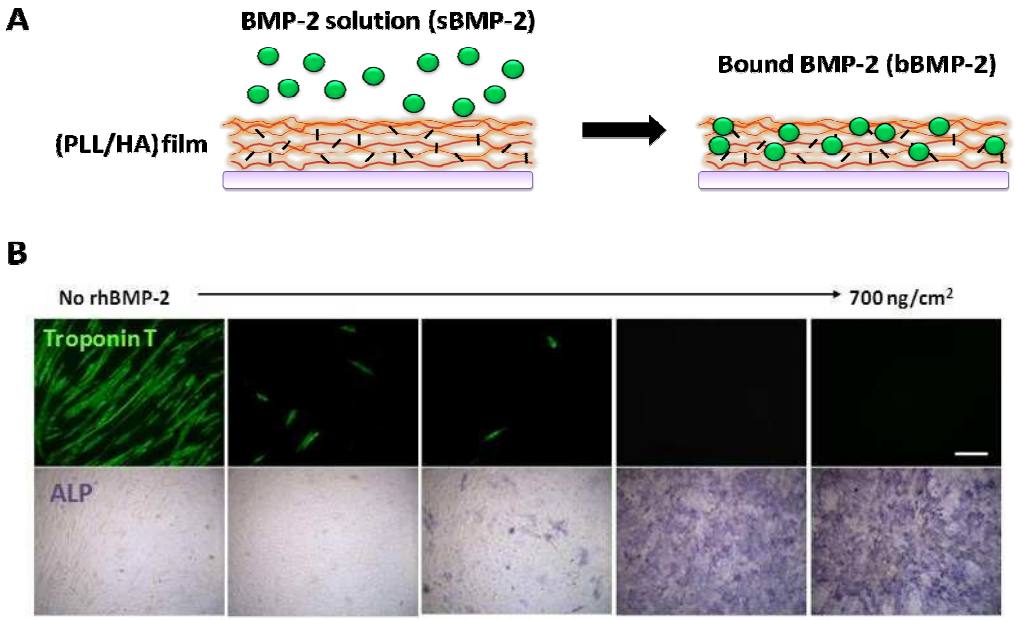

Figure I-37. Effect of BMP-2 loaded into (PLL/HA) films on C2C12 myogenic and osteogenic differentiation. *(A) BMP-2 loading into PLL/HA films. (B) Immunochemical and histochemical staining of troponin T (green) and ALP (alkaline phosphatase, violet) of C2C12 on BMP-2 loaded films for increasing BMP-2 initial concentrations. Adapted from (Crouzier et al. 2009).*

These results show that PEM films constitute an innovative tool allowing to control myoblast adhesion, proliferation and differentiation by modulating chemical/biochemical composition and mechanical properties of the film. The films can also be used for the control of spatial cell organization.

I.D. THESIS SCOPE

In this work, we used layer-by-layer (LbL) assemblies for two goals. The first consisted in the development of multifunctional biomimetic thin films for the control of skeletal muscle cell fate on 2D substrates. We used LbL films made of polypeptides, which can be stiffened by chemical cross-linking (Schneider et al. 2006a) and can be specifically functionalized by grafting of biomimetic peptides onto their surface (Picart et al. 2005).

Our second goal was to explore the potentiality of LbL-coated skeletal muscle cells to form 3D muscle tissues. Here, we used LbL assemblies for the construction of 3D skeletal muscle microtissues by "cell-accumulation technique" (Nishiguchi et al. 2011).

The PhD project is divided in four major parts corresponding to the targeting of different cellular receptors in a 2D environment and to the engineering of 3D muscle tissue (Figure I-38).

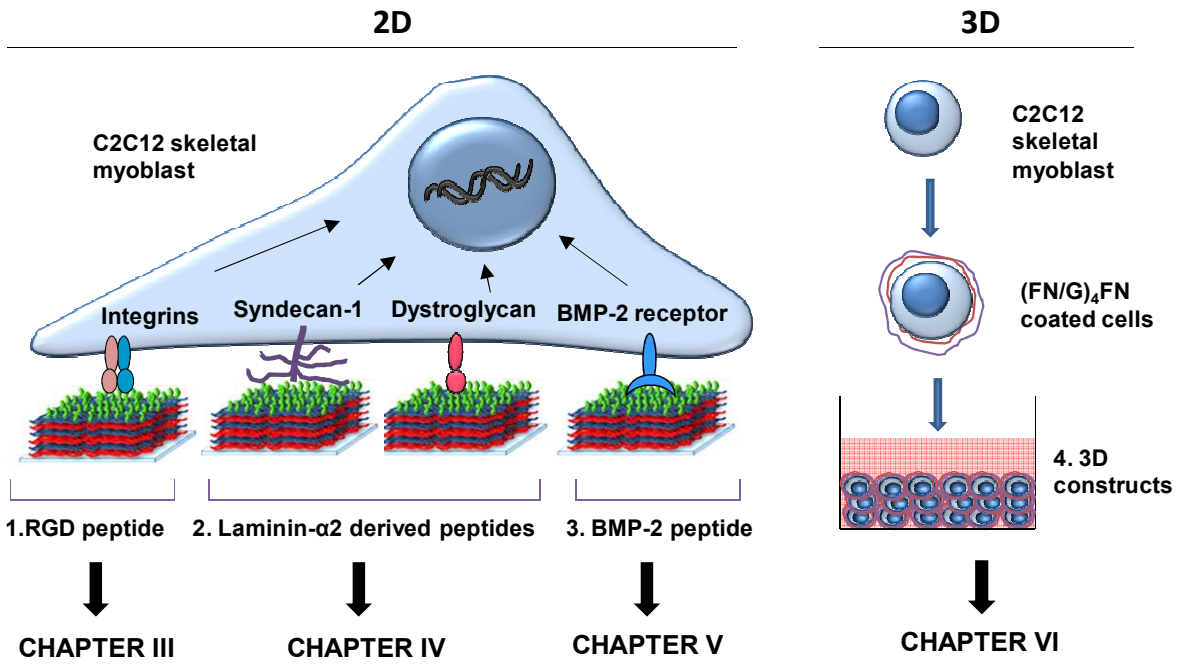

Figure I-38. PEM films as a model biomimetic substrate for the stimulation of skeletal muscle progenitors via various cell surface receptors and for the construction of 3D muscle tissue models*. In 2D: the films with tunable stiffness and grafted with different types of peptides were designed to investigate the effects of peptides on cellular processes, including cell fate. In 3D: construction of thick 3D tissues using LbL protein deposition on the cell surface.*
The manuscript chapters corresponding to each type of film are indicated.

1) Firstly, we wanted to investigate the combined and independent effects of biochemical functionality and mechanical properties of PEM film on cellular processes of skeletal myoblasts. In **chapter III**, we investigate the influence of the substrate stiffness and nanoscale presentation of an integrin-targeting RGD peptide (alone or in combination) on C2C12 myoblast adhesion, proliferation and differentiation (Fig. I-38 (1)).

2) Besides RGD peptide, peptides containing other key sequences are being developed. Among them, laminin-α2 derived peptides targeting syndecans and dystroglycans (Nomizu et al. 1996; Hoffman et al. 1998; Suzuki et al. 2010; Urushibata et al. 2010). In **chapter IV**, we focus on the development of laminin peptide-grafted PEM films for specific targeting of syndecan-1 and dystroglycan (Fig. I-38 (2)).

3) C2C12 myoblasts can differentiate not only into myotubes, but also go towards osteogenic pathway when treated with osteoinductive growth factor BMP-2 (Katagiri et al. 1994). In **chapter V**, we investigate if BMP-2 mimetic peptide presented by PEM films could orient skeletal muscle progenitors towards an osteogenic pathway (Fig. I-38 (3)).

4) Recently, a new technology allowing fast construction of thick 3D tissues using LbL deposition method has been developed (Nishiguchi et al. 2011). In **chapter VI**, we apply the "cell-accumulation technique" to construct 3D muscle tissue models made of C2C12 myoblasts (Fig. I-38 (4)). This work has been conducted in collaboration with Pr Mitsuru Akashi and Dr Michiya Matsusaki from Osaka University.

CHAPTER II – Materials and Methods

This chapter introduces materials and techniques used during the thesis. The principles and details of different experimental methods will be described to allow the reproduction and facilitate the future research.

First, the construction, modification and characterization of bioactive PEM films will be presented. Second, we will focus on fluorescent microscopy, which was widely used in this work. Next, cell culture conditions and the approach for construction of 3D micro-tissues will be described. The last part concerns the different techniques used for the evaluation of the cell behavior on the 2D films and inside 3D constructs.

II.A. CONSTRUCTION OF PEM FILMS

II.A.1. Polyelectrolyte solutions and film buildup

The polyelectrolytes used in this work are polypeptides poly(L-lysine) (PLL, P2636, Sigma) and poly(L-glutamic) acid (PGA, P-4886, Sigma). Their chemical structure is shown in Figure II-1.

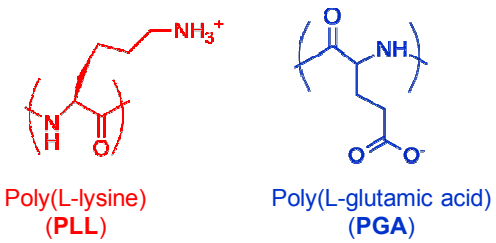

Figure II-1. Chemical structures of poly(L-lysine) (PLL) and poly(L-glutamic) acid (PGA).

Here, we will focus on the construction of (PLL/PGA) multilayer films. Both polyelectrolytes were dissolved at 0.5 mg/mL in a "HEPES-NaCl" buffer (20 mM HEPES, 150 mM NaCl, at pH 7.4). The rinsing solution was composed of 150 mM NaCl (pH 6.5).

For most of the experiments, films were manually constructed in 96-well plates. Such approach allows construction of many films at the same time, to increase the number of conditions and replicates. In addition, the small area of the wells requires smaller amounts of the products. We used the ultrathin bottom plates (Greiner Bio-One), allowing high magnification microscopy observations. The solutions were deposited in the wells with the help of multichannel pipettes. To empty the wells, the plates were turned upside down and shortly shaked to remove the liquid.

A first layer of a positively-charged poly(ethyleneimine) (PEI) dissolved at 5 mg/mL in HEPES-NaCl buffer was deposited to improve the film anchorage. For this, 50 µL of PEI

solution was deposited in the wells and incubated for 20 min at RT. Then, the wells were rigorously rinsed 4 times for 15 min to remove the unbound PEI molecules.

To deposit the subsequent polyelectrolyte layers, 50 µL of the polyelectrolyte solution was deposited in each well and let for 8 min before being rinsed twice for 30 sec and 5 min, respectively, with 100 µL of 150 mM NaCl (pH 6.5). This sequence was repeated until the buildup of a $(PGA/PLL)_6$ film was achieved.

II.A.2. Modification of PEM films

The modifications included modulation of films stiffness by chemical cross-linking and/or functionalization by bioactive peptides.

II.A.2.a) Stiffness modulation

Chemical cross-linking of (PLL/PGA) films is a way to increase their stiffness (Schneider et al. 2006b). The approach is based on carbodiimide chemistry. EDC, or 1-Ethyl-3-(3-dimethylaminopropyl)carbodiimide (Sigma Aldrich E7750), is used as a crosslinker and N-hydroxysulfosuccinimide (Chemrio) as a catalyser. During the reaction, amide bonds between amine groups of PLL and carboxylic groups of PGA are formed (Fig. II-2).

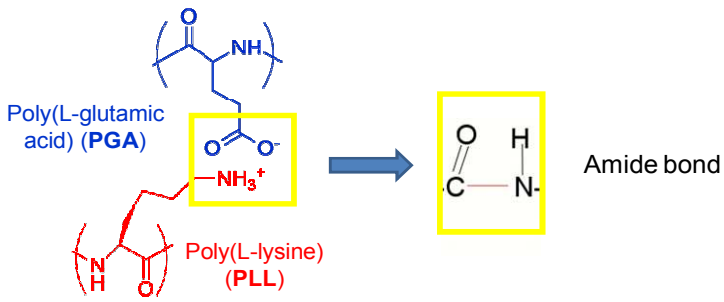

Figure II-2. Schematic presentation of PLL and PGA cross-linking using carbodiimide chemistry.

For the cross-linking, 100 µL of EDC/sulfo-NHS solution in 150 mM NaCl pH 5.5 (mixed v/v with final EDC concentrations of 15 mg/mL and 5.5 mg.mL) were deposited in the wells and incubated at 4° C overnight. Finally, the films were thoroughly washed with the HEPES-NaCl buffer.

II.A.2.b) Functionalization by bioactive peptides

The sequences (Table II-1) were selected according to the existing literature and purchased from GeneCust (Dudelange, Luxembourg). The choice of the sequences will be described in the

next chapters. Cys-Gly (CG) sequence was added at the N-terminus of each peptide to create a "linker" and allow peptide covalent attachment via a cystein residue.

A scrambled L2synd peptide was designed using a tool available at the following link: http://www.mimotopes.com/peptideLibraryScreening.asp?id=97.

Name	Peptide sequence	Targeted receptor	Protein of origin and position	References
RGD	CGPKGDRGDAGPKGA	Integrins	Type I collagen, 728-741	(Picart et al., 2005)
pBMP-2 (1)	CGKIPKASSVPTELSAISTLYL	BMP-2 receptors	rhBMP-2, 73-92 (C78,79S, M89T)	(Saito et al., 2003)
pBMP-2 (2)	CGKIPKACCVPTELSAISMLYL	BMP-2 receptors	rhBMP-2, 73-92	
L2synd	CGKNRLTIELEVRT	Syndecan-1	Laminin-α2, 2780-2791	(Nomizu et al., 1996) (Hoffman et al., 1998)
L2synd scrambled	CGERRTETLVKNIL			
L2dystro	CGVQLRNGFPYFSY	α-Dystroglycan	Laminin-α2, 2812-2823	(Suzuki et al., 2010)

Table II-1. Peptide sequences, targeted receptors and positions in the original protein.

The peptides were grafted to PGA using maleimide chemistry. Peptide grafting to PGA was performed in 2 steps, as described previously (Picart et al. 2005). First, maleimide groups were grafted to PGA; then, cystein-ending peptides could bind to the maleimide (Fig. II-3).

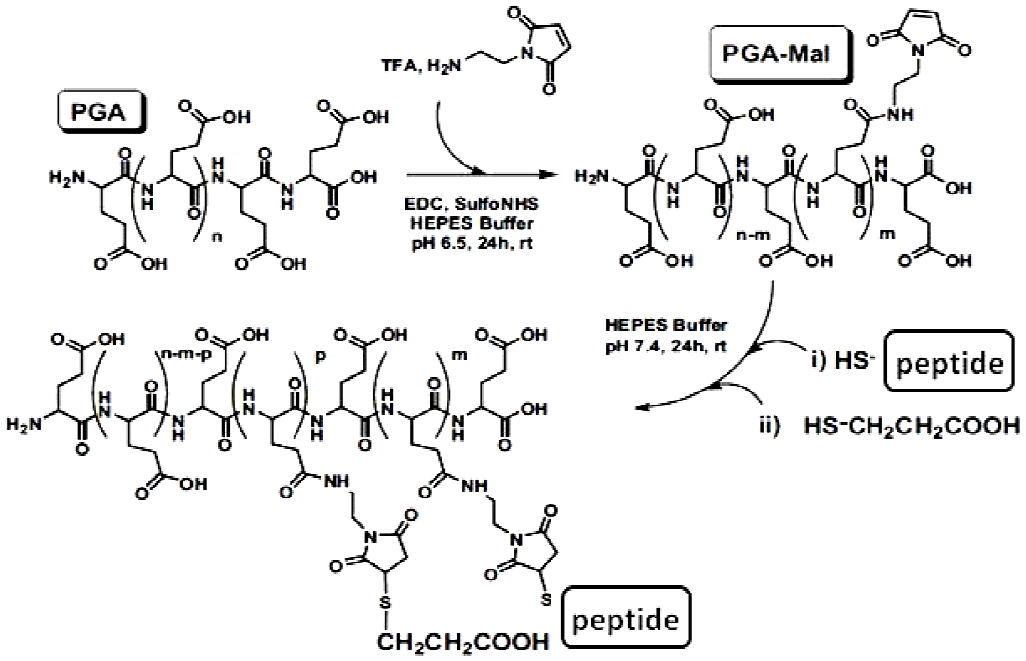

Figure II-3. Two-step protocol for peptide grafting to PGA. Adapted from (Picart et al. 2005).

Step 1. Synthesis of PGA-maleimide

Briefly, to graft maleimide groups onto PGA side chains, PGA is reacted with EDC, sulfo-NHS and maleimide trifluoroacetate in HEPES 10 mM pH 6.5 buffer in an inert atmosphere (nitrogen gas) under magnetic stirring for 24 h. After removal of the byproducts via dialysis against water, the PGA–maleimide is freeze-dried and analyzed by ^{1}H NMR (Fig. II-4). The detailed protocol of the grafting can be found in Annexe III. The average number of maleimide groups bound to PGA was equal to 16% (i.e. in average 16 maleimide groups every one hundred repeating PGA units), as determined via ^{1}H NMR analysis (Annexe IV).

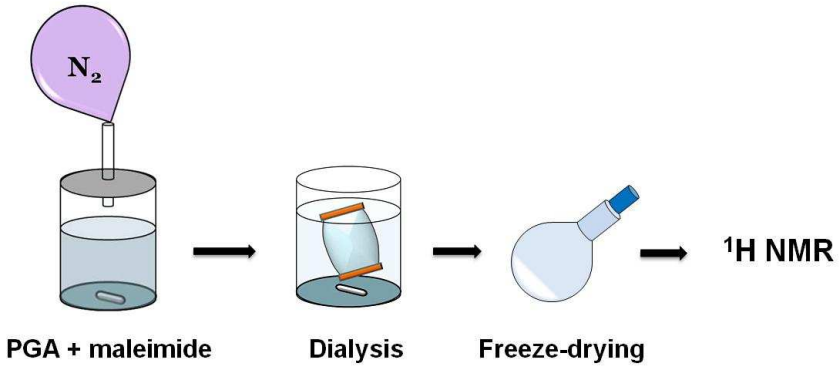

Figure II-4. Procedure of maleimide grafting to PGA.

Step 2: Grafting of the peptides

The further protocol depended on the type of peptides. Briefly, for RGD and BMP-2 peptides, a previously described protocol of peptide grafting to PGA and subsequent PGA-peptide deposition on the films surface was applied (Picart et al. 2005). For laminin-derived peptides, this protocol had to be modified, because L2synd and L2dystro grafting to PGA-maleimide and subsequent freeze-drying led to totally insoluble products. The respective approaches are described below.

RGD- and pBMP-2 functionalized films

For RGD peptides, in the second step, the PGA-maleimide was reacted with the peptide to form the PGA-RGD in HEPES 10 mM pH 7.4 buffer. After 24 h, an excess of mercaptopropionic acid (MPA) was used to neutralize the unreacted maleimide groups. The solution was dialyzed against water, freeze-dried and the final product analysed by ^{1}H NMR (Fig. 5). The detailed protocol of the grafting can be found in Annexe III. The quantitative grafting ratio of the peptide was determined by ^{1}H NMR analysis, and the effective degree of substitution (DS) was found to be 10% (Annexe IV). To obtain PGA-RGD with lower DS, RGD peptide quantities added to the reaction were proportionally decreased.

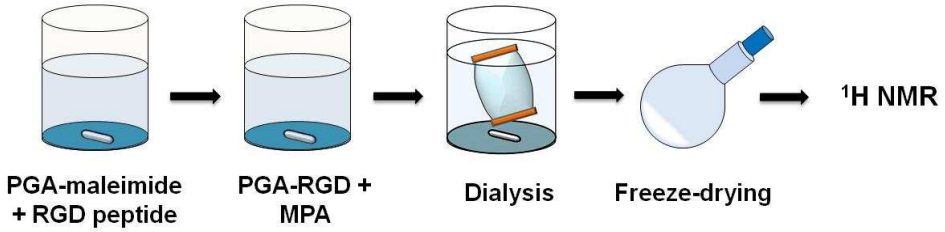

Figure II-5.Procedure of RGD peptide grafting to PGA-maleimide.

After the grafting of RGD was accomplished, the PGA-RGD (0.5 mg/mL in HEPES-NaCl buffer) was deposited on the final layer of (PGA/PLL) films (Fig. 6).

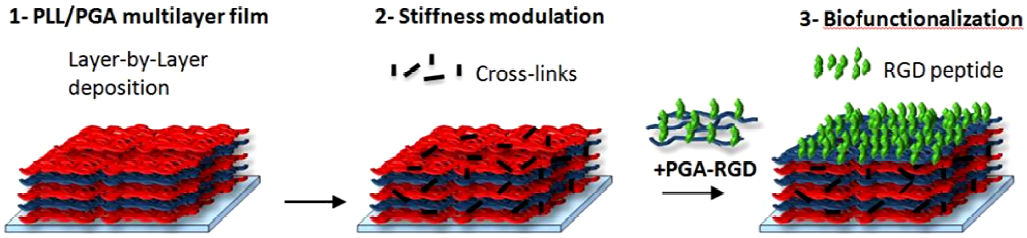

Figure II-6. Design of biomimetic thin film combining physical and biochemical cues. *1- a polyelectrolyte multilayer film (PEM) is built onto a substrate by alternating deposits of PLL and of PGA. 2- The PEM film can be covalently cross-linked using a water-soluble carbodiimide to modulate its stiffness. 3- Biochemical functionality is provided by adding a final layer of PGA grafted with a RGD-containing peptide.*

For films functionalization with pBMP-2, the same grafting procedure was applied. The peptide was grafted to PGA as described above, the quantitative grafting ratio of the peptide was determined by ^{1}H NMR analysis (Annexe IV), and PGA-pBMP-2 was deposited on the final layer of the films.

Laminin peptide-grafted films

For the grafting of laminin-derived peptides and their co-grafting with RGD, previous protocol was slightly modified. The first step consisted, as previously, in grafting maleimide groups onto PGA chains. Then, the obtained PGA-maleimide (0.5 mg/mL in HEPES-NaCl buffer) was deposited on the top of (PGA/PLL) films constructed in 96-well plates.

Next, 100µL of MilliQ water-dissolved 60 µg/mL laminin peptides, 50 µg/mL of RGD peptide or 1:1 (v/v) mix of both were added to the wells (Fig. II-7). The grafting was carried out overnight at RT under agitation, then the films were rinsed twice with MilliQ water to remove the unbound peptide.

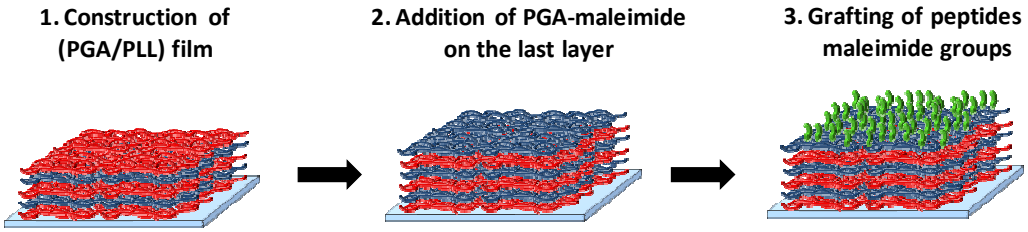

Figure II-7. Construction of laminin peptide-grafted films*. 1- Polyelectrolyte multilayer film is built onto a substrate by alternating deposits of PLL and of PGA. 2- PGA-maleimide is added on the last layer of the film. 3- Biochemical functionality is provided by adding peptides that covalently bind to maleimide group.*

II.A.3. Qualitative assessment of film quality

To check the surface of the constructed films, we used fluorescent PLL (PLL^{FITC}). PLL diffuses into the films and allows to observe the films under fluorescent microscope (Fig. II-8). To this end, 0.5 mg/mL of PLL^{FITC} dissolved in HEPES-NaCl buffer were added to the wells containing constructed films, incubated for 8 min, then rinsed with 150 mM NaCl (pH 6.5). The principle of the fluorescence and fluorescent microscopy are described below (***Part IIB***).

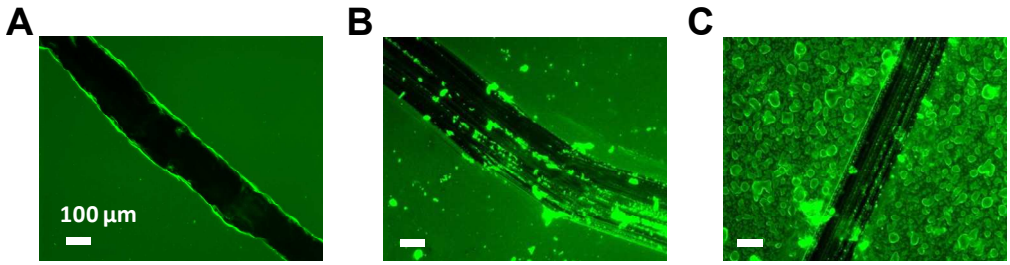

Figure II-8. Scratch on PLL^{FITC} labeled films for a quality control . *(A) The film appears homogeneous and well formed. (B) The film presents aggregates at the surface. (C) The film is not properly formed.*

II.A.4. Film growth monitoring by quartz crystal microbalance

Film buildup was followed by *in situ* quartz crystal microbalance (QCM D300, QSense, Sweden) using a previously published procedure (Crouzier and Picart 2009). PLL, PGA, PGA-maleimide or PGA-RGD, which were prepared at 0.5 mg/mL in the HEPES-NaCl buffer, were successively injected in the cell. They were let to adsorb for 8 min and rinsed for 5 min with the HEPES-NaCl buffer. For L2synd-functionalized films, after adding PGA-maleimide, the films were equilibrated in MilliQ water, and the MilliQ water-dissolved 60 µg/mL L2synd peptide was injected overnight. The unbound peptide was rinced with MilliQ water.

This technique allows to measure film thickness using the Voigt model (Voinova et al. 1999) and to calculate the adsorbed mass. When a mass Δm is adsorbed at the crystal and the measurements are conducted in air, the resulting decrease Δf typically obeys the Sauerbrey equation:

$$\Delta m = -C\Delta f / n$$

where C is the mass sensitivity constant (17.7 ng/cm^2/Hz at 5 MHz), and n is the overtone number.

II.B. FLUORESCENT AND CONFOCAL MICROSCOPY

In many experiments, visualization of the films (Fig. II-8), cells or their components was required. Fluorescent labeling followed by observations using epifluorescent or confocal miscroscope is a common laboratory technique that is used for this goal.

II.B.1. Fluorescence

Fluorescence is a property of a molecule to adsorb a photon and then to re-emit it at a higher wavelength (Fig. II-9). When it is submitted to light excitation at a given wavelength, the fluorescent molecule is brought to an excited electronic state (S_1'). At ambient temperature, the internal conversion induces a partial loss of energy and the molecule falls down to an excited state of lower energy (S1). When the molecule comes back to its stable state (S_o), the associated release of energy takes the form of light. The loss of energy corresponds to the emission of light at a higher wavelength than the initial adsorption wavelength. This phenomenon is known as Stocke's shift.

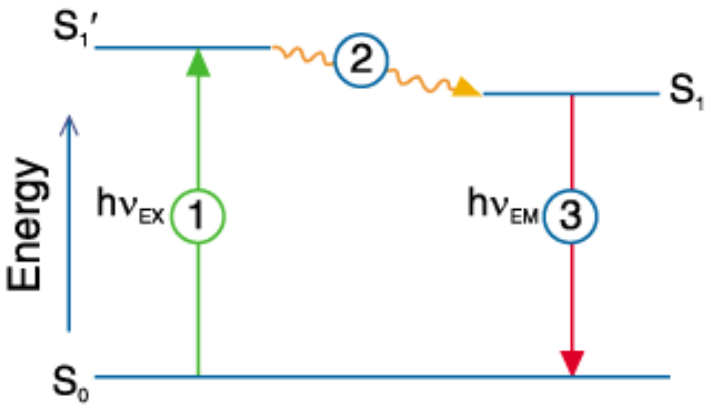

***Figure II-9. Jablonski diagram**. An electron from the fluorophore adsorbs light (1) and becomes excited (stage S_1'). When it is desexcited, there is first a loss of energy by internal conversion (vibration, chock...). The molecule is then a the excitation state (S_1) and comes back to its stable state S_0. This transition corresponds to a release of energy (light) at a higher wavelength (as the energy is lower).*

II.B.2. Epifluorescent microscopy

In epifluorescence microscopy (Fig. II-10A), the light is first filtered through an excitation filter and passes through a dichroic mirror to be sent to the objective. The objective serves as a condenser of the excitation light. The objective is then used to collect the fluorescence light that is emitted by the sample. The emitted light passes through an emission filter before being detected by the camera (or observed by eye using the ocular ports). In this work, we used Zeiss Axiovert 200 inverted epifluorescence microscope equipped with a camera (Fig. II-10B).

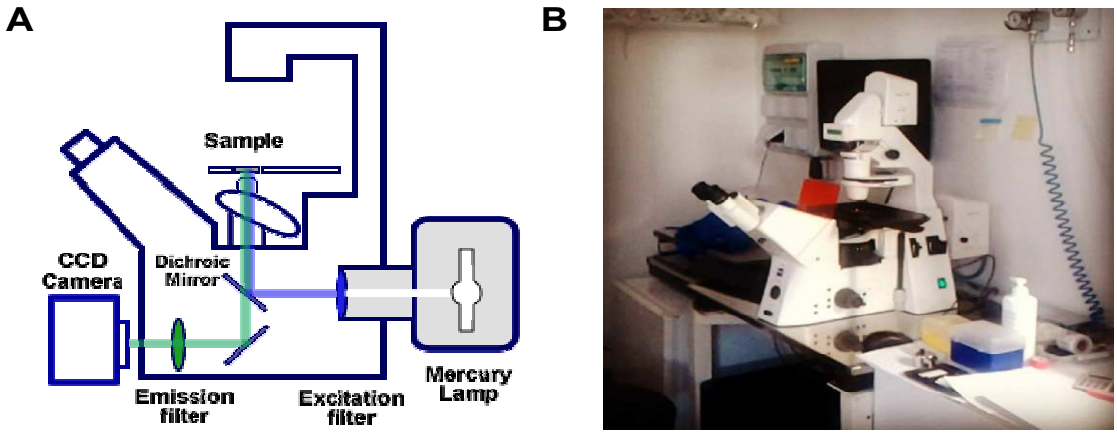

Figure II-10. Epifluorescence microscopy. *(A) Schematic presentation: the light is sent to a dichroic mirror which directs it to the sample. The emitted light from the sample passes through the dichroic mirror before being collected. (B) Zeiss Axiovert 200 inverted epifluorescence microscope equipped with a camera.*

II.B.3. Confocal microscopy

However, the fluorescence coming from the non-focal points is also acquired and a volumetric analysis is not possible. This is the reason why confocal microscopy has been developed by Minsky in 1957. The light source has been replaced by a laser, which allows the light at a precise wavelength to be sent to the sample. However, similarly to epifluorescence microscopy, the sample generates fluorescence out of the focal plane. To avoid this unwanted fluorescence, a pinhole is placed before the detector, which only allows light from the focal plane to be detected (Fig. II-11A). The image obtained in these conditions has a good signal to noise ratio. The scanning of the sample in X,Y direction by the laser allows an image of the focal plane to be taken. This scanning is obtained via motorized mirrors that are disposed on the optical path of the laser. For the scanning in the Z direction, the objective is mounted on a piezo-electric mirror. It is thus possible to obtain images of different focal planes and to reconstitute a 3D structure.

The confocal microscope used is a Zeiss LSM 700 (his name is Hannibal), equipped with four different laser diodes, allowing the simultaneous observation of various fluorophores (Fig. II-11B). Thus, by the appropriate choice of the antibodies and stains, it is possible to visualize different subcellular structures at the same time. He is also equipped with an incubator that allows to maintain the cells at 37°C and 5% CO_2 (Fig. II-11B).

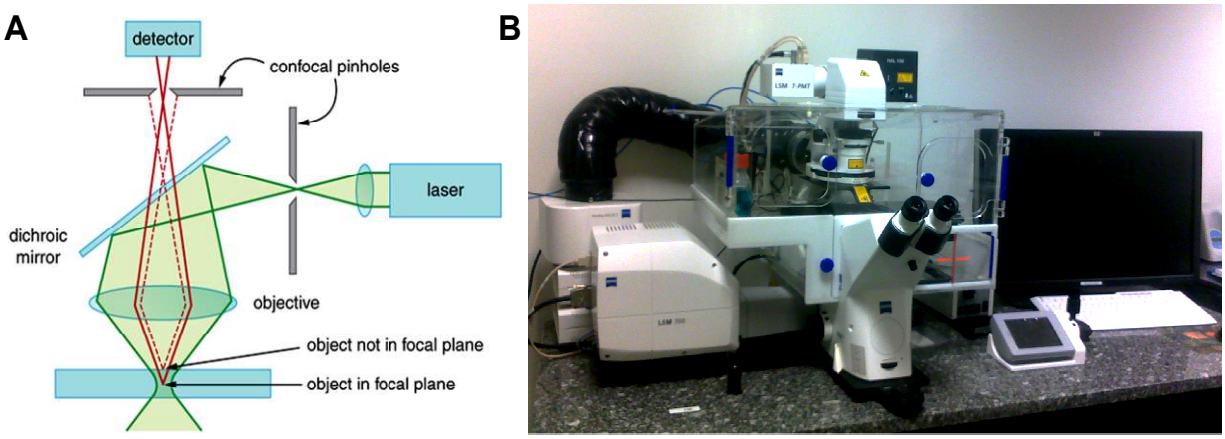

***Figure II-11. Confocal microscopy**. (A) Schematic presentation: the laser source is condensed to a focal point being reflected by the dichroic mirror and after passing through the objective. The fluorescent light is sent collected by a detector. To avoid out of plane fluorescence, a pinhole is placed in the emitted path. (B) Zeiss LSM 700 confocal microscope equipped with an incubator. The system allows to maintain the cells at 37°C and 5% CO_2 during long lasting experiments.*

II.C. CELL CULTURE

Cells are maintained at an appropriate temperature, humidity and gas mixture (typically, 37°C, 5% CO_2 for mammalian cells) in a cell incubator (Fig. II-12).

Figure II-12. Cells grown in an incubator.

Cell culture procedures are performed in sterile conditions. Sterile technique prevents from introducing contaminating microorganisms that can destroy the cells. All cell culture material (dishes, media, pipette tips etc.) are sterile, and all procedures are done in a laminar flow hood (or cell culture hood) that provides an aseptic work area (Fig. II-13).

Figure II-13. Cell culture hood for the work in sterile conditions.

II.C.1. C2C12 myoblasts

Mouse myoblasts (C2C12 cells) were used as a cellular model in most of the studies. These cells are able to reproduce processes that take place during *in vivo* differentiation of skeletal muscle progenitors. C2C12 myoblasts are a subclone of C2 myoblasts (Yaffe and Saxel 1977) which differentiate in culture after serum removal (Blau et al. 1983).

C2C12 cells (purchased from ATCC, used at passages 5-15) were maintained in polystyrene dishes in an incubator at 37° C and 5% CO_2. They were cultured in growth medium (GM) composed of Dulbecco's modified Eagle's medium (DMEM)/F12 medium (1:1; Gibco, Invitrogen, Cergy-Pontoise, France) supplemented with 10% fetal bovine serum (PAA Laboratories, Les Mureaux, France) containing 10 U/mL of penicillin G and 10 µg/mL of streptomycin (Gibco, Invitrogen, Cergy-Pontoise, France). Cells were subcultured prior to reaching 60–70% confluence (approximately every 2 days) in GM (Fig. II-14). Myogenic differentiation was induced by putting the cells at ~80% of confluence into the medium containing 2% of horse serum (HS) (called hereafter DM).

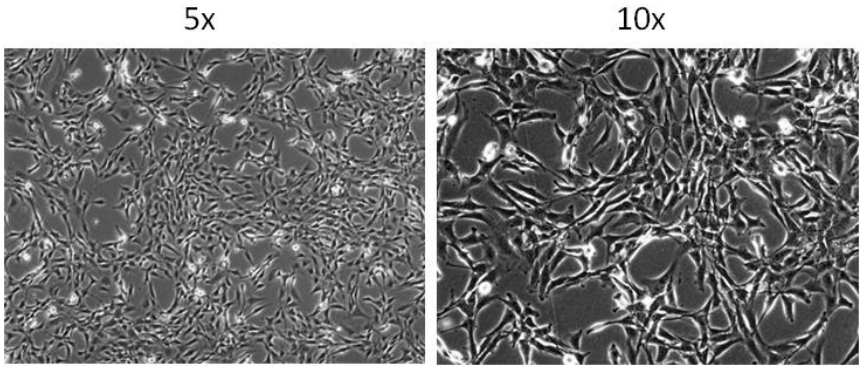

Figure II-14. Phase contrast microscopy observations of C2C12 in culture.

II.C.2. MC3T3 preosteoblasts

MC3T3 murine preosteoblastic cell line is a good model for *in vitro* studying of osteogenic differentiation as they present a similar behavior to primary calvarial osteoblasts. They express high levels of osteoblast-specific markers and are able to mineralize after growth in ascorbic acid-containing medium for several days (Wang et al. 1999).

MC3T3-E1 cells, subclone 4 (CRL-2593, ATCC), were maintained in growth medium composed of αMEM (A1049001, Invitrogen) supplemented with 10% Newborn Calf Serum (N4637-500ML Sigma) and 1% antibiotics (penicillin-streptomycin mix, 15140122 Invitrogen). Confluent culture of MC3T3 is shown in (Fig. II-15)

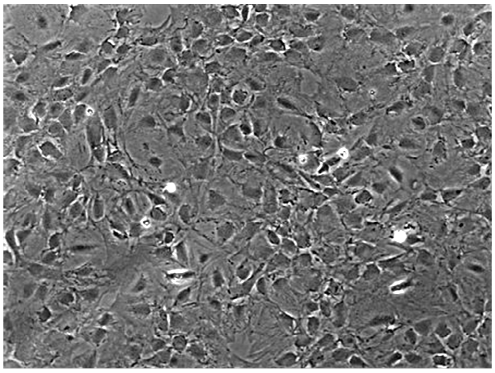

Figure II-15. Culture of MC3T3-E1 pre-osteoblasts after 6 days in osteogenic differentiation medium.

II.C.3. Cell culture on biomimetic PEM films

For all adhesion experiments on the films, C2C12 cells were seeded at 15 000 cells/cm^2 in 96-well plates. Such seeding density allows to have a sufficient cell number for analysis, although maintaining the cells individual.

The cells were allowed to adhere in a serum-free medium (SFM) composed of DMEM/F12 1:1 and supplemented with antibiotics, to eliminate any effect of serum on early adhesion. After

1 h of adhesion, the cells were either fixed, or the SFM was replaced by the GM, depending on the type of experiment (Fig. II-16). For the work on L2synd peptide-grafted films, where a very high degree of specificity was required, the cells were maintained in SFM until 4 h, and only then put in GM, if the experiment (such as migration) required a further culture (Fig. II-16).

For differentiation assays, cells were seeded at 30 000 cells/cm^2 and allowed to adhere for 1 h (or 4 h in the case of L2synd peptide-grafted films) in SFM. Cells were then grown for 1 day in GM to reach about 80% confluence, and then switched to DM (Fig. II-16). The medium was changed twice a week.

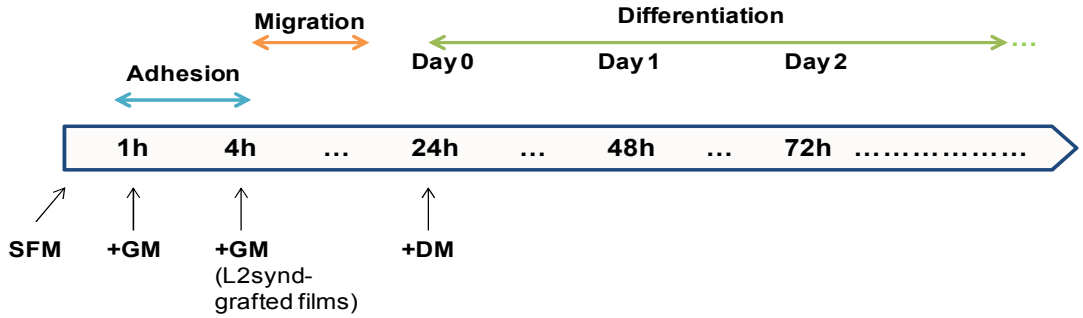

Figure II-16. Chronology of C2C12 culture on PEM films. *The different experiments are indicated by colored arrows. SFM: serum-free medium; GM: growth medium, DM: differentiation medium.*

II.C.4. Construction of C2C12 multilayered tissues

The technique consists in coating the cell surface with fibronectin (FN)/gelatin (G) nanofilms, $(FN/G)_4FN$ (Fig. II-17A), and then seeding the appropriate cell number in 24-well inserts to get the desired number of layers (Fig. II-17B). The inserts with porous bottom allow medium supply to thick multilayered tissues both from the top and from the bottom (Fig. II-17C).

Materials:

- Tris-HCl buffer (50 mM pH 7.4)
- Fibronectin (FN): Sigma, F4759, fibronectin from bovine plasma, 5 mg, MW = 450 kDa
- Gelatin (G): Wako 077-3155, 500g
- 24-well insert: Corning 3470, polyester, pore size 0.4 µm, growth area 0.33 cm^2

Cell coating:

FN and G working solutions are prepared at 0.04 mg/mL in Tris-HCl and stored at 4°C. The cells are detached from culture dishes and washed twice with the GM. After resuspending the cells in Tris-HCl buffer, the cells are subsequently incubated for 1 min using a microtube rotater with 0.04 mg/mL FN or G solutions, then centrifuged at 200 *g* for 1 min, and the supernatant is gently removed by pipetting. After each FN or G deposition step the cells are rinsed in Tris-HCl buffer for 1 min using a microtube rotater, followed by centrifugation.

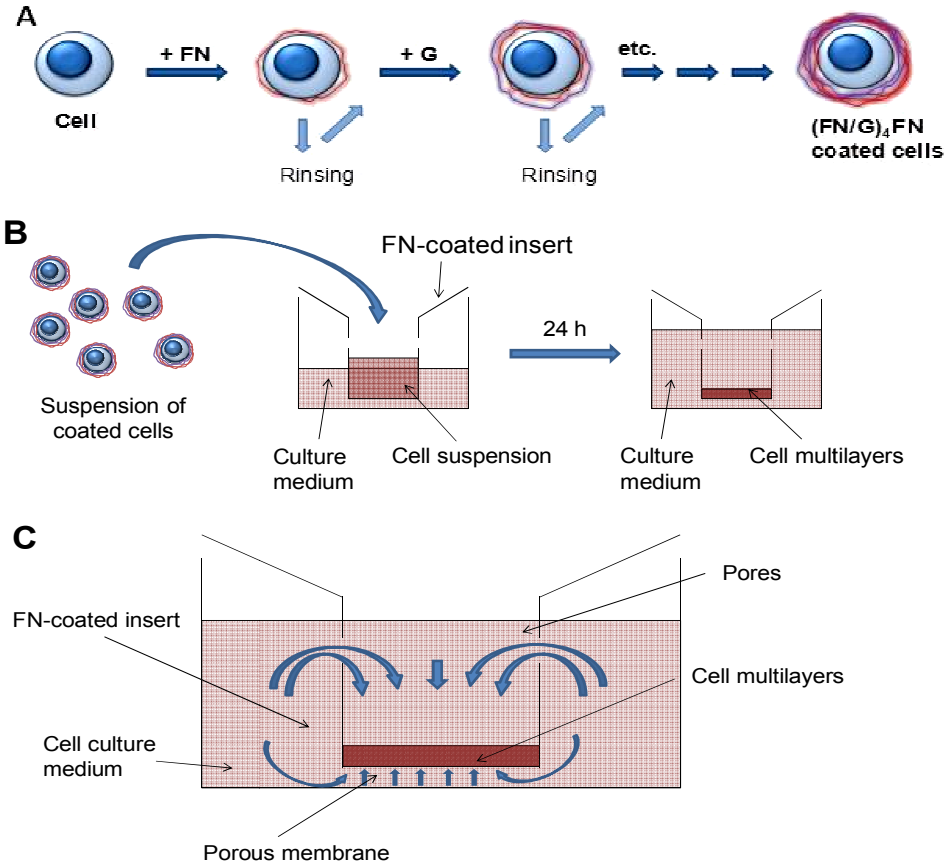

Figure II-17. Schematic presentation of C2C12 multilayered tissues construction by cell-accumulation technique. *(A) Cell coating by $(FN/G)_4FN$ nanofilms. (B) Construction of multilayered tissues in 24-well inserts. (C) The medium is supplied by both sides.*

Cell seeding:

When $(FN/G)_4FN$ nanofilms are formed, the cells are resuspended in GM and 300 µL of cell suspension containing desired cell number (10^5, 5 x 10^5 or 10^6 cells) are deposited into 24-well inserts with a semipermeable membrane coated with FN, and placed into 24-well plates. One milliliter of GM is added in 24-well plate, respectively, outside the inserts (Fig. II-18). The cells are incubated for 1-2 hours at 37°C, then another 1 mL of GM is added to 24-well plate to make a liquid connection between the inside and the outside of the insert (Fig. II-18).

For inserts coating, 100 µL of 0.04 mg/mL FN solution is deposited into the inserts and incubated at 37°C for 30 min, then rinsed once with Tris-HCl buffer.

For the differentiation, the constructs are maintained in GM for 24 h, then switched to DM.

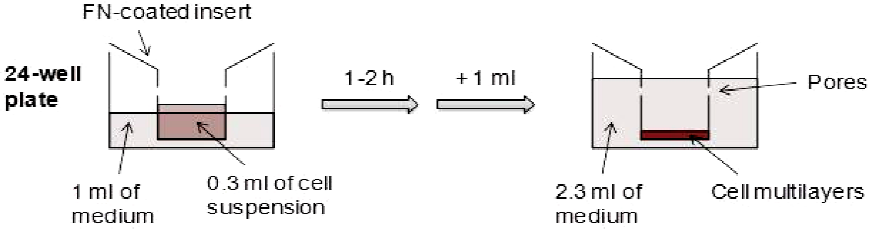

Figure II-18. Schematic presentation of cell seeding into 24-well inserts and culture in 24-well plates.

II.D. EVALUATION OF CELLULAR RESPONSE

The major goal of this work was to study the effects of biomimetic PEM films on different cellular processes: adhesion, migration, proliferation and differentiation. Another goal was to study the internal organization of 3D myoblast structures and to investigate cell behavior in such thick constructs. In this part, we will present different techniques used to evaluate cellular response on 2D biomimetic substrates and in 3D constructs.

II.D.1. Fluorescent cell labeling

II.D.1.a) Principle of immunolabeling

In many assays, visualization of the cells or its components was required. Immunofluorescence (IF) is a common technique that is used to fluorescently label specific components of the cell by antibodies that target specific antigens of cellular proteins (Fig. II-16).

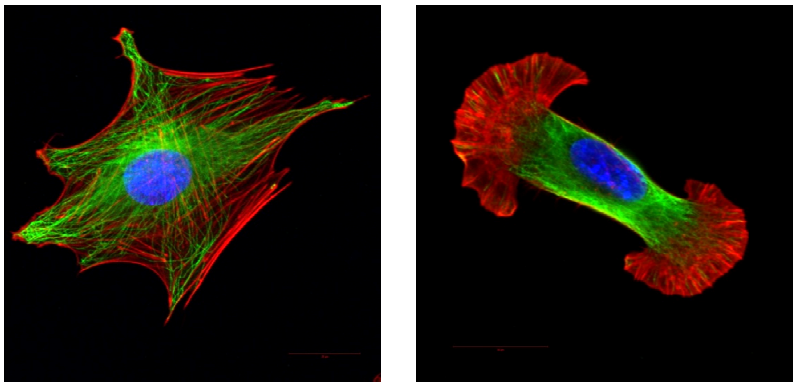

Figure II-16. Examples of fluorescent labeling of specific components of a cell. *The cells were stained for actin (red), tubulin (green) and nuclei (blue).*

The antibody can be coupled to a fluorochrome and can thus be detected by fluorescent microscopy (direct IF, Fig. II-17A). However, usually a secondary antibody coupled to a fluorochrome and recognizing the primary antibody is used (indirect IF, Fig. II-17B). Another possibility is to use a primary antibody coupled to a biotin molecule. In this case, detection is made by a fluorochrome-conjugated streptavidin (Fig. II-17C).

There are also other types of direct fluorescent labeling of cellular components. For instance, phalloidin, a toxin from *Amanita phalloides*, a deadly poisonous fungus, binds F-actin and, if coupled to a fluorochrome, can be detected by fluorescent microscopy. The nuclei can be stained by DAPI or Hoechst fluorescent dyes that bind DNA.

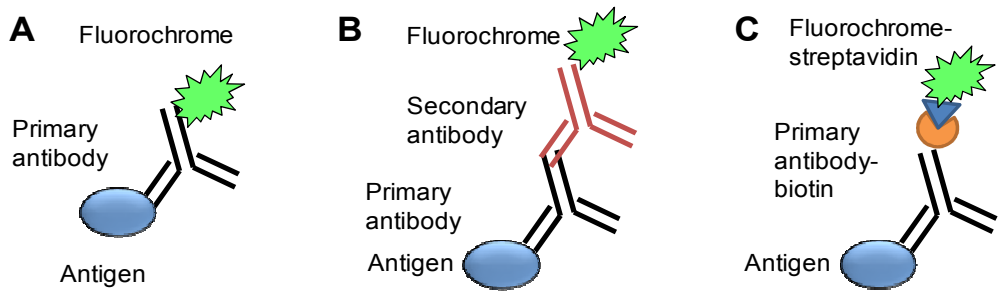

Figure II-17. Different strategies for antigen detection by immunofluorescence*. (A) Direct immuno-fluorescence: a primary antibody coupled to a fluorochrome is used. (B) and (C) Indirect immuno-fluorescence.(B) A secondary antibody coupled to a fluorochrome and recognizing the primary antibody is used.(C) Fluorochrome-conjugated streptavidin binds to a primary antibody coupled to biotin molecule.*

II.D.1.b) Classic immunostaining protocol

Cells were first rinsed in PBS and fixed in 3.7% formaldehyde for 30 min at RT before being permeabilized in 0.5% Triton X-100 for 4 min. After rinsing with PBS, samples were incubated for 1h in 0.1 % BSA in TRIS-buffered saline (TBS, 50 mM TRIS, 150 mM NaCl, 0.1% NaN_3, pH 7.4). Actin was labeled with phalloidin-TRITC (1:800, Sigma) for 30 min. After the incubations with the primary antibodies (diluted in 0.2% TBS-gelatin) for 30 min at RT, cells were washed 3 times in TBS and incubated for 30 min with the secondary antibodies. Cell nuclei were stained with Hoechst 33342 (Invitrogen) at 5 µg/mL for 10 min. A list of used antibodies and their dilutions is provided (Table II-2).

II.D.1.c) Immunostaining protocol to observe adhesion receptors

For Syndecan-1 immunostaining, a protocol adapted from Garcia and coworker was applied (Keselowsky and Garcia 2005). In this protocol, the membrane proteins are cross-linked with the substrate, and intracellular components are removed. Such approach allows better visualization of membrane proteins situated at the basal side of the adherent cell. It has already been applied to cells plated on polyelectrolyte multilayer films, as the film is adding some noise in the fluorescence signal (Ren et al. 2010). Briefly, cells were rinsed in PBS and incubated in ice-cold 1 mM DTSSP (3,3-dithiobis-(sulfosuccinimidyl)propionate, Calbiochem-Merck, Merck Chemicals, Nottingham, UK) in PBS for 30 min. Unreacted cross-linker was quenched with 50 mM Tris in PBS for 15 min, and bulk cellular components were extracted in 0.1% SDS in PBS. The slides were then blocked in BSA (0.1% in TBS). After this, Syndecan-1 was immunostained with 281-2 mouse anti Syndecan-1 (CD138) antibody conjugated to biotin (1:100, BD

Pharmingen, BD Biosciences), and FITC-Streptavidin (1:500, BD Pharmingen, BD Biosciences) was used for visualization (Table II-2).

Primary antibodies					
Antibody	**Reference**	**Provider**	**Animal**	**Clone**	**Final dilution**
Anti-β-Tubulin	T4026	Sigma-Aldrich	Mouse	TUB 2.1	1:200
Anti-CD138 (Syndecan-1)	553713	BD Biosciences	Mouse	281-2	1:100
Anti-FAK pY397	44624G	Invitrogen	Rabbit		1:200
Anti-Fibronectin	F3648	Sigma-Aldrich	Rabbit		1:100
Anti-Myogenin (M225)	sc576	Santa Cruz	Rabbit	M-225	1:60
Anti-N-cadherin	610921	BD Biosciences	Mouse	32/N-Cadherin	1:200
Anti-Skeletal Myosin (Fast)	M4276	Sigma-Aldrich	Mouse	MY-32	1:500
Anti-Troponin T	T6277	Sigma-Aldrich	Mouse	JLT12	1:100

Secondary antibodies				
Antibody	**Reference**	**Provider**	**Animal**	**Final dilution**
Anti-mouse Alexa Fluor 488	A-11008	Invitrogen	Goat	1:1000
Anti-mouse Alexa Fluor 568	A-11004	Invitrogen	Goat	1:1000
Anti-mouse Alexa Fluor 647	A-21235	Invitrogen	Goat	1:1000
Anti-rabbit Alexa Fluor 488	A-11008	Invitrogen	Goat	1:1000
Anti-rabbit Alexa Fluor 568	A-11011	Invitrogen	Goat	1:1000
Anti-rabbit Alexa Fluor 647	A-21244	Invitrogen	Goat	1:1000

Product	**Reference**	**Provider**	**Final dilution**
Phalloidin	P1951	Sigma-Aldrich	1:1000
Hoechst 33342	A3570	Invitrogen	5 µg/mL
Streptavidin-FITC	554060	BD Biosciences	1:500

Table II-2. List of primary antibodies, secondary antibodies, and other products, used for fluorescent cell labeling.

II.D.2. Quantification of cell adhesion

Adhesion is the very first and important step of cell-substrate interactions, which is especially important for anchorage-dependent cells. To evaluate the effects of film stiffness, of peptide functionalization or of specific treatments on cell adhesion, cells were cultured on different types of films in specified conditions for 1 or 4 h. Different parameters such as number of adherent cells, spreading area, morphological parameters and cytoskeletal organization were evaluated.

The data on morphological parameters were manually obtained using a Wacom graphic tablet (named Ginette) which allows to precisely draw the cell contour on microscopy images (Fig. II-18). The data are collected and analysed by ImageJ software (v 1.44p, NIH, Bethesda), which calculates the cell area, circularity and aspect ratio. Cell circularity is a parameter defined by the formula: Circularity = $4\pi(A/P^2)$, (A being the cell area and P its perimeter) that allows to characterize cell morphology: a circularity value of 1.0 indicates a perfect circle and a decrease toward 0 indicates an increasingly elongated polygon. The aspect ratio is a parameter [Major Axis]/[*Minor Axis*] of the particle's fitted ellipse.

Figure II-18. Wacom graphic tablet used for the analysis of cell morphological parameters.

II.D.3. Analysis of cell-film interaction

To evaluate the specificity of cell interaction with L2synd-grafted films, i.e. if the cells specifically recognize the peptide sequence and bind to it via syndecan-1, we performed two competition assays. In the first assay, we pre-incubated the cells with 10 µg/mL of peptide in SFM or with SFM alone for 30 min at 37°C and allowed to adhere on the films grafted with the same peptide for 2 h. In the second assay, we compared cell adhesion on L2synd-grafted films and on the films grafted with a scrambled peptide: a peptide that has the same amino acid composition as L2synd, but not in the same order. For this, the films were grafted with either original or scrambled L2synd peptide, and the cells were allowed to adhere on L2synd-grafted films for 4 h in SFM.

Involvement of proteoglycan adhesion receptors was tested by a competition assay in presence of 1 mg/mL HA MW 360 kDa (Lifecore Biomedical, Chaska, MN, USA) and 200 kDa (gift from Pr Auzély-Velty, CERMAV, Grenoble) and 100 µg/mL heparin (H4784, Sigma). The

cells were pre-incubated for 30 min in SFM alone or containing respective molecules, and allowed to adhere on L2synd-grafted films for 4 h.

Involvement of integrin receptors on different types of PEM films was tested by cell adhesion assay in presence of 2 mM EDTA (Sigma) and 2 mM EGTA (Roth). The cell adhesion via integrin receptors requires divalent ions such as Ca^{2+} and Mg^{2+}. EDTA and EGTA are chelating agents that can inhibit integrin-mediated adhesion by sequestering the divalent cations. The cells were pre-incubated for 30 min in SFM alone or containing respective molecules and allowed to adhere on L2synd-grafted films for 4 h.

For adhesion assays in presence of Rac1 and Cdc42 inhibitors, the cells were allowed to adhere for 4h in absence or in presence of 50 µg/ml of NSC23766 (Rac1 inhibitor) or 10 µM of ML141 (Cdc42 inhibitor) in SFM. DMSO was used as a control for ML141 which is dissolved in DMSO.

II.D.4. Knock-down of integrin receptors using siRNA

The major integrin beta chains in C2C12 myoblasts are β_1-integrin, which is constitutively expressed in skeletal muscle (Hirsch et al. 1998) and β_3 integrin, which was found to be crucial for myogenic differentiation of C2C12 myoblasts (Liu et al., FASEB J., 2011). In order to investigate their possible role in cell adhesion on peptide-grafted films, we performed β_1 or β_3 integrin (or both) knockdown using siRNA approach.

Small interfering RNA (siRNA) are double-stranded RNA molecules, 20-25 base pairs in length. They interfere with the expression of specific genes with complementary nucleotide sequence by inducing their degradation via RNase-containing RISC (RNA-induced silencing complex) (Hamilton and Baulcombe 1999; Elbashir et al. 2001) (Fig. II-19).

Briefly, the cells were transfected with siRNA against β_1 and β_3 integrins (ON-TARGET plus SMARTpool, respectively Mouse ITGB1 and Mouse ITGB3, Thermo Scientific Dharmacon) individually or at the same time, a scrambled siRNA (All Stars negative Control siRNA, Qiagen) being taken as control. For this, the cells were seeded at 30 000 cells/cm^2 in a 6-well plate and cultured in GM (2 mL per well) for 15 h.

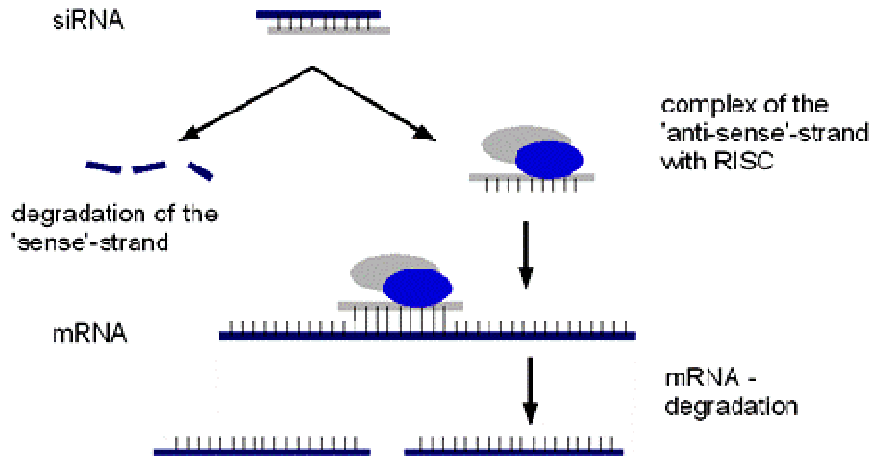

Figure II-19. Mechanism of siRNA interference.

The transfection mix was prepared as following (volumes given for one well):

i) 6 µL of lipofectamine RNAiMAX Reagent (Invitrogen) were added to 305 µL of Opti-MEM medium (Gibco) (= Mix 1);

ii) 0.72 µL of 1 mM siRNA were added to another 305 µL of Opti-MEM medium (= Mix 2);

iii) Mix 1 was gently added to Mix 2 and incubated for 20 min at room temperature.

Previously to transfection, the GM of the wells was replaced by the GM without antibiotics. Then, 610 µL of the final mix were added to each well. After 24 h of incubation at 37°C, the cells were transfected for the second time following the protocol described above and incubated for another 24 h. Then the cells were detached by trypsin-EDTA, seeded in GM at 20 000 cells/cm^2 on the films built in 96-well plate and allowed to adhere for 4 h. Then, the cells were fixed and their area was quantified.

II.D.5. Cell migration assay

To follow cell migration on different types of PEM films, C2C12 cells were seeded at 15 000 cells/cm^2 in 96-well plates, allowed to adhere for 4 h and followed by time-lapse microscopy using Zeiss LSM 700 microscope equipped with an incubator. Images were taken every 10 min during 10 h. For the analysis, at least 20 cells were tracked using ImageJ (v1.45d, NIH, Bethesda) Chemotaxis and Migration Tool. This tool allows to quantify cell velocity and directionality. Directionality is defined as beginning to end distance / total displacement of the cell, and expresses the trajectory of the cell movement. When directionality value is close to 1, this indicates almost straight trajectory; the directionality close to 0 means random movement (Fig. II-20).

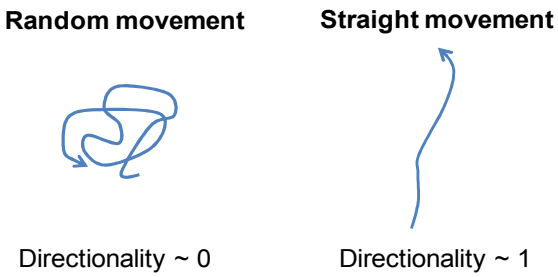

Figure II-20. Cell trajectory characterized by directionality parameter. *Directionality is defined as beginning to end distance / total displacement of the cell.*

II.D.6. BrdU and EdU cell proliferation assays

During myogenic differentiation, a highly ordered process of temporally separable events that begins with the expression of myogenic transcription factors and is followed by cell cycle arrest takes place (Andres and Walsh, J. Cell Biol., 1996). Thus, study of cell proliferation is important for the follow-up of myogenic differentiation, but also for the general evaluation of the proliferative activity.

Cell proliferation was quantified by a BrdU (5-bromo-2'-deoxyuridine) assay (Cell Proliferation Kit, RPN20, GE Healthcare) or by EdU (5-ethynyl-2'-deoxyuridine) assay (Click-iT EdU Imaging Kit, Invitrogen). The principle of BrdU assay is presented in Figure II-21. Briefly, BrdU incorporated into DNA during replication is detected by a primary anti-BrdU antibody, which is detected by a secondary peroxydase-conjugated antibody. Peroxydase substrate giving a colored product is then added.

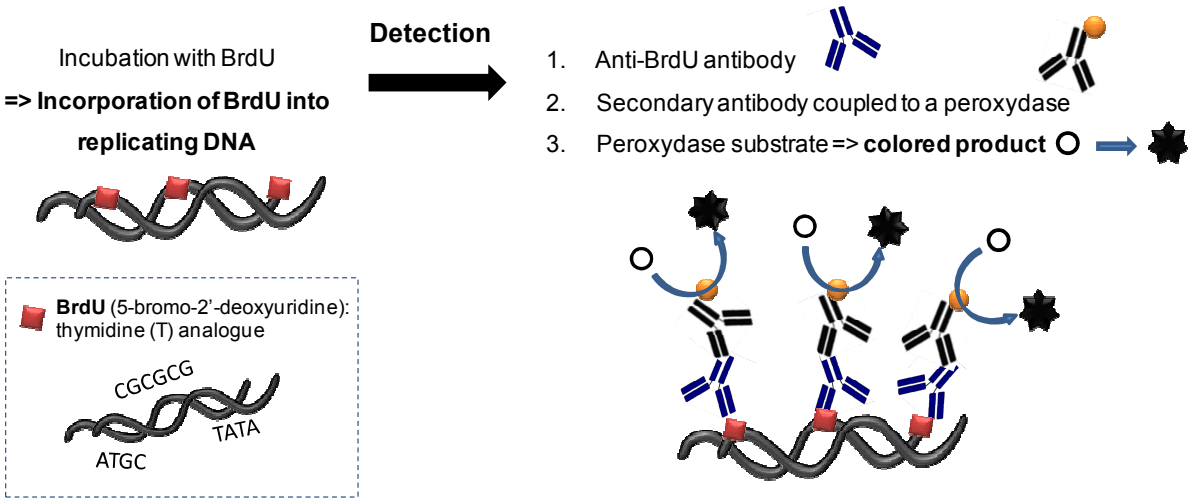

Figure II-21. Mechanism of BrdU proliferation assay.

EdU assay is a novel alternative to the BrdU assay. The detection is based on a click reaction between the alkyne of EdU and azide of Alexa Fluor. In addition, this technique does not require DNA denaturation.

At the chosen time point the cells grown in GM or in DM, on the PEM films or as 3D structures, were incubated with BrdU or EdU diluted at 1/1000 in cell culture medium for 1 h.

The detection was carried out following the manufacturer instructions. At the end, nuclei were counter-stained with Hoechst 33432 (Invitrogen). The images of BrdU-positive nuclei taken by phase contrast microscopy and the images of Hoechst-labeled nuclei taken using an inverted fluorescence microscopy were merged to determine the ratio of BrdU positive nuclei (Fig. II-22A). The images of EdU and Hoechst-labeled nuclei were taken using inverted fluorescence microscopy (Fig. II-22B).

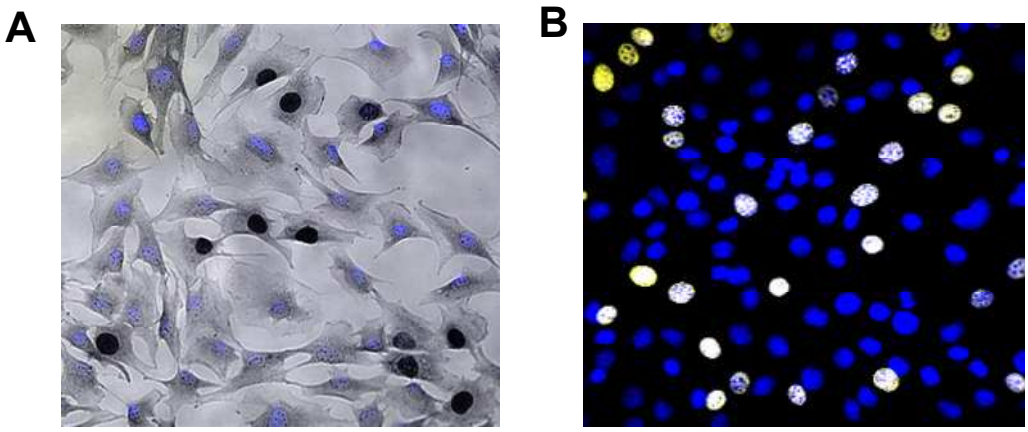

Figure II-22. Exemples of images obtained after BrdU and EdU proliferation assays. *(A) BrdU assay, nuclei of proliferating cells are in black. (B) EdU assay, nuclei of proliferating cells are in yellow.*

II.D.7. Myogenic and osteogenic differentiation assays

II.D.7.a) Myogenic differentiation

Myogenic differentiation was induced by putting the cells at ~80% of confluence into the medium containing 2% of horse serum (HS). This induces the secretion by the cells of different growth factors and promotes cell alignment and fusion into multinucleated myotubes.

To follow the differentiation process, expression of myogenic markers by the cells was analysed at different stages of the differentiation (Fig. II-23). Myogenin was used as an early marker (Day 1 to 3), Troponin T for the early formation of myotubes, and myosin heavy chain was labeled to follow the maturation which as accompanied by the formation of contractile units (“striations”).

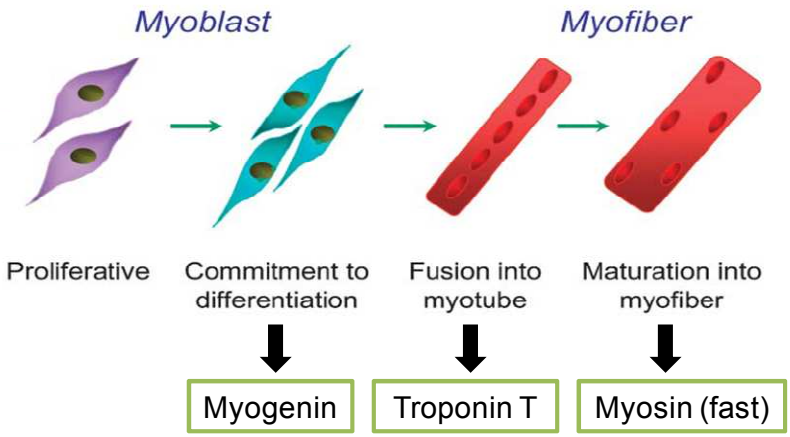

Figure II-23. Markers of different stages of myogenic differentiation. *Adapted from from (Zammit et al. 2006).*

The efficiency of differentiation was characterized by the fusion index, which is a ratio of the nuclei contained in myotubes reported to the total number of nuclei (Charrasse et al. 2007) Fig II-24A). The percentage of striated myotubes was used to evaluate the maturation (Fig II-24B).

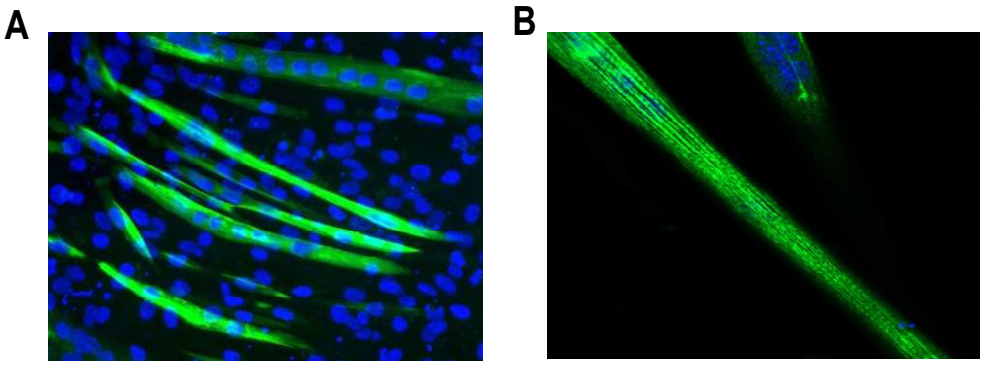

Figure II-24. Methods for characterization of the myogenic differentiation. *(A) Fusion index is a ratio of the nuclei (blue) contained in myotubes (Troponin T, green) reported to the total number of nuclei. (B) Labelling of myosin heavy chain (green) to visualize striations in myotubes, indicating their maturation.*

II.D.7.b) Osteogenic differentiation

C2C12 myoblasts can also undergo osteogenic differentiation when treated with BMP-2 growth factor (Katagiri et al. 1994). In this study, we used the cells seeded on plastic at 30 000 cells/cm^2 in GM supplemented with 500 ng/mL of rhBMP-2 as a positive control of osteogenic differentiation. In this condition, after 2-3 days of culture, the myoblasts start to express ALP that can be dosed by ALP assay or by histochemical staining (Fig.II-25).

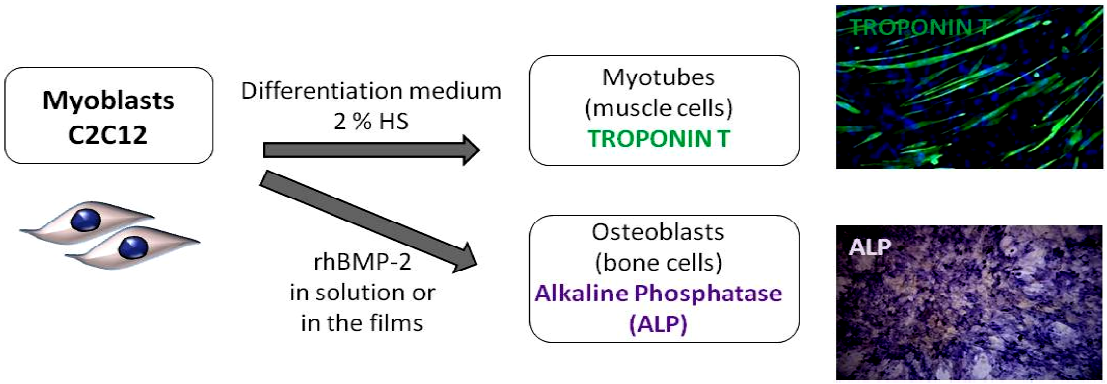

Figure II-25. Differentiation potential of C2C12 myoblasts and some of the usual myogenic and osteogenic markers.

For the induction of osteogenic differentiation of MC3T3 preosteoblasts, the cells were seeded in 24 well-plates at 50 000 cells per well. The medium is supplemented with 50 µg/mL Ascorbic acid (A4403, Sigma) and 10^{-7} M Dexamethasone (D4902, Sigma) and 250 ng/mL rhBMP-2. ALP activity can be measured after 7 days of culture.

The gradual process of osteogenesis can be followed by different proteins being expressed at various time points, comprising early and late genes. In the present study, we used two methods for the evaluation of early osteogenic differentiation of C2C12 myoblasts and MC3T3 pre-osteoblasts in response to BMP-2 derived peptide or rhBMP-2.

The first method consisted in the measurement of alkaline phosphatase (ALP) activity. ALP is a membrane bound hydrolase enzyme responsible for removing phosphate groups, is expressed during osteogenic differentiation (Fig. II-26) and is often used as an early marker.

The second method consists in following the activation of the SMAD pathway (Figure II-26). To this end, we used C2C12-A5 myoblasts transfected with a construct containing luciferase reporter gene placed under Id1 gene promoter (Logeart-Avramoglou et al. 2006); Id1 gene is expressed in response to Smad pathway activation (Fig. II-26).

ALP test

The ALP colorimetric assay is based on monitoring the colour change, as para-nitrophenol phosphate (pNPP), which is colourless, is cleaved by ALP to phosphate and paranitrophenol, which is yellow.

For C2C12 myoblasts, the test was made after 3 days of culture (Fig. II-27) on peptide-grafted PEM films or in presence of soluble pBMP-2. As a positive control, cells seeded on plastic and treated with 500 ng/mL rhBMP-2 were used. For MC3T3 cells, the cells were seeded on plastic ($2{,}5.10^4$ cellules/cm², 24 well-plates) in growth medium supplemented or not with 250

ng/mL of rhBMP-2 or with 200 ng/mL and 500 ng/mL of pBMP-2, and cultured for 7 days (Fig. II-27).

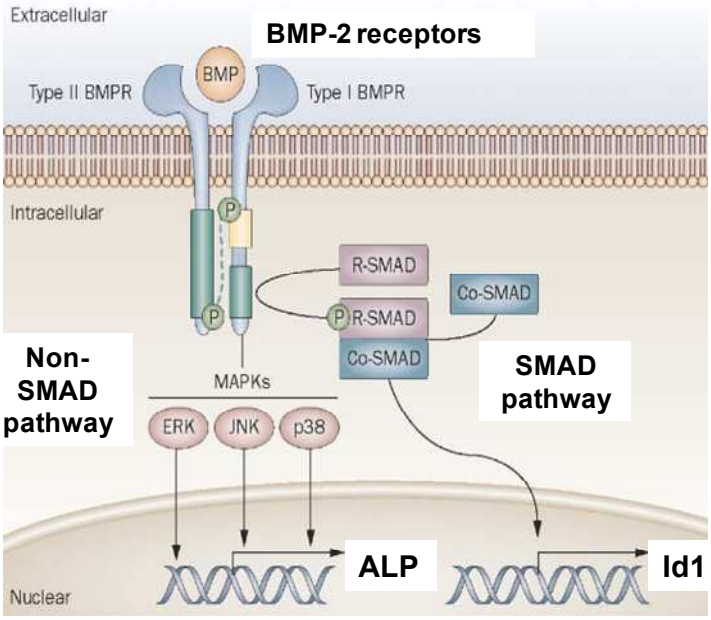

Figure II-26. Early osteogenic markers ALP and Id1 induced via Smad and non-Smad pathways. *Adapted from (Shore and Kaplan 2010).*

Briefly, the cells are lysed in 0.5 mL of 0.1% Triton X100 (Sigma) in PBS for 10 minutes at 4°C. For the test in a 96 well plate (flat, transparent), 20 µL of sample are mixed with 180 µL of working solution prepared as following: 0.1 M 2-amino-2-methyl-l-propanol, 1 mM $MgCI_2$ and 3.34 mg/ml (9 mM) pNPP (*1026,* Euromedex) in MilliQ water and adjusted to pH 10.

The reaction kinetics are followed by the multiwell plate reader (TECAN infinite M1000) using a program that follows the 405 nm absorbance at 405 nm (for p-nitrophenol) every 30 sec for 10 minutes. The cell number is normalized by measuring protein amount by using a BCA protein assay kit (Interchim, France) following manufacturer's instructions. The enzyme activity is expressed as micromoles of p-nitrophenol produced per min per mg of protein (using the slope obtained from the kinetics):

$$\text{ALP (µmol pNPP / min / mg of protein)} = (\text{reaction volume (L)}) \times (\text{slope}) \times (10^{-3} * E(\text{p-nitrophenol}) * l)$$

Reaction volume = 200 µL
E(p-nitrophenol) = 18.75 $mM^{-1}.cm^{-1}.L$
L = 0.2 cm
Molecular Weight: 371.1 $g.mol^{-1}$

Luciferase assay

The activation of Smad pathway was measured using the C2C12 A5 cells with the Bright-Glo™ Luciferase Assay System (E2610, Promega) after 24h of culture (Fig. II-27) on peptide-grafted PEM films or in presence of soluble pBMP-2, in 96-well plates As a positive control, cells seeded on plastic and treated with 500 ng/mL rhBMP-2 were used.

To measure the luminescence, the culture medium is first replaced by 25µl of fresh GM, then 25µl of Luciferase Assay Reagent are added per well, and the measurement is done after 15 min of incubation at room temperature. Cell number is normalized by DNA content measurement using CyQuant NF Proliferation assay kit (Molecular Probes, Invitrogen) following manufacturer's instructions. The method is based on measurement of cellular DNA content via fluorescent dye binding.

Figure II-27 summarizes the different tests used and their time scale.

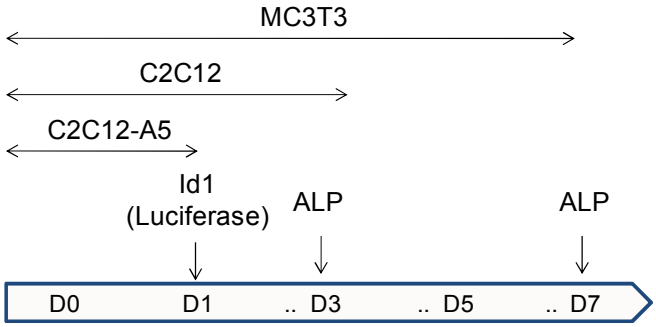

Figure II-27. Time scales of the ALP and luciferase assays used to study early osteogenic differentiation

II.D.8. Statistical analysis

The results represent at least two independent experiments. Data are reported as means ± standard deviation, or as box plots built using SigmaPlot Version 11.0 software.

Statistical comparisons were performed using SigmaPlot Version 11.0 software. Student's t-test was used for comparison of two groups of samples. Analysis for more groups was based on an analysis of variance (ANOVA) followed by an appropriate pairwise comparison or comparison versus control group procedure ($P < 0.05$ was considered significant). Statistically different values are reported on the figures.

CHAPTER III – RGD-functionalized PEM films with tunable stiffness for muscle cell adhesion and differentiation

In this chapter, we studied the effect of a collagen-derived peptide containing RGD adhesive motif on myogenesis using C2C12 skeletal myoblasts as cellular model. We also combined RGD to stiffness modulation of the PEM films, as both biochemical cues and stiffness are known to regulate cell behavior. We explored how the cells respond to peptide-grafted films of different stiffnesses, in order to identify the specific effects of each type of stimuli, biochemical and mechanical, or their synergy. We also studied the effect of RGD grafting ratio variations on cell adhesion and differentiation, and performed cell alignment trials on RGD-functionalized film coated PDMS microgrooved substrates.

III.A. EFFECT OF RGD-FUNCTIONALIZATION AND STIFFNESS MODULATION OF PEM FILMS ON MUSCLE CELL DIFFERENTIATION

III.A.1. Article summary

Satellite cells are now considered as a powerful source for the regeneration of several types of tissues. A major limitation to the study and clinical applications of satellite cells consists in a rapid loss of their stem properties *in vitro*. Moreover, engineering of a functional muscular tissue requires complex environments mimicking *in vivo* niche. Both biochemical cues and matrix stiffness are known to affect muscle cell adhesion, spreading, proliferation and differentiation.

Although RGD substrates have been widely explored in tissue engineering, to date, there is no study investigating the combined effects of RGD nanoscale presentation and matrix stiffness on myogenesis. In this work, we studied the influence of substrate stiffness and RGD nanoscale presentation (alone or in combination) on C2C12 myoblast adhesion, migration, proliferation and differentiation. To this end, we cultured the myoblasts on PEM films made of poly(L-lysine) (PLL) and poly(L-glutamic) acid (PGA) whose rigidity can be tuned by chemical cross-linking (Schneider et al. 2006a). Presentation of a RGD-containing peptide was achieved by chemically grafting the peptide to PGA (Picart et al. 2005) and adsorbing it as final layer of the film. Four different types of films, with or without cross-linking and with or without the RGD-peptide, were constructed and used for cell studies. Architecture and nomenclature of the films is given in the Figure III-1.

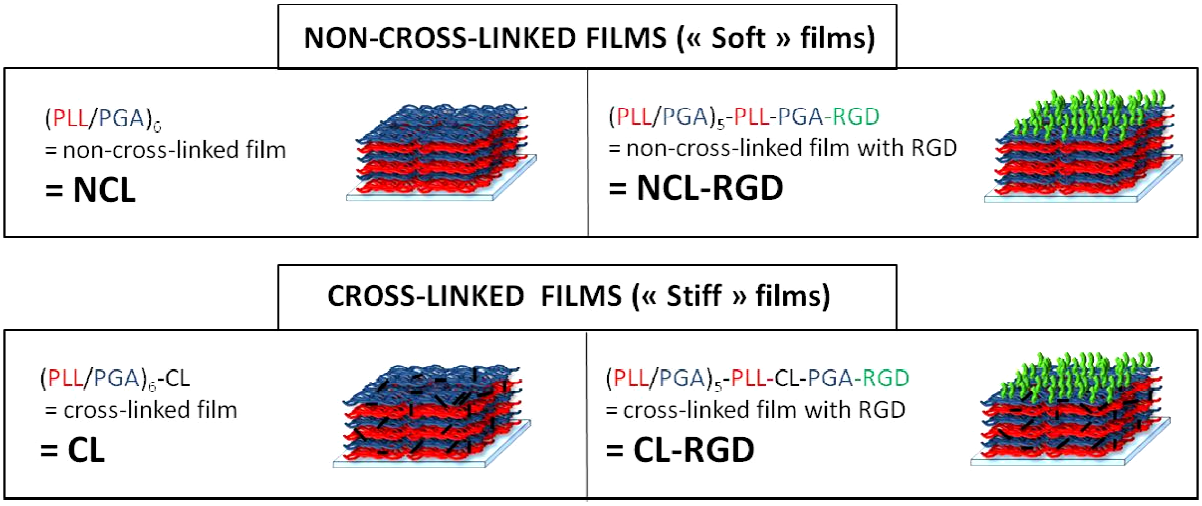

Figure III-1. Four types of films used for investigation of the effects of RGD-functionalization and stiffness modulation of polyelectrolyte multilayer films on muscle cell differentiation.

Cell adhesion assays showed that either cross-linking or RGD-functionalization were sufficient to promote cell adhesion, while non cross-linked film without RGD was non-adhesive. The cells spread more on the RGD-functionalized films, but cell migration speed was enhanced on stiff films. Our results also suggested that soft films with RGD and stiff films recruit different combinations of integrin receptors: while β_3 knockdown alone had an effect on myoblast spreading on NCL-RGD films, the knockdown of both β_1 and β_3 is required to affect myoblast spreading on CL and CL-RGD films.

Differentiation to myotubes was only possible on soft films with RGD peptide, whereas stiff films induced enhanced proliferation and decreased myogenin expression. Moreover, the cells detached from stiff films after few days in differentiation medium, probably because of excessive cell confluence due to absence of cell cycle withdrawal.

Interestingly, myoblast differentiation could be partially rescued on CL films by treatment with ROCK inhibitor, which decreased proliferation level and increased myogenin expression. However, on CL-RGD films, even if the myoblast treated with ROCK inhibitor showed a decreased proliferation level, they were still unable to express myogenin and to differentiate.

Based on our experimental data, we proposed a model for the interplay between mechanical and biochemical stimuli during induction of C2C12 myogenic differentiation. This work suggest that thin films with tunable mechanical and biochemical properties may be a useful tool for biophysical studies of muscle progenitors on controlled 2D microenvironments as well as for their expansion and differentiation *in vitro*.

III.A.2. Article 1

Published in *Acta Biomaterialia*, 2013, **9**(5):6468-80

Effect of RGD-functionalization and stiffness modulation of polyelectrolyte multilayer films on muscle cell differentiation

Varvara Gribova[1, 2], Cécile Gauthier-Rouvière[3], Corinne Albigès-Rizo[4], Rachel Auzely-Velty[2], Catherine Picart[1]

[1]. CNRS UMR 5628 (LMGP), Grenoble Institute of Technology, 3 parvis Louis Néel, F-38016 Grenoble Cedex, France
[2]. Centre de Recherches sur les Macromolécules Végétales (CERMAV-CNRS), affiliated with Université Joseph Fourier, and member of the Institut de Chimie Moléculaire de Grenoble, 601 rue de la Chimie, Domaine Universitaire de Grenoble-St Martin d'Hères, France
[3]. Universités Montpellier 2 et 1, CRBM, CNRS UMR 5237, 1919 Route de Mende, 34293 Montpellier, France
[4]. INSERM U823, ERL CNRS3148, Université Joseph Fourier, Institut Albert Bonniot, Site Santé, BP170, 38042 Grenoble cedex 9, France

Keywords : Extracellular matrix, RGD, substrate stiffness, polyelectrolyte multilayer films, myogenesis

---

Abstract

Skeletal muscle tissue engineering holds promise for the replacement of muscle due to an injury and for the treatment of muscle diseases. Although RGD substrates have been widely explored in tissue engineering, there is no study aimed at investigating the combined effects of RGD nanoscale presentation and matrix stiffness on myogenesis. In the present work, we use polyelectrolyte multilayer films made of poly(L-lysine) (PLL) and poly(L-glutamic) acid (PGA) as substrates of tunable stiffness that can be functionalized by a RGD adhesive peptide to investigate important events in myogenesis, including adhesion, migration, proliferation and differentiation. C2C12 myoblasts were used as cellular models. RGD presentation on soft films and increased film stiffness could both induce cell adhesion, but integrins involved in adhesion were different in case of soft and stiff films. Moreover, soft films with RGD peptide appeared to be the most appropriate substrate for myogenic differentiation while the stiff PLL/PGA films significantly induced cell migration, proliferation and inhibited myogenic differentiation. The ROCK kinase was found to be involved in myoblast response to the different films. Indeed, its inhibition was sufficient to rescue the differentiation on stiff films, but no significant changes were observed on stiff films with the RGD peptide. These results suggest that different signaling pathways may be activated depending on mechanical and biochemical properties of the multilayer films. This study emphasizes the superior advantage of the soft PLL/PGA films presenting the RGD peptide in terms of myogenic differentiation. This soft RGD-presenting film may be further used as coating of various polymeric scaffolds for muscle tissue engineering.

1. Introduction

Regenerative medicine and tissue engineering make use of injected cells or of biomaterials to support cell attachment and to provide them with the appropriate cues to guide their differentiation. Skeletal muscle tissue engineering holds promise for the replacement of muscle due to an injury following a surgery or due to a trauma and for the treatment of muscle diseases, such as muscle dystrophies or paralysis. Adult skeletal muscle progenitor cells are considered as a powerful source for the generation of several tissues, especially skeletal muscles [1] but also smooth muscle [2], bone [3; 4] or fat tissue [5; 6]. The process of muscle formation requires that muscle precursor cells become activated, proliferate, differentiate, and fuse together to form multinucleated myotubes. Proliferation and differentiation of skeletal myoblasts are mutually exclusive events, which are governed by the upregulation of transcriptional activators [7]. A major limitation to the clinical application of muscle progenitors is a rapid loss of their muscle stem cell properties once they are removed from their *in vivo* environment [8].
The development of skeletal muscles is known to depend on the interaction of muscle cells with their surrounding extra-cellular matrix (ECM) [9]. Transmembrane receptors like the dystrophin-glycoprotein complex are known to be important [10; 11]. However, other transmembrane receptors of the integrin family [12] have been shown to be crucial for skeletal muscle development and function [13; 14].

Tissue engineering requires a combination of engineering methods, cell biology and materials. In this context, a goal of biomaterials scientists is to design biocompatible scaffolds in which cells can adhere, proliferate, differentiate and synthesize their own matrix to regenerate tissues. Adhesive properties can be provided either by grafting or by physically adsorbing cell adhesion molecules.

The tripeptide sequence RGD is present in many ECM proteins, including fibronectin, vitronectin, fibrinogen, von Willebrand factor, thrombospondin, laminin, osteopontin, bone sialo protein, and some collagen isoforms [15]. It binds to a wide range of integrin receptors in a non selective manner, i.e. not specifically to a given integrin receptor. To achieve better selectivity and/or target only one type of integrin receptor, several strategies can be applied (for review, see [16]). *In vitro*, ligands containing the RGD peptide have already been used in the field of biomaterials to increase early adhesion of anchorage-dependent cells [17]. This was especially targeted to osteoblasts on peptide-grafted poly(ethylene glycol) hydrogels [18], to fibroblasts on ethylene-acrylic copolymer film with immobilized peptides [19] and to endothelial cells on polyurethane [20].

However, so far, studies of muscle cell differentiation *in vitro* rather used full-length ECM proteins such as fibronectin [21], laminin [22], or collagen [23], which are difficult to couple to synthetic or natural biomaterials. In addition, the functionality of these ECM proteins may be altered by adsorption or chemical coupling onto materials. Mooney and coworkers [24] showed that RGD coupling improved the initial adhesion and enabled the differentiation of myoblast cultured on 2D alginate gels or inside 3D alginate gels.

Besides biochemical cues, matrix stiffness has also been shown to be an important parameter in regulating function of various tissue and cell types, *in vivo* and *in vitro* [25]. Indeed, a number of pathologies, including muscle pathologies, involve changes in matrix properties. In dystrophic muscles, a more fibrotic tissue and an increased rigidity of the diaphragm have been observed as compared to normal diaphragm [26].

In vitro, it is now acknowledged that mechanical properties of the substrate can affect muscle cell adhesion, spreading,

proliferation and differentiation. This has been shown using different types of synthetic and natural materials, such as model synthetic polyacrylamide (PA) gels coated with collagen [23], poly(ethylene glycol) (PEG) hydrogels [27], alginate gels of varying stiffness [24] and polyelectrolyte multilayer films made of biopolymers [28]. Recently, Post and coworkers [29] showed, using PA gels of varying rigidity and protein coating that proliferation was influenced only by rigidity, whereas differentiation was influenced both by rigidity and b[30; 31]y protein coating.

However, to date, there is no study aimed to investigate the combined effects of RGD nanoscale presentation and matrix stiffness in myoblast adhesion, proliferation and differentiation. Polyelectrolyte multilayer films [32] are currently emerging as a new kind of biomaterials coating that can be used to guide cell fate [33; 34]. Advantageously, the architecture of the films, their biodegradability and bioactivity can be controlled [35]. The films can also be micropatterned to have (X-Y) architecture by combining with microfabrication techniques such as photolithography, microcontact printing or microfluidics (Berg_Rubner, Langmuir 2004; Chien, Biomaterials 2009; Monge, Tissue Eng 2012). Furthermore, they can be deposited on various types of supporting materials, including metals, polymers and ceramics, which are already approved as implantable materials [35].

In this study, we investigated the influence of substrate rigidity and RGD nanoscale presentation alone or in combination on C2C12 myoblast adhesion, proliferation and differentiation. To this end, we cultured the myoblasts on polyelectrolyte multilayer films made of poly(L-lysine) (PLL) and poly(L-glutamic) acid (PGA) whose rigidity can be tuned by chemical cross-linking [36]. Moreover, such films are of particular interest since they are made of biodegradable polymers and appear to be biocompatible.

In addition, presentation of a RGD-containing peptide was achieved by chemically grafting the peptide to PGA [37] and adsorbing it as final layer of the film. Such covalent grafting provides a good control of surface composition, a stable link and limits release of the functional group into the culture medium.

We studied the combined effects of RGD nanoscale presentation and matrix stiffness on early adhesion of the myoblasts to their late differentiation in myotubes after 9 days in culture, until the formation of sarcomeres.

2. Materials and methods

2.1. Covalent grafting of RGD adhesion peptide to PGA (poly(L-glutamic) acid)

The type I collagen-derived peptide was chosen according to a published sequence that was shown to induce adhesion of human primary osteoblasts *in vitro* [37]. The 15-amino-acid peptide containing a central RGD (Arg-Gly-Asp) sequence (Cys-Gly-Pro-Lys-Gly-Asp-*Arg-Gly-Asp*-Ala-Gly-Pro-Lys-Gly-Ala, CGPKGD*RGD*AGPKGA) was purchased from GeneCust (Dudelange, Luxembourg). The peptide was grafted as described previously [37]. Briefly, the first step consisted in grafting maleimide groups onto PGA (P-4886, Sigma) chains. To accomplish this grafting, 60 mg of PGA were dissolved in 3 mL of a solution containing 10 mM HEPES buffer (pH 6.5), 20 mg of EDC, and 3 mg of sulfo-NHS in an inert atmosphere (nitrogen gas) under magnetic stirring. Then, 24 mg of N-(2-aminoethyl) maleimide trifluoroacetate was added. The reaction was allowed to proceed at room temperature (RT) for 24 h. After removal of the byproducts via dialysis against water, the PGA–maleimide was freeze-dried. The average number of maleimide groups bound to PGA was equal to 16% ((i.e. in average 16 maleimide groups every one hundred repeating PGA units), as determined via ^{1}H NMR

analysis. In the second step, the PGA-maleimide was reacted with the peptide to form the PGA-RGD: 5 mg of PGA–maleimide were mixed with 5 mg of peptide in 1.5 mL of 10 mM HEPES buffer (pH 7.4) and maintained for 24 h under magnetic stirring at RT. An excess of mercaptopropionic acid was used to neutralize the unreacted maleimide groups. The solution was dialyzed against water and freeze-dried. The quantitative grafting ratio of the peptide was determined by ^{1}H NMR, and the effective degree of grafting was found to be 10% analysis.

2.2. Polyelectrolyte solutions and PEM film buildup

Poly(L-lysine) (PLL, P2636, Sigma) and poly(L-glutamic) acid (PGA, P-4886, Sigma) were dissolved at 0.5 mg/mL in a HEPES-NaCl buffer (20 mM HEPES, 150 mM NaCl, at pH 7.4). For all experiments, films were manually constructed in 96-well plates starting with a first layer of poly(ethyleneimine) (PEI) at 5 mg/ml. To deposit the subsequent polyelectrolyte layers, 50 µL of the polyelectrolyte solution was deposited in each well and let for 8 min before being rinsed twice for 30 sec and 5 min, respectively, with 100 µL of 150 mM NaCl (pH 6.5). This sequence was repeated until the buildup of a $(PGA/PLL)_6$ film was achieved. Then, the last layer of PGA (0.5 mg/mL) or of the PGA-RGD (0.5 mg/mL) was added, giving $(PGA/PLL)_6$-PGA and $(PGA/PLL)_6$-PGA-RGD films.

In order to increase the stiffness, $(PGA/PLL)_6$-PGA films were chemically cross-linked to give $[(PGA/PLL)_6\text{-PGA}]_{CL}$ films. To obtain the cross-linked films functionalized with PGA-RGD, cross-linking was done after $(PGA/PLL)_6$, and PGA-RGD was added after the cross-linking, giving $[(PGA/PLL)_6]_{CL}$-PGA-RGD films. For the cross-linking, 100 µL of EDC/sulfo-NHS solution in 150 mM NaCl pH 5.5 (mixed v/v with final EDC concentrations of 15 mg/mL and 5.5 mg.mL) were deposited in the wells and incubated at 4° C overnight. Finally, the films were thoroughly washed with the HEPES-NaCl buffer. The nomenclature of the film is given in Table 1.

2.3. Quartz Crystal Microbalance with dissipation monitoring (QCM-D)

Film buildup was followed by *in situ* quartz crystal microbalance (QCM D300, QSense, Sweden) using a previously published procedure [38]. PLL, PGA and PGA with grafted RGD peptide prepared at 0.5 mg/mL in the HEPES-NaCl buffer were successively injected in the cell. They were let to adsorb for 8 min and rinsed for 5 min with the HEPES-NaCl buffer.

When a mass Δm is adsorbed at the crystal and the measurements are conducted in air, the resulting decrease Δf typically obeys the Sauerbrey equation:

$$\Delta m = -C\Delta f/n$$

where C is the mass sensitivity constant (17.7 ng ·cm-2 Hz-1 at 5 MHz), and n is the overtone number.

2.4. C2C12 culture

C2C12 cells (from ATCC, used at passages 5-15) were maintained in polystyrene dishes in an incubator at 37° C and 5% CO_2 and cultured in growth medium (GM) composed of Dulbecco's modified Eagle's medium (DMEM)/F12 medium (1:1; Gibco, Invitrogen, Cergy-Pontoise, France) supplemented with 10% fetal bovine serum (PAA Laboratories, Les Mureaux, France) containing 10 U/mL of penicillin G and 10 µg/mL of streptomycin (Gibco, Invitrogen, Cergy-Pontoise, France). Cells were subcultured prior to reaching 60–70% confluence (approximately every 2 days).

For all experiments, C2C12 cells were first allowed to adhere in a serum-free medium (SFM) composed of DMEM/F12 1:1 and supplemented with antibiotics.

Film design			Film architecture	Film nomenclature
PGA	Cross-linking	PGA- RGD		
×			$(PGA/PLL)_6$-PGA	NCL
		×	$(PGA/PLL)_6$-PGA-RGD	NCL-RGD
×	×		$[(PGA/PLL)_6\text{-}PGA]_{CL}$	CL
	×	×	$[(PGA/PLL)_6]_{CL}$-PGA-RGD	CL-RGD

TABLE 1*. Summary of the conditions used for the buildup of the films.*

After 1 h of adhesion, the cells were fixed or the SMF was replaced by the GM, depending on the type of experiment (see below). Cell were differentiated in a differentiation medium (DM) composed of DMEM/F12 (1:1) supplemented with 2% horse serum (PAA Laboratories, Les Mureaux, France) and antibiotics.

2.5. Cell adhesion, proliferation, migration and differentiation assays

For cell adhesion tests, C2C12 cells were seeded at 15 000 cells/cm^2 in 96-well plates and allowed to adhere in SFM for 1 h. For the short-term adhesion tests (1 h), cells were then fixed in 3.7% formaldehyde. For adhesion tests at 4 h, the medium was changed to GM after 1 h and the cells were fixed at 4 h.

Cell proliferation was quantified by a BrdU (5-bromo-2'-deoxyuridine) assay (Cell Proliferation Kit, RPN20, GE Healthcare) following the manufacturer instructions. Three time points were chosen: 4, 24, and 48 h. The cells were incubated for 1 h at 37°C. Nuclei were counter-stained with Hoechst 3342 (Invitrogen). The images of BrdU-positive nuclei taken by phase contrast microscopy and the images of Hoechst-labeled nuclei taken using an inverted fluorescence microscope were merged to determine the ratio of BrdU positive nuclei.

To follow cell migration, C2C12 cells were mixed 1:1 with C2C12 HB1 GFP cells (kindly provided by E.Gomes, Institut de Myology, Paris) and seeded at 15 000 cells/cm^2 in 96-well plates. Images of the fluorescent nuclei were taken every 30 min during 5 h. For analysis, at least 20 cells were tracked using ImageJ (v1.45d, NIH, Bethesda).

For differentiation assays, cells were seeded at 30 000 cells/cm^2 and allowed to adhere for 1 h in SFM. Cells were then grown for 1 day in GM and then switched to DM. The medium was changed twice a week. For the proliferation and differentiation tests in the presence of the ROCK kinase inhibitor (Y-27632, Calbiochem), 5 µM of inhibitor was added at day 1 in DM. Fresh drug was then added every 24 h.

For the quantitative analysis of adhesion and differentiation, at least 50 cells of at least ten different fields (430 µm x 320 µm) were analyzed per condition. To characterize cell adhesion, cell number per field, cell area and circularity were quantified. Cell circularity is a parameter defined by the formula: Circularity = $4\pi(A/P^2)$, (A being the cell area and P its perimeter) that allows to characterize cell morphology: a circularity value of 1.0 indicates a perfect circle and a decrease toward 0 indicates an increasingly elongated polygon.

The differentiation was characterized by the fusion index, which is a ratio of the nuclei contained in myotubes reported to the total number of nuclei [39], and by the percentage of striated myotubes.

2.6. Transfection by siRNA

Cells were transfected with siRNA against β_1 and β_3 integrins (ON-TARGET plus SMARTpool, respectively Mouse ITGB1 and Mouse ITGB3, Thermo Scientific Dharmacon) individually or at the same time, a scrambled siRNA (All Stars negative Control siRNA, Qiagen) being taken as control. For this, the cells were seeded at 30 000 cells/cm^2 in a 6-well plate and cultured in GM (2 mL per well) for 15 h. The transfection mix was prepared as following: for one well, 6 µL of lipofectamine RNAiMAX Reagent (Invitrogen) were added to 305 µL of Opti-MEM medium (Gibco) and 0.72 µL of 1 mM siRNA were added to another 305 µL of Opti-MEM medium. Lipofectamine-containing mix was added to siRNA-containing mix and incubated for 20 min at room temperature. Previously to transfection, the GM of the wells was replaced by the GM without antibiotics. Then, 610 µL of the final mix were added to each well. After 24 h of incubation at 37°C, the cells were transfected for the second time following the protocol described above and incubated for another 24h. Then the cells were detached by trypsin-EDTA, seeded in GM at 20 000 cells/cm^2 on the films built in 96-well plate and allowed to adhere for 4 h. Then, the cells were fixed and their area was quantified.

2.7. Immuno-staining

Cells were first rinsed in PBS and fixed in 3.7% formaldehyde for 30 min at RT before being permeabilized in 0.5% Triton X-100 for 4 min. After rinsing with PBS, samples were incubated for 1 h in 0.1 % BSA in TRIS-buffered saline (TBS, 50 mM TRIS, 150 mM NaCl, 0.1% NaN_3, pH 7.4). Actin was labeled with phalloidin-TRITC (1:800, Sigma) for 30 min. Cell nuclei were stained with Hoechst 33342 (Invitrogen) at 5 µg/ml for 10 min. After the incubations with the primary antibodies (diluted in 0.2% TBS-gelatin) for 30 min at RT, cells were washed 3 times in TBS and incubated for 30 min with the secondary antibodies : rabbit anti-FAK pY397 antibody, (1:200, Invitrogen), myogenin (rabbit anti-myogenin antibody (1:30, Tebu-Bio) and myosin heavy chain (mouse anti-myosin heavy chain (1:500, Sigma) . Alexa-Fluor 388 or 558 conjugated antibodies (Invitrogen) were used at 1:1000. Images were taken by means of Zeiss Axiovert 200 inverted or Zeiss LSM 700 confocal microscope.

2.8. Statistics

The results represent three independent experiments. Data are reported as means ± standard deviation. Student's t-test was performed to compare the different conditions ($p < 0.05$ was considered significant). Statistically different values are reported on the figures.

3. Results

3.1. Density of RGD peptide on the film surface

The principle of film buildup with or without subsequent cross-linking (CL) and/or functionalization with the RGD peptide is depicted in Figure 1A. The four different film architecture studied are given in Table 1: NCL, NCL-RGD, CL and CL-RGD. The film buildup was followed *in situ* by Quartz Crystal Microbalance with dissipation monitoring (QCM-D) (Fig. 1B), which allowed us to measure film thickness using the Voigt model [40]. Film thickness was 120 nm for a film made of 6 layer pairs.

Knowing the grafting density of the RGD peptide to PGA (10%) the amount of RGD peptide present at the film surface was quantified. The adsorbed mass of PGA-RGD was 400 ng/cm^2, which corresponded to a RGD surface density of 0.78 molecules of peptide per nm^2 (or 300 pmol/cm^2). This is a relatively high surface coverage. The Young's modulus of these films deposited on a thick polyelectrolyte cushion has previously been measured to be 51 ± 17 kPa for NCL films and 230 ± 70 kPa for CL ones [36].

3.2. Effect of RGD-functionalization and film cross-linking on C2C12 myoblast adhesion, spreading and morphology

Adhesion is the very first and important step of cell-substrate interactions, which is especially important for anchorage-dependent cells. To evaluate the effect of film stiffness and RGD-functionalization on C2C12 myoblast adhesion, cells were cultured on the four different types of films NCL, NCL-RGD, CL and CL-RGD. The cells were allowed to adhere for 1 h in serum free medium (SFM) to eliminate any effect of serum on early adhesion. The number of adherent cells as well as their spreading area and morphology (circularity) were evaluated. Actin and nuclei staining of C2C12 cells (Fig. 2A) revealed the presence of adherent cells on NCL-RGD, CL and CL-RGD films but of very few cells on NCL ones. In addition, these cells were poorly spread. Quantitative measurements of the number of adherent cells confirmed the microscopy observations with no statistical differences between NCL-RGD, CL and CL-RGD (Fig. 2B). However, after 1 h, cell area was significantly higher on films presenting PGA-RGD (Fig. 2C) as compared to those ending with PGA only. Cells spread also about two times more on CL films as compared to NCL ones. Thus, both substrate stiffness and RGD-functionalization had an effect on cell spreading. The circularity index was significantly lower for films containing the RGD peptide as compared to films without peptide (NCL and CL) (Fig. 2D). This indicated that the presence of RGD but not film stiffness influenced the cell circularity.

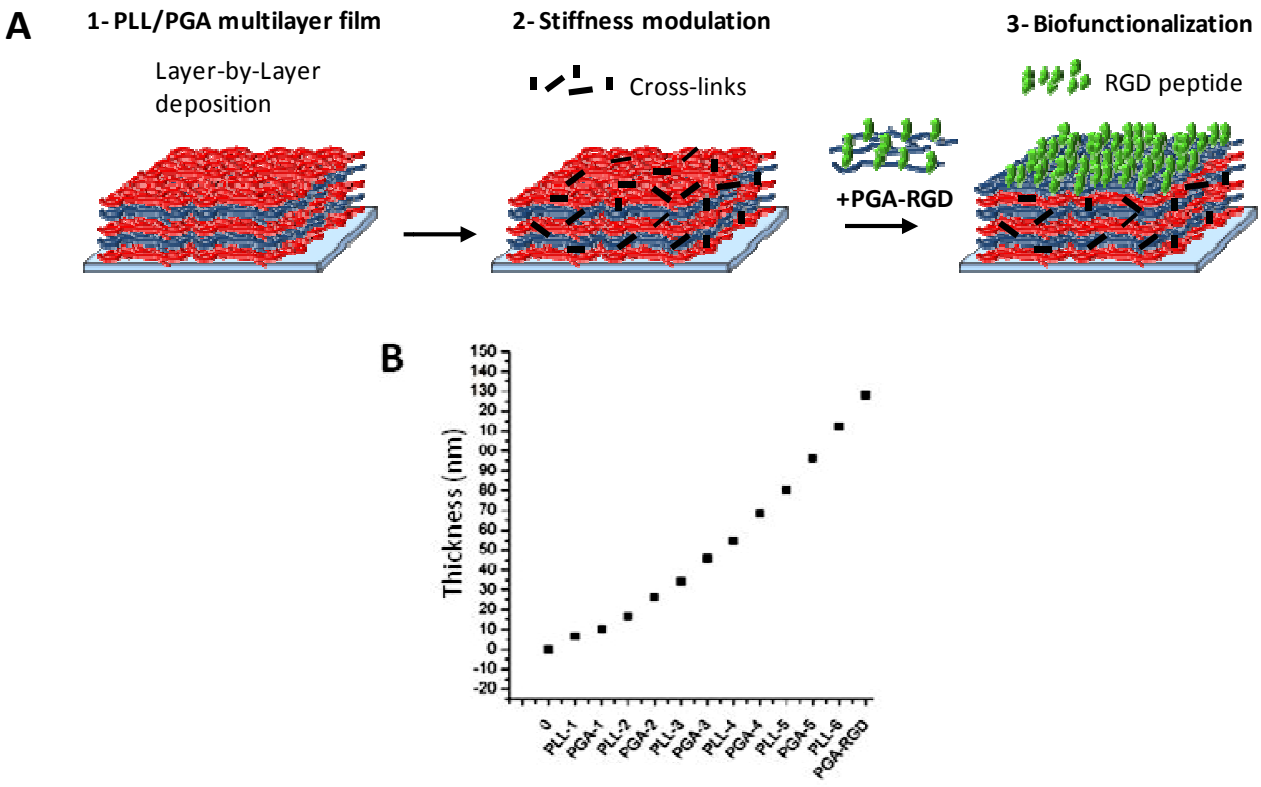

FIGURE 1. Design of biomimetic thin film combining physical and biochemical cues. *(A) 1- a polyelectrolyte multilayer film (PEM) is built onto a substrate by alternating deposits of PLL and of PGA. 2- The PEM film can be covalently cross-linked using a water-soluble carbodiimide to modulate its stiffness. 3- Biochemical functionality is provided by adding a final layer of PGA grafted with a RGD-containing peptide. (B) Exponential growth of the film followed by QCM-D.*

3.3. Characterization of adhesion via integrin receptors and cell migration

The cells are mechano-sensors that actively sense their environment via specific cell surface receptors, especially integrins [41]. Several integrins can interact with RGD ligand, especially $\alpha_5\beta_1$ and $\alpha_V\beta_3$. Cell sensing and integrin activation lead to the formation of focal adhesions (FA), sites where the cells contact with the matrix. FA are enriched in integrins and many other proteins, are linked to actin stress fibers and are a place for cell traction [42; 43].

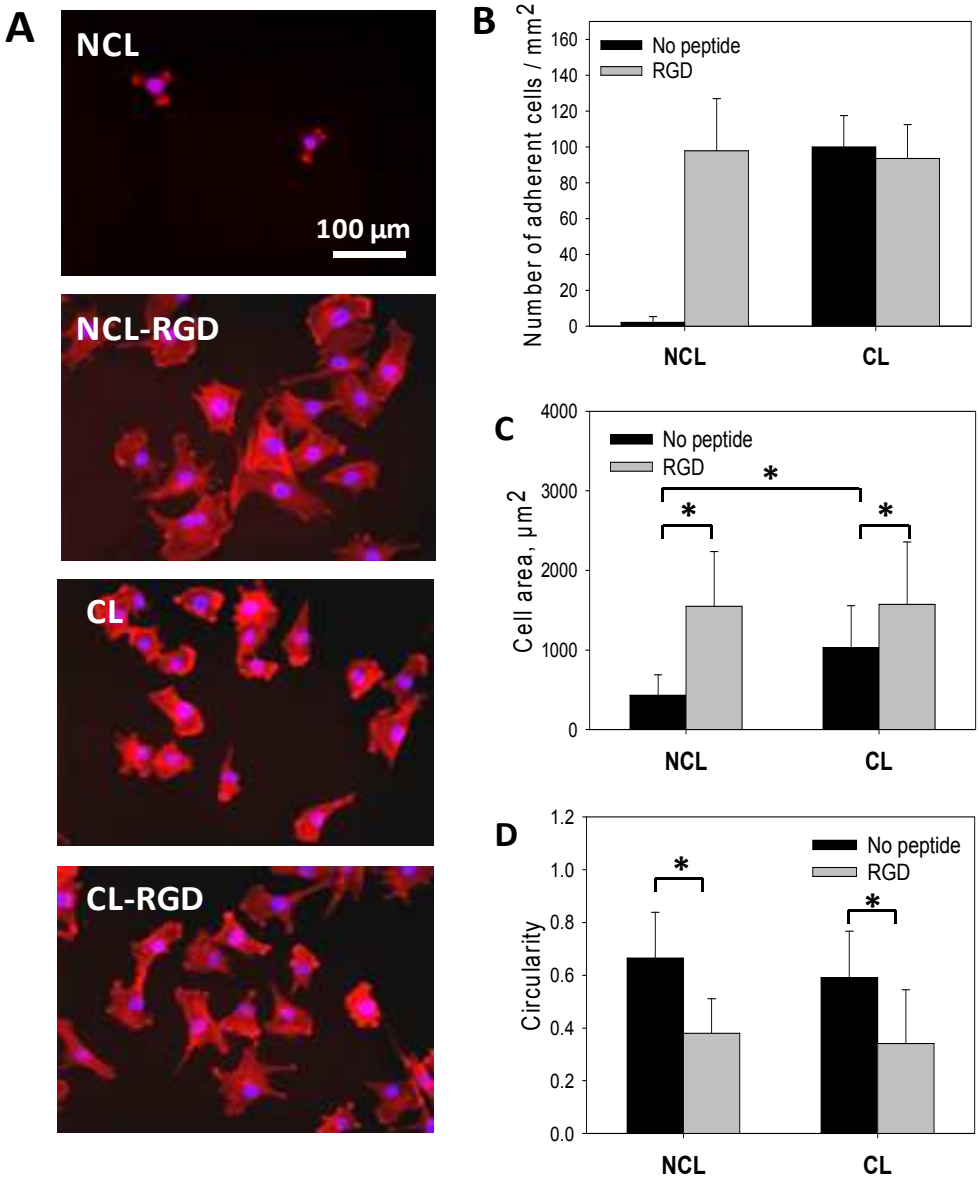

FIGURE 2. Adhesion and spreading of C2C12 myoblasts at early time. *Initial C2C12 cell adhesion and spreading were observed 1 h after plating the cells on NCL, CL, NCL-RGD and CL-RGD films. (A) Actin (red) and nuclei (blue) staining of C2C12 cells to visualize adhesion and spreading on the four types of films (B) Number of adherent cells. (C) Spreading area. (D) Cell circularity quantification. Error bars correspond to SD, * : $p < 0.05$.*

To characterize cell interaction with the substrate via integrin receptors, the formation of stress fibers and the presence of focal adhesions by labeling phosphorylated focal adhesion kinase (pFAK, an important component of mature FA), were first analyzed in C2C12 cells cultured on the different films after 4 h (Fig. 3A and B). After 4 h, stress fibers were observed on all types of films (Fig. 3A). Robust focal adhesions or even fibrillar adhesions (small dashes at the cell periphery) were formed only on NCL-RGD films, while only small and thin focal adhesions or focal complexes (small dots) were visible on CL and CL-RGD films (Fig. 3B). These results showed that both film stiffness and RGD-functionalization played a role in the organization of the actin cytoskeleton and in the formation of focal adhesions as well. The presence of the adhesive ligand on soft films led to the formation of numerous focal and fibrillar adhesions, while only focal complexes formed on the stiffest films, even in the presence of RGD.

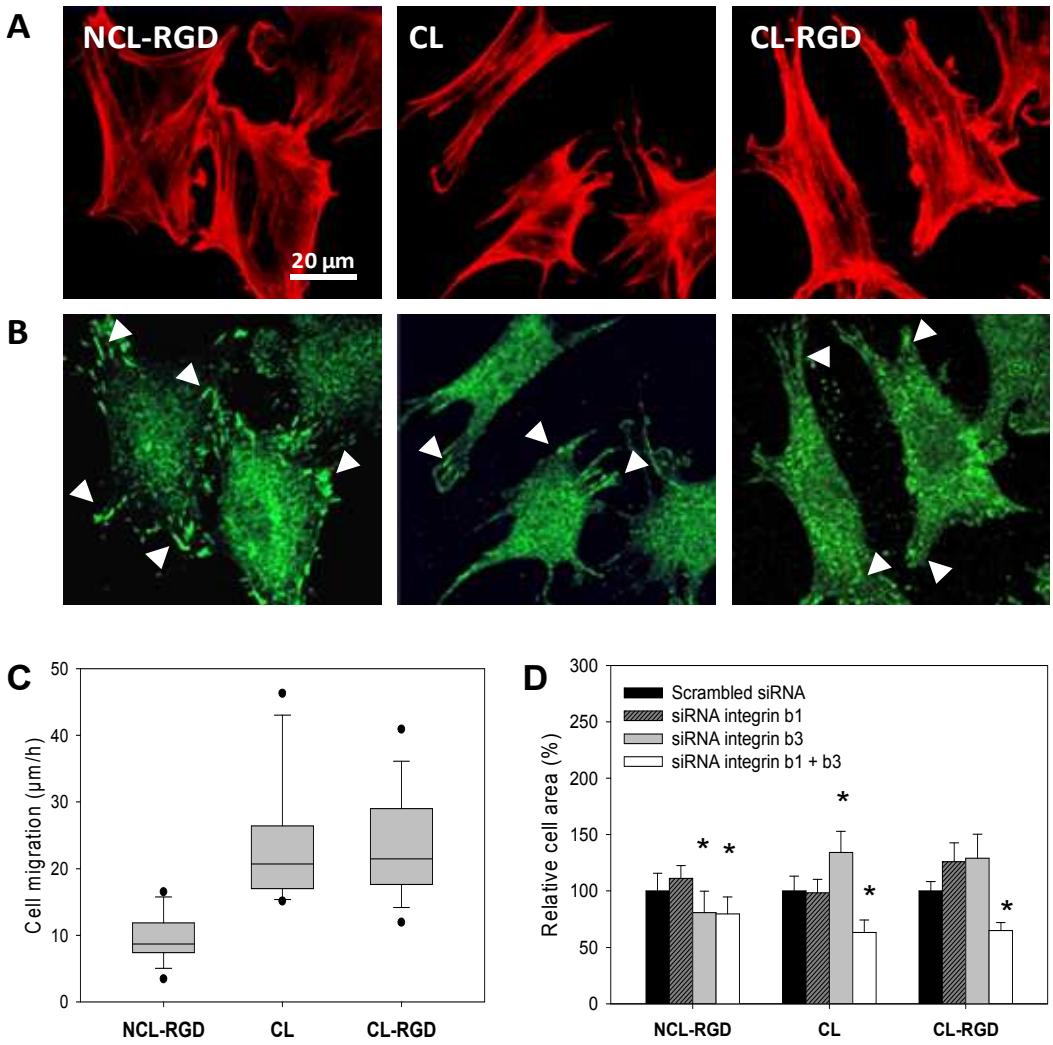

FIGURE 3. Effect of film stiffness and RGD fonctionalization on cytoskeletal organization, focal adhesions and migration. *(A) Staining of actin cytoskeleton (red) after 4 h of culture. (B) Staining of phosphorylated focal adhesion kinase (pFAK Y397, green) after 4 h of culture. (C) Myoblast migration measured over 5 h after seeding. (D) Effect of blocking β_1 and/or β_3 integrins using siRNA: quantification of the cell area after 4 h of adhesion (* $p < 0.05$ compared to scrambled siRNA). Focal adhesions/complexes are indicated by white arrowheads.*

As stress fibers and focal complexes/adhesions play a key role in cell migration, we investigated whether cell migration is influenced by the substrates. To this end, cell migration on the different films over 5 h after cell seeding was followed by tracking individual cells. The results for the migration speed on the different films are shown in Fig. 3C. Cell migrated at ~20 μm/h on stiff films (CL and CL-RGD), which was about two times faster than cells on NCL-RGD films (10 μm/h). Thus, the decrease of focal adhesions on stiff films (CL and CL-RGD) correlated with an enhanced migration on these films.

In order to investigate the possible role of beta chain integrins in cell adhesion, the knockdown of β_1 or β_3 integrin or both using siRNA approach was studied. These integrins are known to be involved in cell mechano-sensing and β_1 and β_3 integrins are present in C2C12 myoblasts [44 45]. The cell area of the transfected cells was quantified after 4 h of adhesion (Fig. 3D). On NCL-RGD films, only β_3 blocking but not of β_1 lead to a slight decrease in cell spreading. Double tranfection of β_1 and β_3 siRNA gave similar results. These data suggested that myoblast interaction with the RGD-containing peptide involved partly β_3 integrins. On CL and CL-RGD films, siRNA against β_1 or β_3 alone did not decrease cell spreading, and even significantly increased it in the case of siRNA β_3 treatment on CL film. However, when the cells were transfected with both β_1 and β_3 siRNA, cell area decreased significantly on CL and CL-RGD films, suggesting that both β_1 and β_3 integrins can be used by the cells in a commutable way to interact with these films. Thus, it appeared that integrins involved in cell spreading on the different films are different.

3.4. Effect of film cross-linking and RGD-functionalization on myogenic differentiation

C2C12 myoblasts are a well-known model for the *in vitro* study of myogenic differentiation due to their ability to reproduce processes that take place during *in vivo* differentiation of skeletal muscle progenitors [46]. The effect of film stiffness and presentation of the RGD ligand on myoblast differentiation in myotubes were studied over 9 days. Phase contrast microscopy images of myogenic differentiation are shown in Fig. 4A. The formation of myotubes was observed on NCL-RGD films, while cell aggregation followed by detachment occurred on both CL and CL-RGD films, after 1-2 days on CL-RGD films and after 2-3 on CL ones. Some detached cells were able to form aggregates that remained adherent until day 9 of differentiation.

Staining of myosin heavy chain (MHC), a late marker of myogenic differentiation [7] was used to characterize myogenic differentiation and the formation of myotubes. MHC was well-expressed only in myoblast cultured on NCL-RGD films, while its expression on CL and CL-RGD films was very weak (Fig. 4B). The fusion index was of 25% of NCL-RGD films and only of 8% for CL and 3% for CL-RGD films (Fig. 4C). Thus, only a small fraction of the remaining cell adhered on CL and CL-RGD films was able to fuse. Moreover, the multinucleated cells on these films neither had the typical elongated morphology of myotubes nor were striated. It was solely for cells grown on NCL-RGD films that striation reached 67% of the myotubes, indicating that their maturation was very good (Fig. 4B, upper image of right column).

These results showed that the soft RGD-functionalized film used in our study was the only film architecture enabling myoblast differentiation and fusion in an efficient manner. Conversely, CL and CL-RGD films were not appropriate for long term differentiation in myotubes.

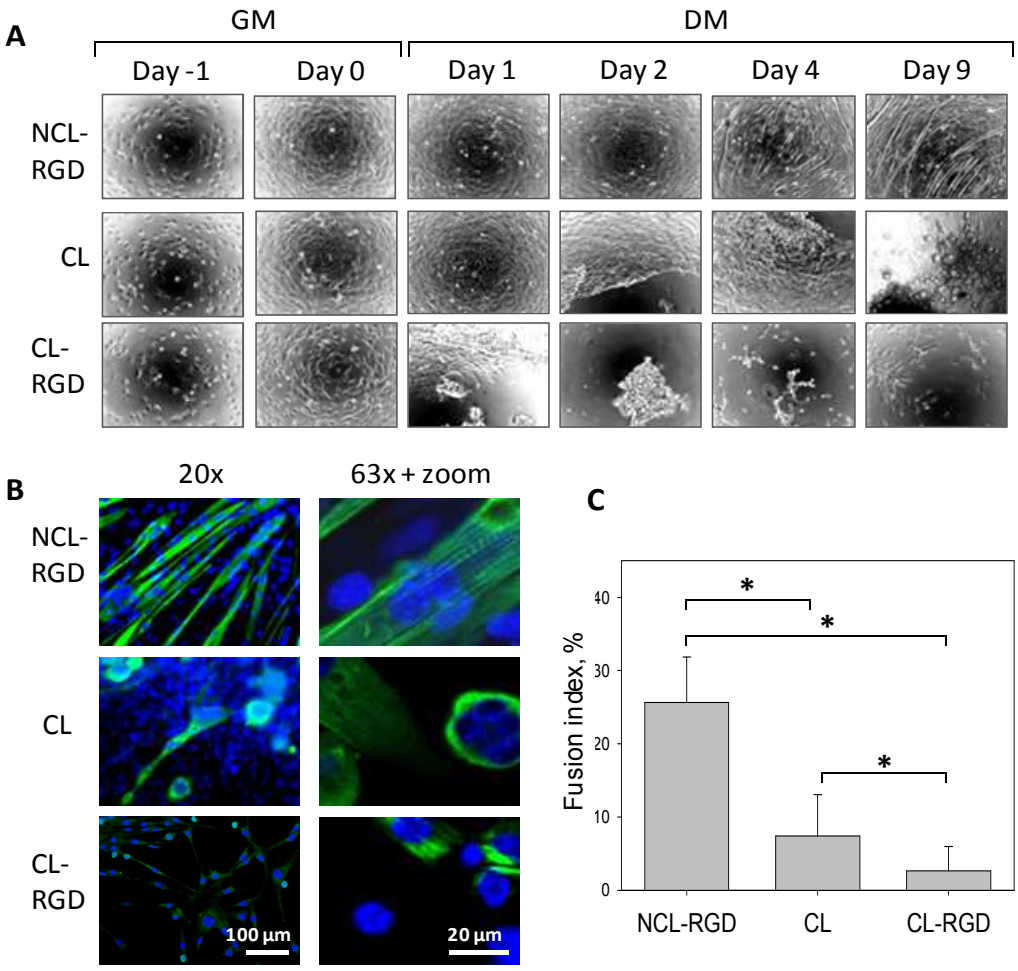

FIGURE 4. Myogenic differentiation of C2C12 myoblasts is effective on NCL-RGD films. *(A) Phase contrast microscopy observations of C2C12 cell differentiation on the NCL-RGD, CL, and CL-RGD films. After 24 h of proliferation in GM (ie Day -1), the cells were put in DM (ie Day 0) and were let to differentiate until Day 9. Cell detachment was observed on CL and CL-RGD films after few days in DM. (B) Myosin heavy chain (green) and nuclei (blue) labeling (20 x and 63 x magnification). (C) Quantification of the fusion index. Error bars correspond to SD, * : $p < 0.05$.*

3.5. C2C12 myoblasts poor differentiation on stiff films is associated with a decreased myogenin expression and enhanced proliferation

For skeletal myoblasts, cell cycle arrest is necessary to undergo differentiation. During myogenic differentiation, a highly ordered process of temporally separable events that begins with the expression of myogenic transcription factors and is followed by cell cycle arrest takes place [7]. In order to further understand the origin of the inappropriate differentiation on stiff films, we quantified the expression of the transcription factor myogenin at early times of the differentiation process (Day 1 to 3) (Fig. 5). On NCL-RGD films, myogenin was already expressed at day 1 (4% of nuclei) and steadily increased until day 3 (13% of nuclei). On CL films, only 1% of nuclei were myogenin-positive at Day 1 and 5% at Day 3. On CL-RGD films, no positive nuclei was detected at Day 1 or 3, but about 2.5% of myogenin-positive cells were observed at Day 2. These results showed that myogenin expression is decreased on stiff films, especially on CL-RGD one where no positive nuclei were found at Day 3.

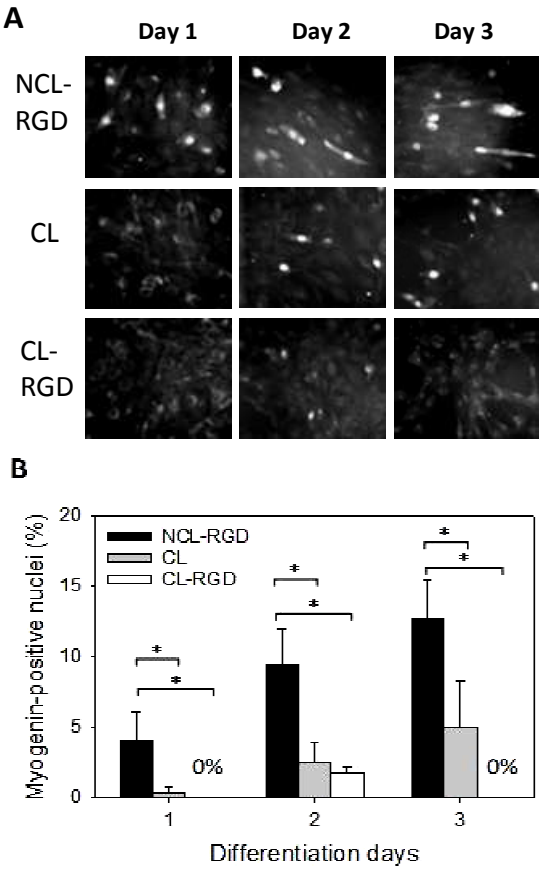

FIGURE 5. Myogenin expression is decreased on stiff films. *After 24 h of proliferation in GM, the medium was changed to DM and cells were let to differentiate for 2 days. (A) Myogenin labeling at day 1, 2 and 3 of differentiation. (B) Quantification of the percentage of myogenin expressing cells. Error bars correspond to SD, * : $p < 0.05$.*

As down-regulation of proliferation is needed for myogenesis to occur [7], we also quantified cell proliferation on the different types of films before and after addition of the DM (Day -1 to 1) by a BrdU incorporation assay (Fig. 6). Day -1 and Day 0 represent the initial growth phase in GM at 4 h and 24 h after cell seeding, respectively, before switching to DM. No difference in the percentage of proliferating cells between the three types of films was observed in GM (Fig. 6B). However, significant differences were observed after 24 h of culture in DM, noted here Day 1. As anticipated, the rate of proliferating cells decreased drastically on NCL-RGD films from 50 % to 10 %, which corresponded to the cell cycle arrest. Conversely, on CL and CL-RGD films, these rates not only failed to decrease but still increased to reach ~90%. As a consequence, at Day -1 and Day 0, the total cell number on the three types of films was similar (Fig. 6C) but at Day 1, the number of cells on stiff films was higher than on NCL-RGD. The highest cell number was found on CL-RGD film.

These results showed that two key events in myogenic differentiation, i.e. myogenin expression and cell cycle arrest, were altered on stiff films. Cells on stiff films bypass the cell cycle exit induced by growth factor deprivation. Cell detachment observed on stiff films may thus be due to enhanced proliferation leading to excessive cell confluence, and/or to enhanced cell migration.

3.6. Effect of inhibition of ROCK kinase on myogenin expression, proliferation and differentiation on stiff films

Previous studies have shown that myoblast differentiation is regulated through Rho/ROCK pathways that must be downregulated to allow myogenesis [47]. These authors have shown that constitutive activation of ROCK resulted in decreased myogenin expression and inhibition of myogenic differentiation in C2C12, while inhibition of ROCK led to an accelerated exit from the cell cycle and induced myogenin expression. These data suggested that ROCK is involved in keeping the myoblasts cycling and prevents commitment to differentiation [48]. We thus hypothesized that decreased myogenin expression and excessive proliferation on CL films, resulting in poor differentiation, may be due to an enhanced ROCK activity. To investigate if ROCK pathway was involved in inappropriate cell differentiation on stiff films, the ROCK inhibitor Y27632 was added at Day 0 of differentiation. Its effect on myogenin expression was evaluated at Days 1, 2 and 3, and on proliferation at Day 1. In addition, MHC was labeled at Day 6.

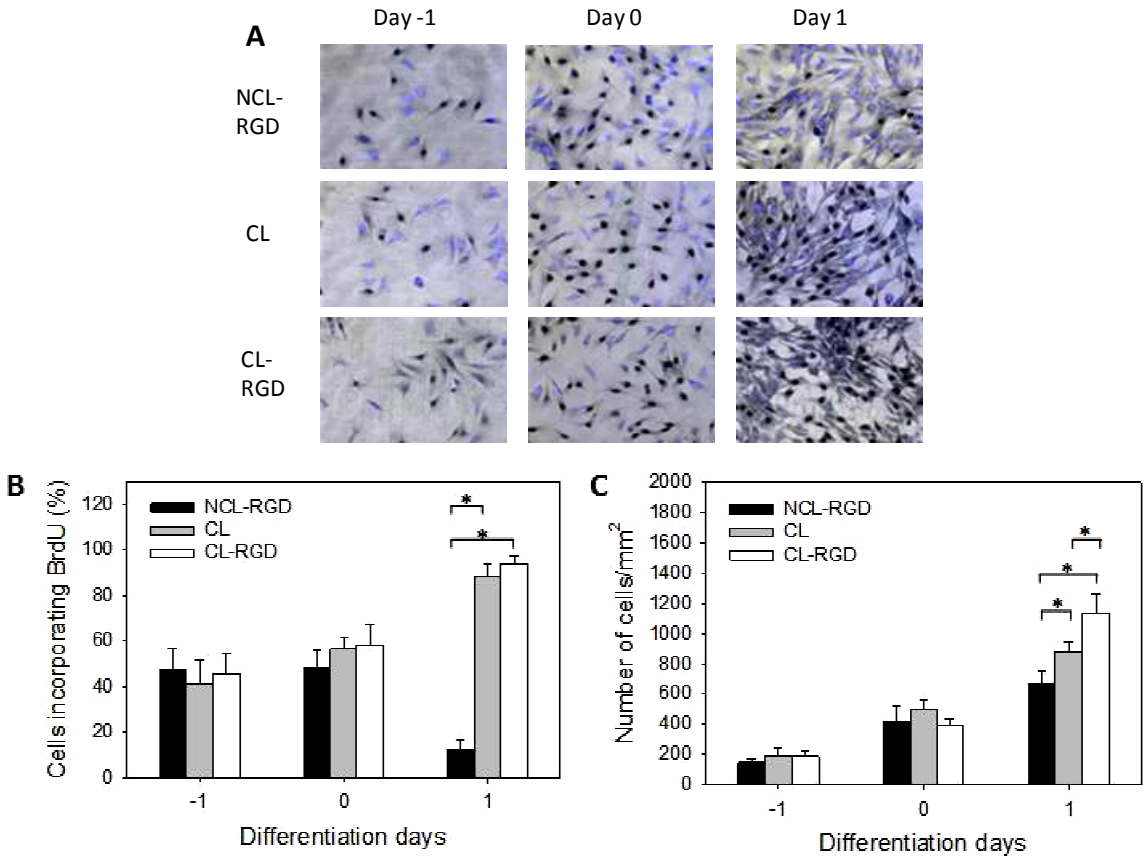

FIGURE 6. Proliferation is enhanced on CL films resulting in an increased cell number. *After 24 h of proliferation in GM (Day -1), the medium was changed to DM (Day 0) and cells were let to differentiate for one day. (A) Staining of BrdU in the nuclei (in black) associated to a fluorescent labeling of total nuclei (blue). (B) Percentage of BrdU-positive cells. (C) Quantification of the total number of adherent cells. Error bars correspond to SD, * : $p < 0.05$.*

First, we studied the effect of ROCK inhibitor on myogenin expression (Fig. 7A-C). On NCL-RGD films, Y27632 treatment did not alter myogenin expression at any time (Fig. 7A). On CL films, a 2-fold increase in myogenin-positive nuclei was observed after 3 days of treatment, reaching 10% (Fig. 7B). On CL-RGD films, myogenin expression remained very weak at less than 3% in any conditions. However, it was still present at Day 3 when treated with ROCK inhibitor, while it was absent in a control (non-treated) condition (Fig. 7C).

The effect of Y27632 on C2C12 myoblast proliferation at Day 1 was also tested (Fig 7D). There was no difference for NCL-RGD films, but we observed a 3-fold decrease in BrdU-incorporating cells on CL and CL-RGD films. This indicated that ROCK was involved in excessive C2C12 proliferation on these films.

MHC expression on NCL-RGD films was not modified by Y27632 treatment (Fig. 7E). In contrast, on CL films, Y27632 treatment was sufficient to prevent cell detachment and to allow myogenic differentiation. Of note, the myotubes formed were not as elongated as on NCL-RGD films and nuclei were more clustered. Finally, no differentiation was observed on CL-RGD films upon Y27632 treatment, suggesting that ROCK inhibition alone was insufficient to restore the differentiation program, and that a more complex molecular mechanism was involved in the cell response to these films.

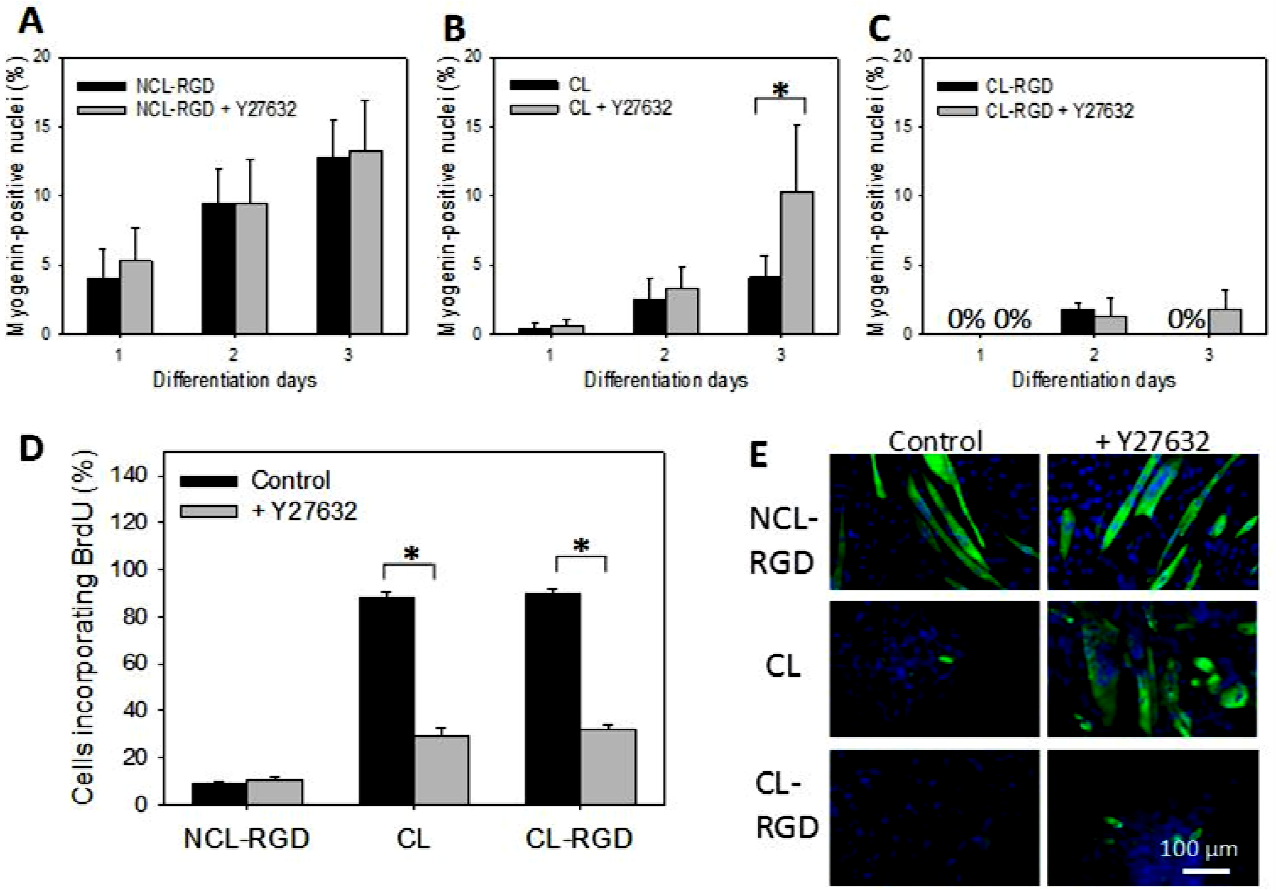

FIGURE 7. ROCK kinase inhibition decreases myoblast proliferation and rescues differentiation on CL films. *After 24 h of proliferation in GM, cells were transferred to DM and let to differentiate for 6 days. (A, B, C) Myogenin labeling at day 1, 2 and 3 in DM. (D) Percentage of BrdU-positive cells at Day 1 of differentiation. (E) Myosin heavy chain labeling at Day 6 of differentiation. Error bars correspond to SD, * : $p < 0.05$.*

4. Discussion

It is becoming increasingly clear that mechanical and biochemical properties of the substrate both play an important role not only in cell adhesion, but in many other processes such as proliferation and differentiation [25]. However, the contribution of each type of signal, i.e substrate stiffness and adhesive ligand, is not always easy to decouple. Mechano-sensitivity studies often use synthetic hydrogels such as PA with ECM proteins or PEG grafted with ECM fragments [49]. It is already acknowledged that mechanical properties of the substrate can affect muscle cell adhesion and differentiation. This has been observed on PA surfaces [23], PEG hydrogels [27] and on PEM films made of PLL and hyaluronan [28; 50]. However, little work has been done on the role of RGD-containing peptides in myogenic differentiation. Rowley and Mooney [51] showed that RGD-peptide was necessary to promote myoblast attachment to alginate hydrogels and that myoblast differentiated only on alginate gels with specific combination of monomeric ratio and RGD grafting density [51]. In addition, RGD-peptides were found to significantly improve myoblast cell adhesion onto grooved polystyrene substrates [52].

Here, we used layer-by-layer films made of polypeptides as modular substrates, which can be stiffened by chemical cross-linking and can be specifically functionalized by grafting a RGD-containing peptide onto PGA [37]. In a previous study, the 15-amino-acid collagen

type I-derived peptide containing an RGD adhesive sequence has been tested for both short-term adhesion properties and long-term proliferation of primary osteoblasts [37]. In the present work, four different types of films with or without cross-linking and with or without the RGD-peptide allowed investigation of the effect of mechanical and biochemical signals and their combinations as well, on important events of myogenesis. We especially focused on the sequence of events involved in C2C12 cell differentiation including early adhesion, migration, proliferation, differentiation and fusion of myoblast into myotubes.

The results obtained by QCM-D regarding (PLL/PGA) film growth (Fig. 1) are consistent with those obtained previously by optical waveguide lightmode spectroscopy on the same films [37], with however a higher thickness measured by QCM-D due to the water incorporated in the films.

While the cells spread more on the RGD-functionalized films, a more detailed analysis of cell interaction with the substrates showed that the stiffness was also very important: only cells on NCL-RGD film exhibited formation of robust focal adhesions and migrated at low speed. The presence of only small focal complexes on stiff films (CL and CL-RGD) (Fig. 3) correlated with an enhanced migration on these films (Fig. 6). Our results also suggested that soft films with RGD and stiff films recruit different combinations of integrin receptors: while β_3 knockdown alone had an effect on myoblast spreading on NCL-RGD films, the knockdown of both β_1 and β_3 is required to affect myoblast spreading on CL and CL-RGD films (Fig 3D). However, the inhibition of cell spreading on the different films was never complete by blocking β_1, β_3 or both integrins at the same time (Fig 3D), suggesting that other integrin or non-integrin receptors may be involved. It has been shown using epithelial cells that β_1 and β_3 integrins promote different migration modes: adhesion by β_3 resulted in static cell-matrix adhesions and persistent migration, while adhesion by β_1 promoted highly dynamic cell-matrix interactions and random migration [53]. These results make a link between cell-surface interactions via specific integrin receptors, focal adhesion dynamics and cell migration. Our results on myoblasts show that there is a correlation between integrins that are recruited, size of focal adhesions/complexes and cell migration speed: involvement of β_3 correlates with robust adhesion and low migration speed, while recruitement of both β_1 and β_3 are related to smaller adhesion complexes and enhanced cell migration (Fig. 3). Our results thus suggests that control of motile strategy by integrins may be a common feature of different cell types.

Interestingly, β_3 integrin was found to be crucial for myogenic differentiation of C2C12 myoblasts, and to mediate satellite cell differentiation [45], while β_1-integrin, which is constitutively expressed in skeletal muscle, has earlier been shown to be dispensable to myogenesis [54]. This is in agreement with our data showing that on the PEM films, the differentiation was only possible on soft films with RGD peptide whereas stiff films offer unfavorable conditions for the differentiation; proliferation was enhanced (Fig. 6) and myogenin expression was decreased on stiff films (Fig. 7). Moreover, the cells detached from stiff films after few days in DM. We hypothesize that cell detachment could be due to enhanced proliferation leading to excessive cell confluence, and/or to enhanced cell migration. The ROCK kinase, which is known to be involved in myogenic differentiation but also in cell blebbing may be responsible for cell detachment (for review, see [55]).

Interestingly, myoblast differentiation could be partially rescued on CL films by treatment with ROCK inhibitor, which decreased proliferation

level and increased myogenin expression (Fig 7B). However, on CL-RGD films, even if the myoblast treated with ROCK inhibitor showed a decreased proliferation level, they were still unable to express myogenin and to differentiate (Fig. 7C). Enhanced ROCK activity on stiff films may be the consequence of the engagement of β_1 integrin on these films since it was reported that β_1 induces a higher RhoA activity than β_3 [53]. Both RhoA and its effector ROCK play a crucial role in myogenic differentiation as both activities must be downregulated to allow myogenesis to occur [47; 48; 56; 57].

In our previous work [28] we evaluated the adhesion and differentiation of C2C12 myoblasts using poly(L-lysine) and hyaluronan (PLL/HA) multilayer films of varying stiffnesses. On these films, formation of focal adhesions was increased on stiff films as compared to soft ones. Evaluation of the adhesive behaviour during the initial steps of spreading showed that blocking β_3, but not β_1 integrins inhibited cell adhesion on stiff (PLL/HA) films [50]. This is different from cross-linked (PLL/PGA) films, which are stiffer than (PLL/HA) films) and for which blocking of both β_1 and β_3 integrins was necessary to inhibit cell spreading. Thus, molecular mechanisms of cell/film interactions involved different integrins depending on film type, film stiffness and presence of a specific ligand (RGD peptide).

Cell adhesion to ECM influences cell proliferation by transducing signals through cell surface integrin receptors, and proliferation is generally low in soft matrix and high in stiff matrix [58; 59]. Proliferation of C2C12 myoblasts was also increased on stiff substrates as compared to soft ones [24; 28]. Here, we showed that the proliferation of C2C12 was significantly increased on stiff films via the activation of ROCK (Fig. 7). Rho/ROCK pathway is also known to be implicated in the remodeling of focal adhesions and migration of tumor cells [60]. Similarly, tumor malignancy and invasion is associated to matrix stiffening [61]. In this context, C2C12 cells on stiff films seemed to acquire some features of cancer cells: they bypassed the cell cycle exit induced by growth factor deprivation, showed an absence of mature focal adhesions and enhanced migration. Thus, CL and/or CL-RGD films may be used as a model basement membrane for studies of cancer cell behavior in response to matrix stiffening. Decreased myogenin expression and absence of exit from the cell cycle observed on cross-linked films could also be a potential tool for *in vitro* amplification of satellite cell while preserving their multiple differentiation potential. Indeed, these primary cells rapidly lose their stem properties and switch to differentiation upon removal from their niche and cultured *in vitro* [8].

Based on our experimental data, we propose a model for the interplay between mechanical and biochemical stimuli during induction of C2C12 myogenic differentiation (Fig. 8). Adhesion on NCL-RGD films involved β_3 integrins and provided favorable conditions for myogenic differentiation of C2C12 cells. Adhesion on stiff films (CL and CL-RGD) involved β_1 integrins in addition to β_3 integrins and promoted ROCK activation. This leads to a high proliferative state without myogenic differentiation. On CL films, ROCK inhibition allowed myogenic differentiation. However, on CL films ending by RGD peptide, ROCK inhibition was not sufficient to induce myogenin expression and to allow cells differentiation. We suggest that mechanical signals (stiffness) on CL-RGD films may affect cell interaction with biochemical signals (RGD peptide), resulting in the inhibition of β_3 integrins by RGD peptide or by β_1 integrins.

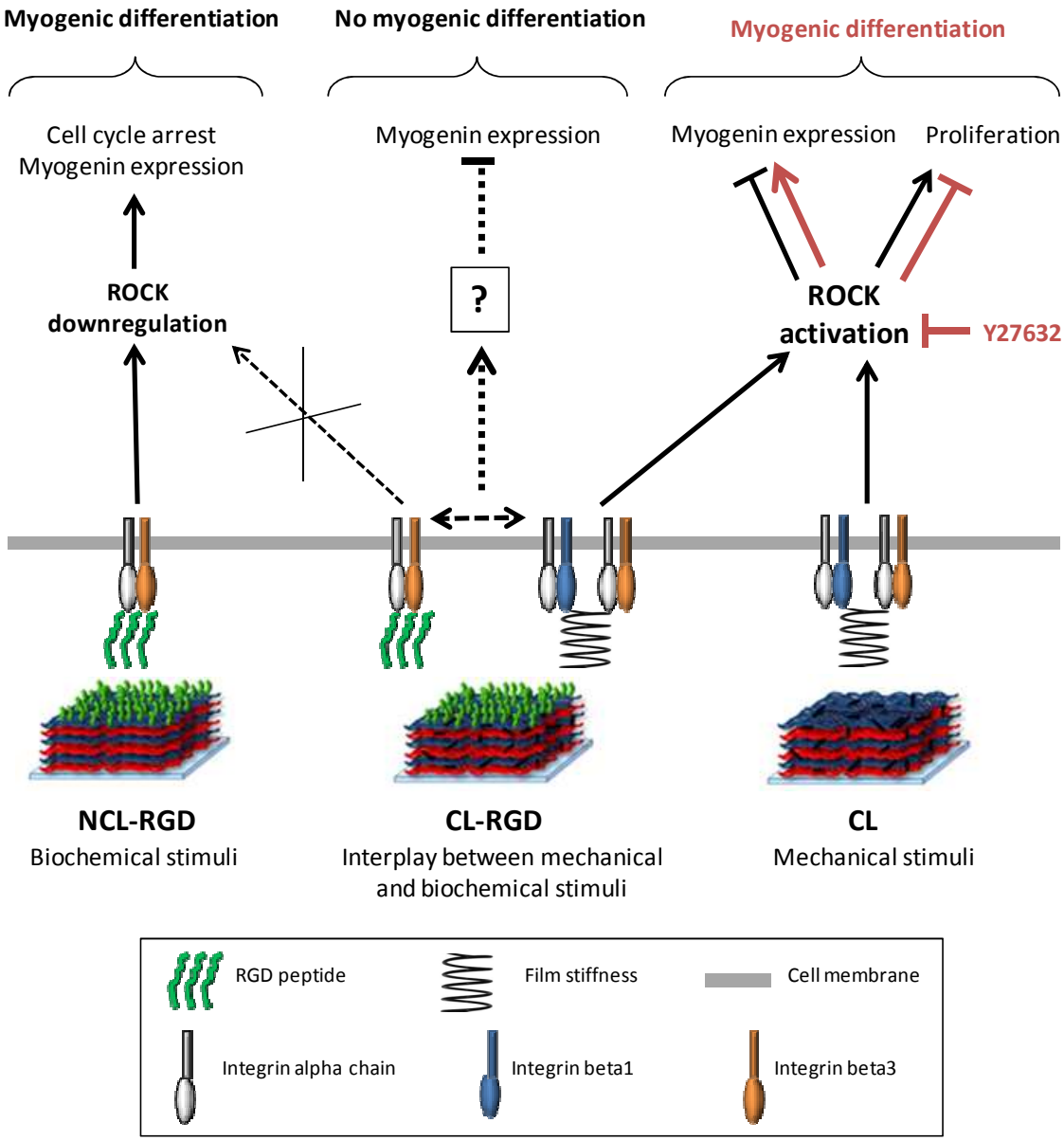

FIGURE 8. Model of the interplay between mechanical and biochemical stimuli during induction of C2C12 myogenic differentiation on soft/stiff films functionalized or not with the RGD peptide. *Adhesion involving β_3 integrins on NCL-RGD films (soft films with covalently attached RGD peptide) provides favorable conditions for myogenic differentiation of C2C12 cells: when the medium is changed to DM, the rate of proliferating cells decreases and that of myogenin increases. Adhesion on CL and CL-RGD films (stiff films) involving β_1 and β_3 integrins promotes ROCK activation leading to a high proliferative state even in DM and to low myogenin expression. When the cells on stiff films are treated with ROCK inhibitor during differentiation, the rate of proliferating cells decreases significantly on both CL and CL-RGD films. Additionally, on CL films, myogenin expression increases, allowing the cells to undergo myogenic differentiation. However, on CL-RGD films, ROCK inhibition was not sufficient to induce myogenin expression and to allow cell to differentiate. We suggest that mechanical signals (stiffness) on CL-RGD films may affect cell interaction with biochemical signals (RGD peptide), resulting in the inhibition of β_3 integrins by RGD peptide or by β_1 integrins.*

Thus, our findings underline the importance of engineering substrates with well-controlled properties, as mechanical signals provided by the substrate can modify cell responses to biochemical cues. In this context, NCL-RGD represents a tool for the study of cell responses to RGD independently of the pathways activated by mechanical signal. Besides, in view of their excellent capacity to support myogenic differentiation, the soft films ending by RGD may be used as coating of various types of scaffolds used in muscle tissue engineering.

5. Conclusions

In the present work, four different types of PEM films, with or without cross-linking and with or without the RGD-peptide, allowed investigation of the effect of mechanical and biochemical signals and their combinations on important events of myogenesis. Soft films with RGD peptide appeared as the most appropriate for myogenic differentiation of C2C12 myoblasts, while stiff films (CL and CL-RGD) induced enhanced migration and proliferation and inhibited myogenic differentiation. ROCK inhibition was sufficient to rescue C2C12 differentiation on CL films but no significant changes were observed on CL-RGD films, showing that different signaling pathways were activated on each type of film depending on their mechanical and biochemical properties. Our model allowed highlighting how important events in myogenesis such as adhesion, migration proliferation, myogenin expression and fusion are regulated by substrate elasticity and presence of an adhesive ligand.

These results suggest that thin films with tunable mechanical and biochemical properties may be a useful tool for biophysical studies of muscle progenitors on controlled 2D microenvironments as well as for their expansion and differentiation *in vitro*. In addition, these films could be very easily be used to coat a wide range of 2D structured materials and 3D scaffolds.

Acknowledgements

This research was supported by Region Rhônes-Alpes via a PhD fellowship to VG. CP and RAV are members of the Institut Universitaire de France (IUF). CP wishes to thank the European Commission for support in the framework of FP7 via an ERC Starting grant 2010 (GA 259370, BIOMIM).

REFERENCES

1. Bischoff, R. (1975). Regeneration of single skeletal muscle fibers in vitro. *Anat Rec* **182**, 215-35.
2. Le Ricousse-Roussanne, S., Larghero, J., Zini, J. M., Barateau, V., Foubert, P., Uzan, G., Liu, X., Lacassagne, M. N., Ternaux, B., Robert, I., Benbunan, M., Vilquin, J. T., Vauchez, K., Tobelem, G. & Marolleau, J. P. (2007). Ex vivo generation of mature and functional human smooth muscle cells differentiated from skeletal myoblasts. *Exp Cell Res* **313**, 1337-46.
3. Katagiri, T., Yamaguchi, A., Komaki, M., Abe, E., Takahashi, N., Ikeda, T., Rosen, V., Wozney, J. M., Fujisawa-Sehara, A. & Suda, T. (1994). Bone morphogenetic protein-2 converts the differentiation pathway of C2C12 myoblasts into the osteoblast lineage. *J Cell Biol* **127**, 1755-66.
4. Schindeler, A., Liu, R. & Little, D. G. (2009). The contribution of different cell lineages to bone repair: exploring a role for muscle stem cells. *Differentiation* **77**, 12-8.
5. Teboul, L., Gaillard, D., Staccini, L., Inadera, H., Amri, E. Z. & Grimaldi, P. A. (1995). Thiazolidinediones and fatty acids convert myogenic cells into adipose-like cells. *J Biol Chem* **270**, 28183-7.
6. Wada, M. R., Inagawa-Ogashiwa, M., Shimizu, S., Yasumoto, S. & Hashimoto, N. (2002). Generation of different fates from multipotent muscle stem cells. *Development* **129**, 2987-95.
7. Andres, V. & Walsh, K. (1996). Myogenin expression, cell cycle withdrawal, and phenotypic differentiation are temporally separable events that precede cell fusion upon myogenesis. *J Cell Biol* **132**, 657-66.
8. Cosgrove, B. D., Sacco, A., Gilbert, P. M. & Blau, H. M. (2009). A home away from home: challenges and opportunities in engineering in vitro muscle satellite cell niches. *Differentiation* **78**, 185-94.
9. Thorsteinsdottir, S., Deries, M., Cachaco, A. S. & Bajanca, F. (2011). The extracellular matrix

dimension of skeletal muscle development. *Dev Biol* **354**, 191-207.
10. Cohn, R. D., Henry, M. D., Michele, D. E., Barresi, R., Saito, F., Moore, S. A., Flanagan, J. D., Skwarchuk, M. W., Robbins, M. E., Mendell, J. R., Williamson, R. A. & Campbell, K. P. (2002). Disruption of DAG1 in differentiated skeletal muscle reveals a role for dystroglycan in muscle regeneration. *Cell* **110**, 639-48.
11. Han, R., Kanagawa, M., Yoshida-Moriguchi, T., Rader, E. P., Ng, R. A., Michele, D. E., Muirhead, D. E., Kunz, S., Moore, S. A., Iannaccone, S. T., Miyake, K., McNeil, P. L., Mayer, U., Oldstone, M. B., Faulkner, J. A. & Campbell, K. P. (2009). Basal lamina strengthens cell membrane integrity via the laminin G domain-binding motif of alpha-dystroglycan. *Proc Natl Ac Sci U S A* **106**, 12573-9.
12. Hynes, R. O. (2002). Integrins: bidirectional, allosteric signaling machines. *Cell* **110**, 673-87.
13. Mayer, U. (2003). Integrins: redundant or important players in skeletal muscle? *J Biol Chem* **278**, 14587-90.
14. Perkins, A. D., Ellis, S. J., Asghari, P., Shamsian, A., Moore, E. D. & Tanentzapf, G. (2010). Integrin-mediated adhesion maintains sarcomeric integrity. *Dev Biol* **338**, 15-27.
15. Ruoslahti, E. (1996). RGD and other recognition sequences for integrins. *Ann Rev Cell Dev Biol* **12**, 697-715.
16. Gribova, V., Crouzier, T. & Picart, C. (2011). A material's point of view on recent developments of polymeric biomaterials: control of mechanical and biochemical properties. *J Mater Chem* **21**, 14354-14366.
17. Hersel, U., Dahmen, C. & Kessler, H. (2003). RGD modified polymers: biomaterials for stimulated cell adhesion and beyond. *Biomaterials* **24**, 4385-415.
18. Benoit, D. S. & Anseth, K. S. (2005). The effect on osteoblast function of colocalized RGD and PHSRN epitopes on PEG surfaces. *Biomaterials* **26**, 5209-20.
19. Hirano, Y., Kando, Y., Hayashi, T., Goto, K. & Nakajima, A. (1991). Synthesis and cell attachment activity of bioactive oligopeptides: RGD, RGDS, RGDV, and RGDT. *J Biomed Mater Res* **25**, 1523-1534.
20. Lin, H. B., Garcia-Echeverria, C., Asakura, S., Sun, W., Mosher, D. F. & Cooper, S. L. (1992). Endothelial cell adhesion on polyurethanes containing covalently attached RGD-peptides. *Biomaterials* **13**, 905-14.
21. Bajaj, P., Reddy, B., Jr., Millet, L., Wei, C., Zorlutuna, P., Bao, G. & Bashir, R. (2011). Patterning the differentiation of C2C12 skeletal myoblasts. *Integr Biol* **3**, 897-909.
22. Serena, E., Zatti, S., Reghelin, E., Pasut, A., Cimetta, E. & Elvassore, N. (2010). Soft substrates drive optimal differentiation of human healthy and dystrophic myotubes. *Integr Biol* **2**, 193-201.
23. Engler, A. J., Griffin, M. A., Sen, S., Bonnemann, C. G., Sweeney, H. L. & Discher, D. E. (2004). Myotubes differentiate optimally on substrates with tissue-like stiffness: pathological implications for soft or stiff microenvironments. *J Cell Biol* **166**, 877-87.
24. Boontheekul, T., Hill, E. E., Kong, H. J. & Mooney, D. J. (2007). Regulating myoblast phenotype through controlled gel stiffness and degradation. *Tissue Eng* **13**, 1431-42.
25. Discher, D. E., Janmey, P. & Wang, Y. L. (2005). Tissue cells feel and respond to the stiffness of their substrate. *Science* **310**, 1139-43.
26. Stedman, H. H., Sweeney, H. L., Shrager, J. B., Maguire, H. C., Panettieri, R. A., Petrof, B., Narusawa, M., Leferovich, J. M., Sladky, J. T. & Kelly, A. M. (1991). The mdx mouse diaphragm reproduces the degenerative changes of Duchenne muscular dystrophy. *Nature* **352**, 536-9.
27. Gilbert, P. M., Havenstrite, K. L., Magnusson, K. E., Sacco, A., Leonardi, N. A., Kraft, P., Nguyen, N. K., Thrun, S., Lutolf, M. P. & Blau, H. M. (2010). Substrate elasticity regulates skeletal muscle stem cell self-renewal in culture. *Science* **329**, 1078-81.
28. Ren, K., Crouzier, T., Roy, C. & Picart, C. (2008). Polyelectrolyte multilayer films of controlled stiffness modulate myoblast cells differentiation. *Adv Funct Mater* **18**, 1378-1389.
29. Boonen, K. J., Rosaria-Chak, K. Y., Baaijens, F. P., van der Schaft, D. W. & Post, M. J. (2009). Essential environmental cues from the satellite cell niche: optimizing proliferation and differentiation. *Am J Physiol Cell Physiol* **296**, C1338-45.
30. Pitaval, A., Tseng, Q., Bornens, M. & Thery, M. (2010). Cell shape and contractility regulate ciliogenesis in cell cycle-arrested cells. *J Cell Biol* **191**, 303-12.
31. Charest, J. L., Garcia, A. J. & King, W. P. (2007). Myoblast alignment and differentiation on cell culture substrates with microscale topography and model chemistries. *Biomaterials* **28**, 2202-10.
32. Decher, G. (1997). Fuzzy Nanoassemblies: Toward Layered Polymeric Multicomposites. *Science* **277**, 1232-1237.
33. Samuel, R. E., Shukla, A., Paik, D. H., Wang, M. X., Fang, J. C., Schmidt, D. J. & Hammond, P. T. (2011). Osteoconductive protamine-based polyelectrolyte multilayer functionalized surfaces. *Biomaterials* **32**, 7491-502.
34. Tan, G.-K., Dinnes, D. L. M., Butler, L. N. & Cooper-White, J. J. (2010). Interactions between meniscal cells and a self assembled biomimetic surface composed of hyaluronic acid, chitosan and meniscal extracellular matrix molecules. *Biomaterials* **31**, 6104-6118.
35. Boudou, T., Crouzier, T., Ren, K., Blin, G. & Picart, C. (2010). Multiple Functionalities of Polyelectrolyte Multilayer Films: New Biomedical Applications. *Adv Mater* **22**, 441-467.
36. Schneider, A., Bolcato-Bellemin, A. L., Francius, G., Jedrzejwska, J., Schaaf, P., Voegel, J. C., Frisch, B. & Picart, C. (2006). Glycated polyelectrolyte multilayer films: differential adhesion of primary versus tumor cells. *Biomacromolecules* **7**, 2882-9.
37. Picart, C., Elkaim, R., Richert, L., Audoin, F., Arntz, Y., Da Silva Cardoso, M., Schaaf, P., Voegel, J. C.

& Frisch, B. (2005). Primary Cell Adhesion on RGD-Functionalized and Covalently Crosslinked Thin Polyelectrolyte Multilayer Films. *Adv Funct Mater* **15**, 83-94.
38. Crouzier, T. & Picart, C. (2009). Ion pairing and hydration in polyelectrolyte multilayer films containing polysaccharides. *Biomacromolecules* **10**, 433-42.
39. Charrasse, S., Comunale, F., Fortier, M., Portales-Casamar, E., Debant, A. & Gauthier-Rouviere, C. (2007). M-cadherin activates Rac1 GTPase through the Rho-GEF trio during myoblast fusion. *Mol Biol Cell* **18**, 1734-43.
40. Voinova, M. V., Rodahl, M., Jonson, M. & Kasemo, B. (1999). Viscoelastic Acoustic Response of Layered Polymer Films at Fluid-Solid Interfaces: Continuum Mechanics Approach. *Phys Scr* **59**, 391.
41. Geiger, B., Spatz, J. P. & Bershadsky, A. D. (2009). Environmental sensing through focal adhesions. *Nat Rev Mol Cell Biol* **10**, 21-33.
42. Garcia, A. J., Vega, M. D. & Boettiger, D. (1999). Modulation of cell proliferation and differentiation through substrate-dependent changes in fibronectin conformation. *Mol Biol Cell* **10**, 785-98.
43. Zamir, E. & Geiger, B. (2001). Molecular complexity and dynamics of cell-matrix adhesions. *J Cell Sci* **114**, 3583-90.
44. Ozeki, N., Jethanandani, P., Nakamura, H., Ziober, B. L. & Kramer, R. H. (2007). Modulation of satellite cell adhesion and motility following BMP2-induced differentiation to osteoblast lineage. *Biochem Biophys Res Commun* **353**, 54-9.
45. Liu, H., Niu, A., Chen, S. E. & Li, Y. P. (2011). Beta3-integrin mediates satellite cell differentiation in regenerating mouse muscle. *FASEB Journal* **25**, 1914-21.
46. Bach, A. D., Beier, J. P., Stern-Staeter, J. & Horch, R. E. (2004). Skeletal muscle tissue engineering. *J Cell Mol Med* **8**, 413-422.
47. Nishiyama, T., Kii, I. & Kudo, A. (2004). Inactivation of Rho/ROCK signaling is crucial for the nuclear accumulation of FKHR and myoblast fusion. *J Biol Chem* **279**, 47311-9.
48. Castellani, L., Salvati, E., Alema, S. & Falcone, G. (2006). Fine regulation of RhoA and Rock is required for skeletal muscle differentiation. *J Biol Chem* **281**, 15249-57.
49. Nemir, S. & West, J. L. (2010). Synthetic materials in the study of cell response to substrate rigidity. *Ann Biomed Eng* **38**, 2-20.
50. Ren, K., Fourel, L., Rouviere, C. G., Albiges-Rizo, C. & Picart, C. (2010). Manipulation of the adhesive behaviour of skeletal muscle cells on soft and stiff polyelectrolyte multilayers. *Acta Biomater* **6**, 4238-48.
51. Rowley, J. A. & Mooney, D. J. (2002). Alginate type and RGD density control myoblast phenotype. *J Biomed Mater Res* **60**, 217-23.
52. Wang, P. Y., Thissen, H. & Tsai, W. B. (2012). The roles of RGD and grooved topography in the adhesion, morphology, and differentiation of C2C12 skeletal myoblasts. *Biotechnol Bioeng* **109**, 2104-15.
53. Danen, E. H., van Rheenen, J., Franken, W., Huveneers, S., Sonneveld, P., Jalink, K. & Sonnenberg, A. (2005). Integrins control motile strategy through a Rho-cofilin pathway. *J Cell Biol* **169**, 515-26.
54. Hirsch, E., Lohikangas, L., Gullberg, D., Johansson, S. & Fassler, R. (1998). Mouse myoblasts can fuse and form a normal sarcomere in the absence of beta1 integrin expression. *J Cell Sci* **111 (Pt 16)**, 2397-409.
55. Fackler, O. T. & Grosse, R. (2008). Cell motility through plasma membrane blebbing. *J Cell Biol* **181**, 879-84.
56. Charrasse, S., Comunale, F., Grumbach, Y., Poulat, F., Blangy, A. & Gauthier-Rouviere, C. (2006). RhoA GTPase regulates M-cadherin activity and myoblast fusion. *Mol Biole Cell* **17**, 749-59.
57. Fortier, M., Comunale, F., Kucharczak, J., Blangy, A., Charrasse, S. & Gauthier-Rouviere, C. (2008). RhoE controls myoblast alignment prior fusion through RhoA and ROCK. *Cell Death Differ* **15**, 1221-31.
58. Mammoto, A. & Ingber, D. E. (2009). Cytoskeletal control of growth and cell fate switching. *Curr Opin Cell Biol* **21**, 864-70.
59. Schaller, M. D. (2010). Cellular functions of FAK kinases: insight into molecular mechanisms and novel functions. *J Cell Sci* **123**, 1007-13.
60. Narumiya, S., Tanji, M. & Ishizaki, T. (2009). Rho signaling, ROCK and mDia1, in transformation, metastasis and invasion. *Cancer and Metastasis Rev* **28**, 65-76.
61. Levental, K. R., Yu, H., Kass, L., Lakins, J. N., Egeblad, M., Erler, J. T., Fong, S. F., Csiszar, K., Giaccia, A., Weninger, W., Yamauchi, M., Gasser, D. L. & Weaver, V. M. (2009). Matrix crosslinking forces tumor progression by enhancing integrin signaling. *Cell* **139**, 891-906.

III.B. COMPLEMENTARY EXPERIMENTS

III.B.1.Effect of RGD density on cell adhesion and differentiation

As shown in previous part, the mass of PGA-RGD adsorbed onto the films surface was 400 ng/cm^2, which corresponded to a RGD surface density of 0.78 molecules of peptide per nm^2 (or 300 pmol/cm^2). This is a relatively high surface coverage.

An integrin molecule being about 8-12 nm in size (Xiong et al. 2002), theoretically, RGD spacing of less than 10 nm is not necessary. The effects of RGD nanospacing was studied using micro- and nanopatterns on non-fouling substrates such as PEG hydrogels with gold nanoparticles positioned at a certain distance. In this case, the RGD peptides are grafted onto gold nanoparticles (Sun et al. 2008). The critical nanospacing for integrin clustering and activation was found to be around 70 nm (Arnold et al. 2004; Sun et al. 2008). Additionally, it is known that the RGD nanospacing within a local cluster is more important than RGD density (Arnold et al. 2004; Huang et al. 2009; Deeg et al. 2011; Schvartzman et al. 2011). RGD spacing and density are known to induce cytoskeleton remodelling (Cavalcanti-Adam et al. 2007; Huang et al. 2009), but also to influence the cell fate (Arnold et al. 2008; Peng et al. 2011; Wang et al. 2013).

In this work, we investigated if a lower RGD density on (PLL/PGA) films could be sufficient for myoblast adhesion and differentiation. Our approach consisted in grafting RDG onto PGA with a lower DS. This was achieved by controlling the RDG quantity allowed to react with PGA, and verified by ^{1}H NMR. The obtained products with a lower DS were deposited onto (PLL/PGA)-PLL films as previously described (Chapter IIIA). Thus, RGD density on the films surface could be varied (Fig. III-2).

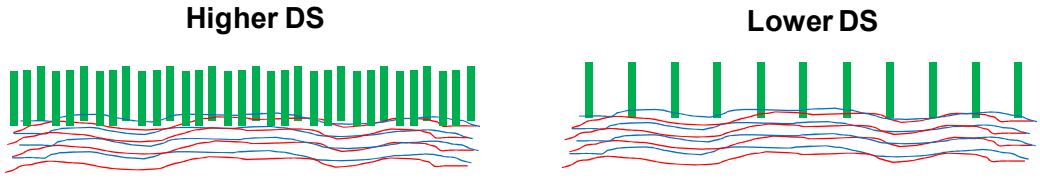

Figure III-2. Control of RGD density on PEM films. *Variation of RGD density by functionalization of the film with PGA-RGD where RDG is grafted onto PGA with different degrees of substitution (DS).*

First, we investigated C2C12 cell adhesion and spreading on the films functionalized with PGA-RGD with DS 10% or 1%. The cells adhered and spread on both RGD densities (Fig. III-3A). The quantifications showed that RGD density had no statistically significant effect on cell number and cell spreading area (Fig. III-3B).

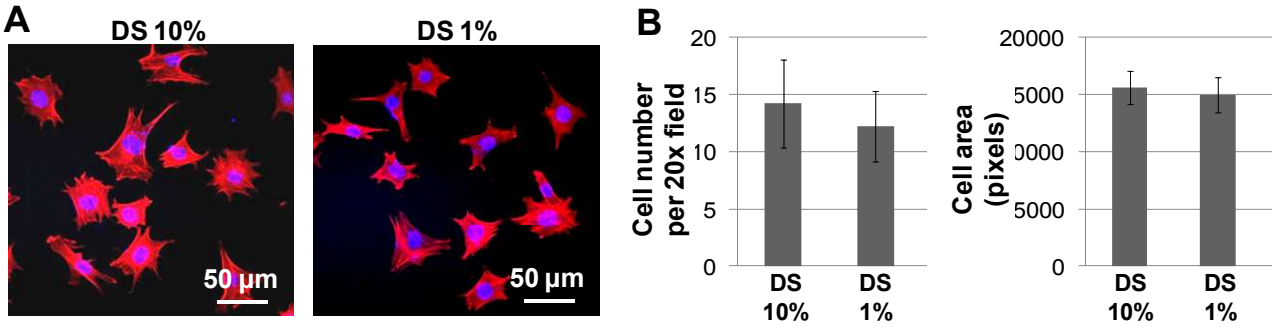

Figure III-3. Cell adhesion on the films with variable RGD density. *Variation of RGD density was achieved by functionalization of the film with PGA-RGD where RDG is grafted onto PGA with different degrees of substitution (DS).The cells were seeded and allowed to adhere for 4h. (A) Staining of actin (red) and nuclei (blue). (B) Quantification of the number of adherent cells and of the cell area.*

It was already shown that cell surface attachment was not sensitive to pattern density, whereas the formation of stable focal adhesions was (Cavalcanti-Adam et al. 2007). We thus visualized focal adhesions on both substrates, DS 10% and DS 1%, by immunolabelling of pFAK (Fig. III-4A). The quantification of the number of focal adhesion per cell showed a statistically significant difference: the cells seeded on the films with higher RGD density (DS 10%) had more focal adhesions per cell (Fig. III-4B).

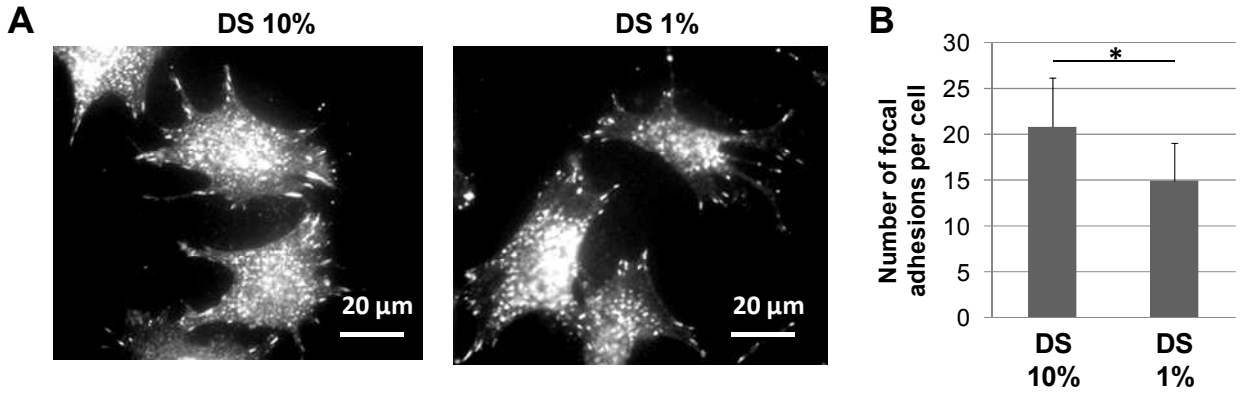

Figure III-4. Formation of focal adhesions on the films with variable RGD density. *The cells were seeded and allowed to adhere for 4h. (A) Staining of pFAK. (B) Quantification of the number of focal adhesions per cell. * $p<0,05$.*

Next, we evaluated the capacity of the films with different RGD densities to support myogenic differentiation. Here, a film functionalized with PGA-RGD DS 7%, that is only slightly lower than the control DS 10%, was added to the study. The C2C12 myoblasts were seeded on different films and allowed to differentiate in DM for 5 days. As described previously (***Chapter IIIA***), myotube formation was observed on the films with PGA-RGD DS 10% (Fig.III-5). On the films with RGD DS 1%, total cell sheet detachment occurred at Day 3. On DS 7% films, partial cell

sheet detachment and cell agregation could be observed, although some myotubes were also present.

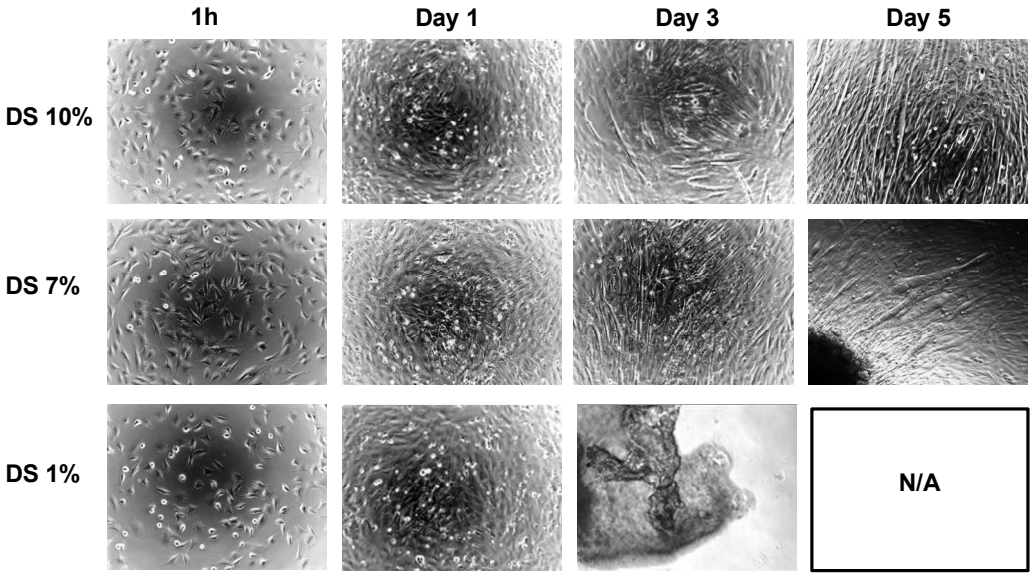

Figure III-5. Effect of RGD density on myogenic differentiation. *Phase contrast microscopy observations of C2C12 cell differentiation on different films. After 24 h of proliferation in GM, the cells were put in DM (i.e. Day 0) and were let to differentiate until Day 5.*

These data show that PGA-RGD DS 10% films are the most efficient for C2C12 myogenic differentiation, although only slight differences were observed for cell adhesion. Although RGD surface density of 0.78 molecules of peptide per nm^2 is a very high surface coverage, a part of RGD peptide molecules is probably inaccessible due to the diffusion of PGA-RGD into the film. Another possibility is that a fraction of the RGD peptides may not have the appropriate conformation to interact with integrins. Indeed, secondary structure of the grafted molecules, and RGD peptides among them, is important for their interactions with the cells. There are currently developments in the modification and grafting of RGD based peptides, in order to improve their affinity, but also to enhance their specificity to a given receptor (Ruoslahti 1996; Hersel et al. 2003).

III.B.2. Adhesion and differentiation on PDMS microgrooved substrates

One of the main challenges in muscle tissue engineering consists to properly organize spatially the tissue. This can be achieved using microfabricated polydimethylsiloxane (PDMS) substrates. PDMS is a biocompatible material that can be easily molded and structured, making it an ideal candidate for both biomedical applications and musculo-skeletal tissue engineering *in vitro* (Dennis and Kosnik 2000). However, due to its hydrophobicity, PDMS is poorly adhesive and requires surface modification. This can be achieved by the adsorption of ECM proteins, such as gelatin (Yim et al. 2010), fibronectin (Peterson and Papautsky 2006) or laminin (Lam et al. 2006), by covalent grafting (Wipff et al. 2009; Mikhail et al. 2010) or polyelectrolyte multilayer (PEM) coating (Kidambi et al. 2007).

In this work, we investigated if NCL-RGD films were a suitable coating for PDMS and could promote C2C12 cell adhesion and myogenic differentiation.

The topographically patterned surface was fabricated by molding PDMS against a silicon mold as described previously (Monge et al. 2012). Before the buildup of films, the PDMS substrates were oxidized by oxygen plasma in a microwave downstream etcher (Plassys) at 1500W power for 10 s. Next, the microgrooved PDMS was coated by (PLL/PGA)-PLL-PGA-RGD multilayer films. The coating was verified by adding PLL^{FITC}. Observations by fluorescent microscopy show homogeneous film deposition onto the PDMS surface (Fig. III-6).

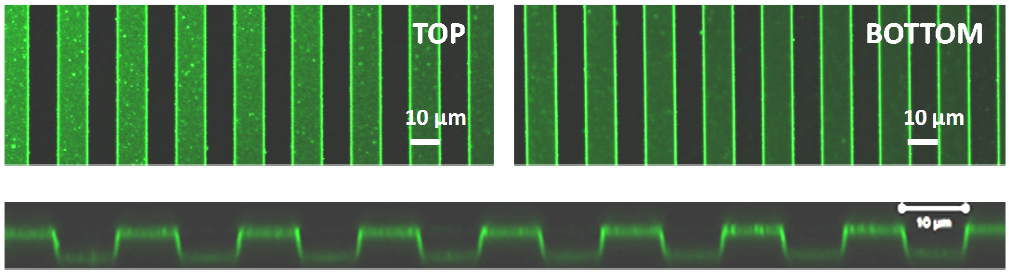

Figure III-6. PEM film-coated PDMS microgrooved substrate. *(PLL/PGA)-PLL--PGA-RGD multilayer films were built on PDMS surface. PLL^{FITC} was added to visualize the films*

Next, we studied C2C12 cell adhesion on PEM-coated PDMS with groove thicknesses of 10 µm and 30 µm (Fig. III-7). On 10 µm grooved substrates, the cells were significantly elongated as compared to flat PDMS substrates (Fig. III-7A). On 30 µm grooves, the cells were more spread than on 10 µm grooves, but were still elongated in the direction of the grooves (Fig. III-7A and B). These results indicated that 30 µm grooves were able to orient the cells without significantly affecting their morphology, as observed on 10 µm grooves. For this reason, we selected 30 µm as a substrate for C2C12 myogenic differentiation.

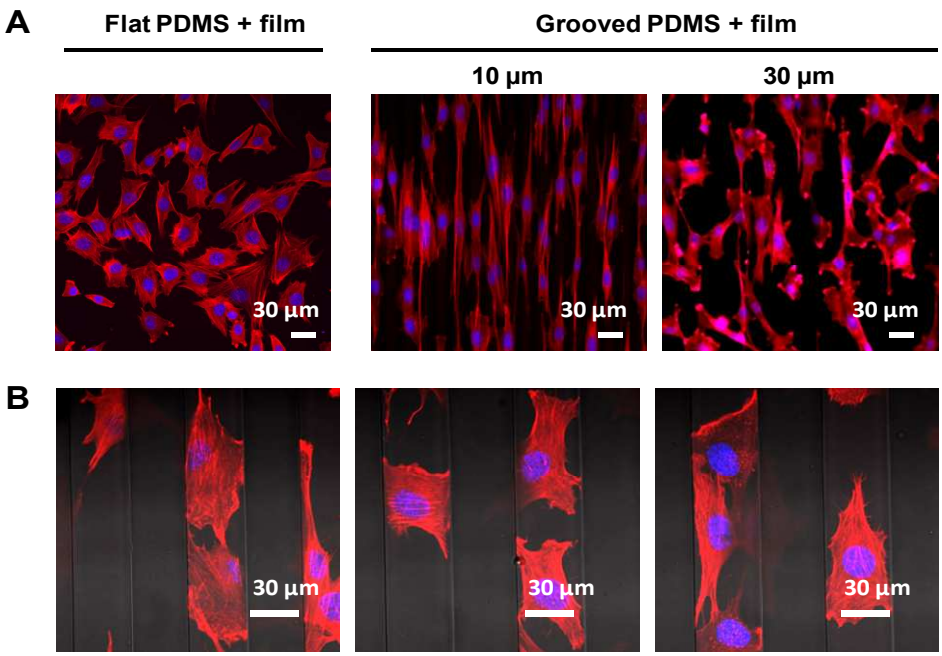

Figure III-7. C2C12 myoblast adhesion on PDMS microgrooved substrates coated with (PLL/PGA)-PLL--PGA-RGD multilayer films. *(A) Cell adhesion on flat PDMS and on PDMS with 10 µm or 30 µm grooves. (B) Cell adhesion on 30 µm grooved PDMS.Red: actin, blue: nuclei.*

To study the effect of PEM-coated PDMS on C2C12 myoblasts differentiation, the cells were seeded on flat PDMS or with 30 µm grooves, and allowed to differentiate for 5 days in DM. Myoblast fusion and Troponin T staining was observed on both substrates (Fig. III-8). However, on flat PDMS, the myotubes were randomly oriented, while on 30 µm grooves PDMS, they were aligned in the direction of the grooves.

These results show that NCL-RGD films can be used as efficient coating for microstructured PDMS, for the alignment of myotubes.

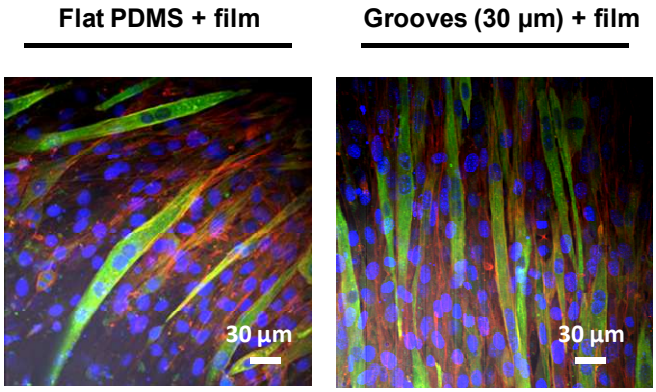

Figure III-8. C2C12 myoblast differentiation on PDMS microgrooved substrates coated with (PLL/PGA)-PLL--PGA-RGD multilayer films. *The cells were seeded on, flat or with 30 µm grooves, and allowed to differentiate for 5 days in myogenic differentiation medium.Green: troponin T, red: actin, blue: nuclei.*

CHAPTER IV – Laminin-derived peptides for targeting of non-integrin cell surface receptors of skeletal myoblasts

In this chapter, we focused on the development peptide-grafted PEM films for specific targeting of non-integrin skeletal muscle receptors such as syndecans and dystroglycans. Besides well-studied integrin receptors, these receptors also play important roles in skeletal muscle development and maintenance. However, their precise roles and functions are not fully understood. We used previously described maleimide chemistry to couple the peptides to PLL/PGA multilayer films and studied their effects on cellular processes of skeletal myoblasts.

IV.A. GENERAL INTRODUCTION

IV.A.1. Physiological importance

The laminin-α2 chain is the predominant laminin alpha chain expressed in adult skeletal muscle and a major component of muscle basement membranes (Miner and Yurchenco 2004). The laminin-α2 chain is involved in anchoring myofibers to the basal lamina, promoting muscle cell integrity and survival (Miyagoe et al. 1997). Mutations in the laminin-α2 gene result in congenital muscular dystrophy type 1A (MDC1A) (Collins and Bonnemann 2010).

Laminin-α2 chains interacts with various cell receptors via globular domains located in their N- and C-terminus (Suzuki et al. 2005). Among them, syndecan-1 (SDC-1) and α-dystroglycan (αDG) (Hoffman et al. 1998; Barresi and Campbell 2006; Urushibata et al. 2010).

Syndecan-1 (SDC-1) was identified as one of laminin receptors interacting with laminin-α2 G-domain (Hoffman et al. 1998). It was found downregulated during myoblast differentiation (Larrain et al. 1997) and its overexpression inhibited myogenic differentiation (Larrain et al. 1998; Velleman et al. 2004) while promoting proliferation (Velleman et al. 2007). Adams et al. showed that syndecan-1 was involved in C2C12 adhesion to laminin and directional migration (Chakravarti et al. 2005). However, the precise mechanism of SDC-1/laminin-α2 interaction and its role in myogenesis remain unclear.

Dystroglycan in muscle cells interacts with laminin-α2 chain and was shown to be crucial for maintaining the integrity of sarcolemma and protecting muscle from damage (Gullberg and Ekblom 1995; Matsumura et al. 1997; Durbeej et al. 1998b; Cohn et al. 2002; Han et al. 2009; Munoz et al. 2010). Mutations that lead to loss of α-dystroglycan (αDG) cause muscular dystrophies (Durbeej et al. 1998a), and defects in the glycosylation of αDG cause muscular dystrophies called dystroglycanopathies (Hewitt 2009; Muntoni et al. 2011).

Non-differentiated cultures of C2C12 myoblasts express low amounts of dystroglycan mRNA, which then progressively appears during myoblast differentiation into myotubes (Kostrominova and Tanzer 1995). However, it was found that satellite cells expressing dystroglycan

supported continued efficient regeneration of skeletal muscle. Besides, maintenance of the regenerative capacity by satellite cells expressing dystroglycan could be responsible for mild progression of muscular dystrophy caused by disruption of posttranslational dystroglycan processing (Cohn et al. 2002).

These data underline the importance of αDG for muscle regeneration. However, its precise role in satellite cell function and myogenic differentiation remains unclear.

IV.A.2. Selection of the peptides

The study of laminin interaction with its partners, SDC-1 and αDG, is rather challenging due to the difficulty of the specific targeting of these receptors by laminin. For instance, cell culture on total laminin-coated substrates does not allow specific targeting of a particular receptor, while overexpression of the receptors in the cells does not exclude the possibility of signaling via other receptors.

To study the specific interactions of laminin-α2 with SDC-1 or αDG, we selected two peptide sequences derived from laminin-α2 chain that were shown to specifically interact with either SDC-1 or αDG (Nomizu et al. 1996; Hoffman et al. 1998; Suzuki et al. 2010; Urushibata et al. 2010). We used these sequences to functionalize PLL/PGA films via covalent grafting by maleimide chemistry to create a either αDG or SDC-1-targeting surfaces. The peptides are named hereafter L2synd and L2dystro for SDC-1 and α-dystroglycan targeting sequences, respectively.

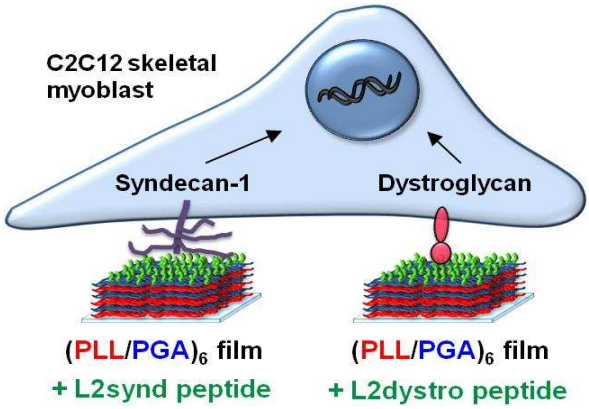

Figure IV-2. Laminin-derived peptide presentation by PLL/PGA multilayer films for SDC-1 and αDG targeting.

In addition, we co-grafted laminin-derived peptides with RGD peptide used in the previous study to investigate the combined effects of signaling via integrin and non-integrin receptors.

IV.A.2. "On-film" grafting method

IV.A.2.a) Effect of grafting method on film quality

The peptide grafting protocol used for RGD had to be slightly modified because L2synd and L2dystro grafting to PGA-maleimide and subsequent freeze-drying led to totally insoluble products. This is probably due to the amino acid composition of the peptide and possible formation of hydrogen/hydrophobic bonds in dry state. Thus, a protocol of direct peptide grafting on the films pre-functionnalized with PGA-maleimide was developed. The detailed grafting procedure is described in ***Chapter II - Materials and methods***. Briefly, it consists in PGA-maleimide deposition on the final layer of $(PGA/PLL)_6$ films and addition of the peptides in solution.

Initially, PGA-RGD was deposited on the film surface in HEPES/NaCl buffer. However, grafting of laminin peptides in HEPES or HEPES/NaCl buffer led to the formation of big aggregates or to film's deterioration, while grafting in water did not affect film's homogeneity, although some small aggregates could be detected (Fig. IV-3).

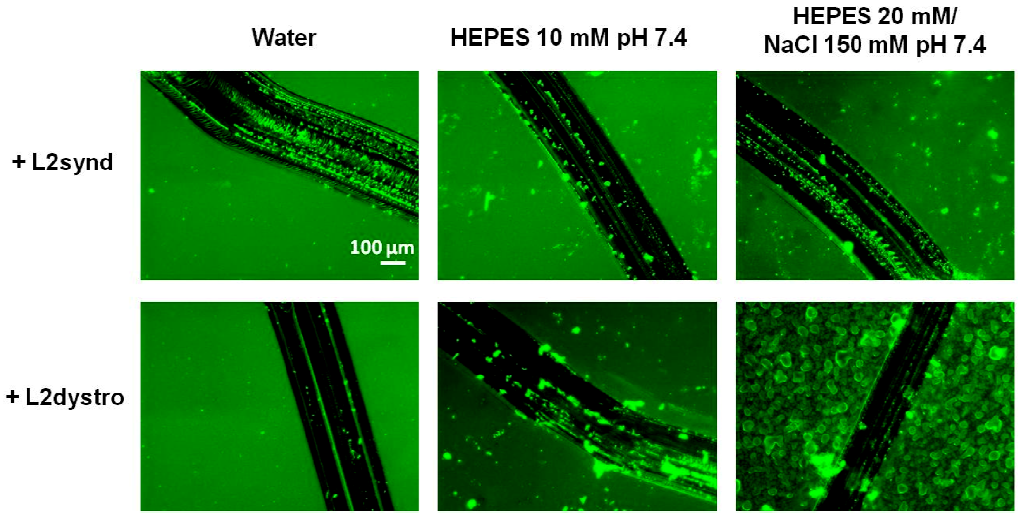

Figure IV-3. Qualitative observation of film formation : Films grafted with L2synd and L2dystro were observed by fluorescence microscopy using PLL-FITC. *The peptides were dissolved in water, HEPES or HEPES/NaCl buffers and added onto $(PGA/PLL)_6$ films pre-functionnalized with PGA-maleimide.*

Thus, the grafting of laminin peptide and of the RGD peptide was further performed in milliQ water. Before studying the effects of laminin-derived peptides on cell adhesion and differentiation, some preliminary tests were performed in order to verify that such protocol did not affect films homogeneity or peptide bioactivity.

To verify the quality of the films, control films used in previous study (NCL and NCL-RGD, last layer deposition in HEPES/NaCl buffer), films functionalized with PGA-maleimide and films grafted with RGD peptide, laminin peptide or their combinations deposited in water were labeled

with PLL-FITC (Fig. IV-4). All the films showed homogeneous surfaces which were comparable to NCL and NCL-RGD films with the last layer deposited in HEPES/Nacl buffer.

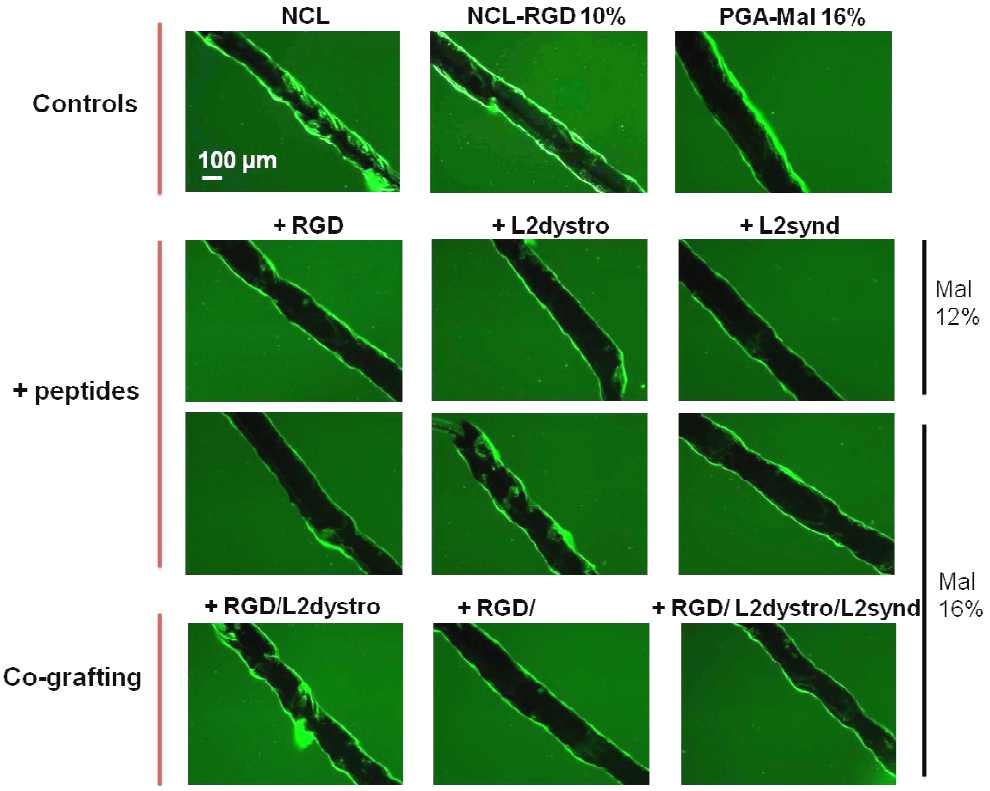

Figure IV-4. Fluorescent labeling of different films using PLL-FITC. For NCL, NCL-RGD and PGA-Mal films, last layer was deposited in HEPES/NaCl buffer. *For the other films, the peptides were dissolved in water and added onto $(PGA/PLL)_6$ films pre-functionnalized with PGA-maleimide with substitution degrees 12% or 16%.*

IV.A.2.b) Validation of the "on-film" grafting protocol

Next, we verified the biological functionality of the films prepared by the new method of "on-film grafting". For this, we compared C2C12 cell adhesion and differentiation on RGD-functionalized films prepared by the "pre-grafting" and the "on-film grafting" methods. To distinguish between the films, we preserved the previously used nomenclature (NCL-RGD) for the film prepared by deposition of pre-grafted PGA. Films prepared by the "on-film grafting" method (deposition of PGA-maleimide, then addition of peptide solution) were called RGD12 and RGD16 for RGD peptide solution deposited on the films functionalized with PGA-maleimide DS 12% and PGA-maleimide DS 16%, respectively.

On all types of films, the cells adhered and spread by forming thick actin stress fibers and focal adhesions (Fig. IV-5A and B). Interestingly, number of focal adhesion per cell was even two-times higher on the films prepared by the new method (Fig. IV-5C).

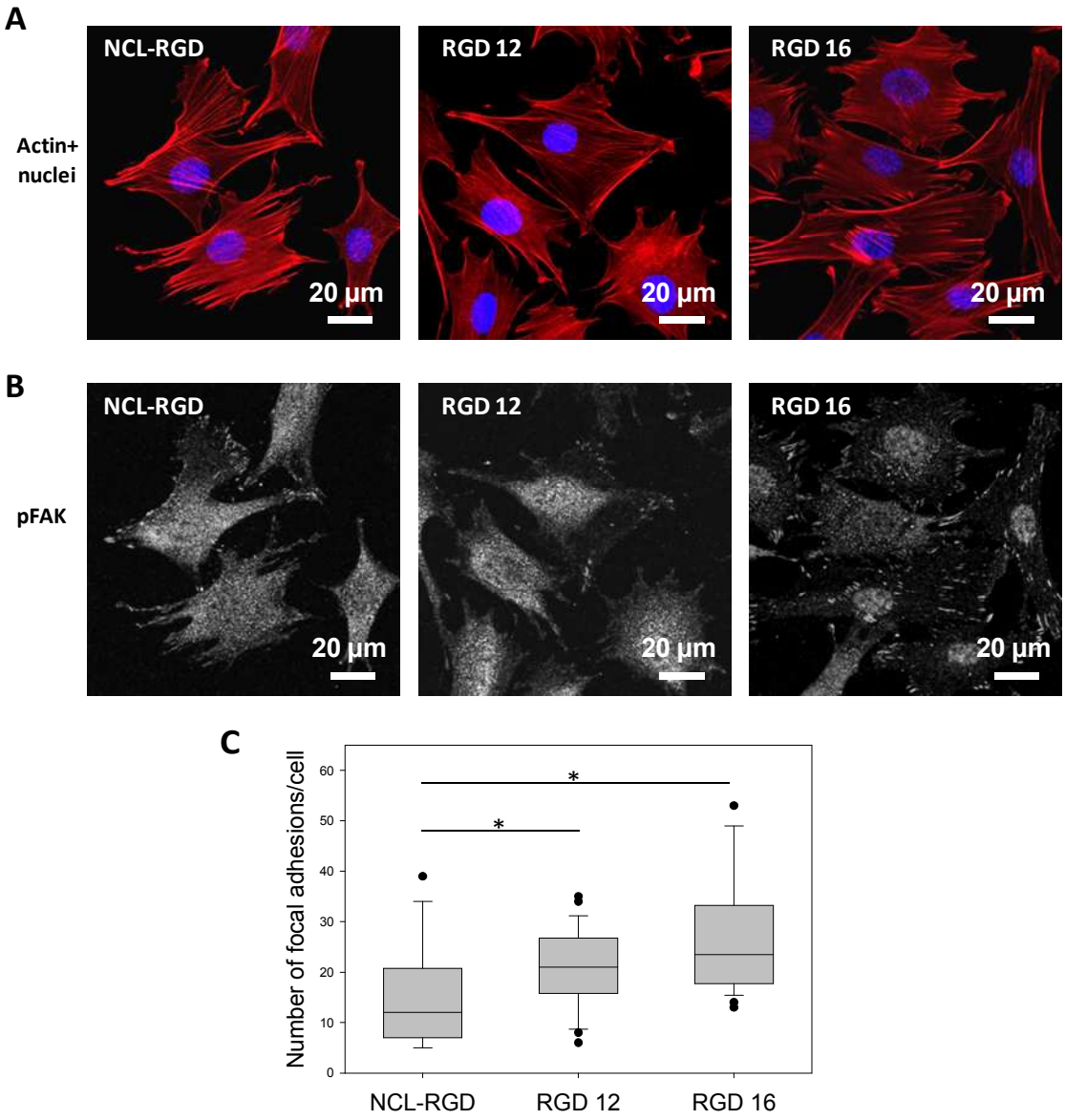

Figure IV-5. C2C12 cell adhesion after 4h on RGD-grafted films prepared by the *the "pre-grafting" and the "on-film grafting" methods. (A) Fluorescent labeling of actin (red) and nuclei (blue). (B) Fluorescent labeling of phosphorylated focal adhesion kinase (pFAK). (C) Quantification of the number of focal adhesions per cell. NCL-RGD: film prepared by PGA-RGD deposition ("pre-grafting" method). RGD12 and RGD16: films prepared by RGD peptide solution deposited on the films functionalized with PGA-maleimide 12% and PGA-maleimide 16%, respectively ("on-film grafting" method).*

The cells were also able to differentiate on all the film types: after 5 days in DM, myotubes were observed on all the film types (Fig. IV-6A). Striations were also observed (Fig. IV-6B). The fusion index was not affected by the RGD grafting method (Fig. IV-6C). However, on RGD16 films, myotubes were slightly longer and wider (Fig. IV-6D and E).

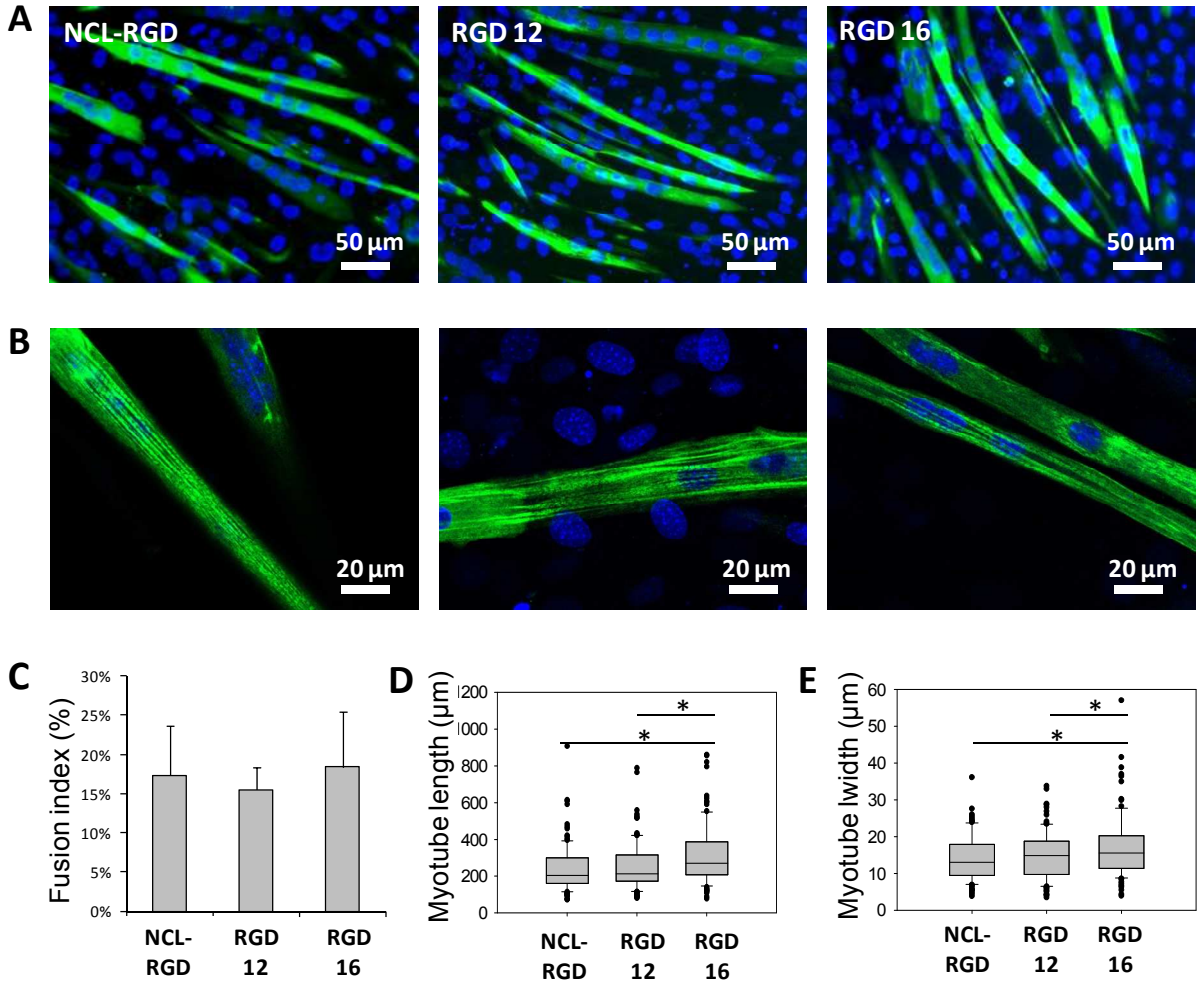

Figure IV-6. C2C12 cell differentiation after 5 days on RGD-grafted films prepared by the "old" and the "new" methods. *(A) and (B) Fluorescent labeling of myosin heavy chain (green) and nuclei (blue). (C) Quantification of the fusion index. (D) Quantification of myotube length. (E) Quantification of myotube width. NCL-RGD: film prepared by PGA-RGD deposition ("old" method). RGD12 and RGD16: films prepared by RGD peptide solution deposited on the films functionalized with PGA-maleimide 12% and PGA-maleimide 16%, respectively ("new" method).*

Based on these data, we concluded that RGD "pre-grafting" and the "on-film grafting" methods were globally equal in terms of C2C12 adhesion and differentiation, and selected RGD16 films as a control myogenic substrate for the further experiments. Similarly, laminin peptides were grafted onto PGA-maleimide 16% pre-functionalized films.

IV.B. PEM FILMS FOR SDC-1 TARGETING IN SKELETAL MYOBLASTS

IV.B.1. Article summary

In this work, we use a 12-amino acid laminin-α2 chain derived peptide (named L2synd) that was shown to specifically interact with SDC-1 (Hoffman et al. 1998). The peptide was grafted to PEM films using maleimide chemistry to create a SDC-1-targeting surface.

Cell adhesion assays showed that RGD peptide induced better cell spreading, while L2synd peptide was responsible for elongated morphology. Interestingly, the cells seeded on mixed RGD/L2synd film presented both of these features: they were as spread as the cells on RGD films and as elongated as on L2synd films. Thus, the peptides can act simultaneously and induce a combination of the effects that each of them induces alone.

We also revealed that, on L2synd films, the cells presented a polarized phenotype with lamellipodia at the leading edge, and increased directional migration. Polarization and directional migration are usually induced by environmental cues such as growth factor or chemokine gradients; here, polarization was induced by a ligand presented from the basal side, and the cells adapted directional migration mode even in absence of classic directionality-inducing factors.

Our data also suggest a crosstalk between SDC-1 and β1-integrin on L2synd-grafted substrate, since cell polarity was inhibited by beta1 integrin blocking, although the substrate did not present any ligands for β1-integrin. Also, polarized cell morphology on L2synd films correlated with the presence of non-centrosomal microtubules and was linked to Rac1 and Cdc42 activity. Interestingly, cell response to Rac1 and Cdc42 inhibition on L2synd-containing films "mimicked" the effect of β1 blocking, suggesting that these are the elements of the same pathway and that β1-integrin – SDC-1 crosstalk results in Rac1 and Cdc42 signaling. Understanding of this cooperation is very important, because both modifications of SDC-1 expression and altered Rac1 activity are observed in many cancer types, leading to increased cell proliferation, loss of polarity and increased motility. Besides, the cells on L2synd films exhibited increased proliferation and absence of cell cycle exit in differentiation medium, decreased myogenin expression and absence of myotube formation.

Finally, we proposed a model of L2synd effect on cytoskeleton organization and cell polarity. We also propose a model according to which some of previously observed effects of laminin presentation or SDC-1 stimulation on skeletal myoblasts can be due to laminin-a2/SDC-1 interaction. This study demonstrates that by combining materials science/chemistry and cell biology approaches it is possible to target specific cell surface receptors and study their roles without changing their normal expression level by transfection or knock-down.

IV.B.2. Article 2

To be submitted

Laminin-peptide grafted polyelectrolyte multilayer films for SDC-1 targeting in skeletal myoblasts

Varvara Gribova[1, 2], Isabelle Paintrand[1], Manuel Théry[4], Rachel Auzely-Velty[2], Cécile Gauthier-Rouvière[3], Catherine Picart[1]

[1]. Grenoble Institute of Technology, CNRS UMR 5628 (LMGP), 3 parvis Louis Néel, F-38016 Grenoble Cedex, France

[2]. Centre de Recherches sur les Macromolécules Végétales (CERMAV, CNRS UPR 5301), affiliated with Université Joseph Fourier, and member of the Institut de Chimie Moléculaire de Grenoble, 601 rue de la Chimie, Domaine Universitaire de Grenoble-St Martin d'Hères, France

[3]. Universités Montpellier 2 et 1, CRBM, CNRS, UMR 5237, 1919 Route de Mende, 34293 Montpellier, France

[4]. Institut de Recherches en Technologies et Sciences pour le Vivant, iRTSV, Laboratoire de Physiologie Cellulaire et Végétale, CNRS/CEA/INRA/UJF, 17, rue des Martyrs, Grenoble 38054, France

Keywords: Extracellular matrix, laminin, Syndecan-1, polyelectrolyte multilayer films, myogenesis

1. Introduction

Tissue engineering is an approach that consists in combining stem cells and biomaterials to create tissues and organs *in vitro*. The goal of biomaterials scientists is to design biocompatible scaffolds in which cells can adhere, proliferate, differentiate and synthesize their own matrix to regenerate tissues [1]. For this, a good understanding of each type of stimulus provided by the matrix, physical or biochemical, as well as interplay and synergy of these signals, is needed.

Skeletal muscle tissue engineering holds promise for the replacement of muscle after an injury, for the treatment of muscle diseases, drug screening or fundamental studies. The process of muscle formation requires that muscle precursor cells become activated, proliferate, differentiate, and fuse together to form multinucleated myotubes [2; 3]. Besides ability to generate the skeletal muscle, adult skeletal muscle progenitor cells can give smooth muscle [4], bone [5; 6] or fat tissue [7; 8]. This makes of them good candidates for engineering of several types of tissues. A major limitation to the clinical application of muscle progenitors is a rapid loss of their stem cell properties once they are removed from their *in vivo* environment [9].

The development of skeletal muscle is known to strongly depend on the interaction of muscle cells with their surrounding extracellular matrix (ECM) [10]. Thus, engineering of a functional muscle tissue *in vitro* requires complex environments mimicking muscle natural extracellular matrix. To this end, substrates with tunable mechanical and chemical/biochemical properties for myoblast expansion and differentiation *in vitro,* as well as for the studies of myogenesis on controlled 2D microenvironments, are crucially needed.

Skeletal muscle ECM consists of the basement membrane that surrounds individual myofibers and of interstitial connective tissue [10; 11; 12; 13]. In adult muscle, satellite cells are situated in a compartment between the myotube membrane (sarcolemma) and the basal lamina [14].

Laminin, which is the major glycoprotein of the basement membranes,[15] consists of

subunits α, β and γ, and contains many distinct domains with different structure and functions [16; 17]. It is known that laminins have effect on myoblasts cell shape, migration, proliferation and differentiation, both *in vitro* and *in vivo* [18; 19 20; 21].

The laminin-α2 chain, a component of laminin-211, -221 and -213, is the predominant laminin alpha chain expressed in adult skeletal muscle [22]. The laminin-α2 chain is involved in anchoring myofibers to the basal lamina, promoting muscle cell integrity and survival [22]. Mutations in the laminin-α2 gene result in congenital muscular dystrophy type 1A (MDC1A) [23]. Among various laminin receptors, integrins [24; 25] are the most characterized and have been shown to be crucial for skeletal muscle development and function [26; 27]. However, other cellular receptors are now recognized to play a role in skeletal muscle regeneration.

Among them, syndecans, transmembrane heparan sulfate proteoglycans (HSPG) that bind a variety of ECM ligands, including fibronectin, laminin, vitronectin, collagen and others [28]. For a long time, syndecans were considered as co-receptors. Recently, their independent role in mediating cell adhesion and signaling has emerged [29]. Besides their numerous roles in different tissues [28; 30], syndecans were shown to play an important role in myogenesis. Syndecan-3 and syndecan-4 specifically mark skeletal muscle satellite cells and are implicated in satellite cell maintenance and muscle regeneration [31]. Syndecan-1 (SDC-1), which was shown to interact with laminin-α2 G-domain [32] was found downregulated during myoblast differentiation [33]. Its overexpression inhibited the differentiation [34; 35] while promoting proliferation [36]. Adams et al. showed that syndecan-1 was involved in C2C12 adhesion to laminin and directional migration [37].

These data demonstrate a crucial role for laminin-α2 and one of its receptor syndecan-1 in muscle regeneration. However, laminins are complex proteins containing many active domains that interact with a variety of cell receptors [38]. A good understanding of various laminin domain functions is thus necessary for targeting precise cell surface receptors, to induce a specific cell response and thus control the cell fate.

The recent developments in the field of biomimetic materials are often aimed to achieve a better selectivity, and make use of biomimetic peptides. Short sequences make it possible to enhance the specificity of the interaction by targeting a particular receptor. Thus, collagen-mimetic peptides [39; 40; 41], laminin-derived peptides [42; 43; 44] and fibronectin-derived peptides or fragments [45; 46] are increasingly used for their high selectivity.

In this work, we use laminin-α2 chain derived peptide that was shown to specifically interact with SDC-1. This peptide was first described by Nomizu et al. as MG-73, a sequence derived from LG4 globular domain of laminin-α2 [47]. Hoffman and al. showed that the peptide bound to syndecan-1 [32].

We grafted to PEM films using maleimide chemistry to create a SDC-1-targeting surface. PEM films [48; 49 50] are a type of highly versatile biomaterials offering numerous advantages for biomedical applications: ease of preparation, capability of incorporating bioactive molecules, functionalization by extracellular matrix components and biopolymers, tunable mechanical properties, and spatio-temporal control over film organization[51]. The advantage of grafting approach is that it provides good control of surface composition, a stable link and limits release of the functional group into the culture medium. Thus, covalent grafting of bioactive peptides allows creation of stable biomimetic and highly-specific surfaces.

We thus propose a model surface for the study of SDC-1 mediated adhesion to laminin and its specific effect on skeletal myoblast cellular

processes. In addition, we combine SDC-1 targeting peptide with a collagen-derived peptide that contains RGD motif, to study the . Its effect on myogenic differentiation of C2C12 myoblasts has been described in our previous work [52].

2. Materials and methods

2.1. PEM film buildup and

Poly(L-lysine) (PLL, P2636, Sigma) and poly(L-glutamic) acid (PGA, P-4886, Sigma) were dissolved at 0.5 mg/mL in a HEPES-NaCl buffer (20 mM HEPES, 150 mM NaCl, at pH 7.4). For all experiments, films were manually constructed in 96-well plates starting with a first layer of poly(ethyleneimine) (PEI) at 5 mg/ml. To deposit the subsequent polyelectrolyte layers, 50 µL of the polyelectrolyte solution was deposited in each well and let for 8 min before being rinsed twice for 30 sec and 5 min, respectively, with 100 µL of 150 mM NaCl (pH 6.5). This sequence was repeated until the buildup of a $(PGA/PLL)_6$ film was achieved.

2.2. PEM films functionalization by adhesion peptides

The laminin alpha2 chain derived peptide L2synd was chosen according to a published sequence that was shown to interact with Syndecan-1 transmembrane proteoglycan [32; 47; 53]. RGD peptide that was previously shown to promote C2C12 adhesion and differentiation [52] was used as a control myogenic peptide. A scrambled L2synd peptide was designed using a tool available at the following website: http://www.mimotopes.com/

The peptides RGD (CGPKGD*RGD*AGPKGA), L2synd (CGKNRLTIELEVRT) and scrambled L2synd (CGERRTETLVKNIL) were purchased from GeneCust (Dudelange, Luxembourg).

Previously published protocol of peptide grafting [41] was slightly modified. Briefly, the first step consisted in grafting maleimide groups onto PGA (P-4886, Sigma) chains. To accomplish this grafting, 60 mg of PGA were dissolved in 3 mL of a solution containing 10 mM HEPES buffer (pH 6.5), 20 mg of EDC, and 3 mg of sulfo-NHS in an inert atmosphere (nitrogen gas) under magnetic stirring. Then, 24 mg of N-(2-aminoethyl) maleimide trifluoroacetate was added. The reaction was allowed to proceed at room temperature (RT) for 24 h. After removal of the byproducts via dialysis against water, the PGA–maleimide was freeze-dried. The average number of maleimide groups bound to PGA was equal to 16% (i.e. in average 16 maleimide groups every one hundred repeating PGA units), as determined via ^{1}H NMR analysis. In the second step, the PGA-maleimide was deposited on the top of PLL-ending films and reacted with 100µl of MilliQ water-dissolved 60µg/mL L2synd peptide, 50µg/mL of RGD peptide or 1:1 (v/v) mix of both. The grafting was carried out overnight at RT under agitation, then the films were rinced twice with MilliQ water to remove the unbound peptide.

2.3. C2C12 culture

C2C12 cells (from ATCC, used at passages 5-15) were maintained in polystyrene dishes in an incubator at 37° C and 5% CO_2 and cultured in growth medium (GM) composed of Dulbecco's modified Eagle's medium (DMEM)/F12 medium (1:1; Gibco, Invitrogen, Cergy-Pontoise, France) supplemented with 10% fetal bovine serum (PAA Laboratories, Les Mureaux, France) containing 10 U/mL of penicillin G and 10 µg/mL of streptomycin (Gibco, Invitrogen, Cergy-Pontoise, France). Cells were subcultured prior to reaching 60–70% confluence (approximately every 2 days). For all experiments, C2C12 cells were first allowed to adhere in a serum-free medium (SFM) composed of DMEM/F12 1:1 and supplemented with antibiotics. After 4 h of adhesion, the cells were fixed or the SMF was replaced by the GM, depending on the type of experiment (see below). Cell were

differentiated in a differentiation medium (DM) composed of DMEM/F12 (1:1) supplemented with 2% horse serum (PAA Laboratories, Les Mureaux, France) and antibiotics.

2.4. Cell adhesion assays

For cell adhesion tests, C2C12 cells were seeded at 15 000 cells/cm^2 in 96-well plates and allowed to adhere in SFM for 4 h, then fixed in 3.7% formaldehyde. For adhesion specificity test using L2synd peptide in solution (sL2synd) the cells were preincubated with 10 µg/mL of peptide in SFM or with SFM alone for 30 min at 37°C and allowed to adhere on L2synd-grafted films for 2h. For adhesion specificity test using scrambled peptide the films were grafted with either original or scrambled L2synd peptide, and the cells were allowed to adhere on L2synd-grafted films for 4h in SFM. Involvement of integrin and proteoglycan adhesion receptors was tested by cell adhesion assay in presence of 2 mM EDTA (Sigma), 2 mM EGTA (Roth), 1 mg/mL HA (MW 360 kDa (Lifecore Biomedical, Chaska, MN, USA)) and 200 kDa (gift from Prof. Auzély-Velty, CERMAV, Grenoble) and 100 µg/mL heparin (H4784, Sigma). The cells were pre-incubated for 30 min in SFM alone or containing respective molecules and allowed to adhere on L2synd-grafted films for 4h.

For adhesion assays in presence of Rac1 and Cdc42 inhibitors, the cells were allowed to adhere for 4h in absence or in presence of 50 µg/ml of NSC23766 (Rac1 inhibitor) or 10µM of ML141 (Cdc42 inhibitor) in SFM. DMSO was used as a control for ML141 which is dissolved in DMSO.

To quantify cell morphology, fluorescence images were analysed with ImageJ software (v 1.44p,NIH, Bethesda) to determine cell area and aspect ratio. Confocal images in Z were analysed to measure the cell height. The aspect ratio is a parameter [*Major Axis*]/[*Minor Axis*] of the particle's fitted ellipse.

Microtubule orientation was quantified after 4h of adhesion in SFV with ImageJ software. Angle θ is defined as the angle between the vector parallel to the microtubule and the vector from the centrosome to the microtubule's closest segment.

2.5. Transfection by siRNA

Cells were transfected with siRNA against β_1 and β_3 integrins (ON-TARGET plus SMARTpool, respectively Mouse ITGB1 and Mouse ITGB3, Thermo Scientific Dharmacon) individually or at the same time, a scrambled siRNA (All Stars negative Control siRNA, Qiagen) being taken as control. For this, the cells were seeded at 30 000 cells/cm^2 in a 6-well plate and cultured in GM (2 mL per well) for 15 h. The transfection mix was prepared as following: for one well, 6 µL of lipofectamine RNAiMAX Reagent (Invitrogen) were added to 305 µL of Opti-MEM medium (Gibco) and 0.72 µL of 1 mM siRNA were added to another 305 µL of Opti-MEM medium. Lipofectamine-containing mix was added to siRNA-containing mix and incubated for 20 min at room temperature. Previously to transfection, the GM of the wells was replaced by the GM without antibiotics. Then, 610 µL of the final mix were added to each well. After 24 h of incubation at 37°C, the cells were transfected for the second time following the protocol described above and incubated for another 24h. Then the cells were detached by trypsin-EDTA, seeded in GM at 10 000 cells/cm^2 on the films built in 96-well plate and allowed to adhere for 4 h in SFM.

2.6. Immuno-staining

Cells were first rinsed in PBS and fixed in 3.7% formaldehyde for 30 min at RT before being permeabilized in 0.5% Triton X-100 for 4 min. After rinsing with PBS, samples were incubated for 1 h in 0.1 % BSA in TRIS-buffered saline (TBS, 50 mM TRIS, 150 mM NaCl, 0.1% NaN_3, pH 7.4). Actin was labeled with phalloidin-TRITC (1:800, Sigma) for 30

min. Cell nuclei were stained with Hoechst 33342 (Invitrogen) at 5 µg/ml for 10 min. After the incubations with the primary antibodies (diluted in 0.2% TBS-gelatin) for 30 min at RT, cells were washed 3 times in TBS and incubated for 30 min with the secondary antibodies. Primary antibodies: mouse anti-β-tubulin antibody (1:200), rabbit anti-FAK pY397 antibody, (1:200, Invitrogen), myogenin (rabbit anti-myogenin antibody (1:30, Tebu-Bio). Secondary antibodies: Alexa-Fluor 488, 594 and 647-conjugated antibodies (Invitrogen) were used at 1:1000. Images were taken by means of Zeiss LSM 700 confocal microscope.

For Syndecan-1 immunostaining, a protocol adapted from Garcia and coworker was applied [55]. Briefly, cells were rinsed in PBS and incubated in ice-cold 1 mM DTSSP (3,3-dithiobis-(sulfosuccinimidyl)propionate, Calbiochem-Merck, Merck Chemicals, Nottingham, UK) in PBS for 30 min. Unreacted cross-linker was quenched with 50 mM Tris in PBS for 15 min and bulk cellular components were extracted in 0.1% SDS in PBS. The slides were then blocked in BSA (0,1% in TBS). After this, Syndecan-1 was immunostained with 281-2 mouse anti Syndecan-1 (CD138) antibody conjugated to biotin (1:100, BD Pharmingen, BD Biosciences) and FITC-Streptavidin (1:500, BD Pharmingen, BD Biosciences) was used for visualization.

2.7. Scanning Electron Microscopy (SEM)

To image the cells on the films by SEM, the films were constructed on 1 x 1 cm silicium wafers. The cells were seeded at 15 000 cells/cm^2 and allowed to adhere for 4 h before fixing them in 2,5% glutaraldehyde in 0,1 M cocadylate buffer pH 7.2 for 30 min. After rinsing with 0,1 M cocadylate buffer pH 7.2, the samples were dehydrated as following: 10 min in 70% ethanol, 10 min in 95% ethanol and 10 min in 100% ethanol. After drying, the samples were imaged by scanning electron microscopy (SEM) using a FEI-Quanta 250 SEM-FEG.

2.8. Cell migration

To follow cell migration, C2C12 cells were seeded at 15 000 cells/cm^2 in 96-well plates. Images were taken every 10 min during 10 h. For analysis, at least 20 cells were tracked using ImageJ (v1.45d, NIH, Bethesda).

2.9. Cell proliferation and differentiation

Cell proliferation was quantified by a EdU (5-ethynyl-2'-deoxyuridine) assay (Click-iT EdU Imaging Kit, Invitrogen). For the evaluation of cell proliferation in GM, the cells were seeded at 15 000 cells/cm^2 and allowed to adhere for 1 h in SFM, then cultured in GM for 24h, 48h or 72h. For proliferation in DM, the cells were seeded at 30 000 cells/cm^2 and allowed to adhere for 1 h in SFM. Cells were then grown for 1 day in GM and then for 1 day in DM. At the chosen time point the cells were incubated with EdU diluted at 1/1000 in cell culture medium for 1h at 37°C. The detection was carried out following the manufacturer instructions. At the end, nuclei were counter-stained with Hoechst 33432 (Invitrogen). The images of EdU and Hoechst-labeled nuclei were taken using a Zeiss LSM 700 confocal microscope For differentiation assays, cells were seeded at 30 000 cells/cm^2 and allowed to adhere for 1 h in SFM. Cells were then grown for 1 day in GM and then switched to DM. The medium was changed every 3 days.

2.10. Statistics

The results represent three independent experiments. For cell morphological measurements, at least 50 cells were analysed. For the ratio of proliferating cells, at least 20 images taken at 20x magnification were analysed. Data are reported as means ± standard deviation. Statistical comparisons were performed using SigmaPlot Version 11.0 software and based on an analysis of variance (ANOVA) followed by an appropriate

pairwise comparison or comparison versus control group procedure ($P < 0.05$ was considered significant). Statistically different values are reported on the figures.

3. Results

3.1. Density of L2synd peptide on the film surface

The principle of film buildup and functionalization with the peptide is depicted in Figure 1A. The film buildup was followed *in situ* by Quartz Crystal Microbalance with dissipation monitoring *(*QCM-D) (Fig. S1), which allowed us to measure film thickness using the Voigt model [56] and to calculate the adsorbed mass of L2synd peptide. Film thickness was about 70 nm for a film made of 6 layer pairs, and the quantity of bound peptide was about 500 ng/cm^2. The Young's modulus of the (PLL/PGA) films deposited on a thick polyelectrolyte cushion has previously been measured and were found 51 ± 17 kPa [57].

3.2. Effect of L2synd functionalization on C2C12 myoblast adhesion and morphology

Adhesion is the very first and important step of cell-substrate interactions, which is especially important for anchorage-dependent cells. To evaluate the effect of L2synd peptide on C2C12 myoblast adhesion, cells were cultured on L2synd-grafted films. RGD-grafted films were used as a positive control for myoblast adhesion [52] and PGA-maleimide functionalized peptide-free films were used as a negative control. In addition, mixed RGD/L2synd-grafted films were prepared to study the interplay between the signals provided by the two peptides. The cells were allowed to adhere for 4 h in serum free medium (SFM) to eliminate any effect of serum on early adhesion. The spreading area and morphology (circularity) were then evaluated. Actin and nuclei staining of C2C12 cells (Fig. 1B) revealed the presence of adherent cells on RGD, L2synd and RGD/L2synd films but of very few cells on PGA-maleimide-functionalized ones. In addition, these cells were poorly spread. Quantitative measurement of the cell area revealed that the area was 1,5 to 2 times higher on films presenting RGD peptide alone or a mix of RGD/L2synd as compared to those grafted with L2synd only (Fig. 1C). However, the aspect ratio was 1,5 times lower for films containing only RGD peptide as compared to films containing L2synd peptide or a mix of RGD/L2synd (Fig. 1D). This results indicated that the presence of RGD promotes cell spreading, while the presence of L2synd renders the cells more elongated.

As only few cells adhered on PGA-maleimide films, these control films were discarded from the subsequent experiments.

3.3. Specificity of cell interaction with L2synd and engaged receptors

We further wanted to verify if cell interaction with L2synd peptide was specific, i.e. if the cells specifically recognized the peptide sequence and bound to it. For this, we performed two competition assays (Fig. 1E and F).

In the first assay (Fig. 1E), we pre-incubated the cells with L2synd peptide in solution (sL2synd) before depositing the cells on L2synd-grafted films, still in presence of sL2synd. The results showed that the number of adherent cells was about 1,5 times lower in presence of sL2synd, as compared to control without sL2synd. This indicates that the peptide in solution competes with the grafted peptide and partially prevents the cells from adhesion onto L2synd-grafted films.

In the second assay (Fig. 1F) we compared cell adhesion on L2synd-grafted films and on the films grafted with a scrambled peptide: a peptide that has the same amino acid composition as L2synd, but not in the same order. The number of adherent cells was about

4 times lower on scrambled peptide as compared to L2synd peptide, showing that amino acid order was important and that the cells regognized quite specifically L2synd sequence.

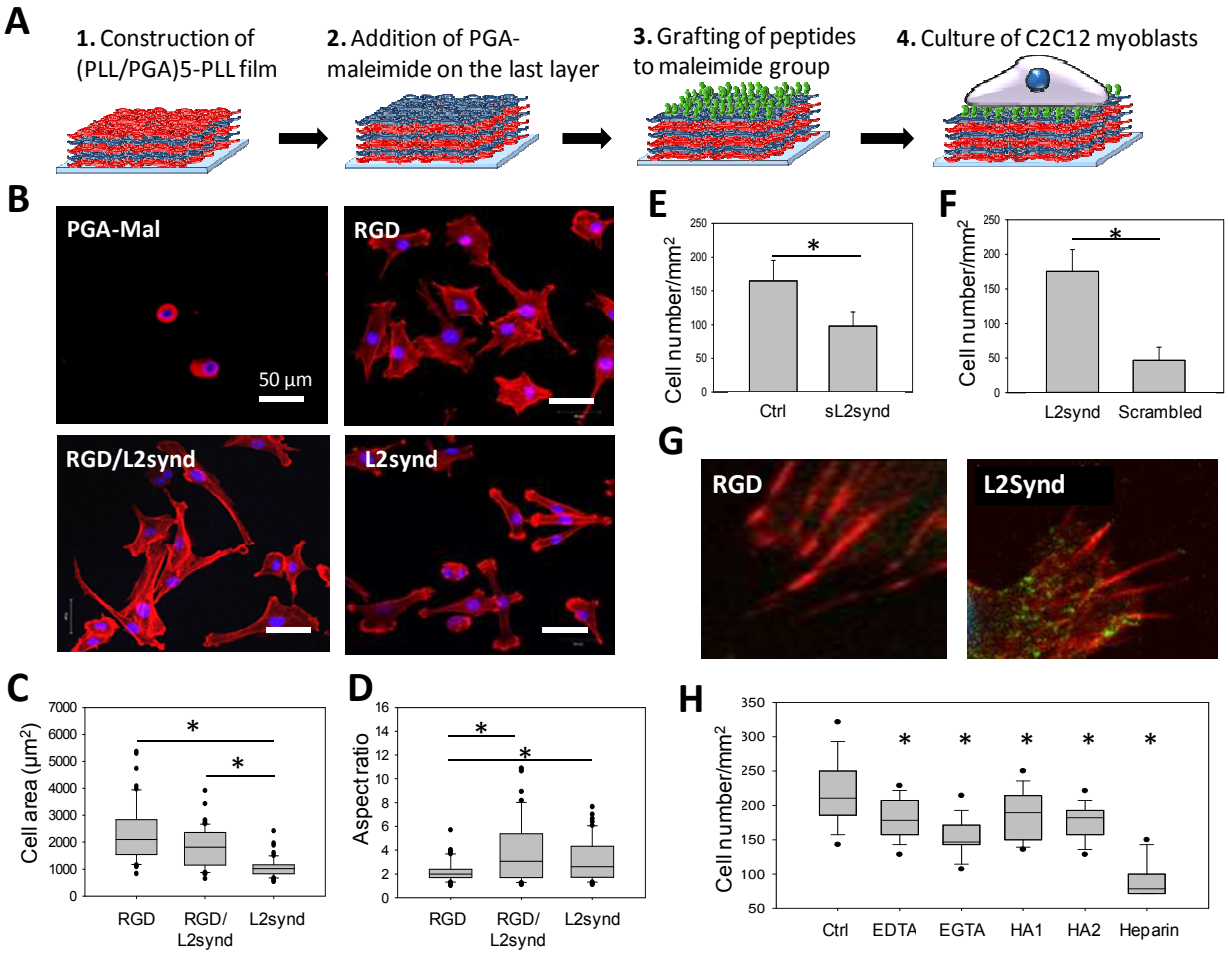

FIGURE 1. Cell adhesion, morphology and specificity of interaction on peptide-grafted films. *(A) Design and characterization of peptide-grafted films. 1- Polyelectrolyte multilayer film is built onto a substrate by alternating deposits of PLL and of PGA. 2- PGA-maleimide is added on the last layer of the film. 3- Biochemical functionality is provided by adding peptides that covalently bind to maleimide group. 4- C2C12 myoblasts are cultured on peptide-grafted films. (B) Actin (red) and nuclei (blue) staining of C2C12 cells to visualize cell adhesion and spreading after 4h of culture on RGD-, RGD/L2synd and L2synd-grafted films. PGA-maleimide functionalized film was used as a peptide-free control. (C) Spreading area after 4h of culture. (D) Aspect ratio after 4h of culture. (E) Adhesion inhibition on L2synd-grafted films by pre-incubating the cells with L2synd peptide in solution (sL2synd); error bars correspond to SD. (F) Adhesion on L2synd-grafted film and on the films grafted with scrambled peptide; error bars correspond to SD. (G) Expression of Syndecan-1 (green) on RGD and L2synd-grafted films; actin is labeled in red. (H) Adhesion inhibition on L2synd-grafted film by EDTA, EGTA, HA1 (MW $4x10^5$), HA2 (MW $2x10^5$) and heparin; conditions that are statistically different from the control are indicated by an asterix. * $p < 0.05$*

Since L2synd peptide was shown to interact with SDC-1 [32], we looked at the SDC-1 expression and localization on L2synd-grafted films and compared it to RGD-grafted films. SDC-1 labeling was detected in cell extremities on L2synd films close to actin bundles (Fig. 1G), but not on RGD films, indicating that SDC-1 is involved in C2C12 myoblast interaction with L2synd peptide, but not with RGD peptide.

Previous studies have demonstrated cooperation between syndecan and integrin receptors in cell adhesion control, although precise mechanisms of their crosstalk remain unclear [58]. In laminin-α1 chain, LG4 module was shown to promote cell attachment through syndecans and cell spreading through integrin α2β1 [59]. In addition, syndecan- and integrin-binding peptides from LG4 module were shown to synergistically accelerate cell adhesion [60]. To determine if integrins were involved in myoblast adhesion to L2synd-grafted films, we evaluated the effect of EDTA and EGTA on cell adhesion (Fig. 1H). Glycosaminoglycans (hyaluronic acid of two different MW and heparin) were used as competitors with SDC-1 polysaccaride side chains to confirm their involvement in cell adhesion to L2synd peptide. Interestingly, all five treatments including EDTA and EGTA decreased the number of adherent cells, although heparin had at least 2-time stronger effect than other treatments. These data showed that integrins may also be involved in cell adhesion to L2synd-grafted films, suggesting the existence of crosstalk between SDC-1 and integrin receptors in myoblasts.

The major integrin beta chains in C2C12 myoblasts are β_1-integrin, which is constitutively expressed in skeletal muscle [61] and β_3 integrin, which was found to be crucial for myogenic differentiation of C2C12 myoblasts [62]. In order to investigate their possible role in cell adhesion to L2synd-grafted films, we performed β_1 or β_3 integrin (or both) knockdown using siRNA approach. RGD-grafted films were used as control: we have recently reported that β_3 integrins were involved in C2C12 myoblast adhesion to RGD peptide-functionalized surface [52]. In addidion, we studied the mixed RGD/L2synd films to evaluate the possible synergy of the signals. The transfected cells cells were stained for actin after 4 h of adhesion and their area and morphology were quantified (Fig. 2). As described previously [52], only β_3 blocking but not of β_1 lead to a decrease in cell spreading on RGD (Fig. 2B-a). Double tranfection of β_1 and β_3 siRNA gave similar results. The same decrease of cell spreading was observed on mixed RGD/L2synd films (Fig. 2B-b). However, neither β_1 nor β_3 blocking had effect on cell spreading on L2synd-grafted films (Fig. 2B-c). Analysis of cell morphology showed that on RGD films only β_1 blocking slightly affected aspect ratio. Interestingly, on L2synd-grafted films β_1 and β_1/β_3 blocking significantly modified cell shape from elongated to very round (Fig. 2A), resulting in 2-fold decrease in the aspect ratio (Fig. 2B-f). The same phenomenon was observed on RGD/L2synd films (Fig. 2B-e). These findings reveal that neither β_1 nor β_3 integrins are involved in cell spreading on L2synd films, but β_1 is responsible for maintaining elongated cell shape on L2synd films. In case of mixed RGD/L2synd films both β_1 and β_3 are involved, with β_3 responsible for cell spreading and β_1 for elongated cell shape.

3.4. Three-dimensional morphology and cytoskeleton organization

To clarify the effects of C2C12 myoblast interactions via syndecan versus integrin receptors, we analysed cell adhesion on RGD and L2synd films in more details. The 3D reconstruction of the cells seeded on RGD or L2synd films revealed a significant difference in cell shape (Fig. 3A). The cells on RGD appeared as homogeneously flat with flattened nucleus, while on L2synd films the cells appeared as polarized with flattened lamellipodium on the leading edge and bulgy nucleus.

Cross-sections in Z done by confocal microscopy (Fig. 3B) were used for the quantification of cell height in nuclear area. The cells on RGD films were ~8 μm high against ~10 μm on L2synd films (Fig. 3C).

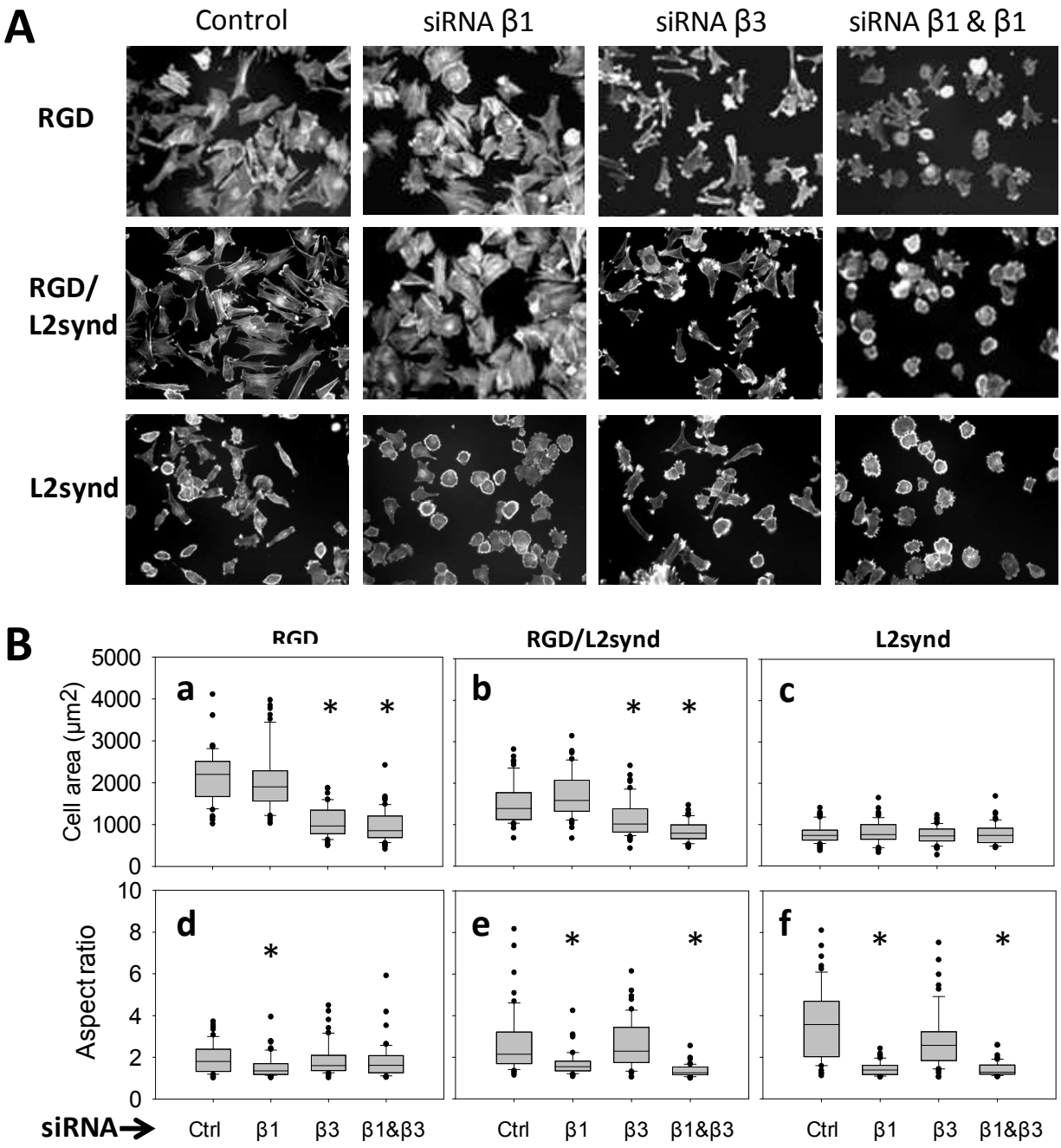

FIGURE 2. Effect of blocking β_1 and/or β_3 integrins on cell spreading on RGD, RGD/L2synd and L2synd-grafted films. *The β_1 and/or β_3 integrins were blocked using siRNA. (A) Actin labeling and (B) quantification of the cell area and aspect ratio after 4 h of adhesion. * $p < 0.05$ compared to control (scrambled siRNA).*

Cell periphery was also differentially organized. SEM images (Fig. 3D) show actin stress fiber extremities on the cell periphery on RGD films and large flat lamellipodia containing actin bundles that orthogonally encounter the leading edge on L2synd films. Actin visualization by fluorescent microscopy (Fig. 3E) confirmed the presence of large stress fibers crossing the cell and ending in filopodia all around cell periphery on RGD films. On L2synd films, a polarized morphology with lamellipodial leading edge, trailing edge and parallel stress fibers between them was observed. The difference in polarity and actin cytoskeleton was associated to different organization of focal adhesions (Fig.

3F). Focal adhesions were visualized by labeling phosphorylated focal adhesion kinase (pFAK), an important component of mature FA. Robust focal adhesions or even fibrillar adhesions (small dashes at the cell periphery) were formed on RGD films, while only focal complexes (small dots) were visible at the leading edge of lamellipodium on L2synd films.

Thus, our data revealed completely different cell adhesion modes on RGD versus L2synd films. On RGD films, cells were well-spread and flattened, attached to the surface by robust adhesions at the extremities of thick actin stress fibers. On L2synd films, cells presented polarized morphology with large and flat lamellipodium at the leading edge, smaller adhesion complexes, thinner actin stress fibers organized in parallel between the leading and trailing edge and bulgy nucleus.

Cooperation between actin cytoskeleton and microtubules (MT) is known to be crucial for cell polarization and lamellipodia formation [63], we thus looked at the organization of MT. The cells on RGD films mostly exhibited radial MT converging to the centrosome, while on L2synd films they seemed differentially organized and oriented in different senses (Fig. 4A).

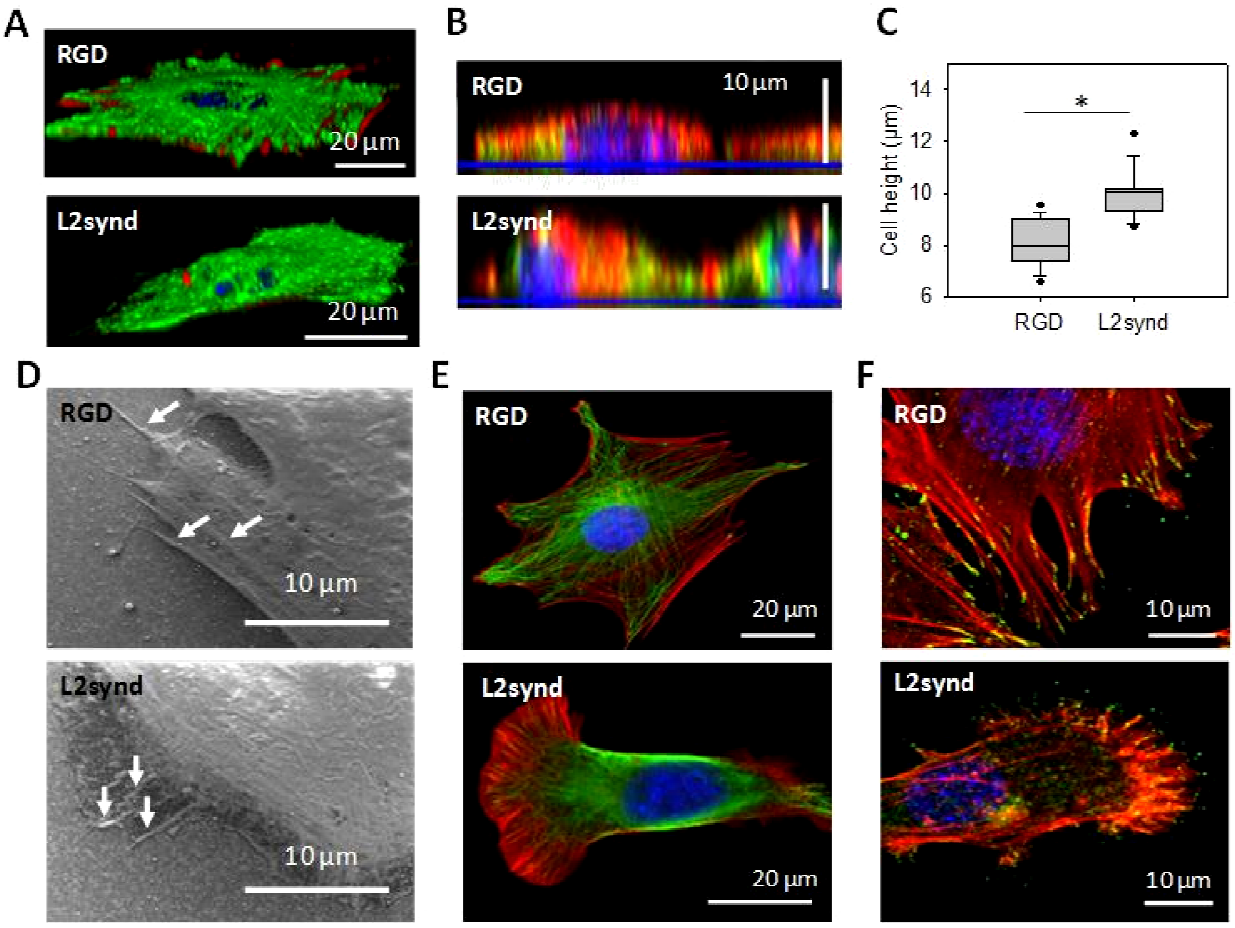

FIGURE 3. Three-dimensional morphology and cytoskeleton organization in the cells seeded on RGD and L2synd-functionalized films after 4h of adhesion. *(A) 3D reconstruction of the cells and (B) cross-sections in Z done using confocal microscopy; beta-tubulin (green), actin (red) and nuclei (blue) were stained. (C) Quantification of cell height, * $p < 0.05$. (D) Scanning electron microscopy (SEM) images, top view. Actin stress fibers (upper image) and actin bundles (lower image) are indicated by white arrows. (E) Staining of actin cytoskeleton (red) and nuclei (blue). (F) Staining of phosphorylated focal adhesion kinase (pFAK Y397, green), actin (red) and nuclei (blue).*

To quantitatively analyse microtubular organization, we measured the angles between the vector parallel to the MT and the vector from the centrosome to the microtubule's closest segment (Fig. 4B) [64]. On RGD films 63% of MT were oriented at less than 30° and 15% at more than 60°, against 33% and 30% on L2synd films, respectively. Globally, on L2synd films, the distribution of the angles was rather homogenous, without predomination of particular orientation. Our results suggest that centrosomal microtubules predominate on RGD films, while on L2synd films they seem to polymerize much more from other non-centrosomal sites.

3.5. Cell migration and directionality

Cell polarity and movement are determined by cooperation between the actin and MT cytoskeletons [63]. The role of non-centrosomal MT in cell architecture and function remains not fully understood. Recently, non-centrosomal MT were shown to regulate actin cytoskeleton organization [64]. Earlier, the balance between MT minus-end capture and release from the centrosome was shown to be critical for efficient cell migration [65].

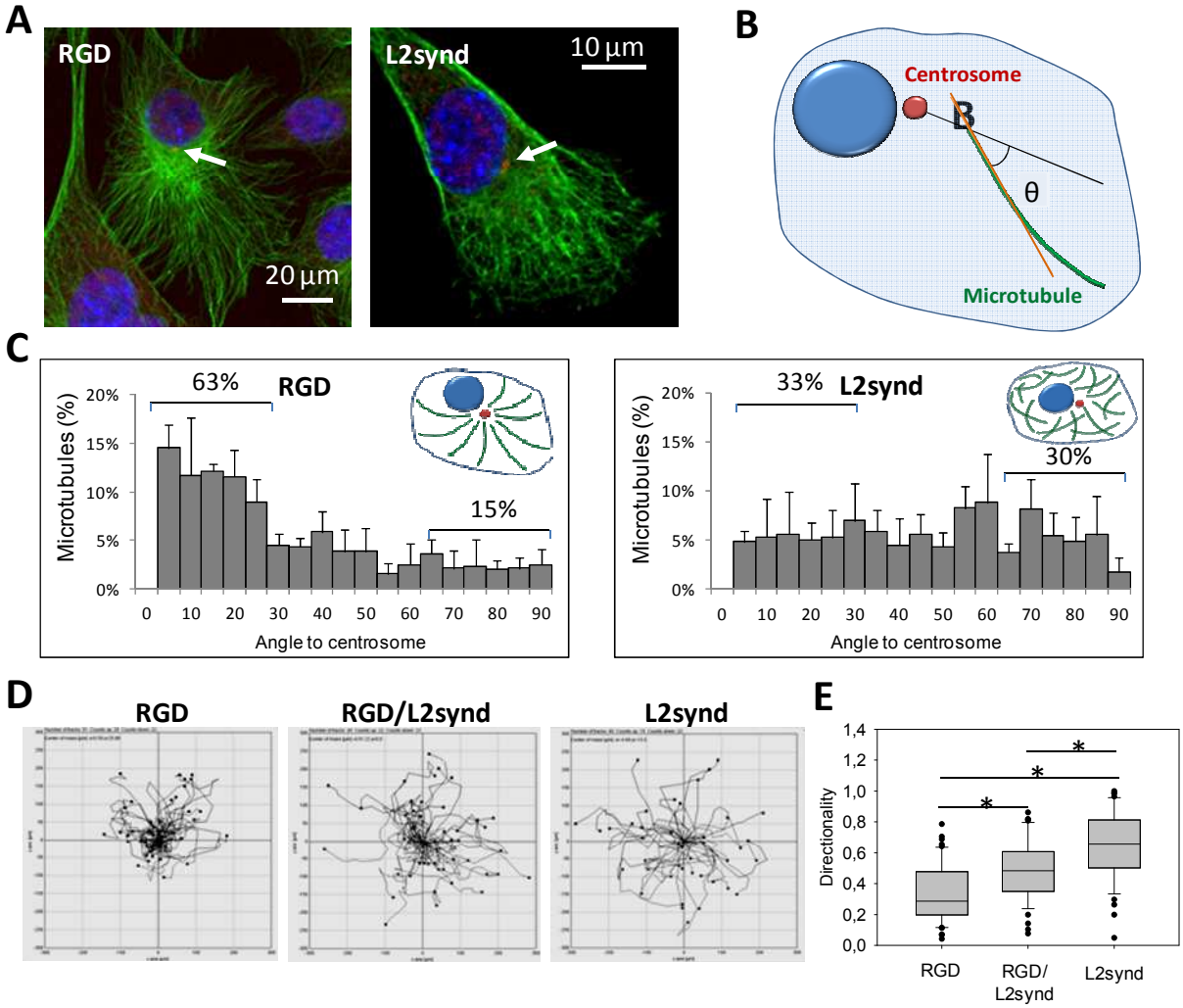

FIGURE 4. Orientation of microtubules and migration on peptide-grafted films *(A) Fluorescent labeling of beta-tubulin (green), ninein (red, indicated by white arrows) and nuclei (blue). (B) Scheme of quantitative measurement of the microtubule organization. Angle θ is defined as the angle between the vector parallel to the microtubule and the vector from the centrosome to the microtubule's closest segment. (C) Quantification of microtubule orientation: the histogram represents a percentage of microtubules with various angles to the centrosome. Data were collected from 5 cells, error bars correspond to SD. (D) Migration was measured for 10h after 4h of adhesion. Migration paths for approximately 20 cells. (E) Quantification of cell directionality (defined as displacement / total path length of the cell). * $p < 0.05$*

To investigate if difference in cell polarity and MT orientation was associated to differences in cell migration, we followed cell migration for 10h on RGD, L2synd and RGD/L2synd-grafted films (Fig. 4D) and quantified both cell velocity and directionality. While there was no significant difference in cell migration speed (Fig. S2), the directionality was higher on L2synd films as compared to RGD films (Fig. 4E). Mixed RGD/L2synd films presented intermediate directionality values. Thus, cell polarity and cytoskeletal organization on L2synd films was associated to an increased directionality.

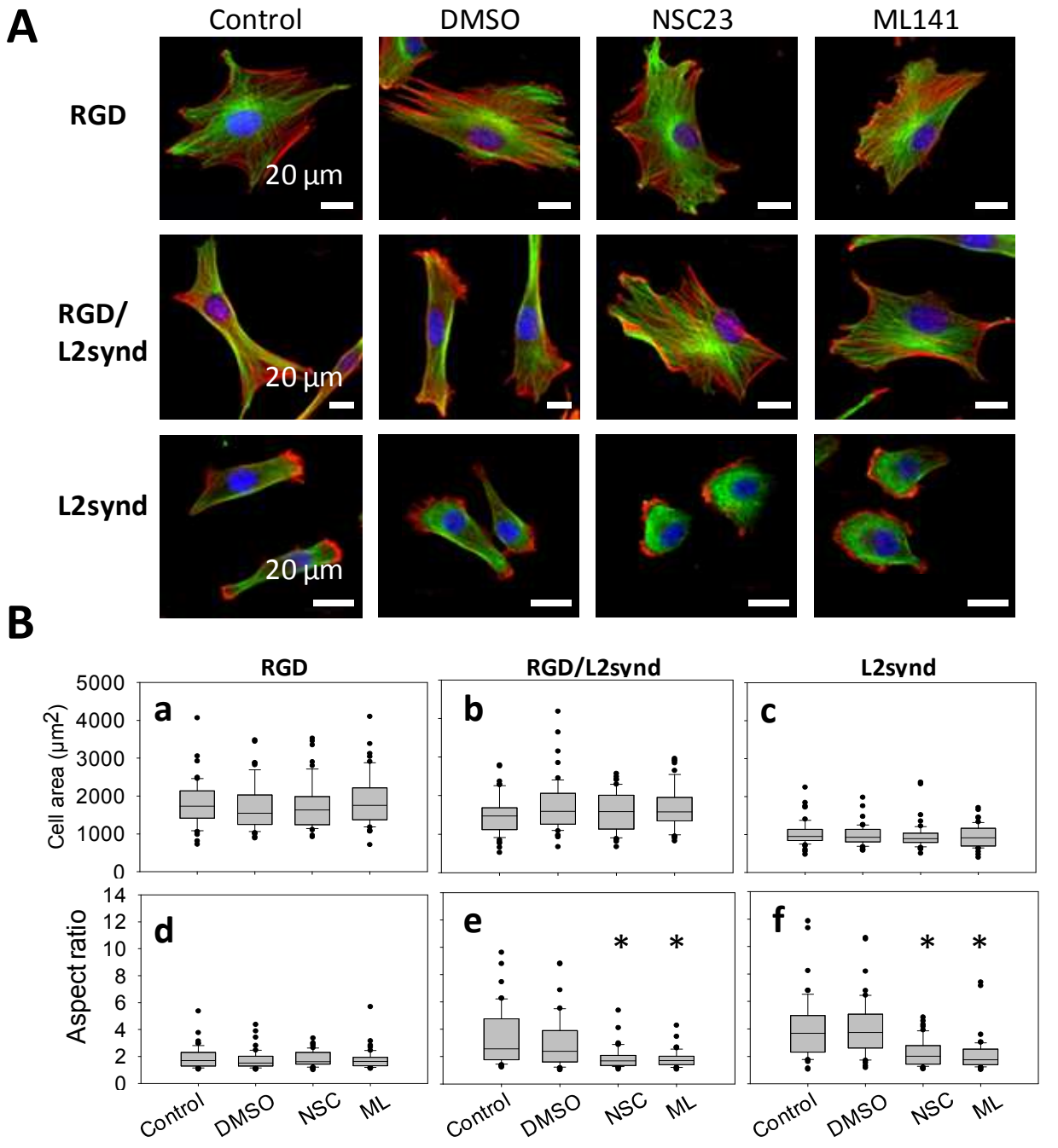

FIGURE 5. Effect of Rac1 and Cdc42 inhibitors on cell morphology on RGD, RGD/L2synd and L2synd-grafted films. *(A) Fluorescent labeling of beta-tubulin (green), actin (red) and nuclei (blue) after 4h of adhesion in absence or in presence of Rac1 inhibitor (NSC23766) or Cdc42 inhibitor (ML141). (B) Quantification of cell area and aspect ratio. * $p < 0.05$ compared to control (DMSO is a control for ML141).*

3.6. Rac1 and Cdc42 are involved in cell polarization on L2synd films

Rho GTPases Rac1 and Cdc42 are implicated in the formation of focal complexes, cell polarization and directed cell movement [66; 67].

To investigate if cell polarization on L2synd-grafted films was related to Rac1 and Cdc42 signaling, we analysed cell spreading and morphology after 4h of adhesion in absence or in presence of Rac1 inhibitor (NSC23766) or Cdc42 inhibitor (Fig. 5). Cell spreading or circularity on RGD films were not affected by any of the inhibitors (Fig. 5B-a and -d). However, on L2synd (Fig. 5B-c and -f) and RGD/L2synd films (Fig. 5B-b and -e), both inhibitors significantly affected cell shape: the aspect ratio decreased while the cell area remained the same. Such cell response to Rac1 and Cdc42 inhibition on L2synd-containing films "mimicks" the effect of beta1 blocking (Fig. 2B-e and -f), suggesting that these are the elements of the same pathway.

3.7. Cell proliferation and differentiation

C2C12 myoblasts are a well-known model for the *in vitro* study of myogenic differentiation due to their ability to reproduce processes that take place during *in vivo* differentiation of skeletal muscle progenitors [68]. Syndecan-1 expression was found downregulated during myoblast differentiation [33], and its overexpression inhibited the differentiation [34; 35] and promoted proliferation [36], we thus tested the effect of L2synd-presenting substrate on C2C12 myoblast proliferation and differentiation.

Cell proliferation in GM was evaluated on RGD, RGD/L2synd and L2synd films using EdU incorporation test (Fig. 6A and B). At 24h, there was no difference in the percentage of proliferating cells. At 48h, proliferation decreased on RGD-grafted films and remained at the same level on L2synd and RGD/L2synd films. At 72h, proliferation decreased on all the films but was about 3 times higher on L2synd films.

Control of cell proliferation by contact inhibition takes place when the cells reach confluence. To ensure that the difference in cell proliferation between L2synd and two other films is not due to different cell density, we labeled actin cytoskeleton and N-cadherin after 72h in GM (Fig. 6C). The images show that the cells form confluent layers on all three film types. However, cell-cell contact organization is different. On RGD, the contacts are visible between all the cells, the cells form a monolayer. However, on L2synd films, no cell-cell contacts are visible, the monolayer is disorganized. On RGD/L2synd films, the organization is intermediate. These data indicate that L2synd peptide has an effect not only on the morphology of individual, but also on the organization of confluent layers.

During myogenic differentiation, a highly ordered process of temporally separable events that begins with the expression of myogenic transcription factors and is followed by cell cycle arrest takes place [2]. In order to verify if the cells were able to undego myogenic differentiation on L2synd films, we quantified the expression of the transcription factor myogenin at early times of the differentiation process (Day 0 to 2) (Fig. 7A). The results show that, while myogenin expression progressively increased from Day 0 to 2 on RGD films, it remained 2 times lower on L2synd and RGD/L2synd films. Down-regulation of proliferation is needed for myogenesis to occur [2], thus we also quantified cell proliferation on the different types of films after addition of the DM (Day 1) by EdU incorporation assay (Fig. 7B). Proliferation at Day 1 was lower on RGD films compared to L2synd and RGD/L2synd films and about 2 times lower than after 24h in GM (Fig. 6B), indicating that the cells exit the cell cycle. On L2synd and RGD/L2synd films the proliferation at Day 1 remained at the same level as after 24h in GM, suggesting the absence of cell cycle exit.

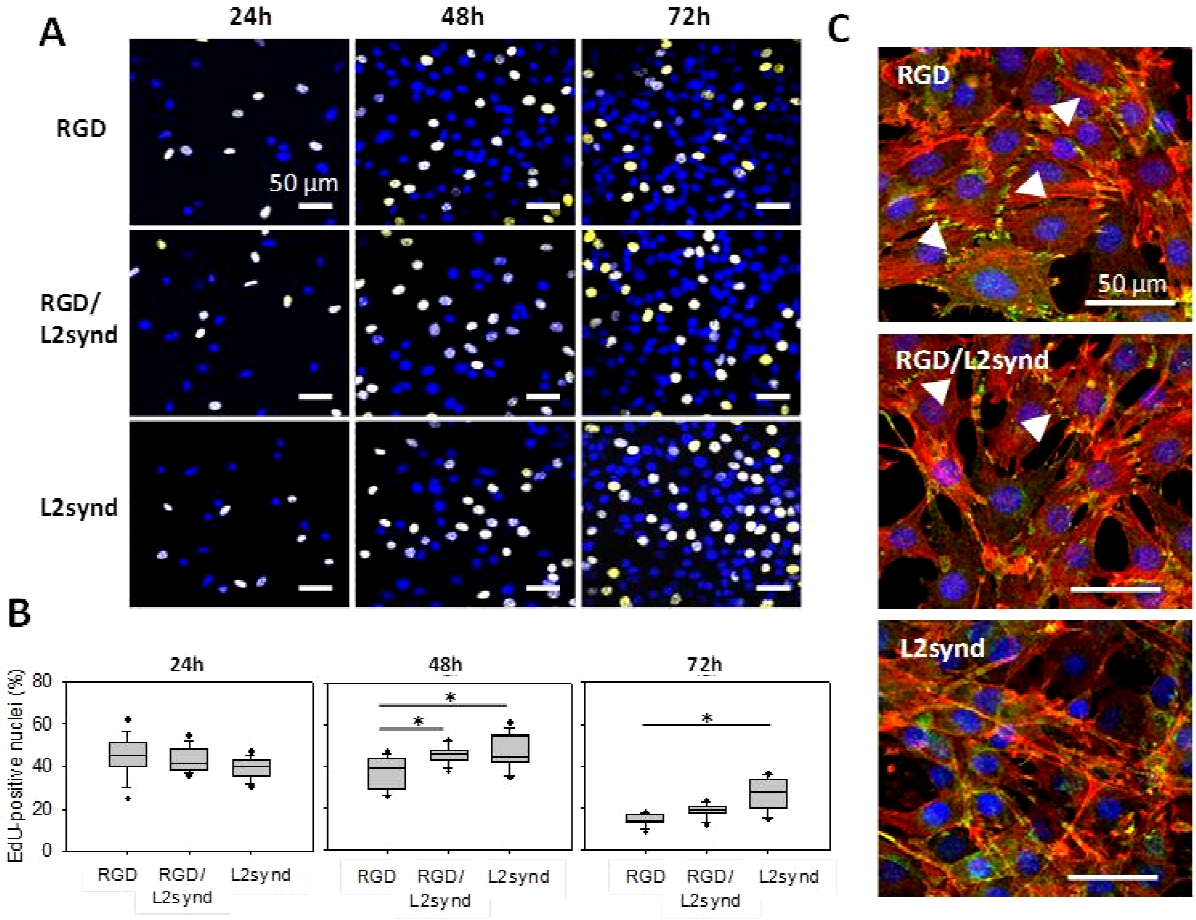

FIGURE 6. Cell proliferation on RGD, RGD/L2synd and L2synd-grafted films. *(A) Staining of EdU in the nuclei (yellow) associated to a fluorescent labeling of total nuclei (blue). (B) Percentage of BrdU-positive cells after 24h, 48h and 72h of culture in GM, * $p < 0.05$. (C) Staining of N-cadherin (green), actin (red) and nuclei (blue) after 72h of culture in GM.*

As we previously showed [52], C2C12 myoblasts differentiated on RGD-grafted films with formation of myotubes after 5 days (Fig. 7C). Some cell sheet detachment was observed on RGD/L2synd films, but the cell were also able to form myotubes. However, on L2synd films, the cell sheet completely detached after 2 days in DM. These data confirm previously described positive effect of the RGD peptide on myogenic differentiation and show that L2synd-grafted films are inappropriate for myogenic differentiation, but rather support cell proliferation. Cells on stiff films bypass the cell cycle exit induced by growth factor deprivation. Cell detachment observed on stiff films may thus be due to enhanced proliferation (Fig. 7B) leading to excessive cell confluence, and/or to enhanced cell migration, together with disorganization of the cellular monolayer and absence of N-cadherin cell-cell contacts (Fig. 6C).

Discussion

It is becoming increasingly clear that biochemical properties of the substrate play an important role not only in cell adhesion, but in many other processes such as proliferation and differentiation [1; 69]. However, in most studies, the substrates are coated by full-length ECM proteins (fibronectin, laminin), their fragments (gelatin) or protein mixtures (Matrigel). Despite the efficacity of this approach for some applications, such as enhancing cell adhesion of primary cells or promoting cell proliferation, it doesn't allow exploring the effect of each type of signal on cellular processes.

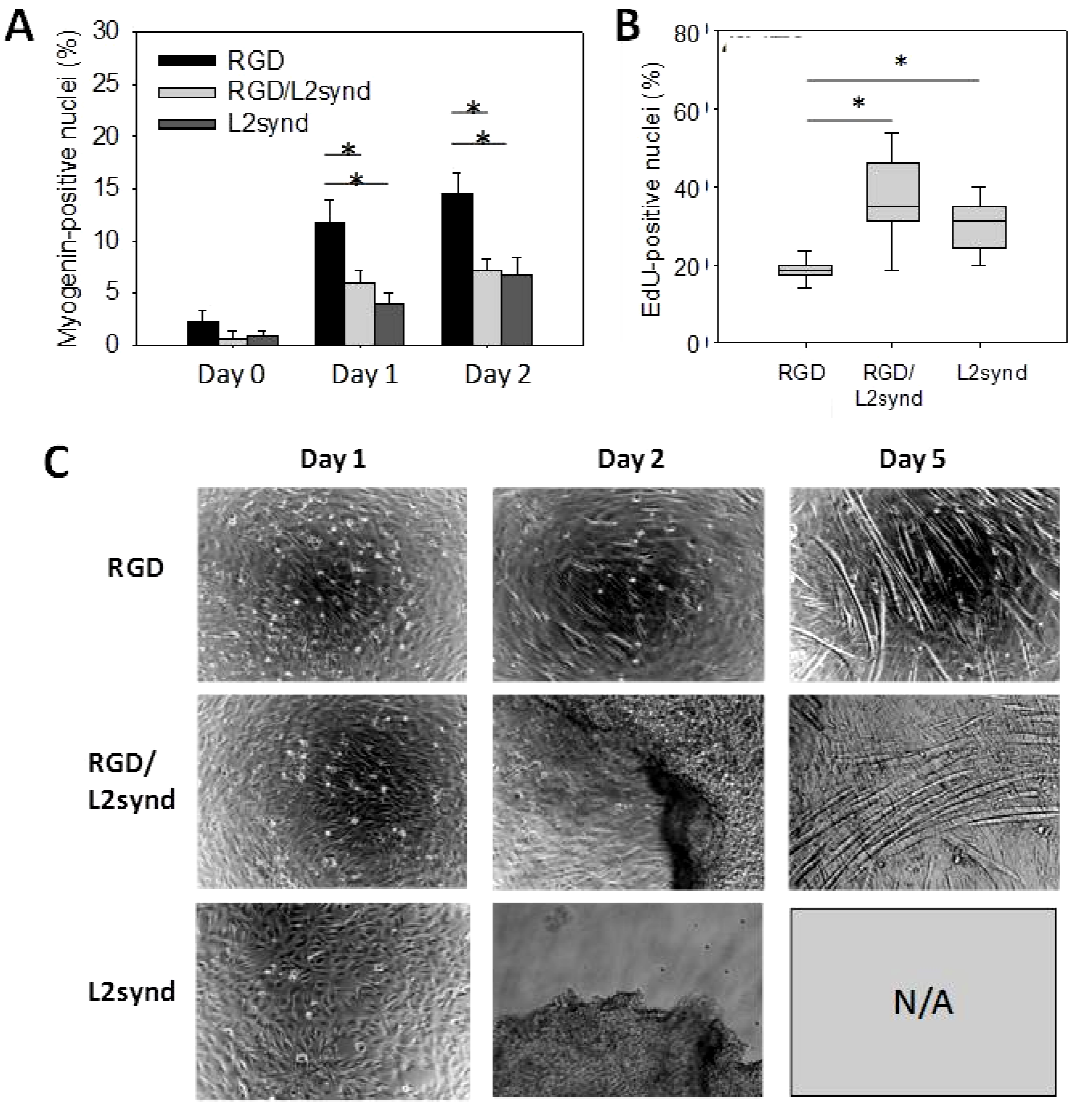

FIGURE 7. Myogenic differentiation on RGD, RGD/L2synd and L2synd-grafted films. *After culture in GM to reach the confluence, the medium was changed to DM (ie Day 0). (A) Quantification of the percentage of myogenin expressing cells at 72h, Day 1 and 2 of differentiation. Error bars correspond to SD, * $p < 0.05$. (B) Percentage of EdU-positive cells after 1 day in DM, * $p < 0.05$. (C) (A) Phase contrast microscopy observations of C2C12 cell differentiation for 5 days. Cell detachment was observed on L2synd-grafted film after 2 days in DM.*

For instance, laminins contain many domains interacting with numerous integrin and non-integrin cell receptors [15; 16; 17]. To control cell processes *in vitro*, the contribution of each adhesive ligand has to be clarified.

In the previous study we described RGD-functionalized "soft" film, compared to stiffer films with or without RGD peptide [52]. Soft RGD-grafted films were shown to recruit beta3 integrins and were favorable for myogenesis. In the present work we targeted a non-integrin laminin receptor SDC-1 whose role in cellular processes of skeletal muscle remains unclear, and compared SDC-1-mediated response to one induced by RGD peptide. We especially focused on the sequence of events involved in C2C12 cell differentiation including early adhesion, migration, proliferation, differentiation and fusion of myoblast into myotubes.

The study of laminin interaction with SDC-1 and its role in myogenesis is rather challenging

due to the difficulty of the specific targeting of SDC-1 by laminin. On the one hand, cell culture on total laminin-coated substrates does not allow specific SDC-1 targeting, as LN possesses many active domains interacting with different receptors. Likewise, SDC-1 overexpression in the cells does not exclude the possibility of signaling via other receptors. On the other hand, when coating the surfaces with anti-SDC-1 antibody [37], interaction site targeted by the antibody (side chains or core protein) may be different from the one that ineracts with laminin, and activate different signaling pathways. Here, we used a novel model surface that allows study of SDC-1 mediated adhesion to laminin in more specific way.

Cell adhesion assays showed that RGD peptide induced better cell spreading, while L2synd peptide was responsible for elongated morphology. Interestingly, the cells seeded on mixed RGD/L2synd film presented both of these features: they were as spread as the cells on RGD films and as elongated as on L2synd films. Thus, the peptides can act simultaneously and induce a combination of the effects that each of them induces alone. Several studies provide evidences that laminin induces elongated/bipolar/polarized cell shape. Ocalan et al showed that culture of MM14 myoblasts on laminin-coated substrate resulted in bipolar cell shape [18]. Thus, our data suggest that polarized cell shape that was previously observed on laminin-coated substrates can be due to cell interaction via SDC-1.

In the previous study, Hoffman and al. showed that adhesion of human submandibular gland (HSG) cells to L2synd peptide was not affected by anti- β1-integrin antibodies [32]. In this study, we observed the effects of EDTA and EGTA on the number of adherent cells, suggesting that a divalent cation-depending adhesion was involved, as well as the effect of β1 blocking siRNA on cell morphology on L2synd-grafted films. Such difference may be explained by the use of different cell types and/or different peptide presentation mode (coating vs grafting). In addition, Hoffman and al. studied only number of adherent cells, but did not look at cell morphology. Our data suggest a crosstalk between SDC-1 and β1 integrin on L2synd-grafted substrate. Synergistic control of cell adhesion by integrins and syndecans have already been described [58], although the mechanisms and precise roles of this interplay remain unclear. Syndecan-1 was shown to support integrin α2β1-mediated adhesion to collagen in Chinese hamster ovary (CHO) cells, suggesting a previously unknown link between integrin-α2β1 and SDC-1 [70]. Hozumi et al. showed that syndecan-1/4 and integrin-α2β1 binding peptides derived from laminin-α1 synergistically accelerated cell adhesion [60]. Our data suggest that this link remains in SDC-1-mediated adhesion of C2C12 myoblasts to laminin-α2 derived sequence. This interaction between integrin-β1 and syndecans may be a common feature of different cell types on different substrates.

We also revealed that, on L2synd films, the cells presented a polarized phenotype with lamellipodia at the leading edge and increased directional migration compared to cells on RGD films. These data are in agreement with the effects of syndecan-1 ligation on lamellipodial spreading and the formation of fascin and actin bundles observed on COS-7 and C2C12 cells [71]. Functional roles of syndecan-1 V region in laminin-dependent C2C12 cell adhesion and polarized cell migration has also been reported [37]. In our study, such cell organization and migration mode was induced by SDC-1 interaction with a precise sequence of laminin-α2. We show that this relatively short 12 amino acid sequence is sufficient to promote cell polarization with formation of leading and trailing edges, lamellipodial spreading and

directional migration, such as observed in previous studies in response to either SDC-1 ligation or coating by total laminin [37; 71]. Interestingly, cell polarization and directional migration are usually induced by environmental cues such as growth factor or chemokine gradients [72; 73]. Here, polarization is induced by an adhesive ligand presented from the basal side, and the cells adapt directional migration mode even in absence of classic directionality-inducing factors.

Microtubule growth and organization are linked to the formation of lamellipodia and cell polarization [63]. Kinases Rac1 and Cdc42 that are known to promote cell polarization and directional migration were shown to be associated to microtubules through a downstream protein linker at the leading edge [74; 75]. In our study, polarized cell morphology on L2synd films correlated with the presence of non-centrosomal microtubules and was linked to Rac1 and Cdc42 activity. The role and functions of non-centrosomal microtubules are not fully understood, and their formation process seems to be dependent on cell type [76].We suggest that non-centrosomal microtubules may be involved in lamellipodia formation and play a role in maintaining cell polarity through Rac1 and Cdc42 pathway.
Interestingly, cell response to Rac1 and Cdc42 inhibition on L2synd-containing films "mimicked" the effect of beta1 blocking, suggesting that these are the elements of the same pathway and that β1 integrin – syndecan-1 crosstalk results in Rac1 and Cdc42 signaling. Such cooperation of integrins and syndecans to regulate Rac1 has been mentioned in several studies [58]. Understanding of this cooperation is very important: both modifications of SDC-1 expression and altered Rac1 activity are observed in many cancer types, leading to increased cell proliferation, loss of polarity and increased motility [66].

Figure 8A represents our model of L2synd effect on cytoskeleton organization and cell polarity. The cells interact with L2synd-grafted film through SDC-1 that cooperates with β1-integrin to activate Rac1 and Cdc42 pathway. Rac1 and Cdc42 contribute to formation of polarized phenotype (microtubule organization and lamellipodia formation), resulting in increased directionality.
Figure 8B represents the state of art concerning regulation of myoblast proliferation and differentiation by SDC-1, integrins and Rac1/Cdc42 pathway (black arrows) and contribution of our study to the understanding of this regulation (red arrows). Several studies have demonstrated that laminin-coated substrates were favorable for myoblast proliferation [18]. Meriane et al. have reported that Rac1 and Cdc42 impaired cell cycle exit of L6 myoblasts, inhibited myogenin expression and myogenic differentiation [77; 78]. On the other hand, SDC-1 overexpression also promoted cell proliferation [36] and inhibited the differentiation [34; 35]. In addition, β3-integrin was found to be crucial for myogenic differentiation [62], while β_1-integrin, which is constitutively expressed in skeletal muscle, has been shown to be dispensable to myogenesis [61]. We demonstrated that the cells on L2synd films exhibited increased proliferation and absence of cell cycle exit in DM, decreased myogenin expression and absence of myotube formation.

Thus, our results make a reconstruction of the events by linking together the previously observed separate effects of laminin, integrin β1 and syndecan-1 receptors and Rac1/ CdC42 pathways on myoblast proliferation and differentiation.

Conclusion and perspectives

Here, we used a novel model surface for the study of SDC-1 mediated adhesion to laminin and its role on skeletal myoblast cellular processes. We especially focused on the

sequence of events involved in C2C12 cell differentiation including early adhesion, migration, proliferation, differentiation and fusion of myoblast into myotubes. This work makes a connection between myoblast interaction with laminins via SDC-1 and signaling through Rac1 and CDC42 pathways that induce changes in cell architecture, enhanced proliferation and inhibition of myogenic differentiation. We also reveal SDC-1 cooperation with beta-1 integrins in maintaining cell polarity and directional migration.

This study demonstrates that by combining materials science/chemistry and cell biology approaches it is possible to target specific cell surface receptors and study their roles without changing their normal expression level by transfection or knock-down. It is also possible to combine two or more ligands targeting different receptors, in order to investigate their combined or synergistic effects. Moreover, biochemical functionality can be further combined to stiffness modulation (PEM films cross-linking), which is now recognized to play a crucial role in many cellular processes, or surface micropatterning. Thus, by using bottom-up approach, multifunctional substrates with perfect control over cell processes can be created. Such substrates are needed for fundamental studies, but also for creating scaffolds for tissue engineering and for stem cell expansion.

Acknowledgements

This research was supported by Region Rhônes-Alpes via a PhD fellowship to VG. CP and RAV are members of the Institut Universitaire de France (IUF). CP wishes to thank the European Commission for support in the framework of FP7 via an ERC Starting grant 2010 (GA 259370, BIOMIM). The authors thank Quentin Lubart for the film characterization by Quartz Crystal Microbalance.

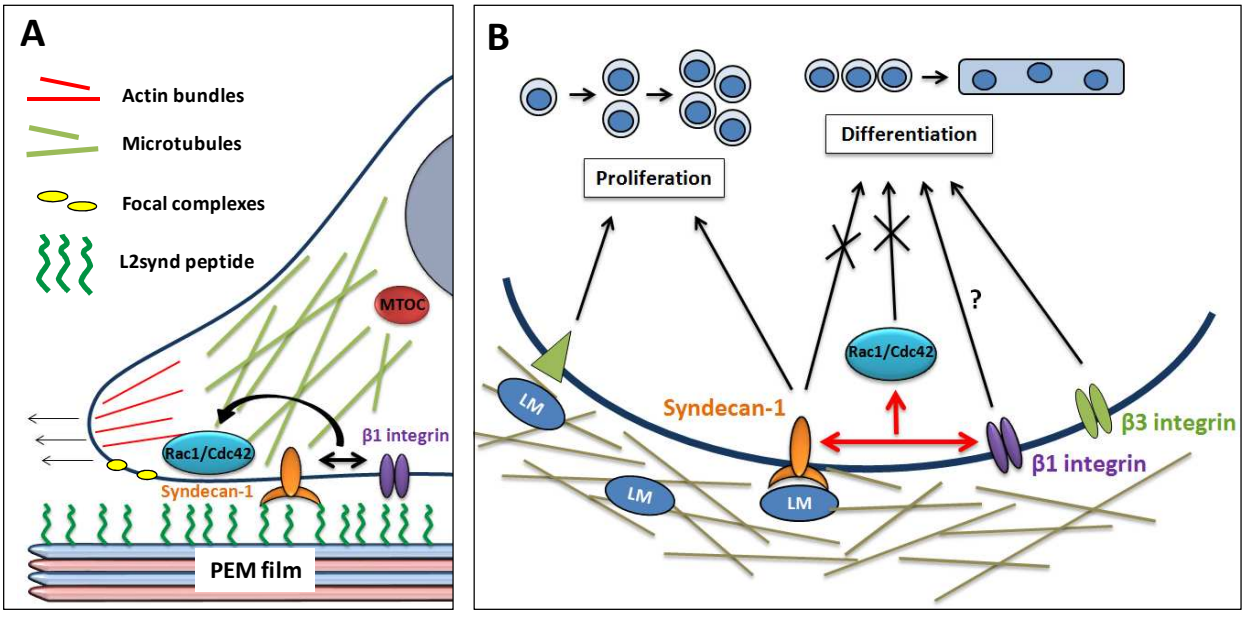

FIGURE 8. Proposed model of L2synd peptide on C2C12 myoblast cytoskeletal organization, proliferation and differentiation. *(A) L2synd-grafted films promote lamellipodia formation, increased cell polarity, presence of non-centrosomal microtubules and directional migration. This interaction involves cooperation between Syndecan-1 and beta-1 integrins and passes through Rho GTPases Rac1 and Cdc42 pathways. (B) Regulation of myoblast proliferation and differentiation by SDC-1, integrins and Rac1/Cdc42 pathway and contribution of our study to the understanding of this regulation (red arrows).*

References

1. Lutolf, M. P. & Hubbell, J. A. (2005). Synthetic biomaterials as instructive extracellular microenvironments for morphogenesis in tissue engineering. *Nat Biotechnol* **23**, 47-55.
2. Andres, V. & Walsh, K. (1996). Myogenin expression, cell cycle withdrawal, and phenotypic differentiation are temporally separable events that precede cell fusion upon myogenesis. *J Cell Biol* **132**, 657-66.
3. Bischoff, R. (1975). Regeneration of single skeletal muscle fibers in vitro. *Anat Rec* **182**, 215-35.
4. Le Ricousse-Roussanne, S., Larghero, J., Zini, J. M., Barateau, V., Foubert, P., Uzan, G., Liu, X., Lacassagne, M. N., Ternaux, B., Robert, I., Benbunan, M., Vilquin, J. T., Vauchez, K., Tobelem, G. & Marolleau, J. P. (2007). Ex vivo generation of mature and functional human smooth muscle cells differentiated from skeletal myoblasts. *Exp Cell Res* **313**, 1337-46.
5. Katagiri, T., Yamaguchi, A., Komaki, M., Abe, E., Takahashi, N., Ikeda, T., Rosen, V., Wozney, J. M., Fujisawa-Sehara, A. & Suda, T. (1994). Bone morphogenetic protein-2 converts the differentiation pathway of C2C12 myoblasts into the osteoblast lineage. *J Cell Biol* **127**, 1755-66.
6. Schindeler, A., Liu, R. & Little, D. G. (2009). The contribution of different cell lineages to bone repair: exploring a role for muscle stem cells. *Differentiation* **77**, 12-8.
7. Teboul, L., Gaillard, D., Staccini, L., Inadera, H., Amri, E. Z. & Grimaldi, P. A. (1995). Thiazolidinediones and fatty acids convert myogenic cells into adipose-like cells. *J Biol Chem* **270**, 28183-7.
8. Wada, M. R., Inagawa-Ogashiwa, M., Shimizu, S., Yasumoto, S. & Hashimoto, N. (2002). Generation of different fates from multipotent muscle stem cells. *Development* **129**, 2987-95.
9. Cosgrove, B. D., Sacco, A., Gilbert, P. M. & Blau, H. M. (2009). A home away from home: challenges and opportunities in engineering in vitro muscle satellite cell niches. *Differentiation* **78**, 185-94.
10. Thorsteinsdottir, S., Deries, M., Cachaco, A. S. & Bajanca, F. (2011). The extracellular matrix dimension of skeletal muscle development. *Dev Biol* **354**, 191-207.
11. Gillies, A. R. & Lieber, R. L. (2011). Structure and function of the skeletal muscle extracellular matrix. *Muscle Nerve* **44**, 318-31.
12. Trotter, J. A. & Purslow, P. P. (1992). Functional morphology of the endomysium in series fibered muscles. *J Morphol* **212**, 109-22.
13. Hinds, S., Bian, W., Dennis, R. G. & Bursac, N. (2011). The role of extracellular matrix composition in structure and function of bioengineered skeletal muscle. *Biomaterials* **32**, 3575-83.
14. Mauro, A. (1961). Satellite cell of skeletal muscle fibers. *J Biophys Biochem Cytol* **9**, 493-5.
15. Miner, J. H. & Yurchenco, P. D. (2004). Laminin functions in tissue morphogenesis. *Annu Rev Cell Dev Biol* **20**, 255-84.
16. Engel, J. & Furthmayr, H. (1987). Electron microscopy and other physical methods for the characterization of extracellular matrix components: laminin, fibronectin, collagen IV, collagen VI, and proteoglycans. *Methods Enzymol* **145**, 3-78.
17. Beck, K., Hunter, I. & Engel, J. (1990). Structure and function of laminin: anatomy of a multidomain glycoprotein. *FASEB J* **4**, 148-60.
18. Ocalan, M., Goodman, S. L., Kuhl, U., Hauschka, S. D. & von der Mark, K. (1988). Laminin alters cell shape and stimulates motility and proliferation of murine skeletal myoblasts. *Dev Biol* **125**, 158-67.
19. Silva-Barbosa, S. D., Butler-Browne, G. S., de Mello, W., Riederer, I., Di Santo, J. P., Savino, W. & Mouly, V. (2008). Human Myoblast Engraftment Is Improved in Laminin-Enriched Microenvironment. *Transplantation* **85**, 566-575 10.1097/TP.0b013e31815fee50.
20. Rooney, J. E., Gurpur, P. B., Yablonka-Reuveni, Z. & Burkin, D. J. (2009). Laminin-111 restores regenerative capacity in a mouse model for alpha7 integrin congenital myopathy. *Am J Pathol* **174**, 256-64.
21. Rooney, J. E., Gurpur, P. B. & Burkin, D. J. (2009). Laminin-111 protein therapy prevents muscle disease in the mdx mouse model for Duchenne muscular dystrophy. *Proc Natl Acad Sci U S A* **106**, 7991-6.
22. Miyagoe, Y., Hanaoka, K., Nonaka, I., Hayasaka, M., Nabeshima, Y., Arahata, K., Nabeshima, Y. & Takeda, S. (1997). Laminin alpha2 chain-null mutant mice by targeted disruption of the Lama2 gene: a new model of merosin (laminin 2)-deficient congenital muscular dystrophy. *FEBS Lett* **415**, 33-9.
23. Collins, J. & Bonnemann, C. G. (2010). Congenital muscular dystrophies: toward molecular therapeutic interventions. *Curr Neurol Neurosci Rep* **10**, 83-91.
24. Hynes, R. O. (2002). Integrins: bidirectional, allosteric signaling machines. *Cell* **110**, 673-87.
25. Hynes, R. O. (1992). Integrins: versatility, modulation, and signaling in cell adhesion. *Cell* **69**, 11-25.
26. Mayer, U. (2003). Integrins: redundant or important players in skeletal muscle? *J Biol Chem* **278**, 14587-90.
27. Perkins, A. D., Ellis, S. J., Asghari, P., Shamsian, A., Moore, E. D. & Tanentzapf, G. (2010). Integrin-mediated adhesion maintains sarcomeric integrity. *Dev Biol* **338**, 15-27.
28. Bernfield, M., Gotte, M., Park, P. W., Reizes, O., Fitzgerald, M. L., Lincecum, J. & Zako, M. (1999). Functions of cell surface heparan sulfate proteoglycans. *Annu Rev Biochem* **68**, 729-77.

29. Couchman, J. R. (2003). Syndecans: proteoglycan regulators of cell-surface microdomains? *Nat Rev Mol Cell Biol* **4**, 926-37.
30. Ruoslahti, E. (1988). Structure and biology of proteoglycans. *Annu Rev Cell Biol* **4**, 229-55.
31. Cornelison, D. D., Filla, M. S., Stanley, H. M., Rapraeger, A. C. & Olwin, B. B. (2001). Syndecan-3 and syndecan-4 specifically mark skeletal muscle satellite cells and are implicated in satellite cell maintenance and muscle regeneration. *Dev Biol* **239**, 79-94.
32. Hoffman, M. P., Nomizu, M., Roque, E., Lee, S., Jung, D. W., Yamada, Y. & Kleinman, H. K. (1998). Laminin-1 and laminin-2 G-domain synthetic peptides bind syndecan-1 and are involved in acinar formation of a human submandibular gland cell line. *J Biol Chem* **273**, 28633-41.
33. Larrain, J., Cizmeci-Smith, G., Troncoso, V., Stahl, R. C., Carey, D. J. & Brandan, E. (1997). Syndecan-1 expression is down-regulated during myoblast terminal differentiation. Modulation by growth factors and retinoic acid. *J Biol Chem* **272**, 18418-24.
34. Larrain, J., Carey, D. J. & Brandan, E. (1998). Syndecan-1 expression inhibits myoblast differentiation through a basic fibroblast growth factor-dependent mechanism. *J Biol Chem* **273**, 32288-96.
35. Velleman, S. G., Liu, X., Coy, C. S. & McFarland, D. C. (2004). Effects of syndecan-1 and glypican on muscle cell proliferation and differentiation: implications for possible functions during myogenesis. *Poult Sci* **83**, 1020-7.
36. Velleman, S. G., Coy, C. S. & McFarland, D. C. (2007). Effect of syndecan-1, syndecan-4, and glypican-1 on turkey muscle satellite cell proliferation, differentiation, and responsiveness to fibroblast growth factor 2. *Poult Sci* **86**, 1406-13.
37. Chakravarti, R., Sapountzi, V. & Adams, J. C. (2005). Functional role of syndecan-1 cytoplasmic V region in lamellipodial spreading, actin bundling, and cell migration. *Mol Biol Cell* **16**, 3678-91.
38. Suzuki, N., Yokoyama, F. & Nomizu, M. (2005). Functional sites in the laminin alpha chains. *Connect Tissue Res* **46**, 142-52.
39. Reyes, C. D., Petrie, T. A., Burns, K. L., Schwartz, Z. & Garcia, A. J. (2007). Biomolecular surface coating to enhance orthopaedic tissue healing and integration. *Biomaterials* **28**, 3228-35.
40. Weber, L. M., Hayda, K. N., Haskins, K. & Anseth, K. S. (2007). The effects of cell-matrix interactions on encapsulated beta-cell function within hydrogels functionalized with matrix-derived adhesive peptides. *Biomaterials* **28**, 3004-11.
41. Picart, C., Elkaim, R., Richert, L., Audoin, F., Arntz, Y., Da Silva Cardoso, M., Schaaf, P., Voegel, J. C. & Frisch, B. (2005). Primary Cell Adhesion on RGD-Functionalized and Covalently Crosslinked Thin Polyelectrolyte Multilayer Films. *Adv Funct Mater* **15**, 83-94.
42. Hozumi, K., Yamagata, N., Otagiri, D., Fujimori, C., Kikkawa, Y., Kadoya, Y. & Nomizu, M. (2009). Mixed peptide-chitosan membranes to mimic the biological activities of a multifunctional laminin alpha1 chain LG4 module. *Biomaterials* **30**, 1596-603.
43. Urushibata, S., Hozumi, K., Ishikawa, M., Katagiri, F., Kikkawa, Y. & Nomizu, M. (2010). Identification of biologically active sequences in the laminin alpha2 chain G domain. *Arch Biochem Biophys* **497**, 43-54.
44. Werner, S., Huck, O., Frisch, B., Vautier, D., Elkaim, R., Voegel, J. C., Brunel, G. & Tenenbaum, H. (2009). The effect of microstructured surfaces and laminin-derived peptide coatings on soft tissue interactions with titanium dental implants. *Biomaterials* **30**, 2291-2301.
45. Petrie, T. A., Raynor, J. E., Reyes, C. D., Burns, K. L., Collard, D. M. & Garcia, A. J. (2008). The effect of integrin-specific bioactive coatings on tissue healing and implant osseointegration. *Biomaterials* **29**, 2849-57.
46. Benoit, D. S. & Anseth, K. S. (2005). The effect on osteoblast function of colocalized RGD and PHSRN epitopes on PEG surfaces. *Biomaterials* **26**, 5209-20.
47. Nomizu, M., Song, S. Y., Kuratomi, Y., Tanaka, M., Kim, W. H., Kleinman, H. K. & Yamada, Y. (1996). Active peptides from the carboxyl-terminal globular domain of laminin alpha2 and Drosophila alpha chains. *FEBS Lett* **396**, 37-42.
48. Decher, G., Hong, J. D. & Schmitt, J. (1992). Buildup of ultrathin multilayer films by a self-assembly process: III. Consecutively alternating adsorption of anionic and cationic polyelectrolytes on charged surfaces. *Thin Solid Films* **210-211**, 831-835.
49. Lvov, Y., Decher, G., Haas, H., Mohwald, H. & Kalachev, A. (1994). X-ray analysis of ultrathin polymer films self-assembled onto substrates. *Physica B* **198**, 89-91.
50. Decher, G. (1997). Fuzzy Nanoassemblies: Toward Layered Polymeric Multicomposites. *Science* **277**, 1232-1237.
51. Boudou, T., Crouzier, T., Ren, K., Blin, G. & Picart, C. (2010). Multiple Functionalities of Polyelectrolyte Multilayer Films: New Biomedical Applications. *Adv Mater* **22**, 441-467.
52. Gribova, V., Gauthier-Rouvière, C., Albigès-Rizo, C., Auzely-Velty, R. & Picart, C. (2012). Effect of RGD-functionalization and stiffness modulation of polyelectrolyte multilayer films on muscle cell differentiation. *Acta Biomater*.
53. Suzuki, N., Hozumi, K., Urushibata, S., Yoshimura, T., Kikkawa, Y., Gumerson, J. D., Michele, D. E., Hoffman, M. P., Yamada, Y. & Nomizu, M. (2010). Identification of alpha-dystroglycan binding sequences in the laminin

alpha2 chain LG4-5 module. *Matrix Biol* **29**, 143-51.
54. Crouzier, T. & Picart, C. (2009). Ion pairing and hydration in polyelectrolyte multilayer films containing polysaccharides. *Biomacromolecules* **10**, 433-42.
55. Keselowsky, B. G. & Garcia, A. J. (2005). Quantitative methods for analysis of integrin binding and focal adhesion formation on biomaterial surfaces. *Biomaterials* **26**, 413-8.
56. Voinova, M. V., Rodahl, M., Jonson, M. & Kasemo, B. (1999). Viscoelastic Acoustic Response of Layered Polymer Films at Fluid-Solid Interfaces: Continuum Mechanics Approach. *Physica Scripta* **59**, 391.
57. Schneider, A., Bolcato-Bellemin, A. L., Francius, G., Jedrzejwska, J., Schaaf, P., Voegel, J. C., Frisch, B. & Picart, C. (2006). Glycated polyelectrolyte multilayer films: differential adhesion of primary versus tumor cells. *Biomacromolecules* **7**, 2882-9.
58. Morgan, M. R., Humphries, M. J. & Bass, M. D. (2007). Synergistic control of cell adhesion by integrins and syndecans. *Nat Rev Mol Cell Biol* **8**, 957-69.
59. Hozumi, K., Suzuki, N., Nielsen, P. K., Nomizu, M. & Yamada, Y. (2006). Laminin alpha1 chain LG4 module promotes cell attachment through syndecans and cell spreading through integrin alpha2beta1. *J Biol Chem* **281**, 32929-40.
60. Hozumi, K., Kobayashi, K., Katagiri, F., Kikkawa, Y., Kadoya, Y. & Nomizu, M. (2010). Syndecan- and integrin-binding peptides synergistically accelerate cell adhesion. *FEBS Lett* **584**, 3381-5.
61. Hirsch, E., Lohikangas, L., Gullberg, D., Johansson, S. & Fassler, R. (1998). Mouse myoblasts can fuse and form a normal sarcomere in the absence of beta1 integrin expression. *J Cell Sci* **111 (Pt 16)**, 2397-409.
62. Liu, H., Niu, A., Chen, S. E. & Li, Y. P. (2011). Beta3-integrin mediates satellite cell differentiation in regenerating mouse muscle. *The FASEB Journal* **25**, 1914-21.
63. Goode, B. L., Drubin, D. G. & Barnes, G. (2000). Functional cooperation between the microtubule and actin cytoskeletons. *Curr Opin Cell Biol* **12**, 63-71.
64. Nagae, S., Meng, W. & Takeichi, M. (2013). Non-centrosomal microtubules regulate F-actin organization through the suppression of GEF-H1 activity. *Genes Cells* **18**, 387-96.
65. Abal, M., Piel, M., Bouckson-Castaing, V., Mogensen, M., Sibarita, J. B. & Bornens, M. (2002). Microtubule release from the centrosome in migrating cells. *J Cell Biol* **159**, 731-7.
66. Sahai, E. & Marshall, C. J. (2002). RHO-GTPases and cancer. *Nat Rev Cancer* **2**, 133-42.
67. Small, J. V. & Kaverina, I. (2003). Microtubules meet substrate adhesions to arrange cell polarity. *Curr Opin Cell Biol* **15**, 40-7.
68. Bach, A. D., Beier, J. P., Stern-Staeter, J. & Horch, R. E. (2004). Skeletal muscle tissue engineering. *J Cell Mol Med* **8**, 413-422.
69. Stevens, M. M. & George, J. H. (2005). Exploring and engineering the cell surface interface. *Science* **310**, 1135-8.
70. Vuoriluoto, K., Jokinen, J., Kallio, K., Salmivirta, M., Heino, J. & Ivaska, J. (2008). Syndecan-1 supports integrin alpha2beta1-mediated adhesion to collagen. *Exp Cell Res* **314**, 3369-81.
71. Adams, J. C., Kureishy, N. & Taylor, A. L. (2001). A role for syndecan-1 in coupling fascin spike formation by thrombospondin-1. *J Cell Biol* **152**, 1169-82.
72. Lortat-Jacob, H. (2009). The molecular basis and functional implications of chemokine interactions with heparan sulphate. *Curr Opin Struct Biol* **19**, 543-548.
73. Kucia, M., Reca, R., Miekus, K., Wanzeck, J., Wojakowski, W., Janowska-Wieczorek, A., Ratajczak, J. & Ratajczak, M. Z. (2005). Trafficking of Normal Stem Cells and Metastasis of Cancer Stem Cells Involve Similar Mechanisms: Pivotal Role of the SDF-1–CXCR4 Axis. *Stem Cells* **23**, 879-894.
74. Fukata, M., Watanabe, T., Noritake, J., Nakagawa, M., Yamaga, M., Kuroda, S., Matsuura, Y., Iwamatsu, A., Perez, F. & Kaibuchi, K. (2002). Rac1 and Cdc42 capture microtubules through IQGAP1 and CLIP-170. *Cell* **109**, 873-85.
75. Watanabe, T., Wang, S., Noritake, J., Sato, K., Fukata, M., Takefuji, M., Nakagawa, M., Izumi, N., Akiyama, T. & Kaibuchi, K. (2004). Interaction with IQGAP1 links APC to Rac1, Cdc42, and actin filaments during cell polarization and migration. *Dev Cell* **7**, 871-83.
76. Bartolini, F. & Gundersen, G. G. (2006). Generation of noncentrosomal microtubule arrays. *J Cell Sci* **119**, 4155-63.
77. Meriane, M., Roux, P., Primig, M., Fort, P. & Gauthier-Rouviere, C. (2000). Critical activities of Rac1 and Cdc42Hs in skeletal myogenesis: antagonistic effects of JNK and p38 pathways. *Mol Biol Cell* **11**, 2513-28.
78. Meriane, M., Charrasse, S., Comunale, F., Mery, A., Fort, P., Roux, P. & Gauthier-Rouviere, C. (2002). Participation of small GTPases Rac1 and Cdc42Hs in myoblast transformation. *Oncogene* **21**, 2901-7.

Supplementary information

Quartz Crystal Microbalance with dissipation monitoring (QCM-D)

Film buildup was followed by *in situ* quartz crystal microbalance (QCM D300, QSense, Sweden) using a previously published procedure [54]. PLL, PGA and PGA-maleimide prepared at 0.5 mg/mL in the HEPES-NaCl buffer were successively injected in the cell. They were let to adsorb for 8 min and rinsed for 6 min with the HEPES-NaCl buffer. After construction the films was allowed to equilibrate in MilliQ water, and the MilliQ water-dissolved 60µg/mL L2synd peptide was injected overnight. The unbound peptide was rinced with MilliQ water.

When a mass Δm is adsorbed at the crystal and the measurements are conducted in air, the resulting decrease Δf typically obeys the Sauerbrey equation:

$$\Delta m = -C\Delta f/n$$

where C is the mass sensitivity constant (17.7 ng/cm^2/Hz at 5 MHz), and n is the overtone number.

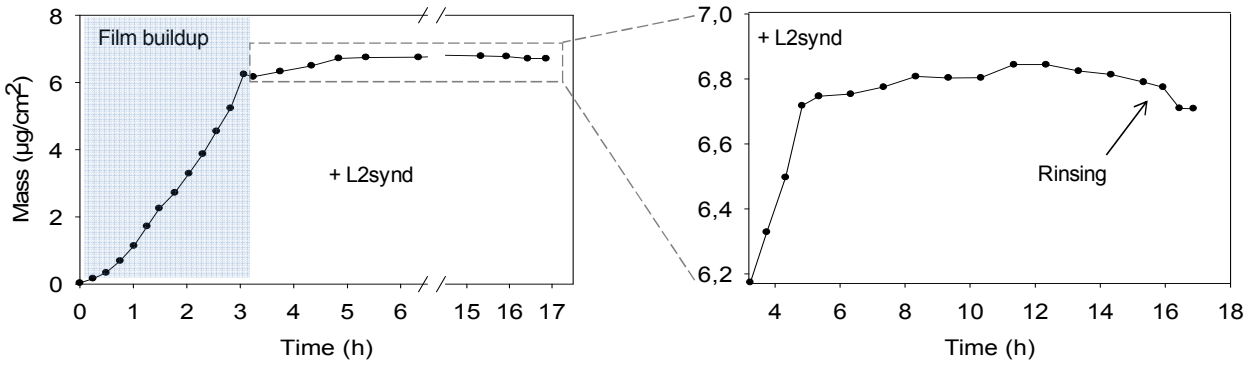

FIGURE S1. *Exponential growth of the film and peptide binding followed by QCM-D.*

IV.C. PEM FILMS FOR α-DYSTROGLYCAN TARGETING IN SKELETAL MYOBLASTS

Recently, two αDG binding sequences in the laminin-α2 chain LG4-5 module were identified, one binding heparin and αDG, and other specifically binding αDG (Suzuki et al. 2010). The peptides specifically inhibited end bud formation of submandibular glands in culture (Suzuki et al. 2010). In this work, we used a 12-amino acid laminin-α2 chain derived peptide (named L2dystro) that was shown to specifically bind αDG (Suzuki et al. 2010). The peptide was grafted to PEM films using maleimide chemistry to create αDG-targeting surface. The L2dystro-functionalized films were used as substrates for C2C12 culture to study the effects of this peptide on cell adhesion, proliferation and differentiation.

IV.C.1. Results

IV.C.1.a) Cell adhesion on L2dystro-functionalized films

To evaluate the effect of L2dystro peptide on C2C12 myoblast adhesion, cells were cultured on L2dystro-grafted films. RGD-grafted films were used as a positive control for myoblast adhesion ***(Chapter III)***. In addition, mixed RGD/L2dystro-grafted films were prepared to study the interplay between the signals provided by the two peptides. The cells were allowed to adhere for 4 h in SFM to eliminate any effect of serum on early adhesion. Actin and nuclei staining of C2C12 cells revealed the presence of adherent cells on RGD, L2dystro and RGD/L2dystro (Fig. IV-7A).

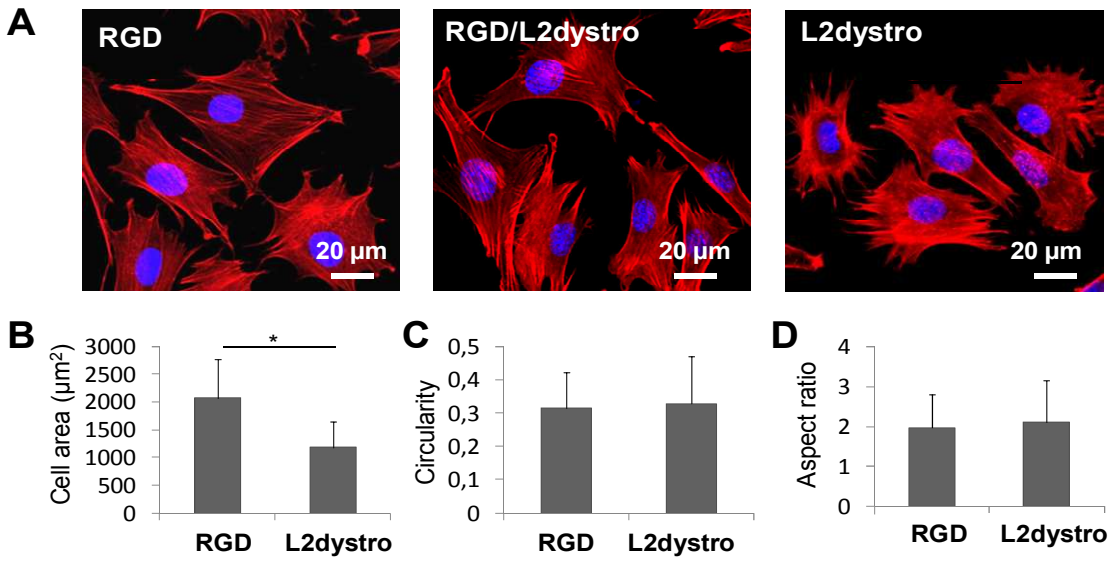

Figure IV-7. C2C12 cell adhesion after 4h on RGD- and L2dystro-grafted films*. (A) Fluorescent labeling of actin (red) and nuclei (blue). (B) Quantification of the cell area. (C) Quantification of the circularity. (D) Quantification of the aspect ratio. * $p < 0.05$*

Next, the spreading area and morphology (circularity and aspect ratio) of the cells on RGD and on L2dystro-grafted films were compared. Quantitative measurement of the cell area revealed that the area was 1.5 to 2 times higher on films presenting RGD peptide as compared to those grafted with L2dystro (Fig. IV-7B). However, there was no difference of either circularity or aspect ratio (Fig. IV-7C and D).

IV.C.1.b) Inhibition of adhesion by addition of soluble peptide

To test if the cells bound to the peptide sequence on the films surface, we performed a competition assay (Fig. I-8). We pre-incubated the cells with L2dystro peptide in solution (sL2dystro) before depositing the cells on L2dystro-grafted films, still in presence of sL2dystro. The results showed that the cell spreading area was about 2 times smaller in presence of sL2dystro (Fig. IV-8A), as compared to control without sL2dystro. This indicates that the peptide in solution competes with the grafted peptide and partially prevents the cells from spreading. However, there was no difference in the number of adherent cells (Fig. IV-8B), suggesting that receptor blocking by the soluble peptide was not complete and still allowed cell interaction of the film.

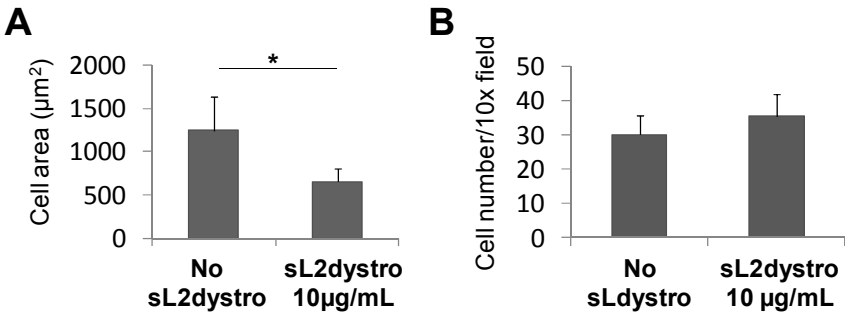

Figure IV-8. C2C12 cell adhesion inhibition on L2dystro-grafted films by pre-incubating the cells with L2dystro peptide in solution (sL2dystro). *(A) Cell spreading after 1h of adhesion. (B) Cell number.*

IV.C.2.c) Migration

To investigate if L2dystro peptide had effect on cell migration, we followed the migration for 10h on RGD, L2dystro and RGD/L2synd-grafted films (Fig. IV-9A) and quantified both cell velocity and directionality (Fig. IV-9B and C). Cell migration speed was higher on L2dystro films as compared to RGD films (Fig. IV-9B). Mixed RGD/L2dystro films presented intermediate velocity values. However, there was no significant difference in the directionality (Fig. IV-9B). Thus, cell culture on L2dystro films was associated to an increased cell migration speed without affecting the directionality.

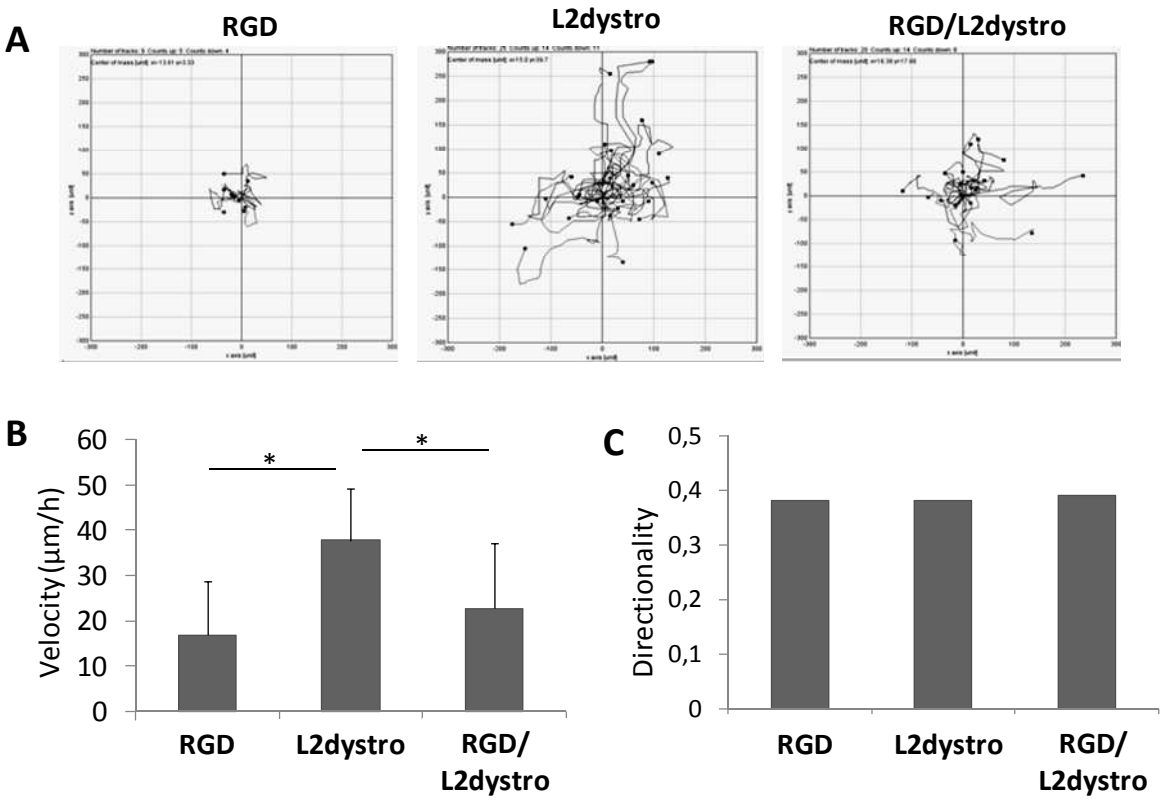

Figure IV-9. Migration on RGD, L2dystro and RGD/L2dystro-grafted films. *Migration was measured for 10h after 4h of adhesion. (A) Migration paths for approximately 15 cells. (B) Quantification of cell velocity. (C) Quantification of cell directionality (defined as displacement / total path length of the cell). * $p < 0.05$*

IV.C.2.d) Differentiation

As we previously showed, C2C12 myoblasts differentiated on RGD-grafted films with formation of myotubes after 5 days. Some cell sheet detachment was observed on RGD/L2dystro films, but the cells were also able to form myotubes. However, on L2dystro films, the cell sheet completely detached after 2 days in DM, showing that only L2dystro-grafted films were inappropriate for myogenic differentiation (Fig. IV-10A and B) and required the presence of additional adhesion ligands. These results are in agreement with previous findings showing that β_3 integrin is crucial for myogenic differentiation of C2C12 myoblasts (Liu et al. 2011). For this reason, RGD or another adhesive peptide needs to be added. Indeed, when L2dystro was mixed with RGD peptide, formation of myotubes could be observed. To avoid partial cell detachment from such RGD/L2dystro mixed surfaces, an appropriate ratio of the peptides has to be determined.

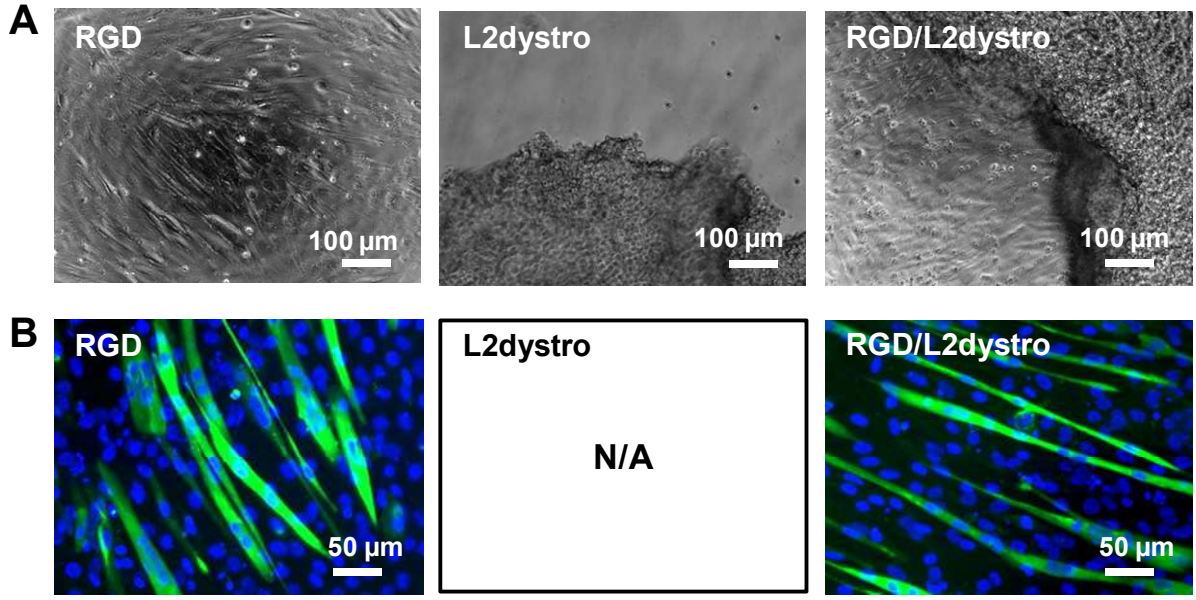

Figure IV-10. Myogenic differentiation on RGD, L2dystro and RGD/L2dystro-grafted films. *After culture in GM to reach the confluence, the medium was changed to DM (ie Day 0). (A) Phase contrast microscopy observations of C2C12 cell differentiation for 5 days. Cell detachment was observed on L2dystro-grafted films after 2 days in DM. (B) Myosin heavy chain (green) and nuclei (blue) labeling.*

IV.C.2. Conclusions and perspectives

In this study, we engineered L2dystro peptide-presenting PEM films. These films were able to promote adhesion, spreading and migration of C2C12 myoblasts, but were inappropriate for myogenic differentiation, indicating that the differentiation process requires the presence of additional adhesion ligands.

As dystroglycan interaction with laminin-α2 chain is crucial for maintaining the function of skeletal muscle, L2dystro-grafted films may become a tool for studying the cellular mechanisms and roles of αDG/laminin-α2 interaction. Different types of dystrophic myotubes may be cultured on L2dystro-grafted films to evaluate the possibility of L2dystro utilization as a therapeutic agent in myopathies. Also, such substrate may be used to follow the restoration of laminin/dystrophin-glycoprotein complex interaction in hybrid myotubes (i.e. myotubes obtained by fusion of normal myoblasts with dystrophic myotubes). This may have important considerations in the design of strategies for both myoblast transplantation and gene therapy of muscular dystrophy.

Besides its role in skeletal muscle, dystroglycan plays diverse roles in Schwann cells. However, the molecular mechanisms are just beginning to be revealed (Masaki et al. 2003; Masaki and Matsumura 2010). Understanding of these mechanisms is promising for the development of effective treatments for human peripheral neuropathies.

CHAPTER V – BMP-2 derived peptide for osteogenic differentiation of skeletal myoblasts

Besides differentiation into myotubes, C2C12 myoblasts can also undergo osteogenic differentiation when treated with BMP-2 growth factor. PEM films with incorporated rhBMP-2 were already shown to orient C2C12 myoblasts towards osteogenic pathway.

In this chapter, our aim was to guide skeletal muscle progenitors towards an osteogenic pathway using BMP-2 derived mimetic peptide. We grafted this peptide to PEM films and evaluated its capacity to induce the osteogenic differentiation of C2C12 myoblasts.

V.A. INTRODUCTION

Saito *et al*. identified the most effective osteogenic peptide derived from BMP-2 amino acid sequence, corresponding to residues 73–92 of the knuckle epitope of BMP-2 (Saito et al. 2003). Osteoinductive activity of this peptide was observed both *in vitro* and *in vivo* (for the review, see (Jabbari 2013)). The sequences used in different studies, their presentation mode and observed effects are shown in Table V-1.

In vitro, the peptide was used in solution (Saito et al. 2003; Kloesch et al. 2007; He et al. 2008a), coated onto cell culture substrate (Saito et al. 2003) or conjugated to synthetic (He et al. 2008a; Zouani et al. 2010; Moore et al. 2011; Zouani et al. 2013) or natural (Saito et al. 2003; Saito et al. 2005; Kloesch et al. 2007) polymers. The peptide induced expression of osteogenic transcription factors and ALP activity, as well as significantly inhibited the binding of rhBMP-2 to both BMP receptors type IA and type II (Saito et al. 2003). The synergistic effect of the BMP-2 peptide with RGD peptide was also studied. The results demonstrated that RGD and BMP peptides, when presented simultaneously, acted synergistically to enhance osteogenic differentiation peptide (He et al. 2008a; Zouani et al. 2010; Moore et al. 2011). Recently, the interplay of substrate stiffness and presentation of BMP-2 peptide was studied (Zouani et al. 2013). BMP-2 peptide showed osteogenic capacity when presented by stiffer substrates. These experiments were conducted using mesenchymal cell lines (Saito et al. 2003; He et al. 2008a; Moore et al. 2011) or MC3T3-E1 pre-osteoblasts (Zouani et al. 2010). However, when C2C12 myoblasts were used for the evaluation of BMP-2 peptide effect in solution or loaded into Collagraft blocks, no osteogenic effect was observed (Kloesch et al. 2007).

In vivo, 73–92 peptide-conjugated alginate gels promoted ectopic calcification in rat calf muscle and repair of rat tibial bone defects (Saito et al. 2003; Saito et al. 2005).

Reference	Sequence	Position (mutation)	Presentation mode	Cells or animal model	Culture medium and duration	Observed effects
rhBMP-2 GenBank: AAB05665, AAF21646.1	KIPKA CCVPT ELSAI SMLYL	73-92				
(Saito et al., 2003)	KIPKA SSVPT ELSAI STLYL	73 – 92 (C78.79S, M89T)	In solution, 50 and 100 µg/well	Murine multipotent mesenchymal cell line C3H10T1/2	Growth medium, 3 days	Expression of osteocalcin mRNA
			Coating of 96-well plate, 100 and 200 µg/well	Murine multipotent mesenchymal cell line C3H10T1/2	Growth medium, 3 days	Elevated alkaline phosphatase (ALP) activity
			Grafting to covalently cross-linked alginate gels	Implanted into rat calf muscle	3 weeks	Ectopic calcification
(Saito et al., 2005)	KIPKA SSVPT ELSAI STLYL	73 – 92 (C78.79S, M89T)	Conjugated to alginate gel (sponge)	Implanted into the rats' tibial bone defects	4 weeks	Bone formation around the surface
			Conjugated to alginate gel (particles)	Implanted into the rats' tibial bone defects	4 weeks	Calcification
(He et al., 2008)	KIPKA SSVPT ELSAI STLYL	73 – 92 (C78.79S, M89T)	In solution, 200 ng/ml of Az-mPEG-BMP peptide (azide functionalized BMP peptide with mini-PEG spacer)	Rat bone marrow stromal cells	Osteogenic medium, up for 21 days	Increase in ALP activity
			Grafted to poly (lactide-co-ethylene oxide-co-fumarate) (PLEOF)hydrogel with or without RGD	Rat bone marrow stromal cells	Osteogenic medium, up for 21 days	Increase in ALP activity and in calcium content
(Zouani et al., 2010)	R KIPKA SSVPT ELSAI SMLYL	R-73-92 (C78.79S)	Co-grafted with RGD onto polyethylene terephthalatate (PET)	Mouse pre-osteoblast like cells MC3T3-E1	Growth medium, 24h	Expression of osteogenic markers, increase in matrix thickness
(Moore et al., 2011)	KIPKA SSVPT ELSAI STLYL	73 – 92 (C78.79S, M89T)	Grafted to octyldimethylchlorosilane self-assembled monolayers (+/-RGD)	Human mesenchymal stem cells	Growth medium, up for 21 days	Bone sialoprotein expression and mineralization when co-grafted with RGD
(Zouani et al., 2013)	R KIPKA SSVPT ELSAI SMLYL	R-73-92 (C78.79S)	Grafted onto (poly(acrylamide-co-acrylic acid) hydrogels with varying stiffness (0.5-3.5, 13-17 and 45-49 kPa)	Human mesenchymal stem cells	Growth medium, 4 days and 4 weeks	Osteogenic differentiation when grafted onto 13-17 and 45-49 kPa
(Kloesch et al., 2007)	KIPKA SSVPT ELSAI STLYL, KIPKA SCVPT ELSAI STLYL	73 – 92 (C78.79S, M89T), 73 – 92 (C78S, M89T)	In solution (1 to 50 µg/mL)	C2C12 myoblasts	5 days	No effect (osteogenic markers measured)
			Loaded into Collagraft blocks (1 to 50 µg/mL)	Implantation into dorsal muscle pockets	4 weeks	No effect (ALP activity measured)

Table V-1. Sequences of BMP-2 derived peptides used in different studies, their presentation mode and observed effects. *The Table is not exhaustive and presents the most important studies on BMP-2 derived peptides.*

In this work, we used BMP-2 derived peptide (pBMP-2) (Saito et al. 2003) to evaluate the capacity of pBMP-2-presenting PEM films of controlled stiffness to induce the osteogenic differentiation of C2C12 myoblasts.

V.B. RESULTS

V.B.1. Cell adhesion and proliferation on BMP-2 peptide-grafted films

BMP-2 derived peptide was grafted to PGA using maleimide chemistry (***Chapter II - Materials and methods***) to obtain PGA-pBMP-2. The final product was analysed by NMR and had substitution degree of 5.5% (Annexe IV).

PGA-BMP-2 was further used to functionalize PLL/PGA films, cross-linked or not. The respective films were called NCL and NCL-pBMP-2 for soft films without and with final layer of PGA-pBMP-2, and CL and CL-pBMP-2 for stiffer films without or with PGA-pBMP-2. NCL films were described in our previous studies as non-adhesive and were used as a negative control. Conversely, CL films were favorable for cell adhesion and proliferation and were used as a positive control.

C2C12 myoblasts were deposited on the films in SFM. After 1h of adhesion, the medium was replaced by GM and the cells were allowed to adhere for 3 more hours, then fixed and stained for actin and nuclei (Fig. V-1). At 4h after seeding, the cells were spread on all the films types, except for NCL which is a negative control for cell adhesion. However, more round cells were observed on NCL-pBMP-2 films compared to both cross-linked films.

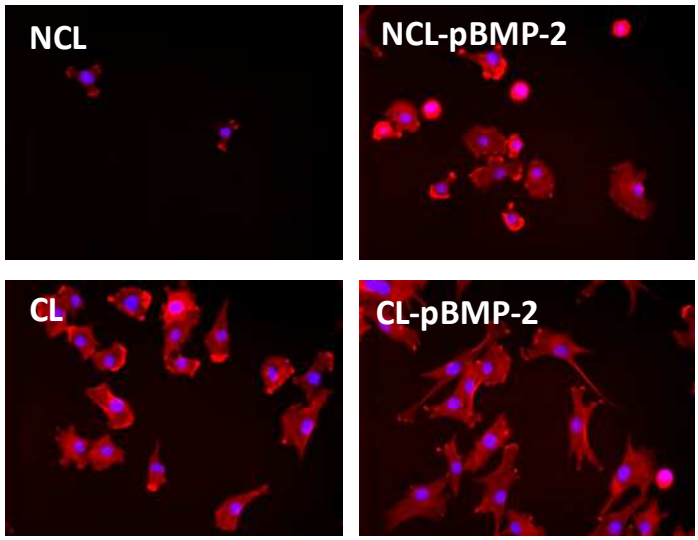

Figure V-1. Adhesion at 4h of C2C12 myoblasts on different types of PLL/PGA films. *The cells were seeded on soft or cross-linked films, with or without PGA grafted with BMP-2 peptide (pBMP-2) deposited on the final layer, and cultured in SFM for 1h, then in GM for 3h.*

Then the cells were cultured for three days to evaluate their capacity to proliferate on different types of films. The cells proliferated on all the film types, although the cell layer was less confluent on NCL-pBMP-2 film compared to both cross-linked films (Fig. V-2). These results show that C2C12 myoblasts were able to recognize pBMP-2 for adhesion and to proliferate on pBMP-2-functionnalized films.

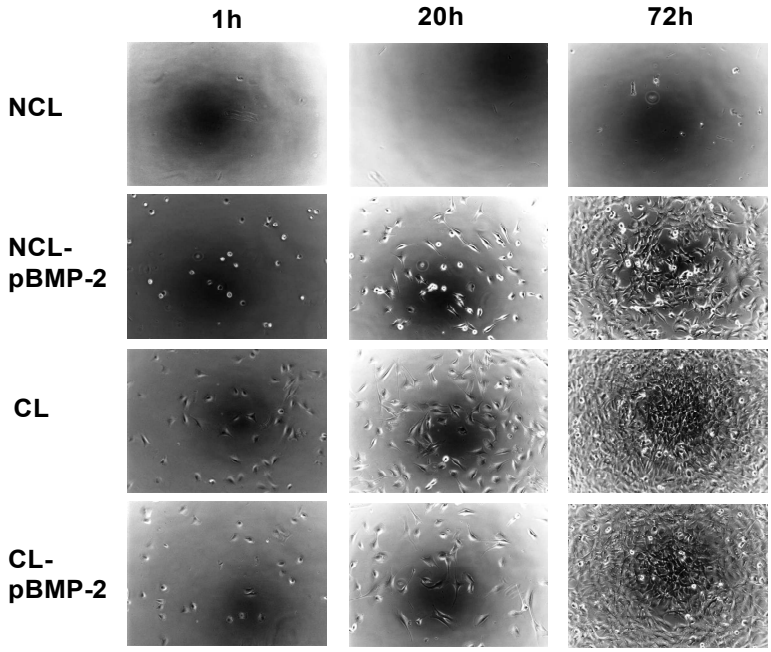

Figure V-2. Proliferation of C2C12 myoblasts on different types of PLL/PGA films. *The cells were seeded on soft or cross-linked films, with or without PGA grafted with BMP-2 peptide (pBMP-2) deposited on the final layer, and cultured in GM for 3 days.*

V.B.2. Evaluation of osteoinductive capacity of BMP-2 peptide-grafted films

We next evaluated the capacity of pBMP-2 grafted surfaces, soft or stiff, to induce ALP expression by C2C12 myoblasts. NCL films, which did not promote any cell adhesion, were discarded from the study. CL films were used as control for stiff films since substrate stiffness is known to affect cell differentiation. Cells seeded on plastic, with or without soluble rhBMP-2 at a concentration known to induce ALP activity, were used as positive and negative controls, respectively. The results showed no effect of pBMP-2-presenting films on ALP activity, which was close to zero and corresponded to the values of negative control (Fig. V-3).

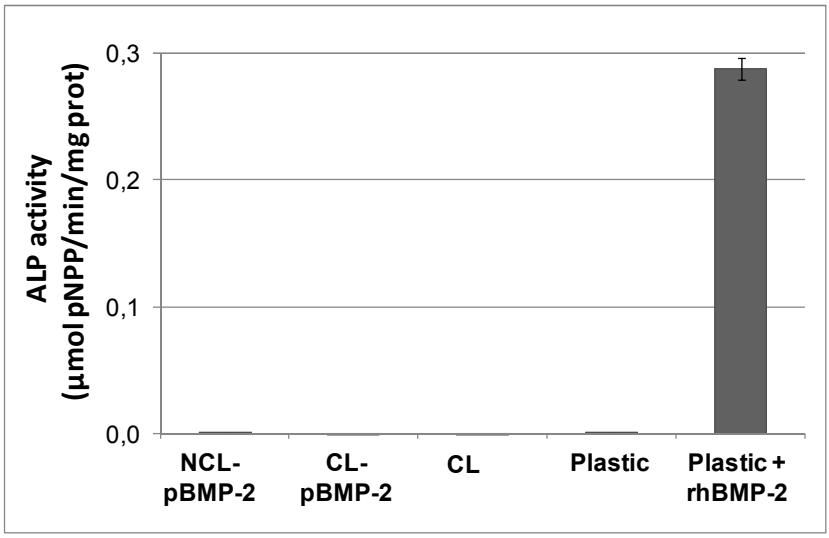

Figure V-3. Effect of BMP-2 peptide presented by PLL/PGA films on induction of ALP in C2C12 cells. *ALP activity was measured after 72 h in GM on different types of substrates. Positive control corresponds to GM supplemented with 500 ng/mL of rhBMP-2.*

In several previous studies, the RGD peptide was shown to synergistically enhance the effect of pBMP-2 (He et al. 2008a; Zouani et al. 2010; Moore et al. 2011). We co-deposited PGA-RGD and PGA-pBMP-2 (mixed at 1:1 v/v) on the last layer to investigate if combined presentation of an adhesive RGD peptide and pBMP-2 could induce ALP activity. However, no difference compared to a negative control could be observed (Fig. V-4).

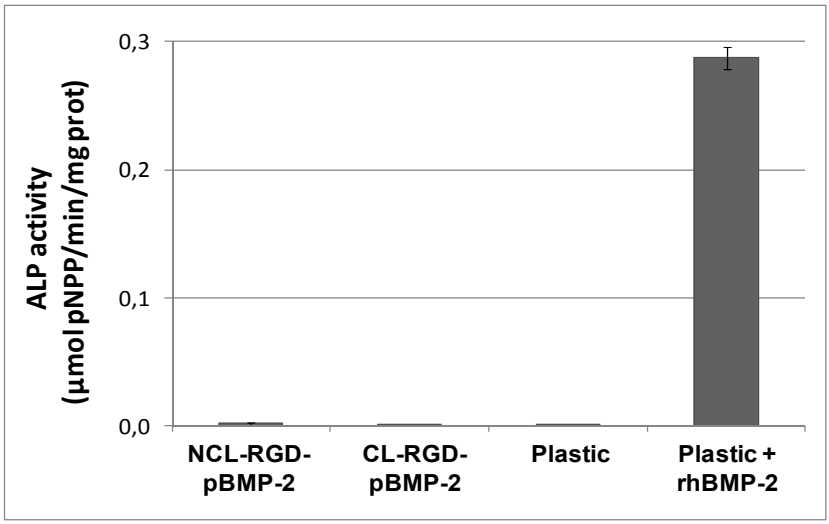

Figure V-4. Effect of RGD and BMP-2 peptide simultaneous presentation on induction of ALP in C2C12 cells. *ALP activity was measured after 72 h of culture in GM on different types of substrates. Positive control corresponds to GM supplemented with 500 ng/mL of rhBMP-2.*

V.B.3. Evaluation of osteoinductive capacity of BMP-2 peptide in solution

We hypothesized that absence of ALP activity in response to pBMP-2 may be due to its presentation mode, because the chemical grafting can influence peptide's bioactivity.

The efficacity of BMP-2 peptide delivered in solution to induce ALP activity was already demonstrated using rat bone marrow stromal cells (He et al. 2008a). The Az-mPEG-BMP-2 peptide concentration used in this experiment was 200 ng/mL. However, in another study, much higher concentrations were used (Saito et al. 2003). Expression of osteocalcin was observed in response to

addition of 100 µg of peptide per well in 96-well plate, which corresponds to a peptide concentration of 1 mg/mL (supposing that 100 µL of medium are used for culture in 96 well-plate). This is a very high concentration that corresponds to rhBMP-2 concentration of approximately 6.5 mg/mL, when considering the same number of knuckle epitopes contained (rhBMP-2: 2 epitopes, MW 26 kDa; BMP-2 peptide: 1 epitope, MW about 2 kDa. Thus, the mass ratio for rhBMP-2 and BMP-2 peptide for 1 epitope is 6.5:1). However, rhBMP-2 concentration used in this study (Saito et al. 2003) as a control was only 50 ng/mL. The concentration used for C2C12 myoblasts to induce ALP expression is 500 ng/mL.

For this reason, we chose a lower peptide concentration of 500 ng/mL that is closer to the concentration used by He *et al.* (He et al. 2008a) and corresponds to approximately 3 µg/mL of rhBMP-2. The peptide was delivered in solution to the cells cultured on the substrates of different stiffnesses that presented or not RGD adhesive peptide. We compared the effect of rhBMP-2 in solution on these films as well.

The NCL-RGD, CL or CL-RGD films alone did not induce any ALP activity (Fig. V-5) indicating that RGD and/or stiffness had no ALP-inductive capacities. When rhBMP-2 was added to the cells cultured on the same films, ALP activity was induced and was comparable to the control (plastic + rhBMP-2). Interestingly, ALP activity on NCL-RGD films was about 2 times higher compared to cross-linked films or positive plastic control. However, still no ALP activity could be observed in response to pBMP-2, here delivered in solution.

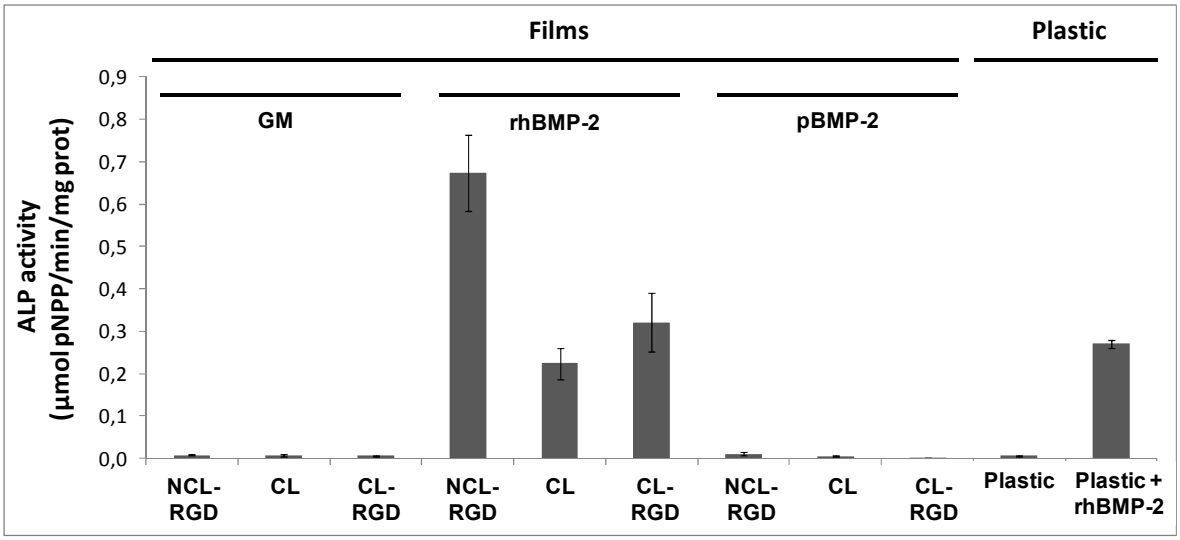

Figure V-5. Effect of BMP-2 peptide in solution on induction of ALP in C2C12 cells cultured on RGD-presenting films. *ALP activity was measured after 72 h of culture on different types of substrates in GM supplemented with 500 ng/mL of BMP-2 peptide (pBMP-2) or 500 ng/mL of rhBMP-2.*

To exclude the possibility that the peptide concentration was too low, we tested much higher concentrations, but still no effect could be observed (Fig. V-6).

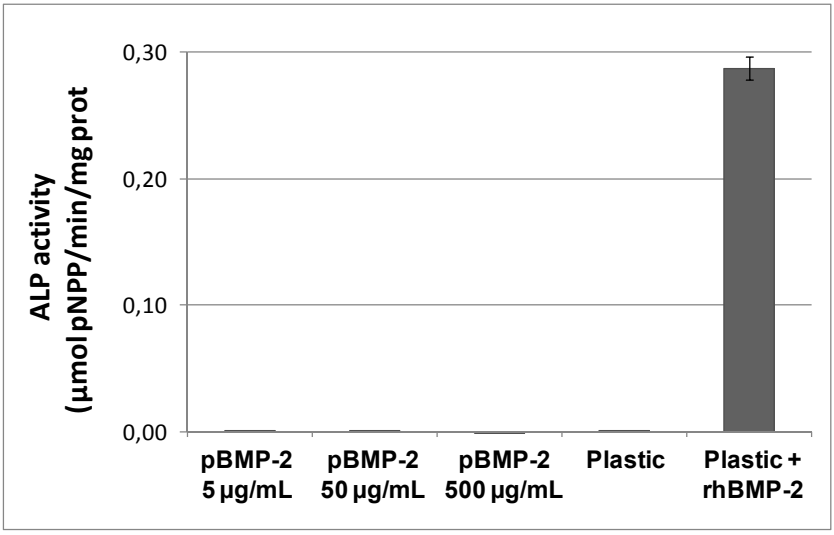

Figure V-6. Effect of different concentrations of BMP-2 peptide in solution on induction of ALP in C2C12 cells. *ALP activity was measured after 72 h of culture on plastic in GM supplemented with different concentrations of BMP-2 peptide (pBMP-2) or 500 ng/mL of rhBMP-2.*

In addition to ALP test, we performed a highly sensitive test using C2C12 A5 myoblast cell line. In response to the activation of Smad pathway, these cells express a reporter gene luciferase. Additionally, we tested a peptide sequence derived from original protein sequence, in which CC and M are not replaced by SS and T.

- pBMP-2(1): KIPKA SSVPT ELSAI STLYL (Saito et al. 2003)
- pBMP-2(2) : KIPKA CCVPT ELSAI SMLYL (GenBank: AAB05665, AAF21646.1)

In positive control (in presence of rhBMP-2), luciferase activity normalized to DNA content was about 12-fold higher than in absence of rhBMP-2 (Fig. V-7). However, no activation of Smad pathway could be detected in response to any of the peptides.

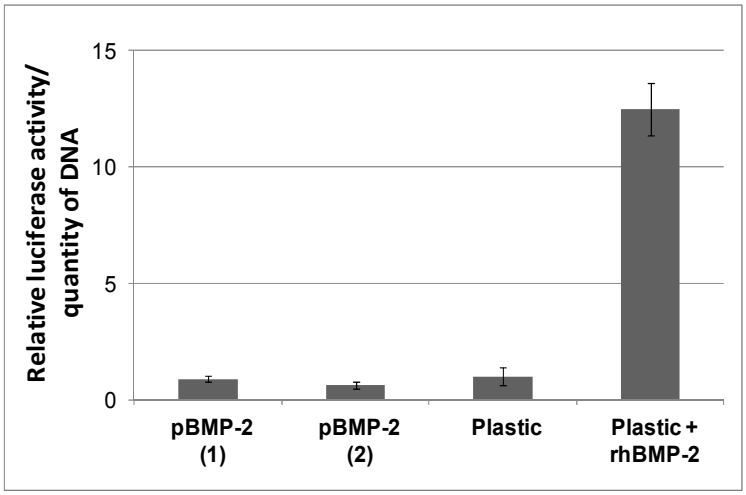

Figure V-7: Effect of different concentrations of BMP-2 peptide in solution on activation of Smad pathway in C2C12 cells. *Luciferase activity normalized to DNA content was measured after 24h of culture in presence of BMP-2 peptides (pBMP-2) or 500 ng/mL of rhBMP-2.*

We also tested if the peptide could induce ALP activity in other cell type than C2C12 myoblasts. We thus evaluated if pBMP-2 could contribute to ALP expression by MC3T3 osteoblastic cell line. In presence of rhBMP-2, ALP activity was more than 2-fold higher compared to negative control, but no effect of pBMP-2 on was observed at any concentration (Fig. V-8).

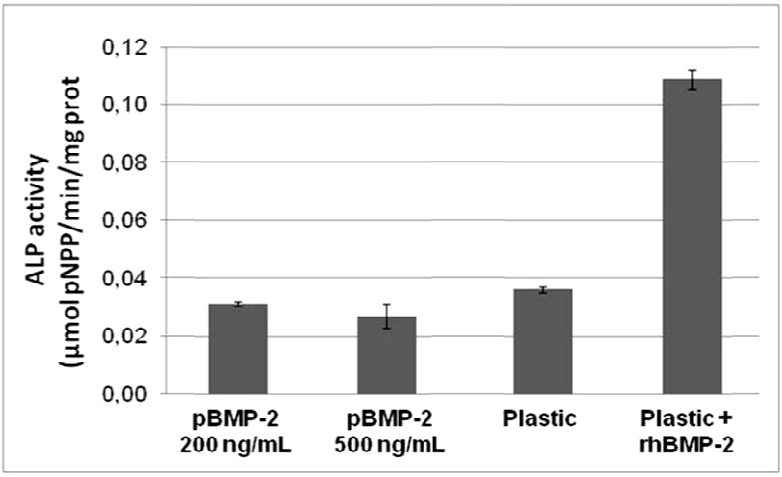

Figure V-8. Effect of different concentrations of BMP-2 peptide in solution on induction of ALP in MC3T3 cells. *ALP activity was measured after 7 days of culture on plastic in osteogenic medium supplemented with different concentrations of BMP-2 peptide or rhBMP-2.*

V.C. DISCUSSION

In this work, we evaluated the capacity of BMP-2 derived peptide to induce the osteogenic differentiation of C2C12 myoblasts. Presented by the films surface, BMP-2 peptide promoted cell adhesion and supported cell proliferation over 3 days. However, BMP-2 peptide, presented alone or with RGD peptide, was not sufficient to induce ALP expression of C2C12 myoblasts. Also, no effect on either ALP expression or on Smad pathway activation could be observed when the peptide was presented in solution at different concentrations.

To better understand the reasons of such results, we carefully analysed the articles published so far in the literature and paid particular attention to the BMP-2 peptide presentation mode, cell models and culture conditions used in different studies. From these different articles, which are are summarized in Table V-1, several observations can be done.

Peptide sequence

The first remark concerns the sequence of the BMP peptide. Amino acids containing thiol or thioether groups (cystein, methionin) from the original BMP-2 sequence (KIPKA **CC**VPT ELSAI S**M**LYL) are being replaced by thiol-free (KIPKA **SS**VPT ELSAI S**M**LYL) (Zouani et al. 2010; Zouani et al. 2013) or both thiol and thioether-free (KIPKA **SS**VPT ELSAI S**T**LYL) (Saito et al. 2003; He et al. 2008a; Moore et al. 2011) amino acids in order to exclude possible reactivity

(formation of disulfide bonds). However, such modifications may affect the secondary structure of the peptide and its functionality.

Effect of the peptide in solution

Another remark concerns the effect of peptide in solution (Saito et al. 2003; He et al. 2008a). In one case (Saito et al. 2003) it was used at very high concentration, providing about 10^6 times more knucle epitopes than rhBMP-2 used in this study as a control. At such concentration, some peptide probably sediment onto the surface and adsorb, thus affecting cell adhesion. In another study (He et al. 2008a), the cells were cultured with Az-mPEG-BMP peptide, and an increased in ALP activity increase was observed after 2 weeks of culture in osteogenic medium. This is a rather long period and one may question to true effect of the peptide. In addition, the medium used was osteoinductive and promotes the differentiation in itself, and the peptides had a mini-PEG + azide modification , which may also play a role.

Presentation of BMP-2 by the surface

In our study, we observed that cell adhrere on BMP-2 peptide grafted soft PLL/PGA films. Without cross-linking or addition of an adhesive ligand, such films are non-adhesive, thus, cell adhesion can be only due to the presence of BMP-2 peptide. Of note, cell spreading on rhBMP-2-loaded soft (PLL/HA) films has already been observed (Crouzier et al. 2011a). Neither BMP-2-free films nor BMP-2 delivery in solution could induce such effect, indicating that the presentation mode is important. However, while matrix-bound rhBMP-2 showed a drastic osteoinductive effect on C2C12 myoblasts, the grafted pBMP-2 did not (Fig. V-1).

In other studies, osteoinductive activity of surface-bound pBMP-2 was observed on peptide-coated substrate (Saito et al. 2003) or on synthetic matrix grafted with pBMP-2 (He et al. 2008a). However, in the latter study, RGD peptide grafted alone increased the expression of osteogenic markers at the same level as pBMP-2 (He et al. 2008a). Interestingly, when pBMP-2 and RGD were co-grafted together, they acted synergistically to enhance osteogenic differentiation (He et al. 2008a; Moore et al. 2011). RGD and pBMP-2 co-grafting was also used by Zouani et al., and induced expression of osteogenic markers (Zouani et al. 2010). However, in this study, the effect of pBMP-2 grafted alone is not shown as control (Zouani et al. 2010).

Based on these results, we hypothesize that BMP-2 peptide may contribute to cell differentiation via its adhesive effect, and that this effect may be significantly improved by the presence of the RGD adhesive peptide. Both peptides may act together to enhance cell adhesion and thus make the substrates more favorable for differentiation. Indeed, the effect of cell adhesion and spreading on osteogenic differentiation was already demonstrated: cell shape regulated commitment

of human mesenchymal stem cells (hMSCs) to adipocytes or osteoblasts (McBeath et al. 2004; Anderson et al. 2011). hMSCs allowed to adhere, flatten, and spread underwent osteogenesis, while unspread, round cells became adipocytes. (McBeath et al. 2004). RGD-functionalized peptide amphiphiles synergistically enhanced osteogenic differentiation in combination with osteogenic medium (Anderson et al. 2011). In addition, the cell fate of MSCs is sensible to ligand density: on patterns of large RGD nanospacing, osteogenesis was predominant (Wang et al. 2013). It was also shown that collagen sponges with bound RGD peptide and loaded with a subfunctional dose of BMP-2 could promote the formation of ectopic bone, while no bone formation was observed with BMP-2 only (Visser et al. 2013). Interestingly, we also observed higher ALP activity in presence of rhBMP-2, when the cells were grown on NCL-RGD films (Fig.V-5).

This may also explain why, when we tested pBMP-2 in solution on MC3T3 cells, we could not observe any increase of ALP activity due to peptide treatment, while in another study that used the same cells, expression of osteogenic markers and increase in matrix thickness were observed (Zouani et al. 2010). These results were obtained for MC3T3 cells cultured on RGD and BMP-2 peptide grafted surfaces (Zouani et al. 2010), where both peptides could be contributing to strong cell adhesion and creating favorable conditions for osteogenic gene expression and matrix synthesis. Similarly, improved bone repair in response to alginate gels grafted with BMP-2 peptide (Saito et al. 2005) may be explained by better adhesive properties of peptide-grafted gels.

Besides RGD adhesive peptide, other characteristics of the material are also known to influence osteogenic differentiation, among them degree of sulfation (Hempel et al. 2012), carboxyle groups (Moore et al. 2011) and substrate stiffness (Zouani et al. 2013). Thus, it is rather difficult to fully decouple the proper osteogenic effect of BMP-2 peptide from the materials chemical and mechanical properties.

Role of the cell type

The last remark concerns the cellular models used in different studies. In the majority of the studies, the cells used were systematically those with a high potential for osteogenic differentiation, such as human MSC or murine C3H10T1/2, or pre-committed such as MC3T3-E1 preosteoblasts. We noted that C2C12 myoblasts, which are widely acknowleged as being BMP-2 responding cells (Katagiri, 1994), were used only once, and pBMP-2 had no osteogenic effect on these cells, neither *in vitro* nor *in vivo* (Kloesch et al. 2007) (Table V-1).

According to the lineage-priming model, stem cells in an undifferentiated state have a basal level of expression of different TF. During differentiation into a cell type, the expression of TF associated to this cell type increases, while the expression of other TF decreases. For instance, in bone marrow MSC, the master transactivator proteins PPARG (adipogenesis), RUNX2

(osteogenesis), and SOX9 (chondrogenesis) are coexpressed before differentiation induction (Delorme et al. 2009). Thus, mesenchymal cells have a basal level of expression of osteoblast-specific genes even in absence of BMP-2. The osteogenic differentiation media for these cells does not necessarily include BMP-2 and is usually based on the addition of dexamethasone, ascorbic acid and β-glycerophosphate. Such conditions induce an increase in *Runx2* expression in both C3H10T1/2 and MC3T3-E1 cells (Tsai et al. 2012). MC3T3-E1 cells express high levels of osteoblast-specific markers and mineralize after growth in ascorbic acid (AA)-containing medium for several days (Wang et al. 1999). C3H10T1/2 cells have a basal level of osteocalcin expression (Zhao et al. 2009). In addition, C3H10T1/2 cells in osteogenic medium synthesize BMP-2 and induce Runx2 expression by autocrine signaling (Phimphilai et al. 2006).

Conversely, C2C12 are committed to a myogenic lineage and express myogenic markers such as MyoD. Unlike mesenchymal and osteoblastic cells, C2C12 cells that start to express osteogenic markers only in response to BMP-2, which makes them a valuable model for the investigation of signaling via BMP-2 receptors (Heining et al. 2011). However, we could not observe induction of osteogenesis in C2C12 by pBMP-2, neither in solution nor in substrate-conjugated form, indicating that pBMP-2 is probably insufficient to induce BMP-2 receptor-mediated signaling. In our point of view, this raises an important question concerning "BMP-2 mimetic" properties of pBMP-2.

Based on these data, we suggest that expression of osteogenic markers in mesenchymal and osteoblastic cells may be induced by synergistic effects between adhesive properties of used materials, osteogenic medium and autocrine signaling, but cannot be fully attributed to the effect of the BMP-2 peptide (Fig.V-9). This could explain why C2C12 cells, which do not express osteogenic markers in absence of proper BMP-2 stimulation, could adhere and proliferate on BMP-2 peptide grafted surface, but did not express osteogenic markers.

We conclude that, although pBMP-2 seems to have favorable effect on osteogenic differentiation, the ability of the BMP-2 peptide to mimic BMP-2 protein osteoinductive function by acting via BMP-2 receptors should be confirmed in further studies.

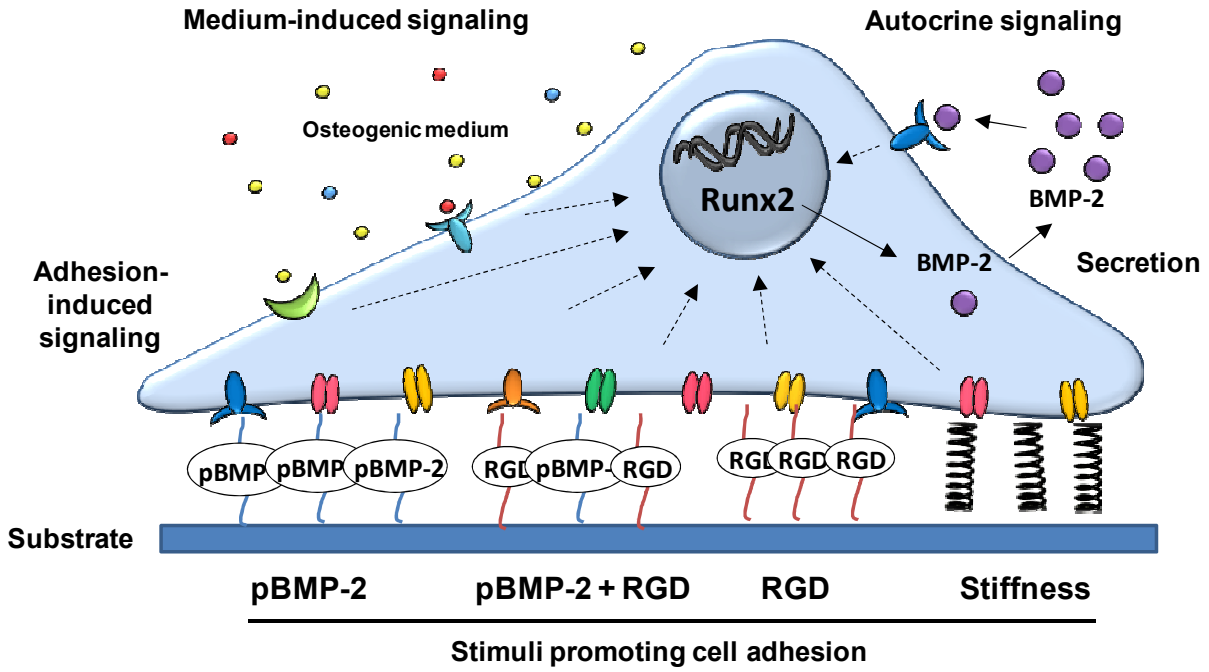

Figure V-9. Model of osteogenesis induction by pBMP-2-presenting substrates. *The increase in expression of osteogenic markers in mesenchymal and osteoblastic cells may be induced by synergistic effects between biochemical and mechanical properties of used materials, osteogenic medium, and autocrine signaling.*

CHAPTER VI – Three-dimensional myoblast tissues fabricated by cell-accumulation method

Althought PEM films are mostly perceived as 2D substrates, LbL deposition method can be also used for the construction of 3D tissue models. In this chapter, we used LbL deposition method to construct 3D skeletal muscle tissue models. This work has been conducted in collaboration with Pr Mitsuru Akashi and Dr Michiya Matsusaki from Osaka University.

VI.A. ARTICLE SUMMARY

Muscle tissue is characterized by a complex three-dimensional (3D) organization of aligned muscle fibers surrounded by an extracellular matrix. One of the current challenges in muscle tissue engineering is to develop techniques for construction of 3D muscle tissues.

Different methods are currently being used, among them hydrogel scaffolds and cell sheet-based techniques; all of the methods present certain advantages, but also drawbacks. For instance, cell sheet-based tissue engineering has limitations due to complicated manipulation of the fragile cell sheets.

Recently, a new technology allowing fast and relatively simple construction of thick 3D tissues using LbL deposition method has been developed. The method, called "cell-accumulation technique", consists in coating the cells with $(FN/G)_4FN$ films and putting them together onto a substrate to form multilayered structures (Nishiguchi et al. 2011). The method allowed successful fabrication of approximately 8L of 3D tissues made of human dermal fibroblasts after only one day of incubation (Nishiguchi et al. 2011).

In this work, we used cell-accumulation method for rapid construction of 3D skeletal muscle tissue models. The multilayered tissues were constructed in the inserts with porous bottom to provide two-sided medium supply to thick multilayers (Fig. VI-1).

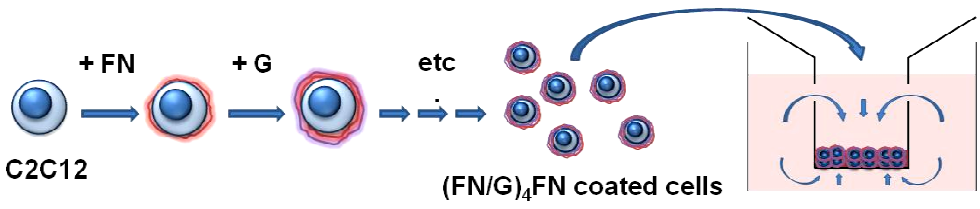

Figure VI-1. Construction of C2C12 multilayered tissues by cell-accumulation method. *Schematic illustration of C2C12 multilayered tissue construction by cell-accumulation technique. Cell are coated by $(FN/G)_4FN$ nanofilms and seeded into 24-well inserts with porous bottom allowing two-sided medium supply.*

As expected, the thickness increased with increasing cell number. The estimated number of layers was 1 layer (1L) for 10^5 seeded cells, 5L for 5 x 10^5 cells and 10L for 10^6 cells. Seeding more

cells (2 x 10^6) did not lead to the formation of a homogeneous cell multilayer and induced the formation of aggregates. This phenomenon seems to be related to nutrient supply and may be overcome by creating a vascular network within the constructs.

Actin stress fiber formation and microtubular network were detected in 1L, 5L and 10L constructs, indicating that the cells were able to bind to the extracellular adhesion ligands and reorganize their cytoskeleton within FN/G matrix. Fibronectin labeling revealed the fibrillar network surrounding the cells: these fibers may include FN secreted by the cells, as the total FN was labeled.

The number of proliferating cells was evaluated after 24h of culture. It decreased with increasing number of layers. In all the constructs, proliferating cells were detectable mostly in the lower part of the multilayer.

Next, we compared differentiation capacity of the constructs made of FN/G-coated or non-coated cells. Expression of nuclear myogenin was detected after 1 day of differentiation in 1L and 5L constructs made of both coated and non-coated cells, but only cytoplasmic myogenin was found in 10L constructs. After 2 more days of differentiation, presence of myotubes and troponin T expression were detected in 1L and 5L constructs made of both coated and non-coated cells. However, differentiated 10L constructs could not be analyzed because of their partial detachment from the periphery and aggregation in the center. We hypothesize that such behavior is due to higher contractile forces in more populated 10L tissues.

Analysis of myotube width and length revealed the advantage of FN/G coating for the formation of 3D skeletal muscle models, as the myotubes were thicker and wider in FN/G-coated constructs compared to non-coated ones. In addition, 5L coated constructs better preserved their thickness over time.

Such muscle constructs fabricated by cell-accumulation method can become a useful model system to study myogenic differentiation in 3D. Because *in vivo* muscle environment can vary in matrix composition depending on muscle type, location and individual variability, cell coating can be additionally adjusted to better mimic specific muscle ECM.

Our approach makes it possible to rapidly form 3D muscle tissues and is promising for the *in vitro* construction of physiologically relevant skeletal muscle tissue models.

VI.B. ARTICLE 3

Short communication
To be submitted

Construction and myogenic differentiation of three-dimensional myoblast tissues fabricated by cell-accumulation method

Varvara Gribova[a], Akihiro Nishiguchi[b], Thomas Boudou[a], Michiya Matsusaki[b], Catherine Picart[a*] and Mitsuru Akashi[b*]

[a] Grenoble Institute of Technology/Minatec, CNRS UMR 5628, 3 Parvis Louis Néel, F-38016 Grenoble Cedex, France
[b] Department of Applied Chemistry, Graduate School of Engineering, Osaka University, 2-1 Yamada-oka, Suita 565-0871, Japan

Keywords: Extracellular matrix, layer-by-layer, myogenesis, tissue engineering

---

Abstract
One of the current challenges in muscle tissue engineering is to develop techniques for construction of three-dimensional (3D) muscle tissues. Muscle tissue is characterized by a complex 3D organization of aligned muscle fibers surrounded by an extracellular matrix (ECM). In the present work, we used a "cell-accumulation method" to fabricate 3D multilayered muscle constructs. The method consists in coating myoblasts cells with fibronectin-gelatin (FN/G) nanofilms mimicking the ECM before seeding them onto a substrate where the cells self-organize. We performed the buildup of up to 10 layers (~40 μm thick) myoblast constructs and analyzed their structure. We demonstrated that the thickness of the constructs depends on the number of seeded cells. We also induced myogenic differentiation and followed the expression of the myogenic markers myogenin and troponin T in the constructs made of either FN/G-coated or non-coated cells. The 3D tissues expressed myogenin after 1 day of culture in differentiation medium and formed multinucleated myotubes after 3 days. Our approach makes it possible to rapidly build 3D muscle tissues and is promising for the *in vitro* construction of skeletal muscle tissue models.

1. Introduction

Skeletal muscle tissue engineering holds promise for the replacement of muscle after an injury or a trauma and for the treatment of muscle diseases. *In vitro* engineered muscle tissue models may also find use for drug screening or for the examination of the functional effects of patient-specific mutations.

The process of muscle formation requires that muscle precursor cells (myoblasts) proliferate, differentiate and fuse together to form multinucleated myotubes. The development of skeletal muscle is known to strongly depend on the interaction of muscle cells with their surrounding extracellular matrix (ECM). Mature skeletal muscle has a complex three-dimensional (3D) organization of aligned muscle fibers surrounded by ECM. Skeletal muscle ECM consists of the basal lamina that

surrounds individual myofibers and of interstitial connective tissue [1; 2; 3]. Skeletal muscle basal lamina contains type IV collagen, laminin and heparin sulfate proteoglycans. The interstitial connective tissue consists mostly of collagens type I, III and V. Fibronectin is detected in both of these compartments [4].

One of the current challenges in muscle tissue engineering engineering is to construct 3D well-organized muscle tissues. Another important challenge consists in vascularizing such engineered tissues, since blood supply is necessary to bring nutritive elements and oxygen to the cells in thick constructs [5]. The most commonly used method for 3D muscle tissue construction consists in myoblast association to polymeric scaffolds.

Some scaffolds made of synthetic materials have been developed [6; 7; 8]. Levenberg et al. have used a polymer scaffold composed of 50% poly- (L-lactic acid) (PLLA) and 50% poly(lactic-glycolic) acid (PLGA) to construct a prevascularized skeletal muscle 3D constructs by co-culturing myoblasts, endothelial cells and fibroblasts [8]. This scaffold was also used to evaluate the effect of the stiffness on myoblasts. The results indicated that compliant scaffolds were insufficient to withstand cell forces, while excessively firm scaffolds could not lead to parallel oriented myotube organization [9].

However, natural matrices such as collagen gels [10], matrigel [11; 12] or fibrin gels [13] present advantages compared to synthetic scaffolds, because they possess cell adhesion ligands that can interact with integrins and thus naturally allow cell anchorage. In addition, some of the scaffolds, e. g. fibrin gels, have the capacity to bind specifically many growth factors [14].

Another widely used method to create 3D muscle constructs is cell sheet-based tissue engineering. A thermoresponsive polymer poly(N-isopropylacrylamide) (PIPAAm), grafted on a cell culture substrate, allows confluent cells to be detached as a single cell sheet and to create scaffold-free 3D tissues by layering multiple cell sheets [15; 16]. Sasagawa et al. developed prevascularized 3D tissues using human umbilical vein endothelial cells (HUVECs) sandwiched between two myoblast sheets [17]. Recently, myoblast sheets with well-aligned orientation were fabricated to create 3D oriented myoblast and myotube constructs [18]. However, this method has limitations due to complicated manipulation of the fragile cell sheets

A new technology allowing fast and relatively simple construction of thick 3D tissues have recently been developed. The method called "cell-accumulation technique" consists in coating the cells with $(FN/G)_4FN$ films and putting them together onto a substrate to form multilayered structures [19]. Nanometer-sized fibronectin-gelatin (FN/G) films prepared by layer-by-layer (LbL) assembly [20] provide the cells with an "artificial ECM" and allow the self-organization of the cells into 3D constructs. As measured by Quartz Crystal Microbalance with Dissipation Monitoring (QCM-D) on a phospolipid bilayer, the thickness of such films is less than 10 nm [21].The method allowed successful fabrication of approximately 8L of 3D tissues made of human dermal fibroblasts after only one day of incubation [19]. Furthemore, vascularized tissues were obtained by a sandwich culture of endothelial cells between fibroblasts assembled by cell-accumulation technique [19].

In this work we report rapid construction of 3D skeletal muscle tissue models using cell-accumulation method. By assembling FN/G-coated C2C12 myoblasts, we were able to build up to 40 μm thick 3D constructs that expressed myogenin after 1 day of culture in differentiation medium and formed multinucleated myotubes after 3 days. Our approach makes it possible to rapidly form 3D muscle tissues and is promising for the *in vitro* construction of physiologically relevant skeletal muscle tissue models.

2. Materials and Methods

2.1. Cell culture

C2C12 cells (from ATCC, used at passages 5-15) cultured in growth medium (GM) composed of Dulbecco's modified Eagle's medium (DMEM)/F12 medium (1:1; Gibco, Invitrogen, Cergy-Pontoise, France) supplemented with 10% fetal bovine serum (PAA Laboratories, Les Mureaux, France) containing 10 U/mL of penicillin G and 10 µg/mL of streptomycin (Gibco, Invitrogen, Cergy-Pontoise, France). Cells were subcultured prior to reaching 60–70% confluence (approximately every 2 days). Cell were differentiated in a differentiation medium (DM) composed of DMEM/F12 (1:1) supplemented with 2% horse serum (PAA Laboratories, Les Mureaux, France) and antibiotics.

2.2. Fabrication of multilayered structures

The cells were detached from culture dishes using trypsin 0,25% EDTA 0,02% and washed twice with the GM. After resuspending the cells in Tris-HCl buffer (Tris-HCl 50 mM pH 7,4), the cells were subsequently incubated for 1 min using a Microtube Rotater with 0,04 mg/mL fibronectin (FN, Sigma–Aldrich, St. Louis, USA) or gelatin (G, Wako Pure Chemical Industries, Osaka, Japan) solutions in Tris-HCl buffer, then centrifuged at 200 *g* for 1 min, and the supernatant was gently removed by pipetting. After each FN or G deposition step the cells were rinsed in Tris-HCl buffer for 1 min using a Microtube Rotater, followed by centrifugation. When $(FN/G)_4FN$ nanofilms were formed, the cells were resuspended in GM and 300 µl of cell suspension containing desired cell number (10^5, 5 x 10^5 or 10^6 cells) were deposited into 24-well inserts with a semipermeable membrane (Corning 3470, 0,4 µm pore size) coated with FN and placed into 24-well plates. For inserts coating, 100 µl of 0,04 mg/mL FN solution was deposited into the inserts and incubated at 37°C for 30 min, then rinsed once with Tris-HCl buffer. One milliliter of GM were added in 24-well plate, respectively, outside the inserts. The cells were incubated for 2 hours at 37°C, then another 1 mL of GM was added to 24-well plate to connect the media between the inside and the outside of the insert (Fig.1A).

2.3. Histological analysis

The tissues were rinsed with phosphate buffered saline (PBS) solution, then incubated in 10% formaldehyde solution at room temperature for 30 min. The samples were then maintained in PBS solution before being mounted in paraffin-embedded blocks. These paraffin-embedded blocks containing layered tissues were cut into 3–4 µm thick sections. The specimens were then stained with hematoxylin and eosin (H&E).

2.4. Immunofluorescence analysis

Cells were first rinsed in phosphate-buffered saline (PBS) and fixed in 4% formaldehyde for 30 min at room temperature before being permeabilized in 0.5% Triton X-100 for 5 min. After rinsing with PBS the samples were incubated for 1 h in 1% bovine serum albumin (BSA) in TRIS-buffered saline (TBS, 50 mM TRIS, 150 mM NaCl, 0.1% NaN_3, pH 7.4). Actin was labeled with phalloidin-TRITC (1:800, Sigma) for 30 min. Cell nuclei were stained with Hoechst 33342 (Invitrogen) at 5 µg/ml for 10 min. After incubation with the primary antibodies diluted in 1% BSA in TBS for 1h at RT the cells were washed three times with TBS and incubated for 2h at RT with the secondary antibodies. Primary antibodies: rabbit anti-myogenin antibody (1:50) (Tebu-Bio), mouse anti-troponin T (1:50) (Sigma), mouse anti-tubulin (1:200) (Sigma) and rabbit anti-fibronectin (1:100, Sigma). Secondary antibodies: goat anti-mouse Alexa-Fluor 488- and Alexa-Fluor 568-conjugated antibodies and goat anti-rabbit Alexa-Fluor 568- and Alexa-Fluor 647-conjugated antibodies

(Invitrogen) were used at 1:1000. Confocal laser scanning microscopy (CLSM) observations were performed using a Zeiss LSM 700 confocal microscope.

2.5. Cell proliferation and differentiation

Cell proliferation was quantified by a EdU (5-ethynyl-2'-deoxyuridine) assay (Click-iT EdU Imaging Kit, Invitrogen). Briefly, the cells were incubated with EdU diluted at 1/1000 in cell culture medium for 1h. The detection was carried out following the manufacturer instructions. At the end, nuclei were counter-stained with Hoechst 33432 (Invitrogen). The images of EdU and Hoechst-labeled nuclei were taken using a Zeiss LSM 700 confocal microscope

2.6. Statistics

Images were analyzed with ImageJ software (v 1.44p,NIH, Bethesda). Data are reported as means ± standard deviation. For thickness quantification, 20 measurements for each sample were collected. For quantification of myotube width, 20 myotubes (3 measurements per myotube) were analyzed. For myotube length, 50 myotubes were analyzed. The differentiation was characterized by the fusion index, which is a ratio of the nuclei contained in myotubes reported to the total number of nuclei [22]. Statistical comparisons were performed using SigmaPlot Version 11.0 software and based on either Student's t-test or on analysis of variance (ANOVA) followed by an appropriate pairwise comparison. Statistically different values ($p < 0.05$ was considered significant) are reported on the figures.

3. Results and discussion

3.1. Build-up of myoblast multilayered structures

The multilayered tissues were constructed by cell-accumulation technique using the inserts with porous bottom to provide two-sided medium supply to thick multilayers (Fig. 1A). Construction of the tissues was followed by phase contrast microscopy. On the image from the top many round cells are visible after 2h of seeding, indicating that the tissues were not formed yet (Fig. 1B), especially on the samples with more cells seeded per insert (5 x 10^5 or 10^6 cells). After 24h, no more round cells can be detected, showing that the cells spread and form homogeneous multilayers. To clarify the relationship between the number of seeded cells and the number of layers obtained, we evaluated the morphology of the constructs by histological analysis (Fig. 1C). As expected, the thickness increased with increasing cell number. These data are in agreement with the previous study [19]. The estimated number of layers was 1 layer (1L) for 10^5 seeded cells, 5L for 5 x 10^5 cells and 10L for 10^6 cells. We also performed 3D reconstruction of the constructs stained for actin and nuclei using confocal microscopy (Fig. 1D). All three constructs presented homogeneous surface and their thickness increased with the number of seeded cells, consistently with the results from histological analysis. Because histological analysis caused partial detachment of 10L tissues (probably during the cutting step), we quantified the thickness from intact cross-sections obtained by confocal microscopy. The thickness of 1L, 5L and 10L tissues after 24h of culture in GM were approximately 12 µm, 22 µm and 37 µm, respectively (Fig. 1E). Interestingly, the maximum thickness (37 µm for 10L) was about the same as described in the previous study [19]. Seeding more cells (2 x 10^6) did not lead to the formation of a homogeneous cell multilayer and induced the formation of aggregates (Fig. S1). These inhomogeneous samples were discarded from the further study. This phenomenon seems to be related to nutrient supply and may be overcome by creating a vascular network within the constructs.

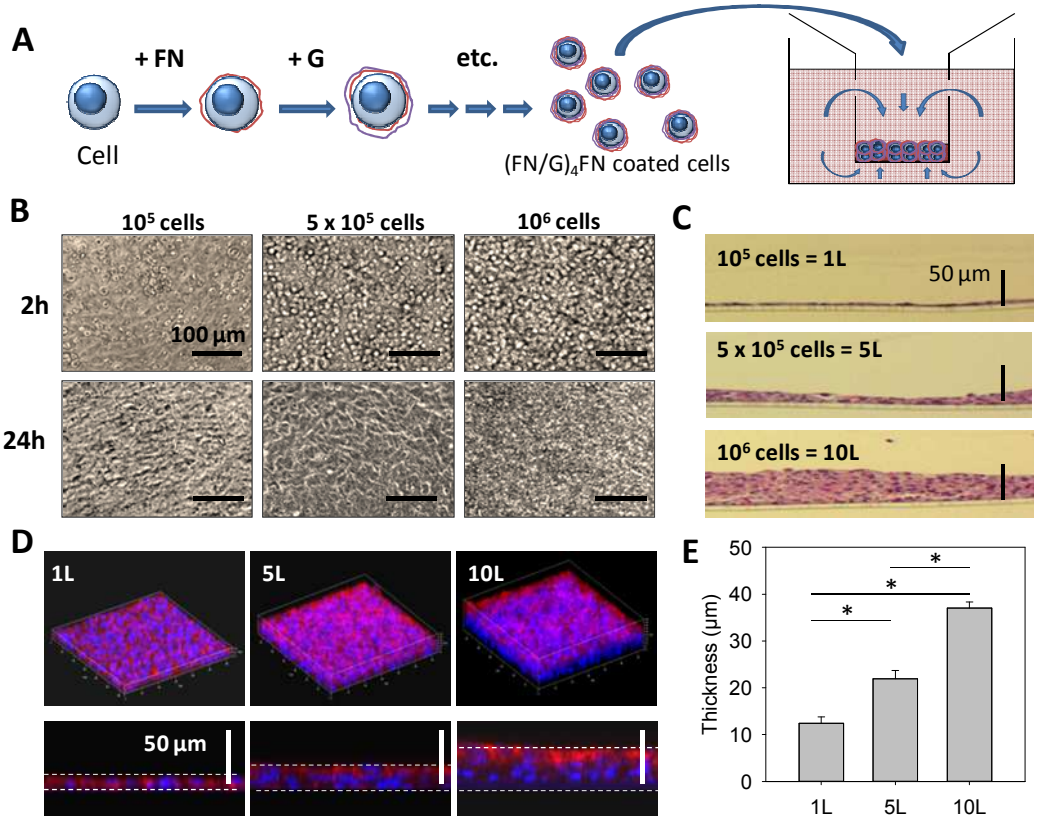

Figure 1. Construction of C2C12 multilayered tissues by cell-accumulation method. *(A) Schematic illustration of C2C12 multilayered tissue construction by cell-accumulation technique. Cell are coated by $(FN/G)_4FN$ nanofilms and seeded into 24-well inserts with porous bottom allowing two-sided medium supply. (B) Phase contrast microscopy observations from the top of 1L, 5L and 10L C2C12 cell constructs after 2h and 24 h of culture in GM. (C) Histological analysis of C2C12 multilayered tissues: phase contrast microscopy observations of hematoxylin-eosin stained cross-sections in Z of 1L, 5L and 10L C2C12 cell constructs after 24 h of culture in GM. (D) 3D reconstruction of 320 x 320 µm fragments of multilayered tissues and cross-sections in Z done using confocal microscopy. Actin (red) and nuclei (blue) are stained. (E) Quantification of the 1L, 5L and 10L thickness. Error bars correspond to SD, * : $p < 0.05$.*

3.2. Cytoskeleton organization and proliferation

The cells are mechano-sensors that actively sense their environment. Cell binding to ECM promotes cytoskeleton reorganization and influences cell proliferation through cell surface receptors, especially integrins [23; 24]. To analyze cell organization within the FN/G matrix, we visualized actin cytoskeleton, microtubules, nuclei and total FN after 24 h of culture (Fig. 2A). Actin stress fiber formation and microtubular network were detected in 1L, 5L and 10L constructs, indicating that the cells were able to bind to the extracellular adhesion ligands and reorganize their cytoskeleton within FN/G matrix. Fibronectin labeling revealed the fibrillar network surrounding the cells, as previously described [25]. These fibers may include FN secreted by the cells, as the total FN was labeled. Interestingly, the cells in 10L constructs had more elongated nuclei, as compared to 1L and 5L constructs. Actin stress fibers were thinner and, like FN fibers, oriented in parallel. This may be due to the particularities of cell organization in thick 3D constructs compared to flatter constructs. It was reported in comparative 2D vs 3D cell adhesion studies that the cells exhibited more elongated shape with less stress fibers on the arrays of large flexible micropillars, as compared to the cells spread on flat surfaces [26; 27].

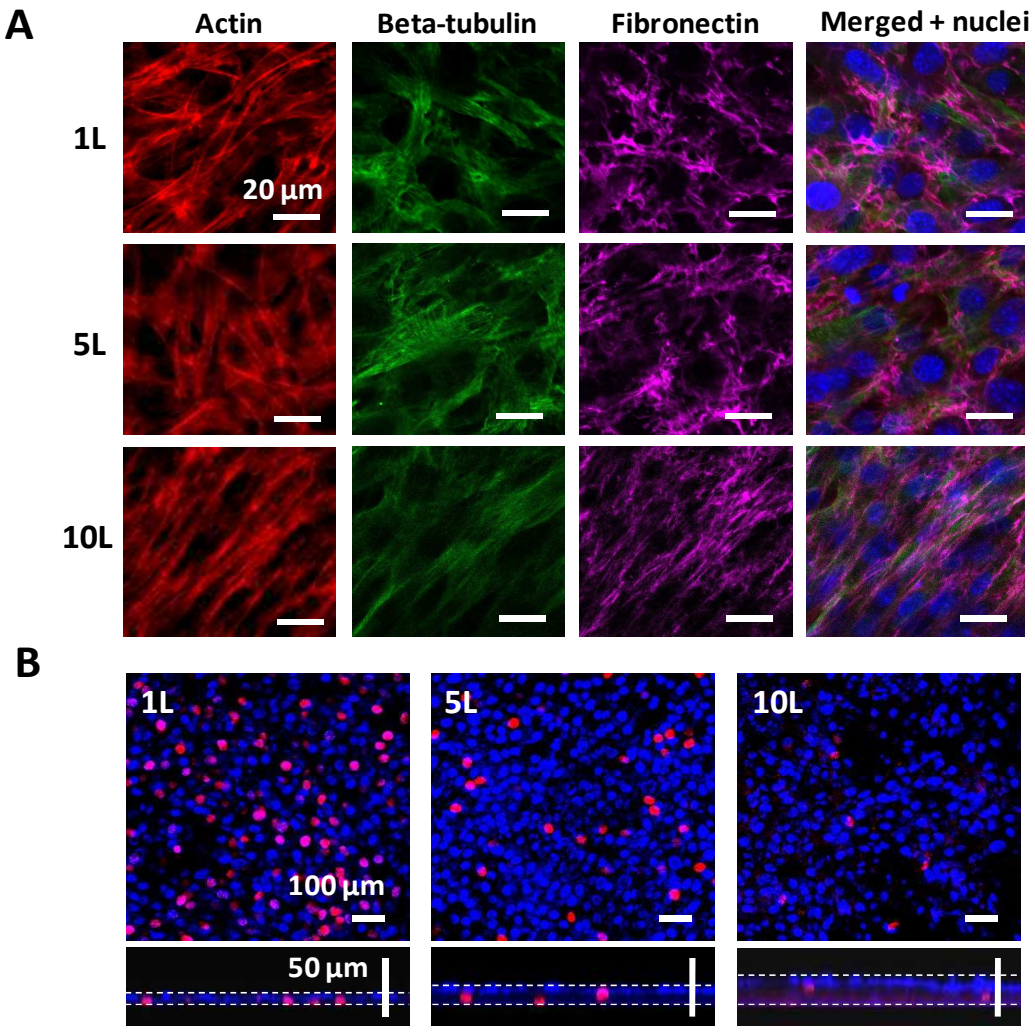

Figure 2. Cytoskeleton and matrix labelling of C2C12 multilayered tissues*. (A) Confocal images of actin (red), beta-tubulin (green), fibronectin (magenta) and nuclei (blue) staining of 1L, 5L and 10L C2C12 cell constructs after 24 h of culture in GM. (B) Cell proliferation: staining of EdU (red) associated to a fluorescent labeling of total nuclei (blue). Upper images: view from the top; lower images: and cross-sections in Z.*

Cell proliferation in GM was evaluated after 24h in GM using EdU incorporation test (Fig. 2B). The number of proliferating cells decreased with increasing number of layers. In all the constructs, proliferating cells were detectable mostly in the lower part of the multilayer. This can be explained by the stiffness of the membrane, because proliferation is generally low in soft matrix and high in stiff matrix [28; 29]. Proliferation of C2C12 myoblasts is also increased on stiff substrates as compared to soft ones [30; 31; 32]. Thus, in the 10L thickest construct where only a small fraction of total myoblasts are in contact with the membrane, the cells undergo faster withdrawal from the cell cycle.

3.3. Myogenic differentiation of myoblast multilayered structures

C2C12 myoblasts are a well-known model for the *in vitro* study of myogenic differentiation due to their ability to reproduce processes that take place during *in vivo* differentiation of skeletal muscle progenitors [33; 34]. For the construction of functional 3D skeletal muscle tissue models *in vitro*, the formation of myotubes is a crucial step.

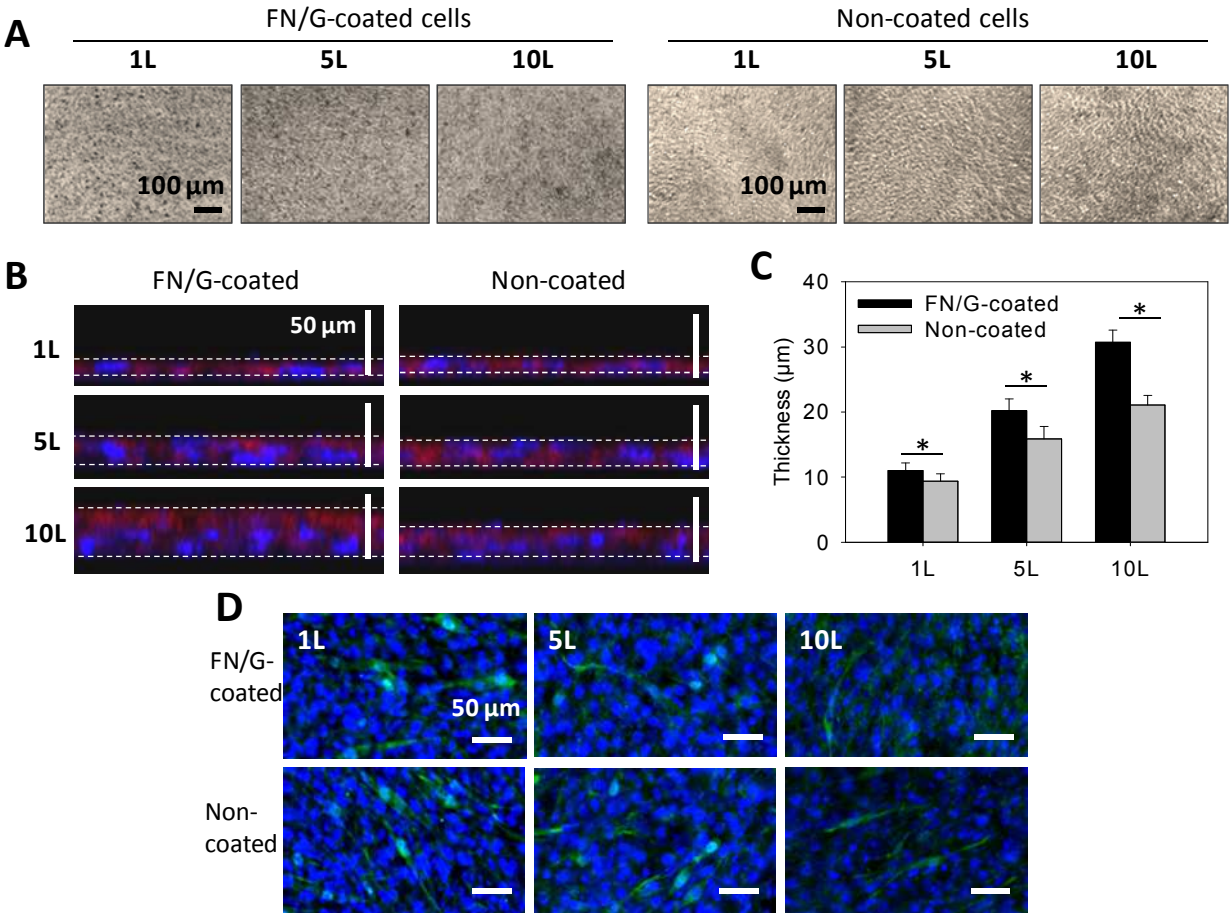

Figure 3. Comparison of C2C12 multilayered tissues prepared by cell-accumulation method from FN/G-coated and non-coated cells at early time of differentiation. *(A) Phase contrast microscopy observations from the top of 1L, 5L and 10L C2C12 cell constructs after 48 h of culture (24h in GM then 24h in DM). (B) Cross-sections in Z with thickness indicated done using confocal microscopy. Actin (red) and nuclei (blue) are stained. (C) Quantification of the thickness. Error bars correspond to SD, * : $p < 0.05$. (D) Myogenin (green) and nuclei (blue) labelling of C2C12 cell constructs after 24h in GM and 24h in DM.*

We studied the ability of the cells to undergo myogenic differentiation in multilayered constructs made of FN/G-coated cells, but also compared them to the constructs made of non-coated cells. When observed from the top at Day 1 of differentiation (24h in GM then 24h in DM), no difference in cell deposition between coated and non-coated constructs could be detected (Fig. 3A). However, the analysis of cross-sections revealed the difference of the thicknesses, although the same cell number was seeded in the beginning (Fig. 3B and C). Thickness was higher for 1L, 5L and 10L constructs made of FN/G-coated cells, compared to non-coated ones. The difference increased with increasing number of layers, reaching about 10 µm for 10L constructs. These results demonstrate the advantage of "artificial ECM" provided by FN/G coating for maintaining 3D structure.

Next, we quantified the expression of the transcription factor myogenin at early time of the differentiation process (Day 1). Myogenin is a marker for entry of myoblasts into the differentiation pathway [33]. Nuclear myogenin expression was detected in 1L and 5L constructs made of both coated and non-coated cells, but only cytoplasmic myogenin was found in 10L constructs (Fig. 3D). Thus, although thickness of the constructs made of FN/G-coated cells was higher, we could not

detect any advantage for differentiation potential at early stage of myogenesis.

We allowed the constructs to differentiate for 2 more days, until formation of multinucleated myotubes could be observed, and performed the staining for troponin T, which is a part of troponin-tropomyosin complex involved in muscle contraction. Presence of myotubes and troponin T expression were detected in 1L and 5L constructs made of both coated and non-coated cells (Fig. 4A). The myotubes were mostly located in the upper part of the constructs. Unfortunately, differentiated 10L constructs could not be analyzed because of their partial detachment from the periphery and aggregation in the center. We hypothesize that such behavior is due to higher contractile forces in more populated 10L tissues.

We further analyzed the thickness of the constructs, fusion index, as well as myotube width and length, to evaluate the functional properties of the resulting tissues. There was no difference of tissue thickness for 1L constructs made of coated or non-coated cells, but 5L constructs made of FN/G-coated cells were 5 µm thicker than those made of non-coated cells (Fig. 4B). The fusion index, which is a ratio of the nuclei contained in myotubes reported to the total number of nuclei, was of 9% for 1L coated and 5L non-coated constructs and of 17% for 1L non-coated and 5L coated constructs (Fig. 4C). Myotubes were slightly larger in non-coated constructs for 1L (11,4 µm for coated and 13,6 µm for uncoated) and about 2 times larger in FN/G-coated constructs for 5L (8,9 µm for uncoated and 14,4 µm for coated) (Fig. 4D). Myotubes length in 5L FN/G-coated constructs was also higher than for 5L non-coated constructs (Fig. 4E). Thus, we reveal the advantage of FN/G coating for the formation of 3D skeletal muscle models *in vitro*. Interestingly, there was more fusion for non-coated 1L and FN/G-coated 5L constructs, demonstrating complexity of cell response to environmental cues (substrate chemistry, mechanical and biochemical properties) in 2D vs 3D systems. In 2D, myoblasts were shown to preferentially differentiate on either stiffer substrates [30; 32] or on softer substrates functionalized with adhesion ligands [31]. The particularities of myoblast differentiation in 3D are not fully understood. Recently, myoblast interaction with 3D fibrin-based matrix was studied [13]. Differentiation kinetics were faster in 3D system, but the pattern of myogenin expression, an early differentiation marker, did not differ between 2D and 3D. These data are consistent with our observations.

Muscle constructs fabricated by cell-accumulation method can become a useful model system to study myogenic differentiation in 3D. The thickness of the coating (~10 nm) [21] is close to the thickness of muscle basement membrane (~18 nm) [35]. Because *in vivo* muscle environment can vary in matrix composition depending on muscle type, location and individual variability, cell coating can be additionally adjusted to better mimic specific muscle ECM.

Conclusion

Here, we performed the buildup of up to 10L (~40µm) 3D myoblast multilayered constructs using murine cell line. We analyzed their structure and expression of myogenic markers. The thickness of the constructs could be successfully controlled by varying the number of seeded cells. We also induced myogenic differentiation and followed the expression of myogenic markers myogenin and troponin T in the constructs made of either FN/G-coated or non-coated cells. The 3D tissues expressed myogenin after 1 day of culture in differentiation medium and formed multinucleated myotubes after 3 days.

Our approach makes it possible to rapidly build 3D muscle tissues and is promising for

the *in vitro* construction of physiologically relevant human skeletal muscle tissue models. 3D muscle constructs with controlled cell organization may help to answer fundamental questions of muscle development by mimicking skeletal muscle *in vivo* environment. Secondly, multilayered muscle tissues may be used as an artificial tissue model for drug response and toxicity assays in pharmaceutics. Moreover, pathological muscle tissue models may be created using this approach to help investigation and treatment of muscle diseases. Finally, development of 3D muscle constructs would be one more step towards *in vitro* engineering of skeletal muscle for the replacement of muscle due to an injury following a surgery, due to a trauma or paralysis.

Acknowledgements

This research was supported by Region Rhônes-Alpes via a PhD fellowship to VG. CP is a member of the Institut Universitaire de France (IUF). CP wishes to thank the European Commission for support in the framework of FP7 via an ERC Starting grant 2010 (GA 259370, BIOMIM). MM and MA wish to thank NEXT Program from JSPS (LR026) and Grant-in-Aid for Scientific Research (S).

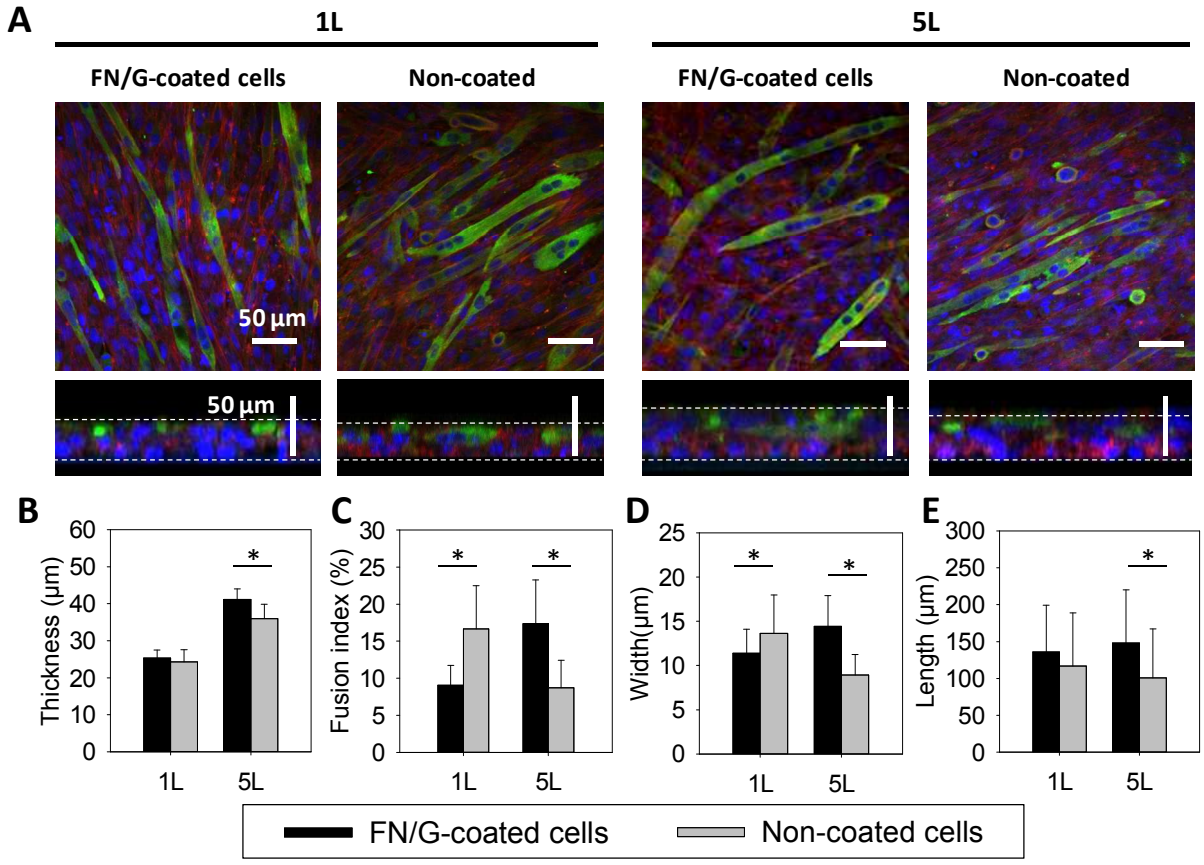

Figure 4. Myogenic differentiation of C2C12 multilayered tissues prepared by cell-accumulation method from FN/G-coated and non-coated cells. *(A) Confocal images of troponin T (green), actin (red) and nuclei (blue) staining of 1L and 5L C2C12 cell constructs after 3 days of differentiation. Upper images: view from the top; lower images: and cross-sections in Z. (B) Quantification of fusion index. (C) Quantification of thickness of the constructs. (D) Quantification of myotube width. (E) Quantification of myotube length. Error bars correspond to SD, * : $p < 0.05$.*

References

1. Gillies, A. R. & Lieber, R. L. (2011). Structure and function of the skeletal muscle extracellular matrix. *Muscle Nerve* **44**, 318-31.
2. Thorsteinsdottir, S., Deries, M., Cachaco, A. S. & Bajanca, F. (2011). The extracellular matrix dimension of skeletal muscle development. *Dev Biol* **354**, 191-207.
3. Hinds, S., Bian, W., Dennis, R. G. & Bursac, N. (2011). The role of extracellular matrix composition in structure and function of bioengineered skeletal muscle. *Biomaterials* **32**, 3575-83.
4. Light, N. & Champion, A. E. (1984). Characterization of muscle epimysium, perimysium and endomysium collagens. *Biochem J* **219**, 1017-26.
5. Koning, M., Harmsen, M. C., van Luyn, M. J. & Werker, P. M. (2009). Current opportunities and challenges in skeletal muscle tissue engineering. *J Tissue Eng Regen Med* **3**, 407-15.
6. Shah, R., Sinanan, A. C., Knowles, J. C., Hunt, N. P. & Lewis, M. P. (2005). Craniofacial muscle engineering using a 3-dimensional phosphate glass fibre construct. *Biomaterials* **26**, 1497-505.
7. Williamson, M. R., Adams, E. F. & Coombes, A. G. (2006). Gravity spun polycaprolactone fibres for soft tissue engineering: interaction with fibroblasts and myoblasts in cell culture. *Biomaterials* **27**, 1019-26.
8. Levenberg, S., Rouwkema, J., Macdonald, M., Garfein, E. S., Kohane, D. S., Darland, D. C., Marini, R., van Blitterswijk, C. A., Mulligan, R. C., D'Amore, P. A. & Langer, R. (2005). Engineering vascularized skeletal muscle tissue. *Nat Biotechnol* **23**, 879-84.
9. Levy-Mishali, M., Zoldan, J. & Levenberg, S. (2009). Effect of scaffold stiffness on myoblast differentiation. *Tissue Eng Part A* **15**, 935-44.
10. Bian, W. & Bursac, N. (2009). Engineered skeletal muscle tissue networks with controllable architecture. *Biomaterials* **30**, 1401-12.
11. Bian, W., Juhas, M., Pfeiler, T. W. & Bursac, N. (2012). Local tissue geometry determines contractile force generation of engineered muscle networks. *Tissue Eng Part A* **18**, 957-67.
12. Vandenburgh, H., Shansky, J., Benesch-Lee, F., Barbata, V., Reid, J., Thorrez, L., Valentini, R. & Crawford, G. (2008). Drug-screening platform based on the contractility of tissue-engineered muscle. *Muscle Nerve* **37**, 438-47.
13. Chiron, S., Tomczak, C., Duperray, A., Laine, J., Bonne, G., Eder, A., Hansen, A., Eschenhagen, T., Verdier, C. & Coirault, C. (2012). Complex interactions between human myoblasts and the surrounding 3D fibrin-based matrix. *PLoS One* **7**, e36173.
14. Janmey, P. A., Winer, J. P. & Weisel, J. W. (2009). Fibrin gels and their clinical and bioengineering applications. *J R Soc Interface* **6**, 1-10.
15. Yamada, N., Okano, T., Sakai, H., Karikusa, F., Sawasaki, Y. & Sakurai, Y. (1990). Thermo-responsive polymeric surfaces; control of attachment and detachment of cultured cells. *Makromol Rapid Commun* **11**, 571-576.
16. Akiyama, Y., Kikuchi, A., Yamato, M. & Okano, T. (2004). Ultrathin poly(N-isopropylacrylamide) grafted layer on polystyrene surfaces for cell adhesion/detachment control. *Langmuir* **20**, 5506-11.
17. Sasagawa, T., Shimizu, T., Sekiya, S., Haraguchi, Y., Yamato, M., Sawa, Y. & Okano, T. (2010). Design of prevascularized three-dimensional cell-dense tissues using a cell sheet stacking manipulation technology. *Biomaterials* **31**, 1646-54.
18. Takahashi, H., Shimizu, T., Nakayama, M., Yamato, M. & Okano, T. (2013). The use of anisotropic cell sheets to control orientation during the self-organization of 3D muscle tissue. *Biomaterials* **34**, 7372-80.
19. Nishiguchi, A., Yoshida, H., Matsusaki, M. & Akashi, M. (2011). Rapid construction of three-dimensional multilayered tissues with endothelial tube networks by the cell-accumulation technique. *Adv Mater* **23**, 3506-10.
20. Decher, G. (1997). Fuzzy Nanoassemblies: Toward Layered Polymeric Multicomposites. *Science* **277**, 1232-1237.
21. Matsusaki, M., Kadowaki, K., Nakahara, Y. & Akashi, M. (2007). Fabrication of Cellular Multilayers with Nanometer-Sized Extracellular Matrix Films. *Angew Chem Int Ed* **46**, 4689-4692.
22. Charrasse, S., Comunale, F., Fortier, M., Portales-Casamar, E., Debant, A. & Gauthier-Rouviere, C. (2007). M-cadherin activates Rac1 GTPase through the Rho-GEF trio during myoblast fusion. *Mol Biol Cell* **18**, 1734-43.
23. Hynes, R. O. (1992). Integrins: versatility, modulation, and signaling in cell adhesion. *Cell* **69**, 11-25.
24. Hynes, R. O. (2002). Integrins: bidirectional, allosteric signaling machines. *Cell* **110**, 673-87.
25. Matsusaki, M., Kadowaki, K., Adachi, E., Sakura, T., Yokoyama, U., Ishikawa, Y. & Akashi, M. (2012). Morphological and histological evaluations of 3D-layered blood vessel constructs prepared by hierarchical cell manipulation. *J Biomater Sci Polym Ed* **23**, 63-79.
26. Ghibaudo, M., Trichet, L., Le Digabel, J., Richert, A., Hersen, P. & Ladoux, B. (2009). Substrate topography induces a crossover from 2D to 3D behavior in fibroblast migration. *Biophys J* **97**, 357-68.
27. Ghibaudo, M., Di Meglio, J. M., Hersen, P. & Ladoux, B. (2011). Mechanics of cell spreading within 3D-micropatterned environments. *Lab Chip* **11**, 805-12.
28. Schaller, M. D. (2010). Cellular functions of FAK kinases: insight into molecular mechanisms and novel functions. *J Cell Sci* **123**, 1007-13.
29. Mammoto, A. & Ingber, D. E. (2009). Cytoskeletal control of growth and cell fate switching. *Curr Opin Cell Biol* **21**, 864-70.
30. Boontheekul, T., Hill, E. E., Kong, H. J. & Mooney, D. J. (2007). Regulating myoblast phenotype

through controlled gel stiffness and degradation. *Tissue Eng* **13**, 1431-42.
31. Gribova, V., Gauthier-Rouvière, C., Albigès-Rizo, C., Auzely-Velty, R. & Picart, C. (2012). Effect of RGD-functionalization and stiffness modulation of polyelectrolyte multilayer films on muscle cell differentiation. *Acta Biomater*.
32. Ren, K., Crouzier, T., Roy, C. & Picart, C. (2008). Polyelectrolyte multilayer films of controlled stiffness modulate myoblast cells differentiation. *Adv Funct Mater* **18**, 1378-1389.
33. Andres, V. & Walsh, K. (1996). Myogenin expression, cell cycle withdrawal, and phenotypic differentiation are temporally separable events that precede cell fusion upon myogenesis. *J Cell Biol***132**, 657-66.
34. Bach, A. D., Beier, J. P., Stern-Staeter, J. & Horch, R. E. (2004). Skeletal muscle tissue engineering. *J Cell Mol Medicine* **8**, 413-422.
35. Osawa, T., Onodera, M., Feng, X. Y. & Nozaka, Y. (2003). Comparison of the thickness of basement membranes in various tissues of the rat. *J Electron Microsc (Tokyo)* **52**, 435-40.

Supplementary Information

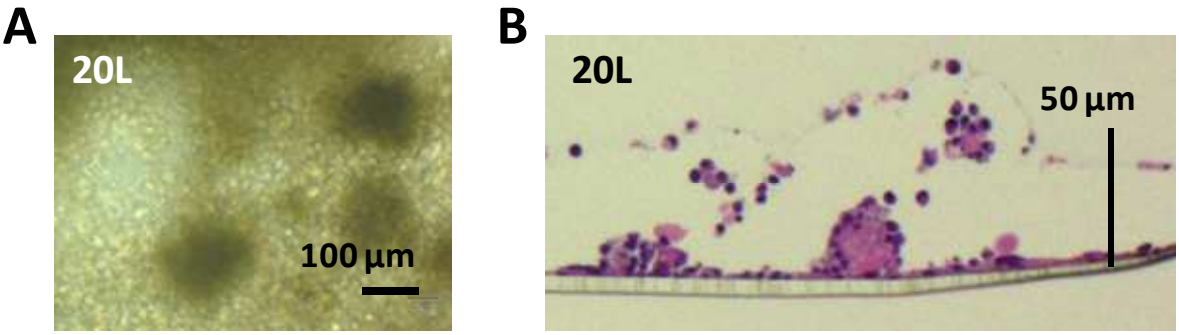

Figure S1. Construction of 20L tissues by cell-accumulation method. *(A) Phase contrast microscopy observations from the top after 24 h of culture in GM. (B) Histological analysis: phase contrast microscopy observations of hematoxylin-eosin stained cross-sections in Z after 24 h of culture in GM.*

CHAPTER VII – Conclusions and directions for future research

VII.A. CONCLUSIONS AND PERSPECTIVES OF THE THESIS WORK

In this work, we used layer-by-layer assemblies for two goals. The first consisted in the development of multifunctional biomimetic thin films for the control of skeletal muscle cell fate on 2D substrates. We used layer-by-layer films made of polypeptides, which can be stiffened by chemical cross-linking and can be specifically functionalized by grafting of biomimetic peptides onto their surface. We showed that such films with tunable mechanical and biochemical properties can be used as a model substrate to study the specific effects of each type of stimuli, or their synergy, on cell adhesion and cell fate. In the second, we used LbL assemblies for the construction of 3D skeletal muscle microtissues by "cell-accumulation technique". The method consists in coating the cells with nano-films made of fibronectin and gelatin using layer-by-layer assembly method and putting them together onto a substrate to form multilayered structures.

Interplay of mechanical and biochemical properties

In the first part, four different types of PEM films, with or without cross-linking and with or without the RGD-peptide, allowed investigation of the effect of mechanical and biochemical signals and their combinations on important events of myogenesis. Mechanical and biochemical properties could be either combined or presented separately. Decoupling of material's mechanical and biochemical properties revealed that these stimuli differentially influence cellular processes. Soft films with RGD peptide appeared as the most appropriate for myogenic differentiation of C2C12 myoblasts, while stiff films induced enhanced migration and proliferation and inhibited myogenic differentiation. Our model allowed highlighting how important events in myogenesis such as adhesion, migration proliferation, myogenin expression and fusion are regulated by substrate elasticity and presence of an adhesive ligand. These results suggest that thin films with tunable mechanical and biochemical properties may be a useful tool for biophysical studies of muscle progenitors on controlled 2D microenvironments as well as for their expansion and differentiation *in vitro*.

In addition, we combined the peptide-grafted films with substrate microtopography, showing that these films can coat microstructured materials. Such approach is promising for the development or multifunctional materials that recapitulate physical, biochemical but also microtopography cues.

Peptide-grafted films for specific targeting of cell surface receptors

Besides well-studied peptides such as RGD peptide, which interact with a wide range of integrin receptors, specific targeting of other types of receptors is important for both understanding of their roles and for the control of the cell fate via these receptors.

In the second part of the work, we selected from the literature specific peptide sequences derived from laminin-α2 chain. One is targeting syndecan-1 cell surface receptors and the other dystroglycan. Both proteins are important for skeletal muscle functions. We performed PEM films functionalization with the peptides (or their combinations with RGD peptide) and focused on the sequence of events involved in C2C12 cell differentiation including early adhesion, migration, proliferation, differentiation and fusion of myoblast into myotubes.

The results showed that cell stimulation by peptide-grafted films induced changes in cell morphology, cytoskeletal organization, migration and affected cell proliferation and myogenic differentiation. We demonstrated that PEM films may serve a tool to investigate cell signaling via non-integrin cell surface receptors. By combining materials science/chemistry and cell biology approaches, it is possible to target specific cell surface receptors. This represents a new experimental approach as compared to the more "traditional" biological techniques, which consist in changing the normal expression level of a protein to study its function (either by overexpression or knock-down). In addition, it is possible to combine two or more ligands targeting different receptors in order to investigate their combined or synergistic effects.

PEM films grafted with GF-derived peptides

Besides adhesion ligands, PEM films can also serve for the presentation of GF-derived peptides. A BMP-2 osteogenic peptide has been identified and its osteoinductive activity was demonstrated by several studies.

In the third part of the work, we evaluated the capacity of BMP-2 derived peptide to induce the osteogenic differentiation of C2C12 myoblasts. Presented by the film surface, BMP-2 peptide promoted cell adhesion and supported cell proliferation over 3 days. However, BMP-2 peptide, presented alone or with RGD peptide, was not sufficient to induce ALP expression of C2C12 myoblasts. Also, no effect on either ALP expression or on Smad pathway activation was observed when the peptide was presented in solution at different concentrations.

We analysed the presentation modes, cellular models and the effects of the peptide in different studies. We hypothesize that expression of osteogenic markers in mesenchymal and osteoblastic cells may be induced by synergistic effects between adhesive properties of used materials, osteogenic medium and autocrine signaling, but may not be fully attributed to the effect of the BMP-2 peptide. The ability of the BMP-2 peptide to mimic BMP-2 protein osteoinductive function by acting via BMP-2 receptors should be confirmed in further studies.

3D muscle tissues

In the last part, we performed the buildup of 3D thick constructs using cells coated with LbL protein films "cell-accumulation method", and analyzed their structure and expression of myogenic

markers. The thickness of the constructs could be successfully controlled by varying the number of seeded cells. We also induced myogenic differentiation and followed the expression of myogenic markers myogenin and troponin T.

Such muscle constructs fabricated by cell-accumulation method can become a useful model system to study myogenic differentiation in 3D. Because *in vivo* muscle environment can vary in matrix composition depending on muscle type, location and individual variability, cell coating can be additionally adjusted to better mimic specific muscle ECM.

Our approach made it possible to rapidly build 3D muscle tissues and is promising for the *in vitro* construction of physiologically relevant skeletal muscle tissue models. Such multilayered muscle tissues may be used as an artificial tissue model for drug response and toxicity assays in pharmaceutics. Finally, development of 3D muscle constructs is promising for *in vitro* engineering of skeletal muscle for the replacement of muscle due to an injury following a surgery, due to a trauma or paralysis.

VII.B. DIRECTIONS FOR THE FUTURE RESEARCH

Development of the materials with controlled properties is important for the field of implantable materials, drug delivery and tissue engineering. PEM films appear as a new type of biomaterial with controlled physical and chemical/biochemical properties and able to trigger a specific cellular response. This can be used for the controlled presentation of bioactive molecules to cells and for unraveling the subtle interplay between cell adhesion receptors, growth factor receptors and mechano-transduction pathways.

Design of specific receptor-targeting biomaterials

Targeting a particular cell surface receptor is important to activate specific signaling pathways. We demonstrated that PEM films can be functionalized with different bioactive peptides or their combinations. Besides the sequences used in this study, other sequences can be selected from the literature to target another cell receptors. By carefully choosing peptide sequences, the films may be used for stem cell maintenance in undifferentiated state, for cell amplification or to induced cell differentiation. For instance, maintaining these cells in a stem state is an important challenge in muscle tissue engineering; films grafted with a peptide sequence targeting syndecan-4, which is a marker of muscle satellite cells, may be explored for satellite cell culture. Such sequences derived from laminin-α1 chain are already available (Suzuki et al. 2003a).

The peptide-functionalized films may be used for the studies of pathological cell models. For instance, dystroglycan interaction with laminin-α2 chain is crucial for maintaining of the

sarcolemma integrity and of the function of skeletal muscle. L2dystro-grafted films may be explored for culture of dystrophic myotubes or for the evaluation of the possibility of L2dystro utilization as a therapeutic agent in myopathies.

Finally, this novel approach can be applied to a variety of cell types. Besides its role in skeletal muscle, dystroglycan is also associated with myelinogenesis in peripheral nerves (Masaki et al. 2003). Films functionalized with L2dystro peptide may be thus used for the investigation of molecular mechanisms and may be promising for the development of effective treatments for human peripheral neuropathies.

Combination with physical properties

Substrates allowing independent adjustment of physical and biochemical properties of different parameters are needed in order to investigate the respective roles of each parameter as well as their synergistic effects.

The peptide presentation by PEM films can be combined with a range of film's stiffnesses, as both factors, biochemical and physical, induce cellular response and can act independently or in synergy. In this work, we used (PLL/PGA) films of crosslinked at two different degrees, leading to soft and stiff films. The control of (PLL/PGA) film cross-linking degree is challenging as these films are very thin (nanometer schale thickness) and have a low hydration. Other types of PEM films allowing a better control of the stiffness, such as (PLL/HA) films, may be used to study the effects of peptide presentation on the substrates of different stiffnesses.

Towards multifunctional substrates

Besides chemical and physical properties, material's topographical cues are important for cell morphology and for collective cell organization. This is particularly important for skeletal muscle, which is a highly aligned tissue. In this work, we used peptide-grafted films for coating of microstructured PDMS, and aligned the myotubes. This approach can also be used for other topographies and other cell types. Creation of RGD peptide gradient using microfluidics technology has already been demonstrated (Almodovar et al. 2013). Creation of double gradients of two different peptides may be useful to explore the effects of the different peptide/peptide ratios. Creation of peptide micropatterns may be achieved by microprinting technology. This may allow investigation of the synergistic effects of cell geometry and biochemical cues.

Such approach is promising for the development of multifunctional materials that combine physical, biochemical and topographic cues.

Development of osteogenic PEM films

Although pBMP-2 seems to have favorable effect on osteogenic differentiation, the ability of the BMP-2 peptide to mimic BMP-2 protein osteoinductive function by acting via BMP-2 receptors remains unclear. Cellular models and experimental conditions have to be carefully controlled to avoid the side effects that may come from the substrate's adhesive properties, osteogenic media or even cell potential to undergo osteogenesis. In this context, C2C12 cells appear to be an appropriate model, as these cells do not express myogenic markers in absence of BMP-2 receptor stimulation.

Besides BMP-2 derived peptide, other osteogenic peptides are being developed, among them BMP-9 derived peptide (Marquis et al. 2008; Bergeron et al. 2009). These sequences can also be employed for PEM film functionalization.

Osteogenic PEM films present an important potential for medical applications in orthopedics. The bioactive films may be coated onto a wide range of materials used as prosthesis and implants, and improve materials integration and bone regeneration.

Development of 3D organized muscle tissue models

One of the current challenges in muscle tissue engineering is to construct 3D well-organized muscle tissues; another important challenge consists in vascularizing such engineered tissues, since blood supply is necessary to bring nutritive elements and oxygen to the cells in thick constructs.

We showed that cell-accumulation technique (Nishiguchi et al. 2011) could be used for the construction of thick 3D structures from skeletal myoblasts and their subsequent differentiation. The same group demonstrated vascularization of such tissues, based on multilayer co-culture system with human umbilical vein endothelial cells (HUVEC) (Nishiguchi et al. 2011). This method may be applied for the development of vascularized 3D muscle tissues. The alignment of the myofibers may be induced by culturing the 3D constructs on micropatterned substrates or by adding pre-aligned layers, a described recently (Takahashi et al. 2013).

Such approach makes it possible to form 3D tissues reproducing *in vivo* muscle organization and make advances in construction of physiologically relevant human skeletal muscle tissue models. Moreover, pathological muscle tissue models may be created using this approach to help investigation and treatment of muscle diseases.

References

Adams JC, Watt FM. 1993. Regulation of development and differentiation by the extracellular matrix. *Development* **117**: 1183-1198.

Akiyama Y, Kikuchi A, Yamato M, Okano T. 2004. Ultrathin poly(N-isopropylacrylamide) grafted layer on polystyrene surfaces for cell adhesion/detachment control. *Langmuir* **20**: 5506-5511.

Allazetta S, Hausherr TC, Lutolf MP. 2013. Microfluidic synthesis of cell-type-specific artificial extracellular matrix hydrogels. *Biomacromolecules* **14**: 1122-1131.

Almodovar J, Crouzier T, Selimovic S, Boudou T, Khademhosseini A, Picart C. 2013. Gradients of physical and biochemical cues on polyelectrolyte multilayer films generated via microfluidics. *Lab Chip* **13**: 1562-1570.

Anderson JM, Vines JB, Patterson JL, Chen H, Javed A, Jun HW. 2011. Osteogenic differentiation of human mesenchymal stem cells synergistically enhanced by biomimetic peptide amphiphiles combined with conditioned medium. *Acta Biomater* **7**: 675-682.

Andres V, Walsh K. 1996. Myogenin expression, cell cycle withdrawal, and phenotypic differentiation are temporally separable events that precede cell fusion upon myogenesis. *J Cell Biol* **132**: 657-666.

Angst BD, Marcozzi C, Magee AI. 2001. The cadherin superfamily: diversity in form and function. *J Cell Sci* **114**: 629-641.

Antipov AA, Sukhorukov GB. 2004. Polyelectrolyte multilayer capsules as vehicles with tunable permeability. *Adv Colloid Interface Sci* **111**: 49-61.

Arnold M, Cavalcanti-Adam EA, Glass R, Blummel J, Eck W, Kantlehner M, Kessler H, Spatz JP. 2004. Activation of integrin function by nanopatterned adhesive interfaces. *Chem Phys Chem* **5**: 383-388.

Arnold M, Hirschfeld-Warneken VC, Lohmuller T, Heil P, Blummel J, Cavalcanti-Adam EA, Lopez-Garcia M, Walther P, Kessler H, Geiger B et al. 2008. Induction of cell polarization and migration by a gradient of nanoscale variations in adhesive ligand spacing. *Nano Lett* **8**: 2063-2069.

Atala A, Bauer SB, Soker S, Yoo JJ, Retik AB. 2006. Tissue-engineered autologous bladders for patients needing cystoplasty. *Lancet* **367**: 1241-1246.

Aviss KJ, Gough JE, Downes S. 2010. Aligned electrospun polymer fibres for skeletal muscle regeneration. *Eur Cell Mater* **19**: 193-204.

Bach AD, Beier JP, Stern-Staeter J, Horch RE. 2004. Skeletal muscle tissue engineering. *J Cell Mol Med* **8**: 413-422.

Bajaj P, Reddy B, Jr., Millet L, Wei C, Zorlutuna P, Bao G, Bashir R. 2011. Patterning the differentiation of C2C12 skeletal myoblasts. *Integr Biol* **3**: 897-909.

Barresi R, Campbell KP. 2006. Dystroglycan: from biosynthesis to pathogenesis of human disease. *J Cell Sci* **119**: 199-207.

Beauvais DM, Rapraeger AC. 2004. Syndecans in tumor cell adhesion and signaling. *Reprod Biol Endocrinol* **2**: 3.

Beck K, Hunter I, Engel J. 1990. Structure and function of laminin: anatomy of a multidomain glycoprotein. *FASEB J* **4**: 148-160.

Becker AL, Johnston APR, Caruso F. 2010. Layer-By-Layer-Assembled Capsules and Films for Therapeutic Delivery. *Small* **6**: n/a-n/a.

Bellin RM, Kubicek JD, Frigault MJ, Kamien AJ, Steward RL, Jr, Barnes HM, Digiacomo MB, Duncan LJ, Edgerly CK, Morse EM et al. 2009. Defining the role of syndecan-4 in mechanotransduction using surface-modification approaches. *Proc Natl Acad Sci U S A* **106**: 22102-22107.

Benoit DS, Anseth KS. 2005. The effect on osteoblast function of colocalized RGD and PHSRN epitopes on PEG surfaces. *Biomaterials* **26**: 5209-5220.

Berg MC, Yang SY, Hammond PT, Rubner MF. 2004. Controlling mammalian cell interactions on patterned polyelectrolyte multilayer surfaces. *Langmuir* **20**: 1362-1368.
Bergeron E, Senta H, Mailloux A, Park H, Lord E, Faucheux N. 2009. Murine preosteoblast differentiation induced by a peptide derived from bone morphogenetic proteins-9. *Tissue Eng Part A* **15**: 3341-3349.
Bernfield M, Gotte M, Park PW, Reizes O, Fitzgerald ML, Lincecum J, Zako M. 1999. Functions of cell surface heparan sulfate proteoglycans. *Annu Rev Biochem* **68**: 729-777.
Bershadsky A, Kozlov M, Geiger B. 2006. Adhesion-mediated mechanosensitivity: a time to experiment, and a time to theorize. *Curr Opin Cell Biol* **18**: 472-481.
Bessa PC, Casal M, Reis RL. 2008. Bone morphogenetic proteins in tissue engineering: the road from laboratory to clinic, part II (BMP delivery). *J Tissue Eng Regen Med* **2**: 81-96.
Bezakova G, Ruegg MA. 2003. New insights into the roles of agrin. *Nat Rev Mol Cell Biol* **4**: 295-308.
Bian W, Bursac N. 2009. Engineered skeletal muscle tissue networks with controllable architecture. *Biomaterials* **30**: 1401-1412.
Bian W, Juhas M, Pfeiler TW, Bursac N. 2012. Local tissue geometry determines contractile force generation of engineered muscle networks. *Tissue Eng Part A* **18**: 957-967.
Bischoff R. 1975. Regeneration of single skeletal muscle fibers in vitro. *Anat Rec* **182**: 215-235.
Blau HM, Chiu CP, Webster C. 1983. Cytoplasmic activation of human nuclear genes in stable heterocaryons. *Cell* **32**: 1171-1180.
Boonen KJ, Rosaria-Chak KY, Baaijens FP, van der Schaft DW, Post MJ. 2009. Essential environmental cues from the satellite cell niche: optimizing proliferation and differentiation. *Am J Physiol Cell Physiol* **296**: C1338-1345.
Boontheekul T, Hill EE, Kong HJ, Mooney DJ. 2007. Regulating myoblast phenotype through controlled gel stiffness and degradation. *Tissue Eng* **13**: 1431-1442.
Boudou T, Crouzier T, Nicolas C, Ren K, Picart C. 2011. Polyelectrolyte multilayer nanofilms used as thin materials for cell mechano-sensitivity studies. *Macromol Biosci* **11**: 77-89.
Boudou T, Crouzier T, Ren K, Blin G, Picart C. 2010. Multiple Functionalities of Polyelectrolyte Multilayer Films: New Biomedical Applications. *Adv Mater* **22**: 441-467.
Bracher M, Bezuidenhout D, Lutolf MP, Franz T, Sun M, Zilla P, Davies NH. 2013. Cell specific ingrowth hydrogels. *Biomaterials* **34**: 6797-6803.
Bruckner-Tuderman L, Has C. 2013. Disorders of the cutaneous basement membrane zone-The paradigm of epidermolysis bullosa. *Matrix Biol*.
Burdick JA, Khademhosseini A, Langer R. 2004. Fabrication of gradient hydrogels using a microfluidics/photopolymerization process. *Langmuir* **20**: 5153-5156.
Butcher DT, Alliston T, Weaver VM. 2009. A tense situation: forcing tumour progression. *Nat Rev Cancer* **9**: 108-122.
Castner DG, Ratner BD. 2002. Biomedical surface science: Foundations to frontiers. *Surf Sci* **500**: 28-60.
Cavalcanti-Adam EA, Volberg T, Micoulet A, Kessler H, Geiger B, Spatz JP. 2007. Cell spreading and focal adhesion dynamics are regulated by spacing of integrin ligands. *Biophys J* **92**: 2964-2974.
Chakravarti R, Sapountzi V, Adams JC. 2005. Functional role of syndecan-1 cytoplasmic V region in lamellipodial spreading, actin bundling, and cell migration. *Mol Biol Cell* **16**: 3678-3691.
Charest JL, Garcia AJ, King WP. 2007. Myoblast alignment and differentiation on cell culture substrates with microscale topography and model chemistries. *Biomaterials* **28**: 2202-2210.
Charrasse S, Comunale F, Fortier M, Portales-Casamar E, Debant A, Gauthier-Rouviere C. 2007. M-cadherin activates Rac1 GTPase through the Rho-GEF trio during myoblast fusion. *Mol Biol Cell* **18**: 1734-1743.
Chen TL, Bates RL, Dudley A, Hammonds RG, Jr., Amento EP. 1991. Bone morphogenetic protein-2b stimulation of growth and osteogenic phenotypes in rat osteoblast-like cells: comparison with TGF-beta 1. *J Bone Miner Res* **6**: 1387-1393.

Chen WL, Simmons CA. 2011. Lessons from (patho)physiological tissue stiffness and their implications for drug screening, drug delivery and regenerative medicine. *Adv Drug Deliv Rev* **63**: 269-276.

Chetprayoon P, Kadowaki K, Matsusaki M, Akashi M. 2013. Survival and structural evaluations of three-dimensional tissues fabricated by the hierarchical cell manipulation technique. *Acta Biomater* **9**: 4698-4706.

Chien HW, Chang TY, Tsai WB. 2009. Spatial control of cellular adhesion using photo-crosslinked micropatterned polyelectrolyte multilayer films. *Biomaterials* **30**: 2209-2218.

Chiron S, Tomczak C, Duperray A, Laine J, Bonne G, Eder A, Hansen A, Eschenhagen T, Verdier C, Coirault C. 2012. Complex interactions between human myoblasts and the surrounding 3D fibrin-based matrix. *PLoS One* **7**: e36173.

Chung TW, Liu DZ, Wang SY, Wang SS. 2003. Enhancement of the growth of human endothelial cells by surface roughness at nanometer scale. *Biomaterials* **24**: 4655-4661.

Cohn RD, Henry MD, Michele DE, Barresi R, Saito F, Moore SA, Flanagan JD, Skwarchuk MW, Robbins ME, Mendell JR et al. 2002. Disruption of DAG1 in differentiated skeletal muscle reveals a role for dystroglycan in muscle regeneration. *Cell* **110**: 639-648.

Collins J, Bonnemann CG. 2010. Congenital muscular dystrophies: toward molecular therapeutic interventions. *Curr Neurol Neurosci Rep* **10**: 83-91.

Cornelison DD, Filla MS, Stanley HM, Rapraeger AC, Olwin BB. 2001. Syndecan-3 and syndecan-4 specifically mark skeletal muscle satellite cells and are implicated in satellite cell maintenance and muscle regeneration. *Dev Biol* **239**: 79-94.

Cosgrove BD, Sacco A, Gilbert PM, Blau HM. 2009. A home away from home: challenges and opportunities in engineering in vitro muscle satellite cell niches. *Differentiation* **78**: 185-194.

Couchman JR. 2003. Syndecans: proteoglycan regulators of cell-surface microdomains? *Nat Rev Mol Cell Biol* **4**: 926-937.

Crouzier T, Fourel L, Boudou T, Albiges-Rizo C, Picart C. 2011a. Presentation of BMP-2 from a soft biopolymeric film unveils its activity on cell adhesion and migration. *Adv Mater* **23**: H111-118.

Crouzier T, Picart C. 2009. Ion pairing and hydration in polyelectrolyte multilayer films containing polysaccharides. *Biomacromolecules* **10**: 433-442.

Crouzier T, Ren K, Nicolas C, Roy C, Picart C. 2009. Layer-by-layer films as a biomimetic reservoir for rhBMP-2 delivery: controlled differentiation of myoblasts to osteoblasts. *Small* **5**: 598-608.

Crouzier T, Sailhan F, Becquart P, Guillot R, Logeart-Avramoglou D, Picart C. 2011b. The performance of BMP-2 loaded TCP/HAP porous ceramics with a polyelectrolyte multilayer film coating. *Biomaterials* **32**: 7543-7554.

Crouzier T, Szarpak A, Boudou T, Auzely-Velty R, Picart C. 2010. Polysaccharide-blend multilayers containing hyaluronan and heparin as a delivery system for rhBMP-2. *Small* **6**: 651-662.

Curtis A, Wilkinson C. 1997. Topographical control of cells. *Biomaterials* **18**: 1573-1583.

Davila J, Chassepot A, Longo J, Boulmedais F, Reisch A, Frisch B, Meyer F, Voegel JC, Mesini PJ, Senger B et al. 2012. Cyto-mechanoresponsive polyelectrolyte multilayer films. *J Am Chem Soc* **134**: 83-86.

Debelle L, Tamburro AM. 1999. Elastin: molecular description and function. *Int J Biochem Cell Biol* **31**: 261-272.

Decher G. 1997. Fuzzy Nanoassemblies: Toward Layered Polymeric Multicomposites. *Science* **277**: 1232-1237.

Decher G, Hong JD, Schmitt J. 1992. Buildup of ultrathin multilayer films by a self-assembly process: III. Consecutively alternating adsorption of anionic and cationic polyelectrolytes on charged surfaces. *Thin Solid Films* **210–211, Part 2**: 831-835.

Deeg JA, Louban I, Aydin D, Selhuber-Unkel C, Kessler H, Spatz JP. 2011. Impact of local versus global ligand density on cellular adhesion. *Nano Lett* **11**: 1469-1476.

Delorme B, Ringe J, Pontikoglou C, Gaillard J, Langonne A, Sensebe L, Noel D, Jorgensen C, Haupl T, Charbord P. 2009. Specific lineage-priming of bone marrow mesenchymal stem cells provides the molecular framework for their plasticity. *Stem Cells* **27**: 1142-1151.

Dennis RG, Kosnik PE, 2nd. 2000. Excitability and isometric contractile properties of mammalian skeletal muscle constructs engineered in vitro. *In Vitro Cell Dev Biol Anim* **36**: 327-335.

Detzel CJ, Larkin AL, Rajagopalan P. 2011. Polyelectrolyte multilayers in tissue engineering. *Tissue Eng Part B Rev* **17**: 101-113.

Discher DE, Janmey P, Wang YL. 2005. Tissue cells feel and respond to the stiffness of their substrate. *Science* **310**: 1139-1143.

Divoux A, Clement K. 2011. Architecture and the extracellular matrix: the still unappreciated components of the adipose tissue. *Obes Rev* **12**: e494-503.

Doran MR, Frith JE, Prowse AB, Fitzpatrick J, Wolvetang EJ, Munro TP, Gray PP, Cooper-White JJ. 2010. Defined high protein content surfaces for stem cell culture. *Biomaterials* **31**: 5137-5142.

Drury JL, Mooney DJ. 2003. Hydrogels for tissue engineering: scaffold design variables and applications. *Biomaterials* **24**: 4337-4351.

Durbeej M. 2010. Laminins. *Cell Tissue Res* **339**: 259-268.

Durbeej M, Henry MD, Campbell KP. 1998a. Dystroglycan in development and disease. *Curr Opin Cell Biol* **10**: 594-601.

Durbeej M, Henry MD, Ferletta M, Campbell KP, Ekblom P. 1998b. Distribution of dystroglycan in normal adult mouse tissues. *J Histochem Cytochem* **46**: 449-457.

Elbashir SM, Harborth J, Lendeckel W, Yalcin A, Weber K, Tuschl T. 2001. Duplexes of 21-nucleotide RNAs mediate RNA interference in cultured mammalian cells. *Nature* **411**: 494-498.

Engel J, Furthmayr H. 1987. Electron microscopy and other physical methods for the characterization of extracellular matrix components: laminin, fibronectin, collagen IV, collagen VI, and proteoglycans. *Methods Enzymol* **145**: 3-78.

Engler A, Bacakova L, Newman C, Hategan A, Griffin M, Discher DE. 2004a. Substrate compliance versus ligand density in cell on gel responses. *Biophys J* **86**: 617-628.

Engler AJ, Griffin MA, Sen S, Bonnemann CG, Sweeney HL, Discher DE. 2004b. Myotubes differentiate optimally on substrates with tissue-like stiffness: pathological implications for soft or stiff microenvironments. *J Cell Biol* **166**: 877-887.

Engler AJ, Sen S, Sweeney HL, Discher DE. 2006. Matrix elasticity directs stem cell lineage specification. *Cell* **126**: 677-689.

Falconnet D, Csucs G, Grandin HM, Textor M. 2006. Surface engineering approaches to micropattern surfaces for cell-based assays. *Biomaterials* **27**: 3044-3063.

Fan VH, Tamama K, Au A, Littrell R, Richardson LB, Wright JW, Wells A, Griffith LG. 2007. Tethered epidermal growth factor provides a survival advantage to mesenchymal stem cells. *Stem Cells* **25**: 1241-1251.

Fan YW, Cui FZ, Hou SP, Xu QY, Chen LN, Lee IS. 2002. Culture of neural cells on silicon wafers with nano-scale surface topograph. *J Neurosci Methods* **120**: 17-23.

Filla MS, Dam P, Rapraeger AC. 1998. The cell surface proteoglycan syndecan-1 mediates fibroblast growth factor-2 binding and activity. *J Cell Physiol* **174**: 310-321.

Frantz C, Stewart KM, Weaver VM. 2010. The extracellular matrix at a glance. *J Cell Sci* **123**: 4195-4200.

Gallant ND, Capadona JR, Frazier AB, Collard DM, García AJ. 2002. Micropatterned Surfaces to Engineer Focal Adhesions for Analysis of Cell Adhesion Strengthening. *Langmuir* **18**: 5579-5584.

Garcia AJ, Vega MD, Boettiger D. 1999. Modulation of cell proliferation and differentiation through substrate-dependent changes in fibronectin conformation. *Mol Biol Cell* **10**: 785-798.

Garza JM, Jessel N, Ladam G, Dupray V, Muller S, Stoltz JF, Schaaf P, Voegel JC, Lavalle P. 2005. Polyelectrolyte multilayers and degradable polymer layers as multicompartment films. *Langmuir* **21**: 12372-12377.

Gautschi OP, Frey SP, Zellweger R. 2007. Bone morphogenetic proteins in clinical applications. *ANZ J Surg* **77**: 626-631.

Genes NG, Rowley JA, Mooney DJ, Bonassar LJ. 2004. Effect of substrate mechanics on chondrocyte adhesion to modified alginate surfaces. *Arch Biochem Biophys* **422**: 161-167.

Ghodadra N, Singh K. 2008. Recombinant human bone morphogenetic protein-2 in the treatment of bone fractures. *Biologics* **2**: 345-354.

Gilbert PM, Havenstrite KL, Magnusson KE, Sacco A, Leonardi NA, Kraft P, Nguyen NK, Thrun S, Lutolf MP, Blau HM. 2010. Substrate elasticity regulates skeletal muscle stem cell self-renewal in culture. *Science* **329**: 1078-1081.

Gillies AR, Lieber RL. 2011. Structure and function of the skeletal muscle extracellular matrix. *Muscle Nerve* **44**: 318-331.

Gingras J, Rioux RM, Cuvelier D, Geisse NA, Lichtman JW, Whitesides GM, Mahadevan L, Sanes JR. 2009. Controlling the orientation and synaptic differentiation of myotubes with micropatterned substrates. *Biophys J* **97**: 2771-2779.

Gorbet M, Postnikoff C. 2013. The impact of silicone hydrogel-solution combinations on corneal epithelial cells. *Eye Contact Lens* **39**: 42-47.

Goudenege S, Lamarre Y, Dumont N, Rousseau J, Frenette J, Skuk D, Tremblay JP. 2010. Laminin-111: a potential therapeutic agent for Duchenne muscular dystrophy. *Mol Ther* **18**: 2155-2163.

Grabarek Z, Gergely J. 1990. Zero-length crosslinking procedure with the use of active esters. *Anal Biochem* **185**: 131-135.

Grabowska I, Szeliga A, Moraczewski J, Czaplicka I, Brzóska E. 2010. Comparison of satellite cell-derived myoblasts and C2C12 differentiation in two- and three-dimensional cultures: changes in adhesion protein expression. *Cell Biol Int* **35**: 125-133.

Gribova V, Auzely-Velty R, Picart C. 2012. Polyelectrolyte Multilayer Assemblies on Materials Surfaces: From Cell Adhesion to Tissue Engineering. *Chem Mater* **24**: 854-869.

Gribova V, Crouzier T, Picart C. 2011. A material's point of view on recent developments of polymeric biomaterials: control of mechanical and biochemical properties. *J Mater Chem* **21**: 14354-14366.

Gribova V, Gauthier-Rouvière C, Albigès-Rizo C, Auzely-Velty R, Picart C. 2013. Effect of RGD functionalization and stiffness modulation of polyelectrolyte multilayer films on muscle cell differentiation. *Acta Biomater* **9**: 6468-6480.

Grossi A, Yadav K, Lawson MA. 2007. Mechanical stimulation increases proliferation, differentiation and protein expression in culture: stimulation effects are substrate dependent. *J Biomech* **40**: 3354-3362.

Guillot R, Gilde F, Becquart P, Sailhan F, Lapeyrere A, Logeart-Avramoglou D, Picart C. 2013. The stability of BMP loaded polyelectrolyte multilayer coatings on titanium. *Biomaterials* **34**: 5737-5746.

Gullberg D, Ekblom P. 1995. Extracellular matrix and its receptors during development. *Int J Dev Biol* **39**: 845-854.

Guvendiren M, Burdick JA. 2010. The control of stem cell morphology and differentiation by hydrogel surface wrinkles. *Biomaterials* **31**: 6511-6518.

Halfter W, Candiello J, Hu H, Zhang P, Schreiber E, Balasubramani M. 2013. Protein composition and biomechanical properties of in vivo-derived basement membranes. *Cell Adh Migr* **7**: 64-71.

Hamilton AJ, Baulcombe DC. 1999. A Species of Small Antisense RNA in Posttranscriptional Gene Silencing in Plants. *Science* **286**: 950-952.

Han R, Kanagawa M, Yoshida-Moriguchi T, Rader EP, Ng RA, Michele DE, Muirhead DE, Kunz S, Moore SA, Iannaccone ST et al. 2009. Basal lamina strengthens cell membrane integrity

via the laminin G domain-binding motif of alpha-dystroglycan. *Proc Natl Acad Sci U S A* **106**: 12573-12579.
He X, Ma J, Jabbari E. 2008a. Effect of grafting RGD and BMP-2 protein-derived peptides to a hydrogel substrate on osteogenic differentiation of marrow stromal cells. *Langmuir* **24**: 12508-12516.
He XZ, Ma JY, Jabbari E. 2008b. Effect of Grafting RGD and BMP-2 Protein-Derived Peptides to a Hydrogel Substrate on Osteogenic Differentiation of Marrow Stromal Cells. *Langmuir* **24**: 12508-12516.
Heining E, Bhushan R, Paarmann P, Henis YI, Knaus P. 2011. Spatial segregation of BMP/Smad signaling affects osteoblast differentiation in C2C12 cells. *PLoS One* **6**: e25163.
Hempel U, Moller S, Noack C, Hintze V, Scharnweber D, Schnabelrauch M, Dieter P. 2012. Sulfated hyaluronan/collagen I matrices enhance the osteogenic differentiation of human mesenchymal stromal cells in vitro even in the absence of dexamethasone. *Acta Biomater* **8**: 4064-4072.
Hern DL, Hubbell JA. 1998. Incorporation of adhesion peptides into nonadhesive hydrogels useful for tissue resurfacing. *J Biomed Mater Res* **39**: 266-276.
Hersel U, Dahmen C, Kessler H. 2003. RGD modified polymers: biomaterials for stimulated cell adhesion and beyond. *Biomaterials* **24**: 4385-4415.
Hertz A, Bruce IJ. 2007. Inorganic materials for bone repair or replacement applications. *Nanomedicine* **2**: 899-918.
Hewitt JE. 2009. Abnormal glycosylation of dystroglycan in human genetic disease. *Biochim Biophys Acta* **1792**: 853-861.
Hinds S, Bian W, Dennis RG, Bursac N. 2011. The role of extracellular matrix composition in structure and function of bioengineered skeletal muscle. *Biomaterials* **32**: 3575-3583.
Hirohashi S, Kanai Y. 2003. Cell adhesion system and human cancer morphogenesis. *Cancer Sci* **94**: 575-581.
Hirsch E, Lohikangas L, Gullberg D, Johansson S, Fassler R. 1998. Mouse myoblasts can fuse and form a normal sarcomere in the absence of beta1 integrin expression. *J Cell Sci* **111 (Pt 16)**: 2397-2409.
Hoffman MP, Nomizu M, Roque E, Lee S, Jung DW, Yamada Y, Kleinman HK. 1998. Laminin-1 and laminin-2 G-domain synthetic peptides bind syndecan-1 and are involved in acinar formation of a human submandibular gland cell line. *J Biol Chem* **273**: 28633-28641.
Hohenester E, Yurchenco PD. 2013. Laminins in basement membrane assembly. *Cell Adh Migr* **7**: 56-63.
Hozumi K, Kobayashi K, Katagiri F, Kikkawa Y, Kadoya Y, Nomizu M. 2010. Syndecan- and integrin-binding peptides synergistically accelerate cell adhesion. *FEBS Lett* **584**: 3381-3385.
Hozumi K, Yamagata N, Otagiri D, Fujimori C, Kikkawa Y, Kadoya Y, Nomizu M. 2009. Mixed peptide-chitosan membranes to mimic the biological activities of a multifunctional laminin alpha1 chain LG4 module. *Biomaterials* **30**: 1596-1603.
Hsiong SX, Boontheekul T, Huebsch N, Mooney DJ. 2009. Cyclic arginine-glycine-aspartate peptides enhance three-dimensional stem cell osteogenic differentiation. *Tissue Eng Part A* **15**: 263-272.
Huang J, Grater SV, Corbellini F, Rinck S, Bock E, Kemkemer R, Kessler H, Ding J, Spatz JP. 2009. Impact of order and disorder in RGD nanopatterns on cell adhesion. *Nano Lett* **9**: 1111-1116.
Huang NF, Lee RJ, Li S. 2010. Engineering of aligned skeletal muscle by micropatterning. *Am J Transl Res* **2**: 43-55.
Huang NF, Patel S, Thakar RG, Wu J, Hsiao BS, Chu B, Lee RJ, Li S. 2006. Myotube assembly on nanofibrous and micropatterned polymers. *Nano Lett* **6**: 537-542.
Hubbell JA. 1999. Bioactive biomaterials. *Curr Opin Biotechnol* **10**: 123-129.
Huebsch N, Mooney DJ. 2009. Inspiration and application in the evolution of biomaterials. *Nature* **462**: 426-432.

Hughes FJ, Collyer J, Stanfield M, Goodman SA. 1995. The effects of bone morphogenetic protein-2, -4, and -6 on differentiation of rat osteoblast cells in vitro. *Endocrinology* **136**: 2671-2677.
Hynes RO. 1992. Integrins: versatility, modulation, and signaling in cell adhesion. *Cell* **69**: 11-25.
-. 2002. Integrins: bidirectional, allosteric signaling machines. *Cell* **110**: 673-687.
-. 2009. The extracellular matrix: not just pretty fibrils. *Science* **326**: 1216-1219.
-. 2012. The evolution of metazoan extracellular matrix. *J Cell Biol* **196**: 671-679.
Ingber D. 1991. Integrins as mechanochemical transducers. *Cur Opin Cell Biol* **3**: 841-848.
Izquierdo A, Ono SS, Voegel JC, Schaaf P, Decher G. 2005. Dipping versus Spraying: Exploring the Deposition Conditions for Speeding Up Layer-by-Layer Assembly. *Langmuir* **21**: 7558-7567.
Jabbari E. 2013. Osteogenic peptides in bone regeneration. *Curr Pharm Des* **19**: 3391-3402.
Jan E, Kotov NA. 2007. Successful differentiation of mouse neural stem cells on layer-by-layer assembled single-walled carbon nanotube composite. *Nano Lett* **7**: 1123-1128.
Janmey PA, Winer JP, Weisel JW. 2009. Fibrin gels and their clinical and bioengineering applications. *J R Soc Interface* **6**: 1-10.
Janzen V, Scadden DT. 2006. Stem cells: good, bad and reformable. *Nature* **441**: 418-419.
Jarvelainen H, Sainio A, Koulu M, Wight TN, Penttinen R. 2009. Extracellular matrix molecules: potential targets in pharmacotherapy. *Pharmacol Rev* **61**: 198-223.
Jensen J, Rustad PI, Kolnes AJ, Lai YC. 2011. The role of skeletal muscle glycogen breakdown for regulation of insulin sensitivity by exercise. *Front Physiol* **2**: 112.
Johansson JA, Halthur T, Herranen M, Soderberg L, Elofsson U, Hilborn J. 2005. Build-up of collagen and hyaluronic acid polyelectrolyte multilayers. *Biomacromolecules* **6**: 1353-1359.
Kandow CE, Georges PC, Janmey PA, Beningo KA. 2007. Polyacrylamide hydrogels for cell mechanics: steps toward optimization and alternative uses. *Methods Cell Biol* **83**: 29-46.
Katagiri T, Yamaguchi A, Komaki M, Abe E, Takahashi N, Ikeda T, Rosen V, Wozney JM, Fujisawa-Sehara A, Suda T. 1994. Bone morphogenetic protein-2 converts the differentiation pathway of C2C12 myoblasts into the osteoblast lineage. *J Cell Biol* **127**: 1755-1766.
Keselowsky BG, Garcia AJ. 2005. Quantitative methods for analysis of integrin binding and focal adhesion formation on biomaterial surfaces. *Biomaterials* **26**: 413-418.
Khademhosseini A, Langer R, Borenstein J, Vacanti JP. 2006. Microscale technologies for tissue engineering and biology. *Proc Natl Acad Sci U S A* **103**: 2480-2487.
Khetan S, Guvendiren M, Legant WR, Cohen DM, Chen CS, Burdick JA. 2013. Degradation-mediated cellular traction directs stem cell fate in covalently crosslinked three-dimensional hydrogels. *Nat Mater* **12**: 458-465.
Kidambi S, Udpa N, Schroeder SA, Findlan R, Lee I, Chan C. 2007. Cell adhesion on polyelectrolyte multilayer coated polydimethylsiloxane surfaces with varying topographies. *Tissue Eng* **13**: 2105-2117.
Klagsbrun M. 1990. The affinity of fibroblast growth factors (FGFs) for heparin; FGF-heparan sulfate interactions in cells and extracellular matrix. *Curr Opin Cell Biol* **2**: 857-863.
Klingler W, Jurkat-Rott K, Lehmann-Horn F, Schleip R. 2012. The role of fibrosis in Duchenne muscular dystrophy. *Acta Myol* **31**: 184-195.
Kloesch B, Hoering B, Dopler D, Banerjee A, van Griensven M, Redl H. 2007. Synthetic peptides derived from the knuckle epitope of hBMP-2 were
evaluated for inducing osteogenic differentiation in vitro and in vivo. *Eur Cells Mater***14**: 70.
Koning M, Harmsen MC, van Luyn MJ, Werker PM. 2009. Current opportunities and challenges in skeletal muscle tissue engineering. *J Tissue Eng Regen Med* **3**: 407-415.
Kostrominova TY, Tanzer ML. 1995. Temporal and spatial appearance of alpha-dystroglycan in differentiated mouse myoblasts in culture. *J Cell Biochem* **58**: 527-534.
Kragstrup TW, Kjaer M, Mackey AL. 2011. Structural, biochemical, cellular, and functional changes in skeletal muscle extracellular matrix with aging. *Scand J Med Sci Sports* **21**: 749-757.

Kucia M, Reca R, Miekus K, Wanzeck J, Wojakowski W, Janowska-Wieczorek A, Ratajczak J, Ratajczak MZ. 2005. Trafficking of Normal Stem Cells and Metastasis of Cancer Stem Cells Involve Similar Mechanisms: Pivotal Role of the SDF-1–CXCR4 Axis. *Stem Cells* **23**: 879-894.

Kutejova E, Briscoe J, Kicheva A. 2009. Temporal dynamics of patterning by morphogen gradients. *Curr Opin Genet Dev* **19**: 315-322.

Lam MT, Sim S, Zhu X, Takayama S. 2006. The effect of continuous wavy micropatterns on silicone substrates on the alignment of skeletal muscle myoblasts and myotubes. *Biomaterials* **27**: 4340-4347.

Lampin M, Warocquier C, Legris C, Degrange M, Sigot-Luizard MF. 1997. Correlation between substratum roughness and wettability, cell adhesion, and cell migration. *J Biomed Mater Res* **36**: 99-108.

Langer R, Vacanti JP. 1993. Tissue engineering. *Science* **260**: 920-926.

Larkin AL, Davis RM, Rajagopalan P. 2010. Biocompatible, detachable, and free-standing polyelectrolyte multilayer films. *Biomacromolecules* **11**: 2788-2796.

Larrain J, Carey DJ, Brandan E. 1998. Syndecan-1 expression inhibits myoblast differentiation through a basic fibroblast growth factor-dependent mechanism. *J Biol Chem* **273**: 32288-32296.

Larrain J, Cizmeci-Smith G, Troncoso V, Stahl RC, Carey DJ, Brandan E. 1997. Syndecan-1 expression is down-regulated during myoblast terminal differentiation. Modulation by growth factors and retinoic acid. *J Biol Chem* **272**: 18418-18424.

Le Guehennec L, Soueidan A, Layrolle P, Amouriq Y. 2007. Surface treatments of titanium dental implants for rapid osseointegration. *Dent Mater* **23**: 844-854.

Le Ricousse-Roussanne S, Larghero J, Zini JM, Barateau V, Foubert P, Uzan G, Liu X, Lacassagne MN, Ternaux B, Robert I et al. 2007. Ex vivo generation of mature and functional human smooth muscle cells differentiated from skeletal myoblasts. *Exp Cell Res* **313**: 1337-1346.

Lee J, Cuddihy MJ, Kotov NA. 2008. Three-dimensional cell culture matrices: state of the art. *Tissue Eng Part B Rev* **14**: 61-86.

Leguen E, Chassepot A, Decher G, Schaaf P, Voegel JC, Jessel N. 2007. Bioactive coatings based on polyelectrolyte multilayer architectures functionalized by embedded proteins, peptides or drugs. *Biomol Eng* **24**: 33-41.

Levenberg S, Rouwkema J, Macdonald M, Garfein ES, Kohane DS, Darland DC, Marini R, van Blitterswijk CA, Mulligan RC, D'Amore PA et al. 2005. Engineering vascularized skeletal muscle tissue. *Nat Biotechnol* **23**: 879-884.

Levental KR, Yu H, Kass L, Lakins JN, Egeblad M, Erler JT, Fong SF, Csiszar K, Giaccia A, Weninger W et al. 2009. Matrix crosslinking forces tumor progression by enhancing integrin signaling. *Cell* **139**: 891-906.

Levy-Mishali M, Zoldan J, Levenberg S. 2009. Effect of scaffold stiffness on myoblast differentiation. *Tissue Eng Part A* **15**: 935-944.

Li Y, Rodrigues J, Tomas H. 2012a. Injectable and biodegradable hydrogels: gelation, biodegradation and biomedical applications. *Chem Soc Rev* **41**: 2193-2221.

Li Y, Wang X, Sun J. 2012b. Layer-by-layer assembly for rapid fabrication of thick polymeric films. *Chem Soc Rev* **41**: 5998-6009.

Light N, Champion AE. 1984. Characterization of muscle epimysium, perimysium and endomysium collagens. *Biochem J* **219**: 1017-1026.

Liu H, Niu A, Chen SE, Li YP. 2011. Beta3-integrin mediates satellite cell differentiation in regenerating mouse muscle. *FASEB J* **25**: 1914-1921.

Logeart-Avramoglou D, Bourguignon M, Oudina K, Ten Dijke P, Petite H. 2006. An assay for the determination of biologically active bone morphogenetic proteins using cells transfected with an inhibitor of differentiation promoter-luciferase construct. *Anal Biochem* **349**: 78-86.

Lortat-Jacob H. 2009. The molecular basis and functional implications of chemokine interactions with heparan sulphate. *Curr Opin Struct Biol* **19**: 543-548.

Lutolf MP, Gilbert PM, Blau HM. 2009. Designing materials to direct stem-cell fate. *Nature* **462**: 433-441.
Lutolf MP, Hubbell JA. 2005. Synthetic biomaterials as instructive extracellular microenvironments for morphogenesis in tissue engineering. *Nat Biotechnol* **23**: 47-55.
Lutolf MP, Lauer-Fields JL, Schmoekel HG, Metters AT, Weber FE, Fields GB, Hubbell JA. 2003a. Synthetic matrix metalloproteinase-sensitive hydrogels for the conduction of tissue regeneration: engineering cell-invasion characteristics. *Proc Natl Acad Sci U S A* **100**: 5413-5418.
Lutolf MP, Raeber GP, Zisch AH, Tirelli N, Hubbell JA. 2003b. Cell-responsive synthetic hydrogels. *Adv Mater* **15**: 888-+.
Lutolf MP, Weber FE, Schmoekel HG, Schense JC, Kohler T, Muller R, Hubbell JA. 2003c. Repair of bone defects using synthetic mimetics of collagenous extracellular matrices. *Nat Biotechnol* **21**: 513-518.
Lvov Y, Decher G, Haas H, Möhwald H, Kalachev A. 1994. X-ray analysis of ultrathin polymer films self-assembled onto substrates. *Physica B: Condensed Matter* **198**: 89-91.
Macdonald ML, Samuel RE, Shah NJ, Padera RF, Beben YM, Hammond PT. 2011. Tissue integration of growth factor-eluting layer-by-layer polyelectrolyte multilayer coated implants. *Biomaterials* **32**: 1446-1453.
Mammoto A, Ingber DE. 2009. Cytoskeletal control of growth and cell fate switching. *Curr Opin Cell Biol* **21**: 864-870.
Mann BK, Schmedlen RH, West JL. 2001. Tethered-TGF-beta increases extracellular matrix production of vascular smooth muscle cells. *Biomaterials* **22**: 439-444.
Marklein RA, Burdick JA. 2010. Spatially controlled hydrogel mechanics to modulate stem cell interactions. *Soft Matter* **6**: 136-143.
Marquis ME, Lord E, Bergeron E, Bourgoin L, Faucheux N. 2008. Short-term effects of adhesion peptides on the responses of preosteoblasts to pBMP-9. *Biomaterials* **29**: 1005-1016.
Masaki T, Matsumura K. 2010. Biological role of dystroglycan in Schwann cell function and its implications in peripheral nervous system diseases. *J Biomed Biotechnol* **2010**: 740403.
Masaki T, Matsumura K, Saito F, Yamada H, Higuchi S, Kamakura K, Yorifuji H, Shimizu T. 2003. Association of dystroglycan and laminin-2 coexpression with myelinogenesis in peripheral nerves. *Med Electron Microsc* **36**: 221-239.
Matsumoto T, Sasaki J, Alsberg E, Egusa H, Yatani H, Sohmura T. 2007. Three-dimensional cell and tissue patterning in a strained fibrin gel system. *PLoS One* **2**: e1211.
Matsumura K, Yamada H, Saito F, Sunada Y, Shimizu T. 1997. The role of dystroglycan, a novel receptor of laminin and agrin, in cell differentiation. *Histol Histopathol* **12**: 195-203.
Matsusaki M, Akashi M. 2009. Functional multilayered capsules for targeting and local drug delivery. *Expert Opin Drug Deliv* **6**: 1207-1217.
Matsusaki M, Kadowaki K, Nakahara Y, Akashi M. 2007. Fabrication of Cellular Multilayers with Nanometer-Sized Extracellular Matrix Films. *Angew Chem Int Ed* **46**: 4689-4692.
Mauro A. 1961. Satellite cell of skeletal muscle fibers. *J Biophys Biochem Cytol* **9**: 493-495.
Mayer H, Scutt AM, Ankenbauer T. 1996. Subtle differences in the mitogenic effects of recombinant human bone morphogenetic proteins -2 to -7 on DNA synthesis on primary bone-forming cells and identification of BMP-2/4 receptor. *Calcif Tissue Int* **58**: 249-255.
Mayer U. 2003. Integrins: redundant or important players in skeletal muscle? *J Biol Chem* **278**: 14587-14590.
McBeath R, Pirone DM, Nelson CM, Bhadriraju K, Chen CS. 2004. Cell shape, cytoskeletal tension, and RhoA regulate stem cell lineage commitment. *Dev Cell* **6**: 483-495.
Meredith SC. 2005. Protein denaturation and aggregation: Cellular responses to denatured and aggregated proteins. *Ann N Y Acad Sci* **1066**: 181-221.
Mikhail AS, Ranger JJ, Liu L, Longenecker R, Thompson DB, Sheardown HD, Brook MA. 2010. Rapid and efficient assembly of functional silicone surfaces protected by PEG: cell adhesion to peptide-modified PDMS. *J Biomater Sci Polym Ed* **21**: 821-842.

Miner JH, Yurchenco PD. 2004. Laminin functions in tissue morphogenesis. *Annu Rev Cell Dev Biol* **20**: 255-284.

Miyagoe Y, Hanaoka K, Nonaka I, Hayasaka M, Nabeshima Y, Arahata K, Nabeshima Y, Takeda S. 1997. Laminin alpha2 chain-null mutant mice by targeted disruption of the Lama2 gene: a new model of merosin (laminin 2)-deficient congenital muscular dystrophy. *FEBS Lett* **415**: 33-39.

Monge C, Ren K, Berton K, Guillot R, Peyrade D, Picart C. 2012. Engineering Muscle Tissues on Microstructured Polyelectrolyte Multilayer Films. *Tissue Eng* **18**: 1664-1676.

Monge C, Saha N, Boudou T, Pózos-Vásquez C, Dulong V, Glinel K, Picart C. 2013. Rigidity-Patterned Polyelectrolyte Films to Control Myoblast Cell Adhesion and Spatial Organization. *Adv Funct Mater* **23**: 3432-3442.

Moon JJ, Saik JE, Poche RA, Leslie-Barbick JE, Lee SH, Smith AA, Dickinson ME, West JL. 2010. Biomimetic hydrogels with pro-angiogenic properties. *Biomaterials* **31**: 3840-3847.

Moore NM, Lin NJ, Gallant ND, Becker ML. 2011. Synergistic enhancement of human bone marrow stromal cell proliferation and osteogenic differentiation on BMP-2-derived and RGD peptide concentration gradients. *Acta Biomater* **7**: 2091-2100.

Morgan MR, Humphries MJ, Bass MD. 2007. Synergistic control of cell adhesion by integrins and syndecans. *Nat Rev Mol Cell Biol* **8**: 957-969.

Mueller TD, Nickel J. 2012. Promiscuity and specificity in BMP receptor activation. *FEBS Lett* **586**: 1846-1859.

Munoz J, Zhou Y, Jarrett HW. 2010. LG4-5 domains of laminin-211 binds alpha-dystroglycan to allow myotube attachment and prevent anoikis. *J Cell Physiol* **222**: 111-119.

Muntoni F, Torelli S, Wells DJ, Brown SC. 2011. Muscular dystrophies due to glycosylation defects: diagnosis and therapeutic strategies. *Curr Opin Neurol* **24**: 437-442.

Narici MV, de Boer MD. 2011. Disuse of the musculo-skeletal system in space and on earth. *Eur J Appl Physiol* **111**: 403-420.

Nemir S, West JL. 2010. Synthetic materials in the study of cell response to substrate rigidity. *Ann Biomed Eng* **38**: 2-20.

Newham P, Humphries MJ. 1996. Integrin adhesion receptors: structure, function and implications for biomedicine. *Mol Med Today* **2**: 304-313.

Nguyen NM, Senior RM. 2006. Laminin isoforms and lung development: All isoforms are not equal. *Dev Biol* **294**: 271-279.

Nikkhah M, Edalat F, Manoucheri S, Khademhosseini A. 2012. Engineering microscale topographies to control the cell-substrate interface. *Biomaterials* **33**: 5230-5246.

Nishiguchi A, Yoshida H, Matsusaki M, Akashi M. 2011. Rapid construction of three-dimensional multilayered tissues with endothelial tube networks by the cell-accumulation technique. *Adv Mater* **23**: 3506-3510.

Nomizu M, Song SY, Kuratomi Y, Tanaka M, Kim WH, Kleinman HK, Yamada Y. 1996. Active peptides from the carboxyl-terminal globular domain of laminin alpha2 and Drosophila alpha chains. *FEBS Lett* **396**: 37-42.

Olugebefola SC, Ryu SW, Nolte AJ, Rubner MF, Mayes AM. 2006. Photo-cross-linkable polyelectrolyte multilayers for 2-D and 3-D patterning. *Langmuir* **22**: 5958-5962.

Ono Y, Calhabeu F, Morgan JE, Katagiri T, Amthor H, Zammit PS. 2011. BMP signalling permits population expansion by preventing premature myogenic differentiation in muscle satellite cells. *Cell Death Differ* 18(2): 222–234.

Ono SS, Decher G. 2006. Preparation of ultrathin self-standing polyelectrolyte multilayer membranes at physiological conditions using pH-responsive film segments as sacrificial layers. *Nano Lett* **6**: 592-598.

Palamà IE, D'Amone S, Coluccia AML, Gigli G. 2013. Micropatterned polyelectrolyte nanofilms promote alignment and myogenic differentiation of C2C12 cells in standard growth media. *Biotechnol Bioeng* **110**: 586-596.

Pelham RJ, Jr., Wang Y. 1997. Cell locomotion and focal adhesions are regulated by substrate flexibility. *Proc Natl Acad Sci U S A* **94**: 13661-13665.
Peng R, Yao X, Ding J. 2011. Effect of cell anisotropy on differentiation of stem cells on micropatterned surfaces through the controlled single cell adhesion. *Biomaterials* **32**: 8048-8057.
Pennakalathil J, Hong JD. 2011. Self-standing polyelectrolyte multilayer films based on light-triggered disassembly of a sacrificial layer. *ACS Nano* **5**: 9232-9237.
Perkins AD, Ellis SJ, Asghari P, Shamsian A, Moore ED, Tanentzapf G. 2010. Integrin-mediated adhesion maintains sarcomeric integrity. *Dev Biol* **338**: 15-27.
Peterson ET, Papautsky I. 2006. Microtextured polydimethylsiloxane substrates for culturing mesenchymal stem cells. *Methods Mol Biol* **321**: 179-197.
Petrie TA, Raynor JE, Reyes CD, Burns KL, Collard DM, Garcia AJ. 2008. The effect of integrin-specific bioactive coatings on tissue healing and implant osseointegration. *Biomaterials* **29**: 2849-2857.
Peyton SR, Raub CB, Keschrumrus VP, Putnam AJ. 2006. The use of poly(ethylene glycol) hydrogels to investigate the impact of ECM chemistry and mechanics on smooth muscle cells. *Biomaterials* **27**: 4881-4893.
Phimphilai M, Zhao Z, Boules H, Roca H, Franceschi RT. 2006. BMP signaling is required for RUNX2-dependent induction of the osteoblast phenotype. *J Bone Miner Res* **21**: 637-646.
Picart C, Elkaim R, Richert L, Audoin F, Arntz Y, Da Silva Cardoso M, Schaaf P, Voegel JC, Frisch B. 2005. Primary Cell Adhesion on RGD-Functionalized and Covalently Crosslinked Thin Polyelectrolyte Multilayer Films. *Adv Funct Mater* **15**: 83-94.
Pitaval A, Tseng Q, Bornens M, Thery M. 2010. Cell shape and contractility regulate ciliogenesis in cell cycle-arrested cells. *J Cell Biol* **191**: 303-312.
Pozos Vazquez C, Boudou T, Dulong V, Nicolas C, Picart C, Glinel K. 2009. Variation of polyelectrolyte film stiffness by photo-cross-linking: A new way to control cell adhesion. *Langmuir* **25**: 3556-3563.
Raeber GP, Lutolf MP, Hubbell JA. 2007. Mechanisms of 3-D migration and matrix remodeling of fibroblasts within artificial ECMs. *Acta Biomater* **3**: 615-629.
Rambaran RN, Serpell LC. 2008. Amyloid fibrils: abnormal protein assembly. *Prion* **2**: 112-117.
Ranella A, Barberoglou M, Bakogianni S, Fotakis C, Stratakis E. 2010. Tuning cell adhesion by controlling the roughness and wettability of 3D micro/nano silicon structures. *Acta Biomater* **6**: 2711-2720.
Ranga A, Lutolf MP. 2012. High-throughput approaches for the analysis of extrinsic regulators of stem cell fate. *Curr Opin Cell Biol* **24**: 236-244.
Ranucci CS, Moghe PV. 2001. Substrate microtopography can enhance cell adhesive and migratory responsiveness to matrix ligand density. *J Biomed Mater Res* **54**: 149-161.
Rapier R, Huq J, Vishnubhotla R, Bulic M, Perrault CM, Metlushko V, Cho M, Tay RT, Glover SC. 2010. The extracellular matrix microtopography drives critical changes in cellular motility and Rho A activity in colon cancer cells. *Cancer Cell Int* **10**: 24.
Reilly GC, Engler AJ. 2010. Intrinsic extracellular matrix properties regulate stem cell differentiation. *J Biomech* **43**: 55-62.
Ren K, Crouzier T, Roy C, Picart C. 2008. Polyelectrolyte multilayer films of controlled stiffness modulate myoblast cells differentiation. *Adv Funct Mater* **18**: 1378-1389.
Ren K, Fourel L, Rouviere CG, Albiges-Rizo C, Picart C. 2010. Manipulation of the adhesive behaviour of skeletal muscle cells on soft and stiff polyelectrolyte multilayers. *Acta Biomater* **6**: 4238-4248.
Reyes CD, Petrie TA, Burns KL, Schwartz Z, Garcia AJ. 2007. Biomolecular surface coating to enhance orthopaedic tissue healing and integration. *Biomaterials* **28**: 3228-3235.
Rezania A, Healy KE. 1999. Biomimetic peptide surfaces that regulate adhesion, spreading, cytoskeletal organization, and mineralization of the matrix deposited by osteoblast-like cells. *Biothechnol Progr* **15**: 19-32.

Ricard-Blum S. 2011. The collagen family. *Cold Spring Harb Perspect Biol* **3**: a004978.
Richert L, Boulmedais F, Lavalle P, Mutterer J, Ferreux E, Decher G, Schaaf P, Voegel J-C, Picart C. 2004. Improvement of stability and cell adhesion properties of polyelectrolyte multilayer films by chemical cross-linking. *Biomacromolecules* **5**: 284-294.
Ricotti L, Taccola S, Bernardeschi I, Pensabene V, Dario P, Menciassi A. 2011. Quantification of growth and differentiation of C2C12 skeletal muscle cells on PSS-PAH-based polyelectrolyte layer-by-layer nanofilms. *Biomed Mater* **6**: 031001.
Rooney JE, Gurpur PB, Burkin DJ. 2009a. Laminin-111 protein therapy prevents muscle disease in the mdx mouse model for Duchenne muscular dystrophy. *Proc Natl Acad Sci U S A* **106**: 7991-7996.
Rooney JE, Gurpur PB, Yablonka-Reuveni Z, Burkin DJ. 2009b. Laminin-111 restores regenerative capacity in a mouse model for alpha7 integrin congenital myopathy. *Am J Pathol* **174**: 256-264.
Rossi CA, Pozzobon M, De Coppi P. 2010. Advances in musculoskeletal tissue engineering: moving towards therapy. *Organogenesis* **6**: 167-172.
Rowley JA, Mooney DJ. 2002. Alginate type and RGD density control myoblast phenotype. *J Biomed Mater Res* **60**: 217-223.
Rozario T, DeSimone DW. 2010. The extracellular matrix in development and morphogenesis: a dynamic view. *Dev Biol* **341**: 126-140.
Ruoslahti E. 1988a. Fibronectin and its receptors. *Annu Rev Biochem* **57**: 375-413.
-. 1988b. Structure and biology of proteoglycans. *Annu Rev Cell Biol* **4**: 229-255.
Ruoslahti E. 1996. RGD and other recognition sequences for integrins. *Annu Rev Cell Dev Biol* **12**: 697-715.
Ruoslahti E, Pierschbacher MD. 1987. New perspectives in cell adhesion: RGD and integrins. *Science* **238**: 491-497.
Saito A, Suzuki Y, Ogata S, Ohtsuki C, Tanihara M. 2003. Activation of osteo-progenitor cells by a novel synthetic peptide derived from the bone morphogenetic protein-2 knuckle epitope. *Biochim Biophys Acta* **1651**: 60-67.
Saito A, Suzuki Y, Ogata S, Ohtsuki C, Tanihara M. 2005. Accelerated bone repair with the use of a synthetic BMP-2-derived peptide and bone-marrow stromal cells. *J Biomed Mater Res A* **72**: 77-82.
Sanes JR. 2003. The basement membrane/basal lamina of skeletal muscle. *J Biol Chem* **278**: 12601-12604.
Sasagawa T, Shimizu T, Sekiya S, Haraguchi Y, Yamato M, Sawa Y, Okano T. 2010. Design of prevascularized three-dimensional cell-dense tissues using a cell sheet stacking manipulation technology. *Biomaterials* **31**: 1646-1654.
Scadden DT. 2006. The stem-cell niche as an entity of action. *Nature* **441**: 1075-1079.
Schaaf P, Voegel JC, Jierry L, Boulmedais F. 2012. Spray-assisted polyelectrolyte multilayer buildup: from step-by-step to single-step polyelectrolyte film constructions. *Adv Mater* **24**: 1001-1016.
Schaller MD. 2010. Cellular functions of FAK kinases: insight into molecular mechanisms and novel functions. *J Cell Sci* **123**: 1007-1013.
Schindeler A, Liu R, Little DG. 2009. The contribution of different cell lineages to bone repair: exploring a role for muscle stem cells. *Differentiation* **77**: 12-18.
Schneider A, Bolcato-Bellemin AL, Francius G, Jedrzejwska J, Schaaf P, Voegel JC, Frisch B, Picart C. 2006a. Glycated polyelectrolyte multilayer films: differential adhesion of primary versus tumor cells. *Biomacromolecules* **7**: 2882-2889.
Schneider A, Francius G, Obeid R, Schwinté P, Hemmerlé J, Frisch B, Schaaf P, Voegel J-C, Senger B, Picart C. 2005. Polyelectrolyte Multilayers with a Tunable Young's Modulus: Influence of Film Stiffness on Cell Adhesion. *Langmuir* **22**: 1193-1200.
Schofield R. 1978. The relationship between the spleen colony-forming cell and the haemopoietic stem cell. *Blood Cells* **4**: 7-25.

Schvartzman M, Palma M, Sable J, Abramson J, Hu X, Sheetz MP, Wind SJ. 2011. Nanolithographic control of the spatial organization of cellular adhesion receptors at the single-molecule level. *Nano Lett* **11**: 1306-1312.

Serena E, Zatti S, Reghelin E, Pasut A, Cimetta E, Elvassore N. 2010. Soft substrates drive optimal differentiation of human healthy and dystrophic myotubes. *Integr Biol* **2**: 193-201.

Shah NJ, Macdonald ML, Beben YM, Padera RF, Samuel RE, Hammond PT. 2011. Tunable dual growth factor delivery from polyelectrolyte multilayer films. *Biomaterials* **32**: 6183-6193.

Shah R, Sinanan AC, Knowles JC, Hunt NP, Lewis MP. 2005. Craniofacial muscle engineering using a 3-dimensional phosphate glass fibre construct. *Biomaterials* **26**: 1497-1505.

Shiratori SS, Rubner MF. 2000. pH-dependent thickness behavior of sequentially adsorbed layers of weak polyelectrolytes. *Macromolecules* **33**: 4213-4219.

Shore EM, Kaplan FS. 2010. Inherited human diseases of heterotopic bone formation. *Nat Rev Rheumatol* **6**: 518-527.

Silva-Barbosa SD, Butler-Browne GS, de Mello W, Riederer I, Di Santo JP, Savino W, Mouly V. 2008. Human Myoblast Engraftment Is Improved in Laminin-Enriched Microenvironment. *Transplantation* **85**: 566-575 510.1097/TP.1090b1013e31815fee31850.

Smith-Petersen MN. 1948. Evolution of mould arthroplasty of the hip joint. *J Bone Joint Surg Br* **30B**: 59-75.

Srivastava S, Kotov NA. 2008. Composite Layer-by-Layer (LBL) assembly with inorganic nanoparticles and nanowires. *Acc Chem Res* **41**: 1831-1841.

Stedman HH, Sweeney HL, Shrager JB, Maguire HC, Panettieri RA, Petrof B, Narusawa M, Leferovich JM, Sladky JT, Kelly AM. 1991. The mdx mouse diaphragm reproduces the degenerative changes of Duchenne muscular dystrophy. *Nature* **352**: 536-539.

Stern-Straeter J, Riedel F, Bran G, Hormann K, Goessler UR. 2007. Advances in skeletal muscle tissue engineering. *In Vivo* **21**: 435-444.

Stevens MM, George JH. 2005. Exploring and engineering the cell surface interface. *Science* **310**: 1135-1138.

Sun J, Graeter SV, Yu L, Duan S, Spatz JP, Ding J. 2008. Technique of surface modification of a cell-adhesion-resistant hydrogel by a cell-adhesion-available inorganic microarray. *Biomacromolecules* **9**: 2569-2572.

Suzuki N, Hozumi K, Urushibata S, Yoshimura T, Kikkawa Y, Gumerson JD, Michele DE, Hoffman MP, Yamada Y, Nomizu M. 2010. Identification of alpha-dystroglycan binding sequences in the laminin alpha2 chain LG4-5 module. *Matrix Biol* **29**: 143-151.

Suzuki N, Ichikawa N, Kasai S, Yamada M, Nishi N, Morioka H, Yamashita H, Kitagawa Y, Utani A, Hoffman MP et al. 2003a. Syndecan binding sites in the laminin alpha1 chain G domain. *Biochemistry* **42**: 12625-12633.

Suzuki N, Nakatsuka H, Mochizuki M, Nishi N, Kadoya Y, Utani A, Oishi S, Fujii N, Kleinman HK, Nomizu M. 2003b. Biological activities of homologous loop regions in the laminin alpha chain G domains. *J Biol Chem* **278**: 45697-45705.

Suzuki N, Yokoyama F, Nomizu M. 2005. Functional sites in the laminin alpha chains. *Connect Tissue Res* **46**: 142-152.

Takahashi H, Shimizu T, Nakayama M, Yamato M, Okano T. 2013. The use of anisotropic cell sheets to control orientation during the self-organization of 3D muscle tissue. *Biomaterials* **34**: 7372-7380.

Teboul L, Gaillard D, Staccini L, Inadera H, Amri EZ, Grimaldi PA. 1995. Thiazolidinediones and fatty acids convert myogenic cells into adipose-like cells. *J Biol Chem* **270**: 28183-28187.

Teixeira AI, Abrams GA, Bertics PJ, Murphy CJ, Nealey PF. 2003. Epithelial contact guidance on well-defined micro- and nanostructured substrates. *J Cell Sci* **116**: 1881-1892.

Thery M, Bornens M. 2006. Cell shape and cell division. *Curr Opin Cell Biol* **18**: 648-657.

Thery M, Racine V, Piel M, Pepin A, Dimitrov A, Chen Y, Sibarita JB, Bornens M. 2006. Anisotropy of cell adhesive microenvironment governs cell internal organization and orientation of polarity. *Proc Natl Acad Sci U S A* **103**: 19771-19776.

Thorsteinsdottir S, Deries M, Cachaco AS, Bajanca F. 2011. The extracellular matrix dimension of skeletal muscle development. *Dev Biol* **354**: 191-207.

Tighe BJ. 2013. A decade of silicone hydrogel development: surface properties, mechanical properties, and ocular compatibility. *Eye Contact Lens* **39**: 4-12.

Trappmann B, Gautrot JE, Connelly JT, Strange DG, Li Y, Oyen ML, Cohen Stuart MA, Boehm H, Li B, Vogel V et al. 2012. Extracellular-matrix tethering regulates stem-cell fate. *Nat Mater* **11**: 642-649.

Trotter JA, Purslow PP. 1992. Functional morphology of the endomysium in series fibered muscles. *J Morphol* **212**: 109-122.

Tryoen-Toth P, Vautier D, Haikel Y, Voegel JC, Schaaf P, Chluba J, Ogier J. 2002. Viability, adhesion, and bone phenotype of osteoblast-like cells on polyelectrolyte multilayer films. *J Biomed Mater Res* **60**: 657-667.

Tsai MT, Lin DJ, Huang S, Lin HT, Chang WH. 2012. Osteogenic differentiation is synergistically influenced by osteoinductive treatment and direct cell-cell contact between murine osteoblasts and mesenchymal stem cells. *Int Orthop* **36**: 199-205.

Tsai WB, Chen RP, Wei KL, Chen YR, Liao TY, Liu HL, Lai JY. 2009. Polyelectrolyte multilayer films functionalized with peptides for promoting osteoblast functions. *Acta Biomater* **5**: 11-11.

Urushibata S, Hozumi K, Ishikawa M, Katagiri F, Kikkawa Y, Nomizu M. 2010. Identification of biologically active sequences in the laminin alpha2 chain G domain. *Arch Biochem Biophys* **497**: 43-54.

Vandenburgh H, Shansky J, Benesch-Lee F, Barbata V, Reid J, Thorrez L, Valentini R, Crawford G. 2008. Drug-screening platform based on the contractility of tissue-engineered muscle. *Muscle Nerve* **37**: 438-447.

Velleman SG, Coy CS, McFarland DC. 2007. Effect of syndecan-1, syndecan-4, and glypican-1 on turkey muscle satellite cell proliferation, differentiation, and responsiveness to fibroblast growth factor 2. *Poult Sci* **86**: 1406-1413.

Velleman SG, Liu X, Coy CS, McFarland DC. 2004. Effects of syndecan-1 and glypican on muscle cell proliferation and differentiation: implications for possible functions during myogenesis. *Poult Sci* **83**: 1020-1027.

Visser R, Arrabal PM, Santos-Ruiz L, Fernandez-Barranco R, Becerra J, Cifuentes M. 2013. A Collagen-Targeted Biomimetic RGD Peptide to Promote Osteogenesis. *Tissue Eng Part A*.

Voinova MV, Rodahl M, Jonson M, Kasemo B. 1999. Viscoelastic Acoustic Response of Layered Polymer Films at Fluid-Solid Interfaces: Continuum Mechanics Approach. *Phys Scr* **59**, 391.

Vuoriluoto K, Jokinen J, Kallio K, Salmivirta M, Heino J, Ivaska J. 2008. Syndecan-1 supports integrin alpha2beta1-mediated adhesion to collagen. *Exp Cell Res* **314**: 3369-3381.

Wada MR, Inagawa-Ogashiwa M, Shimizu S, Yasumoto S, Hashimoto N. 2002. Generation of different fates from multipotent muscle stem cells. *Development* **129**: 2987-2995.

Wang D, Christensen K, Chawla K, Xiao G, Krebsbach PH, Franceschi RT. 1999. Isolation and characterization of MC3T3-E1 preosteoblast subclones with distinct in vitro and in vivo differentiation/mineralization potential. *J Bone Miner Res* **14**: 893-903.

Wang PY, Thissen H, Tsai WB. 2012. The roles of RGD and grooved topography in the adhesion, morphology, and differentiation of C2C12 skeletal myoblasts. *Biotechnol Bioeng* **109**: 2104-2115.

Wang X, Yan C, Ye K, He Y, Li Z, Ding J. 2013. Effect of RGD nanospacing on differentiation of stem cells. *Biomaterials* **34**: 2865-2874.

Weber LM, Hayda KN, Haskins K, Anseth KS. 2007. The effects of cell-matrix interactions on encapsulated beta-cell function within hydrogels functionalized with matrix-derived adhesive peptides. *Biomaterials* **28**: 3004-3011.

Werner S, Huck O, Frisch B, Vautier D, Elkaim R, Voegel JC, Brunel G, Tenenbaum H. 2009. The effect of microstructured surfaces and laminin-derived peptide coatings on soft tissue interactions with titanium dental implants. *Biomaterials* **30**: 2291-2301.

Williamson MR, Adams EF, Coombes AG. 2006. Gravity spun polycaprolactone fibres for soft tissue engineering: interaction with fibroblasts and myoblasts in cell culture. *Biomaterials* **27**: 1019-1026.

Wilson JT, Cui W, Kozlovskaya V, Kharlampieva E, Pan D, Qu Z, Krishnamurthy VR, Mets J, Kumar V, Wen J et al. 2011. Cell Surface Engineering with Polyelectrolyte Multilayer Thin Films. *J Amer Chem Soc* **133**: 7054-7064.

Wipff PJ, Majd H, Acharya C, Buscemi L, Meister JJ, Hinz B. 2009. The covalent attachment of adhesion molecules to silicone membranes for cell stretching applications. *Biomaterials* **30**: 1781-1789.

Wolf K, Friedl P. 2011. Extracellular matrix determinants of proteolytic and non-proteolytic cell migration. *Trends Cell Biol* **21**: 736-744.

Wrana JL, Attisano L, Wieser R, Ventura F, Massague J. 1994. Mechanism of activation of the TGF-beta receptor. *Nature* **370**: 341-347.

Wu YZ, Coyer SR, Ma HW, Garcia AJ. 2010. Poly(dimethylsiloxane) elastomers with tethered peptide ligands for cell adhesion studies. *Acta Biomater* **6**: 2898-2902.

Xiong JP, Stehle T, Zhang R, Joachimiak A, Frech M, Goodman SL, Arnaout MA. 2002. Crystal structure of the extracellular segment of integrin alpha Vbeta3 in complex with an Arg-Gly-Asp ligand. *Science* **296**: 151-155.

Yaffe D, Saxel O. 1977. Serial passaging and differentiation of myogenic cells isolated from dystrophic mouse muscle. *Nature* **270**: 725-727.

Yamada N, Okano T, Sakai H, Karikusa F, Sawasaki Y, Sakurai Y. 1990. Thermo-responsive polymeric surfaces; control of attachment and detachment of cultured cells. *Makromol Chem, Rapid Comm* **11**: 571-576.

Yamaguchi A, Katagiri T, Ikeda T, Wozney JM, Rosen V, Wang EA, Kahn AJ, Suda T, Yoshiki S. 1991. Recombinant human bone morphogenetic protein-2 stimulates osteoblastic maturation and inhibits myogenic differentiation in vitro. *J Cell Biol* **113**: 681-687.

Yamakawa N, Tanaka T, Shigeta M, Hamano M, Usui M. 2003. Surface roughness of intraocular lenses and inflammatory cell adhesion to lens surfaces. *J Cataract Refract Surg* **29**: 367-370.

Yim EK, Darling EM, Kulangara K, Guilak F, Leong KW. 2010. Nanotopography-induced changes in focal adhesions, cytoskeletal organization, and mechanical properties of human mesenchymal stem cells. *Biomaterials* **31**: 1299-1306.

Young JL, Engler AJ. 2011. Hydrogels with time-dependent material properties enhance cardiomyocyte differentiation in vitro. *Biomaterials* **32**: 1002-1009.

Yurchenco PD. 2011. Basement membranes: cell scaffoldings and signaling platforms. *Cold Spring Harb Perspect Biol* **3**.

Zahn R, Thomasson E, Guillaume-Gentil O, Vörös J, Zambelli T. 2012. Ion-induced cell sheet detachment from standard cell culture surfaces coated with polyelectrolytes. *Biomaterials* **33**: 3421-3427.

Zamir E, Geiger B. 2001a. Components of cell-matrix adhesions. *J Cell Sci* **114**: 3577-3579.

-. 2001b. Molecular complexity and dynamics of cell-matrix adhesions. *J Cell Sci* **114**: 3583-3590.

Zammit PS, Partridge TA, Yablonka-Reuveni Z. 2006. The skeletal muscle satellite cell: the stem cell that came in from the cold. *J Histochem Cytochem* **54**: 1177-1191.

Zeisberg M, Kalluri R. 2013. Cellular Mechanisms of Tissue Fibrosis. 1. Common and organ-specific mechanisms associated with tissue fibrosis. *Am J Physiol* **304**: C216-C225.

Zhang J, Senger B, Vautier D, Picart C, Schaaf P, Voegel JC, Lavalle P. 2005. Natural polyelectrolyte films based on layer-by layer deposition of collagen and hyaluronic acid. *Biomaterials* **26**: 3353-3361.

Zhang H, Shih J, Zhu J, Kotov NA. 2012. Layered nanocomposites from gold nanoparticles for neural prosthetic devices. *Nano Lett* **12**: 3391-3398.

Zhao L, Li G, Chan KM, Wang Y, Tang PF. 2009. Comparison of multipotent differentiation potentials of murine primary bone marrow stromal cells and mesenchymal stem cell line C3H10T1/2. *Calcif Tissue Int* **84**: 56-64.

Zouani OF, Chollet C, Guillotin B, Durrieu MC. 2010. Differentiation of pre-osteoblast cells on poly(ethylene terephthalate) grafted with RGD and/or BMPs mimetic peptides. *Biomaterials* **31**: 8245-8253.

Zouani OF, Kalisky J, Ibarboure E, Durrieu MC. 2013. Effect of BMP-2 from matrices of different stiffnesses for the modulation of stem cell fate. *Biomaterials* **34**: 2157-2166.

Annexe I – Review article 1

Published in *Journal of Materials Chemistry*, 2011, **2**1: 4354–14366

A material's point of view on recent developments of polymeric biomaterials : control of mechanical and biochemical properties

Varvara Gribova, Thomas Crouzier and Catherine Picart

LMGP-MINATEC, Grenoble Institute of Technology, 3 parvis Louis Néel, 38016 Grenoble, France

Keywords: polymeric biomaterials, synthetic polymers, biopolymers, substrate stiffness, biochemical functionalization

---

Abstract

Cells respond to a variety of stimuli, including biochemical, topographical and mechanical signals originating from their micro-environment. Cell responses to the mechanical properties of their substrates have since about 14 years been increasingly studied. To this end, several types of materials based on synthetic and natural polymers have been developed. Presentation of biochemical ligands to the cells is also important to provide additional functionalities or more selectivity in the details of cell/material interaction. In this review article, we will emphasize the development of synthetic and natural polymeric materials with well-characterized and tunable mechanical properties. We will also highlight how biochemical signals can be presented to the cells by combining them with these biomaterials. Such developments in materials science are not only important for fundamental biophysical studies on cell/material interactions but also for the design of a new generation of advanced and highly functional biomaterials.

1. Introduction

Our body contains several types of tissues (skin, bone, cartilage…) whose mechanical and biochemical properties depend on their composition. Tissues are composed of cells embedded within an extracellular matrix (ECM) made of proteins, polysaccharides, and other bioactive molecules such as growth factors. The field of tissue engineering, which consists in recreating new tissues by means of a combination of engineering, cell biology and materials, was pioneered about 18 years ago by Langer and colleagues from MIT [1]. A goal of biomaterials scientists is to design biocompatible scaffolds in which cells can adhere, proliferate, differentiate and synthesize their own matrix to regenerate tissue. Molecules promoting cell adhesion have already been included in the design of biomaterials, as it is known that many cells need to adhere for their survival [2].

More recently, other parameters like mechanical properties of biomaterials [3; 4] and delivery of growth factors [5] have also been taken into account. On the other hand, biophysicists have long been studying the process of cell adhesion [6; 7] and the cell's mechanical properties. More recently, cell aggregates and tissues have been studied [8]. To this end, several characterization techniques have been adapted to soft biological materials, including micromanipulation, microrheology [9] and nano-indentations.

How the cells exert forces on to a substrate and how these forces are transmitted at the molecular level inside the cells are key questions, which have been and are still being investigated. Such questions are tackled by a wide range of investigators, from a cell

biology point of view to a mechanical point of view [7; 10].

This has also led to the development of new materials that would, ideally, make possible independent variation in mechanical and biochemical properties. If surface properties of the materials are taken into consideration, they are viewed as 2D materials and cells will interact with them from their basal side. In the case of hydrogel materials, their bulk (volumic) properties are important, as the cells embedded in the hydrogel are fully surrounded by it.

We are now entering a new era where the 3rd dimension is more and more taken into account. In this context, measurements of forces in 3D are starting to be measured. However, it is important to underline that both 2D and 3D studies of cell/material interactions are required, as these studies will provide complementary information.

Although the two scientific communities of biomaterials scientists and biophysicists have different goals and different experimental approaches, they nevertheless share a common interest in designing materials with well-defined mechanical and biochemical properties. For biomaterials scientists, these may serve as new scaffolds to control cell fate and tissue regeneration. For biophysicists, they may be used as toolbox to decorticate and understand the specific effects of different environmental signals on the cell. Until recently, cell biologists commonly used glass substrates or tissue culture polystyrene substrates to investigate cell behavior. Commercial products of model basement membrane-like ECM such as Matrigel are also used and have become popular in cancer cell biology. Matrigel is composed of mainly laminin-111, collagen IV, heparan sulfate proteoglycan, entactin/nidogen, and various growth factors (fibroblast growth factor, transforming growth factor beta, epidermal growth factor, etc.) but is poorly defined. Even though it contains natural biomolecules, it cannot be used to identify the role of specific parameters on cell behavior and to modulate them in a controlled manner.

In this review, we will be writing from a materials point of view. First, we will give an overview of the different types of materials, including synthetic and natural ones, which have been developed for their tunable physical/mechanical and biochemical properties (Table 1).

We will focus on the advances made in the design of 2D and 3D polymeric materials with well-defined mechanical and biochemical properties (Figure 1). We will discuss the range of mechanical properties, depending on type and composition of the material.

We will also present different ways of providing them a biochemical functionality. Two main strategies of functionalization are usually employed: covalent coupling or physical adsorption of the bioactive molecules (entire proteins, fragments or peptides). The coupling strategy is often required for synthetic materials, which do not have any natural interaction with biomolecules. Conversely, natural materials that exhibit low and high affinity interactions with ECM proteins and growth factors, can be favorably exploited to present these stimuli.

The third important aspect concerns spatio-temporal properties of the materials, especially spatial control of stiffness or of ligand presentation. For more information on these aspects, the reader is referred to very interesting recent reviews, which adopt either a “cell point of view” [11] or a “biomaterials point of view” [12].

Finally, the paper will end with some concluding remarks and a short outlook.

2. 2D and 3D materials used for mechano-sensitivity studies

Polymeric materials have been developed both by biophysicists and biomaterial scientists. Controlling and modulating their biochemical and mechanical properties is one of the current challenges, ideally aimed to achieve simultaneous and independent control of each of these properties. First, we should mention that polymeric materials have mechanical properties that are somewhat difficult to compare, due to the various methods used to measure them. Each of these methods, including dynamic shear rheology, dynamic compression for hydrogels and nano-indentations for films, is well-suited to a given type of material.

PROPERTIES	NATURAL	SYNTHETIC
2D 3D	PEM-films Fibrin Collagen Hyaluronan Alginate IPN Composites	PA gels PDMS PEG
Physical/mechanical properties	- Viscoelasticity - Physical architecture - Porosity (nm to µm scale) - Degradability (proteases)	- Pure elasticity - No physical architecture - Small porosity - Non biodegradabile (unless grafted with MMP peptides)
Biochemical properties	- Non specific interactions (electrostatic, H-bonds) - Specific (natural ligands)	- Inertness - Need grafting with ligands
Main disadvantage	- Difficulty to decouple mechanics and chemistry	- High swellability (for PEG) - Stability over time
Main advantage	-Biomimetism (natural presence in tissues)	-Versatility of the control

TABLE 1*. Summary of the main properties of natural and synthetic materials, from 2D to 3D materials, which are used in mechano-sensitivity studies. This includes their physical/mechanical and biochemical properties. Their main disadvantages and advantages are also given.*

The Young's modulus (E_0) is most often measured by traction tests or nano-indentations. The elastic and viscous moduli (G',G") of soft materials are rather measured by oscillatory shear rheology. However, a close look at all values measured for various materials indicates that E_0 or G' lie in the range of a few Pa to hundred MPa, depending on the material (Figure 2A). Indeed, this is in the physiological range of cell and tissue stiffnesses (Figure 2B). It has to be noted that, very often, the strategies employed for modulating mechanical properties also involve changes in the nature or density of the chemical bonds within the materials. Unfortunately, it is simply impossible to fully decouple both. The main strategies for creating ionic or/and covalent crosslinks in polymeric materials are summarized in Figure 3. Incorporation of nano-objects has also been shown to stiffen a polymeric material. However, this method has never been applied in the context of the 2D or 3D materials used for cell mechano-sensitivity studies. Here, we will distinguish between synthetic materials and natural materials, which are made of naturally occurring biomolecules. The main physical/mechanical and biochemical properties, advantages and drawbacks of these two types of materials are summarized in Table 1.

2.1 Synthetic polymeric materials

Synthetic polymers can be tuned in terms of composition, rate of degradation, mechanical and chemical properties. There are four major types of polymers that are used in mechano-sensitivity studies (Figure 2 and Table 1). Three of them are mostly employed as 2D culture substrates, e.g polyacrylamide (PA), polydimethylsiloxane (PDMS) and polyelectrolyte multilayer films made of synthetic polyelectrolytes, whereas the fourth, poly(ethylene glycol) (PEG), is used as a 3D hydrogel with cells embedded in it. We will present below the design strategies for each of these.

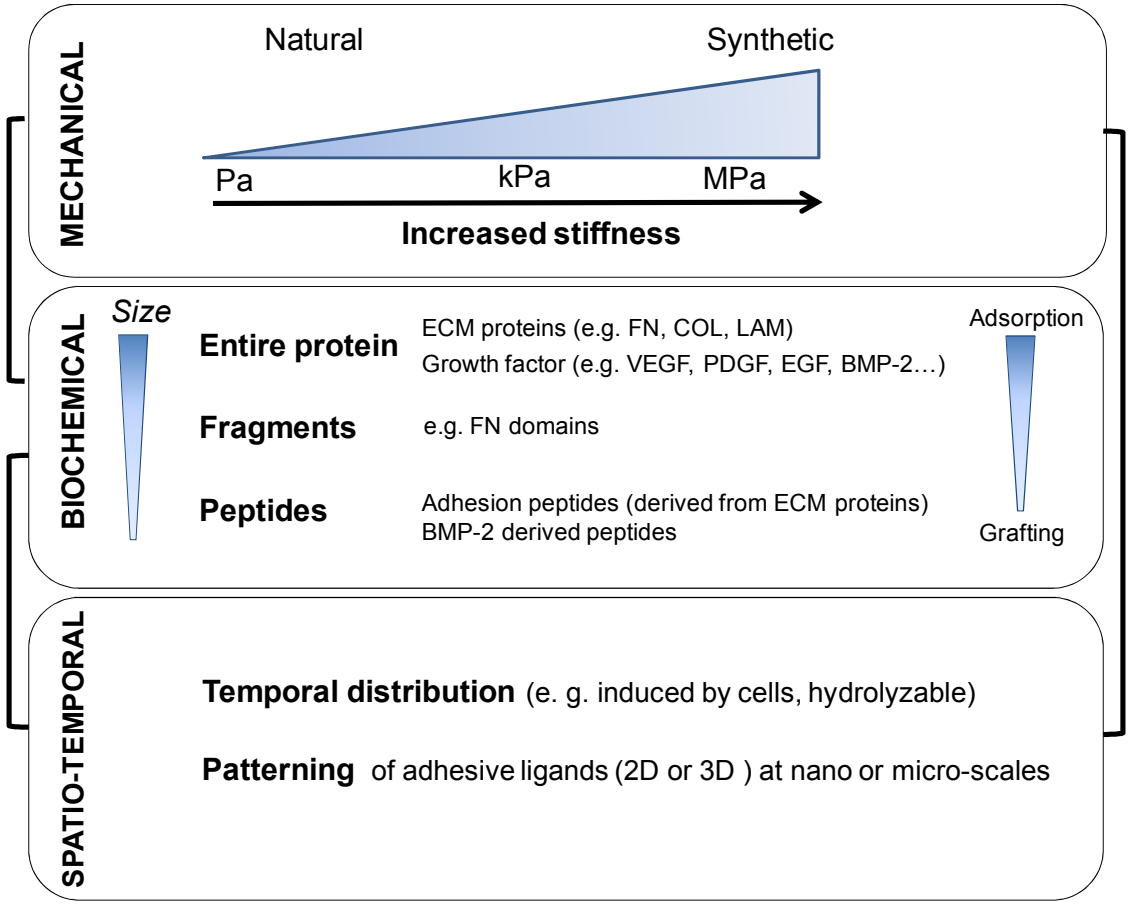

FIGURE 1. *Scheme presenting the possibilities of control of the cell microenvironment using engineered materials : mechanical properties with typical variation in elastic moduli from few Pa to tens of MPa; biochemical properties obtained by adsorbing or grafting entire proteins, protein fragments as well as peptides; spatio-temporal properties, e.g. hydrolytically degradable materials or controlled presentation of ligands by nano and micropatterning.*

2.1.1 Polyacrylamide hydrogels

PA gels, initially used by biologists for protein electrophoresis, have been used for about 14 years for mechano-sensitivity studies [3]. Their stiffness can be adjusted by varying the molar fraction of the bis-acrylamide cross-linker. Cross-linking can be induced by chemicals such as ammonium persulfate to trigger a free radical-dependent polymerization of double bonds (vinyl groups) in the otherwise stable acrylamide and bis-acrylamide monomers. Alternately, cross-linking can be photo-induced (Irgacure is commonly used), leading to E_0 in the range of 10 to 100 kPa. PA hydrogels are relatively simple in their mechanics, and have been extensively characterized by other traditional techniques, including bulk tensile loading, microindentation, and rheology [3; 13]. Classic theory of rubber elasticity would predict that the elastic modulus of a polymer gel scales linearly with cross-linker concentration, which is fairly well validated by experimental measurements [14]. For this reason, PA gels are very popular and have been extensively used to investigate the mechanical effects on cell morphology, adhesion, migration and differentiation in 2D cell cultures. [4; 15; 16]

The chemical inertness of polyacrylamide is one of its greatest advantages and disadvantages. PA doesn't promote any specific cell adhesion when used as a culture substrate, and ligands have to be grafted to control adhesive interactions, which is a clear advantage when demonstrating the mechanical contribution of a given receptor or adhesive protein. Unfortunately, the degree of inertness is also a limitation, as the chemical nature of the PA does not allow easy covalent attachment.

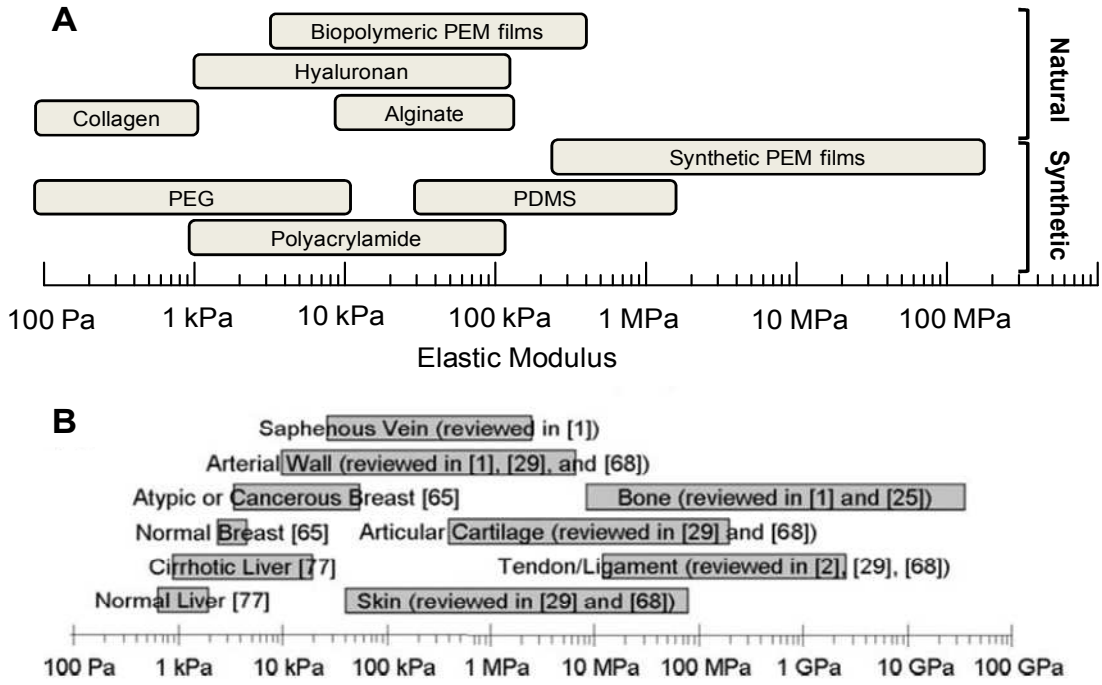

***FIGURE 2**. (A) Range of stiffnesses of the different synthetic and natural materials that are currently employed for mechanosensitivity studies, which are presented in this review. These include both synthetic and natural 2D and 3D materials. (B) Range of stiffnesses found in selected human tissues (from Nemir and West, Annals of Biomed. Eng.(Nemir and West, Ann. Biomed. Eng., 2010)).*

There are additional possibilities offered by PA gels. First, in case of photo-polymerized gels, gradients in mechanical properties can be created by illuminating the gel using photomasks [17].

Second, as cells cannot be entrapped in 3D in PA gels due to the toxicity of acrylamide, a simple approach that involves sandwiching cells between two polyacrylamide hydrogels has been proposed [18; 19]. This method does not fully embed the cells in the environment but it does engage at least part of the dorsal cell receptors, thus mimicking the native 3D environment. Furthermore, it makes it possible to manipulate compliance and measure traction forces. Indeed, microparticles of well-defined sizes can be inserted into PA gels, allowing cell traction forces to be measured, provided that the Young's modulus and the deformation regime of the gels are known [20]. For this reason, PA gels are by far the most commonly used substrate for quantification of traction forces [21].

2.1.2 PDMS

PDMS has arisen from the development of soft lithography. As PDMS is elastically deformable, non toxic and exhibits excellent optical properties, it has become a material of choice to stretch cells in controlled conditions. PDMS is always used as a 2D culture substrate (i.e with cells grown at its surface): this material it too dense for the cells to migrate through in 3D. In addition, it is a non-degradable material and cannot be remodeled by cells. To prepare PDMS, a "base" and a "curing agent", which contains monomers and is also named "cross-linker", are typically mixed in a 10:1 w:w ratio. Thus, to prepare substrates with different elastic moduli, the silicone elastomer base and the cross-linker can be mixed at various ratios, forming gels from 50 kPa to 1.7 MPa [22; 23; 24]. However, PDMS exhibits uncontrolled protein adsorption and can sometimes cause non-specific cell adhesion, depending on its surface properties and cell type. Thus, PDMS surface needs to be chemically modified by various cell adhesion molecules to induce more reproducible adhesion [22; 23]. Various strategies have been developed for this purpose (see paragraph 3.1).

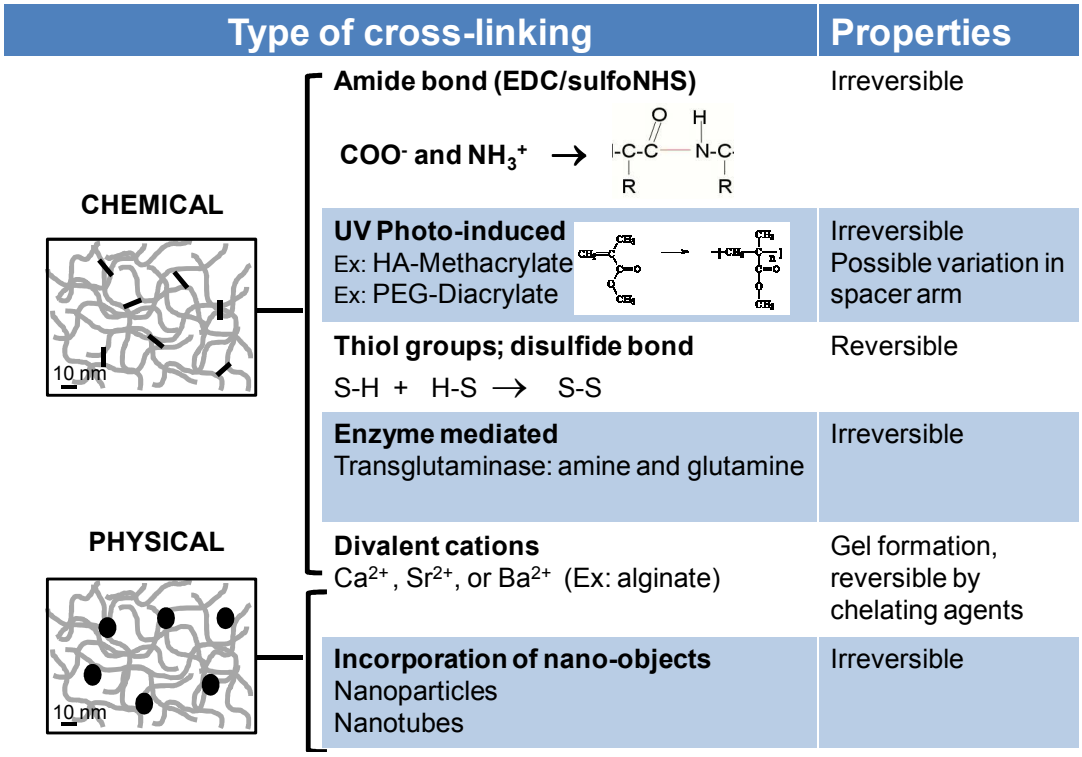

FIGURE 3. *Overview of the main strategies used to modulate mechanical properties of synthetic and natural materials. The methods are essentially based on chemical cross-linking, as physical cross-linking is so far barely employed for biomaterials. We have classified cross-linking by divalent cations at the border between chemical and physical cross-linking, as addition of cations changes the film chemistry but, at the same time, induces a physical gelation (no need for covalent crosslinks).*

2.1.3 Polyelectrolyte multilayer films made of synthetic polymers

Polyelectrolyte multilayer films are a new kind of self-assembled material that emerged almost 20 years ago [25] and has versatile properties depending on the assembly conditions and post-assembly treatments. The thickness of these films can be adjusted in the range of few nm to several µm by varying the deposition conditions (pH, ionic strength and concentration of the polyelectrolytes) and the polyelectrolyte pairs. Using pH-dependent assembly of poly(acrylic acid)/poly(allylamine) (PAA/PAH), Van Vliet *et coll.* evidenced that such films can exhibit elastic moduli E from 200 kPa to 142 MPa (measured by nano-indentation), which is as much as one thousand-fold more compliant than tissue-culture polystyrene. [26]. Extremely stiff films with a high degree of ionic cross-links are obtained at neutral pH whereas soft films are obtained when films are built in acidic pH. [27; 28].

A different strategy was proposed by Senger *et coll.*[29], who prepared a composite film made of a first $(PLL/HA)_{24}$ stratum capped by a second $(PSS/PAH)_n$ stratum (*n* varying between 0 and 12). As the (PSS/PAH) films were much stiffer, the progressive deposition of these layers rendered the composite film stiffer, from roughly 50 to 500 kPa. An apparent elastic modulus was estimated from elasticity measurements by modeling the different strata. These films were recently used to investigate whether substrate elasticity has an effect on nuclear processes such as replication and transcription [30].

2.1.4 PEG-based

To date, there are very few synthetic materials with controlled mechanical properties that can be used for 3D cell studies, because of their high density, low porosity and lack of biodegradability. PEG-based hydrogels with well-controlled molecular properties have been developed for this purpose. These synthetic hydrogels are biologically inert and, as such,

they often require the insertion of adhesion peptides during polymerization [31]. Typically, the hydrogels are formed by Michael-type addition of PEG-diacrylate (PEG-DA) and of thiol-containing peptides on to multiarm PEG-Vinyl sulfone (VS). These gels are very sensitive to their preparation conditions including pH, stoichiometry, precursor concentration, chain length and number of arms of the macromers [31]. PEG gels are known to swell greatly when introduced in solution, with the equilibrium swelling ratio ranging from 10 to 70 and elastic moduli from 0 to 6 kPa as determined by small strain oscillatory shear measurements [31].These parameters were found to be connected by a power law, with more swelling for softer gels. Of note, these gels have a very low viscous component G" and very low porosity (of around 25 nm) as compared to physical hydrogels such as fibrin or collagen [32]. This low porosity renders them resistant to cell migration, as incorporated cells essentially have an isotropic continuum without sensible physical architecture. Subsequent developments of these gels have included the grafting of protease-sensitive peptides (sensitivity to matrix metallo-proteases) with bifunctional groups to be grafted at both of their extremities [33]. Thus, these materials are locally degraded in response to cell-surface proteases, allowing cells to create paths for 3D migration (Figure 4).

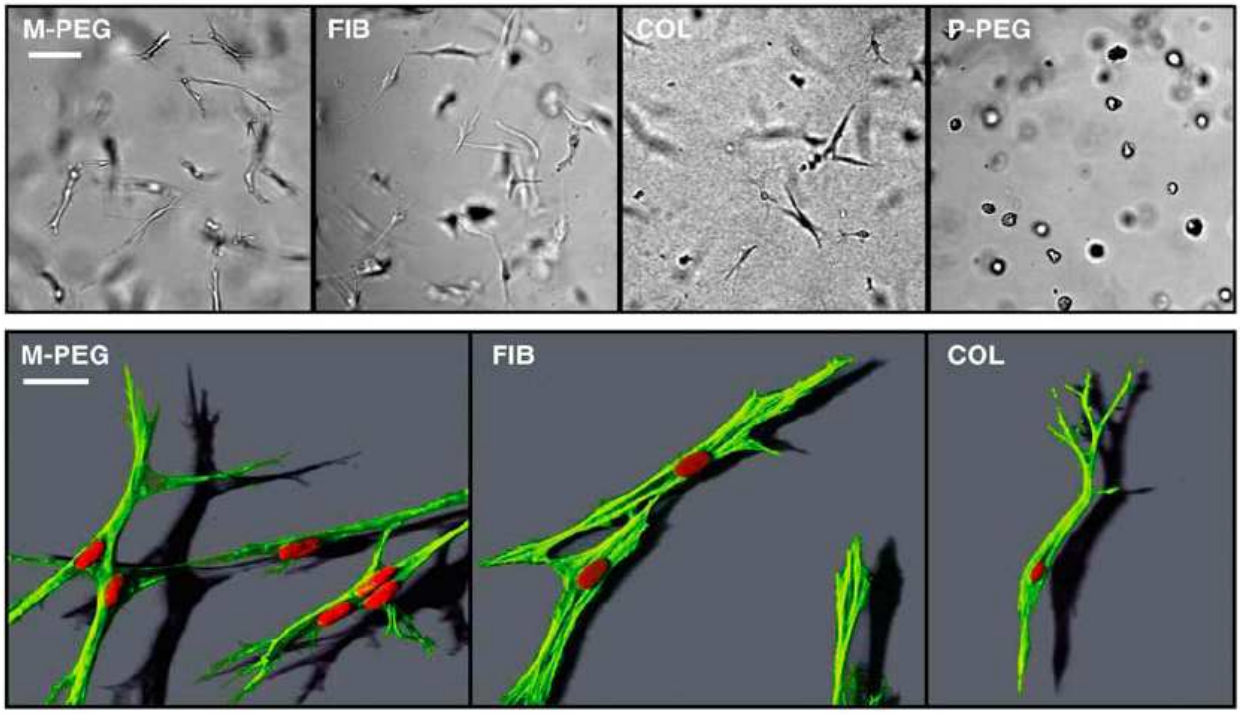

FIGURE 4. *Representative images of human neonatal foreskin fibroblasts (HFFs) cultured within the four materials: two biopolymers, namely collagen I (COL, at 2 mg/mL) and fibrin (FIB, at 2 mg/mL) and PEG hydrogels that possess matrix metalloprotease sequence (MMP-sensitive PEG hydrogels, M-PEG) or plasmin-sensitive PEG hydrogels (P-PEG). Upper row : brightfield images; Lower row : confocal images obtained after staining for F-actin (rhodamine-phalloidin, green) and nuclei (DAPI, red). Scale bars, 100 µm (upper row) and 30 µm (lower row). Of note, the MMP sensitive cross-linker allows HFFs to spread and attain cell shapes in synthetic M-PEG gels (M-PEG) very similarly to HFFs in biopolymers (FIB, COL) (images of the bottom row). In contrast, HFFs are not able to form a spindle-shaped morphology in plasmin-sensitive PEG hydrogels (P-PEG) as seen by the increased compactness and a decrease in projected cell area. (From Hubbell and coll., Biophys J, 2005, copyright Cell Press 2005).*

2.2. Natural materials

Natural biopolymers have the advantage of being components of native ECM matrices, i.e. they provide compositional uniqueness such as stimulating a specific cellular response and serve both as mechanical as well as biochemical signals. Natural materials are also particularly interesting due to their unique structural properties (Table 1). Their nano and microstructure are similar to that of native tissues in terms of functional groups, backbone (presence of neutral and charged groups, chirality) and structural organization (coils, fibers…). Conversely, natural materials have also some drawbacks. They are more fragile, polydisperse, and not always pure. Moreover, their mechanical properties are often difficult to measure mechanically or rheologically as they can exhibit non linear behaviors. In addition, their natural bioactivity makes it fastidious to fully decouple the effect of mechanics from chemistry. The main biopolymers used to study the effect of substrate stiffness on cell behavior are collagen, alginate, fibrin, and agarose (Figure 2 and Table 1). 2D PEM coatings made by self-assembly of polypeptides and polysaccharides are emerging as a new class of materials with well-defined properties. The methods employed to cross-link natural materials are similar to those employed for synthetic materials. They are summarized in Figure 3.

2.2.1 Collagen

Type I collagen is a major protein component of fibrous connective tissues, which provides mechanical support and frameworks for the other tissues in the body. Collagen is a natural ligand for several integrin receptors. Collagen gels exhibiting different mechanical properties can be prepared by varying the pH during hydrogel formation [34] or by varying its concentration [35]. Thus, porosity as well as density of ligands, which are changed simultaneously, are coupled to the material's mechanical properties. Elastic modulus G' of such gels can vary between 5 and 1000 Pa as measured by oscillation rheometry. Collagen gels can be prepared as 2D culture surfaces or 3D matrices [35]. They exhibit a rather organized physical architecture characterized by the presence of fibers.

Grinnel *et al*. recently investigated the effect of 2D and 3D collagen matrices on cell adhesion and migration. They quantified the effects of matrix stiffness and porosity on collagen translocation, fibroblast cell spreading and cell migration for collagen gels with average pore diameter varying from 1.1 to 2.2 μm. Drying collagen fibrils appears to have an impact on cell spreading and proliferation. Plant *et al*. [36] showed that thin films of collagen fibrils can be dehydrated, and when seeded on these dehydrated fibrils, smooth muscle cells spread and proliferate extensively. Indeed, the dehydrated collagen gels were found to be mechanically stiffer than their hydrated counterparts. Tanishita *et al*. found that *in vitro* formation of microvessel networks by endothelial cells was also affected by the mechanical properties of collagen gels [34].

Microbial transglutaminase, an enzyme that catalyzes the formation of a covalent bond between a free amine group (e.g., protein- or peptide-bound lysine) and the gamma-carboxamid group of protein- or peptide-bound glutamine, can also be employed to covalently crosslink collagen I [37]. This resulted in a 6-fold increase in G" (1.3 kPa versus 210 Pa). In terms of cell behavior, these authors showed a significant reduction in the level of cell-mediated contraction of scaffolds with increased concentrations of enzymes.

2.2.2 Alginate

Alginate is a linear polysaccharide of (1-4)-linked β-mannuronic acid and α-guluronic acid monomers, which forms a gel in the presence of certain divalent cations (calcium, strontium, or barium) (Figure 3) [38]. The block structure of alginate dictates the structure of ionic cross-links, and covalent cross-links can also be formed [39; 40; 41]. Due to their biocompatibility, alginate gels have long been used for biomedical purposes, particularly in the manufacture of surgical dressings for exuding wounds. More recently, they were employed as scaffolds for the immunoprotection of transplanted cells. Elastic modulus and toughness can be modulated from 2 to 70 kPa by controlling the parameters for gel cross-

linking. However, alginate needs to be chemically modified to interact specifically with mammalian cells, which is usually achieved by grafting RGD (arginine-glycine-aspartic acid)-containing cell adhesion ligands [42]. In this context, alginate gels were used to investigate the substrate mechanics effect on chondrocyte adhesion [43]. Very recently, the same group demonstrated that the commitment of mesenchymal stem cell populations changes in response to the rigidity of 3D alginate gels, with osteogenesis occurring predominantly at 11-30 kPa [44]. Matrix stiffness was found to regulate integrin binding as well as reorganization of adhesion ligands at the nanoscale. Both were traction-dependent and correlated with osteogenic commitment of mesenchymal stem cell populations.

2.2.3 Hyaluronan and other biopolymers

Hyaluronan (HA) is a non-sulfated glycosaminoglycan (GAG) that is present in different types of tissues and fluids, including synovial fluid, cartilage, tendon and skin. It plays a role in tissue viscoelasticity and hydration, due to its ability to interact with water molecules and to establish multiple hydrogen bonds. [45]. Hyaluronan is also present in the pericellular coat (also called glycocalyx) of different cell types, chondrocytes being a prominent example with a thick coat of ~5 µm [46]. Despite their biocompatibility, native HA gels have poor mechanical properties. Although HA can be cross-linked using 1-ethyl-3-(3-dimethylamino-propyl) carbo-diimide (EDC) [47] before serving as a soft substrate for cell biology experiments, such hydrogel preparations lack long-term stability and have very low elasticity (3 to 250 Pa). To increase its mechanical properties, the Prestwich group has proposed a method that consists in grafting thiol groups to HA (HA–SH) [48] to form disulfide (S-S) bonds in the presence of an oxidizing agent. Adding PEG-DA to the mixture can provide additional cross-links. AFM nano-indentations have been performed on S-S crosslinked HA gels, and moduli were found in the range of 1 to 100 kPa [14]. One of the drawbacks of such gels is the dissociation of the S-S bond over several days. Another is that PEG-DA addition leads to the formation of hydrolytically degradable esters, which may balance the stiffening effect of the cross-links. Engler *et al*. recently compared the growth of pre-cardiac cells on HA and PA gels of similar stiffness [49]. They showed that pre-cardiac cells grown on collagen-coated HA hydrogels exhibit a 3-fold increase in mature cardiac specific markers and form up to 60% more maturing muscle fibers than they do when grown on compliant PA hydrogels over 2 weeks.

Other biomolecules are being developed to investigate the effects of substrate mechanics. Bellamkonda *et al*. used agarose gels at different concentrations (ranging from 0.75 to 2 % wt/vol) to investigate the rate of neurite extension [50], which was found to be inversely correlated to the mechanical stiffness of the gels. Soichet *et coll.* have developed cross-linkable forms of chitosan by grafting methacrylate groups [51]. These hydrogels have been used for the regeneration of neuronal tissue.

2.2.4 Polyelectrolyte multilayer films made of biopolymers as 2D coatings

As mentioned above, polyelectrolyte multilayer films are a new type of self-assembled coating that has found applications for cell studies in the past 10 years [52]. PEM films made of polysaccharides and polypeptides have been engineered and studied [53; 54]. Their mechanical properties can be modulated by several methods. A now popular method is to covalently cross-link carboxylic with amine groups in the films to form covalent amide bonds. This was first applied to poly(L-lysine)/hyaluronan (PLL/HA) films [55] for a fixed cross-linker concentration and subsequently to the same films on a large range of cross-linker concentration [56]. The apparent Young's modulus of the films, as probed by AFM-nano-indentations, could thus be modulated over a range of a few kPa to ~500 kPa. More recently, this strategy has been applied to several other types of multilayer films to obtain mechanical properties that depend on the type of polyelectrolyte pairs, deposition conditions and cross-linker concentrations [57]. Recent developments include the investigation of the effect of film cross-linking on hepatocyte

adhesion [58], on the differentiation of myoblast cells into myotubes [59] and of selective cross-linking on the outer region of the films. This results in a rigid outer "skin" to promote cell attachment, while leaving the film's interior unaffected [60].

Another strategy relies on the use of a natural cross-linking agent such as genipin [61]. The viscoelastic properties of chitosan/hyaluronan (CHI/HA) and chitosan/alginate (CHI/ALG) multilayer films without cross-linking or after cross-linking with genipin have been investigated using quartz crystal microbalance with dissipation monitoring (QCM-D). (CHI/HA) cross-linked films proved to be highly non-adhesive for pre-osteoblasts and fibroblastic skin cells. Conversely, cross-linking (CHI/ALG) films dramatically improved pre-osteoblast and rat fibroblastic skin cell adhesion, especially for high bi-layer numbers and using high concentrations of cross-linker. Finally, photo-crosslinking can be employed to modulate the Young's modulus of (PLL/HA) films that contain a photosensitive derivative of HA (HA-vinyl benzyl) grafted at various percentages [62].

2.3. Mixtures of synthetic/natural

As both synthetic and natural biomaterials have advantages and drawbacks, efforts have also been made to develop composite biomaterials made of mixtures of synthetic and natural materials. In this respect, Putnam *and coll.* developed PEG-conjugated fibrinogen gels [63], by coupling PEG-DA to full-length fibrinogen. These gels can be additionally cross-linked by exogenous cross-linkable PEG-DA (typical range from 0 to 2 wt%) and make possible the simultaneous manipulation of mechanical properties and adhesion ligand density presented to cells. Their bulk compressive moduli ranged from 450 to 5.2 kPa. [63]. However, their mechanical properties decreased over a seven-day immersion period in phosphate buffered saline, and it was probably due to the combined effects of hydrolysis and proteolysis. Adding soluble factors such as ascorbic acid to the gels was found to stimulate matrix remodeling by modulating smooth muscle cells phenotype (induction of contractility), which led to an increase in elastic modulus [64].

Semi-interpenetrating hydrogels (IPNs) are an emerging class of hydrogels, which make it possible to combine the advantages of each component. For instance, photo-cross-linkable hyaluronic acid (HA) and semi-interpenetrating collagen components were found to exhibit superior mechanical properties [65]. The inclusion of the semi-interpenetrating collagen chains provided a synergistic mechanical improvement over unmodified HA hydrogels. These semi-IPNs supported fibroblast adhesion and proliferation and were shown to be suitable for cell encapsulation at high levels of cell viability. They were also employed to fabricate cell-laden microstructures and microchannels. Another example is that of fibroin/collagen hybrid hydrogels [66], which were prepared by cross-linking a fibroin/collagen solution using the water soluble EDC. G' of these gels varied between 3 and 10 kPa. Some mobility of fibroin molecules inside the gels was noticed. These composite gels allowed vascular smooth muscle cells to grow.

3. Biochemical functionalization

A common approach in the field of biomaterials is to start from a "blank slate" [67], i.e. a substrate or material preventing protein adsorption and cell adhesion, and to add a biochemical functionality to the material in a controlled fashion. As mentioned above, cell attachment on many synthetic polymers is very poor, due to their inertness and lack of specific adhesive motifs. Such a low background attachment has been observed for PA, PDMS and PEG hydrogels. In the case of natural materials, although cells may possess specific receptors recognizing the material, their naturally high hydration, softness and the possible lack of accessibility for functional groups often render them poorly adhesive. Such low cell attachment has been observed for hydrated polysaccharides such as HA and ALG.

Researchers have thus designed strategies for giving additional biochemical functionality to different types of synthetic and natural materials. We will distinguish here between three types of biochemical functionality (Figure 1): i) full length ECM proteins, ii) fragments and peptides derived from these

proteins and iii) growth factors (GF). Among the important biomolecules are ECM proteins like fibronectin, collagen and laminin as well as GAGs. These GAGs are negatively charged polysaccharides that can interact with proteins by non covalent and covalent interactions [68]. In this latter case, they form what is called a proteoglycan. In addition, growth factors are an important class of signaling molecules playing a key role in cellular processes including growth, proliferation, differentiation, adhesion and migration [69].

Biochemical functionality can be provided either by grafting or by physically adsorbing the bioactive molecule. Notably, presentation of a biochemical signal from a biomaterial or a substrate in a "matrix-bound" manner is important for mimicking physiological conditions, as many bioactive molecules are bound to the ECM matrix *in vivo* [70]. Indeed, in the ECM, glycosaminoglycans are found immobilized by ionic or covalent cross-links. We will present below the different strategies (grafting *versus* physical adsorption), how they are achieved and what types of biomolecules have been grafted or adsorbed to date.

3.1. Biochemical functionalization by grafting

The advantage of grafting is that it provides good control of surface composition, a stable link and limits release of the functional group into the culture medium. Covalent grafting of short bioactive peptides or protein fragments is more frequently performed than that of full length ECM proteins, which is more difficult to handle. A key issue is to preserve the bioactivity of the grafted molecules, especially entire proteins, because their activity depends on their 3D conformation. Moreover, using harsh solvents and/or high temperatures often leads to the denaturation of biologically active molecules. Thus, selecting the appropriate conjugation strategy and using spacer arms are essential to retain the bioactivity of grafted molecules and provide them with sufficient flexibility and accessibility by the cell receptors.

3.1.1 Major grafting strategies

Grafting of proteins/peptides can be performed in solution on hydrogel components prior to formation of the 2D or 3D biomaterial or directly at the surface of a biomaterial. This latter strategy can only be performed on 2D biomaterials. As mentioned earlier, a key requirement is to preserve the bioactivity of the biomolecules.

3.1.1.1 Targeting amino and carboxylic groups

Proteins can be coupled to polymers via their amino-groups. To this end, sulfo-SANPAH (sulfosuccinimidyl-6-[40-azido-20-nitrophenylamino]hexanoate) can be employed. It is a hetero-bifunctional cross-linker containing a photosensitive phenyl azide group on one end and an amine-reactive N-hydroxysuccinimide on the other end. Proteins can thus react via their amine group with sulfo-SANPAH, which can itself react with the gel [71] upon exposure to UV light. However, the limited solubility, stability and shelf-life of sulfo-SANPAH have urged researchers to look for alternative grafting strategies. Alternatively, the water soluble carbodiimide coupling chemistry can be employed to create a covalent amide bond, which is formed between activated carboxylic groups and ammonium groups [72]. This is, in principle, straightforward coupling chemistry, but several side reactions are known to complicate the subject. These are especially present when the polymer contains a large amount of water, as in the case of HA [73]. Therefore, sulfo-N-hydroxysulfosuccinimide ester is often employed to catalyze the reaction. This strategy has been applied to alginate gels, which contain carboxylic groups [42] to covalently attach a G4RGDSP oligopeptide so as to promote cell-matrix interactions [74]. It has also been used to graft different proteins or fragments (extracted human fibronectin, collagen I or collagen IV; recombinant fragments of fibronectin and vitronectin) on to polyelectrolylte multilayer films containing hyaluronan [75].

3.1.1.2 Targeting cysteine residues

Thiol groups of proteins or peptides are another target for coupling reactions. Maleimides linked to PEG are often used as flexible linker molecules to attach whole proteins, protein fragments or peptides to

surfaces. The double bond of maleimide readily reacts with the thiol group found on cysteine to form a stable carbon-sulfur bond. Attaching the other end of the polyethylene chain to a bead or solid support, or to a polyelectrolyte [76] allows to separate the protein from other molecules in solution, provided that molecules do not also possess thiol groups.

Acrylate groups are often used in Michael addition, which is a conjugate reaction based on the nucleophilic addition of a carbanion or another nucleophile to an alpha, beta unsaturated carbonyl compound. This is one of the most useful methods for the mild formation of C-C bonds and thus for covalently cross-linking acrylated polymers, usually by light activation. Acrylates are also known to react with thiols of cysteines (on peptides or proteins) under defined experimental conditions. This reaction, which belongs to the thiol-ene family of reactions, involves the addition of an S-H bond across a double or triple bond by either a free radical or ionic mechanism. Thus, acrylates are often employed to graft either peptides or full-length proteins. For example, RGD sequences have been incorporated into PEG hydrogel networks through the acrylation of the peptide sequence at the N-terminus, followed by copolymerization of the acrylated peptides with PEG-DA via photocross-linking in aqueous solution [77; 78; 79]. On similar PEG hydrogels, bis-cysteine peptides that contain an additional acrylate group and that are MMP-sensitive (e.g., Ac-GCRD-GPQGYIWGQ-DRCG) or plasmin sensitive (e.g., Ac-GC-YKYNRD-CG) have been prepared [32]. Burdick *et al*. [80] used an acrylate derivative of HA to graft two peptide components: one to support cell adhesion and the other for proteolytic degradability. Full-length fibrinogen was also coupled to PEG-DA at room temperature but in the presence of a strong denaturating agent (urea) [81].

The potentiality of acrylate to serve for cross-linking polymeric chains but also for peptide coupling has recently been shown for acrylated HA hydrogels. These were subjected to two step experimental protocol: the first step was designed to couple peptides to the acrylate groups and the second to initiate free radical polymerization of the remaining acrylate groups by exposure to UV light [80]. The resulting UV-HA hydrogels were expected to prevent remodeling due to the incorporation of non-degradable covalent cross-links from kinetic chain formation and thus to confine encapsulated cells to a rounded morphology.

3.1.2 Grafting of different types of molecules

As mentioned above, we will distinguish here the three types of molecules - full length ECM proteins, protein fragments or shorter peptides (typically from 4 to 20 amino acids) and GF– that can be grafted. Grafting sequences has great advantages over grafting full length molecules. In entire proteins (ECM proteins or GF), many different active sequences there can be recognized by cell surface receptors. Using a bioactive fragment makes it possible to enhance the specificity of the interaction and to target one particular partner to better control cellular processes. The problem is that such short sequences are usually less bioactive than entire molecules because of the loss of active site spatial architecture owing the protein's specific conformation [82].

3.1.2.1 Peptides

The most common grafted peptides are derived from ECM proteins, mainly fibronectin [83], collagen [84], laminin [85; 86] and vitronectin [87] **(Table 2)**. More recently, peptides that exhibit protease sensitive sequences have been grafted to the biomaterials to add biodegradability in response to cellular activity [88].

The tripeptide sequence RGD is very popular, as it is present in many ECM proteins, including fibronectin, vitronectin, fibrinogen, von Willebrand factor, thrombospondin, laminin, osteopontin, bone sialo protein, and some collagen isoforms [82]. It binds to a wide range of integrin receptors in a non selective manner, i.e. not specific to a given integrin receptor. The literature about the various forms of RGD peptides is rich and the reader is referred to more specialized reviews [89]. To achieve better selectivity and/or target only one type of integrin receptor, several strategies have been investigated: i) synthesis of cyclic peptides [90], or peptide multimerization to enhance avidity with particular cell adhesion receptors [91], ii) using a more selective peptide

sequence that is not based on RGD but contains other key sequences or iii) associating two different bioactive peptides derived from the same ECM protein [92] or from different ones [93] (Table 2). Thus, collagen-mimetic peptides [94; 95], laminin-derived peptides [85; 86; 96] and fibronectin-derived peptides or fragments [83; 92] are increasingly used for their higher selectivity.

Garcia *et al*. [97] engineered polymer brushes of oligo(ethylene glycol) methacrylate on PDMS, which resisted biofouling and prevented cell adhesion. These polymer brushes were functionalized to display bioadhesive peptides, which were either tethered uniformly or constrained to micropatterned domains using standard peptide chemistry approaches. Benoit and Anseth [92] showed that associating an RDG-containing peptide to another fibronectin-derived epitope like PHSRN not only made it possible to enhance the bioactivity of the functionalized surface compared to RGD only, but also to specifically target a particular integrin receptor $\alpha_5\beta_1$. Each domain independently contributed little to binding, but when combined, they synergistically bound to $\alpha_5\beta_1$ to provide stable adhesions [92; 98].

We are now progressively entering a new era, where peptides with higher specificity, high biological activity as well as targeting other receptors than integrins are being designed (Table 2). Indeed, it is now acknowledged that besides integrin receptors, other families of receptors including syndecans[99] and growth factor receptors play key roles in early cellular events. Recent developments also include grafting the peptide sequence of growth factors, mostly bone morphogenetic protein 2 (BMP-2) derived peptides [100; 101].

ECM protein	PEPTIDE SEQUENCE	TARGETED RECEPTOR	CELL TYPE	REFERENCE
COLLAGEN (Type I)	GFOGER	Integrin $\alpha2\beta1$	Primary bone marrow stromal cells	Reyes et al., *Biomaterials* 2007 [94]
	CGPKGDRGDAGPKGA	Integrins $\alpha1\beta1$, $\alpha2\beta1$	Primary human osteoblasts	Picart et al. *Adv. Funct. Mater*. 2005 [76]
	DGEA	Integrin $\alpha2\beta1$	MIN6 b-cells	Weber Biomaterials 2007 [95]
FIBRONECTIN (FN)	rhFN fragment FNIII7-10 (with RGD and PHSRN)	Interin $\alpha5\beta1$	Osteoblasts	Petrie et al., *Biomaterials* 2008 [83]
			hESC, hMSC	Doran et al., *Biomaterials* 2010 [75]
	RGD-PHSRN	Inegrin $\alpha5\beta1$	Osteoblasts	Benoit and Anseth, *Biomaterials* 2005 [90]
LAMININ (LAM)	RKRLQVQLSIRT ($\alpha1$ chain LAM-1, LG4 module)	Syndecans	Human dermal fibroblasts, neural PC12	Hozumi et al, *Biomaterials* 2009 [83]
	ATLQLQEGRLHFXFDLGKGR, X: Nle ($\alpha1$ chain, LG4 module)	Integrin $\alpha2\beta1$		
	PPFLMLLKGSTRFC (LG3 of the lam-5 $\alpha3$ chain)	Integrins $\alpha6\beta4$, $\alpha3\beta1$	Oral keratinocyte cell line, TERT-2 OKF-6	Werner et al., *Biomaterials* 2009 [96]
	IKLLI (LAM $\alpha1$ chain)	Integrin $\alpha3\beta1$	MIN6 b-cells	Weber, *Biomaterials* 2007 [95]
	IKVAV (LAM $\alpha1$ chain)	110 kDa laminin receptor protein		
	YIGSR (LAM $\beta1$ chain)	67 kDa laminin receptor protein		
VITRONECTIN	rhVN, N-terminal Somatomedin B and RGD domain	Plasminogen activator inhibitor-1 (PAI-1), integrin receptors	hESC	Doran et al., *Biomaterials* 2010 [75]
Multiple ECM proteins	RGDSPC	Integrins	MC3T3-E1 preostoblasts	Zouani et al., *Biomaterials* 2010 [100]
			Human foreskin fibroblasts	Lutolf et al., *Nature Biotech*. 2003 [84]
	G4RGDSP	Integrins	Primary human bone marrow stromal cells, MC3T3-E1 preosteoblasts, mouse bone marrow stromal D1 cell line	Hsiong et al. *Tissue Eng*. 2009 [92]
	Cyclic RGD: G4CRGDSPC	Integrin receptors, higher specifity for $\alpha V\beta3$		
	MMP-sensitive peptide: Ac-GCRD-GPQGIWGQ-DRCG-NH2	Matrix metalloproteinases (MMP)	Human foreskin fibroblasts	Lutolf et al. *Nature Biotech* 2003 [84]

***TABLE 2**. Peptide sequences used for targeting adhesion receptors of four main ECM proteins (collagen, fibronectin, laminin and vitronectin) as well as for providing degradability (matrix-metalloprotease sequence). The targeted receptor (or receptor family) as well as cell type used in the study are indicated.*

3.1.2.2 Grafting ECM proteins to synthetic surfaces

Synthetic polymers such as PA and PDMS are often biofunctionalized by grafting proteins. For PA gels, three major methods, which are reviewed in [71], are commonly used. The first relies on carbodiimide coupling of proteins to poly(acrylic acid), which has to be inserted into the PA gel during gel formation. Another method uses molecules that have bi-functionality, one end of the molecules mediating the incorporation into polyacrylamide whereas the other end is reactive toward primary amines. Here again, we find acrylate and N-hydroxysuccinimide in the form of acrylic acid N-hydroxysuccinimide ester (NHS-acrylate), which is incorporated into a one-step polymerization reaction [102] during the acrylamide polymerization reaction. Recent developments include the fabrication of a synthetic interfacial hydrogel culture system, termed variable moduli Interpenetrating Polymer Networks (vmIPNs) [103]. The principle is to build at the first step a polyacrylamide gel by varying the concentration of acrylamide and bisacrylamide monomers to synthesize PA gels from 10 Pa to 10 kPa and of low swelling ratio (~2). Then, the IPN is created by polymerizing a second layer of amino-PEG (4 nm thick) within the top few nanometers of the first acrylamide layer for subsequent grafting of adhesion peptides. Such materials were then used to investigate the adhesion, proliferation and differentiation of adult neural stem-cells. Under mixed differentiation conditions with serum, softer gels were found to favor neurons, whereas harder gels promoted glial cultures.

PDMS, if untreated, exhibits high hydrophobicity and extremely low cell attachment [23]. Different methods have thus been developed to biochemically modify the surface of PDMS for cell adhesion. Recently, Hinz *et al*. systematically compared the immobilization of cell-adhesive molecules to PDMS using electrostatic (simple protein adsorption and layer-by-layer deposition) and covalent surface coating procedures [104]. They developed a functionalization protocol that is based on: (1) PDMS oxidation by oxygen plasma treatment, (2) binding of 3-aminopropyltriethoxysilane (APTES) to the oxidized surface and (3) covalent cross-linking of ECM proteins to the silane using glutaraldehyde. They found that the covalent linkage of adhesive molecules was superior to non-covalent methods in providing a coating that resisted to major deformations and that fully transmitted this stretch to cultured cells.

3.1.2.3 Grafting growth factors

There are only a few examples of covalent immobilization of entire growth factors on materials whose mechanical properties can also be modulated. One of the most studied "tethered" growth factor is epidermal growth factor (EGF) [105]. EGF plays an important physiological role in the maintenance of oro-esophageal and gastric tissue integrity. It was initially tethered to poly(methyl methacrylate)-graft-poly-(ethylene oxide) (PMMA-g-PEO) amphiphilic comb copolymers by activation with 4-nitrophenyl chloroformate (NPC) to target the N-terminal amine of murine EGF [105; 106]. In the latest work by this group [106], a biotinylated recombinant protein containing the 53 amino acid human EGF domain was linked to a biotonylated peptide hydrogel by neutravidin. This EGF-containing recombinant protein also contained a protease-resistant 20 amino acid hydrophilic spacer arm to provide optimal bioactivity. Another strategy consists in synthesizing photoreactive EGF via the reaction of primary amine groups in the growth factor with the N-hydroxysuccinimide functionality of Sulfo-SANPAH [107]. In a subsequent step, EGF is covalently tethered to polystyrene by means of UV irradiation.

Nerve growth factor (NGF) has been grafted to 2-hydroxyethy methacrylate (HEMA) gels using ethylene dimethacrylate as crosslinker, ammonium persulfate as initiatior and tetramethy ethylenediamine (TEMED) as accelerator [108]. By modifying these p(HEMA)-NGF gels with pAA, neuronal PC12 cells adhered and responded to the immobilized NGF by extending neuritis in a manner similar to that which is observed with soluble NGF. PC12 cell neurites were even observed to be thicker when cultured on immobilized NGF than when cultured in the presence of soluble NGF. Very recently, vascular endothelial growth factor (VEGF) has been coupled to a

PEG-hydrogel through photo-polymerization via laser scanning lithography [109]. Endothelial cell cultures in these gels underwent accelerated tubulogenesis forming endothelium tubes that possess lumens only in the presence of tethered VEGF.

3.2. Biochemical functionalization by physical adsorption

The complex environment surrounding the cells *in vivo* is composed of ECM components (fibrillar proteins, proteoglycans, adhesion molecules) and soluble biomacromolecules such as cytokines, growth factors and other signaling molecules. Many of these biomolecules interact by non convalent interactions, including electrostatic, Van der Waals, hydrogen bonds and hydrophobic interactions, but also by ligand/receptor interactions. *In vivo*, these biomolecules are often presented by the ECM proteins or glycosaminoglycans in a "matrix-bound" manner. Thus, biomaterial scientists are also trying to associate different components of the *in vivo* cellular microenvironment to reproduce it in a simple way and to create biologically active materials. Three principal types of molecules or their fragments can be physisorbed on 2D biomaterials or entrapped in 3D biomaterials: ECM polysaccharides (glycosaminoglycans), ECM proteins (fibronectin, collagen, laminins) and growth factors (including EGF, VEGF, BMP-2 and fibroblast growth factor FGF2). In this part, we focus on non covalent interactions between proteins and polymers.

3.2.1 Adsorption of ECM proteins and of glycosaminoglycans

Due to the natural interactions between ECM proteins and natural polyelectrolytes, ECM proteins are often simply adsorbed on PEM films. Several parameters, including the amount of adsorbed protein (often in the range of several ng/cm^2), the strength of the interaction (affinity) as well as protein conformation will depend on the physical and chemical parameters of the multilayer film: type of functional groups (sulfate, carboxylic, ammonium…), pH and ionic strength used during film builduip, and type of ending layer. Fibronectin (FN) is often used as an adhesive protein, due to its interaction with different types of integrin receptors. Wittmer *et al*. [110], investigated the LbL formation of films composed of PLL and dextran sulfate (DS), the adsorption of FN on to these films, and the subsequent spreading behavior of human umbilical vein endothelial cells. Overall, the FN-coated PLL monolayer and the FN-coated PLL-terminated multilayer were the best performing films in promoting cell spreading. They concluded that the presence of FN is an important factor (more than film charge or layer number) in controlling the interaction between cells and multilayer films. Semenov *et al*. [111] also adsorbed or chemically coupled FN on to (PLL/HA) cross-linked films and demonstrated that film cross-linking strongly influenced FN surface distribution, leading to denser presentation of adhesion sites for cells.
Chen *et al*. [28] modified synthetic (PAH/PAA) PEM films with type I collagen and the proteoglycan decorin . They showed that this did not alter substrate stiffness, but enhanced the retention of spheroids on surfaces and stabilized hepatic functions (such as albumin and urea secretion). Very interestingly, decorin was found to exhibit unique compliance-mediated effects on hepatic functions, down-regulating the hepatocyte phenotype when presented on highly compliant substrata, while up-regulating hepatocyte functions when presented on increasingly stiffer substrata. Collagen adsorption was also found to be important for the attachment and function of adult rat hepatocytes on cross-linked (PLL/ALG) and (PLL/PGA) multilayer films [58]. Collagen [112] and fibronectin can even be used as building blocks for layer-by-layer film buildup.
Besides ECM proteins, GAGs are more and more often used as main component of new biomimetic coatings and nanoparticles, which were reviewed recently [54; 113]. They are often simply adsorbed and interact by non specific and/or specific interactions with other positively charged biomolecules [68].

3.2.2 Adsorption of growth factors on thin films or matrices.

Due to their utmost importance in signaling processes, GF are now often inserted into 2D and 3D biomaterials to achieve a specific

function: to regulate cell proliferation for FGF2 [114], or promote the formation of new vessels for VEGF [109], induce bone regeneration for BMP-2 or chondrogenesis for TGF-□1. There are several high affinity partners of growth factors among biological materials. Fibrin, a non globular fibrous protein, is involved in a large number of biological processes (blood clotting by polymerization of fibrin, signal transduction, platelet activation) and is a very interesting candidate for growth factor immobilization. Thus, natural interactions of fibrin with FGF, BMP-2 and EGF have been used to present these growth factors in their immobilized form [115; 116; 117] (Figure 5). Desorption experiments using radiolabeled proteins demonstrated that the patterns were retained *in vitro* with less than a 30% loss of growth factor over 9 days [116], which confirms the high affinity of growth factors for fibrin.

The 12th-14th type three repeats of fibronectin (FN III12-14) also appear to be a natural affinity fragment for several GFs [118]. In a recent study, Hubbell *and coll.* [118] showed by surface plasmon resonance that this FN fragment binds to GFs from different families, including most of the GFs from the platelet-derived growth factor (PDGF, VEGF and FGF families and some GFs from the TGF-β and neurotrophin families). Affinities were high in the nanomolar range, without inhibiting GF activity. These authors subsequently employed a fibrin-bound variant of FN III12-14 as 3D biomaterials and showed that it was highly effective as a GF delivery system. For instance, in matrices functionalized with FN III12-14, PDGF-BB-induced sprouting of human smooth muscle cell spheroids was greatly enhanced.

Other natural high affinity binding domains are those derived from heparin. Recently, Chow *et al.* [119] created a self-assembled bioactive hierarchical membrane functionalized with a heparin-binding peptide amphiphile (HBPA). HBPA contains a consensus sequence to bind and display heparin loops on the surface of nanofibers in order to localize and activate potent angiogenic growth factors through their respective heparin-binding domains. Both VEGF and FGF2 are known to have heparin-binding domains along with potent angiogenic activity. Release of these factors was effectively lower in the presence of heparin in the membrane.

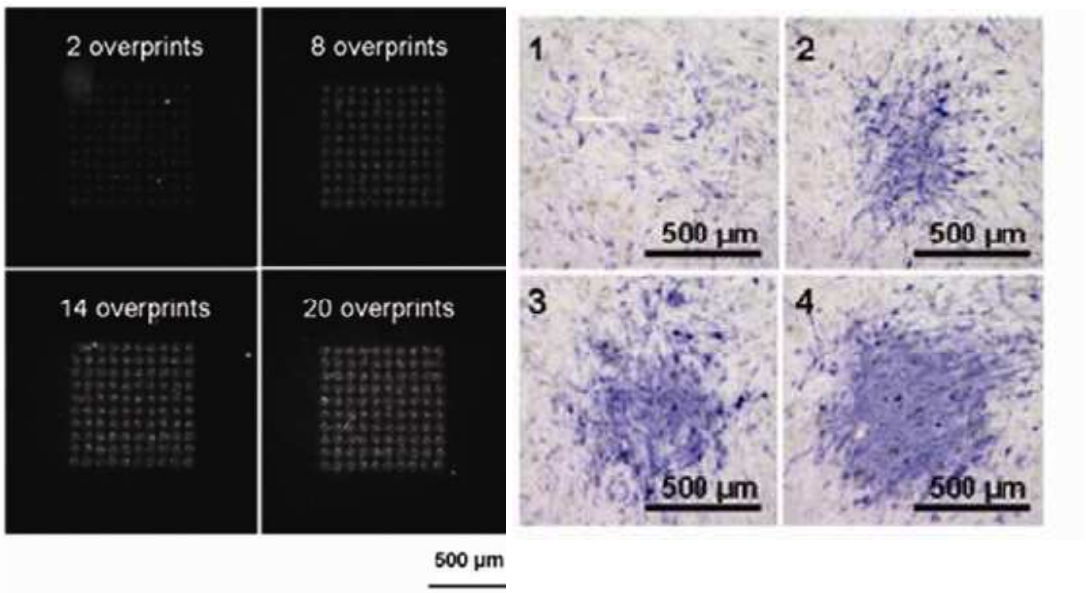

FIGURE 5*. Bioprinting of BMP-2 growth factor, which is here fluorescently labeled, on a fibrin film. Left image: BMP-2 was printed at various surface concentrations by varying the number of overprints, leading to increased fluorescence on the surface. The four images correspond to, respectively: 2, 8, 14 and 20 overprints. Right images: corresponding expression of the bone marker alkaline phosphatase (in blue), which is expressed during differentiation of muscle derived stem cells in bone. (From Campbell and coll., Stem cells, 2007, copyright AlphaMed press)*

Polyelectrolyte multilayer films can also be employed to sequester growth factors and present them to cells in a "matrix-bound" manner. VEGF could be adsorbed on to $(PAH/PSS)_4$ films and was shown to exhibit a specific bioactivity toward endothelial cells [120]. (PLL/HA) crosslinked films or (PLL/HA-heparin) films can be used as a reservoir for BMP-2 delivery and controlled differentiation of myoblasts to osteoblasts [121; 122]. Very interestingly, these films are made of natural components, are biodegradable, and their mechanical properties can also be modulated.

4. Concluding remarks and outlook

Different types of synthetic and natural materials in various forms (thin films or gels) have been and are currently being developed to reproduce *in vitro* the *in vivo* cell microenvironment. Here, we have particularly focused on materials mechanical and biochemical properties. Biochemical functionalization has up to now mostly focused on improving cell adhesion by presenting cell adhesive ligands. However, many ligands are not highly specific and do not target a particular receptor type. Recent developments have begun to focus : i) on targeting a given type of integrin or non-integrin receptors (such as syndecans) and ii) to present not only adhesive signals but also signals triggered by growth factors (FGF, BMP, VEGF…), which affect cell proliferation and cell differentiation. There is no doubt that this direction will be further developed and studied in order to understand how different signals can act in synergy. The control over mechanical and biochemical properties will enable and foster further studies aimed at understanding possible synergies between these signals. Cross-talks between the different signaling pathways may be unveiled in a near future.

Natural materials that have some adhesive sites intrinsically and that can bind growth factors with a high affinity will be particularly interesting candidates as compared to their synthetic counterparts. Indeed, if multiple functionalities have to be added to synthetic materials, the strategy of coupling may become even more tedious and time-consuming. Ease of implementation is an important criterion for biomaterials scientists, as well as for biophysicists and cell biologists. Such experimental constraints should be kept in mind when designing materials, as only simple, easy-to-handle and easy-to-characterize materials would be used by cell biologists.

Creating anisotropic properties to mimic the natural environment is also a current challenge [123]. Gradients in both mechanical properties and growth factors will thus be developed and used to understand how cells respond to these cues, from adhesion and proliferation to differentiation. We have seen that UV light is already widely used for the synthesis of biomaterials. Light-initiated cross-linking steps and gradients will probably be a valuable tool for basic cell-material interaction studies or advanced tissue engineering applications. It is also predicted that new methodological developments emerging from soft lithography and microfluidics will be combined to further develop these 2D and 3D biomaterials [124]. Importantly, these technologies can be applied to a wide range of polymeric biomaterials currently in use. This will make it possible to incorporate spatial control which is crucial for developing complex microenvironments [125]. Ultimately, control over biochemical and mechanical properties in a spatially-controlled manner will be achieved to investigate the respective role of each parameter as well as to produce innovative biomaterials [126].

Acknowledgements

CP is a Junior Member of the "Institut Universitaire de France" whose support is gratefully acknowledged. CP wishes to thank the European Commission for support via an ERC Starting grant 2010 (GA 259370). VG thanks the Rhône-Alpes region for a fellowship via the cluster MACODEV.

Bibliographic references

1. Langer, R. & Vacanti, J. P. (1993). Tissue engineering. *Science* **260**, 920-926.
2. Newham, P. & Humphries, M. J. (1996). Integrin adhesion receptors: Structure, function and implications for biomedicine. *Mol Med Today* **2**, 304-313.
3. Pelham, R. J. & Wang, Y. L. (1997). Cell locomotion and focal adhesions are regulated by substrate flexibility. *Proc Natl Acad Sci U S A* **94**, 13661-13665.
4. Engler, A. J., Sen, S., Sweeney, H. L. & Discher, D. E. (2006). Matrix elasticity directs stem cell lineage specification. *Cell* **126**, 677-89.
5. Fan, V. H., Tamama, K., Au, A., Littrell, R., Richardson, L. B., Wright, J. W., Wells, A. & Griffith, L. G. (2007). Tethered epidermal growth factor provides a survival advantage to mesenchymal stem cells. *Stem Cells* **25**, 1241-51.
6. Bongrand, P., Capo, C. & Depieds, R. (1982). Physics of cell adhesion. *Prog Surf Sci* **12**, 217-285.
7. Rehfeldt, F., Engler, A. J., Eckhardt, A., Ahmed, F. & Discher, D. E. (2007). Cell responses to the mechanochemical microenvironment--implications for regenerative medicine and drug delivery. *Adv Drug Delivery Rev* **59**, 1329-39.
8. Luu, O., David, R., Ninomiya, H. & Winklbauer, R. (2011). Large-scale mechanical properties of Xenopus embryonic epithelium. *Proc Natl Acad Sci U S A* **108**, 4000-4005.
9. Dobrowsky, T. M., Panorchan, P., Konstantopoulos, K. & Wirtz, D. (2008). Live-Cell Single-Molecule Force Spectroscopy. In *Biophysical Tools for Biologists, Vol 2: In Vivo Techniques*, Vol. 89, pp. 411-+. Elsevier Academic Press Inc, San Diego.
10. Janmey, P. A. & Weitz, D. A. (2004). Dealing with mechanics: mechanisms of force transduction in cells. *Trends Biochem Sci* **29**, 364-370.
11. Shoichet, M. S. (2010). Polymer Scaffolds for Biomaterials Applications. *Macromolecules* **43**, 581-591.
12. Nemir, S. & West, J. L. (2010). Synthetic materials in the study of cell response to substrate rigidity. *Ann Biomed Eng* **38**, 2-20.
13. Yeung, T., Georges, P. C., Flanagan, L. A., Marg, B., Ortiz, M., Funaki, M., Zahir, N., Ming, W., Weaver, V. & Janmey, P. A. (2005). Effects of substrate stiffness on cell morphology, cytoskeletal structure, and adhesion. *Cell Motil Cytoskeleton* **60**, 24-34.
14. Engler, A. J., Rehfeldt, F., Sen, S. & Discher, D. E. (2007). Microtissue elasticity: measurements by atomic force microscopy and its influence on cell differentiation. *Methods in Cell Biol* **83**, 521-45.
15. Engler, A. J., Griffin, M. A., Sen, S., Bonnemann, C. G., Sweeney, H. L. & Discher, D. E. (2004). Myotubes differentiate optimally on substrates with tissue-like stiffness: pathological implications for soft or stiff microenvironments. *J Cell Biol* **166**, 877-87.
16. Solon, J., Levental, I., Sengupta, K., Georges, P. C. & Janmey, P. A. (2007). Fibroblast adaptation and stiffness matching to soft elastic substrates. *Biophys J* **93**, 4453-61.
17. Isenberg, B. C., Dimilla, P. A., Walker, M., Kim, S. & Wong, J. Y. (2009). Vascular smooth muscle cell durotaxis depends on substrate stiffness gradient strength. *Biophys J* **97**, 1313-22.
18. Beningo, K. A., Hamao, K., Dembo, M., Wang, Y. L. & Hosoya, H. (2006). Traction forces of fibroblasts are regulated by the Rho-dependent kinase but not by the myosin light chain kinase. *Arch Biochem Biophys* **456**, 224-31.
19. Beningo, K. A., Dembo, M. & Wang, Y. L. (2004). Responses of fibroblasts to anchorage of dorsal extracellular matrix receptors. *Proc Natl Acad Sci U S A* **101**, 18024-9.
20. Boudou, T., Ohayon, J., Picart, C., Pettigrew, R. I. & Tracqui, P. (2009). Nonlinear elastic properties of polyacrylamide gels: Implications for quantification of cellular forces. *Biorheology* **46**, 191-205.
21. Reinhart-King, C. A., Dembo, M. & Hammer, D. A. (2005). The dynamics and mechanics of endothelial cell spreading. *Biophys J* **89**, 676-89.
22. Chou, S. Y., Cheng, C. M. & LeDuc, P. R. (2009). Composite polymer systems with control of local substrate elasticity and their effect on cytoskeletal and morphological characteristics of adherent cells. *Biomaterials* **30**, 3136-42.
23. Brown, X. Q., Ookawa, K. & Wong, J. Y. (2005). Evaluation of polydimethylsiloxane scaffolds with physiologically-relevant elastic moduli: interplay of substrate mechanics and surface chemistry effects on vascular smooth muscle cell response. *Biomaterials* **26**, 3123-9.
24. Tzvetkova-Chevolleau, T., Stephanou, A., Fuard, D., Ohayon, J., Schiavone, P. & Tracqui, P. (2008). The motility of normal and cancer cells in response to the combined influence of the substrate rigidity and anisotropic microstructure. *Biomaterials* **29**, 1541-1551.
25. Decher, G., Lehr, B., Lowack, K., Lvov, Y. & Schmitt, J. (1994). New nanocomposite films for biosensors: layer-by-layer adsorbed films of polyelectrolytes, proteins or DNA. *Biosens Bioelectron* **9**, 677-684.
26. Thompson, M. T., Berg, M. C., Tobias, I. S., Rubner, M. F. & Van Vliet, K. J. (2005). Tuning compliance of nanoscale polyelectrolyte multilayers to modulate cell adhesion. *Biomaterials* **26**, 6836-6845.
27. Thompson, M. T., Berg, M. C., Tobias, I. S., Lichter, J. A., Rubner, M. F. & Van Vliet, K. J. (2006). Biochemical functionalization of polymeric cell substrata can alter mechanical compliance. *Biomacromolecules* **7**, 1990-1995.

28. Chen, A. A., Khetani, S. R., Lee, S., Bhatia, S. N. & Van Vliet, K. J. (2009). Modulation of hepatocyte phenotype in vitro via chemomechanical tuning of polyelectrolyte multilayers. *Biomaterials* **30**, 1113-20.
29. Francius, G., Hemmerle, J., Ball, V., Lavalle, P., Picart, C., Voegel, J., Schaaf, P. & Senger, B. (2007). Stiffening of soft polyelectrolyte architectures by multilayer capping evidenced by viscoelastic analysis of AFM indentation measurements. *J Phys Chem C* **111**, 8299-8306.
30. Kocgozlu, L., Lavalle, P., Koenig, G., Senger, B., Haikel, Y., Schaaf, P., Voegel, J. C., Tenenbaum, H. & Vautier, D. (2010). Selective and uncoupled role of substrate elasticity in the regulation of replication and transcription in epithelial cells. *J Cell Sci* **123**, 29-39.
31. Lutolf, M. P. & Hubbell, J. A. (2003). Synthesis and physicochemical characterization of end-linked poly(ethylene glycol)-co-peptide hydrogels formed by Michael-type addition. *Biomacromolecules* **4**, 713-22.
32. Raeber, G. P., Lutolf, M. P. & Hubbell, J. A. (2005). Molecularly engineered PEG hydrogels: a novel model system for proteolytically mediated cell migration. *Biophys J* **89**, 1374-88.
33. Lutolf, M. P., Raeber, G. P., Zisch, A. H., Tirelli, N. & Hubbell, J. A. (2003). Cell-responsive synthetic hydrogels. *Adv Mater* **15**, 888-+.
34. Yamamura, N., Sudo, R., Ikeda, M. & Tanishita, K. (2007). Effects of the mechanical properties of collagen gel on the in vitro formation of microvessel networks by endothelial cells. *Tissue Eng* **13**, 1443-53.
35. Miron-Mendoza, M., Seemann, J. & Grinnell, F. (2010). The differential regulation of cell motile activity through matrix stiffness and porosity in three dimensional collagen matrices. *Biomaterials* **31**, 6425-35.
36. McDaniel, D. P., Shaw, G. A., Elliott, J. T., Bhadriraju, K., Meuse, C., Chung, K. H. & Plant, A. L. (2007). The stiffness of collagen fibrils influences vascular smooth muscle cell phenotype. *Biophys J* **92**, 1759-69.
37. Halloran, D. O., Grad, S., Stoddart, M., Dockery, P., Alini, M. & Pandit, A. S. (2008). An injectable cross-linked scaffold for nucleus pulposus regeneration. *Biomaterials* **29**, 438-47.
38. Wong, M. (2004). Alginate in tissue engineering. In *Biopolymer Methods in Tissue Engineering*, pp. 77-86.
39. Augst, A. D., Kong, H. J. & Mooney, D. J. (2006). Alginate hydrogels as biomaterials. *Macromol Biosci* **6**, 623-33.
40. Kong, H. J., Wong, E. & Mooney, D. J. (2003). Independent control of rigidity and toughness of polymeric hydrogels. *Macromolecules* **36**, 4582-4588.
41. Lee, K. Y., Rowley, J. A., Eiselt, P., Moy, E. M., Bouhadir, K. H. & Mooney, D. J. (2000). Controlling mechanical and swelling properties of alginate hydrogels independently by cross-linker type and cross-linking density. *Macromolecules* **33**, 4291-4294.
42. Rowley, J. A. & Mooney, D. J. (2002). Alginate type and RGD density control myoblast phenotype. *J Biomed Mater Res* **60**, 217-23.
43. Genes, N. G., Rowley, J. A., Mooney, D. J. & Bonassar, L. J. (2004). Effect of substrate mechanics on chondrocyte adhesion to modified alginate surfaces. *Arch Biochem Biophys* **422**, 161-7.
44. Huebsch, N., Arany, P. R., Mao, A. S., Shvartsman, D., Ali, O. A., Bencherif, S. A., Rivera-Feliciano, J. & Mooney, D. J. (2010). Harnessing traction-mediated manipulation of the cell/matrix interface to control stem-cell fate. *Nat Mater* **9**, 518-26.
45. Jouon, N., Rinaudo, M., Milas, M. & Desbrieres, J. (1995). Hydration of hyaluronic acid as a function of the counterion type and relative humidity. *Carbohydr Polym* **26**, 69-73.
46. Zimmerman, E., Geiger, B. & Addadi, L. (2002). Initial stages of cell-matrix adhesion can be mediated and modulated by cell-surface hyaluronan. *Biophys J* **82**, 1848-57.
47. Ladam, G., Vonna, L. & Sackmann, E. (2003). Micromechanics of surface-grafted hyaluronic acid gels. *J PhysChem B* **107**, 8965-8971.
48. Shu, X. Z., Liu, Y., Luo, Y., Roberts, M. C. & Prestwich, G. D. (2002). Disulfide cross-linked hyaluronan hydrogels. *Biomacromolecules* **3**, 1304-11.
49. Young, J. L. & Engler, A. J. (2011). Hydrogels with time-dependent material properties enhance cardiomyocyte differentiation in vitro. *Biomaterials* **32**, 1002-9.
50. Balgude, A. P., Yu, X., Szymanski, A. & Bellamkonda, R. V. (2001). Agarose gel stiffness determines rate of DRG neurite extension in 3D cultures. *Biomaterials* **22**, 1077-84.
51. Leipzig, N. D. & Shoichet, M. S. (2009). The effect of substrate stiffness on adult neural stem cell behavior. *Biomaterials* **30**, 6867-78.
52. Boudou, T., Crouzier, T., Ren, K., Blin, G. & Picart, C. (2010). Multiple functionalities of polyelectrolyte mulitlayer films : new biomedical applications. *Adv Mater* **22**, 441-467.
53. Picart, C., Mutterer, J., Richert, L., Luo, Y., Prestwich, G. D., Schaaf, P., Voegel, J.-C. & Lavalle, P. (2002). Molecular basis for the explanation of the exponential growth of polyelectrolyte multilayers. *Proc Natl Acad Sci USA* **99**, 12531-12535.
54. Crouzier, T., Boudou, T. & Picart, C. (2010). Polysaccharide-based polyelectrolyte multilayers. *Curr Opin Colloid Interface Sci* **15**, 417-426.
55. Richert, L., Boulmedais, F., Lavalle, P., Mutterer, J., Ferreux, E., Decher, G., Schaaf, P., Voegel, J.-C. & Picart, C. (2004). Improvement of stability and cell adhesion properties of polyelectrolyte multilayer films by chemical cross-linking. *Biomacromolecules* **5**, 284-294.

56. Francius, G., Hemmerle, J., Ohayon, J., Schaaf, P., Voegel, J.-C., Picart, C. & Senger, B. (2006). Effect of cross-linking on the elasticity of polyelectrolyte multilayer films measured by colloidal probe AFM. *Microsc Res Tech* **69**, 84-92.
57. Boudou, T., Crouzier, T., Auzely-Velty, R., Glinel, K. & Picart, C. (2009). Internal composition versus the mechanical properties of polyelectrolyte multilayer films: The influence of chemical cross-linking. *Langmuir* **25**, 13809-13819.
58. Wittmer, C. R., Phelps, J. A., Lepus, C. M., Saltzman, W. M., Harding, M. J. & Van Tassel, P. R. (2008). Multilayer nanofilms as substrates for hepatocellular applications. *Biomaterials* **29**, 4082-4090.
59. Ren, K., Crouzier, T., Roy, C. & Picart, C. (2008). Polyelectrolyte multilayer films of controlled stiffness modulate myoblast differentiation. *Adv Funct Mater* **18**, 1378-1389.
60. Phelps, J. A., Morisse, S., Hindie, M., Degat, M. C., Pauthe, E. & Van Tassel, P. R. (2011). Nanofilm Biomaterials: Localized Cross-Linking To Optimize Mechanical Rigidity and Bioactivity. *Langmuir* **27**, 1123-1130.
61. Hillberg, A. L., Holmes, C. A. & Tabrizian, M. (2009). Effect of genipin cross-linking on the cellular adhesion properties of layer-by-layer assembled polyelectrolyte films. *Biomaterials* **30**, 4463-4470.
62. Pozos Vazquez, C., Boudou, T., Dulong, V., Nicolas, C., Picart, C. & Glinel, K. (2009). Variation of polyelectrolyte film stiffness by photo-cross-linking: A new way to control cell adhesion. *Langmuir* **25**, 3556-3563.
63. Peyton, S. R., Kim, P. D., Ghajar, C. M., Seliktar, D. & Putnam, A. J. (2008). The effects of matrix stiffness and RhoA on the phenotypic plasticity of smooth muscle cells in a 3-D biosynthetic hydrogel system. *Biomaterials* **29**, 2597-607.
64. Kim, P. D., Peyton, S. R., VanStrien, A. J. & Putnam, A. J. (2009). The influence of ascorbic acid, TGF-beta1, and cell-mediated remodeling on the bulk mechanical properties of 3-D PEG-fibrinogen constructs. *Biomaterials* **30**, 3854-64.
65. Brigham, M. D., Bick, A., Lo, E., Bendali, A., Burdick, J. A. & Khademhosseini, A. (2009). Mechanically robust and bioadhesive collagen and photocrosslinkable hyaluronic acid semi-interpenetrating networks. *Tissue Eng Part A* **15**, 1645-53.
66. Lu, Q., Feng, Q., Hu, K. & Cui, F. (2008). Preparation of three-dimensional fibroin/collagen scaffolds in various pH conditions. *J Mater Sci Mater Med* **19**, 629-34.
67. Croll, T. I., O'Connor, A. J., Stevens, G. W. & Cooper-White, J. J. (2006). A blank slate? Layer-by-layer deposition of hyaluronic acid and chitosan onto various surfaces. *Biomacromolecules* **7**, 1610-22.
68. Alberts, B., Bray, D., Lewis, J., Raff, M., Roberts, K. & Watson, J. D. (1994). *Mol Biol Cell*, Garland Publishing Inc, New York.
69. Macri, L., Silverstein, D. & Clark, R. A. (2007). Growth factor binding to the pericellular matrix and its importance in tissue engineering. *Adv Drug Delivery Rev* **59**, 1366-81.
70. Hynes, R. O. (2009). The extracellular matrix: not just pretty fibrils. *Science* **326**, 1216-9.
71. Kandow, C. E., Georges, P. C., Janmey, P. A. & Beningo, K. A. (2007). Polyacrylamide hydrogels for cell mechanics: steps toward optimization and alternative uses. *Methods Cell Biol* **83**, 29-46.
72. Grabarek, Z. & Gergely, J. (1990). Zero-length crosslinking procedure with the use of active esters. *Anal Biochem* **185**, 131-135.
73. Kuo, J. W., Swann, D. A. & Prestwich, G. D. (1991). Chemical modification of hyaluronic acid by carbodiimides. *Bioconjugate Chem* **2**, 232-41.
74. Boontheekul, T., Hill, E. E., Kong, H. J. & Mooney, D. J. (2007). Regulating myoblast phenotype through controlled gel stiffness and degradation. *Tissue Eng* **13**, 1431-42.
75. Doran, M. R., Frith, J. E., Prowse, A. B. J., Fitzpatrick, J., Wolvetang, E. J., Munro, T. P., Gray, P. P. & Cooper-White, J. J. (2010). Defined high protein content surfaces for stem cell culture. *Biomaterials* **31**, 5137-5142.
76. Picart, C., Elkaim, R., Richert, L., Audoin, F., Da Silva Cardoso, M., Schaaf, P., Voegel, J.-C. & Frisch, B. (2005). Primary cell adhesion on RGD functionalized and covalently cross-linked polyelectrolyte multilayer thin films. *Adv Funct Mater* **15**, 83-94.
77. Mann, B. K., Schmedlen, R. H. & West, J. L. (2001). Tethered-TGF-beta increases extracellular matrix production of vascular smooth muscle cells. *Biomaterials* **22**, 439-44.
78. Peyton, S. R., Raub, C. B., Keschrumrus, V. P. & Putnam, A. J. (2006). The use of poly(ethylene glycol) hydrogels to investigate the impact of ECM chemistry and mechanics on smooth muscle cells. *Biomaterials* **27**, 4881-93.
79. Hern, D. L. & Hubbell, J. A. (1998). Incorporation of adhesion peptides into nonadhesive hydrogels useful for tissue resurfacing. *J Biomed Mater Res* **39**, 266-76.
80. Khetan, S. & Burdick, J. A. (2010). Patterning network structure to spatially control cellular remodeling and stem cell fate within 3-dimensional hydrogels. *Biomaterials* **31**, 8228-34.
81. Almany, L. & Seliktar, D. (2005). Biosynthetic hydrogel scaffolds made from fibrinogen and polyethylene glycol for 3D cell cultures. *Biomaterials* **26**, 2467-77.
82. Ruoslahti, E. (1996). RGD and other recognition sequences for integrins. *Annu Rev Cell Dev Biol* **12**, 697-715.
83. Petrie, T. A., Raynor, J. E., Reyes, C. D., Burns, K. L., Collard, D. M. & Garcia, A. J. (2008). The effect of integrin-specific bioactive coatings on tissue healing and implant osseointegration. *Biomaterials* **29**, 2849-57.
84. Lutolf, M. P., Weber, F. E., Schmoekel, H. G., Schense, J. C., Kohler, T., Muller, R. & Hubbell, J.

A. (2003). Repair of bone defects using synthetic mimetics of collagenous extracellular matrices. *Nat Biotechnol* **21**, 513-8.
85. Hozumi, K., Yamagata, N., Otagiri, D., Fujimori, C., Kikkawa, Y., Kadoya, Y. & Nomizu, M. (2009). Mixed peptide-chitosan membranes to mimic the biological activities of a multifunctional laminin alpha1 chain LG4 module. *Biomaterials* **30**, 1596-603.
86. Urushibata, S., Hozumi, K., Ishikawa, M., Katagiri, F., Kikkawa, Y. & Nomizu, M. (2010). Identification of biologically active sequences in the laminin alpha2 chain G domain. *Arch Biochem Biophys* **497**, 43-54.
87. Doran, M. R., Frith, J. E., Prowse, A. B., Fitzpatrick, J., Wolvetang, E. J., Munro, T. P., Gray, P. P. & Cooper-White, J. J. (2010). Defined high protein content surfaces for stem cell culture. *Biomaterials* **31**, 5137-42.
88. Raeber, G. P., Lutolf, M. P. & Hubbell, J. A. (2007). Mechanisms of 3-D migration and matrix remodeling of fibroblasts within artificial ECMs. *Acta Biomater* **3**, 615-29.
89. Hersel, U., Dahmen, C. & Kessler, H. (2003). RGD modified polymers: biomaterials for stimulated cell adhesion and beyond. *Biomaterials* **24**, 4385-4415.
90. Hsiong, S. X., Boontheekul, T., Huebsch, N. & Mooney, D. J. (2009). Cyclic arginine-glycine-aspartate peptides enhance three-dimensional stem cell osteogenic differentiation. *Tissue Eng Part A* **15**, 263-72.
91. Suzuki, N., Nakatsuka, H., Mochizuki, M., Nishi, N., Kadoya, Y., Utani, A., Oishi, S., Fujii, N., Kleinman, H. K. & Nomizu, M. (2003). Biological activities of homologous loop regions in the laminin alpha chain G domains. *J Biol Chem* **278**, 45697-45705.
92. Benoit, D. S. & Anseth, K. S. (2005). The effect on osteoblast function of colocalized RGD and PHSRN epitopes on PEG surfaces. *Biomaterials* **26**, 5209-20.
93. Rezania, A. & Healy, K. E. (1999). Biomimetic peptide surfaces that regulate adhesion, spreading, cytoskeletal organization, and mineralization of the matrix deposited by osteoblast-like cells. *Biotechnol Prog* **15**, 19-32.
94. Reyes, C. D., Petrie, T. A., Burns, K. L., Schwartz, Z. & Garcia, A. J. (2007). Biomolecular surface coating to enhance orthopaedic tissue healing and integration. *Biomaterials* **28**, 3228-35.
95. Weber, L. M., Hayda, K. N., Haskins, K. & Anseth, K. S. (2007). The effects of cell-matrix interactions on encapsulated beta-cell function within hydrogels functionalized with matrix-derived adhesive peptides. *Biomaterials* **28**, 3004-11.
96. Werner, S., Huck, O., Frisch, B., Vautier, D., Elkaim, R., Voegel, J. C., Brunel, G. & Tenenbaum, H. (2009). The effect of microstructured surfaces and laminin-derived peptide coatings on soft tissue interactions with titanium dental implants. *Biomaterials* **30**, 2291-2301.
97. Wu, Y. Z., Coyer, S. R., Ma, H. W. & Garcia, A. J. (2010). Poly(dimethylsiloxane) elastomers with tethered peptide ligands for cell adhesion studies. *Acta Biomater* **6**, 2898-2902.
98. Garcia, A. J., Schwarzbauer, J. E. & Boettiger, D. (2002). Distinct activation states of alpha5beta1 integrin show differential binding to RGD and synergy domains of fibronectin. *Biochemistry* **41**, 9063-9.
99. Bellin, R. M., Kubicek, J. D., Frigault, M. J., Kamien, A. J., Steward, R. L., Jr, Barnes, H. M., Digiacomo, M. B., Duncan, L. J., Edgerly, C. K., Morse, E. M., Park, C. Y., Fredberg, J. J., Cheng, C. M. & LeDuc, P. R. (2009). Defining the role of syndecan-4 in mechanotransduction using surface-modification approaches. *Proc Natl Acad Sci U S A* **106**, 22102-7.
100. He, X. Z., Ma, J. Y. & Jabbari, E. (2008). Effect of Grafting RGD and BMP-2 Protein-Derived Peptides to a Hydrogel Substrate on Osteogenic Differentiation of Marrow Stromal Cells. *Langmuir* **24**, 12508-12516.
101. Zouani, O. F., Chollet, C., Guillotin, B. & Durrieu, M. C. (2010). Differentiation of pre-osteoblast cells on poly(ethylene terephthalate) grafted with RGD and/or BMPs mimetic peptides. *Biomaterials* **31**, 8245-53.
102. Wang, Y. L. & Pelham, R. J., Jr. (1998). Preparation of a flexible, porous polyacrylamide substrate for mechanical studies of cultured cells. *Methods Enzymol* **298**, 489-496.
103. Saha, K., Keung, A. J., Irwin, E. F., Li, Y., Little, L., Schaffer, D. V. & Healy, K. E. (2008). Substrate modulus directs neural stem cell behavior. *Biophys J* **95**, 4426-38.
104. Wipff, P. J., Majd, H., Acharya, C., Buscemi, L., Meister, J. J. & Hinz, B. (2009). The covalent attachment of adhesion molecules to silicone membranes for cell stretching applications. *Biomaterials* **30**, 1781-9.
105. Kuhl, P. R. & Griffith-Cima, L. G. (1996). Tethered epidermal growth factor as a paradigm for growth factor-induced stimulation from the solid phase. *Nat Med* **2**, 1022-7.
106. Mehta, G., Williams, C. M., Alvarez, L., Lesniewski, M., Kamm, R. D. & Griffith, L. G. (2010). Synergistic effects of tethered growth factors and adhesion ligands on DNA synthesis and function of primary hepatocytes cultured on soft synthetic hydrogels. *Biomaterials* **31**, 4657-71.
107. Puccinelli, T. J., Bertics, P. J. & Masters, K. S. (2010). Regulation of keratinocyte signaling and function via changes in epidermal growth factor presentation. *Acta Biomater* **6**, 3415-25.
108. Kapur, T. A. & Shoichet, M. S. (2004). Immobilized concentration gradients of nerve growth factor guide neurite outgrowth. *J Biomed Mater Res A* **68**, 235-43.

109. Leslie-Barbick, J. E., Shen, C., Chen, C. S. & West, J. L. (2011). Micron-scale spatially patterned, covalently immobilized vascular endothelial growth factor on hydrogels accelerates endothelial tubulogenesis and increases cellular angiogenic responses. *Tissue Eng Part A* **17**, 221-229.
110. Wittmer, C. R., Phelps, J. A., Saltzman, W. M. & Van Tassel, P. R. (2007). Fibronectin terminated multilayer films: protein adsorption and cell attachment studies. *Biomaterials* **28**, 851-860.
111. Semenov, O. V., Malek, A., Bittermann, A. G., Voros, J. & Zisch, A. (2009). Engineered polyelectrolyte multilayer substrates for adhesion, proliferation and differentiation of human mesenchymal stem cells. *Tissue Eng Part A* **15**, 2977-2990.
112. Zhang, J., Senger, B., Vautier, D., Picart, C., Schaaf, P., Voegel, J.-C. & Lavalle, P. (2005). Buildup of collagen and hyaluronic acid polyelectrolyte multilayers. *Biomaterials* **26**, 3353-3361.
113. Boddohi, S. & Kipper, M. J. (2010). Engineering Nanoassemblies of Polysaccharides. *Adv Mater* **22**, 2998-3016.
114. Sahni, A., Sporn, L. A. & Francis, C. W. (1999). Potentiation of endothelial cell proliferation by fibrin(ogen)-bound fibroblast growth factor-2. *J Biol Chem* **274**, 14936-14941.
115. Campbell, P. G., Miller, E. D., Fisher, G. W., Walker, L. M. & Weiss, L. E. (2005). Engineered spatial patterns of FGF-2 immobilized on fibrin direct cell organization. *Biomaterials* **26**, 6762-70.
116. Miller, E. D., Fisher, G. W., Weiss, L. E., Walker, L. M. & Campbell, P. G. (2006). Dose-dependent cell growth in response to concentration modulated patterns of FGF-2 printed on fibrin. *Biomaterials* **27**, 2213-21.
117. Phillippi, J. A., Miller, E., Weiss, L., Huard, J., Waggoner, A. & Campbell, P. (2008). Microenvironments engineered by inkjet bioprinting spatially direct adult stem cells toward muscle- and bone-like subpopulations. *Stem Cells* **26**, 127-34.
118. Martino, M. M. & Hubbell, J. A. (2010). The 12th-14th type III repeats of fibronectin function as a highly promiscuous growth factor-binding domain. *FASEB J* **24**, 4711-21.
119. Chow, L. W., Bitton, R., Webber, M. J., Carvajal, D., Shull, K. R., Sharma, A. K. & Stupp, S. I. (2011). A bioactive self-assembled membrane to promote angiogenesis. *Biomaterials* **32**, 1574-82.
120. Muller, S., Koenig, G., Charpiot, A., Debry, C., Voegel, J., Lavalle, P. & Vautier, D. (2008). VEGF-functionalized polyelectrolyte multilayers as proangiogenic prosthetic coatings *Adv Funct Mater* **18**, 1767-1775
121. Crouzier, T., Ren, K., Nicolas, C., Roy, C. & Picart, C. (2009). Layer-by-Layer films as a biomimetic reservoir for rhBMP-2 delivery: controlled differentiation of myoblasts to osteoblasts. *Small* **5**, 598-608.
122. Crouzier, T., Szarpak, A., Boudou, T., Auzely-Velty, R. & Picart, C. (2010). Polysaccharide-blend multilayers containing hyaluronan and heparin as a delivery system for rhBMP-2. *Small* **6**, 651-662.
123. Kutejova, E., Briscoe, J. & Kicheva, A. (2009). Temporal dynamics of patterning by morphogen gradients. *Curr Opin Genet Dev* **19**, 315-322.
124. Lutolf, M. P., Gilbert, P. M. & Blau, H. M. (2009). Designing materials to direct stem-cell fate. *Nature* **462**, 433-441.
125. Marklein, R. A. & Burdick, J. A. (2010). Spatially controlled hydrogel mechanics to modulate stem cell interactions. *Soft Matter* **6**, 136-143.
126. Huebsch, N. & Mooney, D. J. (2009). Inspiration and application in the evolution of biomaterials. *Nature* **462**, 426-32.

Annexe II – Review article 2

Published in *Chemistry of Materials*, 2012, **24**(5): 854−869

Polyelectrolyte multilayer assemblies on materials surfaces: from cell adhesion to tissue engineering

Varvara Gribova[1,2], Rachel Auzely-Velty[2] and Catherine Picart[1]

1. LMGP-MINATEC, Grenoble Institute of Technology, 3 parvis Louis Néel, 38016 Grenoble, France
2. Centre de Recherches sur les Macromolécules Végétales (CERMAV-CNRS), affiliated with University Joseph Fourier, and member of the Institut de Chimie Moléculaire de Grenoble (France)

Keywords: layer-by-layer, polysaccharides, growth factors, cell adhesion cell differentiation, biomaterials, regenerative medicine

Abstract

Controlling the bulk and surface properties of materials is a real challenge for bioengineers working in the fields of biomaterials, tissue engineering and biophysics. The layer-by-layer (LbL) deposition method, introduced 20 years ago, consists in the alternate adsorption of polyelectrolytes that self-organize on the material's surface, leading to the formation of polyelectrolyte multilayer (PEM) films.[1; 2] Due to its simplicity and versatility, the procedure has led to considerable developments of biological applications within the past 5 years. In this review, we focus our attention on the design of PEM films as surface coatings for applications in the field of biomaterials, tissue engineering and for fundamental biophysical studies. This will include a survey of the chemical and physical properties that have emerged as being key points in relation to biological processes. The numerous possibilities for adjusting the chemical, physical and mechanical properties of PEM films have fostered studies on the influence of these parameters on cellular behaviors. Importantly, PEM have emerged as a powerful tool for immobilization of biomolecules with preserved bioactivity.

1. Introduction

Controlling the bulk and surface properties of materials is a real challenge for bioengineers working in the fields of biomaterials, tissue engineering and biophysics.

In the field of implantable biomaterials, the bulk properties of materials are known to be important for the overall properties, especially for mechanical strength, but their surface properties have long been recognized as being of utmost importance. [3] The surface of the material is an interface between the material and the host tissue and is able to trigger a wide variety of processes, from the initial inflammatory reaction to ultimate tissue remodeling. Considerable efforts are thus currently devoted towards functionalization of the surfaces of biomaterials used in biomedical applications (typically metals, polymers, ceramics) in order to render them bioactive, i.e. able to trigger a specific cell response.[4] Polymeric coatings appear especially interesting due to the diversity of the chemical and physical properties they offer. For instance, polymeric coatings have recently been employed for the coating of stents. [5] Natural biopolymers appear promising as biomimetic coatings, due to their natural similarity to human tissues. Lots of efforts are thus dedicated to engineering new forms of biomimetic surfaces. Tissue engineering has grown as a field in its own: its aim is to use a combination of cells, engineering and materials, and, together with suitable biochemical and physico-chemical factors, improve the biological functions of damaged

tissues (bone, cartilage, blood vessels, skin…) or replace them.[6] Here, a scaffold in combination with cells and appropriate biochemical signals are needed to trigger a specific cell response and lead to formation of a new tissue. Synthetic polymeric materials can be employed as scaffolds when mechanical strength is needed and hydrogels can be used for soft tissues.[7] Thus, surface modification of the scaffold may provide it with new functionalities.

Lastly, for more fundamental studies on cellular processes, biophysicists have already developed several tools to control the important properties of surfaces: spatial presentation of extracellular matrix proteins has been designed using microtechnologies to constrain cells in specific areas,[8],biochemical adhesive ligands have been grafted to surfaces in controlled amounts,[9] and more recently, the mechanical properties of the substrate have also been recognized as playing a key role in cell adhesion [10] but also in cell fate.[11] Developments are now dedicated to the combined presentation of several stimuli and to the presentation of new types of biochemical ligands playing a role in cell fate, such as growth factors.[12] This would also help to investigate possible synergies between intracellular signaling pathways. Also, the presentation of biochemical stimuli is traditionally performed for cells grown on stiff substrates such as tissue culture polystyrene or glass. Now, the aim is to present them from softer, more physiological substrates.

Several techniques have thus been developed to design thin films at the molecular level, including Langmuir-Blodgett (LB) and self-assembled monolayers (SAMs). As already indicated by Kotov in his review,[13] both present a certain number of limitations and disadvantages. For biological applications, there was thus a need for easier and more versatile deposition methods. The layer-by-layer (LbL) deposition method, introduced by Moehwald, Decher and Lvov 20 years ago, consists in the alternate adsorption of polyelectrolytes that self-organize on the material's surface, leading to the formation of polyelectrolyte multilayer (PEM) films.[1; 2] The procedure is simple and versatile, as it is possible to control the processing parameters to modulate film growth and internal structure. Thus, the nature of the polyelectrolytes, the nature and number of the functional groups, pH and ionic strength during assembly [14] and the substrate used to build the films can be carefully chosen.[15] PEM film fabrication can be performed under mild conditions in an aqueous environment, which is a great advantage when using biopolymers and bioactive molecules. Film growth can be more or less rapid and films can be either stratified or can exhibit some interdiffusion, which makes it possible to use them either as barriers [16] or as compartments for the loading of bioactive molecules.[17]

Importantly, as will be shown below, PEM films appear highly suitable for immobilization of biomolecules with preserved bioactivity. They have emerged as a new type of coating, besides the more traditionally employed self-assembled monolayers and Langmuir-Blodgett films. [18] In fact, the most problematic are probably the limited amounts of biological molecules incorporated into Langmuir-Blodgett films due to their limited stability. For self-assembled monolayers, these are monolayers and there is a need for the presence of thiols on the substrate (e.g for only noble metals or silane) in order to deposit them. For PEM films, no expensive equipment is required. In addition, surfaces of various chemistry and shape have already been coated with PEM films.[19] As will be shown below, one of the great advantages of the PEM technology is also its ability to preserve the bioactivity of biological molecules and the possibility to deliver large amounts of biomolecules.

For all these reasons, there have been considerable developments in the past 5 years in the field of PEM for biomedical applications. Several reviews that include the biological field have been published recently. They concern either the internal structure of the films [15; 20; 21; 22] or the applications of PEM films at the nanoscale.[23] These applications can be for controlled erosion using biodegradable polymers, [24] protein inspired

nanofilms, [25] biosensors and biomimetics [13] and drug delivery.[26; 27]

In this review, we focus our attention on the design of PEM films as surface coatings for applications in the field of biomaterials, tissue engineering and for fundamental biophysical studies. This will include a survey of the chemical and physical properties that have emerged as being key points in relation to biological processes. The numerous possibilities for adjusting the chemical, physical and mechanical properties of PEM films have fostered studies on the influence of these parameters on cellular behaviors.

We will include the different possibilities for controlling cell behavior by means of film composition, presentation of bioactive molecules, and modulation of mechanical properties. We will focus here on processes that require cell adhesion and will not review the potentiality offered by PEM films in cell transfection [28] or as anti-microbial coatings.[29] Also, due to limited space, we will not review other interesting aspects of controlling cellular processes through spatial organization of cell adhesion. Spatio-temporal control offers other possibilities [19] that may open up new applications for PEM films that will be presented below.

Through selected examples from the recent literature, we will show that PEM films have truly emerged as a promising tool for the confinement of bioactive molecules, while preserving their bioactivity and delivering them locally. Very interestingly, these can be achieved via specific non covalent interactions. By combining the different types of properties of PEM films, it is thus possible to control the early steps in cell adhesion but also longer time scale processes such as cell differentiation and tissue formation. Last but not least, the controlled presentation of bioactive molecules to cells by means of the engineered PEM films offers a new tool for biophysicists who are interested in unraveling the subtle interplay between cell adhesion receptors, growth factor receptors and mechano-transduction pathways.

2. Role of film composition

2.1. Films made of synthetic polymers

2.1.1. Case of (PSS/PAH) films

Synthetic polyelectrolytes such as poly(styrene sulfonate) (PSS, a strong polyelectrolyte), poly(acrylic acid) (PAA) or poly(allylamine hydrochloride) (PAH) have been widely used in cell/film studies. The main advantage of using synthetic polymers is the possibility of adjusting certain parameters, including ionic strength and assembly pH, to a considerable degree. Furthermore, they are easy to modify chemically. In this case, initial cell adhesion is mostly mediated through electrostatic interaction (i.e. non specific) and, more indirectly, via serum proteins adsorbed on to the films.

The most frequently studied synthetic PEM is, by far, linearly growing and dense (PSS/PAH) film. Its thickness can be precisely varied from a few nanometers to a few tens of nanometers [30]. Cell types such as endothelial cells, [31] fibroblasts, [32; 33; 34] osteoblastic cells,[35] and hepatocytes [36] have been cultured on these films. As a general rule, adhesion and proliferation on these films are very good. This may be attributed partly to the presence of sulfonate groups. (PSS/PAH) can be coated on the inner side of cryoperserved arteries [37] (Figure 1). This improved the mechanical properties of the cryopreserved vessel. It also made possible the adhesion and spreading of endothelial cells so that the internal structure of the vessel resembles that of fresh arteries. By looking at the expression of specific endothelial markers, namely PECAM-1 and von-Willebrand-factor (vWF), the authors proved that the phenotype of the endothelial cells was preserved. In a subsequent study of the same group, PEM-treated arteries (rabbit carotids) as grafts bypassed native (untreated) rabbit carotids.[38] The *in vivo* evaluation of cryoperserved human umbilical arteries treated with (PSS/PAH) multilayers demonstrated a high graft patency after 3 months of implantation. Such modified arteries could constitute a useful option for small vascular replacement.

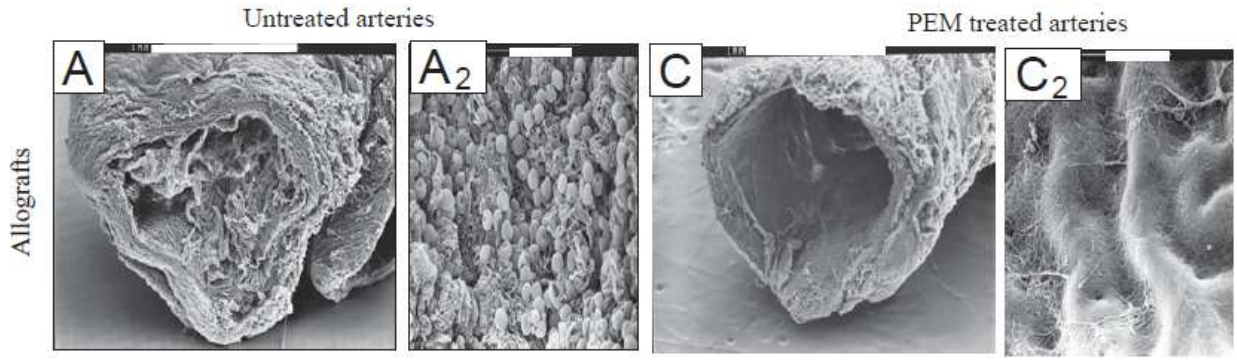

FIGURE 1. Scanning electron microscopy images of untreated and PEM-treated explanted arteries *A) were occluded and with pervasive thrombus (A2) after 1 week of implantation When the artery was treated with a (PSS/PAH) film (C), the internal surface of the treated arteries (C2) showed no adherent cells and platelets. After 12 weeks, the treated internal artery surfaces (E2 and F2) showed a similar morphology to the native carotid internal surface (images not shown). Original magnification 400 (A and C) and 1,000 (A2 and C2) (adapted from Journal of the American College of Cardiology Vol. 52, No. 19, 2008 © 2008, ref 33.), copyright Elsevier 2008).*

In another study, the same group investigated the differentiation potential of endothelial progenitor cells (EPCs), which are currently seen as very promising cells in tissue engineering for the design of autologous vascular grafts. Very interestingly, a rapid differentiation of endothelial progenitor cells (EPCs) into confluent mature endothelial cells was observed on (PSS/PAH) multilayers, which was higher than on conventional surfaces.[39] Indeed, the time needed to obtain these mature cells was reduced from two months to two weeks. Very recently, human mesenchymal stem cells (MSCs) were also found to differentiate into endothelial-like cells after only two weeks of culture on the (PSS/PAH) films, as shown by the expression of PECAM-1 and vWF. Thus, (PSS/PAH) films appears to have potential for vascular tissue engineering.

Recently, also using human MSCs, Guillaume-Gentil et al. showed that (PSS/PAH) films on conductive indium tin oxide (ITO) electrodes can be used as a platform for growing viable cell sheets.[40] In this study, films made of nine layer pairs ending with PSS and of ~20 nm in thickness were used. The resulting stem cell sheets retained their phenotypical profile and mesodermal differentiation potency. The authors showed that both electrochemically-induced local pH lowering and a global decrease in the environmental pH resulted in a rapid detachment of intact stem cell sheets. Furthermore, they evidenced that the recovered stem cells sheets recovered maintained their capacity to differentiate toward the adipogenic and osteogenic lineages.

2.1.2. Other PEM films made of synthetic polyelectrolytes

Another type of popular PEM assembly is the (PAA/PAH) system, which was initially developed by Rubner's group.[41] The thickness of these films can be varied by changing the pH of the assembly.[14] Interestingly, the topography of such films can be modified by post-treatment in acidic solution to render them either nanoporous or sub-microporous.[41] Rajagopalan *et al*. [42] investigated the potential of such films for wound healing in the cornea using corneal epithelial cells as cellular models, as the epithelium presents a physical barrier to external agents. During wound healing, corneal epithelial cells undergo proliferation and migrate to the wound site. In their study, they created pore diameters in the 100–600 nm range by post-treatment of (PAH/PAA) films in solutions of pH ranging from 1.9–2.5 range. Porous surfaces that exhibited either 100 nm or 600 nm pore diameters supported corneal cell adhesion, but the nanoscale porosity significantly enhanced corneal epithelial cellular response. Corneal epithelial cell proliferation and migration speeds were significantly higher on nanoporous topographies. The actin

cytoskeletal organization was well defined and vinculin focal adhesions were found in cells presented with a nanoscale environment. These trends prevailed for fibronectin(FN)-coated surfaces as well suggesting that for human corneal epithelial cells, the physical environment plays a defining role in guiding cell behavior. Of note, FN is a cell-surface protein, which is a very important component of the ECM as it mediates cellular adhesive interactions.

2.2. Films made of natural polymers

Tissues are composed of cells embedded within an extracellular matrix (ECM) made of proteins, polysaccharides, and other bioactive molecules such as growth factors. ECM provides the cells with mechanical and biochemical signals.

ECM proteins, polysaccharides or their fragments can be used in PEM construction to promote cell adhesion and proliferation. Entire films can be made of ECM components; ECM molecules or their fragments can be adsorbed on the film's surface or covalently linked, respectively. A step closer to recreating the original matrix in which cells develop *in vivo* is to use ECM components as building blocks for the films.

Natural biopolymers, such as collagen (COL), [43; 44] gelatin,[45; 46] hyaluronan (HA) [47; 48], chondroitine sulfate (CS) [49 50] or heparin (HEP) [51; 52] can be used as building blocks for PEM films. This type of PEM film provides compositional uniqueness such as stimulating a specific cellular response and serves both as mechanical and biochemical signals.

Type I collagen is a major protein component of fibrous connective tissues, which provides mechanical support and frameworks for the other tissues in the body. Collagen is a natural ligand for several cell receptors in the integrin family. Gelatin is a partially hydrolyzed and denaturated form of collagen.

HA, CS and HEP belong to the family of glycosaminoglycans, which is made of disaccharide repeating units containing a derivative of an amino sugar, either glucosamine or galactosamine. They contain a negatively charged carboxylate and/or sulfate groups. HA and CS are responsible for the unique hydration and mechanical properties of synovial fluid, cartilage and tendons. HA and CS are highly hydrated polymers surrounded by respectively ~20 and ~30 water molecules per disaccharide unit in interaction through hydrogen bonds [53]. Importantly, these polysaccharides are part of the pericellular coat (also called glycocalyx). This coat, which can be up to several μm in thickness,[54] plays a major role in the interactions between a cell and its environment by mediating cellular adhesion and the diffusion of biomacromolecules such as growth factors.[55] HEP has several possibilities for sulfate groups. Some forms act as anticoagulants by binding specifically to antithrombin, which accelerates the sequestration of thrombin. This is why HEP is often used as an anti-coagulant.

In an early study, gelatin was associated with polyethyleneimine (PEI) and deposited on a synthetic degradable poly(DL-lactide) substrate.[56] Chondrocytes were found to attach and proliferate, and their viability was good on these PEM-modified scaffolds.

Gelatin was also associated with chitosan (CHI), a polysaccharide that is not present in the human body but can be found in crustacean shells, and deposited on to titanium films.[46] Here, the authors showed that the proliferation and viability of osteoblast cells on the PEM-modified titanium substrates were better than on control surfaces after one and 7 days of culture *in vitro*.

COL has been associated with HA to build (COL/HA) films.[44] Interestingly, the fibrillar structure of collagen was preserved as observed by AFM imaging of the films. The authors showed that chondrosarcoma cells spread well and synthesized the extracellular matrix components solely on the collagen ending films, whereas no cellular matrix was found for those ending with HA.

The introduction of HEP into PEM films is often applied to coatings of blood-contacting biomaterials. In fact, endothelialization and antithrombogenicity are two key issues in stent implantation. Heparin was initially introduced with PEI.[57] Recently, (COL/HEP) films have been employed as titanium coatings to study endothelial progenitor cell (EPC) attachment and proliferation.[58] *In vitro*, the (COL/HEP)

greatly increased EPC attachment and proliferation as only 3 days were required to form a confluent layer. Furthermore, platelet adhesion was found to be reduced on such coatings.

As CS is an important component of cartilage and bone tissues, the adhesion of bone cells to (CS/HEP) coatings was recently investigated.[59] When CS was used as a film component, the films displayed a low Young's modulus and cell adhesion was poor. However, the cells responded differently when CS was adsorbed on to a stiffer polypeptide PEM basis. Similar films made of (COL/HEP) and (COL/CS) were recently built on poly(dimethylsiloxane) (PDMS) substrates,[60] with COL retaining its fibrillar structure. Whereas (COL/CS) films were stable in culture medium, (COL/HEP) were not. Primary bovine chondrocyctes were found to adhere better on PEM films than on tissue culture polystyrene. Interestingly, these authors showed that □1 integrin antibodies prevented cell spreading, suggesting that cell adhesion and spreading were specifically mediated by interactions with the collagen fibrils.

One advantage of these natural components is their ability to specifically interact with living cells, their bioavailability and their possible biodegradability, as specific enzymes are present in tissue and biological fluids.

2.3 Role of the final layer: surface charge and hydrophobicity

As PEM films are 2D materials, not only their entire composition, but also their surface composition is important. Surface charge can affect protein adsorption (depending on the pI of the protein) and ultimately cell adhesion. The typical functional groups of the polyelectrolytes are carboxylic acid, sulfate, sulfonate as negatively charged groups and amine as positively charged groups. In the case of synthetic polyelectrolytes, PAA-ending films (carboxylic group) were found to be resistant to the adsorption of BSA, fibrinogen or even to lysozyme, which is oppositely charged to PAA.[61] This was explained by the low charge density of PAA but also by its strong hydration, which creates an exclusion volume above the PAA layer. Usually, proteins adsorb preferentially on to films of opposite charge.[61; 62; 63] For instance, PAH-terminated films lead to a very high adsorption of proteins from the serum [64]. On PSS-ending films, certain serum proteins present in the cell culture medium, such as BSA, adsorb weakly [65] and may be implicated in the cell response to PSS-ending films.

However, it now seems to be accepted that protein adsorption alone cannot account for the significant differences in cell adhesion.

Depending on the cell type, cell may prefer positively or negatively charged film-ending layers. For instance, hepatocytes grown on the films made from synthetic polymers poly(dimethyldiallylammonium chloride) (PDDA) as polycation and PSS[66] adhered only to the films terminated with a PSS layer, and not to PDDA-ending films. However, other cells lines, such as fibroblasts, were less sensitive and adhered on both the PDDA and PSS-ending films.

In a different field of application, the differentiation potential of myoblast into myotubes was assessed recently.[67] The authors first investigated the growth of myoblasts on PSS or PAH-ending films with PSS of different molecular weighs. They found better viability and growth on PSS-ending films but observed that there was no difference for PSS of different molecular weights. They also followed differentiation into myotubes over 7 days and observed it was more effective on PSS-ending films, as assessed by the higher fusion index. The molecular weight of the PSS had no influence.

Hydrophilicity/Hydrophobicity are also known to influence protein interactions with the surface and cell adhesion as well. Synthetic polymers were employed by Salloum *et al*. for investigating the combined effects of increasing surface charge and hydrophobicity [68] on vascular smooth muscle cell (SMC) adhesion. On the most hydrophobic surfaces, the A7R75 SMCs spread and were not very motile. Conversely, on the most hydrophilic surfaces, these cells adhered poorly and displayed characteristics of being highly motile.

It was shown that surface wettability, surface charge and lateral structures could be controlled by changing the pH value of the HEP solution to acidic, neutral or alkaline values during multilayer assembly of PEI and HEP multilayer films, resulting in modulation of fibroblast adhesion.[69] All terminal layers were cytophobic, unless pre-adsorption of serum or of FN was achieved. The effect of the serum was more prominent on PEI final layers, probably due to their positive surface charge, whereas the effect of FN was more pronounced on HEP terminated multilayers, possibly due to its ability to bind FN specifically. The PEM films that were initially non adhesive were also found to inhibit fibroblast growth. On the contrary, those favoring cell adhesion also induced higher cell growth and metabolic activity.

To conclude, surface charge and hydrophobicity of PEM films can have a significant impact on cell adhesion, in a manner that depends on the nature of the functional groups and on the cell types, as well.

2.4 Influence of film thickness

Some films are known to grow linearly over a wide range of conditions, whereas other PEM films grow exponentially. This is the case for (PLL/PGA)[70], (PLL/HA)[71] and (PLL/CSA)[49] films built in physiological conditions (pH 7.4, 0.15 M NaCl). Film thickness is related to the ability of the polyelectrolyte to take up water, to the charge matching of the polyelectrolyte pairs and to the affinity of the polyelectrolytes for each other [15]. Usually, PEM films made from highly hydrated polysaccharides and polyaminoacids yield gel-like films. In such cases, the films are very soft and hydrated, and cells adhere poorly to them.[72; 73; 74] On the contrary, as mentioned above (*see 2.1.1.*), cell adhesion is usually good (PSS/PAH) films exhibiting linear growth.

Film thickness can also be modulated by pH variations during film assembly, one of the best characterized PEM films in this category being (PAH/PAA) films. Rubner's group has plotted the film thickness matrix as a function of the pH of each polyelectrolyte solution ,[14] with thick films being formed when the pH of PAA is close to 2, while highly stitched and dense films are formed at neutral pH. (PAH/PAA) films were found to be non adhesive when films were built at pH 2 (thick films), whereas high adhesion was observed for films built at pH 6.5. This was attributed to the ability of the former films to swell. [75; 76]

3. Modulation of film mechanical properties

It is increasingly accepted that cell processes depend on the reciprocal and dynamic interactions of cells with their surrounding microenvironment, which include biochemical and mechanical stimuli defined by neighboring cells and extracellular matrices.[77] Cells are mechano-sensors known to transduce a mechanical signal into a biochemical signal, or *vice versa*. Specific proteins are known to play a key role in this process and among those are integrins. Integrins are trans-membrane receptors that exhibit conformational changes in response to mechanical stimuli.[78] Some components of the adhesive structures of the cells that are formed during adhesion (e.g focal adhesions) can also exhibit conformational changes and transducer forces. Many cell types are sensitive to the mechanical properties of the underlying substrate and respond by increasing their adherence, spreading and proliferation.

In a pioneer study by Discher's group, decoupling (or independent adjusting) of the mechanical and chemical properties has been achieved, using model synthetic gels such as polyacrylamide gels grafted with COL at increasing densities.[79] The same group showed that altering polyacrylamide gel stiffness made possible MSC differentiation into neurons on soft PA gels, bone cells on stiff gels that mimicked collagenous bone,[11] and myoblasts for gels of intermediate stiffness. Other types of synthetic and natural polymeric materials with controlled mechanical properties have been developed, such as poly(ethylene glycol),[80; 81] PDMS, alginate [82] or hyaluronan.[83]

Although a full decoupling of mechanical and chemical properties is the ideal goal, this is in

fact very difficult to achieve. There are several reasons for this: first, many of the cross-linking strategies are based on a chemical modification of the material. Second, biochemical ligands are added by grafting it or by adsorbing it. Grafting involves a chemical modification at the surface of the material and adsorption, which relies on non covalent interactions, is a natural process that depends on the physico-chemical properties of both the material and the protein.

PEM films are materials whose mechanical properties can be controlled in several ways, thus allowing cell studies on the films of different stiffnesses.

Different strategies employed for modulating the mechanical properties of PEM films have already been reviewed recently: adding "stiff" layers,[84] modulating pH during assembly [85], chemical cross-linking by means of glutaraldehyde [86] or by means of a carbodiimide,[72] photo-crosslinking using photosensitive derivatives of the polyelectrolytes,[87; 88] or incorporating nanoobjects into the film.[89] (Figure 2)

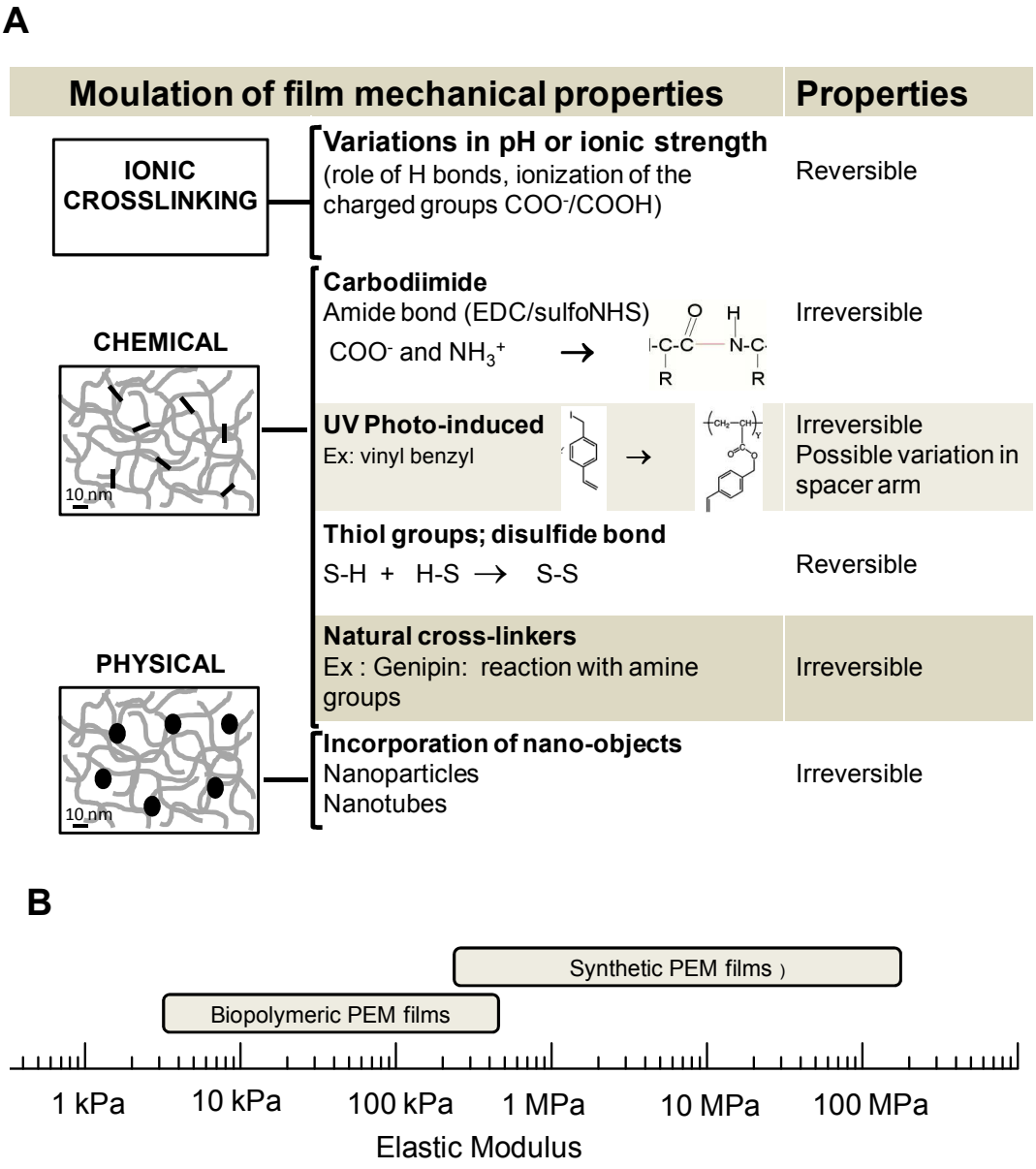

FIGURE 2. *(A)* ***Overview of the main strategies used to modulate mechanical properties of polyelectrolyte multilayer films.*** *The methods are essentially based on ionic cross-linking, chemical cross-linking and physical cross-linking. (B) Range of stiffnesses of the natural and synthetic polyelectrolyte multilayer films.*

As mentioned by Sukhishvili *et al.* [27], cross-linking is often applied to convert PEM films into "surface hydrogels". Often, soft and hydrated films do not exhibit stratification but what is required here is rather a change in their "bulk" properties. The film is seen as a "surface adsorbed hydrogel" whose confinement provides it with very interesting properties for local changes in biochemical and mechanical properties. Of note, this modulation in mechanical properties over one or two orders of magnitude in Young's modulus can only be achieved if the film's stiffness in uncrosslinked conditions is sufficiently low.

3.1. Adding "stiff" layers

For instance, (PSS/PAH) films are already so stiff (Young's modulus of up to 100 MPa) that nobody has tried to stiffen them even more. Instead, they can be employed as a rigid barrier to stiffen (PLL/HA) films.[84; 90] Thus, by adding several layer pairs of (PSS/PAH) on to the (PLL/HA) basis, Vautier *et al.* [90] have shown that the adhesion of kidney epithelial cells progressively increased when the films become stiffer. In a very elegant manner, they have studied the influence of substrate elasticity on replication and transcription, using such PEM films as model substrates. The sequential relationship between Rac1 (a very important protein involved in cytoskeletal changes), vinculin adhesion assembly, and replication becomes efficient at above 200 kPa because activation of Rac1 leads to vinculin assembly, actin fiber formation and, subsequently, to the initiation of replication. Above 50 kPa, transcription was correlated with the engagement of a specific integrin (□v-integrin) together with histone H3 hyperacetylation and chromatin decondensation, allowing little cell spreading. In contrast, soft substrates (below 50 kPa) promoted morphological changes characteristic of apoptosis, including cell rounding, nucleus condensation, loss of focal adhesions and exposure of phosphatidylserine at the outer cell surface.

3.2. Modulating pH during assembly

As shown by Van Vliet *et al.*, the stiffness of (PAH/PAA) films assembled at different pH can be varied from 200 kPa to 142 MPa and can affect cell function.[85] They showed that the adhesion and proliferation of human microvascular endothelial cells strongly increased as the PEM became stiffer.[85] In a recent work, the same group adjusted independently the mechanical and chemical properties of films by modifying the film's surface with COL I or a mixture of COL I/decorin and studying primary hepatocyte adhesion and functions. These cells are widely considered to be ideal for constructing liver tissue models but are known to rapidly (within a few hours or days) lose their viability and phenotype functions upon isolation from the native *in vivo* microenvironment of the liver. They found that, on unmodified (PAH/PAA) surfaces, hepatocyte attachment increased with PEM rigidity,[91] but this trend was canceled when the PEM substrata was modified with COL I or with COL I pre-mixed with the small proteoglycan decorin. They also demonstrated that hepatic albumin secretion (a marker for liver-specific protein synthesis) over two weeks decreased with increasing substrata stiffness, correlating that hepatocytes formed stable, spheroid aggregates preferentially on protein-modified compliant surfaces, whereas cells detached from stiffer substrata after only a few days of culture. Such detachment was presumably due to the dominance of cell–cell over cell–substrata interactions.[91]

3.3. Chemical cross-linking

Chemical cross-linking by means of carbodiimide chemistry has been applied to various PEM films and quantified by means of infrared spectroscopy and AFM nano-indentations [92]. Amine and carboxylic groups are converted into covalent amide bonds [72] in the presence of 1-Ethyl-3-(3-dimethylaminopropyl) carbodiimide (EDC). Chondrosarcomas and chondroytes,[93] osteoblasts,[74] have been found to adhere more when the (PLL/HA) or (PLL/PGA) film [74] stiffness is increased. For SMCs,[94] and skeletal muscle cells,[95] [19] an increase in cell spreading on (PLL/HA) cross-linked films as well as on (PAH/PGA) cross-linked films was observed.

Recently, the behavior of two different types of stem cell was investigated on (PLL/HA)

cross-linked films: MSCs and embryonic stem cells (ESCs). MSCs represent a particularly interesting cell type for research and therapy because of their ability to differentiate into mesodermal lineage cells such as adipocytes, osteocytes, chondrocytes, cardiac muscle, or endothelial cells.[96] Zisch *et al.* observed that native (PLL/HA) (e.g. uncrosslinked) showed poor adhesion for MSCs despite a high surface density of preadsorbed FN.[97] However, MSC adhesion and proliferation was very good on cross-linked (PLL/HA) films. Covalent attachment of FN was necessary to maintain the MSC over weeks for their differentiation. Furthermore, the MSC were capable of differentiating into osteocytes and chondrocytes upon culture with induction factors.

The behavior of ESCs on (PLL/HA) films has also been investigated. ESCs are derived from the inner cell mass (ICM) of the blastocyst at an early stage of embryonic development following the segregation of the embryo into the ICM and the trophectoderm.[98] Blin *et al*. showed that ESC adhesion and proliferation increased on stiffer films. ESCs were also shown to keep their pluripotency when grown on native nanofilms, which prevented their adhesion. Their phenotype was more reminiscent of the ICM stage of embryogenesis. Furthermore, cells grown on native (PLL/HA) films exhibited a better potential for differentiation than cells grown on cross-linked films. These latter cells reached the epiblast stage, which had a more limited repertoire of differentiation.
The chemistry of the native film played an important role in the maintenance of ESC pluripotency. In fact, the native films, but not cross-linked ones, released a small amount of PLL, which was sufficient to induce the expression of ICM genes for ESC cells.
This very small release may be related to the mechanical properties of the native (PLL/HA) film. Indeed, reflection interference contrast microscopy and confocal laser scanning microscopy experiments have evidenced that native (PLL/HA) film is rather a viscoelastic liquid whose equilibrium elastic modulus is zero.[99] This was not observed for EDC-crosslinked films.

3.4. Photo-crosslinking

Photo-crosslinking is another way of modifying a film's mechanical properties after film buildup, provided that one of the polyelectrolytes has a photo-sensitive group.[87] Pozos-Vasquez *et al*. also reported on the preparation of polyelectrolyte films based on PLL and HA derivatives modified by photoreactive vinylbenzyl (VB) groups.[88] The VB-modified HA incorporated into the films was cross-linked on UV irradiation and the force measurements taken by atomic force microscopy proved that the rigidity of the cross-linked films increased up to four times. Adhesion of myoblast cells increased on the stiffest films.

These research papers, studying different cell types on different PEM films, highlight on the one hand the strong dependence of cell processes on both the mechanical and chemical properties of the substrata, and, on the other, the difficulties for decoupling these two distinct properties. Thus, care is needed when concluding from the respective roles of these factors, that they are often correlated.

3.5. Incorporating nanoparticles

Incorporating nanoobjects into an organic matrix is another way of stiffening it, and has already been widely applied to PEM films [100; 101]. Different types of nanoobject have been introduced as film components, including carbon nanotubes [102] [100] and montmorillonite, [103] Evaluating the mechanical properties of these composite films displayed up to 2 orders of magnitude more on Young's modulus when compared with the pure polyelectrolyte.[104] The mechanical properties also depend on the non aggregated or aggregated state of the nanoparticles [105]. Such composite assemblies with interesting mechanical and electrical properties appear particularly interesting for the coating of neuroprosthetic devices .[106] In a first study, Kotov *et al*. showed that thin PEM membranes containing single-walled carbon nanotubes (SWNT) supported extensive neurite outgrowth.[100] Later on, the same group demonstrated that mouse embryonic neural stem cells (NSCs) could be successfully differentiated into neurons, astrocytes and oligodendrocytes with clear formation of

neuritis on the PEI/SWNT multilayer films.[89] NSCs behaved similarly to those cultured on the standard and widely used poly(L-ornithine) substratum in terms of cell viability, development of neural processes, and appearance and progression of neural markers.

More recently, synthetic PEI was replaced by the protein laminin, which is an important component of the extracellular matrix of the brain, to "humanize" the carbon nanocomposite film [107]. The authors found that the adhesion of NSCs up to 7 days in culture depended on the outermost layer and on the post-treatment (heating at 300°C for a very short time) (Figure 3). The (SWNT/laminin) nanocomposites did not support cell adhesion, unless they were stiffened by heating. The substrate that was most conducive to cell adhesion and attachment was the PEM film that contained SWNT as the topmost layer and that was heat treated. Extensive formation of functional neural networks was observed as indicated by the presence of synaptic connections. Importantly, 98% of the cells were found to remain viable. Immuno-staining of specific neuronal markers MAP-2 (for neurons), glial fibrillary acidic protein, GFAP (for astrocytes), and nestin (for NSCs) were performed after 7 days of culture. Interestingly, it was found that differentiated neurons and glial cells were present in large amounts due to spontaneous differentiation caused by the physical properties of the SWNT/laminin composites. Furthermore, calcium imaging of the NSCs revealed generation of action potentials upon the application of a lateral current through the SWNT substrate. All together, these results appear very promising as they indicate that the protein-SWNT composite can serve as the material foundation of neural electrodes with a chemical structure better adapted to long-term integration with the neural tissue.

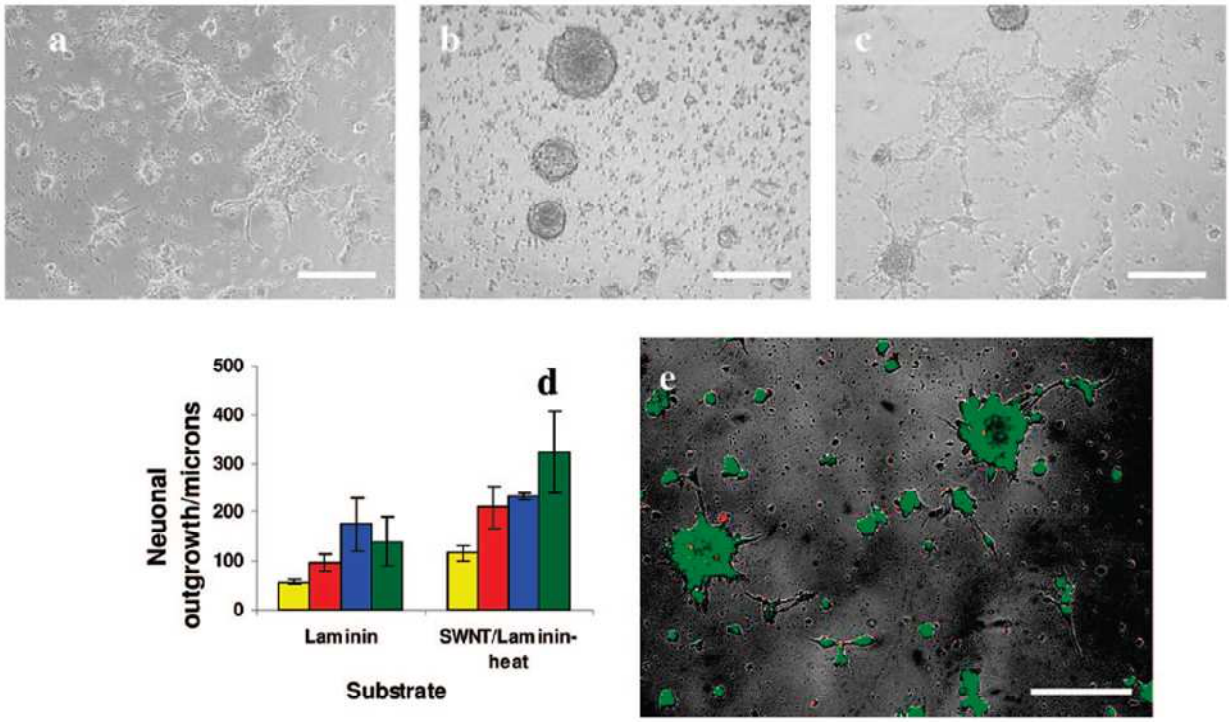

FIGURE 3. Micrograph assessing neural stem cell adhesion and differentiation *72 h after initial seeding on (a) laminin-coated glass slides and on 10 bilayers SWNT/laminin thin films that were (b) used as is or (c) heated at 300 °C for 10 min. (d) Distance of outgrowth from neurospheres after 24 h (yellow), 48 h (red), 72 h (blue), and 120 h (green) on laminin-coated slides and heat-treated SWNT/laminin film on slide. (e) Live-dead viability assay on seeded cells where live cells are stained green and dead cells are red. Scale bars are 200 μm (reproduced with permission from ref Kotov et al, Nanoletters 2009, copyright ACS 2009).*

3.6. Modeling the cell response

There are still only a few models of cell interactions with PEM films. In a recent model of cell adhesive behavior on thin polyelectrolyte multilayers, Chan *et al.* [108] implemented a finite element analysis to help elucidate the trends observed in cell spreading, e.g. decreased cell spreading when the number of layer pairs in the film was increased (for very thin films of less than 100 nm in thickness). The authors correlated the focal adhesion area to the amount of work done by the cell during active mechanosensing. The film was modeled as a linear elastic material. An "effective stiffness" was defined to account not only for its mechanical properties but also for its thickness and for the number of focal adhesions recruited. Their results suggest that the energy consumed by the cells during active probing with a constant adhesion force regulates cell morphology and adhesion behavior.

Further modeling of cell/film interactions may help to better understand the role of various parameters in cell response.

4. Biochemical functionalization

Biochemical functionalization can be achieved in order to activate a specific cellular signal. Presentation of a biochemical signal by the PEM films allows this signal to be spatially controlled at the cell adhesion site. The biochemical signal can also be potentially sustained for a long time period. Different strategies may be employed (Figure 4).

4.1. Modification by ECM molecules

4.1.1. Adsorption of entire ECM proteins on PEM films

To improve cell adhesion on PEM films, adsorption of ECM proteins (Figure 4A) on to multilayers is a useful tool, usually achieved using COL or FN as adhesive proteins. These proteins are widely used by biomaterial scientists,[109; 110], biophysicists [79] and biologists [111] as they are important ECM proteins and probably the best characterized. The aim is to provide specific attachment to the cells via integrin receptors.

Wittmer *et al.* [36] investigated the effect of various parameters on the attachment and function of three different types of hepatic cell, human hepatocellular carcinoma (HepG2) cells, rat hepatocytes and human fetal hepatoblasts. To this end, they chose different types of PEM film, such as (PAH/PSS), (PLL/PGA) or (PLL/ALG) films and systematically studied the influence of composition, terminal layer, and rigidity (using EDC cross-linked films, see 3.3). They also investigated the influence of a terminal layer of COL I or COL IV, a prominent extra-cellular matrix protein within the human liver parenchyma. In a first step, they studied cell attachment and growth over a 7-day period and in a second step, they quantified albumin secretion of the confluent systems. Importantly, all the PEM systems produced albumin, indicating the presence of functional hepatoblasts and/or hepatocytes. The cross-linked $(PLL/PGA)_n$-PLL films promoted the greatest level of function at 8 days. From the large set of conditions they studied, they conclude that film composition, terminal layer, and rigidity are key variables in promoting attachment and function of hepatic cells, while film charge and biofunctionality were somewhat less important.

Using (PAH/PAA) films as a matrix for hepatocyte attachment, Van Vliet *et al.* showed that adsorption of COL on the softest films (PEM built at pH 2) led to enhanced hepatocyte attachment, which was statistically similar to the stiffer, unmodified and protein-modified substrata.[91]

The effect of FN adsorption on to PEM films has also been investigated in some specific cases. For instance, Olenych *et al.* [76] found that FN bound best to PAH-terminated and Nafion-terminated PEMUs, but poorly to PEM films terminated with a copolymer of PAA. A7r5 smooth muscle cells were found to adhere and spread well on the Nafion-terminated PEMU surfaces. In contrast, cells spread less and migrated more on both FN-coated and uncoated PAH-terminated PEM surfaces. Interestingly, these results indicate that A7r5 cell adhesion, spreading, and motility on PEMUs can be independent of FN binding to the surfaces.

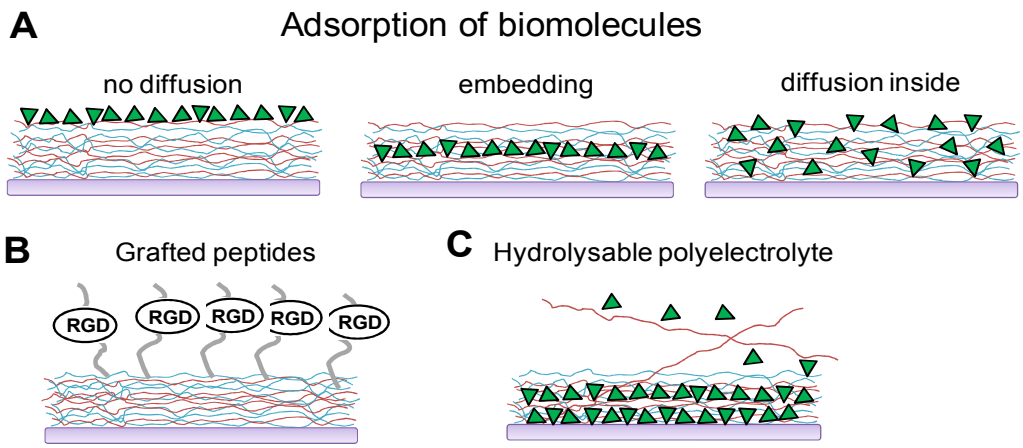

***FIGURE 4**. Scheme representing different possibilities of incorporing bioactive molecules inside or on top of PEM films. (A) Adsorption of the bioactive molecule can be achieved after film buildup or at a certain step during build up. In case of diffusion, the bioactive molecule can be loaded in the "bulk" of the film; (B) Very small molecules such as bioactive peptides can be grafted to one of the polyelectrolytes; (C) if one of the components is hydrolysable, then the bioactive molecule can be delivered in solution.*

Using (PLL/dextran sulfate) PEM films, Wittmer *et al.* [112] also showed, by means of quantitative measurements of FN adsorption, that FN adsorption on PLL-terminated films exceeded that on dextran sulfate-terminated films by 40%, correlating with the positive charge and lower degree of hydration of PLL terminated films. They followed the attachment of endothelial cells (human umbilical vein endothelial cells) and found that PLL-ending films exhibited a greater extent of cell spreading than dextran sulfate-ending films. Furthermore, adsorption of FN led to an increase in cell spreading. For these PEM films, they concluded that the presence of FN was an important factor, more than film charge or layer number, in controlling the interaction between multilayer films and living cells.

Based on all these studies, it appears that it is not possible to draw a unique conclusion. In some cases, film composition and mechanical properties can be more important than the biochemical signal provided by the adsorbed ECM molecules. However, in the case of poorly adhesive films (especially soft PEM films), the biochemical signal may compensate and lead to engagement of integrin cell receptors, leading to increased cell attachment and spreading.

It should be noted that solely quantifying the adsorbed amount of protein is not predictive enough of the conformation of the protein on the PEM films. Indeed, conformational changes that occur upon protein adsorption are difficult to assess with quantitative methods due to the low amount of adsorbed amounts. Garcia *et al.* [113] showed that FN conformational changes can be detected by different antibodies recognizing specific protein motifs. Antibody binding also depends on the state of the molecule (stretched *versus* relaxed).[114] Such FN conformational changes can control switching between proliferation and differentiation. Last by not least, other proteins present in a much lower amount in the serum may act in synergy with the pre-adsorbed proteins.

Recently, gold nanoparticles (AuNPs) were used as a tool for depositing cell adhesion proteins, fibronectin and ephrinB3, on top of PEM films.[115] The authors studied cancer cell adhesion and found that it was affected by nanoparticle density, an optimum being observed for an intermediate nanoparticle density. Drastic changes in cell adhesion were observed, with the formation of protractions (lamellipodia and filopodia). Of note, the influence of the nanotopology here was also higher than the influence of the coating of the Au NP. Interestingly, the authors also studied

ephrin signaling by quantifying the expression of paxillin. They found that it was more effective when ephrin B3 was presented from the Au NP than when it was directly attached to the polymer film.

4.1.2. Grafting ECM-derived peptides

Selectivity, i.e. specificity in adhesion, can be achieved by grafting peptides (Figure 4B) that are known to interact with specific cell adhesion receptors, typically integrins. In this case, only short sequences of ECM proteins are considered. The most prominent example is that of the RGD sequence, RGD being a central integrin-binding region in FN and COL, which has already been grafted to polymers using various strategies.[9] Using PEM, two different strategies have been developed. The first consists in grafting the peptide to one of the polyelectrolytes and then adsorbing the modified polyelectrolyte as a regular layer. The synthetic step is thus performed aside from the film buildup. PEM films with poor adhesion are excellent candidates for such functionalization, which was applied using PAH-RGD and PGA-RGD for cell attachment.[74; 116] PGA-RGD added as the outermost layer was shown to have a beneficial influence on osteoblast adhesion and proliferation.[74] Recently, in an elegant work by Werner *et al*.,[117] it was shown that a laminin5-derived peptide grafted to PGA could induce specific cell adhesive structures in epithelial cells called hemidesmosomes and specifically activate β4 integrins. PAH-RGD was also found to increase adhesion on (PAH/PAA) films.[118] The osteoblasts exhibited a better differentiated phenotype on the pH 2.0 films than the pH 6.5 films with respect to calcium deposition. However, incorporation of another peptide (LHRRVKI) known to be a heparin binding domain did not support cell adhesion, growth or matrix mineral deposition.

The second strategy consists in directly coupling the RGD peptide on to the film using the carbodiimide EDC as coupling agent.[119] This was achieved on (HA/CHI) films deposited on titanium. Osteoblast cells adhered and proliferated much better in the presence of the grafted peptide.

Importantly, however, the question has been raised as to whether these chemical modifications in the polyelectrolytes may alter other physical chemical properties such as protein adsorption or mechanical properties, in turn influencing cell adhesion and proliferation. These points were investigated by Thompson *et al*. [120] and Schneider *et al*. [121] who measured the mechanical properties of the films with or without modified polyelectrolytes.

4.2. PEM films modified with growth factors and hormones

Another way to render the films bioactive and induce specific cell responses is to use bioactive molecules like growth factors and hormones that control cell proliferation and differentiation.

4.2.1. Grafting of hormones

A short peptide hormone, α-MSH (alpha-melanocyte-stimulating hormone), with anti-inflammatory properties, has been successfully integrated into multilayer films. Initially coupled with PLL, α-MSH was effective toward melanoma cells that were induced to produce melanocortin.[122] Then, coupled with PGA and introduced into (PLL/PGA) films, it was efficient in annihilating the effect of a bacterial endotoxin that stimulated an inflammatory response in human monocytic cells.[123] The morphology of the monocytes was also affected by α-MSH as the cells formed many “fiber like” protrusions not visible on standard (PLL/PGA) films.

4.2.2. Presenting matrix-bound growth factors

It should be noted that grafting proteins is more difficult to control than grafting peptides, as the protein should not be denaturated during the reaction. In addition, as the precise active site in a protein is not always known, or requires a special 3D conformation, the presence of the full length protein (and not of a peptide sequence) can be required to achieve bioactivity.

Up to now, two major strategies have been employed to provide films with a specific bioactivity using larger molecules such as growth factors (Figure 4A): i) adsorption of

the bioactive molecule as a regular layer. The deposition step has to be carefully chosen depending on the physico-chemical properties of the protein (isolectric point, solubility depending on solution pH and ionic strength). ii) adsorption and possibly post-loading the bioactive molecule in the as-prepared films. Depending on the film's internal structure (thickness, porosity, internal groups and charges), the bioactive molecule may simply adsorb at the film's surface or diffuse in it. Of note, if the PEM film is made of biodegradable polymers, then the bioactive molecule will be delivered in solution (Figure 4C). If it is not biodegradable, the bioactive molecule may partially diffuse out of the PEM film and is delivered to the basal surface of the cell.

Growth factors, i.e. proteins that can control growth and maturation of tissues, cell proliferation, division and differentiation are especially interesting in this respect.
The first strategy was applied for basic Fibroblast growth factor (bFGF or FGF-2), a factor that is involved in cell proliferation and differentiation of a wide variety of cells and tissues. This factor was also deposited with CS by Shen *et al.* [124], who built (FGF-2/CS) films. These authors showed that approximately 30% of the incorporated FGF-2 was released within 8 days. *In vitro* cell culture found that the fibroblasts showed star-like morphology with plenty of pseudopods on the FGF-2 incorporated collagen film after 1 day of culture, and the collagen films assembled with FGF-2 have better bioactivity than that of the virgin one and the FGF-2 control.
The second strategy of adsorption on top of PEM films was also applied to FGF-2 by Tezcaner *et al*.[49] Using (PLL/CSA) films with adsorbed FGF-2, these authors showed that FGF-2 increased the number of photoreceptor cells attached and maintained the differentiation of rod and cone cells.

(CHI/HEP) film construction was recently achieved in the presence and absence of adsorbed FN and FGF-2.[125] The functional response of bone marrow-derived ovine MSCs to these PEM coatings deposited on TCPS and titanium was investigated. These authors found that FGF-2 adsorbed to heparin-terminated PEMs with adsorbed FN induced greater cell density and a higher proliferation rate of MSCs than any of the other conditions tested, including delivery of the FGF-2 in solution, at an optimally mitogenic dose. This effect was observed for PEM-coated TCPS. However, surprisingly, the same effects were not observed when the FGF-2 was delivered from PEM adsorbed on titanium and the response of ovine MSCs to adsorbed FGF-2 was not as strong as the response to FGF-2 delivered in solution. This requires further investigation.

More recently, the loading and release of FGF-2 from synthetic hydrolytically degradable multilayer thin films of various architectures were explored by Hammond's group.[126] Three parameters were studied: number of layers, counterpolyanion (heparin or chondrotin sulfate), and type of degradable polycation. The incorporated amounts were found in the range 7-45 ng/cm^2 of FGF-2 and the release time varied between 24 h and approximately five days. The effective bioactivity of the released FGF-2 was proved *in vitro* as it promoted the proliferation of MC3T3-E1 preosteoblast cells. Interestingly, FGF-2 released from LbL films demonstrated increased ability of up to 8 times the negative control values to enhance proliferation compared to the free FGF-2 (about 2 times). Importantly, none of the other film components (including CS and HEP) showed any proliferative effect on the preosteoblasts.

FGF-2 adsorption via heparin-based PEM was also recently applied to decellularized porcine aortic heart valve leaflets [127], which are used in the replacement of diseased aortic valves. FGF-2 was found to be released slowly from the valve and was sustained over 4 days while its biological activity was preserved, as proved by increased fibroblast viability.

As the immobilized growth factors can maximally retain their bioactivity, the LBL assembly would be a potential approach for constructing a bioactive substrate for biomedical applications.

Additional bioactivity can be provided for (PSS/PAH) films by adsorbing growth factor on to them or by adding them before the last

deposited layer. Here again, the charge of the polyelectrolyte can influence cell adhesion, metabolic activity and adsorbed growth factor as well. The first proof of effective bioactivity of two nerve growth factors was provided by Vodouhe *et al*.[128] First, the authors showed that better neuron viability was observed on (PSS/PAH) and (PLL/PGA) films in comparison to a simple monolayer. Second, they embedded two nerve growth factors, brain-derived neurotrophic factor (BDNF) and semaphoring 3A (Sema3A) into (PSS/PAH) films before depositing a final PSS layer. The adsorbed protein amounts were 95 ng/cm^2 for BDNF and 25 ng/cm^2 for Sema3A. They evidenced that the embedded proteins remained functional and available, even under two layers of polyelectrolytes. Both proteins modified the growth of the neurons either by increasing it (BDNF) or by reducing neurite length (Sema3A). Such PEM films would allow the direct presentation of growth factors in the injury environment for promoting repair of neuronal tissue.

Vautier *et al*.[129] modified the surface of porous titanium implants with polyelectrolyte multilayer (PEM) films functionalized with vascular endothelial growth factor (VEGF). Of the two PEM systems investigated, poly(L-lysine)/poly(L-glutamic acid) (PLL/PGA) and (PAH/PSS), they selected a (PAH/PSS) film made of four layer pairs ending with PSS for both its high efficiency to adsorb VEGF and its biocompatibility toward endothelial cells. Furthermore, they showed that it stimulated the proliferation of endothelial cells.
They demonstrated that VEGF adsorbed on $(PAH/PSS)_4$ maintains its bioactivity *in vitro* by measuring the phosphorylation of the endothelial VEGF receptor VEGFR2 and the specific activation of the mitogen-activated protein kinases (MAPK) ERK ½ pathway. This effect was correlated with specific activation of intracellular signaling pathways induced by successive phosphorylation of the endothelial VEGF receptor VEGFR2 and mitogen-activated protein kinases (MAPK) ERK1/2.

Cells capable of differentiating and, in particular, stem cells that are multi- or pluripotent cells, are currently the subject of several studies thanks to their potential applications in tissue repair *in situ* and tissue engineering. Here again growth factors are of special interest.
Dierich *et al*.[130] were the first to show the use of PEM films for the differentiation of embryonic bodies (EBs) into cartilage and bone. A poly(L-lysine succinylated)/PGA film, into which BMP-2 (bone morphogenetic 2) and TGFβ1 (transforming growth factor 1) had been embedded was chosen for this purpose. They found that both BMP-2 and TGFβ1 needed to be present simultaneously in the film to trigger proteoglycan production and drive the EBs to cartilage and bone formation. The same authors subsequently investigated the effect of a growth factor, BMP-4, and its antagonist, Noggin, embedded in a PLL/PGA film on tooth development. [131] They showed that these films can induce or inhibit cell death in tooth development and that the biological effects of the active molecules are conserved. The functionalized PEMs could thus act as efficient delivery tools for activating cells. This approach shows promise as it could be used to finely reproduce architectures with cell inclusions as well as to provide tissue organization.

BMP-2 is another member of the BMP family that is particularly interesting for accelerating bone healing.[132] BMP-2 has been inserted into a film as a regular layer, but the successive washing steps do not allow a high amount of BMP-2 to be retained (less than 100 ng per substrate) [133]. When it is combined with hydrolytically degradable polycations (□-aminoesters), several µg can be loaded and 10 µg of BMP-2 are released over a period of two weeks *in vitro*.[134] Of note, there was no initial burst (less than 1% is released in the first 3 h) as compared with commercial collagen matrices which can release up to 60% of BMP-2. BMP-2 released from LbL films retains its ability to induce bone differentiation in MC3T3 pre-osteoblasts, as measured by induction of alkaline phosphatase and stains for calcium. *In vivo*, BMP-2 film coated polymeric scaffolds and implanted intramuscularly in rats were shown to induce bone formation.

The adsorption strategy was also applied to BMP-2, which was shown to diffuse in cross-linked (PLL/HA) films.[17] Indeed, (PLL/HA) films are a reservoir for BMP-2, as very high loaded amounts can be obtained (up to 7 $\mu g/cm^2$) and only a small fraction was released initially. The amount of BMP-2 trapped could be adjusted by varying both the number of layers in the film and the initial BMP-2 concentration in solution. The effective proof of bioactivity was obtained on myoblast cells: cells differentiated into myotubes on cross-linked (PLL/HA) films without BMP-2 in the films, but they differentiated into osteoblasts in a dose-dependent manner when cultured on the BMP-2 loaded films. The expression of alkaline phosphatase, a marker for osteoblastic activity, was dependent on the amount of BMP-2 loaded into the films.[17]

If a mixture of heparin and hyaluronan is used as a polyanion in the film buildup, heparin is found to be preferentially incorporated. In this case, thinner and denser films are obtained, on to which only a small amount of BMP-2 can be adsorbed. Interestingly, the ALP production by myoblast cells was found to be solely correlated to the amount of BMP-2 adsorbed or trapped in the film, independently of the film's internal chemistry.[135] Furthermore, the bioactivity of BMP-2 loaded in cross-linked (PLL/HA) films deposited on TCP/HAP granules, biomaterials used in orthopedic surgery as a bone substitute, was recently confirmed by *in vivo* studies in rats.[136] Induction of bone around the PEM-film coated implant (i.e osteo-induction) was proved to be due to the sole presence of BMP-2, the film itself being inert. In addition, the PEM film did not induce an inflammatory response in the surrounding tissues.

4.3 Other types of specific interactions

A receptor that is especially important for the healing of the endothelium is CD34. In the cardiovascular field, stent implantation is a common procedure, which may subsequently lead to in-stent restenosis (i.e obstruction of the vessel) or even stent thrombosis. It is therefore important to stimulate healing of the endothelium in appropriate conditions. Ji *et al.* developed a strategy to mimic the natural endothelium healing mechanism that consists in stimulating neighboring endothelial cell (EC) migration or capturing the circulating endothelial cells directly from the blood circulation.[86] To this end, they immobilized an anti-CD34 antibody on heparin/collagen multilayers. They found that the PEM coating with or without the anti-CD34 antibody functionalization preserved good hemocompatibility, but also promoted cell attachment and growth notably in a non selective manner. However, the anti-CD34 antibody functionalized heparin/collagen multilayers could specifically promote the attachment and growth of vascular ECs at the expense of smooth muscle cells.

Specificity in the interaction may also be observed for other types of receptor. HA, which is an important polysaccharide component of ECM, is known to interact with several receptors. Among them is CD44, a cell surface glycoprotein involved in cell/cell adhesion, cell adhesion and migration. B lymphocyte adhesion on to (CHI/HA) films was recently investigated by varying the deposition conditions, especially ionic strength and pH.[137] The authors showed that there was a specific interaction between the CD44 receptor in lymphocyte cells and HA. Furthermore, the deposition conditions of the films had an influence on the interaction, low pH and added salt being the preferred conditions for higher cell binding. This interaction was favored in conditions that favor loops and tails in HA. However, they also noticed that CHI-terminated films prepared without NaCl in the deposition solutions presented a similar high lymphocyte binding efficiency, which they attributed to increased electrostatic contributions.
The same group showed that that it is possible to attach a superparamagnetic PEM patch to the membrane of T- and B-lymphocytes using CD44-HA interactions.[138] B-cells responded to an applied magnetic field, and T-cells continued to chemokinetically migrate on intercellular adhesion molecule (ICAM)-coated surfaces following patch attachment.

However, it should be noted that, for other films that contain HA, such as (PLL/HA)

films, no specific interaction with HA receptors has been evidenced.[139] This might be due to the fact that the films are cross-linked, which may affect the presentation of HA to the cell receptors due to its entanglement with PLL chains.

5. Toward multifunctionality

PEM coatings may offer new tools to tissue engineers and biophysicists, who need well controlled and well characterized biomimetic matrices. PEM coatings offer new potentialities when compared to classic synthetic materials such as polyacrylamide gels [10] or poly(ethylene glycol) [140] by making use of both covalent and non covalent interactions. The potentialities for manufacturing multi-functional coatings that combine, for instance, spatial organization and bioactivity, or adjustable stiffness and chemistry, or adjustable stiffness and bioactivity, are apparently unlimited. Recent examples illustrate that we are now entering an area of new developments for the design of multifunctional films.

5.1 Three-dimensional microenvironments containing bioactive films

PEM films can be considered as 2D matrices, even if they can be several tens of micrometer thick, in the sense that they cannot provide a sufficiently porous 3D scaffold for the cells to grow in. However, PEM films can be deposited on porous materials and provide additional properties for the biomaterial surface.

In a recent study describing further efforts to provide stem cells with a biomimetic niche environment, Nichols *et al*. [141] built an elegant scaffold with an inverted colloidal crystal topography reminiscent of bone marrow architecture, which was further coated with albumin/PDDA films. Bone marrow stromal cells were first allowed to attach to the scaffold. Subsequently, CD34+ hematopoietic stem cells were seeded in the scaffold to create a three dimensional co-culture. The authors demonstrated that the scaffold supports CD34+ cell expansion and B lymphocyte differentiation with production of antigen specific IgG antibodies. Recently, the same group achieved a further step toward mimicking the cell microenvironment of the bone marrow and thymus by presenting a Notch ligand (Delta-like 1, DL-1) at the surface of the PEM film.[142] For this purpose, they used mononuclear cells derived from human umbilical cord that were positive for the surface marker CD34 (CD34+). After 28 days of growth on the PEM-coated colloidal scaffolds, the cells were found to be CD4+ and CD8-, an observation that was specifically due to the presence of the DL-1 Notch ligand. Without the DL-1 coating, the cells were shown to express a CD34 for 2 weeks, which indicated that the PEM-coated scaffold stimulated *ex vivo* hematopoietic stem cell expansion without notch signaling. In addition, the cells progressively developed their own ECM.

3D microwells are increasingly used for cell culture arrays.[143] Recently, Lynn *et al.* developed an approach to the fabrication and selective functionalization of amine-reactive polymer multilayers on the surface of 3D-polyurethane-based microwells[144]. These authors prepared film-coated arrays that could be chemically functionalized postfabrication by treatment with different amine-functionalized macromolecules or small molecule primary amines. They showed that spatial control over glucamine functionalization yielded 3D substrates that could be used to confine cell attachment and growth to microwells for periods up to 28 days. A dual functionalization could also be achieved by sequential treatment with two different fluorescently labeled cationic polymers: functionalization of the surface of the wells with one polymer and the regions between the wells with a second. This approach to dual functionalization opens perspectives for the long-term culture and maintenance of cell types, e.g stem cells.

5.2 Bioactivity of two different growth factors

The group of Prof Hammond recently showed that is it possible to release at precise doses two types of potent growth factors, osteogenic BMP-2 (to induce bone regeneration) and angiogenic VEGF165 (to induce neo-vascularization) in different ratios in a

degradable [poly(b-amino ester)/polyanion/ growth factor/polyanion] LbL tetralayer repeat architecture. [145] The amount of biologically active molecules loaded was precisely controlled by varying the number of tetralayers. Very interestingly, both growth factors were shown to retain their bioactivity *in vitro*: BMP-2 initiated differentiation of pre-osteoblastic cells and VEGF induced proliferation of endothelial cells. The authors also showed that the mineral density of the ectopic bone formed was about 33% higher in the case of the dual release (Figure 5) as compared to BMP-2 alone, which they attributed to an increased local vascular network. .

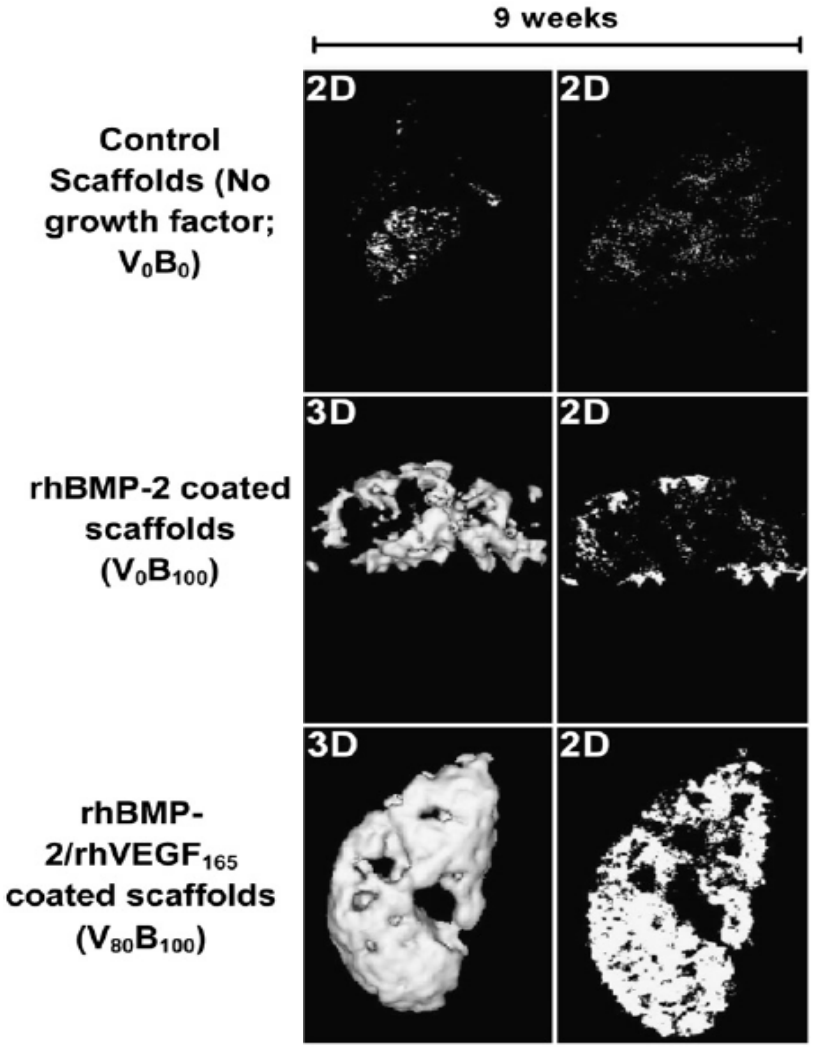

FIGURE 5. Two dimensional microCT scans (2D) and matched three dimensional reconstructions (3D) of excised PCL-bTCP half disc scaffolds, which were implanted in the intramuscular region of rats*. Implants were coated with (i) no growth factor, (ii) 6 µg of single growth factor rhBMP-2 and (iii) 6 µg of single growth factor rhBMP-2 followed by 4 µg of rhVEGF165. The amount of growth factor loaded was determined by fabricating triplicate companion copies along with the implanted scaffolds, releasing the growth factors in vitro and performing ELISA detection assays. (Top row) Control scaffolds without growth factors produce no detectable bone over the duration of the study. Low levels of backscatter is caused by the polymer. (Middle row) In single growth factor rhBMP-2 films lacking rhVEGF165, bone formation is restricted to the periphery of the scaffold at 4 weeks (images not shown) and 9 weeks. (Bottom row) As a result of increased vascularity, scaffolds releasing rhVEGF165 demonstrate a smooth, continuous profile in the ectopically formed bone which matures from 4 weeks to 9 weeks to fill the entire scaffold. In all the images, the bone formed takes the shape of the scaffold and grows inward when VEGF is present. Images are an isosurface rendering at 0.25 surface quality factor at a level threshold of 640, as defined by the proprietary Microview_ software from GE Healthcare. (reproduced with permission from McDonnald et al, Biomaterials 2011, copyright Elsevier 2011)*

5.3. Mechanical stimulation and delivery of bioactive molecules

PEM film properties may also be combined with mechanical stimulation or with electrochemical stimulation. In an elegant study, Lavalle *et al.* showed that (PLL/HA) films coated with PDMS substrates can be stretched and release an enzyme that is loaded in the bulk of the film and capped with a synthetic PEM barrier. [146] The biocatalytic activity of the film could be switched on/off reversibly by mechanical stretching, which exposed enzymes through the capping barrier, similarly to mechanisms involved in proteins during mechanotransduction. This opens new possibilities for triggering the release of bioactive molecules from the film "bulk". Interestingly, a recent study by Schaaf *et al*. [147] showed that the adhesive state of fibroblasts can be changed from cytophobic to cytophilic simply by stretching a film with a cell repellent phosphatidylcholine–PAA layer as the final layer. In the afore-mentioned examples, the substrate supporting the PEM film is stretched in a controlled fashion.

The ability to construct stable ECM-based films on PDMS [148; 149] has particular relevance in mechanobiology, microfluidics and other applications. A combination of PEM with microfluidics appears to be highly promising. It was recently shown that PEM films can be deposited in a microfluidic device and that a pH gradient could be generated during multilayer formation.[150] The authors showed that cells started to migrate from the films built at pH 5 to those built at pH 9. Developments of PEM films in combination with electrochemistry also appear promising as biomolecules can be released from the films [151; 152] as well as whole cell sheets.[153]

Mechanical stimulus can also be provided by varying the film's stiffness. As mentioned previously, cells can respond actively to the rigidity of a substrate by exerting forces on it, which allows them to adhere and spread more or less, depending on the rigidity of the underlying matrix. Recently, using (PLL/HA) films, we have shown that it is possible to combine film stiffness and presentation of the BMP-2 growth factor by the matrix [154]. Here, the PEM film offers the possibility of providing two independent stimuli: a mechanical stimulus and a biochemical stimulus that is known to impact cell differentiation.[17] By preparing films of different stiffness and by loading a known amount of BMP-2, we revealed that BMP-2 has a drastic effect on early cell adhesion (Figure 6A) as well as on cell migration (Figure 6B). This effect was especially potentiated when BMP-2 was presented from soft films. First, this highlights that biochemical stimuli can override mechanical stimuli in certain conditions. Second, this also proves that BMP-2 not only has an effect on cell differentiation but also possibly in the early stages of cell adhesion. This opens a route for studies on the interplay between growth factor presentation from the matrix (and associated cell signaling) and cell adhesion receptors involved in rigidity sensing.

Other types of stimulation such as light-triggered release of activated molecules [155] might also be used in the future to locally delivery bioactive molecules to cells, as they have shown promise in the delivery of cargo from microcapsules adsorbed onto the films [156].

6. Evaluation of toxicity and *in vivo* studies

For translation of PEM-coated surfaces or PEM microcapsules into medicine, both the efficiency and toxicity of the PEM assemblies must be evaluated. It is already known that several single polycations are potentially cytotoxic, depending on the dose and site of injection. This is valid for PEI and PLL [157] and for CHI as well.[158] Systematic studies for each specific case are thus required.

The biocompatibility of a single PEI layer was tested on both fibroblastic and osteoblastic cells. Pure titanium (Ti) and nickel–titanium (NiTi) alloy were coated with PEI and morphology, adhesion and viability were assessed for up to 7 days after seeding. The results show that the cells were less viable and proliferated less on PEI-coated titanium than

on the control, suggesting that PEI is potentially cytotoxic.[159] On the other hand, (PSS/PAH) films deposited on human umbilical arteries showed good grafting behavior and no inflammation in a rabbit model after 12 weeks of implantation.[160] Coronary stents have also been coated with (CHI/HEP) films and they were tested in vitro and *in vivo* in a pig model.[161] This PEM coating was found to be safe and efficient in promoting re-endothelialization and intimal healing after stent implantation in addition to having good hemocompatibility. Similarly, (PLL/PGA) films have been coated on a tracheal prosthesis and implanted for up to three months.[162] For prostheses modified by PGA ending multilayer films, a more regular and less obstructive cell layer was observed on the endoluminal side compared to those modified by PLL ending films. An anti-inflammatory peptide grafted to PGA was found to be bioactive *in vivo*. No inflammation was observed in the case of BMP-2 delivered intramuscularly.[134; 136]

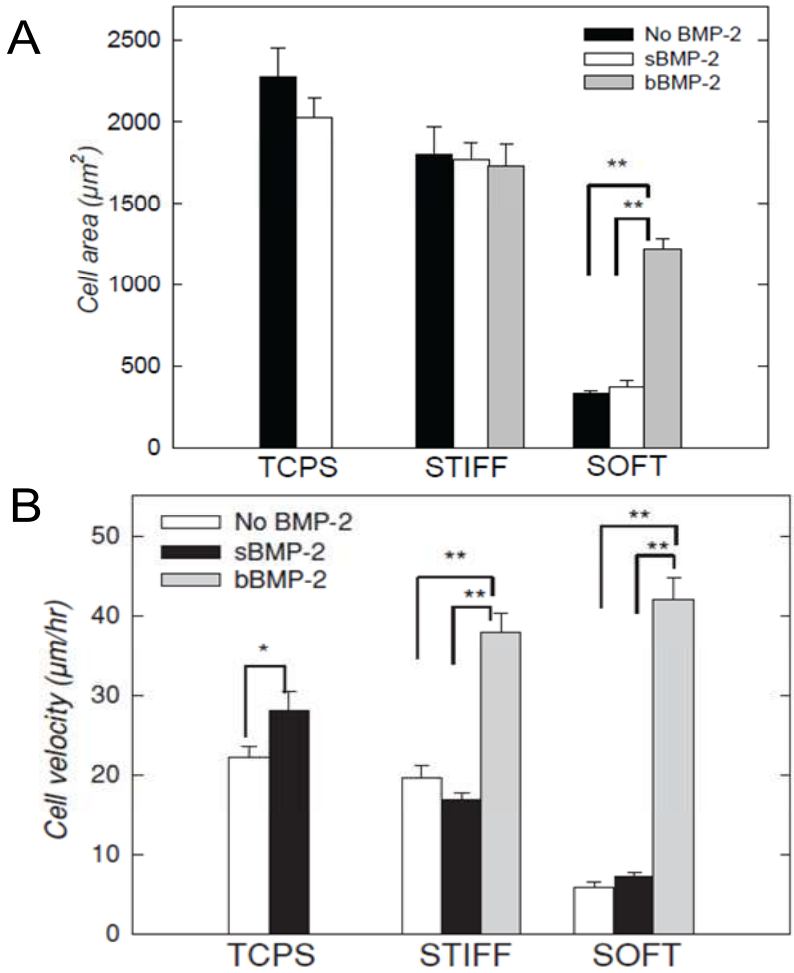

FIGURE 6. Sustained effect of matrix-bound BMP-2 on cell morphology and on cell migration. *Cell morphology is observed 16 hours after plating the cells. Actin and nucleus staining of C2C12 cells revealed a well spread morphology on the glass control substrate as well as on stiff (PLL/HA) films in the presence or in the absence of BMP-2, independently of the presentation mode of BMP-2 ("soluble" versus "matrix-bound"). Conversely, for soft (PLL/HA) films, sBMP-2 did not induce any noticeable effect on cell spreading but bBMP-2 induced a striking increase in cell spreading (images not shown). (A) The cell surface area is plotted for the different conditions. This shows the drastic increase in cell spreading in response to bBMP-2 on soft films is sustained after initial adhesion. (B) Migration velocity (μm/hour) of C2C12 cells cultured on different substrates: standard tissue culture polystyrene (TCPS) and either stiff or soft films. Matrix-bound BMP-2 greatly increases cell velocity on stiff films and even more on soft films with bBMP-2. The soluble form of BMP-2 had no significant effect compared to the condition where no BMP-2 is added, except on TCPS. ** $p<0.005$ (reproduced with permission from Crouzier et al, Adv Materials 2011, copyright Wiley 2011)*

De Geest *et al*. recently carried out an interesting study using a terrestrial slug, namely *Arion lusitanicus* as a nonvertebrate model organism to investigate mucosal irritation.[163] This slug has recently been used to test several pharmaceutical, as well as health care components *in vivo* [164] as an alternative to tests in mice, rabbits or non-human animals. They investigated the mucosal irritation potency of several classes of biopolymers, synthetic polyelectrolytes and the reactive polyelectrolytes of oppositely charged polyelectrolytes, their complexes as well as hollow multilayer capsules, which they intend to use in vaccines.[165] They found that single polyelectrolyte components induced tissue irritation. But, very interestingly, this response was dramatically reduced upon complexation with an oppositely charged polyelectrolyte, regardless of whether the polyelectrolytes were randomly complexed in water or assembled in a controlled fashion in multilayer capsules.

The chemical modification of polycations is also possible for decreasing their potential toxicity. By using PLL modified with PEG groups (PLL-g-PEG) and by assembling them with alginate, Chaikof *et al*. recently showed that individual pancreatic islets can be coated with (PLL-g-PEG/ALG) multilayer films [166]. These authors also demonstrated that additional biological specificity can be provided for the islets by depositing specific groups (such as biotin or azide functionalized-PEG). Very interestingly, they also showed that the functional capacity of islets to release insulin in a glucose-responsive manner was not adversely influenced by the PEM film. Indeed, the islets engineered with PEMs secreted statistically similar amounts of insulin at both basal and high glucose concentrations compared to untreated controls. Furthermore, by implanting these islets *in vivo* into mice through the portal vein and into the liver microvasculature, they proved that the survival and function of these PEM-coated cells.

All together, these studies show that it is possible to design PEM films with bioactive properties *in vivo*, which can be fully integrated *in vivo* without any noticeable toxicity. Here again, each engineered PEM system will have to be studied in the framework of a specific application.

8. Concluding remarks

In the last 5 years, there have been considerable developments in synthetic and natural PEM assemblies for the coating of biomaterial surfaces and tissue engineering. An important aspect is the dynamic nature of mono or multi-cellular systems (interactions between cells or cell/matrix) that occur over several hours, days, and weeks. Based on this survey, it appears that better defined applications and multi-functionalization using several strategies simultaneously have recently emerged. The various strategies that are used to non-covalently localize bioactive adhesion molecules and growth factors appear highly promising for future *in vivo* studies on tissue regeneration as well as for more fundamental mechanistic studies. PEMs may serve as new biomimetic matrices with controlled physical properties and controlled presentation of biochemical moieties, for investigating cell/material or cell/cell interactions. It is now acknowledged that the means of presentation of a bioactive molecule is a key point in its bioactivity and that matrix-bound presentation is much more physiologic than delivering growth factors in solution.[167] As we have seen here that many growth factors retain their bioactivities inside or on top of PEM films, we foresee that PEMs will help answer important biological questions such as: How do matrix-bound molecules interact with cell receptors and transduce biochemical signals, as compared to soluble molecules added in the culture medium? It will also be interesting to unravel the structure of the bioactive molecules inside PEM films and to understand the molecular mechanisms at the basis of their preserved bioactivity. General rules may emerge. This will require the use of new biochemical and biophysical analytical tools. PEMs will undoubtedly find a place alongside other well established materials such as polyacrylamide or polyethylene glycol hydrogels, which require covalent grafting for the coupling of chemical ligands.

The potentialities for manufacturing multi-functional PEM coatings are apparently

unlimited. The design and pertinence of such architectures will rely on a strong multidisciplinary approach and will require collaboration between engineers, physical chemists, organic chemists, biochemists, and cell and stem cell biologists. In the burgeoning field of stem cells, PEM films also appear to offer a tool to maintain stemness or to guide cell differentiation. Besides being a 2D coating, their application in 3D mimetic architectures will be an original means of controlling supra-cellular organization. Thus, the reciprocal interactions between active cells and active PEM surfaces offer tremendous potentialities that will be explored in the future.

Acknowledgements
CP and RAV are Junior Members of the "Institut Universitaire de France" whose support is gratefully acknowledged. CP wishes to thank the European Commission for support via an ERC Starting grant 2010 (GA 259370). VG thanks the Rhône-Alpes region for a fellowship via the cluster MACODEV.

LIST OF ABBREVIATIONS

ALG : alginate
AuNP : gold nanoparticles
BDNF : brain derived neurotrophic factor
BMP : bone morphogenetic proteins
CHI : chitosan
CS : chondroitin sulfate and CSA for chondroitin sulfate A
CLSM : confocal laser scanning microscopy
COL : collagen
EDC : 1-Ethyl-3-(3-dimethylaminopropyl) carbodiimide
EPC : endothelial progenitor cell
ESC : embryonic stem cells
FGF-2 (or bFGF) : basic fibroblast growth factor
FN : fibronectin
ICM : inner cellular mass
HA : hyaluronan
HEP : heparin
LbL : layer-by-layer
MAPK : mitogen-activated protein kinases
MSC : mesenchymal stem cells
α-MSH : alpha-melanocyte-stimulating hormone
NGF : nerve growth factor
PA : polyacrylamide
PDMS : poly(dimethylsiloxane)
PEI : poly(ethylene)imine
PLL : poly(L-lysine)
PAH : poly(allylamine) hydrochloride
PEM : polyelectrolyte multilayer
PSS : poly(styrene) sulfonate
SMC : smooth muscle cells
SWNT : single-walled carbon nanotube
TCPS : tissue culture polystyrene
VB : vinylbenzyl
VEGF : vascular endothelial growth factor

Bibliography

1. Decher, G., Hong, J. D. & Schmitt, J. (1992). Buildup of ultrathin multilayer films by a self-assembly process: III. Consecutively alternating adsorption of anionic and cationic polyelectrolytes on charged surfaces. *Thin Solid Films* **210-211**, 831-835.
2. Lvov, Y., Decher, G., Haas, H., Mohwald, H. & Kalachev, A. (1994). X-ray analysis of ultrathin polymer films self-assembled onto substrates. *Phys B* **198**, 89-91.
3. Castner, D. G. & Ratner, B. D. (2002). Biomedical surface science: Foundations to frontiers. *Surf. Sci.* **500**, 28-60.
4. Hubbell, J. A. (1999). Bioactive biomaterials. *Curr Opin Biotechnol.* **10**, 123-129.
5. Fattori, R. & Piva, T. (2003). Drug-eluting stents in vascular intervention. *Lancet* **361**, 247-9.
6. Langer, R. & Vacanti, J. P. (1993). Tissue engineering. *Science* **260**, 920-926.
7. Drury, J. L. & Mooney, D. J. (2003). Hydrogels for tissue engineering: scaffold design variables and applications. *Biomaterials* **24**, 4337-51.
8. Chen, C. S., Mrksich, M., Huang, S., Whitesides, G. M. & Ingber, D. E. (1997). Geometric control of cell life and death. *Science* **276**, 1425-1428.
9. Hersel, U., Dahmen, C. & Kessler, H. (2003). RGD modified polymers: biomaterials for stimulated cell adhesion and beyond. *Biomaterials* **24**, 4385-4415.
10. Wang, Y. L. & Pelham, R. J., Jr. (1998). Preparation of a flexible, porous polyacrylamide substrate for mechanical studies of cultured cells. *Methods Enzymol* **298**, 489-496.
11. Engler, A. J., Sen, S., Sweeney, H. L. & Discher, D. E. (2006). Matrix elasticity directs stem cell lineage specification. *Cell* **126**, 677-89.
12. Hudalla, G. A. & Murphy, W. L. (2011). Biomaterials that Regulate Growth Factor Activity via Bioinspired Interactions. *Adv Funct Mater* **21**, 1754-1768.
13. Tang, Z., Wang, Y. l., Podsiadlo, P. & Kotov, N. A. (2006). Biomedical applications of layer-by-layer assembly: from biomimetics to tissue engineering. *Adv Mater* **18**, 3203-3224.
14. Shiratori, S. S. & Rubner, M. F. (2000). pH-dependent thickness behavior of sequentially adsorbed layers of weak polyelectrolytes. *Macromolecules* **33**, 4213-4219.

15. von Klitzing, R. (2006). Internal structure of polyelectrolyte multilayer assemblies. *Phys Chem Chem Phys* **8**, 5012-33.
16. Garza, J. M., Jessel, N., Ladam, G., Dupray, V., Muller, S., Stoltz, J. F., Schaaf, P., Voegel, J. C. & Lavalle, P. (2005). Polyelectrolyte multilayers and degradable polymer layers as multicompartment films. *Langmuir* **21**, 12372-12377.
17. Crouzier, T., Ren, K., Nicolas, C., Roy, C. & Picart, C. (2009). Layer-by-Layer films as a biomimetic reservoir for rhBMP-2 delivery: controlled differentiation of myoblasts to osteoblasts. *Small* **5**, 598-608.
18. Kwok, C. S., Mourad, P. D., Crum, L. A. & Ratner, B. D. (2000). Surface modification of polymers with self-assembled molecular structures: multitechnique surface characterization. *Biomacromolecules* **1**, 139-148.
19. Boudou, T., Crouzier, T., Ren, K., Blin, G. & Picart, C. (2010). Multiple functionalities of polyelectrolyte multilayer films: new biomedical applications. *Adv Mater* **22**, 441-67.
20. Schönhoff, M., Ball, V., Bausch, A. R., Dejugnat, C., Delorme, N., Glinel, K., von Klitzing, R. & Steitz, R. (2007). Hydration and internal properties of polyelectrolyte multilayers. *Colloids and Surfaces A: Physicochem. Eng. Aspects* **303**, 14-29.
21. Jaber, J. A. & Schlenoff, J. B. (2006). Recent developments in the properties and applications of polyelectrolyte multilayers. *Curr. Opin. Colloid Interface Sc.* **11**, 324-329.
22. Sukhishvili, S. A., Kharlampieva, E. & Izumrudov, V. (2006). Where polyelectrolyte multilayers and polyelectrolyte complexes meet. *Macromolecules* **39**, 8873-8881.
23. Hammond, P. T. (2004). Form and function in multilayer assembly: New applications at the nanoscale. *Adv Mater* **16**, 1271-1293.
24. Lynn, D. M. (2007). Peeling back the layers: Controlled erosion and triggered disassembly of multilayered polyelectrolyte thin films. *Adv Mater***19**, 4118-4130.
25. Zhang, L., Zhao, W. H., Rudra, J. S. & Haynie, D. T. (2007). Context dependence of the assembly, structure, and stability of polypeptide multilayer nonofilms *ACS Nano* **1**, 476-486.
26. Zelikin, A. N. (2010). Drug releasing polymer thin films: new era of surface-mediated drug delivery. *ACS Nano* **4**, 2494-509.
27. Pavlukhina, S. & Sukhishvili, S. (2011). Polymer assemblies for controlled delivery of bioactive molecules from surfaces. *Adv Drug Delivery Rev* **63**, 822-836.
28. Jewell, C. M. & Lynn, D. M. (2008). Multilayered polyelectrolyte assemblies as platforms for the delivery of DNA and other nucleic acid-based therapeutics. *Adv Drug Delivery Rev* **60**, 979-99.
29. Lichter, J. A., Van Vliet, K. J. & Rubner, M. F. (2009). Design of Antibacterial Surfaces and Interfaces: Polyelectrolyte Multilayers as a Multifunctional Platform. *Macromolecules* **42**, 8573-8586.
30. Picart, C., Gergely, C., Arntz, Y., Schaaf, P., Voegel, J.-C., Cuisinier, F. G. & Senger, B. (2004). Measurement of film thickness up to several hundreds of nanometers using optical wavguide lightmode spectroscopy. *Biosens Bioelectron* **20**, 553-561.
31. Boura, C., Menu, P., Payan, E., Picart, C., Voegel, J.-C., Muller, S. & Stoltz, J.-F. (2003). Endothelial cells grown on thin polyelectrolyte mutlilayered films: An evaluation of a new versatile surface modification. *Biomaterials* **24**, 3521-3530.
32. Mhamdi, L., Picart, C., Lagneau, C., Othmane, A., Grosgogeat, B., Jaffrezic-Renault, N. & Ponsonnet, L. (2006). Study of the polyelectrolyte multilayer thin films' properties and correlation with the behavior of the human gingival fibroblasts. *Mater Sci Eng: C* **26**, 273-281.
33. Brunot, C., Grosgogeat, B., Picart, C., Lagneau, C., Jaffrezic-Renault, N. & Ponsonnet, L. (2008). Response of fibroblast activity and polyelectrolyte multilayer films coating titanium. *Dent Mater* **24**, 1025-1022.
34. Mhamdi, L., Picart, C., Lagneau, C., Othmane, A., Grosgogeat, B., Jaffrezic-Renault, N. & Ponsonnet, L. (2006). Study of the polyelectrolyte multilayer thin films' properties and correlation with the behavior of the human gingival fibroblasts. *Mater Sci Eng: C* **26**, 273-281.
35. Tryoen-Toth, P., Vautier, D., Haikel, Y., Voegel, J.-C., Schaaf, P., Chluba, J. & Ogier, J. (2002). Viability, adhesion, and bone phenotype of osteoblast-like cells on polyelectrolyte multilayer films. *J Biomed Mater Res* **60**, 657-667.
36. Wittmer, C. R., Phelps, J. A., Lepus, C. M., Saltzman, W. M., Harding, M. J. & Van Tassel, P. R. (2008). Multilayer nanofilms as substrates for hepatocellular applications. *Biomaterials* **29**, 4082-4090.
37. Kerdjoudj, H., Boura, B., Moby, V., Montagne, K., Schaaf, P., Voegel, J.-C., Stoltz, J.-F. & Menu, P. (2007). Re-endothelialization of human umbilical arteries treated with polyelectrolyte multilayers: A tool for damaged vessel replacement. *Adv Funct Mater* **17**.
38. Kerdjoudj, H., Berthelemy, N., Rinckenbach, S., Kearney-Schwartz, A., Montagne, K., Schaaf, P., Lacolley, P., Stoltz, J. F., Voegel, J. C. & Menu, P. (2008). Small vessel replacement by human umbilical arteries with polyelectrolyte film-treated arteries in vivo behavior. *J Amer Coll Cardiol* **52**, 1589-1597.
39. Berthelemy, N., Kerdjoudj, H., Gaucher, C., Schaaf, P., Stolz, J. F., Lacolley, P., Voegel, J. C. & Menu, P. (2008). Polyelectrolyte films boost progenitor cell differentiation into endothelium-like monolayers. *Adv Mater* **20**, 2674-2678.
40. Guillaume-Gentil, O., Semenov, O. V., Zisch, A. H., Zimmermann, R., Voros, J. & Ehrbar, M. (2011). pH-controlled recovery of placenta-derived

mesenchymal stem cell sheets. *Biomaterials* **32**, 4376-4384.
41. Mendelsohn, J. D., Barrett, C. J., Chan, V. V., Pal, A. J., Mayes, A. M. & F, R. M. (2000). Fabrication of microporous thin films from polyelectrolyte multilayers. *Langmuir* **16**, 5017 -5023.
42. Hajicharalambous, C. S., Lichter, J., Hix, W. T., Swierczewska, M., Rubner, M. F. & Rajagopalan, P. (2009). Nano- and sub-micron porous polyelectrolyte multilayer assemblies: Biomimetic surfaces for human corneal epithelial cells. *Biomaterials* **30**, 4029-4036.
43. Johansson, J. A., Halthur, T., Herranen, M., Soderberg, L., Elofsson, U. & Hilborn, J. (2005). Buildup of collagen and hyaluronic acid polyelectrolyte multilayers. *Biomacromolecules* **6**, 1353-9.
44. Zhang, J., Senger, B., Vautier, D., Picart, C., Schaaf, P., Voegel, J.-C. & Lavalle, P. (2005). Buildup of collagen and hyaluronic acid polyelectrolyte multilayers. *Biomaterials* **26**, 3353-3361.
45. Ai, H., Lvov, Y., Mills, D., Jennings, M., Alexander, J. & Jones, S. (2003). Coating and selective deposition of nanofilm on silicone rubber for cell adhesion and growth. *Cell Biochem Biophys***38**, 103-14.
46. Cai, K., Rechtenbach, A., Hao, J., Bossert, J. & Jandt, K. D. (2005). Polysaccharide-protein surface modification of titanium via a layer-by-layer technique: characterization and cell behaviour aspects. *Biomaterials* **26**, 5960-71.
47. Thierry, B., Winnik, F. M., Merhi, Y., Silver, J. & Tabrizian, M. (2003). Bioactive coatings of endovascular stents based on polyelectrolyte multilayers. *Biomacromolecules* **4**, 1564-1571.
48. Picart, C., Lavalle, P., Hubert, P., Cuisinier, F. J. G., Decher, G., Schaaf, P. & Voegel, J.-C. (2001). Buildup mechanism for poly(L-lysine)/hyaluronic acid films onto a solid surface. *Langmuir* **17**, 7414-7424.
49. Tezcaner, A., Hicks, D., Boulmedais, F., Sahel, J., Schaaf, P., Voegel, J. C. & Lavalle, P. (2006). Polyelectrolyte multilayer films as substrates for photoreceptor cells. *Biomacromolecules* **7**, 86-94.
50. Crouzier, T. & Picart, C. (2009). Ion pairing and hydration in polyelectrolyte multilayer films containing polysaccharides. *Biomacromolecules* **10**, 433-42.
51. Fu, J., Ji, J., Yuan, W. & Shen, J. (2005). Construction of anti-adhesive and antibacterial multilayer films via layer-by-layer assembly of heparin and chitosan. *Biomaterials* **26**, 6684-92.
52. Boddohi, S., Killingsworth, C. E. & Kipper, M. J. (2008). Polyelectrolyte multilayer assembly as a function of pH and ionic strength using the polysaccharides chitosan and heparin. *Biomacromolecules* **9**, 2021-2028.
53. Servaty, R., Schiller, J., Binder, H. & Arnold, K. (2001). Hydration of polymeric components of cartilage--an infrared spectroscopic study on hyaluronic acid and chondroitin sulfate. *Int J Biol Macromol* **28**, 121-7.
54. Cohen, M., Klein, E., Geiger, B. & Addadi, L. (2003). Organization and adhesive properties of the hyaluronan pericellular coat of chondrocytes and epithelial cells. *Biophys J* **85**, 1996-2005.
55. Evanko, S. P., Tammi, M. I., Tammi, R. H. & Wight, T. N. (2007). Hyaluronan-dependent pericellular matrix. *Adv Drug Deliv Rev* **59**, 1351-65.
56. Zhu, H., Ji, J., Tan, Q., Barbosa, M. A. & Shen, J. (2003). Surface engineering of poly(DL-lactide) via electrostatic self-assembly of extracellular matrix-like molecules. *Biomacromolecules* **4**, 378-386.
57. Tan, Q. G., Ji, J., Zhao, F., Fan, D. Z., Sun, F. Y. & Shen, J. C. (2005). Fabrication of thromboresistant multilayer thin film on plasma treated poly (vinyl chloride) surface. *J Mater Sci* **16**, 687-692.
58. Chen, J. L., Chen, C., Chen, Z. Y., Chen, J. Y., Li, Q. L. & Huang, N. (2010). Collagen/heparin coating on titanium surface improves the biocompatibility of titanium applied as a blood-contacting biomaterial. *J Biomed Mater Res Part A* **95A**, 341-349.
59. Grohmann, S., Rothe, H., Frant, M. & Liefeith, K. (2011). Colloidal Force Spectroscopy and Cell Biological Investigations on Biomimetic Polyelectrolyte Multilayer Coatings Composed of Chondroitin Sulfate and Heparin. *Biomacromolecules* **12**, 1987-1997.
60. Mhanna, R. F., Voros, J. & Zenobi-Wong, M. (2011). Layer-by-Layer Films Made from Extracellular Matrix Macromolecules on Silicone Substrates. *Biomacromolecules* **12**, 609-616.
61. Salloum, D. S. & Schlenoff, J. B. (2004). Protein adsorption modalities on polyelectrolyte multilayers. *Biomacromolecules* **5**, 1089-96.
62. Ladam, G., Schaaf, P., Cuisinier, F. G. J., Decher, G. & Voegel, J.-C. (2001). Protein adsorption onto auto-assembled polyelectrolyte films. *Langmuir* **17**, 878-882.
63. Gergely, C., Bahi, S., Szalontai, B., Flores, H., Schaaf, P., Voegel, J. C. & Cuisinier, F. J. (2004). Human serum albumin self-assembly on weak polyelectrolyte multilayer films structurally modified by pH changes. *Langmuir* **20**, 5575-82.
64. Picart, C., Ladam, G., Senger, B., Voegel, J.-C., Schaaf, P., Cuisinier, F. J. G. & Gergely, C. (2001). Determination of structural parameters characterizing thin films by optical methods: A comparison between scanning angle reflectometry and optical waveguide lightmode spectroscopy. *J Chem Phys* **115**, 1086-1094.
65. Ladam, G., Gergely, C., Senger, B., Decher, G., Voegel, J.-C., Schaaf, P. & Cuisinier, F. J. G. (2000). Protein Interactions with Polyelectrolyte Multilayers: Interactions between Human Serum Albumin and Polystyrene Sulfonate/Polyallylamine Multilayers. *Biomacromolecules* **1**, 674-687.

66. Kidambi, S., Lee, I. & Chan, C. (2004). Controlling primary hepatocyte adhesion and spreading on protein-free polyelectrolyte multilayer films. *J Am Chem Soc* **126**, 16286-16287.
67. Ricotti, L., Taccola, S., Bernardeschi, I., Pensabene, V., Dario, P. & Menciassi, A. (2011). Quantification of growth and differentiation of C2C12 skeletal muscle cells on PSS-PAH-based polyelectrolyte layer-by-layer nanofilms. *Biomed Mater* **6**.
68. Salloum, D. S., Olenych, S. G., Keller, T. C. & Schlenoff, J. B. (2005). Vascular smooth muscle cells on polyelectrolyte multilayers: hydrophobicity-directed adhesion and growth. *Biomacromolecules* **6**, 161-7.
69. Niepel, M. S., Peschel, D., Sisquella, X., Planell, J. A. & Groth, T. (2009). pH-dependent modulation of fibroblast adhesion on multilayers composed of poly(ethylene imine) and heparin. *Biomaterials* **30**, 4939-4947.
70. Lavalle, P., Gergely, C., Cuisinier, F., Decher, G., Schaaf, P., Voegel, J.-C. & Picart, C. (2002). Comparison of the structure of polyelectrolyte multilayer films exhibiting a linear and an exponential growth regime : An in situ atomic force microscopy study. *Macromolecules* **35**, 4458-4465.
71. Picart, C., Mutterer, J., Richert, L., Luo, Y., Prestwich, G. D., Schaaf, P., Voegel, J.-C. & Lavalle, P. (2002). Molecular basis for the explanation of the exponential growth of polyelectrolyte multilayers. *Proc Natl Acad Sci USA* **99**, 12531-12535.
72. Richert, L., Boulmedais, F., Lavalle, P., Mutterer, J., Ferreux, E., Decher, G., Schaaf, P., Voegel, J.-C. & Picart, C. (2004). Improvement of stability and cell adhesion properties of polyelectrolyte multilayer films by chemical cross-linking. *Biomacromolecules* **5**, 284-294.
73. Richert, L., Lavalle, P., Payan, E., Stoltz, J.-F., Shu, X. Z., Prestwich, G. D., Schaaf, P., Voegel, J.-C. & Picart, C. (2004). Layer-by-layer buildup of polysaccharide films : Physical chemistry and cellular adhesion aspects. *Langmuir* **1**, 284-294.
74. Picart, C., Elkaim, R., Richert, L., Audoin, F., Da Silva Cardoso, M., Schaaf, P., Voegel, J.-C. & Frisch, B. (2005). Primary cell adhesion on RGD functionalized and covalently cross-linked polyelectrolyte multilayer thin films. *Adv Funct Mater* **15**, 83-94.
75. Mendelsohn, J. D., Yang, S. Y., Hiller, J., Hochbaum, A. I. & Rubner, M. F. (2003). Rational design of cytophilic and cytophobic polyelectrolyte multilayer thin films. *Biomacromolecules* **4**, 96-106.
76. Olenych, S. G., Moussallem, M. D., Salloum, D. S., Schlenoff, J. B. & Keller, T. C. (2005). Fibronectin and cell attachment to cell and protein resistant polyelectrolyte surfaces. *Biomacromolecules* **6**, 3252-3258.
77. Stevens, M. M. & George, J. H. (2005). Exploring and engineering the cell surface interface. *Science* **310**, 1135-8.
78. Ingber, D. (1991). Integrins as mechanochemical transducers. *Curr Opin Cell Biol* **3**, 841-848.
79. Engler, A., Bacakova, L., Newman, C., Hategan, A., Griffin, M. & Discher, D. E. (2004). Substrate compliance versus ligand density in cell on gel responses. *Biophys J* **86**, 617-628.
80. Lutolf, M. P., Raeber, G. P., Zisch, A. H., Tirelli, N. & Hubbell, J. A. (2003). Cell-responsive synthetic hydrogels. *Adv Mater* **15**, 888-+.
81. Moon, J. J., Saik, J. E., Poche, R. A., Leslie-Barbick, J. E., Lee, S. H., Smith, A. A., Dickinson, M. E. & West, J. L. (2010). Biomimetic hydrogels with pro-angiogenic properties. *Biomaterials* **31**, 3840-3847.
82. Genes, N. G., Rowley, J. A., Mooney, D. J. & Bonassar, L. J. (2004). Effect of substrate mechanics on chondrocyte adhesion to modified alginate surfaces. *Arch Biochem Biophys* **422**, 161-7.
83. Young, J. L. & Engler, A. J. (2011). Hydrogels with time-dependent material properties enhance cardiomyocyte differentiation in vitro. *Biomaterials* **32**, 1002-9.
84. Francius, G., Hemmerle, J., Ball, V., Lavalle, P., Picart, C., Voegel, J., Schaaf, P. & Senger, B. (2007). Stiffening of soft polyelectrolyte architectures by multilayer capping evidenced by viscoelastic analysis of AFM indentation measurements. *J Phys Chem* **111**, 8299-8306.
85. Thompson, M. T., Berg, M. C., Tobias, I. S., Rubner, M. F. & Van Vliet, K. J. (2005). Tuning compliance of nanoscale polyelectrolyte multilayers to modulate cell adhesion. *Biomaterials* **26**, 6836-6845.
86. Lin, Q. K., Ding, X., Qiu, F. Y., Song, X. X., Fu, G. S. & Ji, J. (2010). In situ endothelialization of intravascular stents coated with an anti-CD34 antibody functionalized heparin-collagen multilayer. *Biomaterials* **31**, 4017-4025.
87. Olugebefola, S. C., Ryu, S. W., Nolte, A. J., Rubner, M. F. & Mayes, A. M. (2006). Photo-cross-linkable polyelectrolyte multilayers for 2-D and 3-D patterning. *Langmuir* **22**, 5958-62.
88. Pozos Vazquez, C., Boudou, T., Dulong, V., Nicolas, C., Picart, C. & Glinel, K. (2009). Variation of polyelectrolyte film stiffness by photo-cross-linking: A new way to control cell adhesion. *Langmuir* **25**, 3556-3563.
89. Jan, E. & Kotov, N. A. (2007). Successful differentiation of mouse neural stem cells on layer-by-layer assembled single-walled carbon nanotube composite. *Nano Lett* **7**, 1123-1128.
90. Kocgozlu, L., Lavalle, P., Koenig, G., Senger, B., Haikel, Y., Schaaf, P., Voegel, J. C., Tenenbaum, H. & Vautier, D. (2010). Selective and uncoupled role of substrate elasticity in the regulation of replication and transcription in epithelial cells. *J Cell Sci* **123**, 29-39.

91. Chen, A. A., Khetani, S. R., Lee, S., Bhatia, S. N. & Van Vliet, K. J. (2009). Modulation of hepatocyte phenotype in vitro via chemomechanical tuning of polyelectrolyte multilayers. *Biomaterials* **30**, 1113-20.
92. Schneider, A., Francius, G., Obeid, R., Schwinté, P., Frisch, B., Schaaf, P., Voegel, J.-C., Senger, B. & Picart, C. (2006). Polyelectrolyte multilayer with tunable Young's modulus : influence on cell adhesion. *Langmuir* **22**, 1193-1200.
93. Richert, L., Schneider, A., Vautier, D., Vodouhe, C., Jessel, N., Payan, E., Schaaf, P., Voegel, J. C. & Picart, C. (2006). Imaging cell interactions with native and crosslinked polyelectrolyte multilayers. *Cell Biochem Biophys* **44**, 273-85.
94. Richert, L., Engler, A. J., Discher, D. E. & Picart, C. (2004). Elasticity of native and cross-linked polyelectrolyte multilayers. *Biomacromolecules* **5**, 1908-1916.
95. Ren, K., Crouzier, T., Roy, C. & Picart, C. (2008). Polyelectrolyte multilayer films of controlled stiffness modulate myoblast cells differentiation. *Adv Funct Mater* **18**, 1378-1389.
96. Brooke, G., Cooka, M., Blair, C., Han, R., Heazlewood, C., Jones, B., Kambouris, M., Kollar, K., McTaggart, S., Pelekanos, R., Rice, A., Rossetti, T. & Atkinson, K. (2007). Therapeutic applications of mesenchymal stromal cells. *Semin Cell Dev Biol* **18**, 846-858.
97. Semenov, O. V., Malek, A., Bittermann, A. G., Voros, J. & Zisch, A. (2009). Engineered polyelectrolyte multilayer substrates for adhesion, proliferation and differentiation of human mesenchymal stem cells. *Tissue Eng Part A* **15**, 2977-2990.
98. Niwa, H. (2007). How is pluripotency determined and maintained? *Development* **134**, 635-46.
99. Picart, C., Senger, B., Sengupta, K., Dubreuil, F. & Fery, A. (2007). Measuring mechanical properties of polyelectrolyte multilayer thin films : novel methods based on AFM and optical techniques. *Colloid Surf A* **303**, 30-36.
100. Gheith, M. K., Sinani, V. A., Wicksted, J. P., Matts, R. L. & Kotov, N. A. (2005). Single-walled carbon nanotube polyelectrolyte multilayers and freestanding films as a biocompatible platformfor neuroprosthetic implants. *Adv Mater* **17**, 2663-2667.
101. Jiang, C. & Tsukruk, V. (2006). Freestanding nanostructures via layer-by-layer assembly. *Adv Mater* **18**, 829-840.
102. Tang, Z., Kotov, N. A., Magonov, S. & Ozturk, B. (2003). Nanostructured artificial nacre. *Nat Mater* **2**, 413-418.
103. Podsiadlo, P., Tang, Z., Shim, B. S. & Kotov, N. A. (2007). Counterintuitive effect of molecular strength and role of molecular rigidity on mechanical properties of layer-by-layer assembled nanocomposites. *Nano Lett* **7**, 1224-31.
104. Srivastava, S. & Kotov, N. A. (2008). Composite Layer-by-Layer (LBL) assembly with inorganic nanoparticles and nanowires. *Acc Chem Res* **41**, 1831-41.
105. Skirtach, A. G., Volodkin, D. V. & Mohwald, H. (2010). Bio-interfaces--interaction of PLL/HA thick films with nanoparticles and microcapsules. *Chem Phys Chem* **11**, 822-9.
106. Kotov, N. A., Winter, J. O., Clements, I. P., Jan, E., Timko, B. P., Campidelli, S., Pathak, S., Mazzatenta, A., Lieber, C. M., Prato, M., Bellamkonda, R. V., Silva, G. A., Kam, N. W. S., Patolsky, F. & Ballerini, L. (2009). Nanomaterials for Neural Interfaces. *Adv Mater* **21**, 3970-4004.
107. Kam, N. W. S., Jan, E. & Kotov, N. A. (2009). Electrical stimulation of neural stem cells mediated by humanized carbon nanotube composite made with extracellular matrix protein. *Nano Lett* **9**, 273-278.
108. Mehrotra, S., Hunley, S. C., Pawelec, K. M., Zhang, L. X., Lee, I., Baek, S. & Chan, C. (2010). Cell Adhesive Behavior on Thin Polyelectrolyte Multilayers: Cells Attempt to Achieve Homeostasis of Its Adhesion Energy. *Langmuir* **26**, 12794-12802.
109. Garcia, A. J., Takagi, J. & Boettiger, D. (1998). Two-stage activation for alpha5beta1 integrin binding to surface-adsorbed fibronectin. *J Biol Chem* **273**, 34710-5.
110. Friess, W. (1998). Collagen - biomaterial for drug delivery. *Eur J Pharm Biopharm* **45**, 113-136.
111. Grinnell, F. (2000). Fibroblast-collagen-matrix contraction: growth-factor signalling and mechanical loading. *Trens Cell Biol* **10**, 362-365.
112. Wittmer, C. R., Phelps, J. A., Saltzman, W. M. & Van Tassel, P. R. (2007). Fibronectin terminated multilayer films: protein adsorption and cell attachment studies. *Biomaterials* **28**, 851-860.
113. Keselowsky, B. G., Collard, D. M. & Garcia, A. J. (2003). Surface chemistry modulates fibronectin conformation and directs integrin binding and specificity to control cell adhesion. *J Biomed Mater Res A* **66A**, 247-259.
114. Little, W. C., Schwartlander, R., Smith, M. L., Gourdon, D. & Vogel, V. (2009). Stretched Extracellular Matrix Proteins Turn Fouling and Are Functionally Rescued by the Chaperones Albumin and Casein. *Nano Lett* **9**, 4158-4167.
115. Lee, H., Jang, Y., Seo, J., Nam, J. M. & Char, K. (2011). Nanoparticle-Functionalized Polymer Platform for Controlling Metastatic Cancer Cell Adhesion, Shape, and Motility. *ACS Nano* **5**, 5444-5456.
116. Berg, M. C., Yang, S. Y., Hammond, P. T. & Rubner, M. F. (2004). Controlling mammalian cell interactions on patterned polyelectrolyte multilayer surfaces. *Langmuir* **20**, 1362-1368.
117. Werner, S., Huck, O., Frisch, B., Vautier, D., Elkaim, R., Voegel, J. C., Brunel, G. & Tenenbaum, H. (2009). The effect of microstructured surfaces and laminin-derived peptide coatings on soft tissue interactions with titanium dental implants. *Biomaterials* **30**, 2291-2301.

118. Tsai, W. B., Chen, R. P. Y., Wei, K. L., Chen, Y. R., Liao, T. Y., Liu, H. L. & Lai, J. Y. (2009). Polyelectrolyte multilayer films functionalized with peptides for promoting osteoblast functions. *Acta Biomater* **5**, 3467-3477.
119. Chua, P. H., Neoh, K. G., Kang, E. T. & Wang, W. (2008). Surface functionalization of titanium with hyaluronic acid/chitosan polyelectrolyte multilayers and RGD for promoting osteoblast functions and inhibiting bacterial adhesion. *Biomaterials* **29**, 1412-21.
120. Thompson, M. T., Berg, M. C., Tobias, I. S., Lichter, J. A., Rubner, M. F. & Van Vliet, K. J. (2006). Biochemical functionalization of polymeric cell substrata can alter mechanical compliance. *Biomacromolecules* **7**, 1990-1995.
121. Schneider, A., Bolcato-Bellemin, A.-L., Francius, G., Jedrzejwska, J., Schaaf, P., Voegel, J.-C., Frisch, B. & Picart, C. (2006). Glycated polyelectrolyte multilayer films : differential adhesion of primary versus tumor cells. *Biomacromolecules* **7**, 2882-2889.
122. Chluba, J., Voegel, J. C., Decher, G., Erbacher, P., Schaaf, P. & Ogier, J. (2001). Peptide hormone covalently bound to polyelectrolytes and embedded into multilayer architectures conserving full biological activity. *Biomacromolecules* **2**, 800-805.
123. Jessel, N., Schwinté, P., Falvey, P., Darcy, R., Haïkel, Y., Schaaf, P., Voegel, J.-C. & Ogier, J. (2004). Build-up of polypeptide multilayer coatings with anti-inflammatory properties based on the embedding of piroxicam-cyclodextrin complexes. *Adv Funct Mater* **14**, 174-182.
124. Ma, L., Zhou, J., Gao, C. & Shen, J. (2007). Incorporation of basic fibroblast growth factor by a layer-by-layer assembly technique to produce bioactive substrates. *J Biomed Mater Res B* **83**, 285-292.
125. Almodovar, J., Bacon, S., Gogolski, J., Kisiday, J. D. & Kipper, M. J. (2010). Polysaccharide-Based Polyelectrolyte Multi layer Surface Coatings can Enhance Mesenchymal Stem Cell Response to Adsorbed Growth Factors. *Biomacromolecules* **11**, 2629-2639.
126. Macdonald, M. L., Rodriguez, N. M., Shah, N. J. & Hammond, P. T. (2010). Characterization of Tunable FGF-2 Releasing Polyelectrolyte Multilayers. *Biomacromolecules* **11**, 2053-2059.
127. De Cock, L. J., De Koker, S., De Vos, F., Vervaet, C., Remon, J. P. & De Geest, B. G. (2010). Layer-by-Layer Incorporation of Growth Factors in Decellularized Aortic Heart Valve Leaflets. *Biomacromolecules* **11**, 1002-1008.
128. Vodouhe, C., Schmittbuhl, M., Boulmedais, F., Bagnard, D., Vautier, D., Schaaf, P., Egles, C., Voegel, J. C. & Ogier, J. (2005). Effect of functionalization of multilayered polyelectrolyte films on motoneuron growth. *Biomaterials* **26**, 545-554.
129. Muller, S., Koenig, G., Charpiot, A., Debry, C., Voegel, J., Lavalle, P. & Vautier, D. (2008). VEGF-functionalized polyelectrolyte multilayers as proangiogenic prosthetic coatings *Adv Funct Mat* **18**, 1767-1775
130. Dierich, A., Le Guen, E., Messaddeq, N., Stoltz, S., Netter, P., Schaaf, P., Voegel, J.-C. & Benkirane-Jessel, N. (2007). Bone formation mediated by synergy-acting growth factors embedded in a polyelectrolyte multilayer film. *Adv Mater* **19**, 693-697.
131. Nadiri, A., Kuchler-Bopp, S., Mjahed, H., Hu, B., Haikel, Y., Schaaf, P., Voegel, J. C. & Benkirane-Jessel, N. (2007). Cell apoptosis control using BMP4 and noggin embedded in a polyelectrolyte multilayer film. *Small* **3**, 1577-1583.
132. Paralkar, V. M., Hammonds, R. G. & Reddi, A. H. (1991). Identification and characterization of cellular binding proteins (receptors) for recombinant human bone morphogenetic protein 2B, an initiator of bone differentiation cascade. *Proc Natl Acad Sci U S A* **88**, 3397-401.
133. van den Beucken, J. J., Walboomers, X. F., Boerman, O. C., Vos, M. R., Sommerdijk, N. A., Hayakawa, T., Fukushima, T., Okahata, Y., Nolte, R. J. & Jansen, J. A. (2006). Functionalization of multilayered DNA-coatings with bone morphogenetic protein 2. *J Controlled Release* **113**, 63-72.
134. Macdonald, M. L., Samuel, R. E., Shah, N. J., Padera, R. F., Beben, Y. M. & Hammond, P. T. (2011). Tissue integration of growth factor-eluting layer-by-layer polyelectrolyte multilayer coated implants. *Biomaterials* **32**, 1446-53.
135. Crouzier, T., Szarpak, A., Boudou, T., Auzely-Velty, R. & Picart, C. (2010). Polysaccharide-blend multilayers containing hyaluronan and heparin as a delivery system for rhBMP-2. *Small* **6**, 651-662.
136. Crouzier, T., Sailhan, F., Becquart, P., Guillot, R., Logeart-Avramoglou, D. & Picart, C. (2011). The performance of BMP-2 loaded TCP/HAP porous ceramics with a polyelectrolyte multilayer film coating. *Biomaterials* **32**, 7543-54.
137. Doshi, N., Swiston, A. J., Gilbert, J. B., Alcaraz, M. L., Cohen, R. E., Rubner, M. F. & Mitragotri, S. (2011). Cell-based drug delivery devices using phagocytosis-resistant backpacks. *Adv Mater***23**, H105-H109.
138. Swiston, A. J., Cheng, C., Um, S. H., Irvine, D. J., Cohen, R. E. & Rubner, M. F. (2008). Surface functionalization of living cells with multilayer patches. *Nano Lett* **8**, 4446-53.
139. Ren, K., Fourel, L., Gauthier-Rouviere, C., Albiges-Rizo, C. & Picart, C. (2010). Manipulation of the adhesive behaviour of skeletal muscle cells on soft and stiff polyelectrolyte multilayers. *Acta Biomater* **6**, 4238-48.
140. Lutolf, M. P., Weber, F. E., Schmoekel, H. G., Schense, J. C., Kohler, T., Muller, R. & Hubbell, J. A. (2003). Repair of bone defects using synthetic mimetics of collagenous extracellular matrices. *Nat Biotechnol* **21**, 513-8.

141. Nichols, J. E., Cortiella, J., Lee, J., Niles, J. A., Cuddihy, M., Wang, S., Bielitzki, J., Cantu, A., Mlcak, R., Valdivia, E., Yancy, R., McClure, M. L. & Kotov, N. A. (2009). In vitro analog of human bone marrow from 3D scaffolds with biomimetic inverted colloidal crystal geometry. *Biomaterials* **30**, 1071-1079.
142. Lee, J. & Kotov, N. A. (2009). Notch Ligand Presenting Acellular 3D Microenvironments for ex vivo Human Hematopoietic Stem-Cell Culture made by Layer-By-Layer Assembly. *Small* **5**, 1008-1013.
143. Guillame-Gentil, O., Semenov, O., Roca, A. S., Groth, T., Zahn, R., Voros, J. & Zenobi-Wong, M. (2010). Engineering the Extracellular Environment: Strategies for Building 2D and 3D Cellular Structures. *Adv Mater* **22**, 5443-5462.
144. Broderick, A. H., Azarin, S. M., Buck, M. E., Palecek, S. P. & Lynn, D. M. (2011). Fabrication and selective functionalization of amine-reactive polymer multilayers on topographically patterned microwell cell culture arrays. *Biomacromolecules* **12**, 1998-2007.
145. Shah, N. J., Macdonald, M. L., Beben, Y. M., Padera, R. F., Samuel, R. E. & Hammond, P. T. (2011). Tunable dual growth factor delivery from polyelectrolyte multilayer films. *Biomaterials* **32**, 6183-6193.
146. Mertz, D., Vogt, C., Hemmerle, J., Mutterer, J., Ball, V., Voegel, J. C., Schaaf, P. & Lavalle, P. (2009). Mechanotransductive surfaces for reversible biocatalysis activation. *Nat Mater* **8**, 731-735.
147. Reisch, A., Hemmerle, J., Chassepot, A., Lefort, M., Benkirane-Jessel, N., Candolfi, E., Mesini, P., Letscher-Bru, V., Voegel, J. C. & Schaaf, P. (2010). Anti-fouling phosphorylcholine bearing polyelectrolyte multilayers: Cell adhesion resistance at rest and under stretching. *Soft Matter* **6**, 1503-1512.
148. Brown, X. Q., Ookawa, K. & Wong, J. Y. (2005). Evaluation of polydimethylsiloxane scaffolds with physiologically-relevant elastic moduli: interplay of substrate mechanics and surface chemistry effects on vascular smooth muscle cell response. *Biomaterials* **26**, 3123-9.
149. Wipff, P. J., Majd, H., Acharya, C., Buscemi, L., Meister, J. J. & Hinz, B. (2009). The covalent attachment of adhesion molecules to silicone membranes for cell stretching applications. *Biomaterials* **30**, 1781-1789.
150. Kirchhof, K., Andar, A., Yin, H. B., Gadegaard, N., Riehle, M. O. & Groth, T. (2011). Polyelectrolyte multilayers generated in a microfluidic device with pH gradients direct adhesion and movement of cells. *Lab on a Chip* **11**, 3326-3335.
151. Boulmedais, F., Tang, C. S., Keller, B. & Voros, J. (2006). Controlled electrodissolution of polyelectrolyte multilayers: A platform technology towards the surface-initiated delivery of drugs. *Adv Funct Mater* **16**, 63-70.
152. Wood, K. C., Zacharia, N. S., Schmidt, D. J., Wrightman, S. N., Andaya, B. J. & Hammond, P. T. (2008). Electroactive controlled release thin films. *Proc Natl Acad Sci USA* **105**, 2280-2285.
153. Guillaume-Gentil, O., Akiyama, Y., Schuler, M., Tang, C., Textor, M., Yamato, M., Okano, T. & Voros, J. (2008). Polyelectrolyte coatings with a potential for electronic control and cell sheet engineering. *Adv Mater* **20**, 560.
154. Crouzier, T., Fourel, L., Boudou, T., Albiges-Rizo, C. & Picart, C. (2011). Presentation of BMP-2 from a soft biopolymeric film unveils its activity on cell adhesion and migration. *Adv Mater* **23**, H111-8.
155. Volodkin, D. V., Delcea, M., Mohwald, H. & Skirtach, A. G. (2009). Remote near-IR light activation of a hyaluronic acid/poly(l-lysine) multilayered film and film-entrapped microcapsules. *ACS Appl Mater Interfaces* **1**, 1705-10.
156. Volodkin, D. V., Madaboosi, N., Blacklock, J., Skirtach, A. G. & Mohwald, H. (2009). Surface-supported multilayers decorated with bio-active material aimed at light-triggered drug delivery. *Langmuir* **25**, 14037-43.
157. Fischer, D., Li, Y. X., Ahlemeyer, B., Krieglstein, J. & Kissel, T. (2003). In vitro cytotoxicity testing of polycations: influence of polymer structure on cell viability and hemolysis. *Biomaterials* **24**, 1121-1131.
158. Kean, T. & Thanou, M. (2010). Biodegradation, biodistribution and toxicity of chitosan. *Adv Drug Deliv Rev* **62**, 3-11.
159. Brunot, C., Ponsonnet, L., Lagneau, C., Farge, P., Picart, C. & Grosgogeat, B. (2007). Cytotoxicity of polyethyleneimine (PEI), precursor base layer of polyelectrolyte multilayer films. *Biomaterials* **28**, 632-40.
160. Kerdjoudj, H., Berthelemy, N., Rinckenbach, S., Kearney-Schwartz, A., Montagne, K., Schaaf, P., Lacolley, P., Stoltz, J. F., Voegel, J. C. & Menu, P. (2008). Small vessel replacement by human umbilical arteries with polyelectrolyte film-treated arteries: In Vivo behavior. *J Amer Coll Cardiol* **52**, 1589-1597.
161. Meng, S., Liu, Z. J., Shen, L., Guo, Z., Chou, L. S. L., Zhong, W., Du, Q. G. & Ge, J. (2009). The effect of a layer-by-layer chitosan-heparin coating on the endothelialization and coagulation properties of a coronary stent system. *Biomaterials* **30**, 2276-2283.
162. Schultz, P., Vautier, D., Richert, L., Jessel, N., Haikel, Y., Schaaf, P., Voegel, J. C., Ogier, J. & Debry, C. (2005). Polyelectrolyte multilayers functionalized by a synthetic analogue of an anti-inflammatory peptide, alpha-MSH, for coating a tracheal prosthesis. *Biomaterials* **26**, 2621-2630.
163. De Cock, L. J., Lenoir, J., De Koker, S., Vermeersch, V., Skirtach, A. G., Dubruel, P., Adriaens, E., Vervaet, C., Remon, J. P. & De Geest, B. G. (2011). Mucosal irritation potential of

polyelectrolyte multilayer capsules. *Biomaterials* **32**, 1967-1977.
164. Adriaens, E. & Remon, J. P. (1999). Gastropods as an evaluation tool for screening the irritating potency of absorption enhancers and drugs. *Pharm Res* **16**, 1240-1244.
165. De Koker, S., Naessens, T., De Geest, B. G., Bogaert, P., Demeester, J., De Smedt, S. & Grooten, J. (2010). Biodegradable Polyelectrolyte Microcapsules: Antigen Delivery Tools with Th17 Skewing Activity after Pulmonary Delivery. *J Immunol* **184**, 203-211.
166. Wilson, J. T., Cui, W., Kozlovskaya, V., Kharlampieva, E., Pan, D., Qu, Z., Krishnamurthy, V. R., Mets, J., Kumar, V., Wen, J., Song, Y., Tsukruk, V. V. & Chaikof, E. L. (2011). Cell surface engineering with polyelectrolyte multilayer thin films. *J Am Chem Soc* **133**, 7054-64.
167. Hynes, R. O. (2009). The extracellular matrix: not just pretty fibrils. *Science* **326**, 1216-9.

Annexe III – Grafting protocols

Synthesis of PGA-maleimide

Materials:

- PGA (Poly-(L-glutamic acid)), Sigma 54886, lot 017K5108
- EDC (N-ethyl-N(3-dimethylaminopropylcarbodiimide), Sigma E7750, lot BCBB9878V
- S-NHS (N-hydroxysulfosuccinimide), Sigma 56485, lot BCBB6771
- HEPES, Sigma
- Maleimide : 1) N-(2-aminoethyl maleimide trifluoracetate), Sigma 56951, lot 1442171V; 2) 2-maleimidoethylamine, Aochem (China) E3333, lot 20121129
- Spectra/Por dyalisis membrane, MWCO 6-8,000 , Spectrum Laboratories

Grafting procedure **(**for ~100 mg of the final product):

- Prepare "HEPES 6.5" buffer: HEPES 10 mM pH 6.5 (store at 4°C)
- Dissolve 100 mg of PGA in 2 mL HEPES 6.5 buffer, transfer to a small round-bottom flask (~10-20 mL of total volume) under magnetic stirring (= reaction mixture)
- Dissolve 5 mg of S-NHS in 1 mL HEPES 6.5 buffer and add to the reaction mixture
- Dissolve 33 mg of EDC in 1 mL HEPES 6.5 buffer and add to the reaction mixture
- Place under nitrogen atmosphere
- Dissolve 40 mg (Sigma) or 23 mg (Aochem) of maleimide in 1 mL HEPES 6.5 buffer and add to the reaction mixture under stirring and nitrogen atmosphere (use syringe to inject)
- Incubate for 24h at RT

Purification (dialysis):

- Wash the membrane in Na_2HCO_3 (~1 spoon of powder for 1L of water) at 80°C for 20 minutes, rinse with water
- Add the product and dialyse against water

Freeze-drying:

- Transfer the product to a round-bottom flask for freeze-drying, freeze with liquid nitrogen and insert into the freeze-dryer
- Store the dry product at -20°C

NMR analysis:

- Dissolve ~3-4 mg of the product in 500-600 µL of D_2O
- Analyse by ^1H NMR at 298K

Grafting of RGD peptide

Materials:

- PGA-maleimide DS 16%
- HEPES, Sigma
- RGD peptide: CGPKGDRGDAGPKGA, Genecust
- MPA (3-mercaptopropionic acid), Sigma 145801
- Spectra/Por dyalisis membrane, MWCO 6-8,000 , Spectrum Laboratories

Grafting procedure (for about 10 mg of the final product):

- Prepare the "HEPES 7.4" buffer: HEPES 10 mM pH 7,4 (store at 4°C)
- Dissolve 10 mg of PGA-maleimide in 1,5 mL of HEPES 7.4 buffer
- Dissolve 10 mg of RGD peptide in1,5 mL of HEPES 7.4 buffer
- Mix and incubate under magnetic stirring at RT for 24h
- Add 2 µl of MPA (under the hood!) and incubate under magnetic stirring at RT for 24h
- Purify by dialysis, freeze-dry, analyse by ^{1}H NMR at 298K, store at -20°C

Annexe IV - NMR spectra

PGA, 353 K

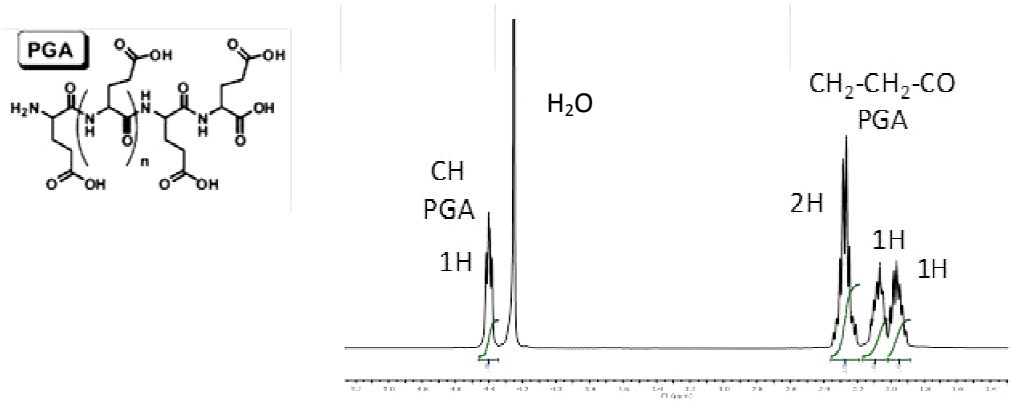

PGA-maleimide, 353 K

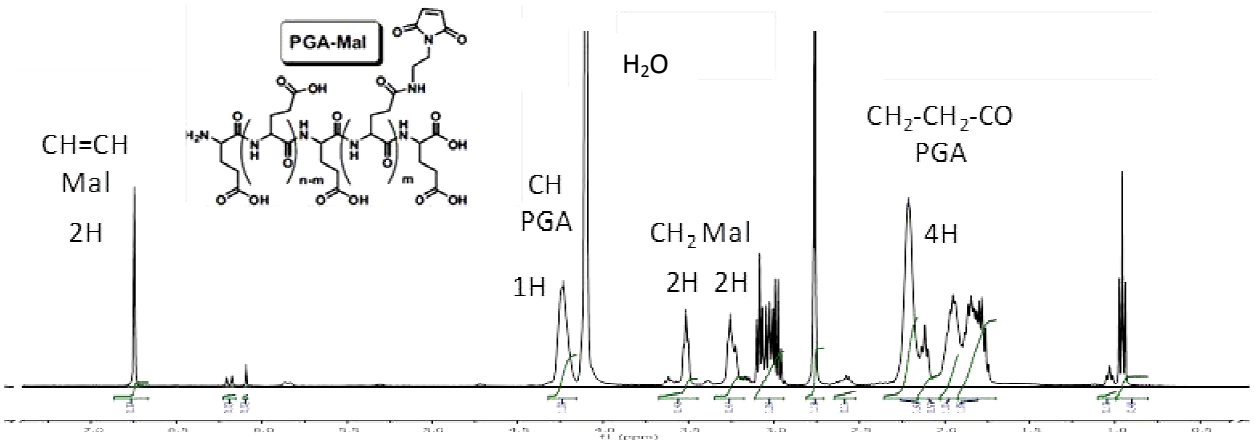

RGD, 298 K

Cys-Gly-Pro-Lys-Gly-Asp-Arg-Gly-Asp-Ala-Gly-Pro-Lys-Gly-Ala

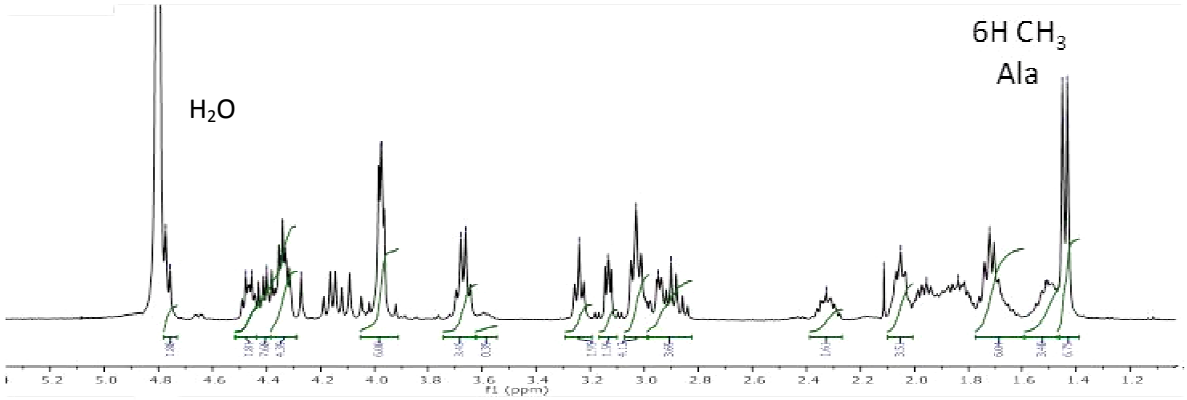

PGA-maleimide-RGD, 298 K

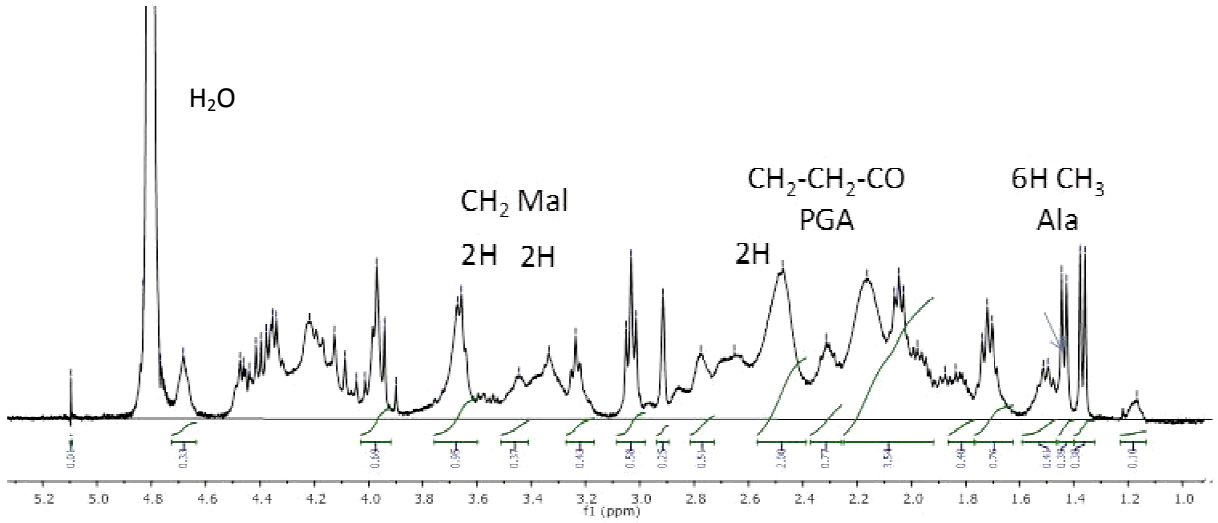

pBMP-2, 298 K

Cys-Gly-Lys-Ile-Pro-Lys-Ala-Ser-Ser-Val-Pro-Thr-Glu-Leu-Ser-Ala-Ile-Ser-Thr-Leu-Tyr-Leu

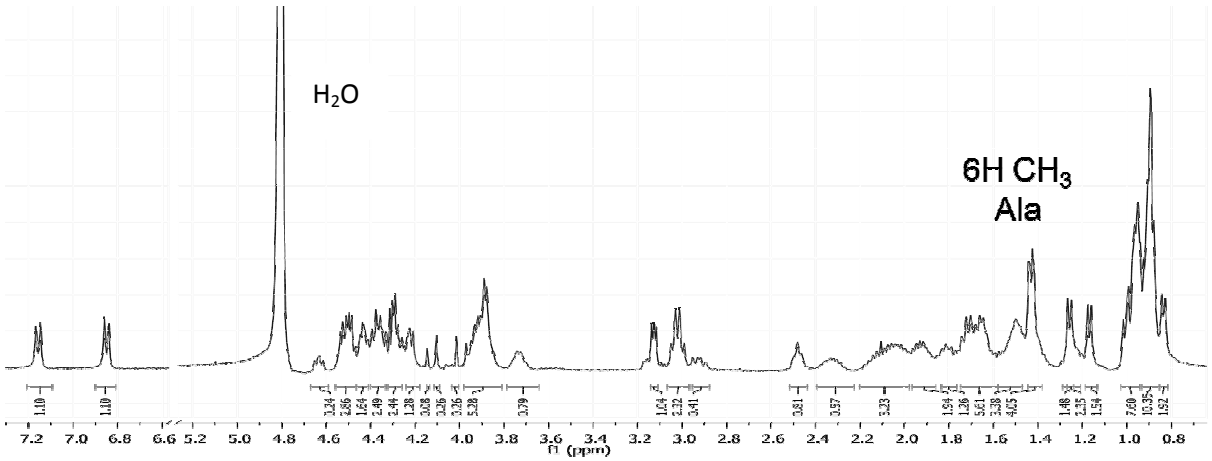

PGA-maleimide-pBMP-2, 298 K

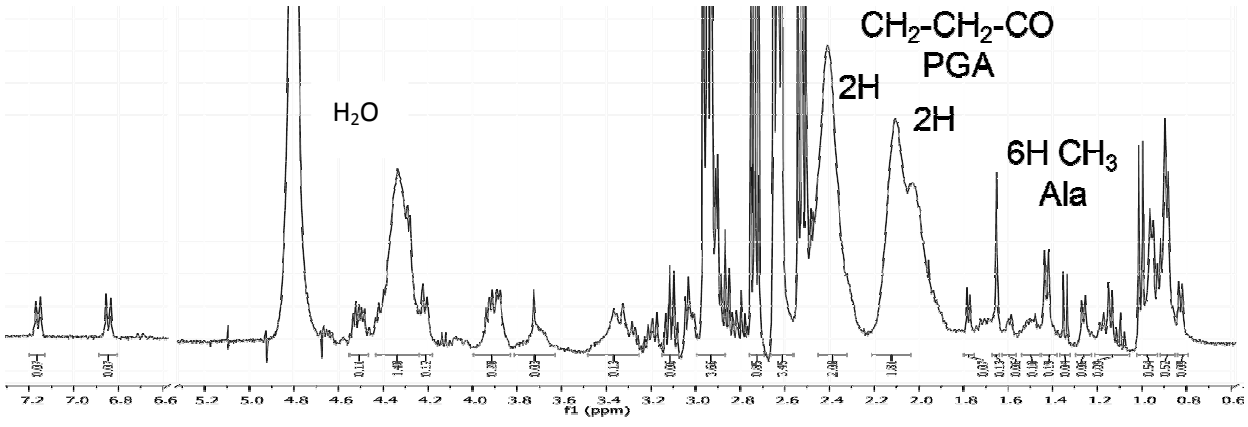

Annexe V - Curriculum Vitae

Varvara GRIBOVA

Born in Vilnius, Lithuania, May 29th, 1985
67 avenue Alsace-Lorraine
38000 Grenoble
Tel : (+33) 06 13 81 89 74
E-mail : varvara.gribova@gmail.com

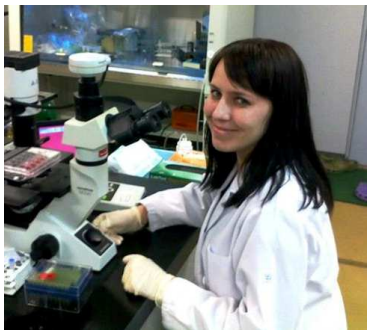

Education

2010 – 2013 **Grenoble Institute of Technology (Grenoble, France)**
Doctorate, Biomaterials & Tissue Engineering

2009 – 2010 **Université de Pierre et Marie Curie (UPMC) /Paris VI (Paris, France)**
Master 2 Cell Biology, Development and Stem Cells

2007 – 2009 **Université de Franche-Comté (Besançon, France)**
Master 1 Biochemistry, Cellular and Molecular Biology

2007 – 2009 **Université de Franche-Comté (Besançon, France)**
Licence 3 Biochemistry, Cellular Biology and Physiology

2003 – 2006 **Lomonosov Moscow State University (Moscow, Russia)**
Faculty of Biology, Zoology Department

1991 – 2003 **Secondary school « Naujamiesčio » (Vilnius, Lithuania)**
High school diploma

Professional experience

2010 – 2013 **Grenoble INP/Minatec**, Laboratory of Materials and Physical Engineering
PhD thesis: Development of biomimetic films for musculo-skeletal tissue engineering applications

2009 – 2010 **INSERM U972,** Laboratory "Stem Cells: from their niches to therapeutic applications" (Kremlin-Bicêtre, Ile-de-France)
Internship (8 months) : Study of differentiation potential of human fetal liver mesenchymal stem cells

2009 **Institute of Developmental Biology and Cancer, CNRS UMR 6543 (Nice)**
Internship (2 months): Proliferation and differentiation of the cells derived from undifferintiated liposarcomas

Languages

- **Russian:** mother tongue
- **French, English:** advanced level
- **Lituanian:** to reactivate; **Japanese**: notions

Interests

Painting, drawing, infographics, scientific illustration, arts and crafts
Personal website: http://biology-art.ucoz.com

Publications

Gribova, V., Crouzier, T. and C. Picart. A material's point of view on recent developments of polymeric biomaterials: control of mechanical and biochemical properties. *Journal of Materials Chemistry*, 2011, **21**: 14354-14366

Gribova, V., Auzely-Velty, A. and C. Picart. Polyelectrolyte multilayer assemblies on materials surfaces: from cell adhesion to tissue engineering. *Chemistry of Materials,* 2012, **24**:854−869

Gribova, V., Gauthier-Rouvière, C., Albigès-Rizo, C., Auzély-Velty, R. and C. Picart. Effect of RGD-functionalization and stiffness modulation of polyelectrolyte multilayer films on muscle cell differentiation. *Acta Biomaterialia*, 2013, **9**(5):6468-80

Conferences

Oral communications:

- 1st ERC Biomim meeting "At the Frontier between Materials and Biology", April 10-12, 2013, Grenoble
- 10th Annual Meeting of the French Society of Myology and Myogenesis Club, November 14-16th, 2012, Grenoble
- 3rd Workshop « Nano & Micro-Environments for Cell Biology » by Nanosciences Fondation of Grenoble, December 15th, 2011, Grenoble

Posters:

- Gordon Research Conference on Signal Transduction by Engineered Extracellular Matrices, July 8-13th, 2012, University of New England, Biddeford ME, USA
- 50th Anniversary of the French Society for Extracellular Matrix Biology, March 29-30th, 2012, Paris
- Myogenesis Club, October 27-28th, 2011, Lyon
- International LbL Symposium "20 Years of Layer-by-Layer Assembly: New Frontiers for Fundamental Science and for Applications", March 10-12th, 2011, Strasbourg

Awards

- Postdoctoral fellowship for North American and European researchers from Japan Society for the Promotion of Science (JSPS) (from January 2014)
- Travel fellowship awarded by the Society for Biology of the Cell – France for participation at Gordon Research Conference (GRC) « Signal Transduction by Engineered Extracellular Matrices » (2012, USA)
- Merit scholarship for academic achievements awarded by the French Ministry of Higher Education and Research for the period of Master program (2008-2010)
- Merit scholarship for academic achievements awarded by the Moscow State University (2004-2006)

Abstract

Tissue engineering approach consists in combining cells, engineering and biomaterials to improve the biological functions of damaged tissues or to replace them. Production of "artificial tissues" is still challenging and requires collaboration of scientists from different domains like cell biology, chemistry, materials and polymer science.

Skeletal muscle tissue engineering holds promise for the replacement of muscle due to an injury and for the treatment of muscle diseases, such as muscle dystrophies or paralysis, but is also required for pharmaceutical assays. To this end, materials with tunable mechanical and biochemical properties for myoblast expansion and differentiation *in vitro,* as well as for the studies of myogenesis on controlled 2D microenvironments or in 3D scaffolds, are crucially needed.

In this work, we used layer-by-layer (LbL) assemblies for two goals. The first consisted in the development of multifunctional biomimetic thin films for the control of skeletal muscle cell fate on 2D substrates. We used LbL films made of polypeptides, which can be stiffened by chemical cross-linking and can be specifically functionalized by grafting of biomimetic peptides onto their surface. In addition, we combined the peptide-grafted films with substrate microtopography. Such approach is promising for the development or multifunctional materials that combine the different stimuli present in *in vivo* ECM, among them physical and biochemical cues, but also microtopography.

In the second part, we use LbL assemblies for the construction of 3D skeletal muscle microtissues. This allows to rapidly build 3D muscle tissues and is promising for the *in vitro* construction of physiologically relevant skeletal muscle tissue models.

Résumé

L'ingénierie tissulaire consiste à assembler de façon intelligente des cellules et des matériaux biocompatibles dans le but de créer des tissus artificiels. Pour la construction de tissus en laboratoire, il est indispensable d'élaborer des matériaux qui miment cet environnement. Dans ce cadre, la collaboration entre les scientifiques de différents domaines (matériaux, chimie, biologie, biochimie) s'avère nécessaire.

L'ingénierie du muscle squelettique est prometteuse pour remplacer le tissu musculaire endommagé et pour le traitement des maladies du muscle, mais aussi pour les essais pharmaceutiques. Dans ce but, les matériaux avec les propriétés mécaniques et chimiques contrôlées sont requis -- pour l'amplification et la différenciation *in vitro* de cellules souches musculaires, mais aussi pour l'étude de la myogenèse sur des microenvironnements contrôlés 2D et dans les matrices 3D.

Dans ce travail, nous avons utilisé la technique d'assemblage couche par couche (LbL, layer-by-layer) pour deux buts. Le premier a été de développer de nouveaux films biomimétiques possédant des propriétés biochimiques et mécaniques parfaitement contrôlées, pour étudier les interrelations entre ces deux paramètres sur les processus cellulaires. En plus, nous avons associé ces films biomimetiques aux substrats avec la topographie contrôlée, afin de guider la formation du tissu.

Dans un second temps, nous avons utilisé la technique LbL pour organiser les cellules en structures 3D. Nous avons ainsi crée des microtissus d'épaisseur contrôlée, qui pourraient être utilisés en tant que modèles de tissus artificiels pour les applications thérapeutiques ou pour les évaluations de médicament en industrie pharmaceutique.